The Signaling Network of the Caleosins and the Heterotrimeric G Proteins in *Arabidopsis thaliana* and The Analysis of the *Esi3/RCI2/PMP3* and *Pirin* Gene Families in *Triticum aestivum*

Sabrina Christina Brunetti

A Thesis
In the Department
of
Biology

Presented in Partial Fulfillment of the Requirements
For the Degree of
Doctor of Philosophy (Biology) at Concordia University
Montreal, Quebec, Canada

November 2022

CONCORDIA UNIVERSITY
SCHOOL OF GRADUATE STUDIES

This is to certify that the thesis prepared

By: *Sabrina Christina Brunetti*

Entitled:*The Signaling Network of the Caleosins and the Heterotrimeric G Proteins in Arabidopsis thaliana and The Analysis of the Esi3/RCI2/PMP3 and Pirin Gene Families in Triticum aestivum*

and submitted in partial fulfillment of the requirements for the degree of

DOCTOR OF PHILOSOPHY (*Biology*)

complies with the regulations of the University and meets the accepted standards with respect to originality and quality.

Signed by the final examining committee:

_____ Chair
Dr. Wayne Brake

_____ External Examiner
Dr. Virginia Walker

_____ Examiner
Dr. William Zerges

_____ Examiner
Dr. Paul Joyce

_____ Examiner
Dr. Jin Suk Lee

_____ Thesis Supervisor
Dr. Patrick Gulick

Approved by _____
Dr. Robert Bertrand Weladji, Graduate Program Director

January/09/2023 _____
Dr. Pascale Sicotte, Dean
Faculty of Arts and Science

Abstract

The Signaling Network of the Caleosins and the Heterotrimeric G Proteins in Arabidopsis thaliana and The Analysis of the Esi3/RCI2/PMP3 and Pirin Gene Families in Triticum aestivum

Sabrina C. Brunetti, Ph.D

Concordia University 2023

Plants have complex mechanisms of response to environmental stresses that contribute to stress tolerance. This work is directed at the characterization of four classes of genes that encode proteins involved in the response to environmental stresses: caleosins, the α subunit of heterotrimeric G proteins (*GPA1*), *Pirins and Early-Salt-stress-Induced-3* (*Esi3*) genes. The work investigates these genes in the model species, Arabidopsis, or the crop specie, wheat. It also characterizes the physical and genetic interaction of members of the caleosins family, GPA1, and Pirin1, to decipher their potential role in signalling pathways related to stress response in plants. The gene families encoding the *Pirins* and *Esi3s* were also characterized in hexaploid wheat to investigate possible roles in stress responses.

This work reports that the Arabidopsis caleosins RD20/CLO3 and CLO7 interact both physically and genetically with the Gα subunit, GPA1. The interactions were characterized by Bimolecular Fluorescence Complementation and yeast two-hybrid assays. Interactions were enhanced by both calcium and the GTP bound state of GPA1. *RD20*/*CLO3* and *GPA1* play a role in hypocotyl elongation in the dark and in leaf morphology. *CLO7* and *GPA1* play a role in seed germination in response to ABA treatment and osmotic stress. The *clo7 gpa1* double mutant is embryo lethal and cannot be recovered. *RD20*/*CLO3* affects root architecture in response to ABA treatment. Both *RD20*/*CLO3* and *CLO7* affect flowering time under long day conditions.

Members of the *Triticum aestivum Esi3* and *Pirin* gene families were implicated in stress response pathways by their differential expression in response to stress treatment. The *Esi3* gene family is comprised of 29 family members with 10 paralogs each with a copy in the A, B and D genome except for *Esi3-2* which is missing a B copy. All members of the *Esi3* gene family have altered gene expression in response to abiotic and biotic stress conditions. The *Pirin* gene family is comprised of 18 genes with six paralogous gene copies, each having an A, B and D homeolog. The members of the *Pirin* gene family have specialized expression and play differing roles in response to abiotic and biotic stress.

Acknowledgements

I would like to first and foremost thank my supervisor, Dr. Gulick. Dr. Gulick has been a great mentor and supervisor, he has taught me a great deal in my time working with him. His endless support will always be appreciated and never forgotten. He has given me all the tools necessary to be an independent researcher. I thank you from the bottom of my heart.

I would also like to thank my fiancé, James, for his never-ending support, motivation, and patience throughout this entire journey. A big thank you to my parents for providing me with this opportunity and for always believing in me. You have all been a great support network and I would not have been able to accomplish this without you all.

To my committee members, Dr. Zerges and Dr. Lee, who have guided me throughout this journey, I thank you both. You have both taught me a great deal which has contributed greatly to my work and thesis.

To all my labmates, past and present, I thank you all for the great journey we had and the lasting memories. In particular to Michelle, this journey has made it so I leave with a best friend. Your help in the lab is beyond appreciated and the good times we had while doing it will always be remembered.

Lastly, thank you to all the wonderful faculty and staff at Concordia that I have had the pleasure of meeting and working with.

Contribution of Authors

Chapter 2

The published work presented in Chapter 2 entitled "The stress induced caleosin, RD20/CLO3, acts as a negative regulator of GPA1 in Arabidopsis" has multiple authors whose contributions are as follows; PJG designed the project. SCB, ZW, JAW, and HBK participated in the experimental design. SCB created the *rd20 gpa1* double mutant, created the transgenic lines (over-expression), carried out the BiFC and yeast two-hybrid assays, created the RD20/CLO3 calcium mutations, carried out the hypocotyl elongation experiments and the leaf morphology

experiment, carried out the RNA analysis, assisted in the protein purifications and GTPase assay and carried out the *in vitro* binding experiment. SCB analyzed, compiled the data, carried out the statistical analysis and created the figures, SCB wrote the manuscript and contributed to the revisions. MKMA assisted in the BiFC and yeast two-hybrid assays, analyzing the hypocotyl data and contributed to the writing and revision. ZW, HBK, and GG created the non-mutant BiFC clones and the transgenic GUS line. ME, JR and MJL performed the protein purifications and GTPase experiments and analyzed the data. JAW performed the preliminary leaf morphology experiment and contributed to the writing of the initial draft. PJG contributed to the writing and revision of the manuscript as well as data analysis and project supervision.

Chapter 3

The work presented in Chapter 3 entitled "The caleosin CLO7 and its role in Heterotrimeric G-protein signaling" has three authors whose contributions are as follows: S.C.B, and M.K.M.A participated in the experimental design. SCB and MKMA performed the following experiments: the BiFC and yeast two-hybrid, the germination and pollen viability assay, and created the transgenic lines (35S and RNAi lines). SCB carried out the GFP localization, the semi-quantitative RT-PCR, performed crossed to generate the *clo7 gpa1* double mutant and analysed the seed from the cross. SCB compiled all the data, ran the statistical analysis, and created all the figures, wrote the manuscript, and contributed to the revisions. PJG. designed the project, analyzed the data, contributed to writing and revision of the manuscript as well as project supervision.

Chapter 4

The work presented in Chapter 4 entitled "The caleosin *RD20/CLO3* regulates abscisic acid affects on lateral root development and in conjunction with the caleosin *CLO7* regulates flowering time" has three authors whose contributions are as follows: SCB. participated in the experimental design, created the GUS lines, created the *CLO7* and *RD20/CLO3* transgenic lines, carried out the BiFC, yeast two-hybrid, root, *RD20/CLO3* and *CLO7* GUS and flowering time assays. SCB carried out the RNA-Seq analysis and ran the stastical analysis on the data. SCB compiled the data and created all the figures. MKMA assisted in creating the *CLO7* transgenic lines, in the BiFC, *CLO7* GUS and flowering-time assay.

MKMA carried out the *CLO7* root analysis. P.J.G. designed the project, analysed the data, contributed to the writing and revisions, and supervised the project.

Chapter 5

The work presented in Chapter 5 entitled "Characterization of the *Esi3*/*RCI2*/*PMP3* gene family in the Triticeae" has three authors whose contributions are as follows: SCB, MKMA and PJG retrieved the sequences for the gene family. SCB ran the phylogenetic analysis, carried out the statistical analysis, ran the RNA-Seq analysis and half of the microarray analysis. SCB compiled the data and created all the figures. MKMA ran half of the microarray analysis and carried out the database comparison and created the table for the comparison. SCB, MKMA and PJG analysed the data, contributed to the writing and revision of the manuscript and supervised the project.

Chapter 6

The work presented in Chapter 6 entitled "Characterization and expression of the *Pirin* gene family in *Triticum aestivum*" has three authors whose contributions are as follows: SCB, MKMA and PJG retrieved the gene family sequences. SCB carried out the phylogenetic, RNA-Seq, promoter and statistical analyses. SCB created all the figures and tables, wrote the manuscript, and contributed to the revisions. MKMA assisted in the gene structure analyses and carried out the database comparison work and contributed to the revisions. PJG analysed the data, contributed to the writing and revision of the manuscript, and supervised the project.

Table of Contents

List of Figures

List of Tables

List of Abbreviations

ABA	Abscisic acid
ABF	Arabidopsis ABA-responsive element-binding Factor gene
ABI	Arabidopsis ABA-insensitive 1 gene
ABRE	ABA-Responsive Element
AP2/EREBP	APETALA2/ Ethylene-Responsive Element Binding Proteins
AGB1	Arabidopsis G protein β subunit 1 gene
AGG1	Arabidopsis G protein γ subunit 1 gene
AGG2	Arabidopsis G protein γ subunit 2 gene
AGG3	Arabidopsis G protein γ subunit 3 gene
Blt101	Barley low temperature gene
BR	Brassinosteroid(s)
CBF/DREB	C-repeat Binding Factor/Drought Responsive Element-Binding protein
CLO	Arabidopsis caleosin gene
Clo	Triticum caleosin gene
EFA27	EF-hand, Anchored 27 the rice caleosin gene
ER	Endoplasmic Reticulum
Esi3	Wheat Early Salt Induced gene
FAOH	Fatty acid hydroxides
G protein	Heterotrimeric GTP-binding protein
GA	Gibberellin(s)
GAI	Arabidopsis Gibberellin Insensitive gene
GAP	GTPase-activating protein

GPA1	Arabidopsis G protein α subunit gene
GPCR	G-protein-coupled receptor
GDP/GTP	Guanosine diphosphate/triphosphate
Lhcb	light-harvesting chlorophyll a/b-binding protein
OB	Oil body
OsLti6	*Oryza sativa* low-temperature-induced 6 gene
Pirin1	Arabidopsis cupin domain protein 1
RCI	Arabidopsis Rare Cold Inducible gene
RGS	Regulator of G-protein Signaling
ROS	Reactive oxygen species
WT	Wild-type Arabidopsis plant
ZmRCI2	*Zea Mays* Rare Cold Inducible gene

Preface

This work is directed at expanding our understanding of the role of stress regulated genes in a plants response to environmental stress and in plant development. The first objective of this study was to characterize the interaction between the Gα subunit of the Heterotrimeric G-protein complex, GPA1, and the caleosins RD20/CLO3 and CLO7 (Chapter 2 and 3). The RD20/CLO3 gene in known to be strongly induced by drought and ABA treatment, and the heterotrimeric G proteins have been shown to affect a number of stress responses. The investigation was undertaken to understand the relationship between these genes in relation to regulatory pathways involved in development and stress responses. The caleosins are calcium-binding proteins with EF-hand calcium binding motifs. Both RD20/ CLO3 and CLO7 were found to interact with GPA1 in a calcium-dependent manner and based on the GTP- or GDP-bound state of GPA1. In Chapter 2, *RD20/CLO3* was characterized as a negative regulator of *GPA1*, and both were found to play a role in hypocotyl elongation in dark-grown seedlings and in leaf morphology (Chapter 2). Chapter 3 focuses on the caleosin *CLO7.* Both *CLO7* and *GPA1* were implicated in seed germination in response to both ABA and osmotic stress and the double mutant *clo7 gpa1* leads to embryo lethality (Chapter 3). *RD20/CLO3* was also found to contribute to lateral root development in response to ABA treatment and the *CLO7*-RNAi/*rd20* and the *RD20*-RNAi/*clo7* have a strikingly early flowering time (Chapter 4).

A secondary objective of this study was to characterize the *Early salt induced 3* (*Esi3)* and *Pirin* gene family in the important crop species, *Triticum aestivum* (Chapters 5 and 6). The studies involve *in situ* analysis of the gene families using a combination of RNA-Seq and microarray datasets highlighting differential gene expression in different tissue types and in response to both biotic and abiotic stress conditions. Lastly, the studies highlight the importance of manually curated gene families to overcome the pitfalls of automated gene annotations (Chapter 5 and 6).

Chapter 1. Introduction

1.1 The Heterotrimeric G proteins

The Heterotrimeric G proteins play important roles in the animal and plant kingdoms. The Heterotrimeric G protein complex is a trimer with an alpha subunit (Gα) and a beta-gamma dimer (Gβ-Gγ). The G proteins are present in a trimeric state when the Gα subunit is GDP bound. When a signal occurs via a G-protein coupled receptor (GPCR) the Gα subunit undergoes guanine exchange in which the GDP is exchanged for GTP (Figure 1A). This exchange is facilitated by a guanine-nucleotide exchange factor (GEF) protein which can catalyze the release of GDP and the binding of GTP (Sprang, 2001). Subsequently, the trimer separates into a Gα subunit and a Gβ-Gγ dimer, and these interact with downstream effectors. The Gα subunit can undergo GTP hydrolysis with the aid of a GTPase accelerating protein (GAP) and can hydrolyze GTP into GDP and the trimer can re-associate (Figure 1B). The GAP proteins involved in G-protein signaling are referred to as Regulator of G-protein Signaling (RGS). Heterotrimeric G protein signaling has been implicated in many signaling and regulatory functions in animals and in microorganisms including *Saccharomyces cerevisiae*. Some of these functions are as follows, signal transduction systems leading to a diversity of physiological functions such as modulation of synaptic transmission, hormone action and release, perception of sensory information, regulation of cell contraction and migration or cell growth and differentiation (Wettschurek and Offermanns, 2005). There are many known G-protein coupled receptors (GPCRs) and they have been used as drug targets (Sriram and Insel, 2018). According to Sriram and Insel, (2018) in 2017 there were 134 GPCRs that had been used as drug targets in the United States and the European Union and 35% of the approved drugs target GPCRs. One interesting example of the G-proteins functionality is in mammalian sweet and umami tasting. These taste sensations are mediated by taste-specific G protein coupled receptors (GPCRs)

(Chandrashekar et al., 2006). The GPCR's responsible for these taste sensations are the class C GPCR taste receptors (TIR3, TIR2 and TIR1), these receptors are comprised of a large N-termini domain which form structures similar to a "Venus flytrap" (Liman et al., 2015). These N-termini domains are linked to the transmembrane sections by a cysteine-rich domain that is responsible for ligand binding and receptor activation (Liman et al., 2015). Different domains of the TIR2/TIR3 receptors are targets of different sweeteners, for example some artificial sweeteners target the transmembrane domain meanwhile sweet proteins target the cysteine-rich domains (Liman et al., 2015). The TIR1 and TIR3 GPCR sugar receptors were also discovered in hummingbirds and are responsible for their affinity towards sweet nectar (Jiang and Beauchamp, 2014). Many bird species don't taste sugars, but the TIR1-TIR3 heterodimer which is part of the umami taste receptor system has been repurposed in hummingbirds to function as a carbohydrate receptor through mutations to both receptor units (Baldwin et al., 2015). A homology model of the TIR3 Venus flytrap domain compared to a known GPCR, metabotropic glutamate receptor 1 (mGluR1), predicted 19 sugar response- conferring substitutions in TIR3 (Baldwin et al., 2015). These substitutions caused dramatic changes to the TIR1-TIR3 protein surface which allowed for the detection of carbohydrates in hummingbirds (Baldwin et al., 2015).

The G-protein gene family in humans is comprised of 23 different Gα subunit family members, six Gβ subunit family members and 12 Gγ subunit family members allowing for more than 1300 possible heterotrimer combinations, which is a stark contrast compared to the Arabidopsis genome which contains only one α subunit, one β and three γ subunits (Jones, 2002; Temple and Jones, 2007). Therefore, an interesting function of the G-proteins in some animal species is the association of the beta/gamma dimer with other proteins to create many different

combinations (Gautam et al., 1990). One example of this is the $G\beta_5$ subunit which can bind to an RGS subfamily which contain Gγ-like domains (Witherow et al., 2000). This class of RGS proteins are not capable of binding to the Gα subunit with high affinity as most RGS proteins, however it is still capable of inhibiting G-protein signaling through GAP activity to a specific Gα subunit, $G\alpha_o$, but not $G\alpha_i$ or $G\alpha_q$ (Witherow et al., 2000).

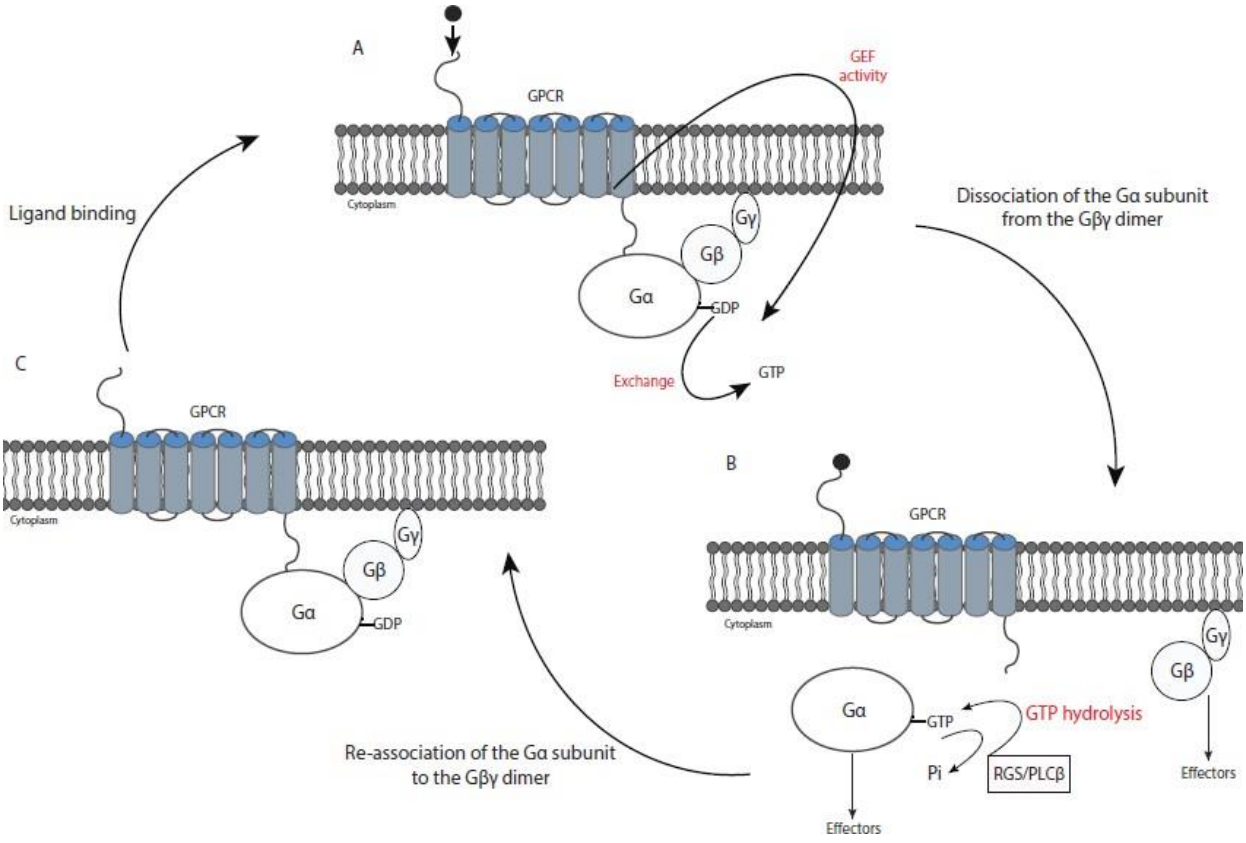

Figure 1. The classical model of G protein signaling. **(A)** The GPCR binds an external ligand causing guanine exchange in Gα which is mediated by a GEF (Guanine Exchange Factor). The

Gα subunit exchanges GDP for GTP and dissociates from the GβGγ. Both the Gα and the GβGγ can activate downstream effectors. **(B)** An RGS/PLCβ GAP aids Gα in GTP hydrolysis, converting GTP back to GDP allowing **(C)** the G-protein subunits to re-associated. Adapted from Urano et al. (2013).

G proteins are encoded in all plant species whose genomes have been characterized including, *Triticum aestivum* (bread wheat), *Oryza sativa* (rice), *Zea mays* (maize), *Brachypodium distachyon* and the model organism *Arabidopsis thaliana*. The G proteins are also found in the last common ancestor of eukaryotes and are a major part of eukaryotic signaling pathways (de Mendoza et al., 2014). In plants the G protein α subunit was discovered to be a dwarf gene during the green revolution which occurred in the 1960s-1970s. During the green revolution crop yields were dramatically increased by plant breeding efforts and the use of fertilizers which became common practice among farmers. The increased use of fertilization caused an increase in plant height and lodging, falling over, resulting in yield losses in cereals. To minimize crop losses there was extensive breeding work done to discover genes that could cause dwarfism. Genes were found in crop plants such as rice, maize and wheat that could reduce plant height yet maintain high biomass production and high yields due to an abnormal response to gibberellic acid (GA) a plant hormone involved in plant growth (Peng et al., 1999). It was later discovered that the Gibberellin-insensitive dwarf gene (*Dwarf1)* in rice is the α-subunit of the Heterotrimeric G protein complex, an ortholog of the Arabidopsis Gibberellin Insensitive gene, *GAI* (Peng et al.,1999; Ashikari et al., 1999). In maize, mutations in the Compact Plant 2 gene (*Ct2*), which is the G-alpha subunit were linked to dwarfed stature, increased leaf number, more ears and more female inflorescence (Urano et al., 2015). The heterotrimeric G proteins in *Triticum aestivum* are encoded by three Gα genes, three Gβ and 12 Gγ genes giving a total of 18 genes encoding the G proteins in the hexaploid wheat

(Gawande et al., 2022). The G-protein members in *T. aestivum* are both transcriptionally up-regulated or down-regulated in response to different abiotic and biotic stress conditions, such as heat and cold stress as well as a response to the fungus *Fusarium graminearum* (Gawande et al., 2022). The heterotrimeric G proteins have been implicated in a multitude of regulatory pathways controlling multiple phenotypes in Arabidopsis (Pandey, 2019).

As indicated previously, there are similarities between G-protein signaling in plants and animals, there are also many differences between the animal G-proteins and the plant G-proteins. In Arabidopsis there is one alpha subunit GPA1, one beta subunit AGB1 and three gamma subunits AGG1, AGG2, and AGG3, however animal genomes contain gene families for the heterotrimeric G protein subunits, for example in the human genome, there are 23 different Gα subunits, six Gβ subunits and 12 Gγ subunits (Jones, 2002; Temple and Jones, 2007). Another marked difference is that Arabidopsis has only three known G gamma subunits, and the GβGγ dimers are not known to dissociate (Gautam et al., 1998). The GβGγ combinations in Arabidopsis are believed to give the GβGγ dimer its functional selectivity since mutations in the different gamma subunits lead to different phenotypes (Thung et al., 2013). Mutations in *AGG1* or *AGG2* lead to early bolting, heat-stress induced flowering, hypersensitivity to osmotic stress assayed by D-mannitol treatment and hypersensitivity to auxin-mediated induction of lateral roots (Thung et al., 2013; Trusov et al., 2007). There were "orphan" phenotypes of *AGB1* that could not be replicated by either *AGG1* or *AGG2* mutant alleles, which led to the discovery of the third Gγ subunit AGG3 (Chakravorty et al., 2011; Trusov et al., 2007). These phenotypes were abscisic acid (ABA)- hyposensitivity seen in the stomatal guard cells as well as ABA hypersensitivity during seed germination. The *agg3* mutant had a similar phenotype to the *agb1* mutation regarding these phenotypes, solidifying its distinct role as one of the Gγ subunits (Wang et al., 2001; Fan et al., 2008; Pandey et al., 2006; Chakravorty et al., 2011). This third

gamma subunit (AGG3) was also distinct in its protein structure and was placed in the group III of Gγ proteins since it is twice the size of the other two γ-subunits (AGG1 and AGG2) and it has a γ-like domain on its N-terminus followed by a transmembrane domain and a cysteine rich C-terminus (Thung et al., 2012).

Another marked difference in G-protein signaling in Arabidopsis is that there are no reports of GPCRs that have been widely accepted as reliable. It was believed that many genes could be GPCRs based on their seven transmembrane (TM) domains, however after further investigation, the support for their candidacy as GPCRs was not strong (Jones and Assmann, 2004; Urano and Jones 2013). Urano and Jones, (2013) highlight that the amino acid conservation among GPCRs is poor even within species and evidence based only on sequence similarity is not conclusive. There is also a lack of biochemical assays similar to those used with animal GPCRs that can be used on the homologs to the plant GPCRs since fast, millisecond-duration cell-based assays for plant G proteins are not well established (Pandey, 2019). Arabidopsis does not require GPCR association for GDP/GTP exchange since GPA1 has an intrinsic guanine nucleotide exchange rate >100-fold greater than the animal $G\alpha_{i1}$ (Jones et al,. 2012). This intrinsic guanine exchange allows GPA1 to self-activate and dissociate from the GβGγ dimer without the need for a GPCR. This indicates that the ligand-binding receptor model in fungi and animals s not appropriate for plant heterotrimeric G protein signaling (Figure 2A). GPA1 also has a slow rate of GTP hydrolysis [kcat = 0.05 min−1] (Urano and Jones. 2014), thus GTPase activating proteins (GAPs) are hypothesized to play an important role in the regulation of heterotrimeric G protein signaling in plants (Figure 2B). In Arabidopsis the only known GAP is RGS1 (Regulator of G protein Signaling 1) which is capable of inducing the GTPase activity of GPA1 (Johnston et al., 2007).

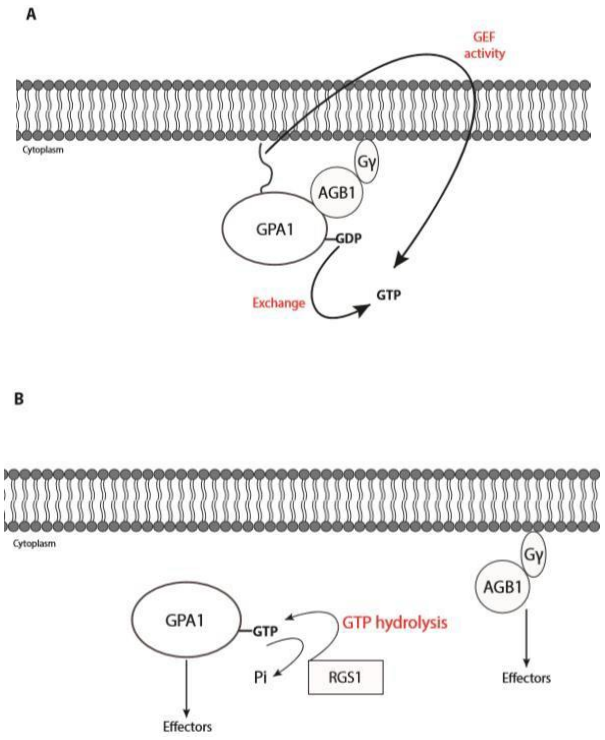

Figure 2. The plant G-protein signaling model. **(A)** The Gα subunit, GPA1, has high intrinsic guanine exchange and can undergo GDP exchange without a 7TM receptor. The exchange of GDP for GTP causes the GPA1 subunit to separate from the AGB1/Gγ dimer. **(B)** The Gα monomer and the AGB1/Gγ dimer are able to regulate down-stream effectors. Association between RGS1 and GPA1 facilitates GTP hydrolysis, converting GTP back to GDP. This hydrolysis will cause GPA1 to re-associate with the AGB1/Gγ dimer, and cycle to an inactive state.

The Gα subunit in Arabidopsis, GPA1, has been linked to different plant traits and has been implicated in stress response pathways. GPA1 plays a role early in plant development by affecting germination (Ullah et al., 2001; Ullah et al., 2002). The *gpa1* mutant is less sensitive to stimulation of germination by GA or Brassinosteroids (BR), two plants hormones that act in synchrony to promote seed germination, as well, the *gpa1* mutant has a hypersensitivity to ABA

inhibition of germination (Ullah et al., 2001; Ullah et al., 2002; Lapik and Kaufman, 2003). This suggests that *GPA1* plays a role in seed germination, and it is postulated it may act *via* an interaction with *Pirin1*. Pirin is a protein with two cupin domains comprised of beta barrels, and is part of the diverse cupin superfamily comprised of 18 functional classes of proteins such as bacterial enzymes, seed desiccation-tolerance, dioxygenases and much more (Dunwell et al., 2004). A yeast two-hybrid assay revealed that *Pirin1* interacts with *GPA1* and that the *pirin1* mutant has a similar germination phenotype to *gpa1*, suggesting that it is a possible downstream effector of the Gα subunit (Lapik and Kaufman, 2003). Aside from GPA1s role in germination it also plays a role in early seedling development by regulating cell division and elongation (Ullah et al., 2001). When the *gpa1* mutant was subjected to conditions of darkness the hypocotyl, the organ between the leaves and root, was shorter compared to the wild-type (WT) plants; therefore, indicating that *GPA1* is involved in hypocotyl extension (Ullah et al., 2001). This is a common characteristic of germinating seedlings which occurs when a young seedling is searching for light, and plays an important role in seedling emergence from soil and in shade avoidance. *GPA1* has been shown to affect hypocotyl elongation by stimulating increased cell division (Ullah et al., 2001). The *gpa1* mutant had a reduced number of elongated cells in the hypocotyl region (Ullah et al., 2001). *GPA1* is also implicated in lamina (expanded blade or leaf) shape by affecting cell division. The *gpa1* mutants have a rounder leaf shape compared to a WT Arabidopsis leaf (Jones et al., 2003; Ullah et al., 2001). This phenotype which results from fewer and larger leaf cells, suggests there was an increase in cell expansion to compensate for the lack of cell division (Ullah et al., 2001). Ullah et al. (2001) make the compelling argument that the *GPA1* over-expression line causes ectopic expression and in some areas, such as meristematic regions, there was an increase in cell division.

The G-protein complex also plays a role in alterations in root growth both in response to ABA treatment and under normal growth conditions (Chen et al., 2006). In Arabidopsis the primary root emerges as one of the first post-embryonic structures, known as the radicle; the matured pericycle cells can then proliferate and differentiate to create a lateral root (Malamy and Benfey, 1997). The developing lateral root, characterized by a cluster of cells whose divisions are perpendicular to the axis of growth of the primary root, are known as the lateral root primordium, it is only after the primordium emerges from the primary root via cell elongation that it is considered a lateral root (Malamy and Benfey, 1997). The *gpa1* mutant has a reduced number of lateral root primordia, while the mutant for *agb1* has an enhanced number of lateral root primordia, which will ultimately affect the overall lateral root numbers (Ullah et al., 2003). The *agb1* roots have approximately 2-fold higher primordia density than the WT and the *gpa1* mutation has the opposite affect with a 2-fold decrease in primordia (Ullah et al., 2003). This suggests an increase in cell division in the *agb1* mutant (Ullah et al., 2003). However, this is not the sole mechanism affecting root development. The lateral roots of the *agb1* mutant are longer suggesting an increase in cell elongation (Ullah et al., 2003). Root architecture is controlled by cell division and elongation which are controlled by plant hormones, such as auxin and ABA, and on nutrient and water availability (Casimiro et al., 2003). ABA is known to inhibit the development of lateral roots. Mutants of both *GPA1* and *AGB1* exhibit a greater reduction in number of lateral roots and reduced primary root elongation in the presence of ABA compared to WT plants, *i.e.* hypersensitivity to ABA inhibition of primary root elongation (Pandey et al., 2006). According to the working model of Chen et al. (2006); when the G-protein complex has dissociated, the free Gβ/Gγ complex can inhibit lateral root development, and when the trimer has reformed there is a stimulation of lateral root development since Gβ is inactive when it is

bound to the trimeric complex. The primary root is directly affected by the state of the Gα subunit (Chen et al., 2006). When the subunit is bound to GTP there is an increase in cell elongation in the primary root (Chen et al., 2006). This working model gives an insight into how the G-proteins may be functioning in controlling root architecture in Arabidopsis.

1.2 The Caleosin Gene Family

The caleosins are a family of calcium-binding proteins with a single EF-hand motif found in both monocots and dicots. The caleosins are found in the monocots *Triticum aestivum* (bread wheat), *Oryza sativa*, *Secale cereale* (rye), *Hordeum vulgare* (barley), *Brachypodium distachyon* and the dicot *Arabidopsis thaliana* (Khalil et al., 2014; Naested et al., 2000). In Triticum there are eleven caleosin family members known as *Clo1-Clo11* (Khalil et al., 2014). Each member has homeologous copies for the A, B and D chromosomes of the allohexaploid wheat genome, totaling 34 caleosins (Khalil et al., 2014). In *S. cereale* and *H. vulgare*, like *T. aestivum*, there are 11 caleosin family members and these family members share 90% and 99% sequence similarity with their homologs found in wheat (Khalil et al., 2014). All of the caleosins in the monocots have a single EF-hand domains (174 amino acids) responsible for calcium binding which is comprised of 36 amino acids with a chelating calcium loop and calcium-ligating residues (Khalil et al., 2014). Additionally, *T. aestivum*, *H. vulgare* and *B. distachyon* caleosins contain a transmembrane domain, GS loop, and a transcription termination factor (Khalil et al., 2014). In wheat, the caleosins are found in a variety of tissue types and developmental stages, for example *Clo9* is highly expressed in root tissue and *Clo6* and *Clo7* have high expression in the anther (Khalil et al., 2014). The caleosins were also found to be expressed in response to conditions of abiotic stress in wheat, barley and rye (Khalil et al., 2014).

In salt-stressed *S. cereale* plants, there was a high level of *Clo9* expression, there was a strong induction of *Clo3* in winter wheat shoots after cold treatment at 4℃, and *Clo10* and *Clo11* in *H. vulgare* had increased expression in response to ABA (Khalil et al., 2014). *Clo3* in wheat was also shown to interact with the α-subunit (GA3) of the G-proteins and the interaction between the two proteins was enhanced by high Ca^{2+} levels (Khalil et al., 2011). It appears that the caleosins have a diverse expression pattern in the monocot plant species and that they may play a critical role in adapting to different stress conditions.

In the dicot *Arabidopsis thaliana*, the CLO gene family is comprised of seven members known as *CLO1-CLO7*. The caleosin, *CLO3*, is also referred to as *RD20* (*Responsive to dehydration/desiccation20*) as it is induced in response to drought and high salinity conditions (Takahashi et al., 2000). The caleosins in Arabidopsis contain single EF-hand motifs in their N-terminal regions responsible for calcium binding (Aubert et al., 2010; Takahashi et al., 2000), a proline knot motif believed to be the peptide motif signal required for oil body (OB) association, as well as a membrane domain and a C-terminal domain with phosphorylation sites (Figure 3, Aubert et al., 2010; Abell et al., 1997; Chen and Tzen 2001).

In plants, oil bodies are rich in triacylglycerols (TAGs) which are an important energy source during germination and post-germination growth (Chen et al., 1999). Oil bodies are found in many tissue types including the seed and their structure and function remains intact due to the presence of oleosins, steroleosins and caleosins which cover the surface of the oil body (Chen et al., 1999). Oil bodies are also found in leaf tissue and the caleosins have been found within the oil bodies associated with the leaves (De Domenico et al., 2011). Leaf oil bodies are considered to be primarily associated with the Endoplasmic Reticulum (ER) and the Arabidopsis *CLO2* is a caleosin that was shown to be ER-localized and associated with leaf oil

bodies (De Domenico et al., 2011). It has been proposed that the caleosins localize to the ER and from there they are incorporated on newly synthesized immature OBs, and these may then fuse in a calcium-dependent manner to become mature OBs (Frandsen et al., 2001). In addition to ER-localized caleosins there are also some caleosins, such as the rice caleosin, EFA27 (EF-hand, Anchored 27), that are associated with the membrane and are believed to play a role in membrane fission and/or fusion related to ER trafficking (Frandsen et al., 1996; Frandsen et al., 2001). Another ER-associated caleosin is *CLO1* and *CLO1* expression was also detected in OBs, developing embryos, mature seeds as well as the root tip of Arabidopsis (Naested et al., 2000). Oleosins and *CLO1* were both recovered from the membrane of the oil body, suggesting co-localization and that both oleosins and caleosins have the same binding affinity for oil bodies (Naested et al., 2000).

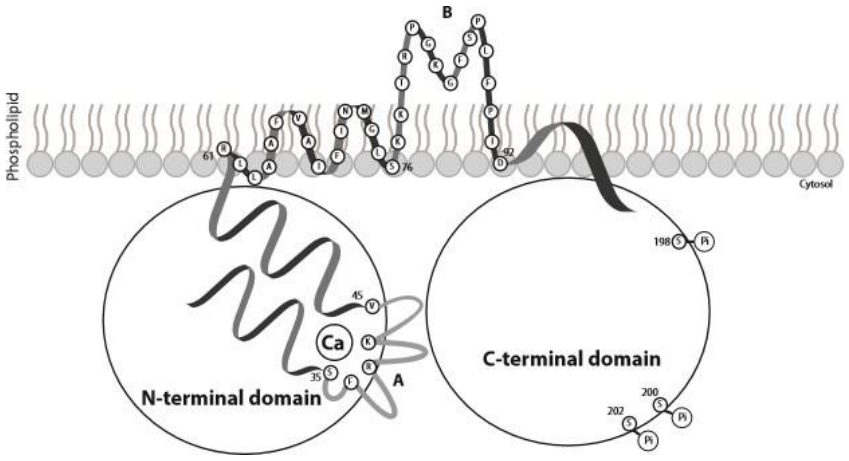

Figure 3. Structure of a caleosin on an oil body. **(A)** N-terminal EF-hand domain to binds Ca^{2+}. This is followed by a transmembrane domain leading to **(B)** the proline knot motif, and then the C-terminal domain with phosphorylation sites. Figure inspired by Frandsen et al. (2001) and the caleosin CLO7 (At2g23240) is depicted.

CLO4 is another caleosin from Arabidopsis that was shown to localize to seed oil bodies and, like *CLO1*, also showed expression in tissues other than the seed, and was found in the radicle (the short root of a germinating seed), leaf, stem and inflorescence as well as the primary and lateral roots (Kim et al., 2011). The expression of *CLO4* was down-regulated in response to both ABA and salt (Kim et al., 2011). In the *clo4* mutant, the ABA regulatory genes, *ABF3* and *ABF4* (*ABA-responsive element-binding Factors 3* and *4*), which are known transcription factors involved in ABA-dependent pathways, were shown to be up-regulated (Kim et al., 2011 and Sreenivasulu et al., 2007). The *clo4* mutant also displayed expression of *ABI1* (*ABA-insensitive 1*), which is a negative regulator of the ABA response and may play a role in the repression of *CLO4* in an ABA-dependent manner (Kim et al., 2011). At the germination stage of development, the *clo4* mutant was found to be hypersensitive to ABA suggesting *CLO4* negatively regulates ABA inhibition of seed germination (Kim et al., 2011). Additionally, the *clo4* mutant was more drought tolerant than the WT, indicating an enhanced response to conditions of water-deficit due to enhanced stomatal closing (Kim et al., 2011). These data suggests that *CLO4* is not only a seed/oil body caleosin but also a stress-responsive caleosin, something not seen in earlier studies on *CLO1* or *CLO2*.

RD20/CLO3 is one of the most studied caleosins in Arabidopsis. It was first analyzed by Takahashi et al. (2000) and was shown to be induced by ionic (salt), osmotic (mannitol), hormonal (ABA) and drought stresses. *RD20/CLO3* was also found to be expressed in above ground tissues, such as flowers, leaves and stomatal guard cells on the leaves, and was up-regulated in these tissue types in response to dehydration, salt, and ABA (Takahashi et al., 2000; Partridge and Murphy, 2009; Aubert et al., 2010). RD20/CLO3, like all caleosins, has the affinity to bind calcium, however this protein can also bind phosphate (Partridge and Murphy,

2009). It appears that in leaves of non-stressed plants there was a low level of phosphorylated RD20/CLO3, however in salt or ABA-stress-treated leaves the phosphorylated levels of RD20/ CLO3 were significantly higher (Partridge and Murphy, 2009). This suggests that the RD20/ CLO3 C-terminal domain may be phosphorylated in response to abiotic stress. In genetic studies the *rd20/clo3* mutant had a higher transpiration rate due to increased stomatal aperture compared to the WT and not an increase in stomatal density (Aubert et al., 2010). Therefore, the mutant had higher water loss when subjected to conditions of water deficit and had decreased tolerance to drought (Aubert et al., 2010). Aubert et al. (2010) tested the mutant plants under drought conditions and observed an increased in wilting of the above ground tissues in the *rd20/clo3* mutant compared to the WT plants.

Given that *RD20/CLO3* is also induced by salt, the mutant was subjected to high NaCl treatment and the *rd20/clo3* mutant had a significantly higher number of senescent leaves, indicating that the mutant is more sensitive to salt stress and does play a role in salt response in Arabidopsis (Aubert et al., 2010). *RD20/CLO3* has also been implicated in the control of cell death during pathogen response, gibberellin-dependent flowering time, ABA sensitivity, oxidative stress tolerance and ABA-dependent germination and seed dormancy (Hanano et al., 2015; Blée et al., 2014). RD20/CLO3 is also known as a peroxygenase with a preference for lipophilic molecules as substrates (unsaturated fatty acids and their hydroperoxide derivatives). Therefore, RD20/CLO3 is involved in oxylipin metabolism during times of biotic and abiotic stress by generating oxidized fatty acids found in stress signaling pathways triggered by salt, ABA, and GA and in response to biotic stress such as fungal attack (Partridge and Murphy, 2009; Hanano et al., 2015; Blée et al., 2014). *RD20/CLO3* is a fatty acid hydroperoxide reductase that allows for the formation of endogenous fatty acid hydroxides (FAOH) leading to oxylipin accumulation, and these FAOHs decrease the accumulation of reactive oxygen species (ROS)

(Hanano et al., 2015). The peroxygenase activity of RD20/CLO3 is due to a conserved histidine (His) residue at position 133 (Hanano et al., 2006; Blée et al., 2014). Plants with a mutation changing the His to alanine (Ala) created plants similar to the WT in terms of oxylipin accumulation (Hanano et al., 2006; Blée et al., 2014). The plants over-expressing *RD20/CLO3* flowered 33 days earlier than WT plants under short day conditions (Blée et al., 2014). The H133A mutant *RD20/CLO3* plants which were under the control of a 35S promoter did not have any changes in flowering time relative to the WT plants indicating that increased amounts of inactive *RD20/CLO3* is not enough to influence flowering time (Blée et al., 2014). Therefore, it appears the early flowering phenotype of the over-expressing *RD20/CLO3* plants is due to oxylipin accumulation (Blée et al., 2014). GA is also a class of hormones known to regulate floral transition and is more effective in doing so under short day conditions (Blée et al., 2014; Wilson et al., 1992). The *RD20/CLO3* over-expressor had an increase in the GA deactivating genes, *GA2ox1* and *GA2ox2*, and an increase in *LEAFY* (*LFY*), a gene known to promote flowering (Blée et al., 2014). The observed flowering time phenotypes seen in the over-expressing *RD20/CLO3* plants as well as the H133A mutant *RD20/CLO3* over-expressing plants confirms that *RD20/CLO3* is involved in the ROS-associated early gibberellin-dependent flowering of Arabidopsis (Blée et al., 2014).

RD20/CLO3 also plays a role in seed germination, the *rd20/clo3* mutant germinated at a higher rate than the WT seed when subjected to ABA, suggesting that the *rd20/clo3* mutant is insensitive to the ABA inhibition of seed germination (Blée et al., 2014). However, if the mutant and WT plants were cold treated prior to ABA treatment this phenotype was abolished, suggesting *RD20/CLO3* may impact seed dormancy by enhancing sensitivity to ABA (Blée et al., 2014). RD20/CLO3 also plays a role in biotic stress due to its peroxygenase activity, which allows it to modulate oxidative stress and cell death (Hanano et al., 2015). When mutant *rd20/*

clo3 leaves were subjected to the fungus *Alternaria brassicicola* the fungus spread throughout the leaves, whereas the *RD20/CLO3* over-expression line had confined circular spots of infection due to alterations in the leaf cuticle wax components (Hanano et al., 2015). It appears that the generated FAOH by *RD20/CLO3* may reduce the growth of *A. brassicicola* and to further test this *rd20/clo3* mutant plants were inoculated with *Pseudomonas syringae* (Hanano et al., 2015). The *rd20/clo3* mutation had the opposite effect when inoculated with Pseudomonas; it appeared to protect the leaf from severe damage suggesting that *RD20/CLO3* plays a role in biotic stress response (Hanano et al., 2015). Furthermore, a caleosin discovered in *Aspergillus flavus*, AfPXG, with peroxygenase activity was capable of severely decreasing fungal development and detrimental aflatoxin accumulation (Hanano et al., 2018). It appears that the caleosins are not only beneficial to plants, but to humans and animals. Though the caleosins were initially identified as components of oil bodies in the seed, expression and genetic analyses suggest that the caleosins may play additional roles in abiotic and biotic stress responses.

1.3 The *Early Salt Induced* Genes (*Esi3*)

Chapter 5 of the thesis describes the characterization of the *Early Salt Induced 3 (Esi3)* gene family in *T. aestivum.* The *Early Salt Induced 3*, *Esi3* genes were found to play a role in response to salt stress in *Lophopyrum elongatum,* a highly salt tolerant relative of wheat (Gulick and Dvořák 1992. *Esi3* was found to be induced as little as two hours after treatment leading to the name 'early salt induced' (Gulick and Dvořák 1992).*Esi3* transcripts were also detected in wheat in response to salt treatment however the levels of expression were 2-fold lower than the expression observed in L. elongatum (Galvez et al., 1993). The *Esi3* expression level is also increased by treatments of KCl , ABA and mannitol, suggesting the *Esi3* genes are stress

responsive (Galvez et al., 1993). The *Esi3* genes were later identified in other plant species such as *Hordeum vulgare* (barley), *Arabidopsis thaliana*, *Zea mays* (maize), *Medicago truncatula*, *Oryza sativa* (rice) and the alkali grass, *Puccinellia tenuiflora*, and they were also identified in the yeast *Saccharomyces cervisiae* (Goddard et al., 1993; Rocha et al., 2015; Fu et al., 2012; Long et al., 2015; Morsy et al., 2005; Zhang et al., 2008). One *Esi3* homolog was identified in barley, *Blt101*, as a gene induced in response to low temperature conditions and was shown not to be induced by drought or ABA (Goddard et al.,1993). It was also reported that *Btl101* was expressed in shoot meristems, mature leaves, and the roots of cold treated barley plants, suggesting a widespread expression pattern and a potential for adaptability to colder climates (Goddard et al., 1993).The first two Arabidopsis *Esi3*-like genes reported as homologs to the barley *blt101* and the *L. elongatum Esi3* sequences were named *AtRCI2A* and *AtRCI2B* (*Rare Cold Inducible*) since they were induced by low non-freezing temperatures (Capel et al.,1997). *AtRCI2A* and *AtRCI2B* were also found to be induced by ABA and dehydration, and that expression of these genes could be induced by low temperature in ABA-deficient and ABA-insensitive genetic backgrounds, suggesting some role in the ABA pathways that regulate low temperature responsiveness (Capel et al., 1997). In Arabidopsis the family of At*RCI2* genes encode small, 54 amino acid, hydrophobic proteins with two transmembrane domains which are regulated at the transcriptional level (Medina et al., 2001). Using *AtRCI2A* and *AtRCI2B* promoter fusions to the GUS gene, expression was localized to guard cells, in the vascular system of stems, namely in protoxylem cells, pollen grains, developing seeds, and the abscission zone of petals and sepals, suggesting that they may play a role under normal growth conditions (Medina et al, 2001).

After the characterization the two Arabidopsis genes, six more *AtRCI2* genes were reported (*AtRCI2C-H*) (Medina et al., 2007). Expression analysis suggests that these different *AtRCI2* genes have distinct roles in response to abiotic stress, since the gene family has differential expression in different tissue types (Medina et al., 2007). All *AtRCI2*s, with the exception of *AtRCI2H,* were expressed in the leaf, stem and root, and *AtRCI2E*, *-F* and *-H* are expressed in the seed (Medina et al., 2007). *AtRCI2A-F* were all induced by cold, ABA, dehydration, and salt, suggesting that the *AtRCI2* genes may have different roles in these tissue types in response to stress (Medina et al., 2007). To better understand the conservation of the *AtRCI2*s it was previously shown that *AtRCI2A-C* and *AtRCI2H*, which lack C-terminal hydrophilic tails were able to complement the deletion of *PMP3* (*Plasma Membrane Protein 3*), the yeast *AtRCI2*-related gene, indicating that the *AtRCI2* genes are functional and conserved in yeast (Navarre and Goffeau 2000). Some members of the *AtRCI2* gene family encode longer proteins with extra C-terminal extensions (*RCI2D-F*) and most members of this subgroup did not complement the Δ*pmp3* mutation in yeast (Medina et al., 2007). When *AtRCI2D* was truncated to eliminate its C-terminal domain and this truncated version was able to complement the Δ*pmp3* mutation (Medina et al., 2007). Taken together these data indicates that the presence of the N-terminal half of the protein without the C-terminal domain facilitates the complementation of the Δ*pmp3* mutation seen with the *AtRCI2*s (Medina et al., 2007). Deletion of *PMP3* caused an increase in plasma membrane potential and sensitivity to cytotoxic cations such as Na^+ (Navarre and Goffeau 2000). Although the function of *PMP3* is not well elucidated, these data suggest that the protein contributes to the regulation of intercellular ion homeostasis by preventing excessive Na^+ influx, in turn leading to salt tolerance in yeast (Navarre and Goffeau 2000). To further

understand this salt tolerance, *AtRCI2A*, a homolog of *PMP3*, was tested under salt stress conditions in Arabidopsis plants. The *rci2a* mutant had higher levels of increase in internal Na^+ than the WT plants when subjected to salt stress treatment (Mitsuya et al., 2005). This was associated with a higher reduction in shoot growth (Mitsuya et al., 2005). The phenotype of the *rci2a* mutant suggests that *AtRCI2A* plays a role in decreasing the over-accumulation of Na^+ ions and like *PMP3*, contributes to salt tolerance (Mitsuya et al., 2005).

Eight homologous copies of the *PMP3* genes were also found in the genome of *Zea mays*, these eight genes known as *ZmPMP3-1* to *-8* were placed into three groups based on phylogenetic analysis (Fu et al., 2012). Group I contained *ZmPMP3-1, -5*, *-7* and *-8* which are 56-58 amino acids in length and they were more closely related to *AtRCI2A* than to the other *ZmPMP3*s (Fu et al., 2012). Group II is compromised of two members, *ZmPMP3-4* and *-6*, which are 54 amino acids in length and lastly, *ZmPMP3-2* and *-3* belong to group III which are 72 and 73 amino acids in length, respectively (Fu et al., 2012). The *ZmPMP3* family members are responsive to various abiotic stresses*; ZmPMP3-1*, *-2*, *-6*, *-7* and *-8* were up-regulated in response to drought, *ZmPMP3-1*, *-2*, *-4* and *-6* were responsive to cold and *ZmPMP3-2*, *-4*, *-5* and *-6* were responsive to ABA (Fu et al., 2012). The tassel, ear, stalk, root, leaf, and silk of maize were analysed and all eight of the *ZmPMP3*s had transcript levels at their highest in the young organs and tissues (Fu et al., 2012). A few notable expression patterns are seen with *ZmPMP3-4* having the highest levels of expression in the tassel and *ZmPMP3-6* with the highest levels of expression in the silk, suggesting different members have functions in different organs under normal or stress conditions. (Fu et al., 2012). Similar to the Arabidopsis *AtRCI2* genes, all *ZmPMP3*s were able to complement the Δ*pmp3* mutation in yeast and enhance its growth under

salt stress which would aid in conserving its cell physiological function (Fu et al., 2012). To solidify these *ZmPMP3*s as homologs of the *PMP3* family *ZmPMP3-1* was overexpressed in Arabidopsis and conferred salt tolerance in plants at the reproductive stage (Fu et al., 2012). The Arabidopsis *AtRCI2* gene family was used to find more homologous copies in *Zea mays*, and 10 gene copies were found in the maize genome and this gene family was annotated as *ZmRCI21-10* (Zhao et al., 2014).

Two genes induced by low temperatures in early seedlings were isolated from rice, *OsLti6a* and *OsLti6b* (*Low-temperature-induced a* and *b*), and they are close relatives of the Arabidopsis *AtRCI2A* and *AtRCI2B* genes and the barley *Blt101* (Morsy et al., 2005). Like the other *Esi3/RCI2* homologs, these genes from rice also play a role in the stress response pathways. Promoter analysis of *OsLti6a* and *OsLti6b* indicates that they have the potential to be components of cold stress response mediated by CBF/DREB-like (C-repeat Binding Factor/Drought Responsive Element-Binding protein) transcription activators, since induction of the two genes seemed to be synchronized with the expression of CBF (Morsy et al,, 2005). CBF/ DREB are a group of transcription factors that contain AP2/EREBP DNA-binding domains, these factors bind to the C-repeat/Drought Responsive Element in the promoters of *cor/rd* genes (*cold regulated/responsive to desiccation*) (Morsy et al., 2005). The *OsLti6a* and *OsLti6b* genes were also induced by ABA, a result that corroborates the presence of a putative ABA-Responsive Element (ABRE) in the promoter of *OsLti6a* (Morsy et al., 2005). In addition to *OsLti6a* and *OsLti6b*, another 12 *RCI2*-like genes were identified in rice, and they were annotated as *OsRCI21-12*, in a similar manner to maize, *OsRCI2-6* and *OsRCI2-10* were previously annotated as *OsLti6b* and *OsLti6a*, respectively. (Medina et al., 2007). Through the extensive analysis conducted, the *Esi3/RCI2/PMP3* genes are stress-responsive genes found in many plant species which play a role in controlling the stress response in many tissues.

1.4 The *Pirin* Gene Family

Pirin1 in Arabidopsis has been shown to interact with GPA1, the α subunit of the heterotrimeric G protein complex and Chapter 6 of this thesis is based on the characterization of the *Pirin* gene family in *T. aestivum*. It is common that some genes share sequence similarity which may imply conservation in function. Some genes are also present in superfamilies with diverse functions sharing some sequence similarity or characteristics, and one such example is the cupin superfamily. This superfamily was given its name based on the presence of a conserved β-barrel fold since '*cupa'* is the Latin term for small barrel (Dunwell et al., 2004). This superfamily was discovered based on sequence similarity to the wheat protein, germin, which is a thermostable protein involved in early germination (Dunwell et al., 2004). Further similarity of germin to other stress-related proteins from a wide range of organisms including the slime mould, *Physarum polycephalum,* and enzymes found in some microbes, revealed the presence of a β-barrel shape, placing an already diverse group of stress proteins into the cupin family (Dunwell and Ganes, 1998). The cupin family was characterized based on four conserved β-barrel motifs with an intervening loop that is less conserved (Dunwell et al., 2004). The length of the inter-motif region varies greatly with a minimum size of 11 amino acids in microbial enzymes, approximately 50 amino acids in non-enzymatic seed storage proteins, and greater than 100 amino acids in some eukaryotic transcription factors and dioxygenases (Dunwell et al., 2000; Dunwell et al., 2001). To further characterize this family, early research suggests the presence of two motifs with conserved sequences; motif 1 was G(X)5HXH(X)3,4E(X)6G and motif 2 was G(X)5PXG(X)2H(X)3N, however advances in 3D protein structures and sequencing have led to the understanding that the sequences of these two motifs are much less conserved (Dunwell et al., 2004). Nonetheless, the cupin superfamily is

comprised of many subgroups based on the number of cupin domains, ranging from single cupin domains, double domains (bicupin) or multiple domains (multicupin) (Dunwell et al., 2004). A small non-exhaustive example of some members of the cupin superfamily include the following: dioxygenases which are enzymes that catalyze a variety of reactions, auxin-binding proteins, seed-storage proteins and nuclear proteins (Dunwell et al., 2004).

A small gene family found in plants, mammals, and prokaryotes encodes the cupin protein Pirin. Pirin was first identified in humans due to its interaction with a nuclear I/CCAAT box transcription factor known as NFI/CTF1, which is responsible for adenovirus DNA replication and RNA polymerase II-driven transcription (Wendler et al., 1997). Based on the nuclear localization of Pirin and its interaction with the transcription factor NFI/CTF1, it has been deemed a transcriptional co-factor in humans (Wendler et al., 1997). The *Pirin* mRNA was expressed in low levels in all human tissues tested (skeletal muscle, heart, etc.) and about 15% of the *Pirin* cDNAs contain a 34-base pair (bp) insertion in the 5' untranslated region (UTR) which is indicative of an alternative splicing process (Wendler et al., 1997). The human Pirin has also been implicated in cell apoptosis via its interaction with the human oncogene *Bcl-3* and helps stabilize a quaternary complex involving *Bcl-3* and anti-apoptotic transcription factors (Warpeha et al., 2007; Foo and Nolan, 1999; Wulczyn et al., 1996).

The N-terminal region of Pirin appears to be conserved in plants, fungi, and prokaryotes (Wendler et al.,1997). An ortholog of the human Pirin, At-*Pirin1* was discovered in Arabidopsis after a yeast two-hybrid screen using the α subunit of the heterotrimeric G-protein complex, GPA1, as bait (Lapik and Kaufman, 2003). Additionally, this yeast two-hybrid showed that At-

Pirin1 (*PRN1*) is an interactor of the α subunit (Lapik and Kaufman, 2003). It was also shown that the C-terminal domain truncation of At-*Pirin1* (170 amino acids of C-terminal domain), which lacks the cupin domain, interacts with GPA1 suggesting that the first 117 amino acids of the N-terminal portion and the cupin domain are not necessary for the interaction (Lapik and Kaufman, 2003). Based on sequence analysis of the 5' regulatory region of At-*Pirin1* a few potential cis-regulatory elements are present which include two ACGT elements and one TT motif (located 308, 430 and 512-bp upstream of the ATG, respectively) (Lapik and Kaufman, 2003). The ACGT elements are 8- to 10-bp in length with the core sequence being ACGT (Busk and Pages, 1998; Leung and Giraudat, 1998). One notable ACGT element is the ABRE-like elements (Abscisic Acid–Responsive Elements) which are found in a number of ABA and stress-inducible gene promoters (Leung and Giraudat, 1998). It was also found that At-*Pirin1* has a 5- fold increase in expression in response to ABA and a 3-fold increase in response to a single pulse of low-fluence red flight, indicating a potential role in abiotic regulatory pathways (Lapik and Kaufman, 2003). This transcript level increase in response to ABA corroborates the presence of ABA-inducible regulatory elements in the At-*Pirin1* promoter region (Lapik and Kaufman, 2003).

At-*Pirin1* also plays a role in seed germination and the At-*pirin1* mutant has a similar phenotype to the *gpa1* mutant in having delayed germination in response to ABA and in the absence of stratification (Lapik and Kaufman, 2003.) This suggests that both *GPA1* and *Pirin1* play a role in overcoming the ABA inhibition of seed germination and aid in breaking seed dormancy via stratification. Given the implication of ABA in pathways triggered by salt (NaCl) and osmotic stress (mannitol and polyethylene glycol), the *gpa1* and At-*pirin1* mutant seed were tested for germination rates in response to these abiotic conditions, and it was found that no

differences occurred in seed germination or seedling growth in response to these factors (Lapik and Kaufman, 2003). Lapik and Kaufman (2003) suggest that At-*Pirin1* acts downstream of *GPA1* in controlling these seed germination phenotypes.

At-*Pirin1* is also implicated in regulating quercetin and specific light and UV responses in early seedling development. Quercetin is a flavonol that accumulates in the Arabidopsis seedlings, cotyledonary node, hypocotyl/root transition zone and root tip (Agati et al., 2012). Flavonols are known to induce auxin accumulation (Zhang et al., 2020). Quercetin is cleaved by quercetinase proteins, and studies carried out using the human and bacterial Pirin indicated that Pirin has quercetinase activity (Adams and Jia, 2005). At-Pirin1 was shown to also have quercetinase activity when bound to an inactive GPA1 (GDP bound), and that the quercetin accumulation in the dark-grown At-*pirin1* mutants was higher after UV induction (Orozco-Nunnelly., 2014). These data suggests that At-*Pirin1* may play a role in regulating quercetin levels which may affect growth of young seedlings (Orozco-Nunnelly. 2014). *GPA1* and At-*Pirin1* are also implicated in a signal transduction chain involving the nuclear factor Y heterotrimer which is comprised of A5, B9 (LEC1) and C9 subunits and is present in imbibed seed and affects germination rates (Warpeha et al., 2007). The NF-Y (Nuclear Factor Y) has been shown to bind the CCAAT box, and the human *Pirin* ortholog was shown to interact with NF-Y (Wendler et al.,1997). Another nuclear-encoded gene that may be involved in the *GPA1* and At-*Pirin1* cascade is *light-harvesting chlorophyll a/b-binding* (*Lhcb*), which is activated by a 10-bp sequence containing a CCAATT box which indicates that a CCAATT-binding protein, such as NY-F may be involved in this activation (Folta and Kaufman, 1999). *Lchb* is activated by blue light (BL), and it is believed that ABA is able to mimic the effects of BL in a pathway mediated by GPA1 via its downstream effector Prephenate Dehydratase 1 (PD1) (Warpeha et al., 2007).

The *nf-y-a5*, *-b9, b6* and *–c4* mutants display hypersensitivity to ABA and cause delayed germination (Warpeha et al., 2007). Using *in vitro* co-precipitation experiments and yeast two-hybrid assays it was shown that Pirin1 interacts with NF-Y-B6. Taken together these data suggest that a signal cascade for ABA seed germination involves *GPA1*, *Pirin1*, and *NF-Y-B6*, ultimately leading to an effector response, however it is unclear what the initial ABA signaling molecule is (Warpeha et al., 2007).

In addition to At-*Pirin1* there are three other members of the *Pirin* gene family in Arabidopsis, At-*Pirin2*, *3*, and *4*. At-*Pirin2* was found to be a suppressor of S-type lignin in Arabidopsis stems and hypocotyls and is expressed in cells next to vessel elements, further solidifying its role in noncell-autonomous lignification of xylem vessels (Zhang et al., 2020). This indicates that the two Arabidopsis *Pirins* studied (*Pirin1* and *2*) have distinct tissue specific expression and functions displaying low redundancy in the gene family. *Pirin* has also been characterized in tomato (*Lycopersicon esculentum* Mill.) designated as Le-*pirin* whose mRNA increased in response to cell death triggered by a mycotoxin, however it was not affected by stress-related chemicals such as ethylene, methyl jasmonate or salicylic acid, suggesting Le-*pirin* plays a role in programmed cell death (Orzaez et al., 2001). *Pirin* orthologs to those found in Arabidopsis and tomato have been mentioned in other dicots and monocots, indicating conservation of the *Pirin* gene family however no further work has been reported on these gene families (Orzaez et al., 2001, Bandaranayake et al., 2012).

Purpose

The purpose of this study is to characterize gene families that are stress-responsive and may lead to adaptations that alter plant survival and fitness. An understanding of these genes could ultimately have applications in agriculture and improve crop yields during times of

abiotic and biotic stress. *Arabidopsis thaliana* is a model organism amenable to genetic manipulation and findings within this species may be applied to crop plants such as *Triticum aestivum*. An example of such a possibility is the work being done on the Heterotrimeric G-protein α-subunit, GPA1, where the ability of Arabidopsis to undergo mutagenesis and to yield seed in a short period of time has allowed extensive work to be done on the G-proteins. This can further help understand G-protein signaling in other plant species like *Oryza sativa*, where it is known that Gα is a dwarf gene and can help overcome crop loss associated with lodging. The caleosin study can further help understand G-protein signaling and could lead to the investigation of the role of the caleosins and G-protein in crop species. This is especially promising since some of the caleosins are affected by biotic and abiotic stresses. The studies on gene families such as *Esi3* and *Pirin* give an insight into their roles in *T. aestivum,* an important crop species, and this information can be used as a stepping stone to further understand genes that aid in crop resistance to environmental stress.

Chapter 2: **The stress induced caleosin, RD20/CLO3, acts as a negative regulator of GPA1 in Arabidopsis** was first published at Plant Molecular Biology Volume 107:159-175, 2021, by Springer Nature.

Brunetti, S. C., Arseneault, M.K.M., Wright, J. A., Wang, Z., Ehdaeivand, M. R., Lowden, M. J., Rivoal, J., Khalil, H. B., Garg, G., and Gulick, P. J. (2021). The stress induced caleosin, *RD20/CLO3*, acts as a negative regulator of *GPA1* in Arabidopsis. Plant Mol. Biol. https://doi.org/10.1007/s11103-021-01189-x

Plant Molecular Biology (2021) 107:159–175
https://doi.org/10.1007/s11103-021-01189-x

The stress induced caleosin, RD20/CLO3, acts as a negative regulator of GPA1 in Arabidopsis

Sabrina C. Brunetti[1] · Michelle K. M. Arseneault[1] · Justin A. Wright[1] · Zhejun Wang[1] · Mohammad-Reza Ehdaeivand[1] · Michael J. Lowden[1] · Jean Rivoal[2] · Hala B. Khalil[1,3] · Gajra Garg[1,4] · Patrick J. Gulick[1]

3.

Received: 25 March 2021 / Accepted: 5 September 2021 / Published online: 2 October 2021

Abstract

Key message **A stress induced calcium-binding protein, RD20/CLO3 interacts with the alpha subunit of the heterotrimeric G-protein complex in Arabidopsis and affects etiolation and leaf morphology.**

Abstract Heterotrimeric G proteins and calcium signaling have both been shown to play a role in the response to environmental abiotic stress in plants; however, the interaction between calcium-binding proteins and G-protein signaling molecules remains elusive. We investigated the interaction between the alpha subunit of the heterotrimeric G-protein complex, GPA1, of *Arabidopsis thaliana* with the calcium-binding protein, the caleosin RD20/CLO3, a gene strongly induced by drought, salt and abscisic acid. The proteins were found to interact in vivo by bimolecular fluorescent complementation (BiFC); the interaction was localized to the endoplasmic reticulum and to oil bodies within the cell. The constitutively GTP-bound GPA1 ($GPA1^{QL}$) also interacts with RD20/CLO3 as well as its EF-hand mutant variations and these interactions are localized to the plasma membrane. The N-terminal portion of RD20/CLO3 was found to be responsible for the interaction with GPA1 and $GPA1^{QL}$ using both BiFC and yeast two-hybrid assays. RD20/CLO3 contains a single calcium-binding EF-hand in the N-terminal portion of the protein; disruption of the calcium-binding capacity of the protein obliterates interaction with GPA1 in in vivo assays and decreases the interaction between the caleosin and the constitutively active $GPA1^{QL}$. Analysis of *rd20/clo3* mutants shows that *RD20/CLO3* plays a key role in the signaling pathway controlling hypocotyl length in dark grown seedlings and in leaf morphology. Our findings indicate a novel role for RD20/CLO3 as a negative regulator of GPA1.

Keywords Heterotrimeric G-protein alpha subunit · Gα protein · GPA1 · Calcium-binding protein · RD20/CLO3 · Signal transduction · Protein–protein interaction · Etiolation

Introduction

Plants have developed a variety of mechanisms to enhance survival and reproduction under conditions of abiotic stress, and the response to stress involves mechanisms controlled by the regulation of several hundred stress-response genes (Kreps et al. 2002; Oono et al. 2003). The plant heterotrimeric GTP-binding protein (G protein) complex has been shown to play a role in the response to a number of stress conditions, including high salinity, drought (Misra et al. 2007), hypoxia, and ethylene treatment (Steffens and Sauter 2010), as well as biotic stress (Aharon et al. 1998). Components of the heterotrimeric G-protein complex have also been shown to act in signaling pathways regulated by abscisic acid (ABA) (Ritchie and Gilroy 2000; Wang et al. 2001; Pandey et al. 2006), jasmonic acid (Okamoto et al. 2009), and gibberellin (Ullah et al. 2003). G proteins and G-protein

✉ Patrick J. Gulick
patrick.gulick@concordia.ca

1 Department of Biology, Concordia University, 7141 Sherbrooke W., Montreal, QC H4B 1R6, Canada

2 Institut de Recherche en Biologie Végétale, Université de Montréal, 4101 Sherbrooke Est, Montréal, QC H1X 2B2, Canada

3 Present Address: Department of Genetics, Faculty of Agriculture, Ain-Shams University, Shoubra El-khema, Cairo, Egypt

4 Present Address: Department of Biotechnology & Microbiology, Mahatma Jyoti Rao Phoole University, Jaipur, Rajasthan, India

regulators have been shown to be involved in alterations in root growth (Chen et al. 2003, 2006), transpiration efficiency (Nilson and Assmann 2010), cell proliferation affecting hypocotyl and leaf growth (Ullah et al. 2003; Chen et al. 2003), and a plethora of other physiological and morphological responses (Pandey 2019; Perfus-Barbeoch et al. 2004). Therefore the investigation of the role of G proteins into the stress signaling networks is an important area of research.

Heterotrimeric G proteins have also been implicated in numerous signaling pathways in animals, but in stark contrast to animals which have small gene families for all G-protein subunits, plant species' genomes encode single or few heterotrimeric G proteins. The Arabidopsis genome encodes a single G alpha and beta subunit and only three G gamma subunits, whereas the human genome encodes 23 alpha, six beta and 12 gamma subunits (Jones 2002). The genome also contains three genes encoding extra-large G proteins capable of binding to the Gβγ dimers and which are functional within the heterotrimeric G protein complex signaling pathway (Chakravorty et al. 2015). The complexity of signaling associated with plant G proteins is likely modulated through association with other proteins. The heterotrimeric G proteins in Arabidopsis have been shown to be part of a large multi-protein complex with a molecular mass of approximately 700 kDa (Wang et al. 2008), whereas the Gα, Gβ and Gγ subunits alone have a combined molecular mass of approximately 100 kDa. In plants null for the Gβ subunit, Gα forms a complex with a molecular weight of 200–400 kDa indicating that the formation of the larger complex is dependent on Gα's binding to the Gβγ dimer (Wang et al. 2008). In rice the heterotrimeric G protein complex was shown to have a molecular mass of 400 kDa also indicating an association with other proteins (Kato et al. 2004). Some of the Gβγ subunits were found to be present in a dimer not associated to the Gα subunit and therefore not being part of the 400 kDa complex (Kato et al. 2004). In Arabidopsis, a number of proteins have been reported to be associated with the Gα subunit including RGS1 (Regulator of G-protein signaling 1), THF1 (Thylakoid Formation), PRN1 (Pirin1) and PLDα1 (Phospholipase D alpha 1) (Klopffleisch et al. 2011). PLDα1 interacts with GPA1, the Arabidopsis gene encoding the α-subunit of the heterotrimeric G proteins, via the DRY motif and the interaction is nucleotide dependent with PLDα1 having a higher affinity for GPA1 in a GDP-bound state (Temple and Jones 2007). PLDα1 is also believed to interact with AGB1, the Gβ subunit, when AGB1 is present in its heterodimer form bound to a Gγ subunit (AGG1, AGG2 or AGG3) (Gookin and Assmann 2014).

GPA1 has been shown to have a role in the regulation of cell proliferation and development in the aerial tissues of the plant; the *gpa1* mutant has impaired cell division in the leaf tissue, with fewer larger cells present leading to a more round leaf shape. In response to dark treatment the *gpa1* mutant has shorter hypocotyls due to impaired cell division of the hypocotyl cells, resulting in fewer elongated cells when compared to the wild type (Ullah et al. 2001). The *GPA1* Q222L ($GPA1^{QL}$) mutant contains a mutation in the conserved GTPase domain inhibiting GTP hydrolysis and causing GPA1 to be in a constitutively active GTP-bound state. Expression of the $GPA1^{QL}$ mutant form has the opposite effect on cell proliferation compared to the *gpa1* mutant (Ullah et al. 2003; Chen et al. 2003). Expression of $GPA1^{QL}$ causes an increase in hypocotyl length due to an increase in cell division, and the *rgs1* mutant phenocopies the $GPA1^{QL}$ mutant for this trait (Chen et al. 2003). This indicates that an active *GPA1* is responsible for the increase in hypocotyl length in dark-grown seedlings. *GPA1* has also been implicated in hypocotyl development in response to the combination of sugar and brassinosteroid signaling (Peng et al. 2018). The presence of glucose mediates the interaction between *GPA1* and brassinosteroid receptors including Brassinosteroid insensitive 1 (*BRI1*) and *BRI1*-associated kinase 1 (*BAK1*) (Peng et al. 2018). Media supplemented with glucose and brassinosteroid inhibitors led to differences in the development of leaf-like structures and the rate of hypocotyl development in dark-grown seedlings (Peng et al. 2018).

RD20/CLO3 (At2g33380) in Arabidopsis, which is a member of the caleosin gene family, is strongly induced under a variety of abiotic stress conditions including dehydration, salt, and ABA treatment (Takahashi et al. 2000). The *rd20/clo3* mutant exhibited decreased tolerance to drought and salt conditions, and *RD20/CLO3* has been suggested to act as a stress-signaling hub that triggers or regulates a plant's stress response mechanisms (Aubert et al. 2010). Most recent work has linked *RD20/CLO3* to peroxygenase activity towards hydroperoxides of unsaturated fatty acids, which reduces levels of reactive oxygen species (ROS) and cell death aiding in biotic stress tolerance (Blée et al. 2014; Hanano et al. 2015). In addition to abiotic and biotic stress responses, RD20/CLO3, similar to the other caleosins, plays a role in the structure and function of lipid/oil droplets (LD) (Chapman et al. 2012). The biogenesis of a lipid droplet is initiated at the endoplasmic reticulum (ER) and is encompassed by a single phospholipid layer embedded with lipid droplet-associated proteins, oleosins, caleosins and steroleosins, which span the outer and inner portions of the droplet (Frandsen et al. 2001). The caleosins were first found to be associated with LDs in a study involving sesame seeds, and they have structural homology to oleosins (Chen et al. 1999; Chapman et al. 2012). The N- and C-terminal domains sit on the cytosolic side of the droplet while anchored via a small membrane-spanning region and a proline knot, which faces the internal triacylglycerol (TAG) matrix (Frandsen et al. 2001). The caleosin has an N-terminal region which is

slightly larger than that of an oleosin and contains a single EF-calcium binding hand, and the C-terminal portion contains phosphorylation sites (Naested et al. 2000; Frandsen et al. 2001). The LDs are a source of TAGs utilized under germination and other developmental conditions (Chapman et al. 2012). There are also some plant species like cycads (sago palms) and mosses, as well as single-celled algae and fungi which only have caleosins present on the LD, suggesting that caleosins are ancestral to oleosins (Huang et al. 2009; Frandsen et al. 2001; Naested et al. 2000).

A homolog of *RD20/CLO3* in *Triticum aestivum*, *Clo3*, was shown to physically interact with the Gα subunit of wheat (*GA3*) (Khalil et al. 2011) suggesting that the caleosins play a regulatory role in G-protein signaling. Both *RD20/CLO3* and *GPA1* have been shown to be regulators of transpirational water loss in Arabidopsis (Aubert et al. 2010; Nilson and Assmann 2010). It was shown that enhanced transpiration efficiency of the *gpa1* mutants is likely due to reduced stomatal density, and not to the altered response of stomata opening or closing in response to drought (Nilson and Assmann 2010). The overexpression of *RD20/CLO3* in transgenic Arabidopsis increased transpiration efficiency, while the *rd20/clo3* mutant decreased efficiency, however neither stomatal density nor stomatal regulation were assayed in that study (Aubert et al. 2010). In addition, mutants in ABA biosynthesis genes in Arabidopsis that have reduced ABA levels have increased transpiration rates and increased stomatal density, suggesting that ABA plays a role in stomatal development (Chater et al. 2014).

The present study investigates the physical interaction between the Arabidopsis GPA1 and the caleosin RD20/CLO3 and characterizes the genetic interaction of the two genes with respect to the regulation of hypocotyl elongation in the dark and leaf morphology. The role of *RD20/CLO3* as a negative regulator of *GPA1* in controlling etiolation and leaf morphology was further investigated.

Methods

Plant material

The mutant line *rd20/clo3* in the Wassilewskija ecotype (WS) background was obtained from the ABRC stock centre (Ohio State U; FLAG_237F07); the *gpa1* mutant line in the WS background was a gift from Dr. Alan Jones (North Carolina State U). An *Arabidopsis thaliana* transgenic line with the *GPA1* promoter::*GUS* reporter fusion was kindly provided by Dr. Sarah Assmann (Pennsylvania State U). The *rd20/clo3* and *gpa1* single mutants were crossed and F1, F2 and F3 generations were characterized. The P35S:*RD20/rd20* line used in this study was kindly provided by Dr. Elizabeth Blée (Université de Strasbourg).

Plant growth conditions

To characterize leaf morphology, Arabidopsis plants were grown in a soil mixture containing two parts black earth, one part peat moss and one part vermiculite that was heat treated at 130 °C for 90 min. Seeds were sown in soil and stratified in the dark at 4 °C for three days. Pots were then placed in a growth chamber and the plants were grown at 22 °C, with light at 95–110 $\mu mol \cdot m^{-2} \cdot s^{-1}$ and maintained in a light cycle of 16 h light and 8 h dark. The length and width of each leaf were measured 7 weeks post germination to ensure all rosette leaves had fully developed.

To characterize hypocotyl growth, plants were grown on Murashige and Skoog (MS) agar media in growth chambers with 95–110 $\mu mol \cdot m^{-2} \cdot s^{-1}$ of light under long day conditions (16 h light:8 h dark). Seeds were sterilized by vortexing in 70% ethanol followed by a sterilization solution (4% bleach, 1% Triton X-100) for 5 min, washed 5 times with sterile distilled water, and stratified in the dark at 4ºC for 48 h. Seeds were plated on Petri dishes containing ½ MS control media which is; 0.5X Murashige and Skoog basal salt mixture, 1% (w/v) sucrose, 0.05% MES hydrate (4-Morpholineethanessulfonic acid), 0.4% Gelzan™ CM agar substitute gelling agent, adjusted to pH 5.7 with KOH and left to grow for two days in a growth chamber. After two days plates were wrapped in aluminum foil to block all light and left in a growth chamber for an additional two days of growth. After four days the hypocotyls of the plants were imaged and hypocotyl lengths measured using ImageJ software (Rasband 1997–2014; http://imagej.nih.gov/ij/). Hypocotyl lengths were measured over three independent experiments with an average of 38 independent plants measured per genotype. For the hypocotyl cell length, the plants were subjected to the same conditions as described above and the cells were imaged using the Zeiss Axioplan Fluorescence Microscope with a 10X objective, cells were then measured using ImageJ software. An average of 56 cells was measured for each genotype. For the hypocotyl tissue localization of p*RD20/CLO3*::*GUS* and p*GPA1*::*GUS* expression, seeds were plated on ½ MS media with 1% sucrose for two days and then wrapped in the dark for an additional two days. The plants were then transferred to an X-Gluc staining solution according to the protocol described by Jefferson et al., 1987. Samples were then de-stained in 70% ethanol and imaged using the Nikon SMZ1500 Stereomicroscope with a 0.75X to 11.25X zoom range and a 10X eyepiece with total magnification of 7.5X to 112.5X.

Construction of vectors

Two mutated forms of RD20/CLO3 with amino acid changes to replace a critical glutamic acid or aspartic acid residue in the EF-hand domain and block the calcium-binding capacity

(Xiong et al. 2010; Piazza et al. 2017) were developed using assembly-PCR with the primers found in Table S4 and recombined into pDonor-201 or pDonor-207 using the Gateway® BP Clonase II Enzyme system (Invitrogen). The coding regions of *RD20/CLO3*, the *RD20/CLO3* N-terminal portion of the protein from amino acids 1 to 90, *GPA1* and $GPA1^{QL}$ were PCR amplified from cDNA clones and recombined into pDonor-201 or pDonor-207 vectors using the Gateway® BP Clonase II Enzyme system (Invitrogen) and all entry clones were transformed into the TOP10 *E. coli* strain. Gateway® LR reactions were used to transfer the inserts from entry clones to pK7FWG2 (Karimi et al. 2002), a binary destination vector to generate eGFP C-terminal fusions as well as to pBatTL-cYFP, and pBatTL-B-sYFP-N (Uhrig, et al. 2007), the BiFC vectors used to create C-terminal half yellow fluorescent protein (YFP) and N-terminal half-YFP fusions, respectively. The *RD20/CLO3* coding region was also cloned into the pFAST G02 expression vector to create 35S promoter overexpression constructs (Shimada et al. 2010). For yeast two-hybrid analysis the full-length coding region and N-terminal half (from amino acids 1–90), N-terminal half EF-hand mutants with substitutions D70A or E81R, C-terminal (amino acids 124–237) truncations of *RD20/CLO3* as well as the full-length *GPA1* and $GPA1^{QL}$ were cloned into pGADT7-GW and pGBKT7-GW vectors (Lu et al. 2010). For expression of GPA1 in *E. coli*, the coding region of the two genes were resynthesized with *E. coli* codon optimized sequences by Life Technologies (Grand Island, USA) and were cloned into pDonor-207 and subsequently into the pGex-6p1 GST-fusion expression Gateway vector using the Gateway cloning system. The *RD20/CLO3 E. coli* optimized coding sequence was directionally cloned into the pRsetA 6xHis tag expression vector (Life Technologies) using SacI and NcoI restriction enzymes. The *GUS* reporter construct for *RD20/CLO3* was made by PCR amplifying a 1123 nt DNA fragment upstream of the translational start site of *RD20/CLO3* and cloned by the Gateway system into the binary plant expression vector, pKGWFS7 (Karimi et al. 2002). All constructs were verified by PCR, and entry clones were verified by sequencing. Primers used to generate the expression clones are listed in Table S4.

Transgenic Arabidopsis lines

P35S:*RD20* and *RD20/CLO3* promoter::*GUS* (pRD20::*GUS*) homozygous transgenic lines were generated by transforming the constructs into WS wild type plants or the *gpa1* mutant line in the WS background using the Arabidopsis floral dip method from Clough and Bent (1998). The P35S:*RD20* in the *rd20* mutant background was developed by Blée et al. (2014). Transgenic P35S:*RD20* T1 and subsequent homozygous lines were screened using the pFAST GFP vector system (Shimada et al. 2010) where transgenic seeds expressing GFP were detected using the Zeiss Axioplan Fluorescence Microscope with the GFP Filter Cube #1,031,346. Two independent homozygous T_3 lines with single transgene insertions were identified for P35S:*RD20/CLO3* in WS and P35S:*RD20/CLO3* in the *gpa1* mutant background (P35S:*RD20/gpa1*). Four p*RD20/CLO3*::*GUS* lines were identified using plant antibiotic resistance screening (½ MS media supplemented with 25 µg/ml Kanamycin).

PCR screening of recombinant lines

The *rd20/clo3* and *gpa1* single mutant lines were crossed and the F1, F2 and F3 generations were screened via PCR using gene specific primers and T-DNA left and right border primers recommended by the SALK Institute (La Jolla, USA). Leaf tissue from seedlings was frozen in liquid nitrogen and ground to a fine powder and DNA was extracted using a detergent-based extraction buffer according to Edwards et al. (1991). An 80–100 ng aliquot of plant DNA was assayed by PCR with primer pairs to detect the T-DNA insertional mutations of *gpa1* and *rd20/clo3* (Table S4). In the F2 generation one independent recombinant line was identified that was heterozygous for the *rd20/clo3* mutation and homozygous for the *gpa1* mutation. Three out of the 18 F3 offspring were homozygous for both mutations.

RNA analysis

The P35S:*RD20/CLO3* lines were screened semi-quantitatively for *RD20/CLO3* expression levels by Reverse Transcription PCR (RT-PCR) (Table S5). RNA was extracted from Arabidopsis plants using the RNeasy Plant extraction kit (Sigma), as per the manufacturer protocol. A 1 µg RNA aliquot was incubated with 50 µM oligo dT at 70 °C for 5 min, placed on ice, and subsequently reverse transcribed with 400 µM dNTPs, 1X RT buffer and 20 units of M-MuLV reverse transcriptase (New England BioLabs) and placed in a thermal cycler at 37 °C for 5 min, 40 °C for 60 min, 55 °C for 20 min, and 70 °C for 10 min. The *RD20/CLO3* cDNA was then amplified in 1X Taq buffer with 200 µM dNTPs, 3 mM $MgCl_2$, 10 µM forward and reverse primer and 2.5 units of Taq polymerase in the thermal cycler for 30 and 35 cycles. Each RNA sample was duplicated, and RT-PCR was repeated independently in two reaction sets. Gene specific primers used for the reactions are presented in Table S4.

Protein interaction by Bimolecular Fluorescence Complementation and localization

Nicotiana benthamiana plants were grown in soil prepared as mentioned above for Arabidopsis and grown in the greenhouse at 22 °C, with natural light supplemented

after sundown and before sunrise and with artificial light at 86.70–95 µmol·m^{-2}·s^{-1}, to maintain a light cycle of 16 h light and 8 h dark. Plants were also grown in growth chambers with 95–110 µmol·m^{-2}·s^{-1} of light under long day conditions (16 h light:8 h dark, 22 °C). Electrocompetent Agrobacterium strain AGL1 was transformed with *RD20/CLO3*, *RD20/CLO3*^{D70A}, *RD20/CLO3*^{E81R}, the *RD20/CLO3* N-terminal (amino acids 1 to 90), *GPA1,* and *GPA1*^{QL} fluorescent fusion constructs to study their transient expressions and interactions in vivo. For the pBatTL vector system the cultures were grown and treated as previously described in Kapila et al. (1997) and Khalil et al. (2011) with the following modifications: the Agrobacterium cultures carrying the YFP fusions and p19 were diluted to an OD_{600} of 0.5, the PM-mCherry fusion was diluted to an OD_{600} of 0.01 and the ER-mCherry fusion was diluted to an OD_{600} of 0.2. The agroinfiltration mixtures were incubated for 4 h at room temperature. The agroinfiltration mixtures were co-infiltrated into the abaxial side of leaves of three to four-week-old *N. benthamiana* plants, the plants were incubated in the greenhouse for 24–49 h. Sections of Agrobacterium-infiltrated *N. benthamiana* leaf tissue approximately 2 mm × 2 mm were imaged within the time points stated above. The images for Figs. 1, 2, 3, S1 panel C, D and E, S2 and S3 panel A were taken with the Olympus FluoView FV10i laser scanning microscope (Olympus, USA) fitted with 60x/1.35 oil (pixel size 0.27 µm). A 473 nm laser was used to observe the eGFP fused proteins and N/C-YFP fused proteins, with the eGFP filter (Ex 489 nm / Em 510 nm) and YFP filter (Ex 480 nm/ Em 527 nm), respectively. The markers included the signal peptide of the cell wall-associated kinase 2 with an ER retention signal, AtWAK2, fused to the fluorescent mCherry protein and the mCherry-AtPIP2A, plasma membrane aquaporin, were imaged with the 559 nm laser and the red narrow filter (Ex 559 nm/ Em 570-620 nm). The images from 0.5 to 1.5 µm spaced z-stacks were converted to maximum z-projections using ImageJ. BiFC Figure S1 panels A and B were taken by the Leica DMI6000B Spinning Disc 2 (SD2) confocal microscope using the objective HCX PL APO CS 20X/1.25 oil pH 3 DIC. YFP fluorescence was viewed with a 25 mW diode laser at 491 nm excitation with BP 540–543 emission filter. The 25 mW diode laser at 561 nm with BP 624–640 filter was used to detect RFP signals. Samples with GFP constructs were excited by 25 mW diode laser at 491 nm with BP 520–535 filter. EM CCD 512 × 512 BT camera was used to record images.

Protein interaction by yeast two-hybrid (Y2H)

The yeast strain AH109 (MATa trp1-901 leu2-3,112 ura3-52 his3-200 gal4 gal80 URA3::MEL1UAS-MELTATA-LacZ LYS2::GAL1UAS-GAL1TATA-HIS3 GAL2UAS-GAL2TATA-ADE2) (Clontech Inc, USA) was transformed with GPA1 and GPA1^{QL} in the AD fusion vector and the RD20/CLO3 N-terminal portion, N-terminal EF-hand mutants, D70A and E81R in the region including amino acids 1 to 90, C-terminal portion, and full-length (CDS) in the BD fusion vector, and the negative and positive controls (empty AD and BD vectors or the AGB1/AGG3(γ) in the BD vector, respectively) using the lithium acetate transformation protocol from Ito et al. (1983), with the following modifications: the pellet was washed twice with 1X TE, after the addition of 1X lithium acetate the yeast cells were left at room temperature for an hour without shaking, carrier DNA (herring sperm DNA, 10 mg/ml leading to a 300 µg DNA final concentration) was added prior to the plasmid, and cells were immediately plated after a 5 min 42°C incubation. Samples were then plated on double drop out media (SD minus leucine and tryptophan) and triple drop out media (SD minus leucine, tryptophan and histidine). Colonies from the double drop out plates were stamped on triple drop out plates with varying concentrations of 3-Amino-1,2,4,-triazole (3-AT, 0 mM to 60 mM).

A β-Galactosidase assay was carried out on triple drop out plates to confirm the GPA1, GPA1^{QL} and RD20/CLO3 N-terminal interactions. Plates with colonies were placed upside down over an area containing 5–10 ml of chloroform for 5 min. The plates were then overlaid with 1.5–2 ml chloroform and left until the chloroform had evaporated. An 8.5 ml aliquot of 0.1% agar was dissolved, cooled to 40℃ and mixed with 1 ml of potassium-phosphate buffer (1 M K_2HPO_4 and 1 M KH_2PO_4) and 0.5 ml of X-Gal solution (20 mg/ml X-Gal in Dimethylformamide (DMF)), which was overlaid on the plate with yeast colonies. The plates were then wrapped in aluminum foil to block light and left at room temperature for 24 h.

Purification of GPA1-GST

The recombinant GPA1-GST protein was expressed in *E. coli* strains HB101 and BL21 (DE3) and it was determined that the recovery of the soluble form was greatly improved by co-expression with the GroES-GroEL chaperones encoded by the pGro7 plasmid (Takara Bio, Mountain View, CA) under induction conditions previously described by Auslender et al. (2015). For protein samples used for GTPase assays, the frozen cell pellet from a 175 ml culture was thawed and resuspended in a pH 7.3 buffer containing 10 mM Na_2HPO4, 1.8 mM KH_2PO_4, 2.7 mM KCl, 140 mM NaCl, 0.1% (v/v) Triton X-100, 30 µM $AlCl_3$, 20 mM NaF, 1 mM DTT, complete EDTA-free protease inhibitor (Roche) and 1 mM PMSF. Cells were disrupted twice at 4 °C using a French Press (18,000 psi) and the supernatant obtained after centrifugation (30 min at 10,000 × *g*) was filtered using

a 0.22 µm pore size cellulose acetate filter. The filtrate was absorbed batch wise to glutathione agarose resin (GoldBio, 0.5 ml settled bed volume, previously equilibrated in extraction buffer). The slurry was poured in a disposable column (0.5 cm diameter) and the resin was washed with 15 ml extraction buffer followed by 15 ml extraction buffer containing 5 mM ATP and 10 mM $MgCl_2$ to dissociate the chaperone bound to the column (Auslender et al. 2015). Proteins were eluted from the column with 5 ml buffer containing 50 mM Tris–HCl pH 8.0, 0.1% (v/v) Triton X-100, 30 µM $AlCl_3$, 20 mM NaF, 1 mM DTT, complete EDTA-free protease inhibitor from Roche, 1 mM PMSF and 10 mM reduced glutathione. After elution, the presence of GPA1-GST in collected fractions (0.5 ml) was assessed by SDS-PAGE analysis. Affinity purified GPA1-GST was transferred to a buffer containing 20 mM Tris–HCl (pH 8.0), 1 mM dithiothreitol (DTT), 25 µM GDP and 5% (v/v) glycerol by diafiltration using an Amicon Ultra-4 centrifugal filter. The protein was further purified by negative chromatography on a MonoQ HR5/5 column equilibrated in the same buffer. Protein in the flow through was incubated with 2 mM EDTA for 5 min, after which 5 mM GTP was added to the sample for 30 min. Protein samples were then subjected to diafiltration against a buffer containing 20 mM Tris–HCl pH 8.0, 10 µM $CaCl_2$ and 25 mM KCl on an Amicon Ultra-4 centrifugal filter. The protein was then used in the GTPase assay.

Purification of (6xHis) RD20/CLO3

The (6xHis) RD20/CLO3 protein was expressed in *E. coli* BL21 (DE3). The RD20/CLO3 culture was induced using an auto-induction protocol adapted from Studier (2005). An RD20/CLO3 starter culture was grown overnight in LB media with 50 µg/ml ampicillin at 37 °C and shaking at 200 rpm. A 2.5 ml aliquot of the starter culture was transferred to 400 ml ZY media (8 g Bio-Tryptone, 4 g Yeast extract) supplemented with 16 ml 50×5052 solution (25% (w/v) glycerol, 2.5% (w/v) glucose and 10% (w/v) α-lactose), 16 ml 50xM solution (1.25 M Na_2HPO_4, 1.25 M KH_2PO_4, 2.5 M NH_4Cl and 0.25 M Na_2S0_4), 1.6 ml 1 M $MgSO_4$ and with ampicillin at 40 µg/ml. The culture was incubated at 37 °C while shaking at 200 rpm for 8 h. The temperature was then reduced to 18 °C overnight. Cells were harvested by centrifugation for 25 min at 10,000 × *g* and the pellets were stored at -80 °C. The pellets were purified using B-PER lysis buffer (Pierce, USA) as per manufacturer guidelines with the addition of 0.25% (v/v) nonyl phenoxypolyethoxylethanol (NP-40), 2500 U of deoxyribonuclease (DNase) and complete EDTA-free protease inhibitor tablet. The supernatant was purified by immobilized metal affinity chromatography using nickel agarose beads (GoldBio) according to Pandey et al. (2009). For use in the GTPase assay, (6xHis) RD20/CLO3 was further purified using ion exchange chromatography on a 1 mL HiTrap Q FF Sepharose (GE Healthcare). For this, the protein was desalted against buffer A (20 mM Tris–HCl pH 8, 0.1% (v/v) TWEEN-20) and applied to the column equilibrated in buffer A. Protein bound to the column was eluted using buffer B (buffer A containing 1 M NaCl) under the following conditions: a 100 mL linear gradient of 0 to 50% (v/v) buffer B in buffer A, followed by 10 mL at 50% (v/v) buffer B and 20 mL at 100% (v/v) buffer B. Fractions of 5 mL were collected and analyzed by SDS-PAGE to identify (6xHis) RD20/CLO3 elution position (typically around 0.3 M NaCl in the gradient). Fractions were concentrated using a 10 kDa MWCO spin filter (Pierce concentrator from Thermo Scientific) and applied to a Superdex 75 26/60 gel filtration column developed using buffer A containing 50 mM NaCl. Proteins in collected fractions were acid precipitated and analyzed by SDS-PAGE. Fractions containing pure (6xHis) RD20/CLO3 were frozen and kept at − 80 °C until use.

GTPase activity assays and protein determination

GTPase activity assays for GPA1-GST were conducted using a spectrophotometric coupled enzyme assay similar to that used for nucleoside diphosphate kinase (Dorion and Rivoal 2003). The reaction medium contained 10 mM Tris–HCl, pH 7.5, 1 mM ethylenediaminetetraacetic acid (EDTA), 10 mM $MgCl_2$, 10 µM GTP, 10 µM $CaCl_2$, 50 mM KCl, 0.32 mM nicotinamide adenine dinucleotide, 4 mM phosphoenolpyruvate, 0.4 unit rabbit muscle pyruvate kinase, and 1 unit rabbit muscle lactate dehydrogenase in a final volume of 0.2 ml. Following hydrolysis by a GTPase, the GDP produced in this assay is recycled to GTP by pyruvate kinase concomitantly with the synthesis of pyruvate, which is detected by a coupled reaction with lactate dehydrogenase. GDP recycling could be important since GDP has been reported to inhibit the activity of some GTPases in the µM range (De Vendittis et al. 1999). Assays were carried out at 25 °C on a calibrated VERSAmax microplate reader (Molecular Devices, Sunnyvale, CA) and the reaction was monitored at 340 nm for 40 min to measure the disappearance of NADH.

In vitro binding of GPA1-GST and (6xHis) RD20/CLO3

In vitro binding of GPA1-GST and (6xHis) RD20/CLO3 was performed by transferring the protein fractions obtained from the protocol above to a buffer containing 10 mM Tris–HCl pH 7.5, 10 mM $CaCl_2$ and 50 mM KCl loading onto an Amicon Ultra-4 centrifugal filter. The glutathione agarose resin (GoldBio, 0.02 mL settled bed volume) was also equilibrated with the same buffer. The GPA1-GST fraction was added to the resin at a final concentration of 0.015 mg/ml and placed at 4 °C while rocking for 1 h. The (6xHis) RD20/CLO3 fraction, eluted from the nickel resin

described above was added at a 1:1 molar ratio and left to rock at 4 °C for an additional 2 h. The flow through was then collected and the column was washed 5 × with a GST wash buffer containing 10 mM Na_2HPO4, 1.8 mM KH_2PO_4, 2.7 mM KCl, 140 mM NaCl. Samples were then eluted using 50 mM Tris–HCl pH 8.0, and 10 mM reduced glutathione. Fractions were analyzed by SDS-PAGE and stained with Coomassie blue.

Statistical analysis

For hypocotyl length and leaf morphology a one-way ANOVA (Analysis of Variance) was carried out to measure the significance of differences between genotypes and was followed by a Tukey's test, using IBM SPSS Statistics version 19 (http://www-01.ibm.com/software/analytics/spss/products/statistics/). The Tukey's post hoc test allows for pair-wise comparisons between the different genotypes and treatments. The samples that share common letters on graphs do not have significant differences, while samples that do not share a common letter have significant differences. The level of significance for all the tests is $\alpha = 0.05$, and p values below 0.05 were considered significant.

Results

Interaction between RD20/CLO3, RD20/CLO3 EF-hand mutants, GPA1 and GPA1^{QL} and cellular localization

The potential for interaction between GPA1 and the caleosin RD20/CLO3 was investigated by bimolecular fluorescence complementation (BiFC) by which protein–protein interactions are detected via the formation of a fluorescent complex when two proteins fused to the N- and C-terminal of a fluorescent protein interact with each other. When RD20/CLO3 and GPA1 were co-expressed as fusions to the two halves of the yellow fluorescent protein (YFP) in the epidermal cells of a *Nicotiana benthamiana* leaf, their interaction was apparent by the fluorescence in both the visible endoplasmic reticulum (ER) network structure and by co-localization with a fluorescently labelled ER marker (Arabidopsis wall-associated kinase 2 signal peptide (AtWAK2) with an HDEL ER retention signal; Fig. 1A, Figure S1, S2, S3 and Table S1). This localization was surprising since both GPA1 and GPA1^{QL} fused to the full-length enhanced green fluorescent protein (eGFP), was localized to the plasma membrane (PM) (Fig. 1E and F and Table S1). This indicates that the GPA1 that interacts with RD20/CLO3 is a subpopulation of the protein that is not associated with the PM. The RD20/CLO3 and GPA1 interaction was also visible in punctate structures surrounding the ER, the puncta also emitted fluorescence when stained with Nile Red, a lipophilic stain (Fig. 2A). The puncta and the Nile Red stain are shown to overlap; this indicates localization to oil/lipid droplets, a characteristic of the caleosin gene family. To further understand the nucleotide dependency of the GPA1 and RD20/CLO3 interaction, BiFC was carried out using the GPA1^{QL} mutant fused to C-YFP. The GPA1^{QL} mutant has normal GTP binding however it cannot undergo GTP hydrolysis due to a mutation in its conserved GTPase domain (Ullah et al. 2003). The interaction between RD20/CLO3 and GPA1^{QL} appears to be localized to the plasma membrane (PM), indicating the localization of the interaction is dependent on the nucleotide-bound state of GPA1 (Fig. 1B). The N-terminal half of RD20/CLO3 was also shown to interact with GPA1 via BiFC and the interaction was localized to the plasma membrane (Fig. 1C). The C-terminal half of RD20/CLO3 did not display any interaction with GPA1 (Fig. 1D). To investigate the effects of calcium on the RD20/CLO3 and GPA1 or GPA1^{QL} interactions, mutations in RD20/CLO3 were created for amino acids critical for calcium-binding in the EF-hand domain (Xiong et al. 2010; Piazza et al. 2017). The aspartic acid at amino acid position 70 was changed to alanine (D70A) and an independent mutation of a glutamic acid to arginine at amino acid position 81 (E81R) were created. Both RD20/CLO3^{D70A} and RD20/CLO3^{E81R}-N-YFP no longer showed an interaction with the GPA1-C-YFP, however they still interact with the GPA1^{QL}-C-YFP and the interactions remained localized to the PM (Fig. 3 and Figure S3). These results suggest that the GPA1^{QL} and RD20/CLO3 interaction is calcium-independent whereas the interaction between the non-mutated GPA1 and RD20/CLO3 is calcium-dependent (Fig. 3).

RD20/CLO3 fused to the full-length eGFP expressed in *N. benthamiana* (Fig. 1G and Table S1) was localized to the ER as seen by co-localization with the fluorescently labelled ER marker (AtWAK2), and by its distribution in a network structure in the upper focal planes of the cell, characteristic of the ER. RD20/CLO3 also localized to LDs as shown by the overlap with Nile Red stain, which is an indicative characteristic of a caleosin (Chapman et al. 2012) (Fig. 2B, C). The positive interaction control, GPA1 and RGS1 (Regulator of G-protein signaling) expressed as BiFC constructs were clearly seen to interact at the PM (Figure S1). The negative interaction control which was the ER-localized protein P24B1-C-YFP showed no interaction with RD20/CLO3-N-YFP. The individually YFP-tagged BiFC constructs of RD20/CLO3 and GPA1 protein fusions that were used with complementing YFP vectors without fusion partners as negative controls showed no interaction in the BiFC assay (Figure S2; Table S2). Taken together, this indicates that the YFP signals detected when GPA1 and RD20/CLO3 are present in vivo are due to the specific interaction between the two proteins. This was further corroborated by

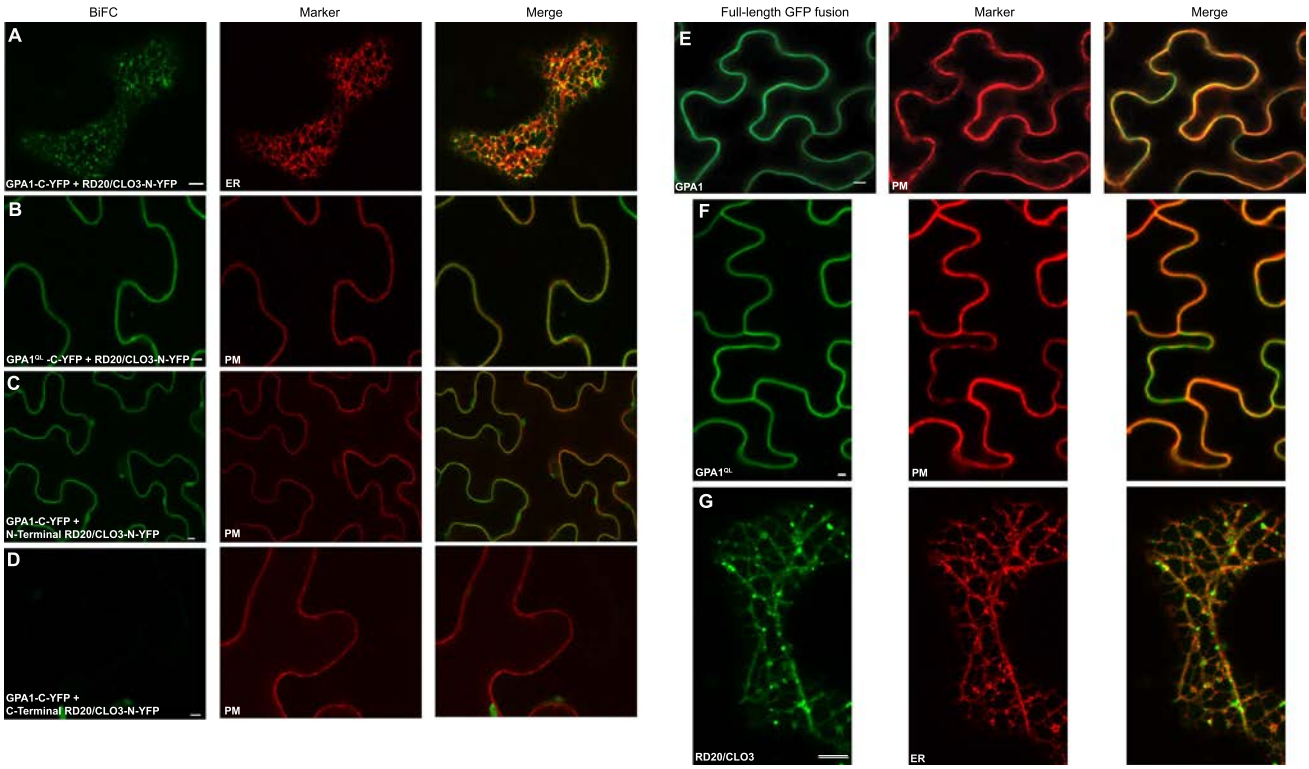

Fig. 1 BiFC interactions and GFP subcellular localizations of GPA1, GPA1^{QL} and RD20/CLO3 in tobacco epidermal leaf tissue. **A** GPA1-C-YFP and RD20/CLO3-N-YFP interaction co-localized with the ER marker AtWAK2-mCherry (ER-mCherry). **B** GPA1^{QL}-C-YFP and RD20/CLO3-N-YFP interaction co-localized with the PM marker AtPIP2A-mCherry (PM-mCherry). **C** GPA1-C-YFP and the N-terminal truncation of RD20/CLO3-N-YFP interaction co-localized with the PM-mCherry marker. **D** GPA1-C-YFP and the C-terminal truncation of RD20/CLO3-N-YFP interaction co-localized with the PM-mCherry marker. **E** GPA1-eGFP fusion co-localized with the PM-mCherry marker. **F** GPA1^{QL}-eGFP fusion co-localized with the PM-mCherry marker. **G** RD20/CLO3-eGFP fusion co-localized with ER-mCherry marker. Bar = 10 µm

the in vitro assay of on-column binding between GPA1-GST and (6xHis) RD20/CLO3 (Figure S4).

Yeast two-hybrid interaction of the N-terminal halves of RD20/CLO3 and RD20/CLO3 EF-hand mutants with GPA1 and GPA1^{QL}

Caleosins have an N-terminal domain with a single EF-hand calcium-binding motif, a membrane domain followed by a proline knot and a C-terminal domain. The truncated version of the protein containing the N-terminal domain lacking the membrane domain and proline knot of RD20/CLO3 (amino acid 1 to 90) was shown to interact with GPA1 by BiFC as well as yeast two-hybrid (Y2H) (Fig. 4A). The N-terminal truncation also interacts with GPA1^{QL} via a yeast two-hybrid (Fig. 4B). The N-terminal half was fused to the binding domain (BD) of the GAL4 transcription factor and shown to interact with GPA1 and GPA1^{QL} bound to the activating domain (AD) of GAL4. The protein–protein interaction between the RD20/CLO3 N-terminal and GPA1 displayed high affinity as was shown with the addition of 3-AT which was added to the media at levels from 1 to 30 mM and the cultures only showed reduced growth at 30 mM 3-AT (Fig. 4A). The N-terminal RD20/CLO3 and GPA1 interaction also showed a stronger colorimetric change after a β-galactosidase assay compared to the positive control of GPA1 AD and AGB1/AGG3(γ) BD truncation (residues 1–112) (Chakravorty et al. 2015), further suggesting a strong interaction between the two proteins (Figure S5). The interaction between RD20/CLO3 N-terminal and the GPA1^{QL} mutant displayed an even higher binding affinity withstanding up to 60 mM 3-AT, indicating a possible preference for GPA1 in an active GTP-bound state (Fig. 4B). The RD20/CLO3 C-terminal (amino acid 124 to 237) domain and the full-length protein did not show an interaction with GPA1 or GPA1^{QL} via Y2H (Fig. 4A, B). The EF-hand N-terminal mutants of RD20/CLO3^{D70A} and RD20/CLO3^{E81R} display a severe negative impact on the interaction between RD20/CLO3 and GPA1 or GPA1^{QL} indicating a calcium dependency (Figs. 5, S3). Both mutated forms, RD20/CLO3^{D70A} and RD20/CLO3^{E81R}

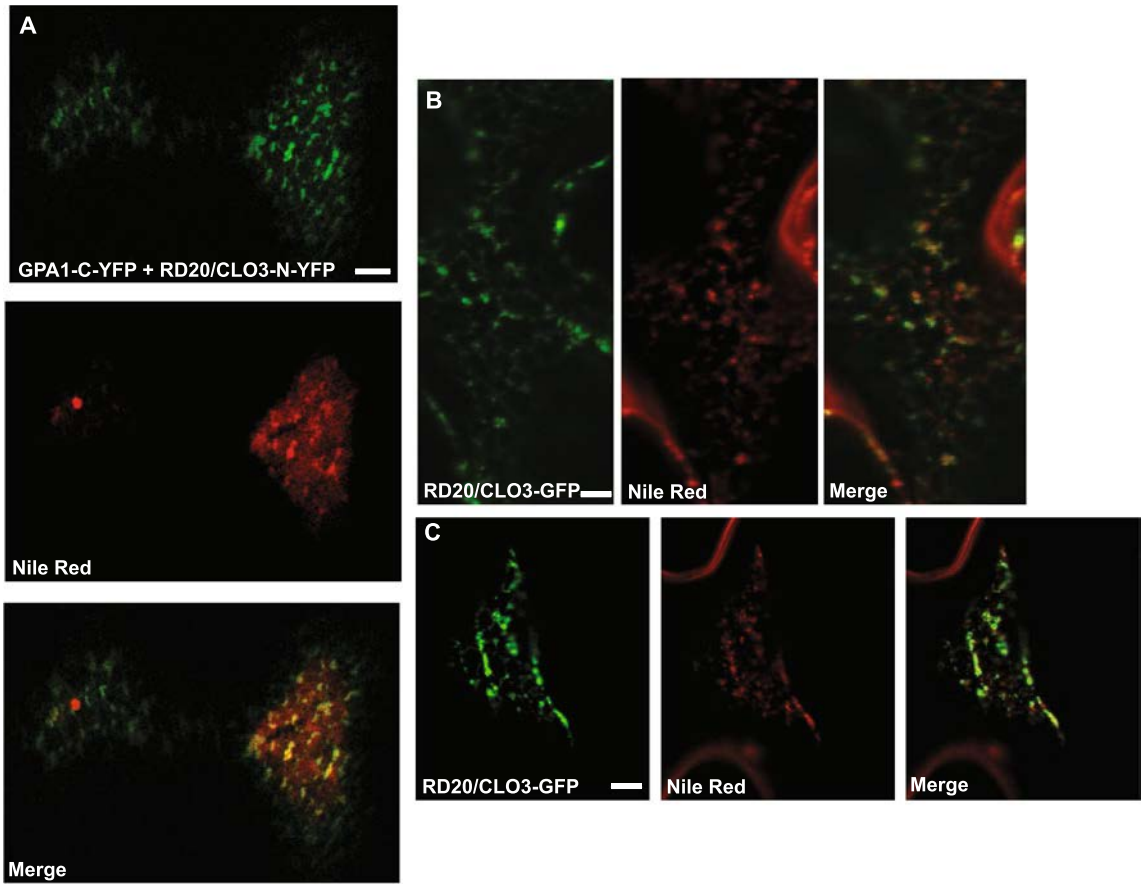

Fig. 2 Oil body localization of RD20/CLO3 eGFP fusion and the RD20/CLO3-N-YFP and GPA1-C-YFP interaction overlapped with the Nile Red lipid stain. **A** RD20-N-YFP interacting with GPA1-C-YFP. **B** and **C** Both panels are showing RD20/CLO3-eGFP fusions. Bar = 10 µm

showed that the disruption of calcium-binding abolished the interaction with GPA1, whereas the interaction with the non-mutant form of RD20/CLO3 showed a positive interaction between the caleosin and GPA1 in the presence of 3-AT up to the highest levels tested (Figs. 3, 5). The interaction between RD20/CLO3^{D70A} and RD20/CLO3^{E81R} with GPA1^{QL} growth is barely detectable and is unable to withstand 3-AT at the lowest level tested (Figs. 5, S3). Overall, the interaction between RD20/CLO3 and GPA1 is calcium-dependent whereas the interaction between mutated forms of RD20/CLO3 with a disrupted EF calcium-binding domain and GPA1^{QL} is markedly reduced though not completely abolished.

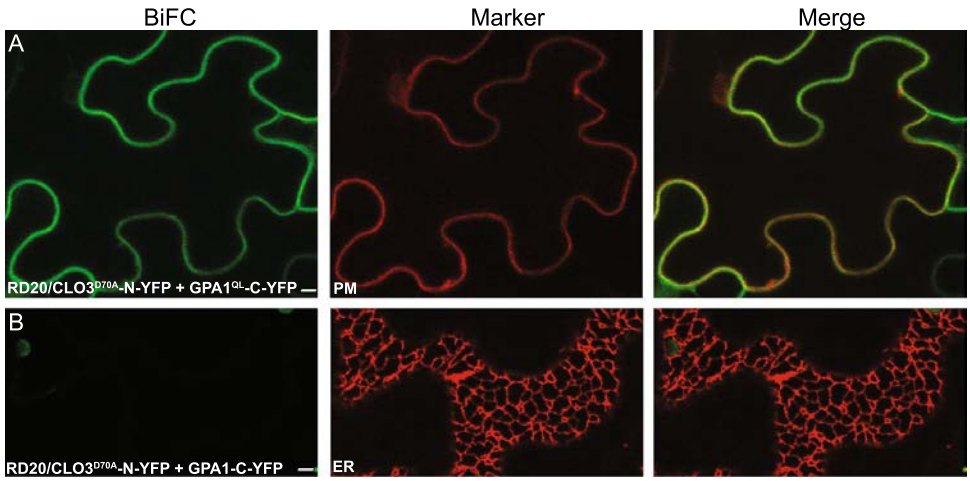

Fig. 3 BiFC interaction between RD20/CLO3^{D70A} and GPA1 or GPA1^{QL}. **A** Interaction between RD20/CLO3^{D70A}-N-YFP and GPA1^{QL}-C-YFP localized to the plasma membrane (PM marker = AtPIP2A-mCherry). **B** Lack of interaction with RD20/CLO3^{D70A}-N-YFP and GPA1-C-YFP, co-transformed with the ER-mCherry marker (AtWAK2-mCherry). Bar = 10 µm

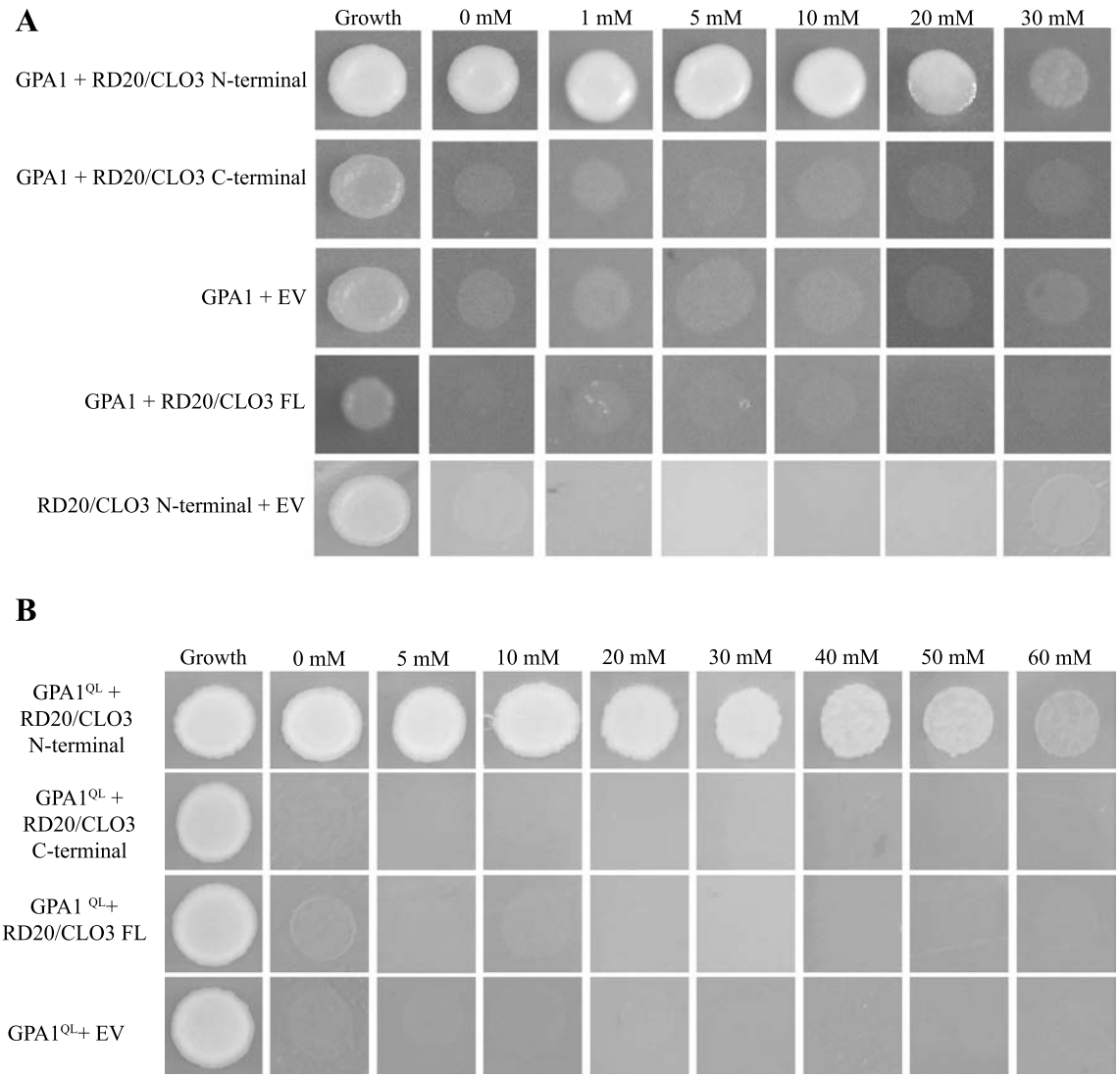

Fig. 4 Yeast two-hybrid assay testing the interaction between **A** GPA1-AD and the N-terminal half of RD20/CLO3-BD (amino acids 1 to 90). **B** GPA1^{QL} -AD and RD20/CLO3 N-terminal half-BD. Yeast growth (Growth) was confirmed on SD-Trp-Leu and the interactions were assayed on SD-Leu-Trp-His supplemented with 3-AT concentrations ranging from 0 to 60 mM. The lack of growth at elevated levels of 3-AT indicates weak interaction between the two proteins. FL = Full-length, EV = empty vector

GTPase assay of GPA1 and RD20/CLO3

Biochemical assays were carried out to characterize the GPA1 and RD20/CLO3 interaction and explore the potential of RD20/CLO3 as a GTPase accelerating protein (GAP). GPA1 and RD20/CLO3 were expressed in *E.coli* as GST and His_6 fusion proteins, respectively, and purified by affinity anion-exchange chromatography followed by a GTPase assay. GPA1 showed low GTPase activity as expected and as previously reported (Johnston et al. 2007), however the addition of RD20/CLO3 did not significantly affect this activity (Table S3 and S3A). These results indicate that RD20/CLO3 does not act as a GAP for GPA1.

RD20/CLO3 mutants respond to the dark with increased hypocotyl lengths

Hypocotyl elongation in dark-grown plants was compared between the *rd20/clo3* and *gpa1* single mutants, the *rd20/gpa1* double mutant, P35S:*RD20* overexpressor lines in the WS wild type (WT), *rd20/clo3* or *gpa1* mutant background to investigate hypocotyl growth rates. The dark-grown *rd20/clo3* had significantly longer hypocotyls than the *gpa1* single mutant or the WS wild-type plants (Fig. 6A). These extended hypocotyls appear to be a factor of elongated cells since the *rd20/clo3* mutant had significantly longer cells than both the WT and the *gpa1* single mutant (Fig. 4B). The double mutant had a significant reduction in hypocotyl

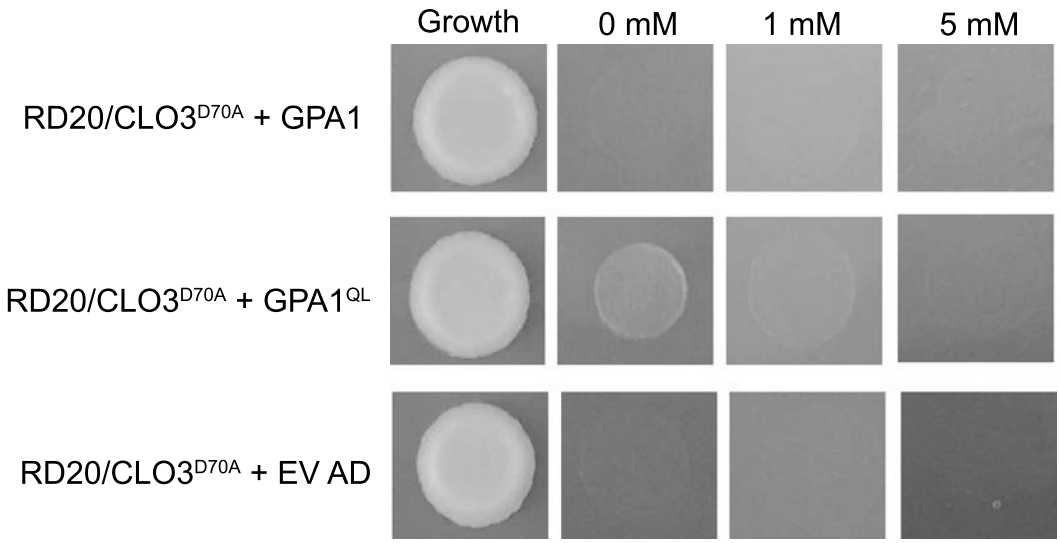

Fig. 5 Yeast two-hybrid assay testing the interaction between GPA1-AD or GPA1^{QL}-AD and the N-terminal half (amino acids 1 to 90) of the EF-hand mutant RD20/CLO3^{D70A}-BD. Yeast growth (Growth) was confirmed on SD-Trp-Leu and the interactions were assayed on SD-Leu-Trp-His supplemented with various 3-AT concentrations (0–5 mM). The lack of growth at elevated levels of 3-AT indicates weak interaction between the two proteins. FL = Full-length, EV = empty vector

length compared to the wild-type and had a hypocotyl length similar to the *gpa1* single mutant (Fig. 6). The reduced cell elongation and shortened hypocotyls seen in the double mutant suggest that *GPA1* is downstream of *RD20/CLO3* in the pathway leading to the increase in hypocotyl length triggered by darkness (Fig. 6A, B). When overexpressing *RD20/CLO3* in the *gpa1* mutant background the phenotype is that of the *gpa1* single mutant, further suggesting that *GPA1* is downstream of *RD20/CLO3.* When *RD20/CLO3* was overexpressed in the WT background, the hypocotyl lengths and the overall cell lengths were significantly decreased compared to both the wild type and the single *rd20/clo3* mutant again suggesting *RD20/CLO3* is a negative regulator of *GPA1* for this trait (Fig. 6A, B). The *rd20/clo3* phenotype was recovered in the complementation line (P35S:*RD20/rd20*) yielding hypocotyl lengths that are not significantly different from the wild type (Fig. 6). Both *RD20/CLO3* and *GPA1* show tissue localization to the hypocotyl area further supporting a mechanism of hypocotyl control by both genes (Fig. 6C–F). These phenotypes suggest that *RD20/CLO3* is upstream and can act as a negative regulator to *GPA1* and that both genes play a role in cell elongation in the hypocotyls in response to darkness.

RD20/CLO3 mutants have altered leaf development

The effect of the *rd20/clo3* mutation was seen to have an opposite phenotype compared to the observed effect of the *gpa1* mutation on leaf morphology. The leaves of the *rd20/clo3* mutants were significantly narrower than the wild type leaves; the mutant had a length-to-width (L:W) ratio of 2.3 while the ratio of the wild type plant leaves was 1.7 (Fig. 7A and B). Leaves of the *gpa1* mutants have a more rounded lamina shape, with an average L:W ratio of 1.3, which corroborates previously published data (Ullah et al. 2001 and Jones et al. 2003) (Fig. 7A and B). The *rd20*/*gpa1* double mutant has an L:W ratio identical to that of the *gpa1* single mutant, 1.3 (Fig. 7A and B), suggesting that *GPA1* is downstream of *RD20/CLO3* in the regulation of this trait. The *RD20/CLO3* overexpressor lines in all backgrounds (WS, *gpa1* or *rd20/clo3* mutant) have a L:W of 1.5–1.6, a ratio that is not significantly different from the wild type or the *gpa1* single mutant (Fig. 7A and B). This further supports the hypothesis that *RD20/CLO3* is a negative regulator of *GPA1*.

Discussion

RD20/CLO3 plays a role in cell growth

G-protein signaling has been shown to play a role in regulating cell growth during hypocotyl elongation in dark-grown seedlings and in cell division of the aerial tissues (Johnston et al. 2007; Ullah et al. 2001). When plants are subjected to light it allows them to begin de-etiolation which is part of photomorphogenic development, allowing for chloroplasts to develop. Plants grown in dark conditions will be etiolated causing the plants to have a long, thin and characteristically white hypocotyl (Ullah et al. 2001). The number of

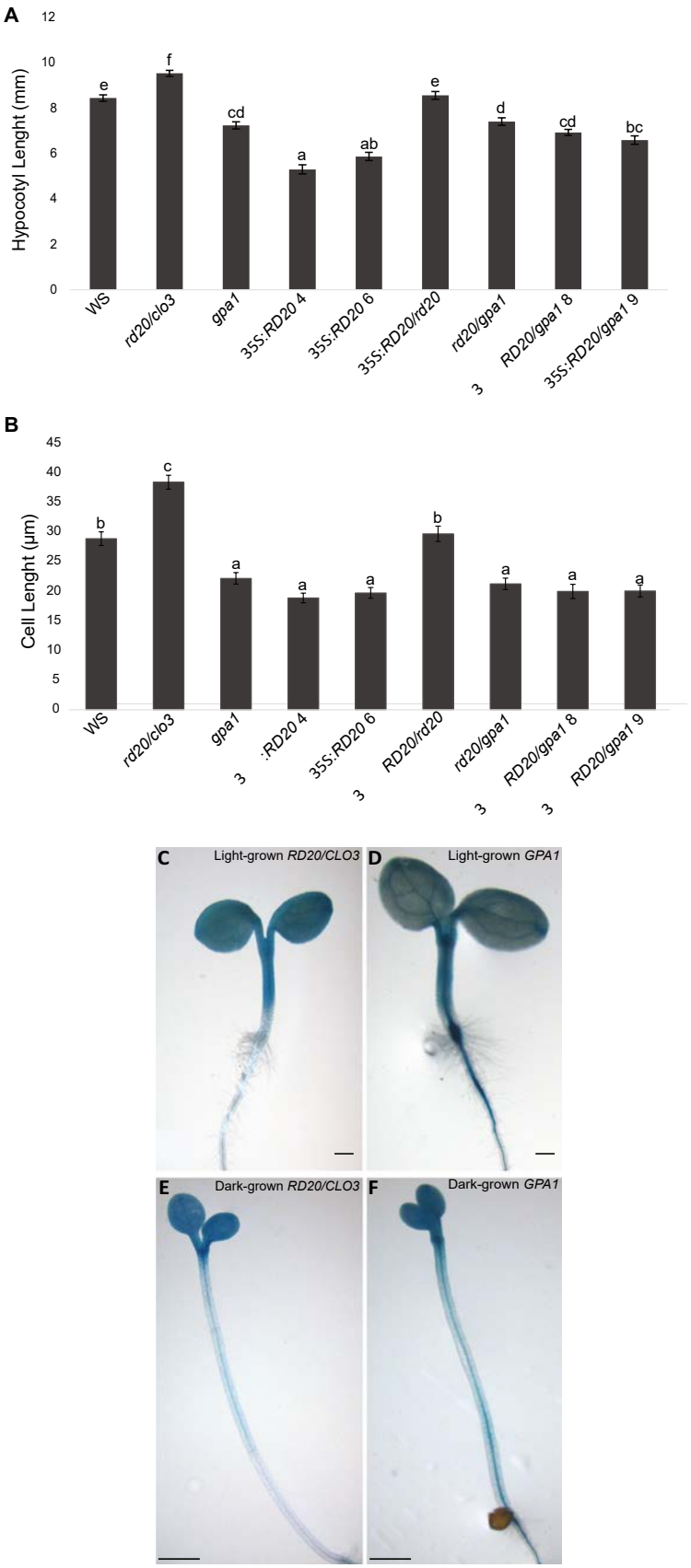

Fig. 6 Hypocotyl analysis of two-day dark grown seedlings in response to darkness of the following genotypes; WS, *rd20/clo3*, and *gpa1* single mutants, the *gpa1/rd20* double mutant and P35S:*RD20/CLO3* (in the WS, *gpa1*or *rd20/clo3* background). **A** Average hypocotyl lengths of dark-grown seedlings. **B** The average length of the cells within the hypocotyls. Staining of the **C** *RD20/CLO3* promoter::*GUS* fusion and **D** *GPA1* promoter::*GUS* fusion, showing expression in the upper hypocotyls region in light-grown conditions. Staining of the **E** *RD20/CLO3* promoter::*GUS* fusion and **F** *GPA1* promoter::*GUS* fusion showing expression throughout the hypocotyl in response to dark conditions. Scale Bar = 1 mm. Rankings determined by Tukey's post-hoc test ($p \leq 0.05$); bars which do not share a common letter are significantly different and indicate that genotypes have significantly different responses to dark growth conditions. Error bars are the SE of the mean

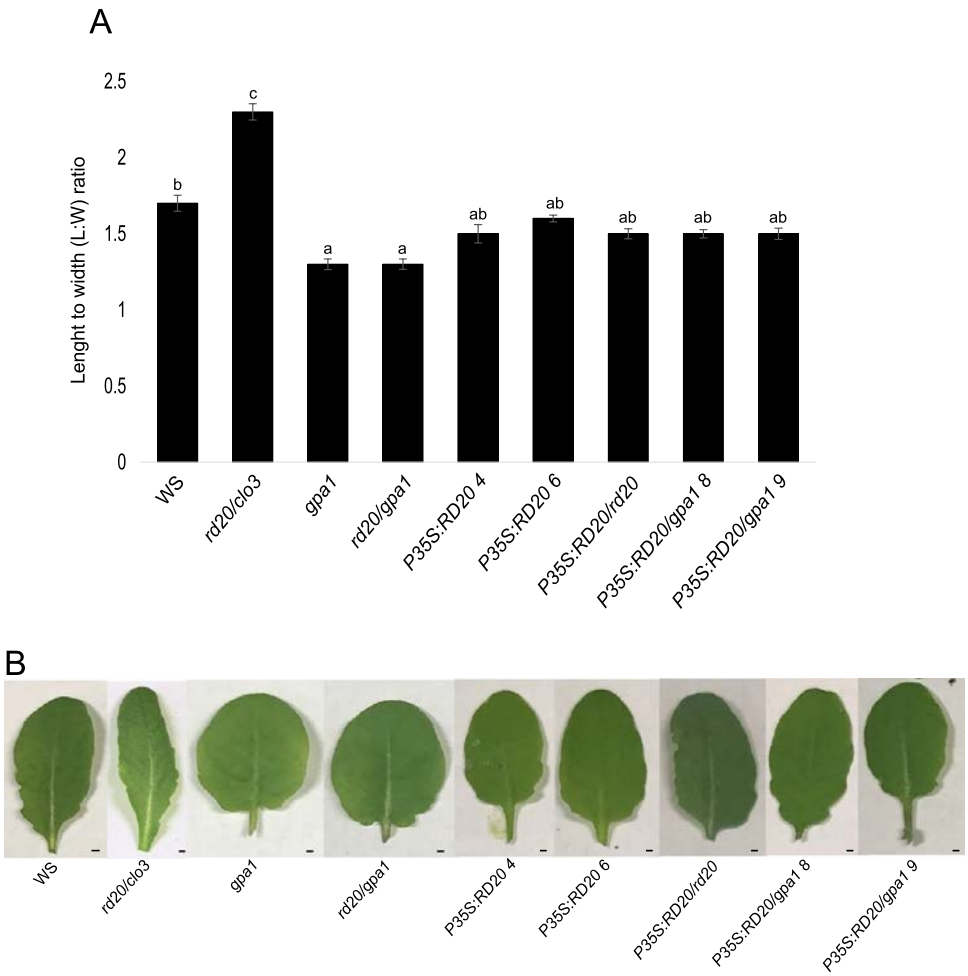

Fig. 7 Leaf morphology of the wild type (WS), *gpa1* and *rd20/clo3* single mutants, P35S:*RD20/CLO3* lines in the WS, *gpa1* or *rd20/clo3* background and the double *rd20/gpa1* mutant. **A** Leaf size represented as a length to width ratio (L:W). **B** Phenotypic differences in the leaf shape. Rankings determined by Tukey's post-hoc test ($p \leq 0.05$) and are denoted by different letters and demonstrate the significant differences between genotypes. Error bars are the SE of the mean. Scale bar = 1 mm

hypocotyl cells that a plant will have been determined during embryogenesis and the length of the hypocotyl is determined exclusively by cell elongation post-germination (Gendreau et al. 1997). The *gpa1* mutant has been previously reported to have shorter hypocotyls in response to darkness due to a decrease in the number of elongated cells, as a by-product of impaired cell division in the mutant (Ullah et al. 2001). It appears that the *agb1* mutant has a decrease in axial cell division with an increase in circumferential division leading to thicker hypocotyls, suggesting that both the *GPA1* and *AGB1* subunits play a role in regulating hypocotyl development in dark conditions (Ullah et al. 2003). Dark-grown single *rd20/clo3* and *gpa1* mutants showed opposite etiolation effects. The dark-grown *rd20/clo3* seedlings had a significant increase in hypocotyl length, as a result of increased cell elongation compared to wild type plants; the *gpa1* single mutant had a decrease in hypocotyl length relative to the wild type. This data suggests that *RD20/CLO3* is a negative regulator of hypocotyl elongation in darkness while *GPA1* appears to be a positive regulator of this phenotype. The constitutively active *GPA1* line, *GPA1*^{QL}, has an increased hypocotyl length due to an increase in cell elongation, the *rgs1* mutant phenocopies the *GPA1*^{QL} line when it comes to this hypocotyl phenotype (Chen et al. 2003). This phenotype suggests that GPA1 is GTP-bound and free from the trimer while causing the extended hypocotyl phenotype and it is possible that an active RD20/CLO3 bound to GPA1 diminishes this phenotype. This theory is supported by the overexpression of *RD20/CLO3* which leads to significantly reduced hypocotyl lengths, suggesting *RD20/CLO3* plays a role in etiolation of seedlings by decreasing hypocotyl cell elongation and may be doing so through its interaction with *GPA1*. This is further supported by the in vivo interaction of RD20/CLO3 with the GPA1^{QL} mutant. The *rd20/gpa1* double mutant had hypocotyl lengths which were significantly reduced and similar to the *gpa1* single mutant. When *RD20/CLO3* was overexpressed in a *gpa1* mutant background, the overexpression of *RD20/CLO3* had no effect, and the hypocotyl lengths are similar to *gpa1*. This suggests that *GPA1* is downstream of *RD20/CLO3* in controlling hypocotyl cell elongation in darkness and that *RD20/CLO3* is a negative regulator of *GPA1* in controlling hypocotyl elongation in dark grown plants. No marked differences were seen in hypocotyl girth in any of the *RD20/CLO3* transgenic lines,

implying that the effect on hypocotyls is a factor of its interaction with GPA1 and not through effects on *AGB1*. *RD20/CLO3* promoter::*GUS* and *GPA1* promoter::*GUS* analysis shows localization of both genes to the hypocotyl region, indicating that both *RD20/CLO3* and *GPA1* are expressed and present at the same time in the hypocotyls.

Similarly to the effect on hypocotyl cells, *GPA1* affects cell expansion and division during leaf morphogenesis (Ullah et al. 2001). There are many different leaf morphologies in Arabidopsis including variations in leaf flatness, leaf serration and leaf width or length and all are controlled by gene networks. Two genes that play a role in leaf width and length are AGUSTIFOLIA3 (AN3) and ROTUNDIFOLIA3 (ROT3), respectively (Tsuge et al. 1996). The mode of action for each of these genes involves cell elongation in either the vertical or horizontal plane leading to extensions in width or length (Tsuge et al. 1996). It is quite possible that the expression of these genes may be affected by *GPA1* since mutations in *rot3* give rise to round leaf shapes similar to the *gpa1* mutant suggesting a possibility that *ROT3* levels are decreased if *gpa1* is mutated (Ullah et al. 2001 and Kim et al. 1998). The mutation in *an3* causes a narrow leaf similar to the leaf shape of the *rd20/clo3* mutant leading to the possibility that *RD20/CLO3* binding to *GPA1* affects *AN3* expression (Tsuge et al. 1996). The overexpression of *RD20/CLO3* regardless of the background (WS, *gpa1* or *rd20/clo3* mutant) has a leaf shape that was an intermediate between WT and the *gpa1* single mutant and not statistically different from either suggesting a minor recovery of epidermal cell development. This could be due in part to the fact that caleosins constitute a multi-gene family in which other members of the family also affect this trait and/or due to ectopic overexpression. A second hypothesis is that since the *agb1* mutant shares a similar phenotype to the *gpa1* mutant, having a round leaf shape, this implies that both the GPA1 and AGB1 subunits are able to cause a narrower leaf shape and the presence of a functional AGB1 subunit might override the overexpression of *RD20/CLO3*. The *rd20/gpa1* double mutant has a leaf shape identical to the *gpa1* single mutant with leaves that have a significantly round appearance, this data is congruent with placing *GPA1* downstream of *RD20/CLO3* in controlling cell division.

In addition to its role in cell division, *GPA1* plays a role in hypocotyl stage development in response to glucose and brassinosteroid signaling. GPA1 is a known interactor of the brassinosteroid receptors BRI1 and BAK1 and plays a role in sugar-responsive growth (Peng et al. 2018). Moreover, the G proteins and the BR receptors appear to function in the same pathway controlling the developmental stages of the hypocotyls in dark-grown Arabidopsis seedlings (Peng et al. 2018). The presence of glucose allows for the phosphorylation of BRI1 and BAK1 which in turn causes phosphorylation of the AGB1/AGG dimer which ultimately leads to the dissociation of the heterotrimer, causing sugar-responsive growth and development (Peng et al. 2018). The potential role of RD20/CLO3 in the brassinosteroid signaling pathway would be an interesting subject for further investigation.

Protein localization and protein–protein interaction suggests that RD20/CLO3 affects both nucleotide-bound states of GPA1 and that calcium-binding affects the interaction

The classical model of heterotrimeric G-protein signaling suggests several steps at which protein–protein interaction may be important for the regulation of Gα; these include the initial trafficking and complex formation at the PM, release from the heterotrimeric complex, interaction with modulating proteins affecting GTPase and GDP/GTP exchange activity, interaction with downstream signaling proteins such as phospholipases C and D, and reconstitution of the G protein complex at the PM. The ER was reported to be the site for the initial formation of the heterotrimeric complex as well as for Gα palmitoylation before transport to the PM (Marrari et al. 2007). The ER is also the site of TAG formation and has been a key organelle in the subsequent biogenesis of oil/lipid bodies (Chapman et al. 2012). In the work reported here, the GFP-tagged GPA1 and GPA1^{QL} was localized to the PM, while GFP-tagged RD20/CLO3 was localized to the ER and to LDs found in or around the ER which is a characteristic of the caleosin gene family. BiFC data showed that the interaction between the two proteins takes place in or on the ER and within lipophilic droplets around the ER. This raises the possibility that this interaction occurs after the release of GPA1 from the PM. To further test this interaction and to confirm its ER localization a second BiFC vector set was used which is believed to significantly reduce the non-specific assembly of proteins (Gookin and Assmann 2014). However, this vector system gave the same results; RD20/CLO3 and GPA1 interact and this interaction was localized to the ER, corroborating the interaction described above (data not shown). An in vitro on column binding assay was also performed which verified the interaction seen by the BiFC assay (Figure S4).

In the classic models of heterotrimeric G-protein signaling, the release of Gα from the complex stimulates its activation and is associated with an exchange of GDP for GTP, and its subsequent inactivation is stimulated by its inherent GTPase activity and its association with GAP proteins; the hydrolysis of GTP into GDP precedes its re-association with Gβγ (Jones 2002). The GPA1^{QL} mutant lacks GTPase activity causing the α-subunit to be abundant in the GTP-bound state. It appears that RD20/CLO3 also interacts with the GPA1^{QL} mutant suggesting a lack of nucleotide dependency. Furthermore, this interaction is localized to the PM, a

marked difference from the ER localization of the interaction with the WT form of GPA1, implying the ER interaction is occurring with a GPA1 GDP-bound subunit. The PM localization with the GTP-bound GPA1 suggests that RD20/CLO3 is redirected from the ER to bind to an active GPA1 subunit. This interaction is not localized to LDs or the ER when GPA1 is in its GTP-bound state, suggesting that RD20/CLO3 and GPA1 have some function in LDs when GPA1 is GDP-bound. These interactions suggest RD20/CLO3 binding to GPA1 may have many downstream effects dependent on the nucleotide state of GPA1, ultimately leading to differences in cellular localization. It is also evident through the study of the EF-hand mutations in RD20/CLO3 (D70A and E81R) that the interaction with GPA1 is calcium-dependent, and the binding interaction is enhanced both by the GTP binding to GPA1 and calcium-binding to RD20/CLO3 as seen in both the Y2H and BiFC assays. The dependence on calcium is significant since stress has been shown to induce calcium fluxes within the cell (Tuteja and Mahajan 2007) and because RD20/CLO3 is induced by several biotic and abiotic stresses, it is plausible that the interaction between RD20/CLO3 and GPA1 occurs as a result of stress induction. There is a basal level of calcium within the cell and RD20/CLO3 is a calcium-binding protein (Takahashi et al. 2000), therefore its interaction with GPA1 may occur in the presence or absence of a stress signal. As seen with the $GPA1^{QL}$ and RD20/CLO3 interaction, calcium enhances the binding between these proteins. This was also observed with the proteins encoded by orthologous genes in *Triticum aestivum,* G-α (GA3) and Clo3 where high calcium levels were shown to enhance the interaction (Khalil et al. 2011).

The N-terminal portion of RD20/CLO3 is sufficient for the interaction with GPA1 and it was shown to interact in both BiFC and Y2H assays. However, the N-terminal construct was the only version of RD20/CLO3 that was able to interact with GPA1 in the Y2H assay. Membrane-associated proteins usually do not show interaction in Y2H assays if the membrane-associated domains are left intact. Hence the membrane domain in the full-length RD20/CLO3 is likely the cause for a lack of interaction between this protein and GPA1. The N-terminal portion of RD20/CLO3 also has a very strong interaction with GPA1 given that it can withstand 30 mM 3-AT in the Y2H assay, further suggesting the N-terminal is responsible for the interaction between the two proteins. The RD20/CLO3 N-terminal also interacts with $GPA1^{QL}$ via Y2H, this interaction is able to withstand a higher dose of 3-AT (60 mM) a clear distinction from the RD20/CLO3 and WT GPA1 interaction. The loss of the RD20/CLO3 C-terminal end caused the RD20/CLO3 and GPA1 interaction to occur at the PM, rather than at the ER. Analysis of the RD20/CLO3 protein sequence by Phobius Software did not detect any ER retention signal in the C-terminal portion of the protein. It is highly plausible that the deletion of the membrane domain and the proline knot in RD20/CLO3 has caused RD20/CLO3 to no longer associate with LDs since this localization is highly dependent on the presence of a proline knot which causes targeting to LDs (Chapman et al. 2012). The deletion of the proline knot in mutated versions of oleosins led to localization to the PM and loss of association with LDs whereas the full-length versions of the protein localize to the ER and LDs (Frandsen et al. 2001; Abell et al. 1997). Therefore, this N-terminal truncation would be a form of RD20/CLO3 which is free from oil bodies and able to interact with GPA1 at the PM. This further shows that RD20/CLO3 is not only an LD-localized caleosin but that it can have a function outside of LDs and play an role in the downstream effects of the active GPA1. Overall, RD20/CLO3 appears to play a role in the regulation of GPA1 and this regulation appears to be based on the nucleotide-bound state of GPA1 and the presence of calcium.

Chapter 3**: The caleosin CLO7 and its role in the heterotrimeric G-protein signalling network** was first published at the Journal of Plant Physiology which can be accessed using the following DOI: https://doi.org/10.1016/j.jplph.2022.153841

Brunetti, S. C., Arseneault, M., and Gulick, P. J. (2022). The caleosin CLO7 and its role in the heterotrimeric G-protein signalling network. *Journal of plant physiology*, *279*, 153841. Advance online publication. https://doi.org/10.1016/j.jplph.2022.153841

Journal of Plant Physiology 279 (2022) 153841

Contents lists available at ScienceDirect

Journal of Plant Physiology

journal homepage: www.elsevier.com/locate/jplph

The caleosin CLO7 and its role in the heterotrimeric G-protein signalling network☆

Sabrina C. Brunetti, Michelle K.M. Arseneault, Patrick J. Gulick *

Biology Department, Concordia University, 7141 Sherbrooke W. Montreal (Quebec) H4B 1R6, Canada

ARTICLE INFO

Keywords:
Interaction with GPA1
Caleosin
CLO7
Germination
Embryo lethal

ABSTRACT

The investigation of the caleosin *CLO7* in relation to heterotrimeric G-protein signalling in Arabidopsis showed that the gene plays a role in seed germination and embryo viability. The caleosin *CLO7* belongs to a multi-gene family of calcium-binding proteins which are characterized by single EF-hand motifs. Other members of the caleosin gene family have been shown to affect transpiration and seed germination as well as play a role in both abiotic and biotic stress responses. The proteins are associated with lipid droplets/oil bodies and some members of the gene family have been shown to have peroxygenase activity. Members of the gene family have also been shown to interact with the α subunit of the heterotrimeric G protein complex. In this study, we further expand on the diversity of physiological responses in which members of this gene family play regulatory roles. Utilizing BiFC and Y2H protein-protein interaction assays, CLO7 is identified as an interactor of the heterotrimeric G protein α subunit, GPA1. The full-length CLO7 is shown to interact with both the wild-type GPA1 and its constitutively active form, $GPA1^{QL}$, at the plasma membrane. Point mutations to critical amino acids for calcium binding in the EF-hand of CLO7 indicate that the interaction with GPA1 is calcium-dependent and that the interaction with $GPA1^{QL}$ is enhanced by calcium. Protein-protein interaction assays also show that CLO7 interacts with Pirin1, a member of the cupin gene superfamily and a known downstream effector of GPA1, and this interaction is calcium-dependent. The N-terminal portion of CLO7 is responsible for these interactions. GFP-tagged CLO7 protein localizes to the endoplasmic reticulum (ER) and to lipid bodies. Characterization of the *clo7* mutant line has shown that *CLO7* is implicated in the abscisic acid (ABA) and mannitol-mediated inhibition of seed germination, with the *clo7* mutant displaying higher germination rates in response to osmotic stress and ABA hormone treatment. These results provide insight into the role of *CLO7* in seed germination in response to abiotic stress as well as its interaction with GPA1 and Pirin1. *CLO7* also plays a role in embryo viability with the *clo7 gpa1* double mutant displaying embryo lethality, and therefore the double mutant cannot be recovered.

1. Introduction

To cope with the persistent exposure to a wide variety of abiotic and environmental stresses, plants have evolved intricate and complex stress response systems; one of these responses involves the signalling pathway mediated by the heterotrimeric G protein complex. Mutations in the Gα (*GPA1*) and Gβ (*AGB1*) subunits of the complex in *Arabidopsis thaliana* have been shown to have altered stress response phenotypes, although their larger role within the stress response framework has yet to be fully elucidated. The G proteins have been implicated in response pathways for auxin-controlled lateral root development (Ullah et al., 2003; Jones et al., 2003), ABA-stimulated stomatal closure (Wang et al., 2001), leaf shape (Ullah et al., 2001), and both gibberellic acid and ABA responses during seed germination (Ullah et al., 2002). In the animal model of G-protein signalling, a ligand binds the G-protein coupled receptor (GPCR), causing Gα to exchange GDP for GTP, allowing Gα to separate from the Gβγ dimer, and thus activating downstream signals. The subunit is inactivated when GTP is hydrolyzed, usually mediated by GTPase activating proteins (GAPs), which are known as regulators of G-protein signalling (RGS). The GDP/GTP exchange for activation is the rate-limiting step in the cycle of heterotrimeric G-protein signalling, and a GPCR is necessary for nucleotide exchange. Contrary to the animal

☆ The author responsible for distribution of materials integral to the findings presented in this article in accordance with the policy described in the Instructions for Authors is Patrick J. Gulick (patrick.gulick@concordia.ca)

* Corresponding author. Department of Biology, Concordia University, 7141 Sherbrooke W. Montreal (Quebec) H4B 1R6, Canada.
E-mail address: patrick.gulick@concordia.ca (P.J. Gulick).

https://doi.org/10.1016/j.jplph.2022.153841
Received 18 June 2022; Received in revised form 7 October 2022; Accepted 8 October 2022
Available online 14 October 2022

model, the Gα subunit in *Arabidopsis thaliana*, GPA1, has a high intrinsic nucleotide exchange rate, more than 100-fold greater than that of the animal Gαi1 (Jones et al., 2012). However, GPA1 has a slow intrinsic hydrolysis rate [kcat = 0.05 min−1] (Urano and Jones, 2014), making GTP hydrolysis a rate-limiting step in the regulation of GPA1 in the plant model. Since hydrolysis is the rate-limiting step, GAPs are thought to play a critical role in the deactivation of GPA1; to date there has only been one GAP discovered in Arabidopsis, known as Regulator of G-protein Signalling 1 (RGS1). The GTP-bound GPA1, disassociated from the heterotrimer, has been shown to activate and/or interact with some potential downstream effectors (Klopffleisch et al., 2011), such as Phospholipase D alpha 1 (PLDα1) (Zhao and Wang, 2013), Pirin1 (PRN1) (Lapik and Kaufman, 2003), Thylakoid Formation 1 (THF1) (Huang et al., 2006), and Response to Dehydration/Desiccation 20/Caleosin 3 (RD20/CLO3) (Brunetti et al., 2021). In Arabidopsis, there is one Gα subunit (GPA1), one Gβ subunit (AGB1), and three Gγ subunits (AGG1, AGG2 and AGG3) (Wang and Botella, 2022). There are also three genes encoding extra-large G proteins, XLG1, XLG2, and XLG3 (Chakravorty et al., 2015). XLG3 has multiple regions with similar protein structure to GPA1 and has been shown to compete for binding to the Gβγ dimer (Chakravorty et al., 2015).

Mutations in *GPA1* have been linked to a plethora of phenotypes in Arabidopsis, including hypersensitivity to abscisic acid (ABA) and sugar inhibition of germination (Lapik and Kaufman, 2003; Ullah et al., 2002), shorter hypocotyls in response to darkness (Chen et al., 2004), decreased lateral root primordia production, rounder leaves, and insensitivity to ABA inhibition of stomatal opening (Ullah et al., 2001), as well as changes in root growth and transpiration efficiency (Nilson and Assmann, 2010; Chen et al., 2006a). *GPA1* also plays a role in seed germination in response to ABA; the *gpa1* mutant is hypersensitive to the ABA inhibition of germination (Perfus-Barbeoch et al., 2004). The *GPA1* Q222L (*GPA1*^{QL}) mutant, which inactivates the inherent GTPase activity of GPA1 and leads to a constitutive GTP-bound state, complements the ABA hypersensitivity in the *gpa1* mutant during germination (Ullah et al., 2003; Maruta et al., 2019). Mutations in the Gβ subunit, *agb1,* decrease sensitivity to gibberellic acid (GA) and the brassinosteroid (BR) stimulation of germination, suggesting that the different heterotrimeric G protein subunits play different roles in seed germination in response to plant hormones (Perfus-Barbeoch et al., 2004). Pirin1, a cupin domain protein, has been shown to physically interact with GPA1 and to also be involved in seed germination (Lapik and Kaufman., 2003). The *pirin1* mutant phenocopies the *gpa1* mutant in that it shows hypersensitivity to ABA in the inhibition of seed germination and is believed to act downstream of *GPA1* in the seed germination pathway (Lapik and Kaufman., 2003). *Pirin1* is believed to have a positive effect on germination by allowing germination pathways to be activated or to overcome the inhibition by ABA (Lapik and Kaufman, 2003; Perfus-Barbeoch et al., 2004). The Gα homolog in rice, *RGA1*, affects seed germination via the GA pathway that regulates a Ca^{2+}-ATPase and α-amylase, which are crucial for seed germination (Ueguchi-Tanaka et al., 2000). It has also been suggested that mutations in two of the Gγ subunits, *AGG1* and *AGG2*, affect root architecture, early bolting, heat stress induction of flowering, and cause hypersensitivity to D-mannitol and auxin-mediated induction of lateral roots (Thung et al., 2013; Trusov et al., 2007). Since there are multiple phenotypes observed by mutations in different Gγ subunits; it is thought that the Gγ subunits impart functional selectivity to the Gβγ dimer (Thung et al., 2013).

Members of the caleosin gene family have been shown to interact with the Gα subunit in Arabidopsis and *Triticum aestivum* (Khalil et al., 2011; Brunetti et al., 2021). Caleosins are a family of calcium-binding proteins that have a single conserved calcium-binding EF-hand domain. They were initially identified as proteins associated with oil bodies in seed tissue, but subsequently have been shown to be expressed in a wide range of tissues (Partridge and Murphy, 2009; Aubert et al., 2011; Kim et al., 2011; Brunetti et al., 2021). There are seven caleosin gene family members in Arabidopsis and three of these have been characterized; *Responsive to Dehydration/Dessication 20/Caleosin 3* (*RD20/CLO3*), *Caleosin 1* (*CLO1*), and *Caleosin 4* (*CLO4*). RD20/CLO3 has been reported to interact with GPA1 and has been shown to be a negative regulator of *GPA1* in controlling leaf morphology and hypocotyl elongation in the dark (Brunetti et al., 2021). *RD20/CLO3* has also been shown to be induced by salt stress, drought, and abscisic acid (ABA) (Takahashi et al., 2000), is capable of regulating transpiration and plays a role in drought tolerance (Aubert et al., 2010), and influences the time to flowering under short day conditions (Blée et al., 2014). The *rd20/clo3* mutant is more sensitive to inhibition of germination in the presence of ABA (Aubert et al., 2011). More recently, *RD20/CLO3* has been shown to have peroxygenase activity, capable of reducing endogenous fatty acid hydroperoxides into hydroxyl-derivatives of fatty acids (FAOH), which in turn aid in ameliorating oxidative stress (Hanano et al., 2015). Another member of the gene family, *CLO4,* is down-regulated by ABA and NaCl treatments. The *clo4* mutant is more resistant to drought stress through the regulation of stomatal aperture and is hypersensitive to ABA inhibition of germination (Kim et al., 2011). A third member of the gene family, *CLO1,* was detected outside of seed oil bodies in ER cellular fractions and in plant tissues (Naested et al., 2000). The caleosins also play a role in the structure and function of lipid droplets, vesicles containing triacylglycerols (TAG) that act as energy reserves which are mobilized in processes such as germination (Chapman et al., 2012). The members of the caleosin gene family share similarities in structure; an N- and C-terminal domain localized outside of the lipid droplet, and a central region including a membrane-spanning segment and a proline knot, which is localized within the TAG matrix (Frandsen et al., 2001). The caleosin *CLO7* (AT1G23240.1) has not been studied in depth, however its expression has been detected within the pollen coat, and this expression profile sets *CLO7* apart from the other caleosins studied (Partridge and Murphy, 2009). The aim of this study is to investigate the role of the caleosin *CLO7* in plant developmental processes including seed germination and embryo viability. The study also characterizes the interaction between CLO7 and GPA1, since GPA1 has been found to affect a number of developmental events and physiological responses to growth regulators. We hypothesize that the diverse activity of GPA1 is modulated by interactions with different regulatory proteins. Therefore, the investigation of the caleosin gene family members as interactors and potential regulators of GPA1 can provide insight into its diverse role in plant development. Previous work had reported Pirin1 to interact with GPA1 and to affect seed germination (Lapik and Kaufman., 2003). In this work we further investigated the role of CLO7 in the G-protein interaction network and found the novel interaction between CLO7 and Pirin1, suggesting CLO7 may play role in a higher order complex that modulates GPA1. The overall purpose of this research is to explore how *CLO7*, *GPA1,* and *Pirin1* may interrelate with one another, and assess the role these genes play in seed germination in response to abiotic stress conditions.

2. Material and methods

2.1. Plant growth conditions

The Arabidopsis and *Nicotiana benthamiana* plants assayed in this study were grown in a soil mixture comprised of black earth, peat moss and vermiculite in a 2:1:1 ratio, respectively. The soil was then baked at 130 °C for 90 min prior to use. Arabidopsis seed were sown and stratified at 4 °C for 3 days. Pots were placed in a growth chamber at 22 °C with 90–100 μmol $m^{-2}{\cdot}s^{-1}$ of artificial light on a long day cycle (16 h light: 8 h dark). *Nicotiana benthamiana* plants were grown in a greenhouse at 22 °C with natural light supplemented with 45–51 μmol $m^{-2}{\cdot}s^{-1}$ artificial light to maintain a long day light cycle (16 h light: 8 h dark). For the Arabidopsis germination assay, the seed were plated on ½ Murashige and Skoog (MS) media plates. All seed were sterilized by vortexing in 70% ethanol and then placed in a sterilization solution (4% sodium

hypochlorite and 1% Triton X-100) for 5 min and washed 5 times with sterile distilled water. The ½ MS media used in this study contains 0.5X MS basal salts, 0.05% MES hydrate, 1% (w/v) sucrose and 0.4% Gelzan^{Tm} CM agar set to a pH of 5.7 using KOH.

2.2. Generation of vectors and transgenic Arabidopsis lines

The expression vectors used in this work were constructed using Gateway® cloning technology (Invitrogen). Sequences were cloned into either the pDonor-207 or pDonor-201 entry vectors using the Gateway® BP Clonase II Enzyme and transformed into the TOP10 *E. coli* strain. Gateway® LR reactions were then used to transfer the inserts from entry clones to the expression vectors. The *CLO7* EF-hand mutant forms, *CLO7*^{D37A} and *CLO7*^{E48A}, were created by assembly PCR using the primer set in Supplemental Table 1. The full-length, N-terminal truncation (amino acids 1 to 76) and C-terminal truncation (amino acids 233 to 633) of *CLO7* as well as the full-length *CLO7*^{D37A} and *CLO7*^{E48A} were cloned into the bimolecular fluorescence complementation (BiFC) vector pBatTL-B-sYFP-N. The full-length *Pirin1* was cloned into the BiFC vectors, pBatTL-B-sYFP-N and pBatTL-cYFP, and the full-length *GPA1* and *GPA1*^{QL} were cloned into pBatTL-cYFP for BiFC analysis (Uhrig et al., 2007). For localizations using fusions to the full-length GFP, both *CLO7* and *GPA1* were cloned into pK7WGF2 (Karimi et al., 2002). The *CLO7* coding region was also cloned into the pFAST G02 and pFAST G03 expression vectors for over-expression in plants with the 35S promoter and RNAi constructs, respectively (Shimada et al., 2010). The promoter:*GUS* reporter construct for *CLO7* was made by PCR amplifying a 1184 nt DNA fragment that extends from the gene's second exon to 777 nt upstream of the translational start site of *CLO7* and cloned into the pFAST G04 vector (Shimada et al., 2010). For yeast two-hybrid analysis the full-length coding region, N-terminal domain (amino acids 1 to 67) and C-terminal domain (amino acids 273 to 633) of *CLO7*, the N-terminal domain of *CLO7*^{D37A} and *CLO7*^{E48A}, the full-length and C-terminal domain (the last 170 amino acids) of *Pirin1*, as well as the full-length *GPA1* and *GPA1*^{QL} were cloned into the pGADT7-GW and pGBKT7-GW vectors (Lu et al., 2010). All the constructs were verified by PCR, and entry clones were verified by sequencing (Supplemental Table 1).

Transgenic Arabidopsis lines with the promoter*CLO7*:GUS, 35:*CLO7* and *CLO7*-RNAi constructs were developed using the floral dip method by Clough and Bent (1998) in the WT Colombia (Col), *clo7* and *gpa1* mutant background plants. Transgenic plants transformed with the pFAST vectors can be detected by green fluorescence in the seed coat (Shimada et al., 2010). Transgenic T1 and subsequent homozygous lines were screened using a Zeiss Axioplan Fluorescence Microscope with the GFP Filter Cube #1031346. Two independent homozygous lines for each transgene were selected and used in this study.

2.3. Semi-quantitative reverse transcription-PCR (RT-PCR)

The following transgenic lines were assayed using semi-quantitative RT-PCR for *CLO7* expression: *CLO7*-RNAi in Col, *CLO7*-RNAi *gpa1*, 35S:*CLO7*, 35S:*CLO7 gpa1* and the 35S:*CLO7 clo7*. RNA was extracted from leaf tissue using the RNeasy Plant Mini Kit (Qiagen) and 0.6–1 μg of total RNA was converted to cDNA using the protocol described by Brunetti et al. (2021). The expression levels of each transgenic line can be found in Supplemental Table 2.

2.4. Bimolecular fluorescence complementation (BiFC) and GFP localizations

Protein-protein interactions were assayed by BiFC in *Nicotiana benthamiana* leaves. The N-terminal and C-Terminal YFP constructs harboring *CLO7*, *CLO7*^{D37A}, *CLO7*^{E48A}, *Pirin1*, *GPA1*, and *GPA1*^{QL} were transformed into the *Agrobacterium tumefaciens* strain AGL1 via electroporation and the cultures were grown and infiltrated into leaves of *Nicotiana benthamiana* as previously described by Kapila et al. (1997), and as modified by Brunetti et al. (2021). The plants were monitored and imaged 24–56 h post-infiltration. Images were taken with the Olympus Fluoview FV10i laser scanning microscope (Olympus, USA) fitted with a 60x/1.35 oil lens (pixel size 0.27 μm). A 473 nm laser was used to observe the eGFP fused proteins (eGFP filter Ex 489 nm/Em 510 nm) and N/C-YFP fused proteins (YFP filter Ex 480 nm/Em 527 nm). The markers, a signal peptide of the cell wall-associated kinase 2 fused to mCherry (At-WAK2-mCherry), and which targets the proteins to the ER, and the plasma membrane aquaporin fused to mCherry (At-PIP2A-mCherry), were imaged with the 559 nm laser (red narrow filter Ex 559 nm/Em 570–620 nm). The 0.5 μm–1.0 μm spacing z-stacks were converted to maximum z-projections using ImageJ (https://imagej.nih.gov/ij/). The CLO7 protein was verified to have no ER retention signal using Phobius Software (https://phobius.sbc.su.se/).

2.5. Yeast two-hybrid

Protein-protein interaction was detected by fusing GPA1 and GPA1^{QL} to the AD, activating domain vector, pGADT7 (pGADT7-*GPA1* and pGADT7-*GPA1*^{QL} fusions), and the full-length and truncated versions of CLO7 (N-terminal domain, amino acids 1 to 67 and C-terminal domain, amino acids 273 to 633) as well as the N-terminal domain EF-hand mutants *CLO7*^{D37A} and *CLO7*^{E48A} were cloned into the DNA-binding domain, BD vector, pGBKT7 (pGBKT7-*CLO7*). The full-length and C-terminal domain (the last 170 amino acids) of *Pirin1* were cloned into the BD vector pGBKT7 and the AD vector pGADT7 (pGBKT7-*Pirin1* and pGADT7-*Pirin1*, respectively). Constructs were transformed into the yeast strain AH109 (MATa, trp1-901, leu2-3, 112, ura3-52, his3-200, gal4Δ, gal80Δ, LYS2::GAL1UAS-GAL1TATAHIS3, GAL2UAS-GAL2TATA-ADE2, URA3::MEL1 UASMEL1TATA-lacZ, MEL1) using the PEG/lithium acetate method described in Ito et al. (1983) and as modified by Brunetti et al. (2021). Transformants that grew on minimal synthetic defined (SD) media lacking leucine and tryptophan were transferred to interaction SD media lacking histidine, tryptophan, and leucine. To further test the strength of the interaction SD-histidine-tryptophan-leucine media was supplemented with varying concentrations of 3-amino-1, 2, 4-triazole (3-AT 0 mM–60 mM). To further assay the interaction a β-galactosidase plate assay was carried out to test the relative affinity of the interaction of GPA1 and the CLO7 N-terminal domain lacking the full transmembrane domain and the positive control of GPA1-AD and AGB1/AGG3(γ)-BD, in which the AGG3 protein was truncated keeping only residues 1–112 (Chakravorty et al., 2015). Plates with yeast colonies were inverted over 5–10 mL of chloroform for 5 min. The yeast colonies were then overlaid with 1–2 mL of chloroform, which was left to evaporate. A 1 mL aliquot of potassium-phosphate buffer (1M K_2HPO_4 and 1M KH_2PO_4) and 0.5 mL X-Gal (20 mg/mL) was added to 8.5 mL of melted 1% agarose cooled to 40 °C and poured over the yeast colonies. The plates were kept in the dark at room temperature for 24 h.

2.6. β-glucuronidase (GUS) assay

The tissue expression of *CLO7* was characterized using promoter-*CLO7*:GUS plants grown on ½ MS media. For analysis of the shoots and roots, the promoter*CLO7*:GUS seed were sterilized and stratified in the dark at 4 °C for 48 h before being plated on ½ MS media with 1% sucrose and grown in a growth chamber at 22 °C with 95–115 μmol $m^{-2}{\cdot}s^{-1}$ light intensity and long day conditions (16 h light: 8 h dark). To monitor expression in the seed coat, the seed were sterilized and plated on ½ MS media with 1% sucrose as a control and ½ MS media with 1% sucrose supplemented with either 2 μm ABA as a hormone treatment, 150 mM D-mannitol or 200 mM NaCl as abiotic stress treatments. Plants or seed were removed from plates in a time course beginning 24 h after sowing up to 15 days of age and placed in X-Gluc staining solution overnight (Jefferson et al., 1987). The next day the staining solution was replaced with 70% ethanol to remove chlorophyll. Photos of aerial tissues and

small seedlings were taken using a Nikon SMZ1500 stereomicroscope with a total magnification of 7.5× to 112.5X. The GUS-stained seed and young radicles were imaged using a Canon SX620 HS camera with autofocus settings.

2.7. Germination assays

The seed germination rates of the genotypes Col, *gpa1*, *clo7*, *CLO7*-RNAi in Col and *gpa1* backgrounds, and 35S:*CLO7* in Col, *gpa1* and *clo7* backgrounds were assayed. Seed were harvested from plants grown under the conditions described above and all seed that were assayed were of the same age. The seed were collected and allowed to dry at room temperature under the same conditions for 4–6 weeks. The seed were then sterilized and plated on ½ MS media with 1% sucrose as control plates and on ½ MS media with 1% sucrose supplemented with 400 mM D-Mannitol or 2 μm ABA. The seed were stratified at 4 °C on plates in the dark for 4 days. The plates were then placed under LED lights at 21 °C with 130–145 μmol $m^{-2}{\cdot}s^{-1}$ artificial light on a long day cycle (16 h light: 8 h dark). The seed germination assays were performed in duplicate. For the ABA treatment, between 70 and 250 seed were scored per genotype per assay. For the mannitol treatment, between 93 and 387 seed were score per genotype per assay. A seed was scored as germinated once a visible radicle had emerged from the seed coat. The number of germinated seed were counted every day until the germination rates reached 100%.

2.8. The clo7 x gpa1 double mutant cross

The seed of the *clo7* and *gpa1* single mutants were sown on soil and stratified as described above and then placed in a growth chamber at 22 °C with 90–100 μmol $m^{-2}{\cdot}s^{-1}$ of artificial light on a long day light cycle (16 h light: 8 h dark). The F1, F2 and 118 F3 plants derived from an F2 plant that was heterozygous for *clo7* and homozygous recessive for *gpa1* (*clo7/+ gpa1*) were analyzed for zygosity. The zygosity screen was carried out by PCR using the LBb1.3 T-DNA border primer recommended by the SALK Institute (La Jolla, USA) and gene-specific primers (Supplemental Table 1). DNA was extracted from leaf tissue according to Edwards et al. (1991). Aliquots of 50–100 ng of plant DNA was assayed by PCR using primer pairs to detect the presence or absence of T-DNA insertions.

The siliques from multiple plants from an F3 line that were identified as *clo7/+ gpa1*, as well as those of the WT (Colombia) and the two single mutants, *gpa1* and *clo7*, were harvested before maturation. The siliques were opened with dissecting forceps and the seed within the siliques were observed using 2.75× magnification eyewear. The number of abnormal or aborted seed were scored for each silique. In wild type plants seed have uniform spacing in the silique; empty spaces in the silique that corresponded to the normal position of a seed were scored as aborted seed.

A semi–*in vitro* pollen tube growth assay was carried out on pollen from F3 plants that were identified as *clo7/+ gpa1*, WT (Colombia) plants, as well as the two single mutants, *gpa1* and *clo7*, as described in Palanivelu and Preuss (2006). *In vitro* culture media was used in an attempt to germinate the *clo7/+ gpa1* abnormal seed. Sterilized seed were plated on media containing 0.5X MS, 10% sucrose, 0.3% phytagel adjusted to pH 5.9 using KOH. The media was autoclaved and then cooled to 50 °C and the following components were added: filter sterilized glutamine (400 mg/L) and 0.1 mg/L 1-naphthaleneacetic acid (NAA). The plates were then stratified at 4 °C for 72 h and then placed at 21 °C with 130–145 μmol $m^{-2}{\cdot}s^{-1}$ artificial light on a long day cycle (16 h light: 8 h dark). After 5 days the seed and seedlings were moved to ½ MS plates supplemented with 1% sucrose.

2.9. Statistical analysis

The data was analyzed using IBM SPSS Statistics version 25 (http://www-01.ibm.com/software/analytics/spss/products/statistics/). All the data for the seed germination assays was analyzed by a two-way ANOVA to assay genotype and treatment effects. This was followed by a one-way ANOVA with a Tukey's *post-hoc* test; *p* values below 0.05 were considered significant ($\alpha = 0.05$).

3. Results

3.1. CLO7 interacts with the Gα subunit (GPA1) and Pirin1 in vivo

CLO7 was shown to interact with the Gα subunit of the heterotrimeric G protein complex (GPA1) using bimolecular fluorescence complementation (BiFC). The full-length and N-terminal truncation (amino acids 1 to 76) of CLO7 interacts with GPA1 at the plasma membrane (PM), indicated by co-localization with the PM marker, At-PIP2A-mCherry (Fig. 1A and B, Supplemental Fig. 1, Supplemental Fig. 2, and Supplemental Table 3). This N-terminal truncation of CLO7 has the intact transmembrane domain but lacks the proline knot motif. The full-length CLO7 also interacts with the constitutively GTP-bound $GPA1^{QL}$, and this interaction is also localized to the plasma membrane (Fig. 2B). The interaction with GPA1 is calcium-dependent, as seen by the lack of interaction with mutant versions of CLO7 in which calcium binding was disrupted by mutations to the EF-hand. One of the mutations is an aspartic acid to alanine at amino acid position 37 ($CLO7^{D37A}$), and the second is a glutamic acid to alanine at amino acid position 48 ($CLO7^{E48A}$); both are amino acids critical for calcium binding (Piazza et al., 2017) (Fig. 3A and D). However, the interaction with $GPA1^{QL}$ is still observed with CLO7 versions that have the EF-hand mutations (Fig. 3B and E). CLO7 also weakly interacts with the full-length Pirin1, a known interactor and downstream effector of GPA1 (Fig. 2C). The interaction between CLO7 and Pirin1 is calcium-dependent; neither $CLO7^{D37A}$ nor $CLO7^{E48A}$ interact with Pirin1 (Fig. 3C and F). Pirin1 interacts with $GPA1^{QL}$ but not the wild-type GPA1 (Fig. 2A). For subcellular localization, the full-length CLO7 was fused to the full-length green fluorescent protein (GFP), and CLO7 was shown to localize to the endoplasmic reticulum (ER) as indicated by co-localization with the ER marker, At-WAK2-mCherry, as well as the evident network structure of the ER (Fig. 1C, Supplemental Fig. 1, Supplemental Fig. 2, and Supplemental Table 3). The CLO7-GFP fusion also localized to punctate structures near the ER, and treatment with the lipophilic stain Nile Red indicated that these punctate structures are lipid droplets (Fig. 1E). A fusion of GPA1 to the full-length GFP molecule showed localization to the PM (Fig. 1D).

3.2. The CLO7 N-terminal region interacts with GPA1, $GPA1^{QL}$ and Pirin1

CLO7 protein truncations tested as fusions with the binding domain (BD) in yeast two-hybrid (Y2H) vectors indicated an interaction between the N-terminal domain of CLO7 (amino acids 1 to 67) and the full-length GPA1 fused with the activation domain (AD-GPA1), as well as with the AD-GPA1 mutant in a GTP-bound state ($GPA1^{QL}$), and with AD-Pirin1, corroborating the interactions seen using BiFC (Fig. 4). The CLO7 N-terminal domain truncation lacks the proline knot motif and twelve amino acids of the transmembrane domain. The BD-fused full-length CLO7 and the C-terminal truncation did not show interaction with AD-GPA1 in the Y2H system (Fig. 4A). The former is likely due to the membrane-associated domains which normally interfere with Y2H assays, and the latter due to the lack of domains necessary for the interaction with GPA1. The same BD-CLO7 N-terminal portion that interacted with AD-GPA1 also interacted with AD-Pirin1 (Fig. 4B). The BD-CLO7 N-terminal portion interacts with both the full-length AD-Pirin1 protein as well as a C-terminal portion of the protein (the last 170 amino acids) (Fig. 4B).

The positive interaction between AD-GPA1 and the BD-CLO7 N-terminal domain was observed with 3-AT concentrations in the media as

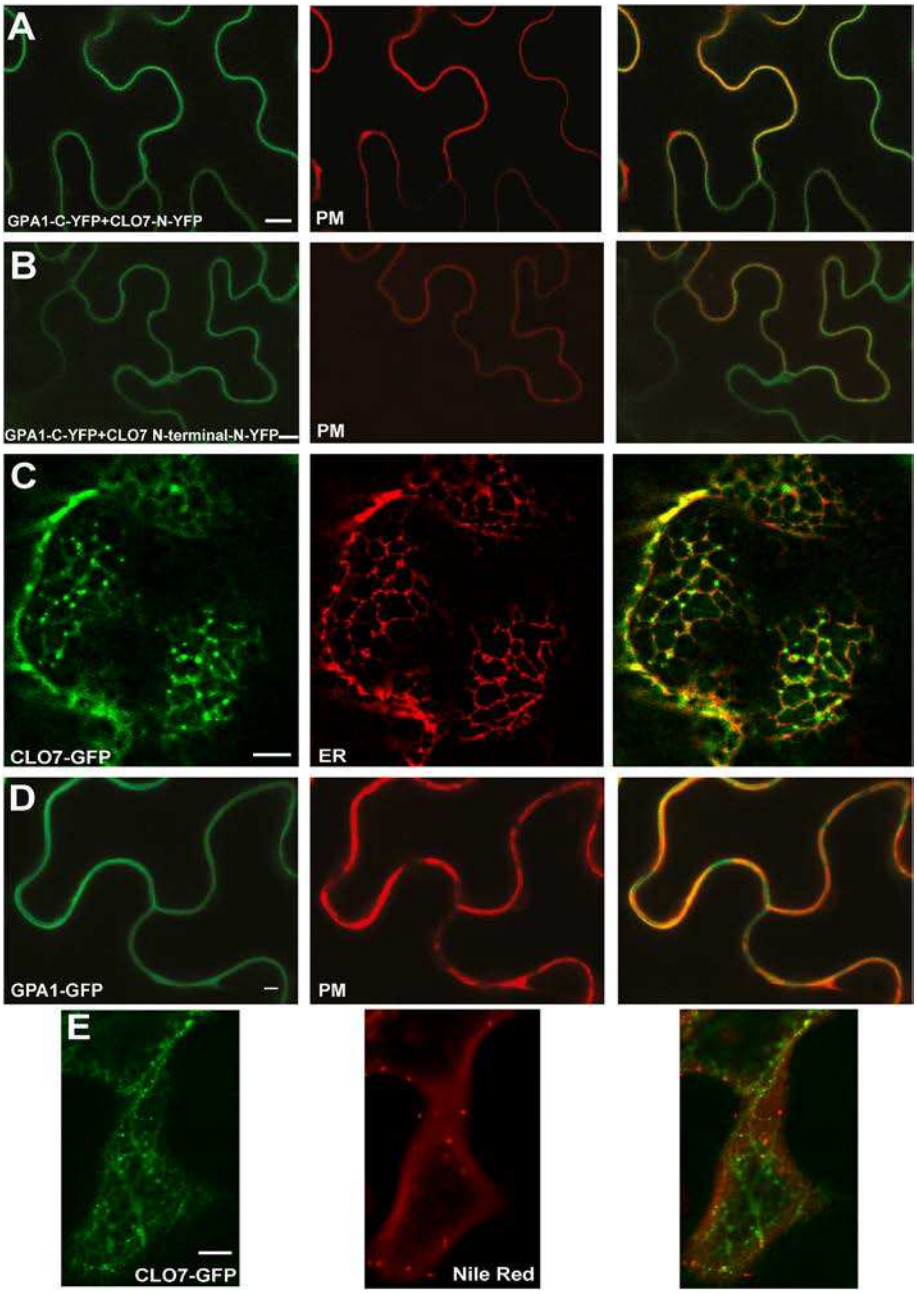

Fig. 1. Bimolecular fluorescence complementation (BiFC) assay showing interaction between **(A)** the full-length CLO7-N-YFP and GPA1-C-YFP localized to the plasma membrane (PM); the At-PIP2 plasma membrane protein fused to mCherry was used as a PM marker. **(B)** The N-terminal domain of CLO7-N-YFP (amino acids 1 to 76) interaction with GPA1-C-YFP also localized to the PM. **(C)** The full-length GFP fusion of CLO7 (CLO7-GFP) localized to the endoplasmic reticulum (ER) of the cell (At-WAK2-mCherry ER marker). **(D)** The full-length GFP fusion of GPA1 localized to the PM. **(E)** CLO7-GFP overlapping with the Nile Red lipophilic stain. Bar = 10 μm. (For interpretation of the references to colour in this figure legend, the reader is referred to the Web version of this article.)

high as 10 mM, indicating a moderately strong interaction between the two proteins, whereas the interaction between AD-GPA1^{QL} and the BD-CLO7 N-terminal appears to be weaker as it only withstands 5 mM 3-AT (Fig. 4A). The N-terminal portion of the CLO7 mutants that disrupt calcium binding (BD-CLO7^{D37A} and BD-CLO7^{E48A}, amino acids 1 to 67) do not interact with AD-GPA1, suggesting that the interaction is calcium-dependent (Fig. 5). The interactions between the N-terminal portion of the CLO7^{D37A} and CLO7^{E48A} mutants with AD-GPA1^{QL} is not abolished, however it is highly impacted since it can only withstand 1 mM 3-AT, indicating a marked reduction in binding affinity between these two proteins if the calcium-binding domain of CLO7 is disrupted (Fig. 5). As mentioned above, the BD-CLO7 N-terminal domain also interacts with AD-Pirin1 and this interaction was unable to withstand more than 1 mM 3-AT, indicating an even weaker interaction than that seen between AD-GPA1 and the BD-CLO7 N-terminal domain (Fig. 4B). Similar to the interaction with GPA1, the CLO7 full-length and C-terminal domain do not interact with Pirin1 (Fig. 4). Mutations that remove the calcium-binding capacity of the N-terminal domain of CLO7 (CLO7^{D37A} and CLO7^{E48A}) prevent the interaction with Pirin1, indicating that the CLO7 and Pirin1 interaction is calcium-dependant (Fig. 5). The AD-GPA1^{QL} and BD-Pirin1 full-length interaction can withstand up to 50 mM 3-AT, suggesting a very strong interaction between the two proteins (Fig. 4B).

To further verify the interaction between AD-GPA1 and the BD-CLO7 N-terminal domain as well as the AD-GPA1^{QL} interaction with the BD-CLO7 N-terminal domain and BD-Pirin1 full-length, a β-Galactosidase plate assay was carried out. This resulted in reporter gene expression and blue colonies (Supplemental Fig. 3). The BD-CLO7 N-terminal portion with the AD-Pirin1 C-terminal and AD-Pirin1 full-length also showed reporter gene expression (Supplemental Fig. 3).

3.3. Tissue-specific expression of CLO7

CLO7 expression was mainly seen in the leaves, in post-germination

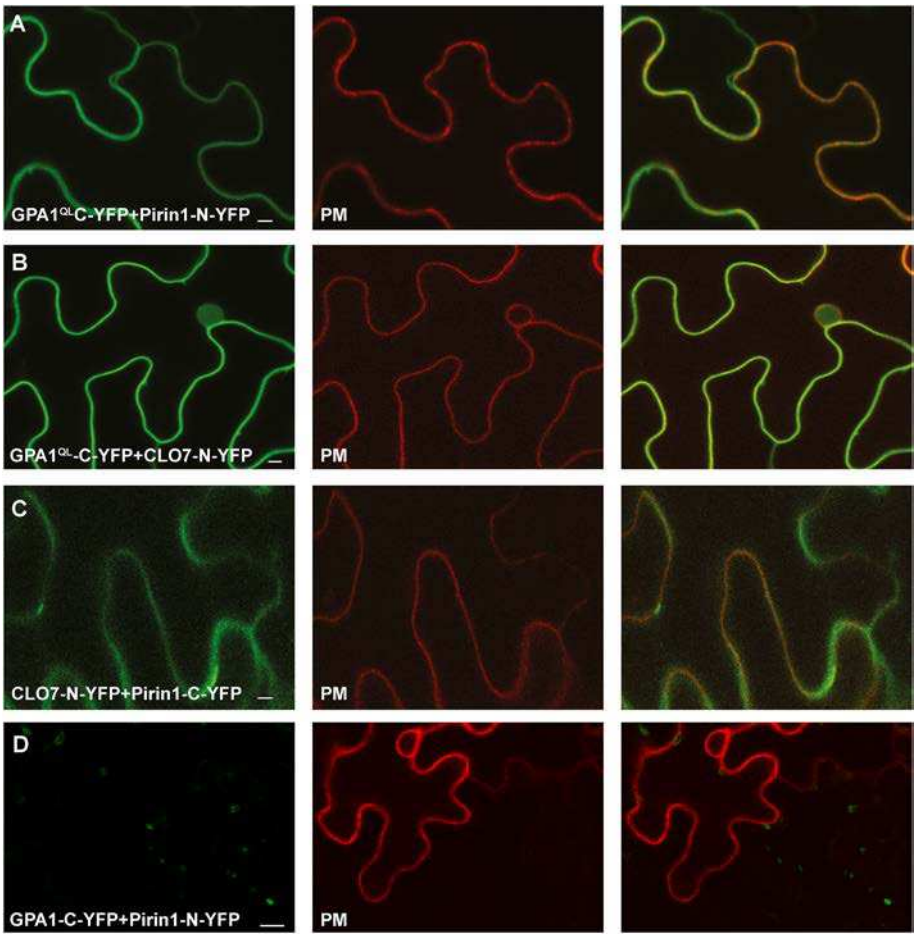

Fig. 2. Bimolecular fluorescence complementation (BiFC) assay showing interaction between **(A)** GPA1^{QL}-C-YFP and the full-length Pirin1-N-YFP localized to the plasma membrane using the mCherry marker (PM). **(B)** GPA1^{QL}-C-YFP and the full-length CLO7-N-YFP localized to the PM. **(C)** The full-length CLO7-N-YFP with the full-length Pirin1-C-YFP localized to the PM. **(D)** The lack of an interaction with GPA1-C-YFP and the full-length Pirin1-N-YFP. Bar = 10 μm.

embryonic tissues, and in the seed coat. Transgenic plants with the promoter*CLO7*:GUS gene reporter fusion showed strong expression in the radicle in germinating seed, followed by a loss of expression in the root and expression in the aerial tissues until the plant was five days post-germination (Fig. 6). Expression that was monitored up to day 15 indicated that *CLO7* is not expressed in seedling tissues after day 5 of control conditions (Fig. 6E). This suggests *CLO7* plays a role in the early developmental stages of the plant. *CLO7* also has expression in the seed coat when seed are placed on control media or when placed on media containing 2 μm ABA, 150 mM mannitol or 200 mM NaCl, indicating that *CLO7* expression is not induced in response to these conditions (Supplemental Fig. 4). This suggests that *CLO7* may play a role in seed germination and early plant development.

3.4. *The clo7 gpa1 double mutant cross displays embryo lethality*

The physical interaction between CLO7 and GPA1 suggests that the two gene products may act in the same signalling pathway. The double *clo7 gpa1* mutant appears to be lethal since the attempt to produce a homozygous double mutant by crossing the two single mutants did not result in the recovery of a double mutant line. The *CLO7* locus is on chromosome 1 and *GPA1* is on chromosome 3, thus linkage is not a factor affecting the recovery of the double mutant. The self pollination of a line heterozygous for *clo7* and homozygous recessive for *gpa1* (*clo7*/+ *gpa1*) would produce ¼ of the plants as double homozygous mutants if the line had been segregating in a Mendelian 1:2:1 ratio; however out of the 118 plants screened a segregation ratio of 30:88:0 was observed for plants homozygous for *CLO7*, heterozygous *clo7*/+ and no double homozygous mutants, respectively.

To further understand the lack of double mutants in the segregating populations, the seed development in the siliques of multiple *clo7*/+ *gpa1* plants were observed and compared to siliques of the WT (Col) and the two single mutants (*clo7* and *gpa1*). The *clo7*/+ *gpa1* lines had many aborted seed, indicated by gaps within the silique where seed had not developed, and other seed that were smaller, dehydrated, and darker than the other seed in the same silique, whereas the occurrence of abnormal seed in the siliques from WT plants was extremely rare (Fig. 7). The *clo7*/+ *gpa1* line had 13% aborted seed and 4% abnormal small and shriveled seed compared to the 0% aborted seed and 0.3% small and shriveled seed seen in the WT. These anomalies, totalling 17% of the seed in the *clo7*/+ *gpa1* line, suggest that the double homozygous mutant is lethal (Fig. 7). The small, shriveled seed were collected and incubated on recovery media; however, none of the abnormal seed germinated (Supplemental Fig. 5).

3.5. *CLO7 affects germination rates in response to ABA and osmotic stress*

The expression of *CLO7* in the seed tissue as indicated by the p*CLO7*:GUS assay motivated an analysis of the involvement of *CLO7* in seed germination in response to ABA treatment and osmotic stress. *CLO7* affects germination rates in response to 2 μm ABA; the *clo7* mutant has significantly higher germination (95%) than the WT (Col, 61%) and the *gpa1* (35%) single mutant on day 2 of ABA treatment (Fig. 8A and Supplemental Table 4). As previously reported, the *gpa1* single mutant

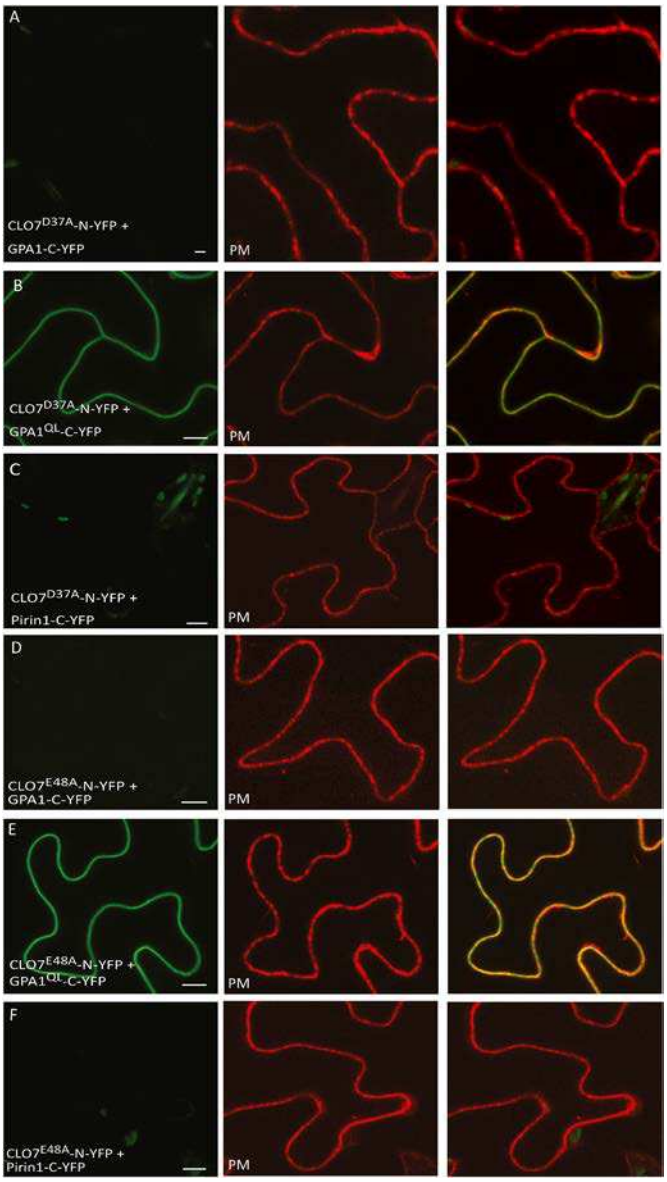

Fig. 3. Bimolecular fluorescence complementation (BiFC) assay showing differences in the interactions between the EF-hand mutants, CLO7^{D37A} and CLO7^{E48A}, with GPA1, GPA1^{QL} and Pirin1. **(A)** Lack of an interaction with CLO7^{D37A}-N-YFP and GPA1-C-YFP, shown with the plasma membrane marker (PM). **(B)** Interaction with CLO7^{D37A}-N-YFP and GPA1^{QL}-C-YFP localized to the PM. **(C)** Lack of an interaction with CLO7^{D37A}-N-YFP and Pirin1-C-YFP, shown with the PM marker. **(D)** Lack of an interaction with CLO7^{E48A}-N-YFP and GPA1-C-YFP, shown with the PM marker. **(E)** Interaction with CLO7^{E48A}-N-YFP and GPA1^{QL}-C-YFP localized to the PM. **(F)** Lack of an interaction with CLO7^{E48A}-N-YFP and Pirin1-C-YFP with the PM marker. Bar = 10 μm.

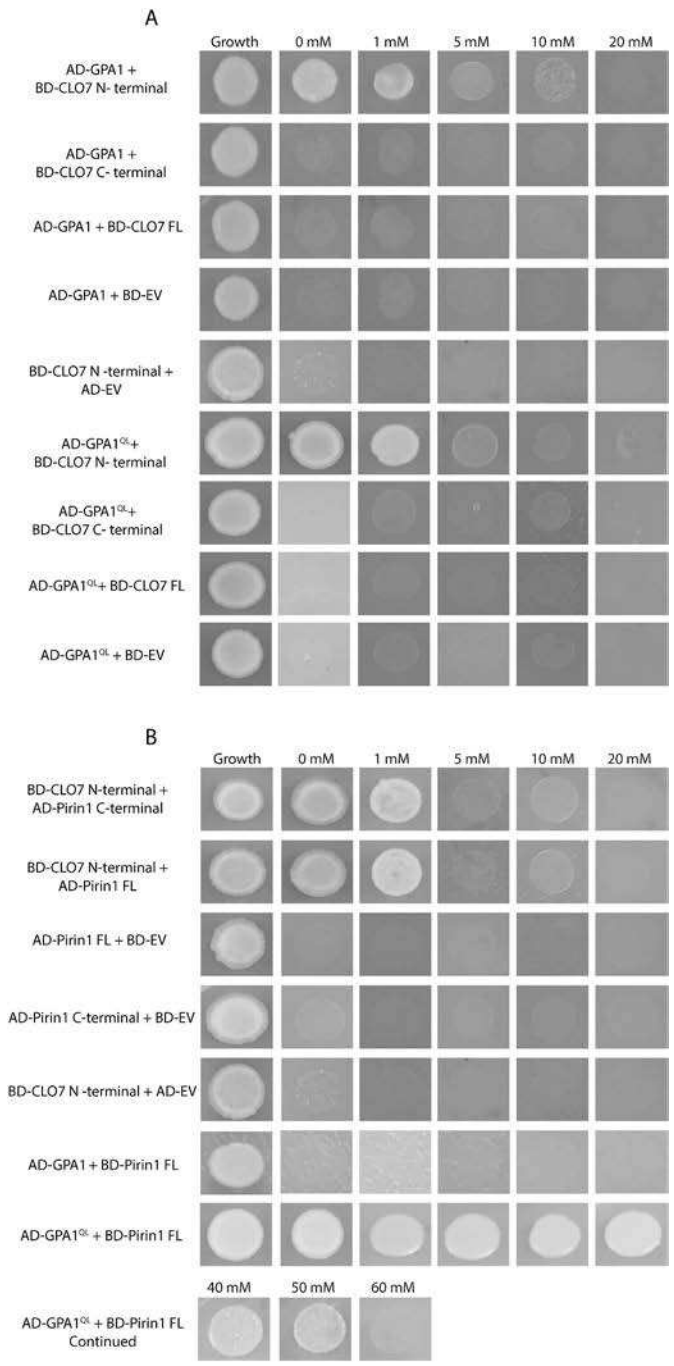

Fig. 4. Yeast two-hybrid interaction of **(A)** the full-length BD-CLO7 protein as well as the BD-N-terminal (amino acids 1 to 67) and C-terminal truncated fragments (amino acids 273 to 633) of CLO7 with AD-GPA1 and AD-GPA1^{QL}. **(B)** Interaction of the BD-CLO7 N-terminal with AD-Pirin1 FL and AD-Pirin1 C-terminal (last 170 amino acids) as well as the interaction between AD-GPA1^{QL} and BD-Pirin1 FL. The growth panel shows growth on SD media lacking leucine and tryptophan which indicates the presence of the two plasmids. The concentrations signify the amount of 3-amino-1, 2, 4-triazole (3-AT) supplemented to SD plates lacking histidine, leucine and tryptophan. EV stands for empty vector and FL stands for full-length.

has a lower germination rate as it is hypersensitive to ABA inhibition of seed germination (Fig. 8A) (Perfus-Barbeoch et al., 2004). The two *CLO7*-RNAi lines, which both have a 60% reduction in gene expression, as determined by semi-quantitative RT-PCR, have phenotypes similar to the *clo7* null mutant with marked insensitivity to ABA inhibition of germination (Fig. 8A and Supplemental Table 4). The two *CLO7*-RNAi lines in the *gpa1* mutant background (*CLO7*-RNAi *gpa1*) display a germination rate similar to the *gpa1* single mutant (Fig. 8A). Similarly, the line with over-expression of *CLO7* in the *gpa1* mutant background (35S:*CLO7 gpa1*) has a reduced germination rate which is not significantly different than the *gpa1* single mutant (Fig. 8A and Supplemental Table 4). The two over-expression lines (35S:*CLO7*) have lower germination rates compared to the WT, confirming *CLO7*'s role in germination inhibition when treated with ABA (Fig. 8A). The recovery line which has the over-expression of *CLO7* in the *clo7* mutant background restores the germination rates to that of the WT indicating that *CLO7* plays a role in seed germination in response to ABA (Fig. 8A). The same trends are observed from day 1 to day 4 of ABA treatment, however

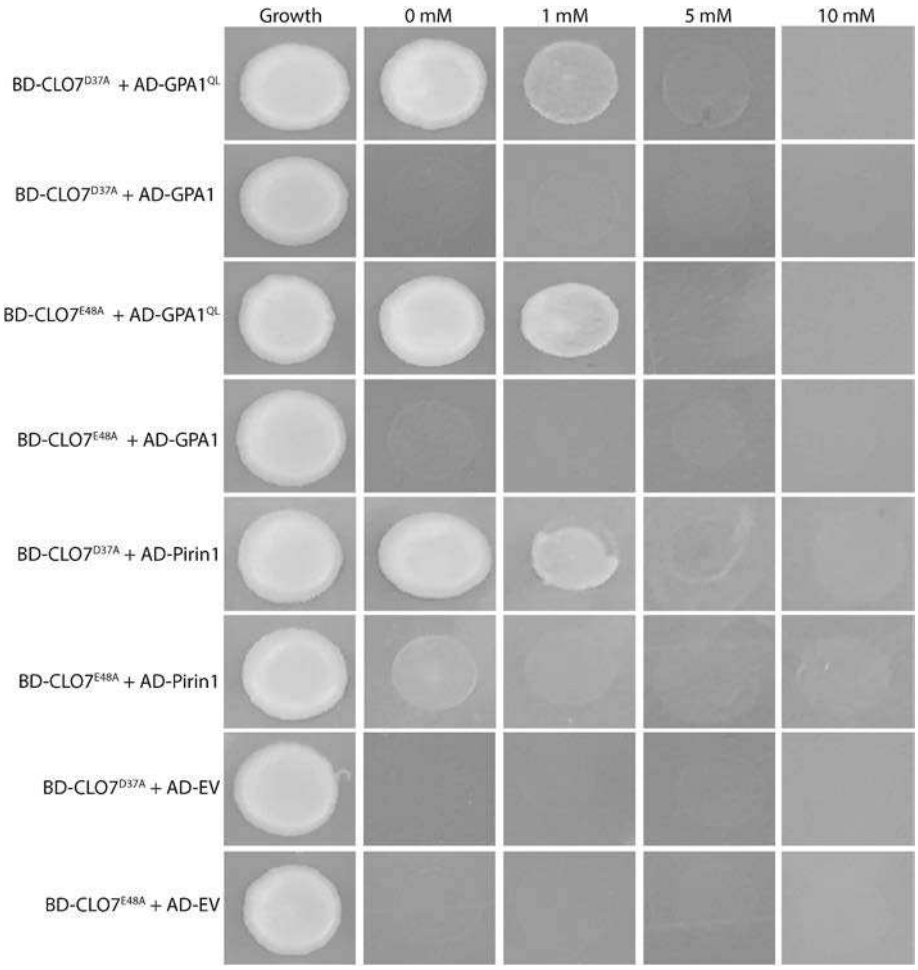

Fig. 5. Yeast two-hybrid interaction of the BD-N-terminal domain of CLO7^{D37A} and CLO7^{E48A} with the full-length AD-GPA1, AD-GPA1^{QL} and AD-Pirin1. The growth panel shows growth on SD media lacking leucine and tryptophan and indicates the presence of the two plasmids. The concentrations signify the amount of 3-amino-1, 2, 4-triazole (3-AT) supplemented to SD plates lacking histidine, leucine and tryptophan. EV stands for empty vector.

the largest differences are seen on day 2 (Supplemental Table 4). All lines used in this assay have 100% germination within 24 h on the control media.

CLO7 also plays a role in germination in response to mannitol, a form of osmotic stress; the *clo7* mutant has a significantly higher germination rate than the WT and *gpa1* mutant after 3 days on 400 mM mannitol (Fig. 8B and Supplemental Table 5). The *clo7* mutant has a 75% germination rate compared to the 67% germination rate seen in the WT and the 46% germination rate seen in the *gpa1* single mutant (Fig. 8B and Supplemental Table 5). The *CLO7*-RNAi lines in the WT (Col) and *gpa1* mutant backgrounds have a higher germination rate, 73%, which is not significantly different from the *clo7* mutant (Fig. 8B and Supplemental Table 5). The 35S:*CLO7* lines in both the WT and *gpa1* mutant background have lower germination rates, 59%, compared to both the WT and *clo7* mutant, however the germination rates are higher than the *gpa1* single mutant (Fig. 8B and Supplemental Table 5). The recovery line, 35S:*CLO7* in the *clo7* mutant background, restored germination rates to that of the WT (Fig. 8B and Supplemental Table 5). The same significant trend is observed on day 2 of mannitol treatment, with the *clo7* mutant having a higher germination rate, however the percent differences between genotypes is not as great (Supplemental Table 5). There is no significance between genotypes by day 4 and day 5 as the germination rates approach 100% (Supplemental Table 5). On control media, all genotypes reach 100% germination 24 h after being subjected to warm temperatures and light. Taken together this data indicates that *CLO7* inhibits germination in response to osmotic stress.

4. Discussion

4.1. Protein-protein interactions between CLO7, GPA1, GPA1^{QL}, and Pirin1

The heterotrimeric G protein complex has an elaborate network of protein-protein interactions leading to a multitude of downstream effectors being activated or inactivated (Klopffleisch et al., 2011). This mechanism of interaction is the core of G-protein signalling and the functionality of the heterotrimer. The identification of CLO7 as an interactor of GPA1 adds to the richness of G-protein functionality and can contribute to the understanding of the role of CLO7 and GPA1 *in planta*. Here we have demonstrated that the caleosin CLO7 not only interacts physically with GPA1 but that it regulates seed germination in response to ABA treatment and under conditions of high osmolarity. *CLO7* acts as a negative regulator of *GPA1*, as *clo7* mutations lead to increased germination under ABA or osmotic stress, whereas the *gpa1* mutation causes a delay in germination under the same conditions. The epistatic relationship of the two genes is complex; in response to ABA treatment both the *CLO7*-RNAi and *CLO7* over-expression lines in the *gpa1* background have phenotypes similar to *gpa1* indicating that *GPA1* is acting downstream of *CLO7*. However, in response to mannitol treatment the *CLO7*-RNAi in the *gpa1* mutant background has a phenotype similar to the *clo7* single mutant. Additionally, the *CLO7*-RNAi lines in the WT background and the 35S:*CLO7* in the *gpa1* background are similar to the 35S:*CLO7* in the WT background, indicating

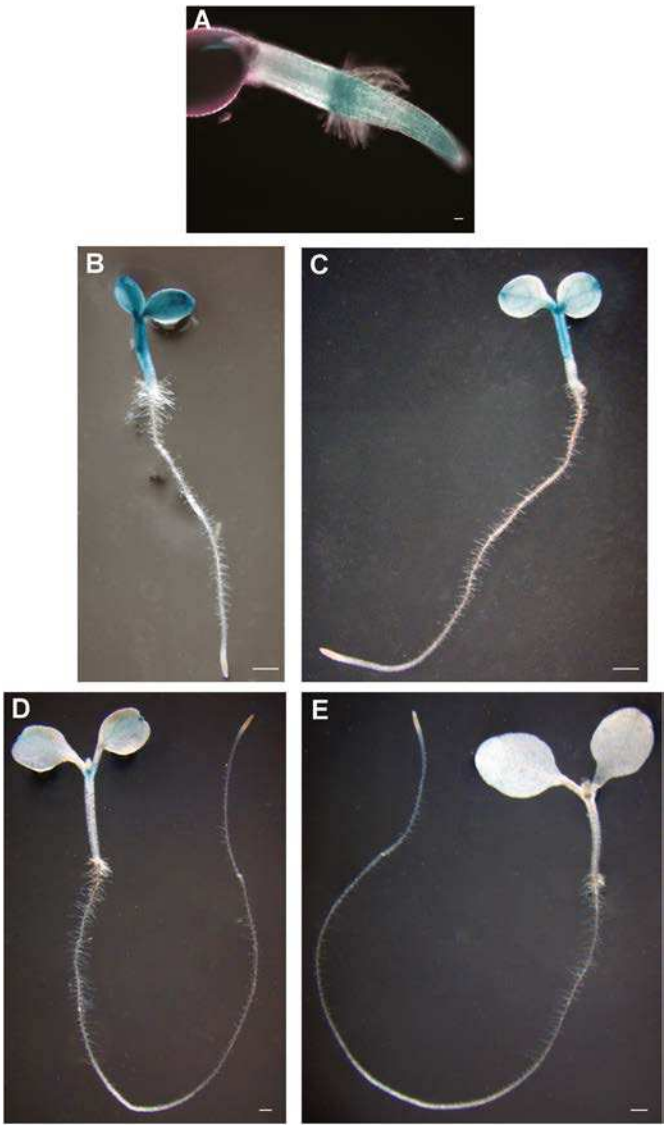

Fig. 6. Tissue-specific expression using the promoter*CLO7*:GUS reporter system. Plants were grown on ½ MS with 1% sucrose for **(A)** 24 h, **(B)** two days, **(C)** three days, **(D)** four days and **(E)** five days. Scale bar for panel **(A)** = 10 μm. Scale bar for panels **(B–E)** = 1 mm.

that *CLO7* is acting downstream of *GPA1*. This suggests that the role of *CLO7* is different in the ABA signalling pathway and the ABA-independent osmotic stress signalling pathways. The CLO7 interaction with GPA1 likely modulates the interaction of GPA1 with other protein partners in these pathways and this may account for the differences observed. An interaction screen using multiple Arabidopsis Y2H libraries reported over 30 proteins that interacted with GPA1 (Klopffleisch et al., 2011). Several protein-protein interactions with GPA1 have been characterized in detail (Klopffleisch et al., 2011), including interactions with Phospholipase D alpha 1 (PLDα1) (Zhao and Wang, 2013), Pirin1 (PRN1) (Lapik and Kaufman, 2003), Thylakoid Formation 1 (THF1) (Huang et al., 2006), and RD20/CLO3 (Response to Dehydration/Desiccation 20/Caleosin 3) (Brunetti et al., 2021). Aside from the few interactors mentioned above, the G protein complex has many more potential effectors and interacting partners. This is evident in that the complex itself has a molecular mass of 100 kDa yet it has been shown to be part of a larger complex with a molecular mass of 700 kDa (Wang et al., 2008). These reports imply many possible interaction combinations that could be affected by the interaction observed between CLO7 and GPA1.

The interaction between CLO7 and Pirin1 contributes to the complexity of the possible modes of regulation of CLO7 in GPA1-centered signalling. Lapik and Kaufman, (2003), previously reported the interaction of GPA1 and Pirin1 and this interaction was confirmed in this study with the use of Y2H and BiFC. Additional analysis presented here sheds light on the nucleotide-dependent state of this interaction since Pirin1 only interacts with $GPA1^{QL}$. *Pirin1* is a downstream effector of *GPA1* and the *pirin1* mutant phenocopies the *gpa1* mutant with a reduction in germination in response to ABA treatment, and therefore is believed to be downstream of *GPA1* (Lapik and Kaufman, 2003). The *clo7* mutant has an opposite phenotype with a higher germination rate in response to ABA, suggesting *CLO7* may be a negative regulator of both *GPA1* and *Pirin1* in the ABA inhibition of germination by either affecting the interaction of Pirin1 with GPA1 or directly through binding to Pirin1.

4.2. *The clo7 and gpa1 cross displays embryo lethality*

The apparent synthetic lethality of the double *clo7 gpa1* mutant implicates the role of the interaction between GPA1 and CLO7 in critical developmental processes in addition to seed germination. Self-pollination of the *clo7*/+ *gpa1* line did not produce any offspring that were homozygous for the mutant alleles for both genes but did produce a substantial number of abnormal or aborted seed, an indication of a synthetic lethal phenotype. Since double homozygous mutant lines could not be recovered from the self-pollination of the line, we presume that the 17% of seed with aberrant development observed in the siliques from those plants represent the seed that were double homozygous for *gpa1* and *clo7*. The frequency of affected seed from a heterozygous line is usually 25%, however the frequency of synthetically lethal offspring has been known to range from as little as 5%–50% depending on the alleles involved (Meinke, 2020). Recently, a curated set of 510 EMBRYO-DEFECTIVE (EMB) genes have been reported in Arabidopsis, highlighting that an elaborate network of genes can play a role in embryo survivability (Meinke, 2020). The report also noted only 83 combinations of double mutations that cause embryo lethality (Meinke, 2020). CLO7's expression has been reported in the male organs, stamens, and sperm cells (Schmid et al., 2005; Partridge and Murphy, 2009), however, the pollen of the *clo7*/+ *gpa1* plants was assayed and there were no apparent abnormalities in pollen grain number or phenotype. It is more plausible that the lethality arises from early embryo development or maternal/female gametophyte development, such as embryo sac development, pollen tube guidance defects and fertilization (Pagnussat et al., 2004). The large number of aborted seed and the

Fig. 7. Affected seed phenotype of the wild-type (WT) Col, single *gpa1* and *clo7* mutants and the seed heterozygous for *clo7* and homozygous recessive for *gpa1* (*clo7*/+ *gpa1*). Some of the seed in the *clo7*/+ *gpa1* line appear dehydrated when compared to the WT, *clo7* or *gpa1* mutant seed.

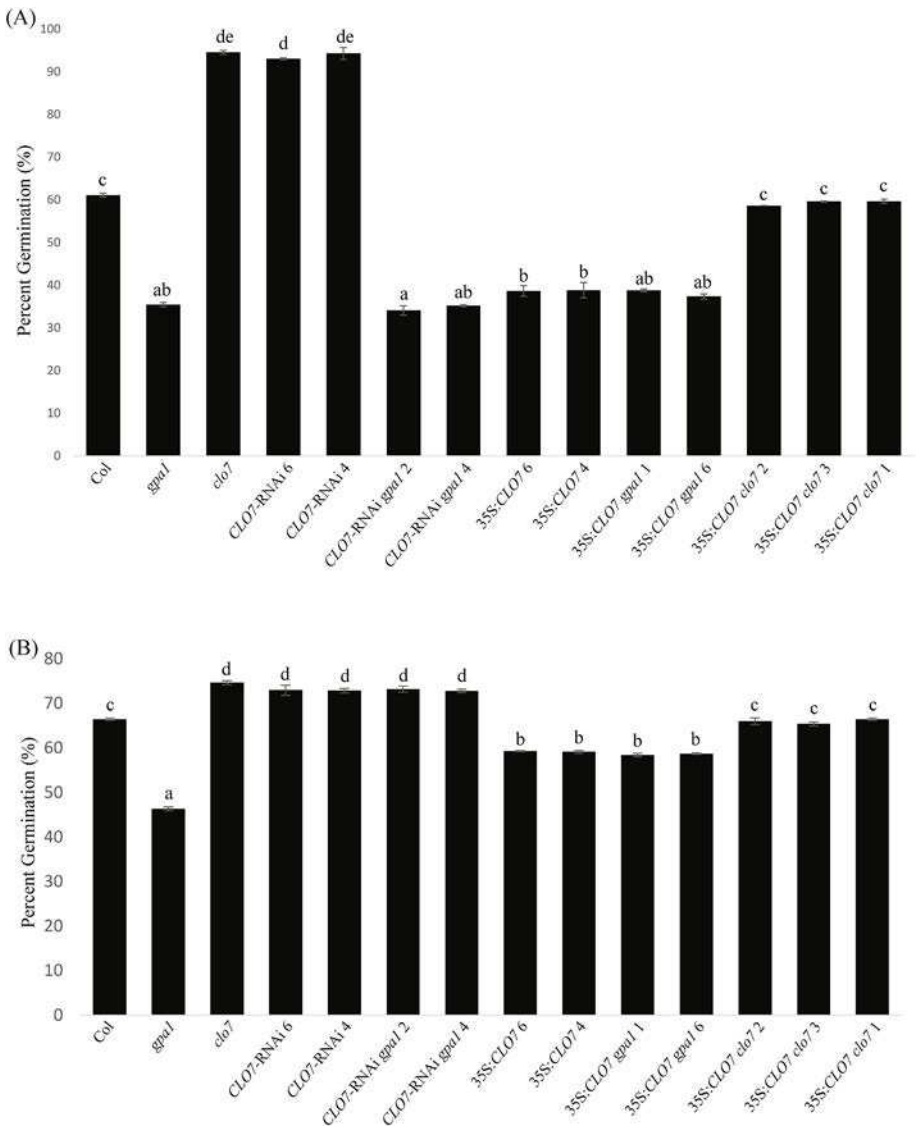

Fig. 8. The percent germination of the wild-type Col, *clo7* and *gpa1* single mutants, the *CLO7*-RNAi lines in the WT and *gpa1* mutant background and the 35S: *CLO7* lines in the WT, *gpa1* and *clo7* mutant backgrounds in response to **(A)** 2 μm ABA and **(B)** 400 mM mannitol. The letters above the bars represent the significant differences between genotypes inferred by a Tukey's *post-hoc* test. Any genotype sharing the same letter indicates non-significant differences in germination percentage. Error bars = standard error of the mean.

small size of the affected seed seen in the cross indicates a defect in embryogenesis with an arrest in development post-fertilization. In a study of genes required for female gametophyte development and function, 48% of the mutants identified displayed defects in embryogenesis and they were deemed MEE (Maternal Effect Embryo arrest) mutants (Pagnussat et al., 2004). The G-protein interactome notes that GPA1 interacts with RACK1 *(*Receptor for Activated C Kinase 1), which is implicated in plant development and interacts with *MEE58* (Maternal Effect Embryo Arrest 58), a maternal embryo defective gene (Klopffleisch et al., 2011; Fetchko and Stagljar, 2004). In Arabidopsis, there are three homologous genes, *RACK1A*, *RACK1B*, and *RACK1C* (Guo and Chen, 2008). RACK1 in Arabidopsis, which is a negative regulator in ABA signalling (Guo et al., 2009), has a similar structure to the β subunit of the heterotrimeric G protein complex, AGB1, in that it has circular seven bladed propeller structures with one TRP-ASP 40 (WD40 repeat) unit on each blade. However, it lacks the N-terminal helix found in AGB1 which is critical for its interaction with the Gγ subunit (Chen et al., 2006b). Chen et al. (2006b), suggests that it is possible that RACK1 and the G proteins may constitute a signalling complex responsible for different plant responses. RACK1 does not directly bind to GPA1, however the Gβγ dimer and Gαβγ trimer form a complex with RACK1 with its affinity for the trimer being much higher than with the dimer (Dell et al., 2002; Ullah et al., 2008). It is possible that CLO7's interaction with GPA1 may affect the interaction of RACK1 with the heterotrimeric G protein complex and affect the downstream interactions with MEE58 causing a maternal embryo lethal phenotype.

5. Conclusion

The current study adds to previous evidence for interactions between members of the caleosin gene family and the α subunit of the heterotrimeric G protein complex, GPA1. *CLO7* is one of the seven caleosin gene family members in the Arabidopsis genome. The characterization of the interaction between CLO7, GPA1 and Pirin1 and its relationship to seed germination and to embryo viability expands our understanding of the role of this class of calcium-binding proteins. This complements analyses of other members of the gene family, particularly RD20/CLO3, which has also been shown to physically interact with GPA1 and to modulate its regulation of Arabidopsis hypocotyl elongation in dark-grown seedlings as well as leaf morphology (Brunetti et al., 2021). The diversity of the caleosin gene family contributes to the diversity of GPA1 signalling; in addition, the caleosins play a role in signalling pathways without the involvement of GPA1. A striking difference in the interactions between CLO7 and RD20/CLO3 with GPA1 is the localization of the interaction within the plant cell. The interaction between RD20/CLO3 and GPA1 is localized to the ER whereas in this study CLO7

was found to interact with GPA1 at the PM (Brunetti et al., 2021). The mechanisms that regulate the localization of the interaction of these proteins and how they modulate plant development and response to environmental stresses remain important questions. The CLO3 ortholog in the monocot *T. aestivum* has also been shown to interact with GA3, the heterotrimeric G protein α subunit in that species (Khalil et al., 2011). This indicates that the interaction between caleosins and the hetero-trimeric G proteins is an evolutionarily conserved phenomena in plants and is likely to have relevance to other important plant species.

Supplementary data

Supplementary data to this article can also be found online at https://doi. org/10.1016/j.jplph.2022.15384

Chapter 4: **The caleosin *RD20/CLO3* regulates abscisic acid affects on lateral root development and in conjunction with the caleosin *CLO7* regulates flowering time**

The caleosin *RD20/CLO3* regulates abscisic acid affects on lateral root development and in conjunction with the caleosin *CLO7* regulates flowering time

Sabrina C. Brunetti[1], Michelle K.M. Arseneault[1] and Patrick J. Gulick[1]†

[1] Biology Department, Concordia University
7141 Sherbrooke W.
Montreal (Quebec) H4B 1R6, Canada

† Author to whom correspondence should be addressed:

Patrick J. Gulick,

Department of Biology,

Concordia University

7141 Sherbrooke W.

Montreal (Quebec) H4B 1R6, Canada

Tel. (514) 848-2424 ext. 3407; Fax (514) 848-2881

Email: patrick.gulick@concordia.ca

ORCID iD: 0000-0001-7587-4616

Keywords: calcium-binding protein, *RD20/CLO3*, *CLO7*, caleosin, root architecture, ABA

The author responsible for distribution of materials integral to the findings presented in this article in accordance with the policy described in the Instructions for Authors is: Patrick J. Gulick (patrick.gulick@concordia.ca, ORCID iD: 0000-0001-7587-4616)

Abstract

The caleosins are encoded by multi-gene families in *Arabidopsis thaliana* and other plant species. This work investigates the role of two family members, *RD20/CLO3* and *CLO7*, in root development in response to ABA treatment and flowering transition. Gene expression of the caleosin *RD20/CLO3* is induced by ABA in the root tissues and *RD20/CLO3* has a negative affect on the total number of lateral roots as well as the length of the lateral roots in response to ABA. The *rd20/clo3* mutant has more and longer lateral roots in response to ABA treatment compared to the wild-type, showing that *RD20/CLO3* plays a role in the ABA signaling pathway affecting this trait. In contrast, the caleosin *CLO7* is not expressed in the roots and does not affect root architecture in response to ABA treatment. However, the *CLO7*-RNAi/*rd20* or the *RD20/CLO3*-RNAi/*clo7* knockdown-mutants display a dramatic early flowering phenotype under long day conditions. Both yeast two-hybrid and bimolecular fluorescence complement-ation showed that both RD20/CLO3 and CLO7 interact with each other and can form homodimers and heterodimers. Taken together, these findings suggest that members of the caleosin gene family play both different and redundant roles in plant development.

Introduction

Plants have a wide range of biological responses to environmental cues and abiotic stresses. Many of these responses are mediated by members of multigene families that may have different expression patterns, affinities and substrate specificities; they may also function in synchrony, antagonistically or may have redundant functions (Meng et al., 2017; Lachowiec et al., 2018). One such example of a gene family are the caleosins, a family of calcium-binding proteins which to date have been shown to affect different plant responses with some members interacting with the α subunit of the heterotrimeric G proteins (Brunetti et al., 2021; Khalil et al., 2011). The caleosin gene families have been described in both monocots and dicots including *Arabidopsis thaliana*, *Triticum aestivum* and *Hordeum vulgare* (Khalil et al., 2016) and are widespread in the plant kingdom, and they have been found in *Aspergillus flavus*, AfPXG (Hanano et al., 2018). The caleosins were first discovered based on their sequence similarity to oleosins, and like oleosins, were shown to be components of lipid/oil bodies which contribute to seed viability and germination; some members of the gene family have been shown to be highly induced in response to abscisic acid (ABA) and osmotic stress (Frandsen et al., 1996; Purkrtova et al., 2015; Naested et al., 2000). The sequence similarity to oleosins combined with structural modeling indicates that the functional EF-hand calcium-binding motif in the N-terminal domain of the caleosins is in the cytosol, whereas the central hydrophobic region containing an amphipathic α–helix preceding a pair of anti-parallel β–strands followed by a proline-knot motif anchors the caleosins to the oil bodies (Chen et al., 1999; Hanano et al., 2006). The C-terminal domain is also cytosolic and contains phosphorylation sites and a conserved cysteine residue (Frandsen et al., 1996; Chen et al., 1999).

In Arabidopsis the caleosin gene family includes seven members, annotated as *CLO1-CLO7*. *CLO1* is a primary example of functional specificity distinction from the other caleosins since CLO1 is suggested to play a role in the degradation of storage lipids within vacuoles and to participate in oil body/vacuole interaction during seed germination (Poxleitner et al., 2006). Although the caleosins were initially identified as seed oil body-associated proteins, they are also found in non-seed tissues, for example *CLO1* is found in pre-embryonic and post-embryonic tissues including developing embryos and root tips (Naested et al., 2000).

The Arabidopsis *CLO4*, has been shown to act as a negative regulator of ABA responses (Kim et al., 2011). Like *CLO1*, *CLO4* is found in non-seed tissues including but not limited to; guard cells, rosette leaves, roots, petals and sepals (Kim et al., 2011). The *clo4* mutant displays hypersensitivity to ABA, salt and mannitol inhibition of germination, suggesting that *CLO4* plays a role in alleviating the inhibitory effects of some abiotic stress on seed germination (Kim et al., 2011). The *clo4* mutant also displayed tolerance to conditions of drought, believed to be linked to the mutants decreased stomatal aperture in response to ABA (Kim et al., 2011). Some ABA responsive genes were found to be upregulated in the *clo4* mutant, including *ABF3* (*ABA-responsive element-binding Factor 3*), ABF4 (*ABA-responsive element-binding Factor 4*), and ABI1 (*ABA insensitive 1)*, further suggesting CLO4 is a negative regulator of the ABA response (Kim et al., 2011).

The most extensively studied caleosin *RD20/CLO3* (*Responsive to Dehydration /Dessication 20*, At2G33380) in Arabidopsis has been shown to be an important component in the response to a wide variety of abiotic stress conditions, including dehydration, salt, cold, and ABA treatment (Takahashi et al., 2000). It has also been identified as a regulator of stomatal aperture, and *rd20/clo3* mutants exhibited decreased tolerance to drought and salt conditions (Aubert et al., 2010). The gene has been suggested to act as a stress-signaling hub that triggers or regulates a plant's stress response mechanisms (Aubert et al., 2010). The expression of *RD20/CLO3* has been localized to above-ground tissues including the leaf tissue, guard cells, flowers, and siliques, again indicating that the caleosins play roles outside of seed oil bodies (Aubert et al., 2010). *RD20/CLO3* also impacts biotic stress tolerance by responding to pathogen infection via its peroxygenase activity which reduces fatty acid hydroperoxides into their corresponding alcohols. RD20/CLO3s ability to reduce these oxylipins allows for the control of reactive oxygen species and cell death, a major contribution to survival of pathogen attack (Partridge and Murphy, 2009; Hanano et al., 2015). The peroxygenase activity is dependent on the histidine residue at position 133 and a mutation at this residue abolishes the activity (Blée et al., 2014). The over-expression of *RD20/ CLO3* causes early flowering transition in response to short day conditions, believed to be caused by gibberellic acid (GA) mediated effects since this phenotype is not observed under long day conditions (Blée et al., 2014). GA mediates early flowering by controlling the transcriptional activation of the floral meristem gene *LEAFY* (*LFY*, Wilson et al., 1992; Blée et al., 2014). The expression of *LFY* was up-regulated while GA-deactivating genes (*GA2 ox1* and

GA2 ox2) were down-regulated leading to the possibility of GA accumulation (Blée et al., 2014). The *rd20/clo3* mutant also displayed an increased germination rate relative to wild-type (WT) plants in response to ABA treatment, which normally inhibits germination, whereas the seeds of over-expression lines germinated at a lower rate than WT seed when treated with ABA (Blée et al., 2014). The *rd20/clo3* mutant also germinated at a higher frequency without stratification (cold treatment), indicating that *RD20/CLO3* plays a role in seed dormancy by having enhanced sensitivity to ABA (Blée et al., 2014). RD20/CLO3 has also been shown to be a negative regulator of the heterotrimeric G-protein alpha subunit (GPA1), and to physically interact with GPA1 (Brunetti et al., 2021). RD20/CLO3 has also been localized to the endoplasmic reticulum (ER) and to oil bodies surrounding the ER (Brunetti et al., 2021). *RD20/CLO3* has been implicated in hypocotyl development in dark-grown seedlings as well as leaf morphology and to be a negative regulator of *GPA1* in relation to these traits (Brunetti et al., 2021). *CLO7* (AT1G23240) is a member of the caleosin gene family that has not been investigated. This study is directed to the investigation of the roles of the caleosins *RD20/CLO3* and *CLO7* in response to ABA and their effects on root architecture as well as their effects on early flowering.

Materials and Methods

Plant Growth for Early-Flowering

The Arabidopsis transgenic plants used to assess flowering time were grown in a 3:1:1 mixture comprised of black earth, peat moss and vermiculite, respectively. Seed were sown on the soil mixture and vernalized in the dark at 4°C for three days. The pots were then placed in a growth chamber under long day conditions, 16 h light and 8 h dark at 22°C, with a light intensity of 95-110 $\mu mol \cdot m^{-2} \cdot s^{-1}$. The leaf numbers were counted once the primary bolt appeared on the plants.

Vector Construction and Transgenic Arabidopsis Lines

The expression vectors used in this study were created using Gateway® cloning technology (Invitrogen). The gene sequences were cloned into pDonor-207 entry clones using the Gateway® BP Clonase II Enzyme and transformed into the TOP10 *E. coli* strain via

electroporation. Gateway® LR reactions were then used to move the inserts into expression vectors. For the 35S:*CLO7*, 35S:*CLO7/clo7* and 35S:*RD20* constructs the coding regions were inserted into the pFAST G02 vector harboring a 35S promoter (Shimada et al., 2010). For the gene knock-downs (*CLO7*-RNAi, *RD20*-RNAi, *CLO7*-RNAi/*rd20*, and *RD20/CLO3*-RNAi/*clo7)* the coding regions were inserted into the pFAST G03 RNAi vector (Shimada et al., 2010). The transgenic lines with gene over-expression (35S:*RD20*, 35S:*CLO7*, 35S:*CLO7/clo7)*, or gene knock-down (*CLO7*-RNAi, *RD20*-RNAi, *CLO7*-RNAi/*rd20*, and *RD20/CLO3*-RNAi/*clo7)*, were generated by transforming the constructs into WS or Col wild-type plants, the *rd20/clo3* mutant line in the WS background, or the *clo7* mutant in the Col background using the Arabidopsis floral dip method from Clough and Bent, (1998). The transgenic T_1 and subsequent lines were screened to identify homozygous lines using the pFAST GFP vector system (Shimada et al., 2010) where transgenic seeds expressing GFP were detected using the Zeiss Axioplan Fluorescence Microscope with the GFP Filter Cube #1031346. Two independent homozygous T_3 lines with single transgene insertions were identified. The p*RD20/CLO3*:*GUS* was created by and described in Brunetti et al., (2021). The p*CLO7*:*GUS* construct was made by PCR amplifying a 1184 nucleotide (nt) DNA fragment that extends from the gene's second exon to 777 nt upstream of the translational start site of *CLO7* and cloned into the pFAST G04 GUS vector (Shimada et al., 2010) and screened using GFP as described above. The 35S:*RD20* in the *rd20* mutant background was developed as described by Blée et al., (2014) and kindly provided by E. Blée.

For the Y2H assay the CLO7 N-terminal domain (amino acids 1 to 67) or the C- terminal domain (amino acids 273 to 633) was cloned into pGADT7-GW or pGBKT7-GW vectors (Lu et al., 2010). For the BiFC assay the CLO7 full-length sequence was cloned into either the pBatTL-B-sYFP-N or pBatTL-cYFP vectors (Uhrig et al., 2007). The RD20/CLO3 N- terminal and C-terminal domain Y2H constructs as well as the N-YFP and C-YFP constructs are described in Brunetti et al., (2021).

Yeast two-Hybrid (Y2H) and Bimolecular Fluorescent Complementation (BiFC) Assays

Both the Y2H and BiFC assays were carried out according to Brunetti et al., (2021). In brief, for the Y2H assay the vectors expressing the N- or C-terminal domains of CLO7 or RD20/ CLO3 were transformed into the yeast strain AH109 using a lithium acetate transformation protocol. The transformed yeast cells were then plated on selective medium to screen for an

interaction and then stamped onto selective medium with varying concentrations of 3-amino-1,2,4-triazole (3-AT). For the BiFC assays the CLO7 and RD20/CLO3 N-YFP and C-YFP constructs were transformed into the Agrobacterium strain AGL1 and the abaxial side of a *Nicotiana benthamiana* leaf was infiltrated with an agroinfiltration solution containing the respective C-YFP and N-YFP combinations. The BiFC was then imaged 46-50 hours post infiltration using the Olympus Fluoview FV10i laser scanning microscope (Olympus, USA) fitted with a 60x/1.35 oil lens (pixel size 0.27 µm). A 473 nm laser was used to observe the N/C-YFP fused proteins (YFP filter Ex 480nm/ Em 527nm). The marker, the C-terminus of c-TIP-mCherry, an aquaporin of the vacuolar membrane fused to mCherry was imaged with the 559 nm laser (red narrow filter Ex 559nm/ Em 570-620nm). For Nile red stained samples, the leaf tissue was incubated with 5 mg/ml of Nile red for 2 minutes and imaged using the 559 nm laser (Texas red filter Ex 595nm/ Em 612nm).

Root Analysis

To measure root growth, the *rd20/clo3* and *clo7* single mutants, the 35S:*RD20*/*CLO3* and 35S:*CLO7* in the wild-type and mutant backgrounds, as well as the wild-types, WS and Col, were grown on Murashige and Skoog (MS) medium. Seeds were sterilized by adding 70% ethanol and vortexing. After two minutes in ethanol, the ethanol was replaced by a sterilization solution (4% bleach, 1% Triton X-100) for 5 minutes. Seeds were then washed five times in sterile distilled water, covered and stratified at 4°C for 48 hours. The seed were then plated on ½ MS control medium: 0.5X Murashige and Skoog basal salt mixture, 1% (w/v) sucrose, 0.05% MES hydrate (4-Morpholineethanesulfonic acid), 0.4% Gelzan^{Tm} CM agar substitute gelling agent, adjusted to pH 5.7 with KOH. The plated seed were left to germinate in a growth chamber at 22ºC, with a light intensity of 95-110 µmol·m-2·s-1 and maintained with a light cycle of 16 h light and 8 h dark. Thirty-six hours post-germination seedlings were transferred to either control plates or treatment plates supplemented with 1 µm ABA, and grown for twelve days on plates positioned vertically in the growth chamber at 22ºC, 95-110 µmol·m-2·s-1 light with a light cycle of 16 h light and 8 h dark. After twelve days of growth, the plants were photographed and the total number of lateral roots and their lengths were measured using ImageJ software (Rasband 1997-2014: https://imagej.nih.gov/ij/).

Localization of Gene Expression with β-glucuronidase (GUS) Reporter Assay

The p*RD20/CLO3*:*GUS* and p*CLO7*:*GUS* plants were germinated on control ½ MS medium with 1% sucrose. Thirty-six hours post-germination, plants were transferred to the ½ MS plates supplemented with 1 µm ABA, or to control medium. The plants were analyzed at time points between two and fifteen days, and then transferred to an X-Gluc staining solution according to the protocol described by Jefferson et al. (1987). Samples were then de-stained in 70% ethanol and imaged using the Nikon SMZ1500 stereomicroscope with a 0.75X to 11.25X zoom range and a 10X eyepiece with total magnification of 7.5X to 112.5X.

Statistical Analysis

The statistical analysis was carried out using IBM SPSS Statistics version 25 (http://www-01.ibm.com/software/analytics/spss/products/statistics/). For the ABA root assay, a two-way ANOVA was carried out followed by a one-way ANOVA with a Tukey's *post-hoc* test; *p* values below 0.05 were considered significant (α=0.05). For the early-flowering phenotype a one-way ANOVA with a Tukey's *post-hoc* test was carried out.

RNA-Seq data

The RNA-Seq data for the *RD20*/*CLO3* (At2g33380) and *CLO7* (At1g23240) expression in the *soc ful* and *elf6-3 ref6C* flowering double mutants was retrieved from the Arabidopsis RNA-Seq Database (Zhang et al., 2020; http://ipf.sustech.edu.cn/pub/athrna/). The data was retrieved using the caleosins' sequence identifiers, At2g33380 and At1g23240, to query the database, for the *RD20/CLO3* expression the data are from the BioProject accession PRJNA284739 by Davin et al. (2016) and the *CLO7* expression data are from the BioProject accession PRJNA418578 by Yan et al. (2018).

Results

RD20/CLO3 is expressed in the leaves and hypocotyls and is induced in the roots by ABA treatment and *CLO7* is expressed in the leaves and not responsive to ABA

Transgenic plants expressing β-*glucoronidase* (*GUS*) under the regulation of the *RD20/CLO3* promoter were used to investigate whether *RD20/CLO3* gene expression in roots is affected by ABA. The expression of *RD20/CLO3* was found to be induced by ABA treatment in a developmentally regulated fashion. In early root development, when seedlings have only primary roots, ABA treatment induced *RD20/CLO3* expression in the primary root tip from two days to five days post-germination (Figure 1A). In contrast, in six-day-old plants, which had both long lateral roots and shorter emerged lateral roots, *RD20/CLO3* gene expression remains induced in the primary root tip, and it is not induced in lateral roots in response to ABA (Figure 1B). After 8 days of ABA treatment the plants showed relatively strong *RD20/CLO3* expression in the elongated lateral roots, but weak expression in the primary root tip, and no expression in short emerged but not elongated lateral roots (Figure 1C). Plants that were not treated with ABA showed no *RD20/CLO3* expression in the root system, however expression is seen in the leaves up to 15 days and in the hypocotyls of plants up to 8 days post-germination, as was also observed in the ABA treated plants (Figure 1).

RD20/CLO3 expression remained high in the lateral roots, in the zone of cell division and the zone of elongation with ABA treatment up to 15 days post-germination (not shown). There was no expression of *RD20/CLO3* in the small lateral root primordia. Altered root growth patterns in response to several stresses including mild NaCl stress are characterized by an inhibition of primary root elongation and stimulation of lateral root emergence (Zolla et al., 2010). Thus, the differential expression of *RD20/CLO3* between the primary root and the lateral roots in response to ABA treatment is an intriguing element of the plant's stress response and suggests that *RD20/CLO3* plays a role in the differentiation between primary and lateral roots in response to environmental stress.

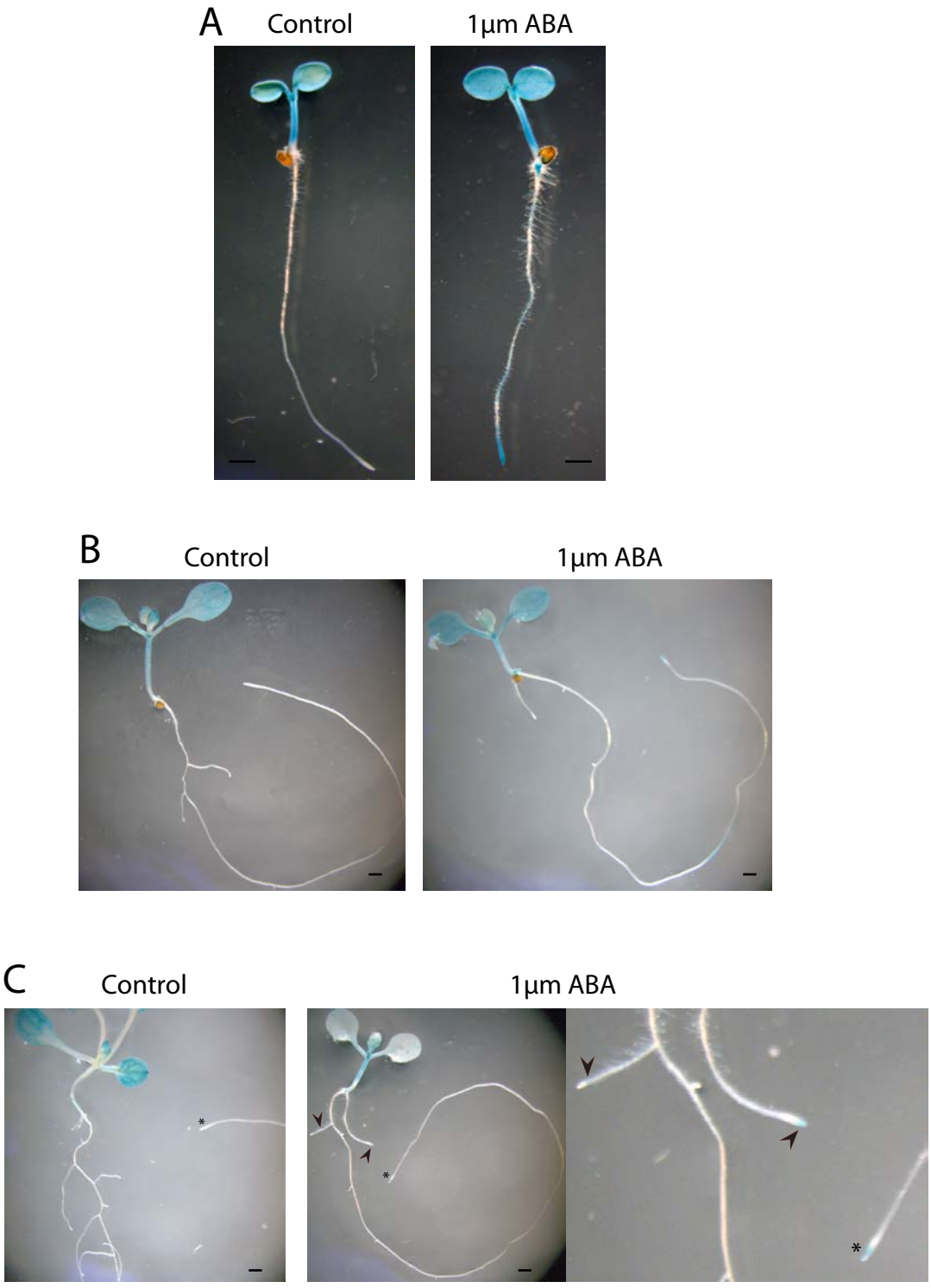

Figure 1. Histochemical GUS staining of transgenic plants transformed with an *RD20/CLO3* promoter:*GUS* reporter construct. Seedlings, 36 h post-germination, were transferred to ½ MS plates with or without 1 µm ABA or control plates for **(A)** two days, **(B)** six days, and **(C)** eight days. The eight day ABA treated plant is represented as a whole and as an inset to the right for a closer view of the roots. *RD20/CLO3* expression was detected in the root system of the plant and throughout root development as displayed. Arrows indicate GUS staining in the lateral roots and * is above the primary root tip. Bar = 1 mm.

To explore *CLO7*'s potential role in root formation in response to ABA the p*CLO7*:*GUS* fusions were used to assay gene induction and tissue localization. The expression of *CLO7* is seen in the aerial tissues of the plant from day 1 to day 5 under control conditions and showed no difference in expression in plants with ABA (Figure 2). *CLO7* expression was not observed in the aerial tissue after day 5 up to day 12 (not shown). *CLO7* expression was never detected in the root tissue and was not induced in response to ABA in the days tested (day one to twelve) (Figure 2 and not shown). The aerial tissue expression is not affected by ABA treatment, indicating that *CLO7*'s involvement in this tissue is independent of ABA (Figure 2). The expression of *CLO7* as seen in young seedlings suggests it plays a role in early development. This expression pattern is different from the expression of *RD20/CLO3*, suggesting that these two caleosins play distinct roles in plant development.

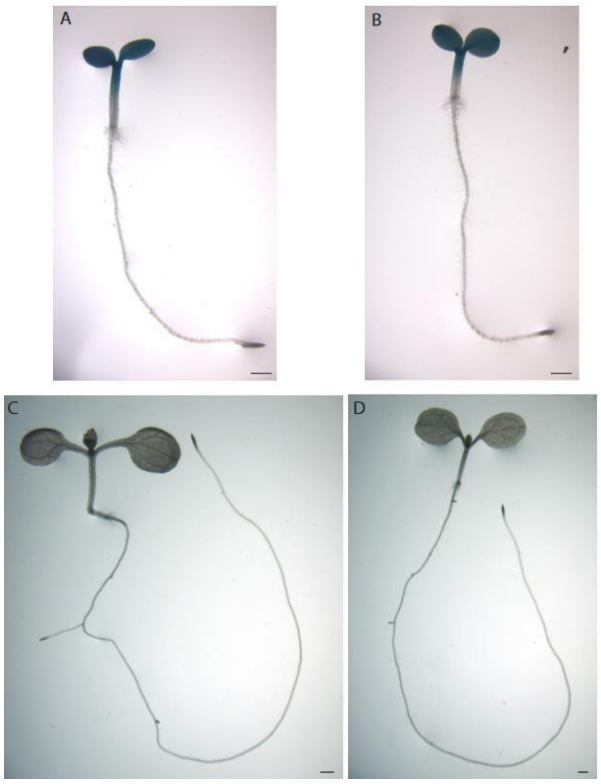

Figure 2. Histochemical GUS staining of transgenic plants transformed with a *CLO7* promoter:*GUS* reporter construct. Seedlings, 36 h post-germination, were transferred to ½ MS plates with or without 1 µm ABA. **(A)** Two-day old seedling on control medium, **(B)** two-day old seedling on medium supplemented with 1 µm ABA, **(C)** five-day old seedling on control medium and **(D)** five-day old seedling on medium supplemented with 1 µm ABA. Bar = 1 mm.

***RD20/CLO3* alters lateral root formation in response to ABA**

The effect of *RD20/CLO3* on lateral root formation in response to ABA treatment was measured by comparing root growth in the *rd20/clo3* mutant and the *RD20/CLO3* over-expressing lines (35S:*RD20/CLO3*), as well as the *RD20/CLO3* over-expressor in the *rd20/clo3* mutant background (35S:*RD20/rd20*). In the comparison of the five genotypes, seedlings were germinated on normal ½ MS medium and transferred to ABA-containing medium 36 h after germination and assessed after twelve days of treatment. Normally, ABA treatment suppresses lateral root (LR) formation. In the growth experiments, mutants for *rd20/clo3* had a significantly greater degree of LR formation under ABA treatment than the wild-type, WS (Figure 3A, and B). All plants had a reduction in the total number of lateral roots, compared to untreated plants, and the lateral roots that did emerge generally had suppressed elongation (Figure 3A and B). When treated with ABA, there was a decrease in the number of lateral roots for the *rd20/clo3* mutant, as well as for WS, although the number of lateral roots for *rd20/clo3* was significantly greater than in WS (Figure 3A). The great majority of lateral roots in all genotypes under ABA treatment were quite short, but a striking feature of the *rd20/clo3* mutant was the development of long lateral roots in ABA treated plants, whereas the wild-type had very short lateral roots (Figure 3B).

The 35S:*RD20/CLO3* lines in the WS background had lateral root numbers and total lateral root lengths similar to that of the WT in response to ABA (Figure 3A and B). When *RD20/CLO3* is over-expressed in the *rd20/clo3* mutant background (35S:*RD20/rd20*) the lateral root elongation phenotype is rescued, with plants having a total lateral root length similar to that of the wild-type plants, indicating that *RD20/CLO3* plays a role in controlling elongation in response to ABA (Figure 3B).

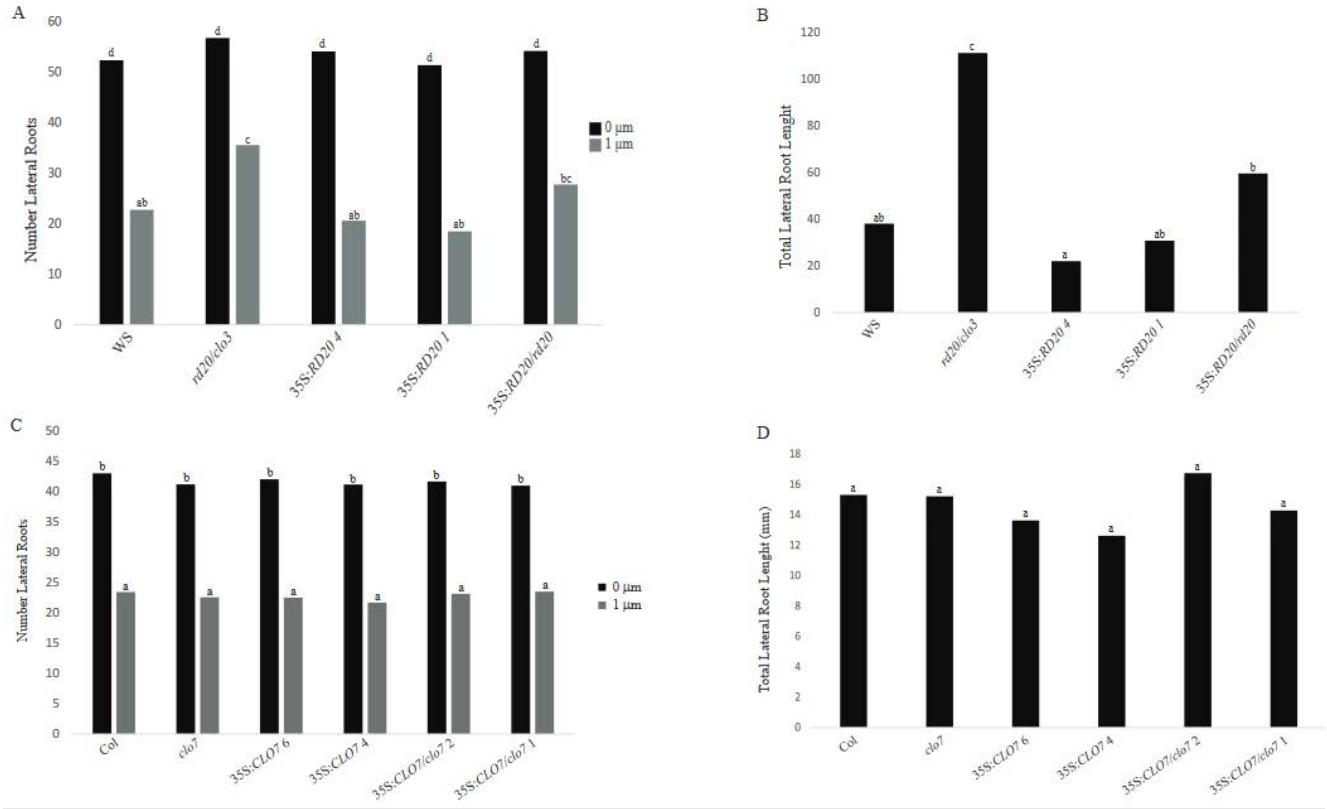

Figure 3. Root phenotypic analysis of the *clo7* and *rd20/clo3* single mutants and the *RD20/CLO3* and *CLO7* over-expressor lines. Seeds were germinated on ½ MS medium and transferred ½ MS medium plus 1 µm ABA plates or to control plates (0 µm ABA) 36 h after germination. **(A)** Total number of lateral roots recorded after twelve days. **(B)** Total length of the lateral roots for each genotype treated with 1 µm ABA. **(C)** Total number of lateral roots after twelve days of growth. **(D)** The total length of all lateral roots for *clo7* and the over-expressor lines treated with 1 µm ABA; control plates are not shown, control plants showed no significant differences in lateral root lengths between the genotypes tested. Rankings determined by Tukey's *post-hoc* test ($p \leq 0.05$) and values that do not share a common letter are significantly different.

CLO7 has no effect on lateral root formation in response to ABA

Unlike *RD20/CLO3*, *CLO7* has no effect on lateral root (LR) development in response to ABA (Figure 3C and D). When the *clo7* mutant and over-expression lines (35S:*CLO7*, 35S:*CLO7/clo7*) were treated with 1 µm ABA the overall length and number of lateral roots were the same as those of the wild-type plants (Col, Figure 3C and 3D). ABA treatment causes an overall reduction in the number of lateral roots as well as the length of the LRs, and the *CLO7* transgenic lines and single mutant displayed the same marked effects with an overall

reduction in LR development (Figure 3C and 3D). The *clo7* mutant and 35S:*CLO7* over-expression lines also had no effect on root architecture under control conditions (Figure 3C and 3D). These data suggests that the two gene family members, *RD20/CLO3* and *CLO7*, are not functionally redundant relative to the control of lateral root development in response to ABA treatment.

RD20/CLO3 and CLO7 interact with each other and are capable of forming homodimers

Protein-protein interaction assays showed that both RD20/CLO3 and CLO7 can form homodimers with themselves, or they can interact with each other forming a heterodimer. The use of a yeast two-hybrid (Y2H) assay initially revealed that RD20/CLO3 and CLO7 can interact with themselves by tagging the N- and C-terminal portions of the proteins to the activating domain (AD) and binding domain (BD) of the GAL4 promoter. The RD20/CLO3 N-terminal domain was able to interact with itself and withstand 40 mM of 3-AT, a competitive inhibitor of histidine biosynthesis, indicating a strong binding affinity to form a homodimer (Figure 4A and 4B). The RD20/CLO3 N-terminal domain also interacted with the C-terminal domain and was able to withstand 40 mM 3-AT (Figure 4A). The RD20/CLO3 C-terminal domains were also able to interact however they were unable to withstand even 1 mM 3-AT (Figure 4A). Similarly, the CLO7 N-terminal was able to form a homodimer and the CLO7 N-terminal domain was able to interact with the C-terminal domain, and these interactions were able to withstand 10 mM 3-AT which indicates a moderate binding affinity (Figure 4B). The CLO7 C-terminal domain could interact with itself however it also could not withstand even 1 mM 3-AT (Figure 4B).

When the CLO7 N-terminus was fused to the AD domain and the RD20/CLO3 N-terminal domain was fused to the BD domain the two proteins interacted and withstood 50 mM 3-AT, indicative of a strong binding affinity between the two caleosins (Figure 4C). The same result was seen when the CLO7 C-terminal portion was fused to the AD domain and the RD20/CLO3 N- terminal portion was fused to the BD domain (Figure 4C). The C-terminal domains did not interact with each other (Figure 4C).

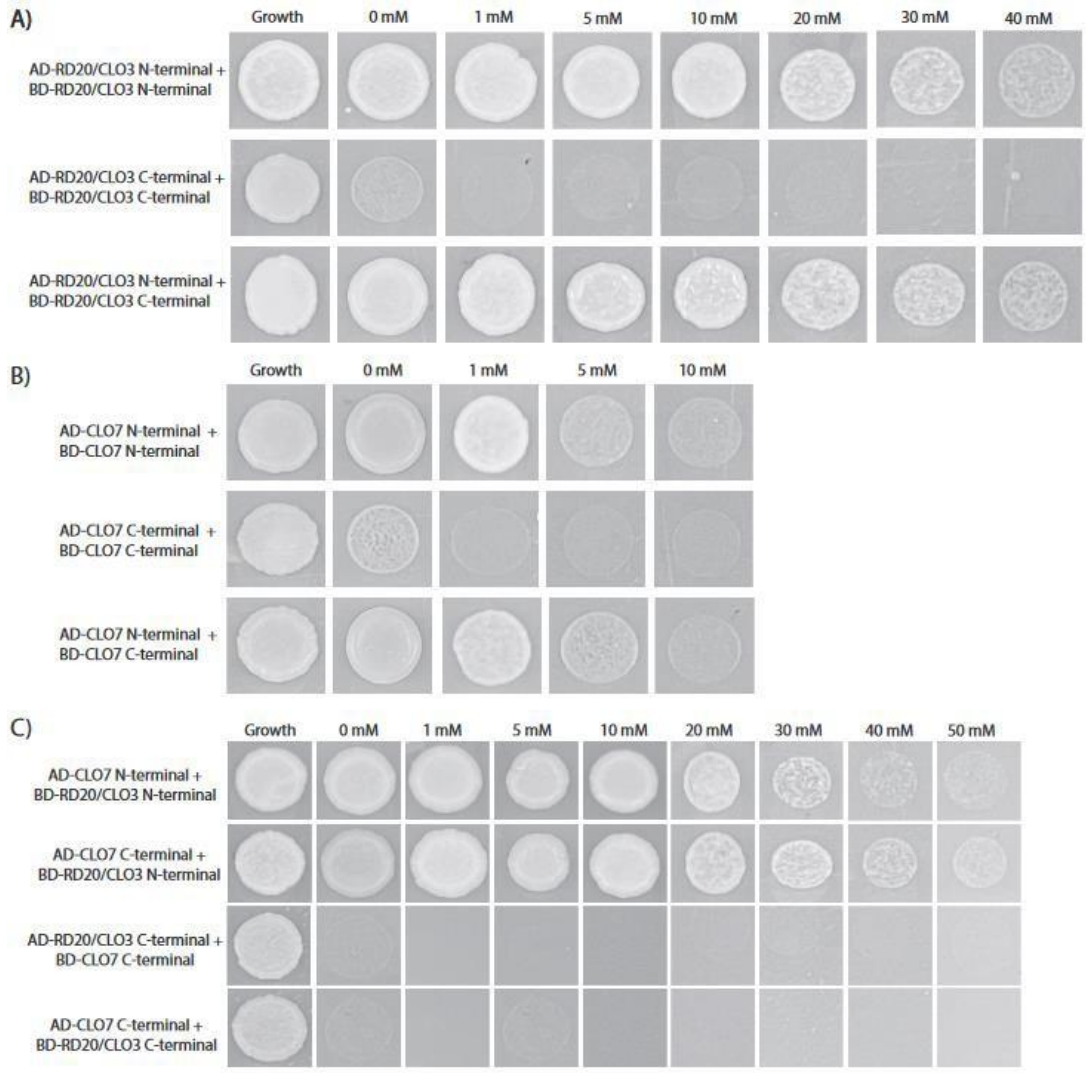

Figure 4. Yeast two-hybrid assay showing the homodimer and heterodimer formation between RD20/CLO3 and CLO7. **(A)** RD20/CLO3 N-terminal and C-terminal domains fused to the AD and BD domains. **(B)** CLO7 N-terminal and C-terminal domains fused to the AD and BD domains. **(C)** CLO7 N-terminal and C-terminal domains fused to the AD and BD domains and RD20/CLO3 N-terminal and C-terminal domains fused to the AD and BD domains. Growth indicates the presence of both the AD- and BD-caleosin fused constructs. The rows with mM concentrations represent the concentration of 3-AT.

By the use of bimolecular fluorescent complementation (BiFC) the full-length proteins showed a similar result in that they are able to form homo- and heterodimers (Figure 5). The

RD20/CLO3-N-YFP interacts with the RD20/CLO3-C-YFP and the interaction is localized to the tonoplast which can be seen with co-localization with an mCherry-fused tonoplast marker (the C-terminus of c-TIP, an aquaporin of the vacuolar membrane) (Figure 5A). The CLO7-N-YFP fusion interacts with the CLO7-C-YFP fusion and this interaction is also localized to the tonoplast (Figure 5C). Lastly, the RD20/CLO3-N-YFP fusion interacts with the CLO7-C-YFP fusion at the tonoplast (Figure 5B). These results corroborate the results seen in the Y2H assay and indicate that CLO7 and RD20/CLO3 form homo- and heterodimers which localize to the tonoplast. During the BiFC assay, large punctate structures which appear to be vesicles were identified and overlap with the Nile Red lipophilic stain suggesting the puncta have lipid membranes (Figure 5D-F). The vesicle structures appeared when CLO7 formed a homodimer, during its interaction with RD20/CLO3, as well as in the interaction of RD20/CLO3 with itself (Figure 5D-F).

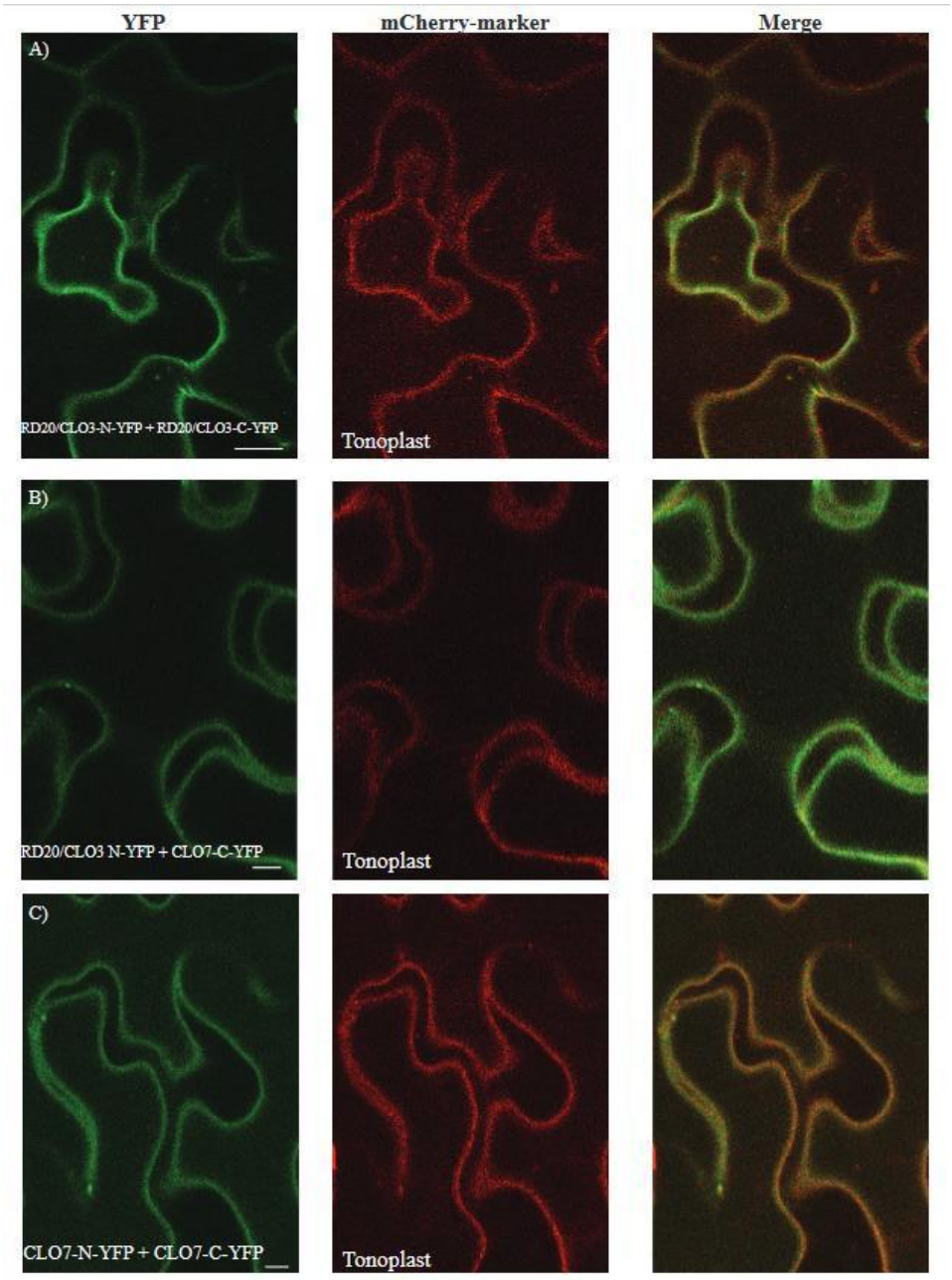
YFP
mCherry-marker
Merge
A)
RD20/CLO3-N-YFP + RD20/CLO3-C-YFP
Tonoplast
B)
RD20/CLO3 N-YFP + CLO7-C-YFP
Tonoplast
C)
CLO7-N-YFP + CLO7-C-YFP
Tonoplast

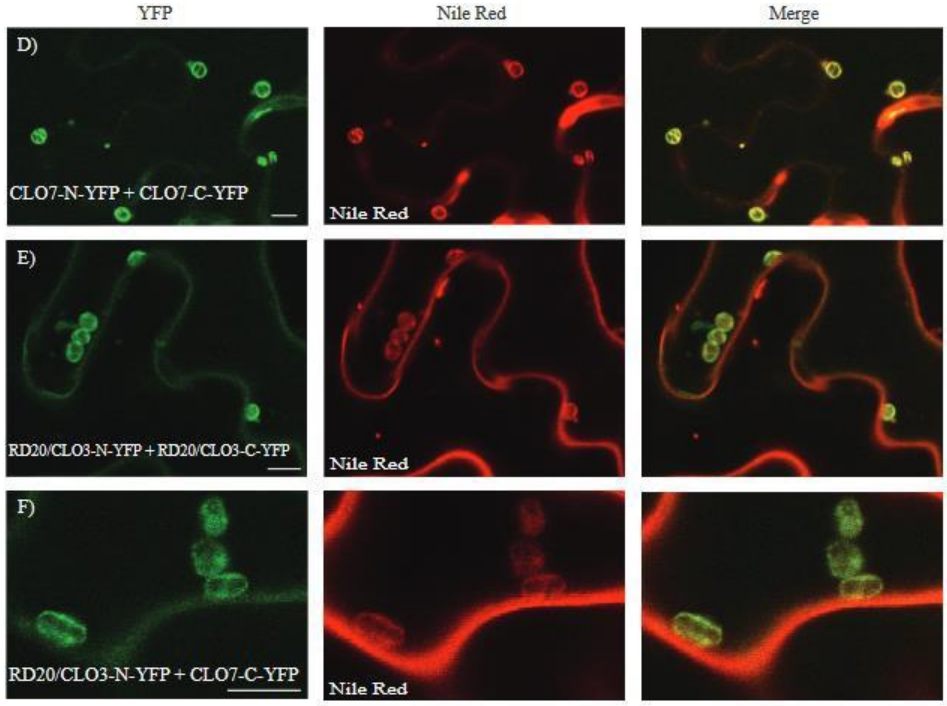

Figure 5. BiFC assay for the homodimer and heterodimer formation of RD20/CLO3 and CLO7. **(A)** RD20/CLO3-N-YFP and RD20/CLO3-C-YFP interaction taking place at the tonoplast as seen with the merge/overlap with the tonoplast-mCherry marker. **(B)** RD20/CLO3-N-YFP and CLO7-C-YFP interaction at the tonoplast. **(C)** CLO7-N-YFP and CLO7-C-YFP interaction at the tonoplast. **(D)** CLO7-N-YFP and CLO7-C-YFP interaction stained with Nile Red, the lipophilic stain showing puncta/vesicle formation. **(E)** RD20/CLO3-N-YFP and RD20/CLO3-C-YFP interaction stained with Nile Red. **(F)** RD20/CLO3-N-YFP and CLO7-C-YFP interaction stained with Nile Red. Bar = 10 µm.

RD20/CLO3 **and** ***CLO7*** **affect bolting times**

The *CLO7*-RNAi knock-down in the *rd20/clo3* mutant background and the *RD20/CLO3*-RNAi knock-down in the *clo7* mutant background (*CLO7*-RNAi/*rd20* or *RD20/CLO3*-RNAi/*clo7*) display an early-flowering phenotype under long day conditions (16 h light:8h dark). Both the *CLO7*-RNAi/*rd20* lines tested produced a flowering stem after developing ten leaves and the two *RD20/CLO3*-RNAi/*clo7* lines flowered after developing 11 leaves, whereas the wild-type plants, Col and WS, flowered after developing 21 and 20 leaves, respectively (Figure 6). This trait was tested using a knock-down in either *CLO7* or *RD20/CLO3* expression in a null

rd20/clo3 or *clo7* background since the two single mutants are in different wild-type backgrounds. The single mutants neither delayed nor accelerated flowering; the *clo7* single mutant had 21.5 leaves at flowering and the *rd20/clo3* mutant averaged 20.5 leaves (Figure 6). The *CLO7*-RNAi lines flowered with 21 leaves, and the *RD20/CLO3*-RNAi lines flowered with an average of 20 leaves, which represent times to flowering that are not significantly different than the wild-type plants. Similarly, the *clo7* and *rd20/clo3* single mutants did not differ from the wild-type. The over-expression lines in all backgrounds tested also displayed no differences in number of leaves at flowering (35:*CLO7*, 35:*RD20/CLO3*, 35:*CLO7*/*clo7* and 35:*RD20*/*rd20*) (Figure 6). Only a reduction in both *CLO7* and *RD20/CLO3* resulted in the early- flowering phenotype. This suggests that both *CLO7* and *RD20/CLO3* are redundant for this trait and that one caleosin can compensate for the other.

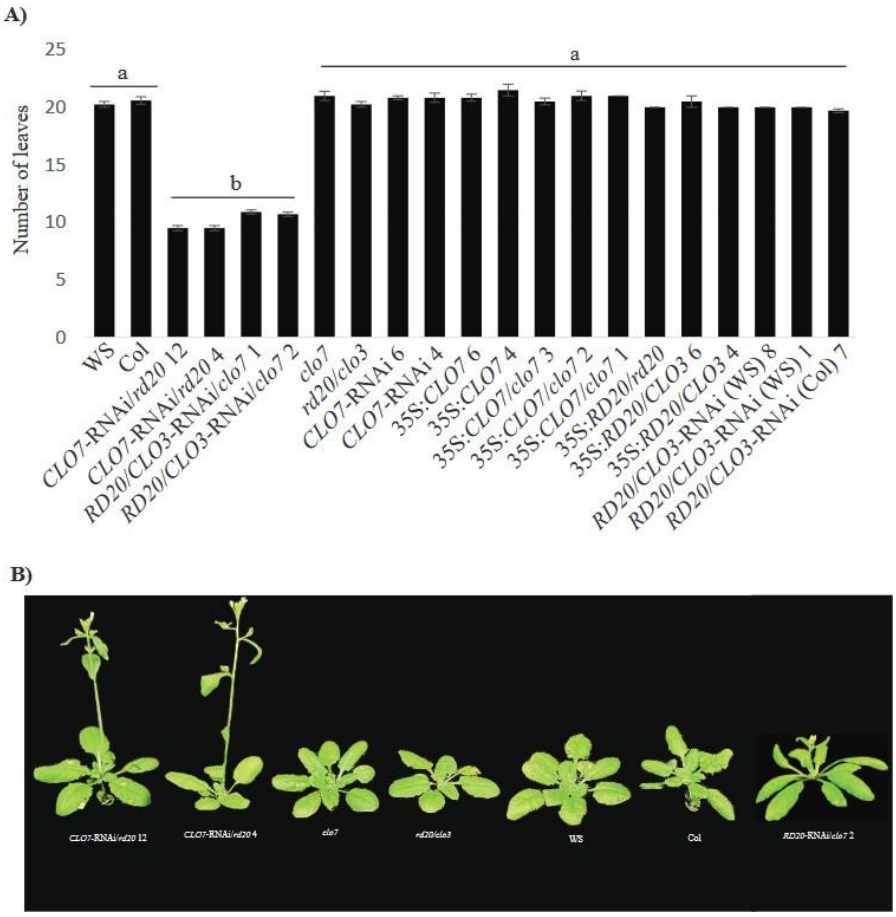

Figure 6. Early-flowering of the *CLO7*-RNAi/*rd20* and *RD20/CLO3*-RNAi/*clo7* compared to the wild-type plants, WS and Col, as well as the single gene mutants, *rd20/clo3* and *clo7,* gene over-expression and knock-down (RNAi) lines. **(A)** Number of leaves at flowering. **(B)** Images

of the wild-types, WS and Col, *rd20/clo3* and *clo7* single mutants, as well as the *CLO7*-RNAi/ *rd20* and the *RD20:*RNAi/*clo7* plants approximately 11 days after planting. The letters represent significant differences between genotypes concluded by a Tukey's *post-hoc* test following a one-way ANOVA. Error bars = standard error of the mean.

Discussion

Altered expression of RD20/CLO3 results in altered root architecture

The changes in root architecture observed in the *rd20/clo3* single mutant and the *RD20/CLO3* over-expressor lines in response to ABA treatment indicate that the induction of the wild-type allele of *RD20/CLO3* would be expected to suppress lateral root development in response to stress. ABA is a stress hormone released by plants when they are subjected to both abiotic and biotic stress, and ABA is known to cause a decrease in the number of lateral roots (Signora et al., 2001; De Smet et al., 2003). Our results show that the *rd20/clo3* plants have an increase in the total number of lateral roots suggesting that *RD20/CLO3* affects the initiation of lateral roots in response to ABA, and when *RD20/CLO3* is not present the plant is less sensitive to the inhibition of ABA lateral root development. Thus, *RD20/CLO3* appears to be a negative regulator of root initiation when there is an increase in ABA levels in the root tissue.

The ABA-induced expression of *RD20/CLO3* in the matured lateral root elongation zone suggests a role in regulating the elongation of the lateral roots in response to stress, a notion that is strongly reinforced by the examination of root architecture. The formation of lateral roots is regulated by a delicate balance involving proliferation of matured pericycle cells into lateral root primordia (LRP) combined with re-differentiation to create new organs (Malamy and Benfey, 1997). The process of lateral root development has been characterized in eight stages, with the beginning stages involving the differentiation of a small number of founder cells at the pericycle which then develop into lateral root primordia (LRP). It isn't until the emerged LRP are extended 10 cells out of the epidermis that it can be considered a matured lateral root (LR), and therefore matured lateral roots are any LRs that are longer than 10 cells and visible to the naked eye (Malamy and Benfey, 1997). The *rd20/clo3* mutant has fewer LR primordia when subjected to ABA which corroborates the fact that the mutant also had more emerged LRs. These data sugge-

sts that the *rd20/clo3* mutant had more primordia develop into matured LRs compared to the wild- type plants. RD20/CLO3 is an interactor of GPA1 (Brunetti et al., 2021), the Gα subunit of the heterotrimeric G protein complex, and the heterotrimeric G-proteins have been shown to play a role in root development in response to ABA. Genetic analysis of the *RD20/CLO3* and *GPA1* single and double mutants did not indicate that they are acting in the same signaling pathway for lateral root development (data not shown).

The *rd20/clo3* mutant also has significantly longer lateral roots when compared to the wild-type, suggesting *RD20/CLO3* is a negative regulator of elongation in matured lateral roots. The induction pattern of the *RD20/CLO3*promoter:*GUS* reporter in the elongation zone of lateral roots, and the low level of expression throughout some of the root system and the primary root tip (Figure 1A and B), are consistent with a role for *RD20/CLO3* as an inhibitor of lateral root elongation. It is also worth noting that lateral roots that underwent initiation and emerged but did not elongate did not show expression in the GUS studies. However, long-term ABA treatments of 15 days or longer indicated that *RD20/CLO3* expression decreases and eventually becomes undetectable.

The initial induction of *RD20/CLO3* in the primary root tip is yet to be understood since there were no significant differences in primary root length when subjected to ABA. Although Aubertet al. (2010) didn't observe expression of *RD20/CLO3* in the roots, this was likely due to the limited number of environmental conditions under which expression was tested in that study. Currently, *RD20/CLO3* appears to be the sole caleosin that is induced in response to abiotic and biotic stress and its role in the larger framework of stress response is still to be elucidated.

A deficiency in both RD20/CLO3 and CLO7 results in an early-flowering phenotype

When either *CLO7* or *RD20/CLO3* expression is knocked-down and *CLO7* or *RD20/CLO3* are null the plants display an early-flowering phenotype under long day conditions. Neither the single *rd20/clo3* or *clo7* mutant nor the *CLO7*-RNAi and *RD20/CLO3*-RNAi lines show altered flowering time. Thus it appears that *RD20/CLO3* and *CLO7* act redundantly in affecting flowering time. In Arabidopsis, flowering consists of at least three flowering pathways; the long-day, autonomous and vernalization pathways (Koornneef et al., 1998a; Levy and Dean, 1998; Mouradov et al., 2002; Simpson and Dean, 2002). Within these flowering networks there are three important genes, SUPPRESSOR OF OVEREXPRESSION OF CO 1 (SOC1), Flower Locus T (FT) and LEAFY (LFY), which act as flowering pathway integrators.

The *RD20/CLO3* overexpression lines have been shown to have increased levels of *LFY* (Blée et al., 2014). *LFY* regulates floral meristem identity and if it is over-expressed it causes early-flowering, and *LFY* expression has been known to be altered by genes in the long-day pathway (Nilson et al., 1998, Blázquez and Weigel, 2000; Blázquez et al., 1998; Weigel and Nilsson, 1995; Moon et al., 2003). However, the increase in *LFY* seen in the *RD20/CLO3* over-expression lines suggests that the mutant would have reduced levels; this would imply delayed bolting which is the opposite of the phenotype recorded here. It is possible that a reduction in *CLO7* affects the levels of either *LFY* or one of the other flowering genes mentioned above. Therefore, the *rd20/clo3* mutant may have reduced levels of *LFY* and the reduction in *CLO7* reduces or increases the levels of another key flowering-time gene and together the effects result in early-flowering times. However, this rationale is less likely since RNA-Seq data shows a down-regulation of *RD20/CLO3* in a *soc ful* double mutant and a down-regulation of *CLO7* in an *early flowering 6 relative of early flowering 6* (*elf6 ref6C)* double mutant (Supplementary Table 1 and 1a). As previously mentioned, *SOC1* is a floral transition gene and *FUL* acts in the same way as *SOC1* and both of these genes are involved in the long-day flowering pathway. *ELF6* is a repressor of the photoperiod pathway and *REF6* is a repressor of FLOWERING LOCUS C (*FLC)*, with *FLC* being the main gene of the autonomous flowering pathway (Noh et al., 2004). *FLC* inhibits *SOC1* and in turn inhibits flowering, therefore an important role of the autonomous pathway is to repress *FLC* (Noh et al., 2004). It is possible that both *RD20/CLO3* and *CLO7* are needed to affect flowering time since they appear to be affected by genes in both the photoperiod and autonomous flowering pathways.

Aside from flowering time genes, plant hormones play a role in the transition to flowering. Gibberellic acid (GA) is an important hormone that controls flowering, most specifically under short-day conditions. For GA signaling, once GA binds the receptor, two genes are affected, SPINDLY (SPY) and PHOTOPERIOD RESPONSE 1 (PHOR1) (Mouradov et al., 2002). SPINDLY (SPY) is a gene identified as a negative regulator of GA signaling and mutations in the *spindly* (*spy*) gene have been shown to cause constitutively active GA signaling, which in turn causes early-flowering under both short and long days. PHOR1 has the opposite affect and causes a delay in flowering (Qin et al., 2011). *RD20/CLO3* over-expression plants had a down-regulation of GA-deactivating genes, suggesting an accumulation of GA which may be a cause for the early-flowering phenotype seen with the P35S:*RD20/CLO3* (Blée et al., 2014). However, RD20/CLO3 alone was unable to affect flowering under long-day

conditions, implying that the GA accumulation was not enough to affect long-day flowering (Blée et al., 2014). It is possible that both *RD20/CLO3* and *CLO7* affect the levels of *SPY* and a reduction in both caleosins causes a decrease in *SPY* resulting in early flowering under long-day conditions, however the GA pathway converges on the floral integrator genes but most specifically on *SOC1* (Corbesier and Coupland, 2006), therefore it is more likely that both *RD20/CLO3* and *CLO7* affect the levels of *SOC1*.

Protein-protein interactions between the caleosin RD20/CLO3 and CLO7

The protein-protein interactions tested in this study indicate that RD20/CLO3 and CLO7 are capable of interacting with each other. However, it seems that *RD20/CLO3* regulates stress responses, such as the negative regulation of root growth in response to ABA without genetic interaction with *CLO7.* In contrast to *RD20/CLO3*, the caleosin *CLO7* has no effect on root architecture when subjected to ABA. The tissue localization and timed expression pattern of *CLO7* suggests a role in early development. The lack of expression in the root and localization in combination with the lack of a root phenotype indicates that *CLO7* does not affect this trait with *RD20/CLO3*. Although the caleosins are members of a multi-gene family, these data in combination with the work done on *CLO1* and *CLO4* suggests that these caleosins play very differing roles and that the gene family does not display high functional redundancy. However the early-flowering time phenotype suggests a genetic interaction between *CLO7* and *RD20/CLO3* . In combination with the interaction between RD20/CLO3 and CLO7 resulting in the formation of heterodimers, it also appears that the proteins are capable of forming homodimers. The caleosins are present on the membrane of oil bodies in a network of caleosin, oleosin and stereolosin (Frandsen et al., 1996; Chapman et al., 2012). This network causes the oil body to maintain its structure, and caleosins forming homodimers would not be surprising since the proteins are very close together and this interaction may aid in structure maintenance. The CLO1 protein has been found to be associated with intracellular membrane compartments such as endosomes, Golgi complexes, the tonoplast (vacuolar membrane) and the ER (Purkrtova et al., 2015). It has been suggested that the phospholipid membrane of the oil body becomes associated with the tonoplast membrane of the vacuole while it is expanding (Frandsen et al., 2001). Therefore, the presence of the RD20/CLO3 and CLO7 interactions on the tonoplast appear to be a characteristic

of the caleosin gene family and oil body-associated proteins. The localization of CLO1 to endosomes also suggests that the large puncta seen in the homo- and heterodimer formations, which resembles vesicles, may be endosomes. However, it is more likely these vesicles are the formation of mature oil bodies since they appear to be two vesicles fusing. Taken together, the caleosins RD20/CLO3 and CLO7 play distinct and redundant roles *in planta* and the interactions observed further solidify their roles as oil body-associated proteins.

Chapter 5: **Characterization of the *Esi3*/*RCI2*/*PMP3* gene family in the Triticeae**

Brunetti et al. BMC Genomics (2018) 19:898
https://doi.org/10.1186/s12864-018-5311-8

BMC Genomics

RESEARCH Open

Characterization of the *Esi3/RCI2/PMP3* gene family in the Triticeae

Sabrina C. Brunetti, Michelle K. M. Arseneault and Patrick J. Gulick*

Abstract

Background: Members of the *Early Salt Induced 3* (*Esi3/RCI2/PMP3*) gene family in plants have been shown to be induced in response to both biotic and abiotic stresses and to enhance stress tolerance in both transgenic plants and *Saccharomyces cerevisiae*. *Esi3* was first identified as a salt stress induced gene in the salt tolerant wild wheat grass, *Lophopyrum elongatum*, and subsequently homologous genes in many other species were found to be members of the gene family. These include *Arabidopsis thaliana* and *Oryza sativa* where they are referred to as *Rare Cold Inducible 2* (*RCI2*), and *Zea mays* where they are referred to as *Plasma Membrane Protein 3* (*PMP3*). This study characterizes the *Esi3* family members in *Triticum aestivum* and explores the tissue specific expression patterns of the gene family members as well as their response to a variety of environmental stresses.

Results: The *Esi3* gene family was found to have a total of 29 family members comprised of ten paralogous groups in the hexaploid *T. aestivum*. Each paralogous group contains three homeologous copies, one in each of the A, B and D genomes with the exception of *Esi3−2* which is missing the B copy. The genes of the *Esi3* gene family were also identified in four other monocot species, *Aegilops tauschii*, *Hordeum vulgare*, *Secale cereale* and *Sorghum bicolor*, and were confirmed or corrected for *Brachypodium distachyon, Oryza sativa* and *Zea mays,* as well as the dicot *Arabidopsis thaliana*. Gene expression of the *Esi3*s was analyzed using tissue-specific, abiotic and biotic stress RNA-Seq 454 sequence libraries and Affymetrix microarray data for *T. aestivum*.

Conclusions: Members of nearly all paralogous groups of the *Esi3* genes in *T. aestivum* have altered gene expression in response to abiotic or biotic stress conditions. In addition, there are modest differences in gene expression among homeologous members of the gene family. This suggests that the *Esi3* gene family plays an important role in the plants response to the stresses presented in this study. The *Esi3−9* in *T. aestivum* has a unique N terminal extension placing it into Group III, a new group for the *Esi3/RCI2/PMP3* gene family.

Keywords: Early salt induced gene family, *Esi3*, Tissue-specific expression, *Rare Cold Inducible 2*, *RCI2*, *Plasma Membrane Protein 3*, *PMP3*, RNA-seq

Background

Members of the *Esi3/RCI2/PMP3* gene family have been shown to be up-regulated by environmental stresses and to contribute to stress tolerance in studies using model species. The *Early Salt-Induced 3* (*Esi3*) gene was initially identified as a salt-stress induced gene in *Lophopyrum elongatum*, a salt tolerant and close relative of bread wheat, *Triticum aestivum* (Gulick et al. 1992). It was reported to be more strongly induced by stress in *L. elongatum* than the less tolerant *T. aestivum* and the intermediately salt tolerant amphiploid derived from a cross between *L. elongatum* and *T. aestivum* (Galvez et al. 1993). A close homolog was also identified as a low temperature induced gene in *Hordeum vulgare* (barley), *Blt101* (Goddard et al. 1993). The genes encode small molecular weight hydrophobic proteins that are members of gene families that have been identified in a wide range of eukaryotic and prokaryotic organisms including more than 150 plant species (Medina et al. 2007). The homologous gene family in *Arabidopsis thaliana*, referred to as *Rare Cold Inducible 2* (*RCI2*) (Rocha 1993), has been shown to be up-regulated by environ- mental stresses such as low temperature, salt and dehydration (Capel et al. 1997; Navarre et al. 2000; Morsy et al. 2005). The eight gene family members in *Arabidopsis* have been divided into two groups; Group I, which encode proteins of 52 to 64 amino acids, and Group II which encode longer proteins, of approximately 60 to 89 amino

* Correspondence: Patrick.gulick@concordia.ca
Biology Department, Concordia University, 7141, Sherbrooke, W. Montreal (Quebec) H4B 1R6, Canada

acids, with longer C terminal hydrophobic extensions which contain charged amino acids (Medina et al. 2007). A homologous gene has also been described in *Saccharomyces cerevisiae*, known as *Plasma Membrane Protein 3* (*PMP3*), the deletion of which resulted in a decrease in plasma membrane potential and caused sensitivity to Na^+ and cytotoxic cations such as tetramethylammonium and hygromycin B. This suggests that this protein contributes to the regulation of intercellular ion homeostasis by controlling plasma membrane potential and preventing excessive Na^+ influx (Navarre et al. 2000). The Arabidopsis *RCI2A* gene was shown to complement the deletion of yeast *PMP3*, indicating that they are functionally interchangeable (Navarre et al. 2000; Morsy et al. 2005; Medina et al. 2001). The *Δpmp3* mutation in *S. cerevisiae* can be complemented by many but not all members of the gene families from other plant species including *Zea mays* (Fu et al. 2012), *Medicago truncatula* (Long et al. 2015), *Oryza sativa* (Morsy et al. 2005) and the alkali grass, *Puccinellia tenuiflora* (Zhang et al. 2008).

Overexpression of *RCI2A* in transgenic Arabidopsis plants was shown to decrease Na^+ uptake, mitigate the salt-induced damage and enhance growth under salt stress conditions (Mitsuya et al. 2006), whereas the disruption of *RCI2A* led to over-accumulation of Na^+ and increased salt sensitivity (Mitsuya et al. 2005) which suggests that RCI2 proteins play major roles in ion homeostasis in response to salt stress. These results were confirmed by experiments in which the *MpRCI2* from plantain, *Musa paradisiaca*, was overexpressed in Arabidopsis (Liu et al. 2012). Overexpression of *RCI2* in *Nicotiana tobacum* increased tolerance to low temperatures (Feng et al. 2009). The overexpression of the *Z. mays* gene *ZmPMP3–1* in the *A. thaliana rci2* mutant background resulted in higher levels of salt tolerance than either the *rci2* mutant or wild type (WT) plants (Fu et al. 2012). In response to NaCl treatment, the transgenic plants showed lower levels of Na^+ accumulation and enhanced K^+ accumulation relative to the mutant or the WT, though the increased K^+ accumulation phenotype was not observed in lines that overexpressed *AtRCI2A* (Mitsuya et al. 2006).

While the mechanisms by which these proteins act are not well known, seven of the *A. thaliana RCI2* proteins (Medina et al. 2007), eight *RCI2*-like proteins identified in *Zea mays* (Fu et al. 2012) as well as several *RCI2*-like genes from *M. truncatula* (Long et al. 2015) have been shown to localize to the plasma membrane when they are transiently expressed as green fluorescent protein (GFP) fusion proteins in onion epidermal cells. The Arabidopsis and *M. truncatula* studies also reported single members of the gene family that were also localized to internal cellular membranes (Medina et al. 2007; Long et al. 2015). The Esi3/RCI2/ PMP3 proteins are not thought to directly affect sodium transporters; combining the *Δpmp3* deletion with the deletion of the two major Na^+ expelling transporters in *S. cerevisiae*, *Δpmr2* and *Δnha1*, increased salt sensitivity of the mutants which suggests that PMP3 does not likely act directly in conjunction with those ion pumps.

The *Esi3/RCI2/PMP3*-encoded proteins are predicted to have two transmembrane domains which alone would not be sufficient to form transmembrane pores, though oligomeric complexes have been hypothesized to have a potential to do so (Rocha 2015). Recent studies carried out with PMP3 in Saccharomyces suggest that it plays a role in plasma membrane organization and is part of the regulatory mechanism for vesicle movement between the plasma membrane and vacuole (De Block et al. 2015). Additionally, it is in- volved in the regulation of levels of phosphoinositides and sphingolipids (De Block et al. 2015).

Members of the *Esi3/RCI2/PMP3* gene families studied in *A. thaliana* and *Z. mays* displayed differential expression in developing tissues and in response to various abiotic stresses, which suggests that they are involved in separate signaling pathways and that those gene family members may play divergent roles (Rocha 2015; Fu et al. 2012; Zhao et al. 2014). The *Esi3*s that were first identified in the highly salt tolerant *L. elongatum* are thought to be members of a small gene family in the genomes of the closely related Triticeae species and to have gene family members represented in the three genomes of hexaploid bread wheat, *T. aestivum*. The allohexaploid genome of *T. aestivum* is the result of two polyploidization events. The first event occurred between the diploid *Triticum urartu* and a species thought to be closely related to *Aegilops speltoides*, which donated the A and B genomes respectively, and which resulted in the tetraploid species *Triticum turgi- dum*. The second allopolyploid speciation event involved a cross between *T. turgidum* and *Aegilops tauschii*, which contributed the D genome and occurred approxi- mately 8000 years ago (Huang et al. 2002; Matsuoka et al. 2011; Khalil et al. 2014). The three genomes have a high degree of synteny and DNA sequence similarity.

Here we report the identification of all homologous sequences of *Esi3* genes within the genome of *T. aestivum*, and analyze the differential expression patterns of these genes. *Esi3* gene family members were identified in cDNA and genomic databases. In addition, gene expression levels in response to stress treatments were characterized from microarray and transcriptome sequence sources. To elucidate the evolutionary relationships between the *Esi3* homologues across plant species, the gene sequence simi- larity was compared to those of other monocot species including *Ae. tauschii*, *Sorghum bicolor*, *Brachypodium distachyon*, *Hordeum vulgare*, *Secale cereale*, *O. sativa*, *Z. mays*, and to the dicot *A. thaliana*.

Results

Esi3 genes in *Triticum aestivum*

Twenty-nine *Esi3/RCI2/PMP3* genes were found in the hexaploid genome of *T. aestivum*. These represent ten paralogous loci in the haploid genome, each with three homeologous copies in the A, B and D genomes with the exception of *Esi3–2* for which the B copy was notidentified (Table 1). In most cases, the sequences of the gene family members were confirmed in three independent sequence databases, the International Wheat Genome Sequencing Consortium (IWGSC) database of genomic chromosomal survey sequences (IWGSC 2014), and the transcriptome shotgun assembly (TSA) and expressed sequence tag (EST) databases for *T. aestivum* at the National Center for Biological Information (NCBI). Additional confirmation of genome assignment and delineation of coding sequences (CDS) were obtained from the databases for other species of the Triticeae tribe. There was no evidence for an *Esi3–2-B* gene copy in the B genome of *T. aestivum* found in the IWGSC genomic sequence database, the EST or TSA databases at NCBI nor in the databases for other B genome-containing species, *T. turgidum* and *Aegilops speltoides*. All members of the gene family had two exons and one intron. Annotations for twenty-four of these gene family members agreed with the most current annotation of the *T. aestivum* genome assembly at the Ensembl Plants database (Enesembl Plants) with the exception of five genes (*Esi3–6-B* and *-D*, *7-B*, *10-A* and *10-D*). The genes that did not agree with our annotations have either extended N terminal domains, mismatches in the protein sequence, or a lack of annotations as protein coding regions; these differences are listed in Additional file 1 Table S1.

Table 1 *Esi3* genes of *Triticum aestivum*

Gene	Genome	EST identifier	TSA identifier	Chromosome	Start Codon[b]	Alignment	Exon 1[a]	Intron	Exon 2[a]	a.a[c]
Esi3–1	A	CJ595172	JP881209.1	4AS	122,736,187	+/–	83	98	82	54
	B	JZ888897.1	JP881208	4BL	424,862,167	+/+	81	98	84	54
	D	CJ697409.1	JP881207.1	4DL	343,061,456	+/+	81	95	84	54
Esi3–2	A	CD881671.1	HAAB01071723.1	4AS	122,627,489	+/–	81	99	84	54
	D	BU099288.1	HAAB01071724.1	4DL	343,088,889	+/+	81	99	84	54
Esi3–3	A	CV767975.1	HP633215.1	5AL	561,693,119	+/+	88	140	134	73
	B	CJ925039.1	JP824371.1	5BL	541,736,786	+/+	88	110	134	73
	D	CJ595273.1	GFFI01135300.1	5DL	444,852,365	+/+	90	119	132	73
Esi3–4	A	CA665474.1	ND	1AS	65,759,553	+/–	84	161	84	55
	B	CJ901293.1	JV986506.1	1BS	108,210,663	+/–	84	162	84	55
	D	CJ685142.1	JV989019.1	1DS	66,987,844	+/–	84	191	84	55
Esi3–5	A	BE497086.1	HAAB01033003.1	2AS	100,129,674	+/–	90	93	84	57
	B	CN010305.1	JV846264.1	2BS	152,175,965	+/–	90	105	84	57
	D	CJ854183.1	HP629889.1	2DS	100,318,450	+/–	90	140	84	57
Esi3–6	A	CJ671046.1	HAAB01051397.1	7AL	692,509,547	+/–	93	110	138	76
	B	CJ562290.1	HAAB01051396.1	7BL	679,884,026	+/–	96	136	138	77
	D	CJ559253.1	HAAB01051398.1	7DL	600,502,457	+/–	96	123	138	77
Esi3–7	A	BJ261574.1	GFFI01140352.1	7AS	102,537,985	+/–	96	109	135	76
	B	CJ725702.1	GFFI01052110.1	7BS	55,853,830	+/–	99	96	144	79
	D	CJ825516.1	GFFI01131578.1	7DS	100,281,019	+/–	96	96	132	76
Esi3–8	A	CD909025.1	ND	1AS	42,505,283	+/–	81	95	84	54
	B	ND	HAAB01084472.1	1BS	62,681,663	+/+	81	120	84	54
	D	CJ648786.1	HAAB01084471.1	1DS	42,845,718	+/–	81	115	84	54
Esi3–9	A	ND	HAAB01083453.1	2AL	775,064,923	+/+	240	170	84	107
	B	BJ243843	ND	2BL	785,821,555	+/–	318	171	84	133
	D	BJ243706.1	GAEF01014403.1	2DL	649,781,640	+/–	276	170	84	119
Esi3–10	A	HX161660.1	GFFI01106676.1	5AL	561,688,908	+/+	90	141	126	71
	B	CA611646.1	HAAB01089382.1	5BL	541,683,185	+/+	90	1111	126	71
	D	BJ278420.1	HAAB01084536.1	5DL	444,743,823	+/+	90	984	126	71

Notes: *ND* not determined/not detected. GenBank EST and TSA identifiers are representative. The database has multiple matches for most *Esi3*s

[a]Exon lengths are the CDS, the UTRs are not included

Esi3–9-B has a non-consensus splice site sequence. The *Esi3–9-D and Esi3–10-A* EST has partial coverage

[b]Position (bp) of start codon (ATG) on pseudomolecules on IWGSC RefSeq v1.0 database

[c] a.a - amino acid

All members of the *Esi3* gene family have a core conserved protein sequence encoding two transmembrane domains. The gene family can be delineated into three groups based on the presence or absence of C terminal or N terminal extensions of the CDS. Group I includes five of the paralogous gene sets, *Esi3-1, -2, -4, -5,* and *-8*, which encode proteins of the classical *Esi3/RCI2/PMP3* lengths of 54–57 amino acids with two conserved transmembrane domains. Group II contains four paralogous sets of genes, *Esi3-3, -6, -7*, and *-10* which encode proteins between 71 to 79 amino acids in length that include C terminal extensions between 14 and 20 amino acids similar to the Group II genes described in Arabidopsis and other species (Rocha 2015). These extensions are rich in hydro- phobic amino acids but also contain charged amino acids. Group III contains *Esi3-9-A, -B* and *-D* genes that encode N terminal extensions of 49–79 amino acids relative to the other members of the gene family. These N terminal extensions were rich in hydrophobic amino acids and have charged amino acids distributed throughout, a pattern that is similar to the C terminal extensions seen in *Esi3-3*, *-6, -7*, and *-10*. At the junction between the N terminal extensions and the conserved domains the proteins had runs of five consecutive valines followed by five prolines. Esi3–9-like proteins with long N terminal extensions similar to those described above are not found in Arabidopsis nor in the *Esi3/RCI2/PMP3* gene families in other well characterized species, and so we have designated them as Group III.

The degree of nucleotide sequence similarity for paralogous copies of the *Esi3* genes of *T. aestivum* within the core conserved sequences, excluding the N or C terminal extensions, for paralogous members of the gene family ranged from 62 to 95% (Additional file 2: Table S2). Amino acid sequences among paralogous gene copies ranged between 47 to 93% identity. The three homeologous gene copies for each of the paralogous groups had amino acid sequence identity ranging from 95 to 100%. The Group I genes, *Esi3-1, -2, -4, -5,* and *-8*, had 100% amino acid sequence identity among homeologous copies (Additional file 2: Table S2). Homeologous copies of *Esi3* genes were localized to homeologous chromosomes. The ten paralogous *Esi3* genes were localized to five different chromosomes. Two pairs of genes appear to be in tandem arrangement. The two most similar pairs of paralogs, *Esi3-1* and *Esi3-2*, which share approximately 92% nucleic acid identity, were both localized to chromosome 4. The two genes are approximately 109 kb and 27 kb apart on the short arm of chromosome 4A and the long arm of chromosome 4D, respectively. *Esi3-3* and *Esi3-10* which are approximately 90% identical are roughly 4 kb, 54 kb and 109 kb apart on chromosomes 5A, 5B and 5D, respectively (IWGSC 2014). In the *Ae. tauschii* genome assembly *Esi3-1* and *Esi3-2* are 20 kb apart on chromosome 4, and *Esi3-3* and *Esi3-10* are approximately 57 kb apart on chromosome 5 (Luo et al 2017; aegilops.wheat.ucdavis.edu).

Genes with high sequence similarity to the *Esi3/RCI2/PMP3* gene family members are found in a wide range of plant species including monocots, dicots, and mosses. *Esi3-9*-like genes, which have long N terminal extensions with high sequence similarity, were only identified in other species in the Triticeae. Searches in the GenBank protein databases identified homologous gene family members with similar N termini in *Ae. tauschii, H. vulgare* and *Secale cereale* (XP_020160007.1, BAK07288.1, GCJW01018134.1, respectively; Additional file 3: Table S3) though an *Esi3*-like gene with a long N terminal extension but with low sequence similarity in this domain was identified in the salt tolerant dicot *Eutrema salsugineum* (formerly *Thellungiella halophile,* GBKH01000241.1). *Esi3*s encoding proteins with C terminal extensions, like those of *Esi3-3, -6, -7* and *-10* were found in the EST databases for many other monocotyledonous and dicotyledonous species but not in the moss, *Physcomitrella patens*.

Esi3/RCI2/PMP3 gene family members were also identified in other monocotyledonous species in which the complete *Esi3/RCI2/PMP3* gene families were not previously described. Using the nucleotide collection, EST and TSA databases at GenBank, ten *Esi3* gene family members were identified in two other species of the Triticeae: *Secale cereale* and *Ae. tauschii*. The gene family in *H. vulgare* is comprised of nine members and includes two genes that had previously been reported (Goddard et al. 1993; Khurana et al. 2015). The complete *Esi3* gene family composition is sum- marized in Additional file 3: Table S3. Seven *Esi3/RCI2/ PMP3* gene family members were also identified in *Sor- ghum bicolor*, one of which was reported by Khurana et al., 2015 (Additional file 3: Table S3). Two novel *Esi3/RCI2/PMP3* gene family members were identified in *B. distachyon* in addition to the six gene family members previously described (Rocha 2015). A small number of dis- crepancies were found between the previously described *Esi3/RCI2/PMP3* gene families for *O. sativa* and *Z. mays* and the Ensembl Plants database. There were also a number of differences between our compiled amino acid sequences and the annotation of the genes in BLAST at Ensembl Plants (Ensembl Plants); these are summarized in Additional file 3: Table S3 and Additional file 1: Table S1. Protein sequences for the *Esi3/RCI2/PMP3* gene families for these species can be found in Additional files 4 and 5: Sequences S4 and S5.

Tissue-specific expression of *Esi3* genes

The members of the *Esi3* gene family showed varied tissue-specific patterns of gene expression in both transcriptome and microarray datasets. One transcriptomic analysis of five tissues including developing seed, root,

leaf, stem and inflorescence (Pingault et al. 2015) was assayed for the 29 gene family members; expression levels ranged from 151.8 RPKPM to undetectable (Fig. 1 and Additional file 6: Table S4). Homeologous groups within *Esi3–1, −2, −3, −4, −5* and *−10* had relatively high level of expression compared to *Esi3–6, −7, −8,* and *−9*. Most paralogous groups that were highly expressed had high levels of expression in more than one tissue type. For example, *Esi3–5*, the most highly expressed paralogous group, was highly expressed in the root, leaf and stem. *Esi3–5* was also expressed in the seed and inflorescence but at lower levels. In tissues in which *Esi3* gene expression was detected, all three mem- bers of the homeologous groups were detected, though at different levels, with the exception of *Esi3–10-A*. The genome of origin of the most highly expressed homeolog varied from among the paralogs, for example for both *Esi3–1* and *Esi3–2* the A homeolog was more highly expressed than the B or D copy, whereas for *Esi3–10* the D homeolog was detected at higher levels than its corresponding homeologs in all tissues with the exception of the seed (Fig. 1). The extensive transcriptome analysis of seventy-one tissue types in Azhurnaya Spring Wheat also showed that each paralog has varying expression across the tissue panel (Additional file 7: Table S5) (Ramírez-González et al. 2018). Anther tissue showed relatively high levels of expression of *Esi3– 1-A, Esi3–4-A, -B, −D, Esi3–5-A, −D* and *Esi3–9-A, -B* (Additional file 7: Table S5). *Esi3–8-A* had high levels of expression in different tissues of grains at various stages of development but was undetected in most other tissue types. *Esi3–6* had low levels of expression across all tissue types assayed (Additional file 7: Table S5). *Esi3–5-A, -B* and *-D* had high expression levels in root tissues at differ- ent stages of development with the highest levels in the root at the seedling stage (Additional file 7: Table S5). This extensive analysis indicates that the *Esi3* gene family members have very dynamic tissue specific and develop- mentally regulated patterns of expression.

Tissue-specific expression was also analyzed in a panel of thirteen tissue types (Additional file 8: Figure S1 and Additional file 9: Table S6) assayed by the Affymetrix 61 k wheat microarray dataset described by Schreiber et al., 2009. All paralogous gene family groups were represented on the microarray with the exception of *Esi3–6*. We note that the microarray cannot distinguish between homeologous gene copies in wheat and expression levels were taken as those of homeologous groups that include the A, B and D copy of each paralogous group. The most striking result from the microarray data was the high level of expression of *Esi3–9* in the anthers and its low levels of detection in any other tissue (Additional file 8: Figure S1 and Additional file 9: Table S6). Gene family members *Esi3–1* to *Esi3–5* have relatively high levels of expression in all tissues, a finding that was similar to the RNA-seq data noted above. In addition low

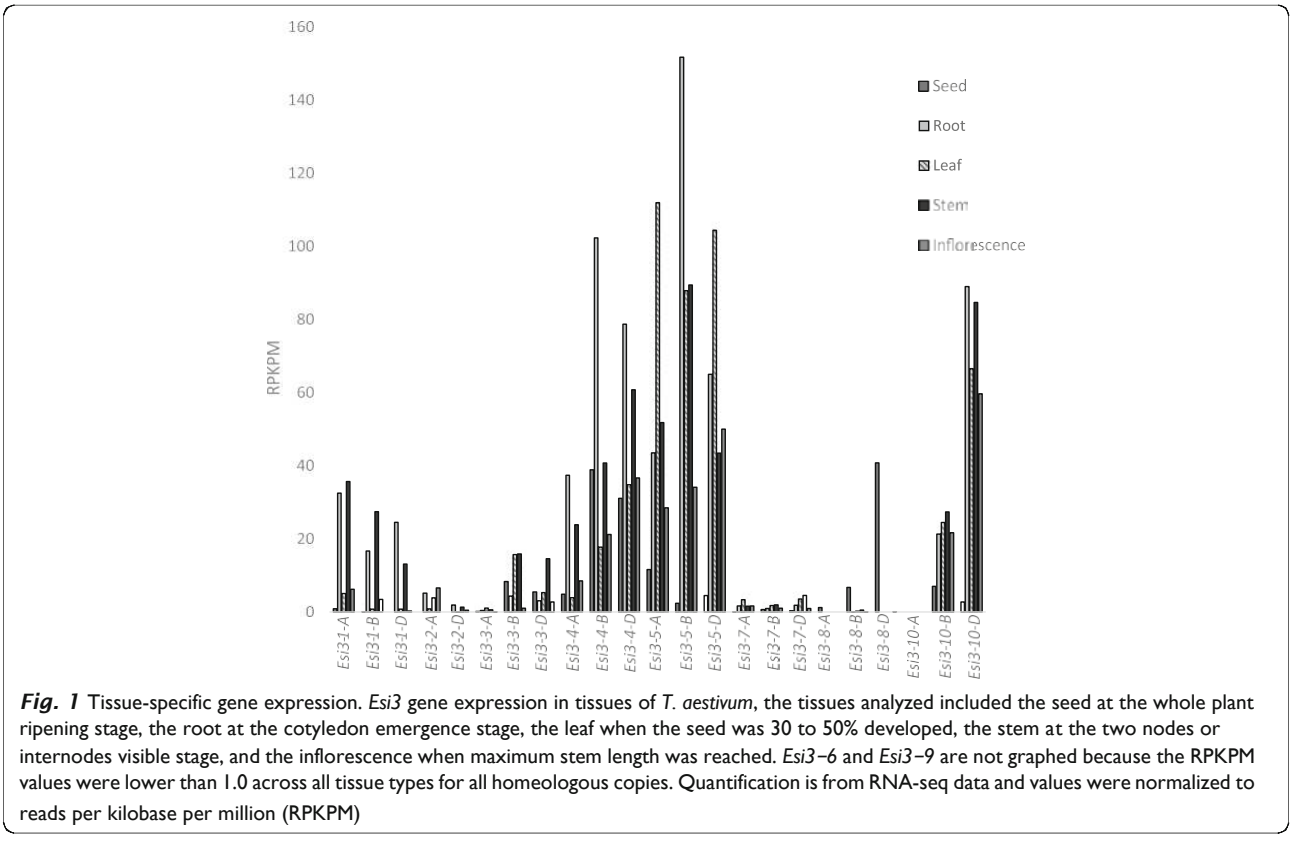

Fig. 1 Tissue-specific gene expression. *Esi3* gene expression in tissues of *T. aestivum*, the tissues analyzed included the seed at the whole plant ripening stage, the root at the cotyledon emergence stage, the leaf when the seed was 30 to 50% developed, the stem at the two nodes or internodes visible stage, and the inflorescence when maximum stem length was reached. *Esi3–6* and *Esi3–9* are not graphed because the RPKPM values were lower than 1.0 across all tissue types for all homeologous copies. Quantification is from RNA-seq data and values were normalized to reads per kilobase per million (RPKPM)

levels of expression of *Esi3–1*, *−8* and *−10* were detected in the anthers, and there were low levels of expression of *Esi3–2, −3* and *−9* in the immature inflorescence. *Esi3–3* showed low levels of expression in the caryopsis 3–5 days after pollination. *Esi3–7* and *Esi3–10,* overall have very low levels of expression across all tissue types assayed.

Expression of *Esi3* genes under drought and temperature stress conditions

The *Esi3* gene family's expression in leaf tissue in response to osmotic stress and high temperature identified five homeologous groups of the gene family that had significant changes in expression (Fig. 2 and Additional file 10: Table S7). Transcriptomic data from Liu et al., 2015 characterized global changes in gene expression in response to short term osmotic stress treatment with PEG and high temperature treatments in seedlings grown on petri dishes. The experiments revealed a strong induction of gene expression for members of the homeologous groups *Esi3–1* and *−3*, and modest induction of *Esi3–2, −4,* and *−7*. All three homeologs of *Esi3–1* were up-regulated more than two fold by one hour of osmotic stress and up-regulated over 20 fold by six hours of stress. The *Esi3–1-A* copy had the highest level of expression in control conditions and was induced 20 fold with six hours of osmotic stress, whereas the B and D copies of the gene had much lower levels of expression in the control plants but were induced 44 and 89 fold, respectively. Nevertheless, the *Esi3–1-A* copy had the highest absolute level of expression in the stressed plants. The *Esi3–1* homeologs were down-regulated by heat treatment and by combined osmotic stress and heat treatment of one hour, however the A copy of the gene was induced two fold by six hours of the combined heat and osmotic stress treatment (Fig. 2 and Additional file 10: Table S7). Similarly, the *Esi3–3-B* copy was highly up-regulated under six hours of osmotic stress. All homeologs of *Esi3–5* had relatively high levels of expression in control conditions, and were down-regulated by drought, up-regulated by heat treatment and up-regulated by combined drought and heat treatment (Additional file 10: Table S7). Alternatively, all homeologs of *Esi3–2* were highly induced after 6 h of drought meanwhile the homeologs are unaffected by the other stress conditions (Fig. 2). *Esi3–10-D* was up-regulated 5 fold after six hours of mixed heat and drought stress, compared to the 0.5–2-fold induction under the other conditions (Additional file 10: Table S7). *Esi3–4* and *Esi3–7* were moderately up-regulated by drought, heat and combined drought and heat treatment (Fig. 2). Most of the homeologous members of the *Esi3* gene family responded similarly to stress conditions, though the absolute level of expression and the degree of change in response to stress varied a few fold among the members of the homeologous groups. The *Esi3* gene family's expression in leaf tissue in response to long term drought and high temperature stress was also analyzed in the microarray datasets for two durum wheat, *T. turgidum*, cultivars that differed in their degree of water use efficiency. The Cappelli cultivar has high water use efficiency and Ofanto has low water use efficiency (Aprile et al. 2013). The abiotic stress regimes were applied to soil-grown plants at booting stage. Though the changes of expression for the *Esi3* genes were generally similar in the two cultivars, there were a few striking differences (Fig. 3 and Additional file 11: Table S8). Cappelli had higher expression of *Esi3–3* under control conditions, though it had higher levels of induction in Ofanto in response to drought treatment. Nevertheless, the resulting levels of expression in Cappelli remained higher than Ofanto after being subjected to drought stress. *Esi3–1* was down-regulated by drought in Cappelli but up-regulated in Ofanto. The drought tolerant cultivar Cappelli had higher levels of expression of *Esi3–8* than the Ofanto cultivar under control, drought and heat treatments, but Ofanto showed *Esi3–8* expression levels similar to Cappelli under mixed drought and heat treatment. *Esi3–5* was more strongly induced by heat stress in Cappelli than in Ofanto, inversely *Esi3–10* was down-regulated by heat in Ofanto. *Esi3–8* was induced by combined drought and heat treatment in Ofanto. The response to mixed drought and heat treatments was complex, in the case of *Esi3–5* the induction due to heat was similar to the gene induction seen with heat and drought in Cappelli. In other cases, the induction due to treat- ments appears to be partially additive, as in Cappelli's *Esi3–8*, or synergistic in the case of *Esi3–8* and *−5* in Ofanto (Fig. 3 and Additional file 11: Table S8). The differences in changes in *Esi3* expression in the two cultivars in response to heat and drought suggests that drought tolerant genotypes may have adaptive gene expression patterns.

Esi3 gene expression patterns in response to drought were also compared between the *T. aestivum* cultivar Chinese Spring, the tetraploid *T. turgidum* cultivar Creso, and a Chinese Spring genetic line with the partial deletion of the long arm of chromosome 5AL (CS_5AL-10), based on microarray datasets of Aprile et al., 2009. The two species are closely related, the tetraploid *T. turgidum* being an ancestral species to *T. aestivum* and sharing the A and B genomes and genes with approximately 99% sequence identity. The *T. aestivum* cultivar Chinese Spring has higher water use efficiency than the *T. turgidum* cultivar Creso (Aprile et al. 2009) and other studies have shown a general trend for *T. aestivum* to be more drought tolerant than *T. turgidum* (Gavuzzi et al. 2007). The comparison demonstrated different

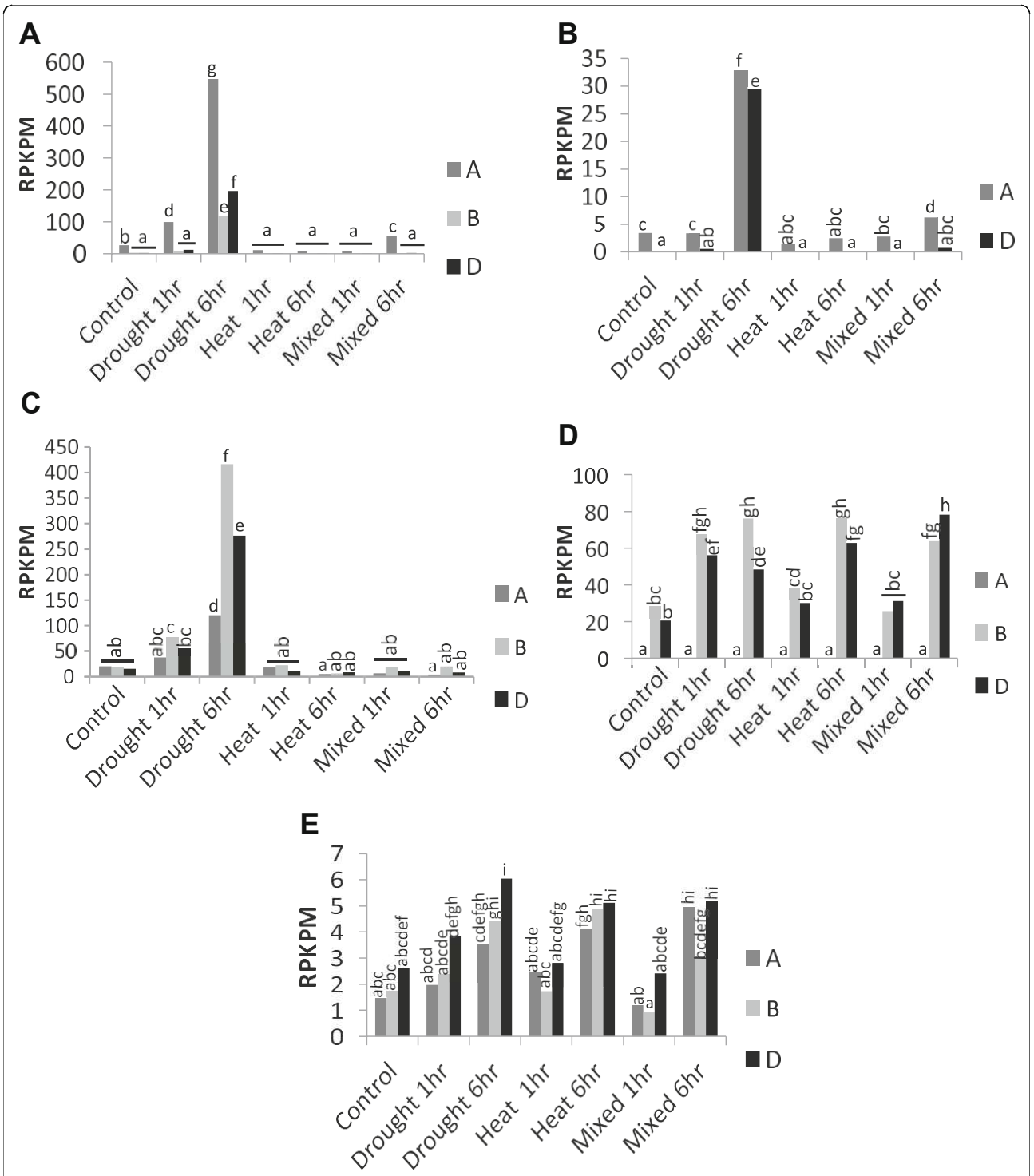

Fig. 2 Short term osmotic and heat stress. *Esi3* gene expression in seedling leaves in response to drought, heat, and combined drought and heat at 1-h and 6-h treatment times. Measurements are based on RNA-seq data. Gene expression differences for a *Esi3−1*, b *Esi3−2*, c *Esi3−3*, d *Esi3−4*, and e *Esi3−7* are represented in reads per kilobase per million (RPKPM). *Esi3s* with significant expression changes are shown. Letters signify Duncan's multiple range values

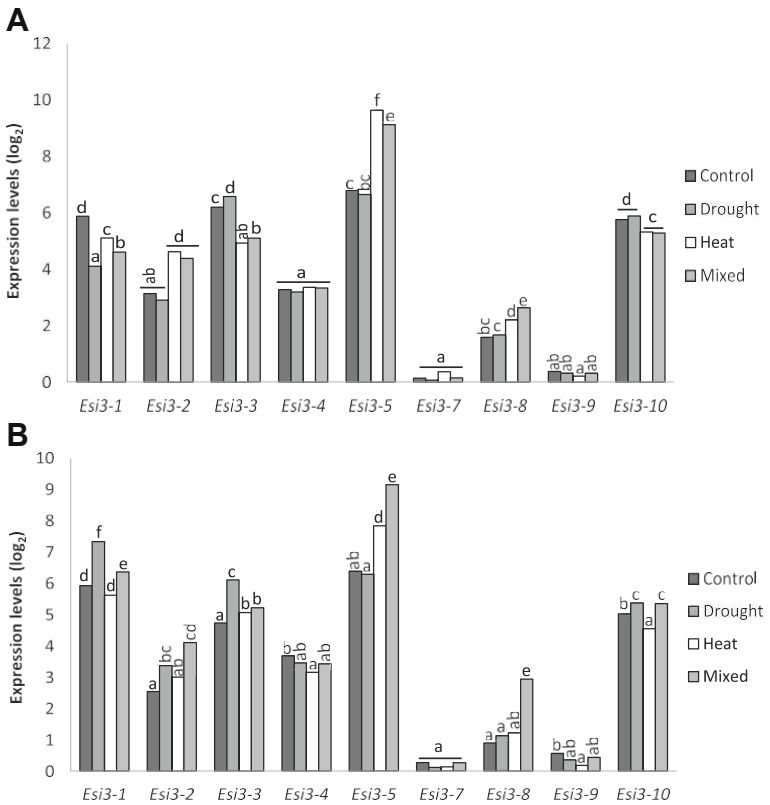

Fig. 3 Long term drought stress. *Esi3* expression in response to drought, heat and both stresses combined compared between (a) Cappelli an efficient water use line and (b) Ofanto a water use inefficient line. Data is from Affymetrix microarray analysis. Values are in log_2 units, thus an increase by 1 unit represents a two-fold increase, background of 3.4 subtracted from each value. Conditions were those described in Aprile et al., 2013 [31]; in brief, plants were stressed at booting stage by withholding water to 12.5% soil water content. Heat treatment was done by incremental increases to 40 °C, and the combined treatment used the same two conditions. Letters signify Duncan's multiple range values

responses to drought stress for *Esi3*s in these two closely related species (Fig. 4 and Additional file 12: Table S9). *Esi3-1* and *Esi3-3* had significantly higher constitutive levels of expression in Creso than in Chinese Spring. *Esi3-10* only has generally high expression levels in Creso and lacks expression in the other cultivars assayed. *Esi3-1* was up-regulated 1.4 fold in Chinese Spring in response to drought treatments, and moderately down-regulated in Creso (Fig. 4 and Additional file 12: Table S9). *Esi3-3* was more strongly up-regulated in Chinese Spring than in Creso. *Esi3-8* has moderately higher levels of mRNA in Chinese Spring in control conditions but it was more strongly induced in Creso than it was in Chinese Spring. Comparisons between Chinese Spring and a derivative genetic line with the 5AL chromosome partially deleted showed a similar induction of *Esi3-1* but showed expression for *Esi3-3* that was approximately 1/10th than that observed in other genotypes (Fig. 4 and Additional file 12: Table S9). The *Esi3-3* and *Esi3-10* genes are located on the long arm of chromosomes 5. Thus the deletion of chromosome 5AL may lower the level of expression for the homeologous group by nature of the deletion of the *Esi3-3-A* and *Esi3-10-A* gene copy. However, the high level of the reduction in expression suggests that it is due to the loss of a regulatory gene on chromosome 5AL that affects the expression of *Esi3-3* and *Esi3-10,* as this chromosome has been reported to contain several genes associated with the response to abiotic stress (Cattivel et al. 2002).

Members of the *Esi3* gene family were also shown to have altered levels of expression in wheat leaf tissue in response to cold treatment (Fig. 5 and Additional file 13: Table S10). *Esi3-1-A, -B* and *-D* copies showed more than 6, 12 and 30-fold increase in expression levels, respectively, as well as high absolute levels of expression in leaf tissue of plants after they were shifted to growth from 23 ° C to 4 °C for two weeks (Fig. 5 and Additional file 13: Table S10) (Li et al. 2015). *Esi3-2-A, Esi3-3-B, Esi3-3-D,* and *Esi3- 10-D* also showed significant increased levels of expression though their absolute levels of expression were lower than *Esi3-1*'s. *Esi3-4-B* and *-D* as well as *Esi3-5-A, -B* and *-D* showed significant reduction in the levels of transcripts in response to cold treatment. In most cases homeologous copies of gene family members responded similarly, they tended to be either all induced or all repressed by cold treatment, though their absolute level

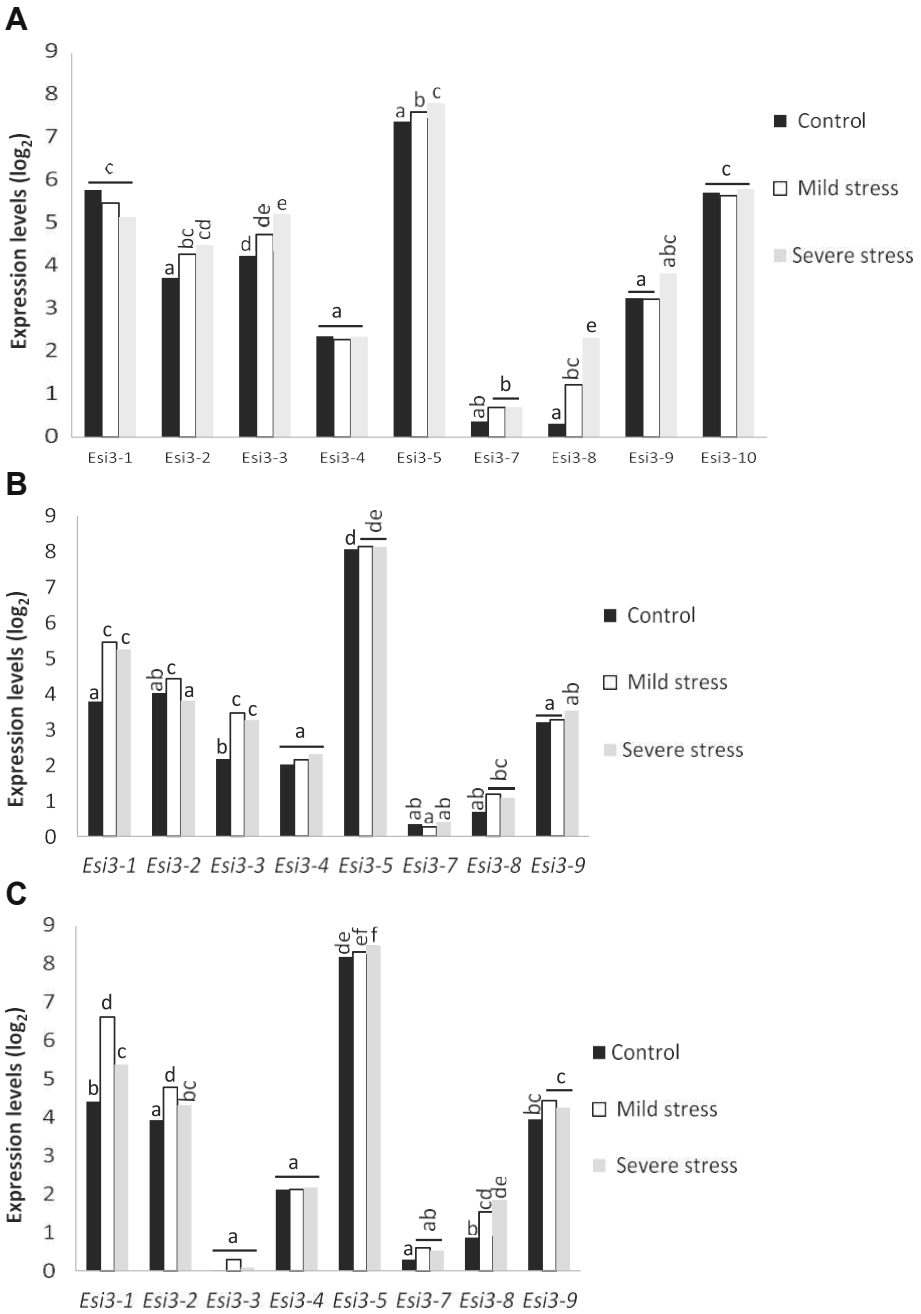

Fig. 4 Long term drought stress. *Esi3* response to mild and severe drought stress in (a) the *T. turgidum* cultivar Creso, (b) the *T. aestivum* cutivar Chinese Spring (CS) and (c) a Chinese Spring line with a deletion in the 5AL chromosome (CS_5AL-10). *Esi3* expression was quantified with Affymetrix microarrays, *Esi3−10* is not represented on CS and CS_5AL-10 graphs since values are zero. Plants were grown as described by Aprile et al., 2009; briefly, soil grown plants were treated at anthesis at different levels of stress: Control field capacity 28% water content, mild stress 18% water content or severe stress at 12.5% water content. Background of 3.3 subtracted from all values, values are in log_2 units. Letters signify Duncan's multiple range values

of expression and the degree of change in expression within homeologous groups varied several fold; in multiple cases the changes in expression for some members of the homeologous groups were not statistically significant.

Fusarium graminearum infection

Analysis of gene expression profiles by transcriptome sequencing for developing spikes inoculated with *Fusarium graminearum* (Steiner et al. 2017) showed striking up-regulation for *Esi3−4-A* and *Esi3−4-D* at 24 and 48h after inoculation. The up-regulation observed in

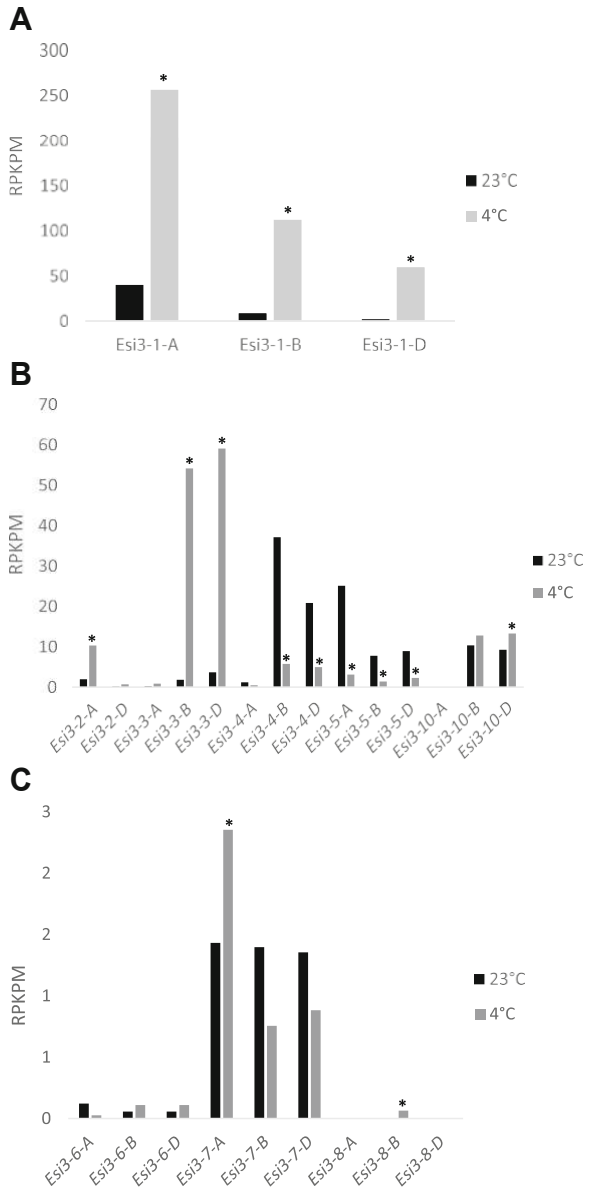

Fig. 5 Short term cold treatment. Gene expression changes in *Esi3* in response to cold treatment at 4 °C. (a) *Esi3−1*, (b) *Esi3−2*, *−3*, *−4*, *-5*, and *−10* (c) *Esi3−6*, *−7*, and *−8* expression in response to cold treatment. The *Esi3s* are separated into three graphs due to large differences in gene expression corresponding to large differences in Y-axis values. *Esi3−9* is not graphed since there was no gene expression detected. * indicates significant changes in gene expression determined by a one-way ANOVA. Values are normalized to reads per kilobase per million (RPKPM)

both the *Fusarium* resistant line NIL 38 and the susceptible line NIL 51 was statistically significant, particularly at 48 h post inoculation (Fig. 6 and Additional file 14: Table S11). *Esi3–5-A, -B*, and *-D* as well as *Esi3–9-A* and *-B* showed higher absolute levels of expression than the *Esi3−4*s, but levels were not significantly changed in response to pathogen inoculation (Additional file 14: Table S11).

However, the D copy for *Esi3−3* was up-regulated 6.5 fold 24 h post inoculation in the susceptible line NIL 51, however there was no induc- tion in the resistant line NIL 38 (Additional file 14: Table S11). In fact, the only tissues in which *Esi3−9* expression was detected was in the spike and, as mentioned above, in the anthers.

Discussion

The members of the *Esi3* gene family identified in *Triticum aestivum* in this study likely represent all members of the family. Whole genome sequencing for *T. aestivum* (IWGSC 2014) and the extensive transcriptome databases for *T. aestivum* and other Triticum species were thoroughly searched for *Esi3*-like sequences. The resulting gene sequence set was verified in the recently released diploid genome for the D genome donor, *Ae. tauschii*, for which the full pseudomolecule sequences for the seven chromosomes are available (Luo et al. 2017). The identification of homeologous genes in the A, B and D genomes for each family member provides additional confidence for the completeness of the searches. The set was compiled and refined through a series of iterative searches, and expanded when it was apparent that there may be members of the family missing from the dataset, such as an absent homeolog or a missing ortholog to a gene family member identified in closely relates species. Orthologs for all members of the *Esi3/RCI2/PMP3* gene family were also identified in closely related diploid species belonging to the Triticeae tribe, *Secale cereale*, *H. vulgare* and *Ae. tauschii*. The high degree of similarity among homeologous gene copies is similar to that described for other gene families in *Triticum aestivum*, alpha tubulins and caleosins, i.e. approximately 97% nucleotide sequence identity and 99–100% amino acid sequence identity for many homeologous sets (IWGSC 2014; Ridha et al. 2007). The degree of sequence similarity among homeologous gene copies is also similar to that among orthologs to the *Esi3* genes in other species of the Triticeae, *H. vulgare* and *Secale cereale*.

The comparison of the structure of the proteins predicted for the gene family members in *Triticum* indicate that species in the Triticeae contain a novel class of Esi3-like proteins in addition to the two groups of *Esi3/RCI2/PMP3* gene family members previously identified in other species (Rocha 2015). *Esi3−9* constitutes a new class of proteins, Group III, characterized by long extensions of coding sequence on their N terminal ends. *Esi3−9*-like genes were also identified in the closely related species *H. vulgare, Secale cereale*, *Ae. tauschii* as well as *T. turgidum*. *Esi3*-like genes with the Group II structure were not iden- tified in Arabidopsis nor in other monocot species sur- veyed which include *Z. mays*, *S. bicolor*, *O. sativa*, and *B. dystachion*. Other genes in the *Esi3* gene family can be

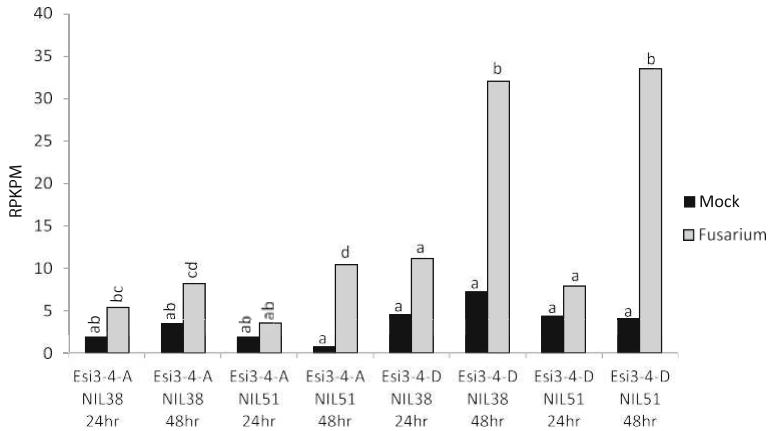

Fig. 6 *Fusarium graminearum* inoculation. *Esi3–4-A* and *Esi3–4-D* changes in gene expression in NIL 38, a disease resistant line and NIL 51, a disease susceptible line, in response to *F. graminearum* inoculation after 24 and 48 h. Letters correspond to Duncan's multiple range values to highlight significant differences in gene expression. Values are normalized to reads per kilobase per million (RPKPM)

classified into groups previously described in other species (Rocha 2015). The *Esi3* genes were dispersed in the genome, however two pairs of genes were found to be localized in tandem. *Esi3–1* was localized near *Esi3–2,* and *Esi3–3* was localized near *Esi3–10* in the A, B and D ge- nomes of *T. aestivum* as well as in *Ae. tauschii*. In *H. vulgare* the *Esi3–1* and *Esi3–2* genes are approximately 200 kb apart, but the species did not contain a copy of *Esi3–3* (Ensembl Plants). Other paralogous *Esi3* genes located on the same chromosomes are quite far from each other. The size of the *Esi3/RCI2/PMP3* gene family is similar in the other species studied; there were ten *Esi3/RCI2/ PMP3* genes in *Ae. Tauschii* and *Secale cereale*, nine in *H. vulgare*, eight in *B. dictachyon,* and *A. thaliana*, seven in *Sorghum bicolor,* 11 in *Z. mays,* and 12 in *O. sativa*. The gene families for *A. thaliana, B. distachyon*, *O. sativa,* and *Z. mays* have been previously described (Rocha 2015).

The phylogenetic tree created with the nine species suggests that there have been independent radiations of the gene family among the monocot species (Additional file 15: Figure S2). Among the Triticeae most gene family members are common, with the exception of *Esi3–2* which is not present in the B genome of *T. aestivum* and *T. turgidum*, which suggests that it was deleted in these lineages (Additional file 16: Figure S3). Overall this pattern indicates that the ten-member gene family evolved to its current number before the divergence of the members of the Triticeae tribe. Though the dicot Arabidopsis has eight members of the *Esi3/RCI2/PMP3* gene family they do not have a close relationship with the gene family members in the Triticeae and other monocot species. The phylogenetic tree suggests that there have been a number of gene duplication events since the divergence of monocots and dicots and there have been additional gene duplication and gene losses since the divergence of *O. sativa, Z. mays, B. distachyon* and the Triticeae.

Accuracy of gene annotation

The importance of manual annotation of gene families is apparent from the miss-annotation of the *Esi3/RCI2/PMP3* gene family members in several full genome annotation databases. This underscores the challenge of perfecting automated annotation of extensive DNA sequence sets. Automated gene annotations are particularly troublesome with genes with short coding sequences such as the *Esi3*s. Some miss-annotations detected in the whole genome database appear to be based on a preference for long open reading frames (ORFs). Several of the miss-annotated loci were identified with incorrect long ORFs that overlapped those of *Esi3/RCI2/PMP3* genes that would encode hypothetical proteins that have no similarity to those in other species. The genome for *S. cereal* is not annotated at Ensembl Plants (Ensembl Plants); these discrepancies are summarized in Additional file 3: Table S3. The annotations reported here relied heavily on the availability of transcript sequences from EST and TSA databases for gene identification and the demarcation of intron/exon junctions. Additional considerations included the detection of open reading frames, sequence and gene structural conservation among family members. We expected sequence similarity among homeologous groups of genes to be higher than 95% in most cases (Khalil et al. 2014; Ridha et al. 2007). When they are available, the transcript sequence is an important consideration in gene annotation. The transcripts in the TSA database were extremely useful because of the exceptional depth of the second generation sequences, as well as the accuracy of their assembly. However, they have a tendency to have excessively long 5′ and 3′ untranslated regions (UTR) sequences that

do not appear to realistically represent the UTRs. These may be due to rare extended transcripts that are detected in the high depth of sequences available from second generation sequencing and that are included in the automated assemblies of transcripts. These extended UTR sequences are generally not seen in the EST databases which have traditionally contained sequences obtained from the Sanger sequencing methods on individual cDNA clones. It is advisable that these two types of transcript sequences remain separated in the public databases.

Expression

Nearly all members of the *Esi3* gene family showed differential expression in response to abiotic or biotic stresses; this differential gene expression is taken as an indicator of the role these genes play in stress tolerance. The constitutive overexpression of select members of the *Esi3/RCI2/PMP3* gene family in Arabidopsis (Fu et al. 2012; Mitsuya et al. 2006; Mitsuya et al. 2005; Liu et al. 2012) and *Nicotiana tobacum* (Feng et al. 2009) have demonstrated that these genes can increase abiotic stress tolerance and reduce Na^+ accumu- lation in transgenic plants. Similarly, the expression of a large number of plant *Esi3/RCI2/PMP3* gene family mem- bers in Saccharomyces demonstrated that they can im- prove salt stress tolerance and complement the deletion of the yeast *PMP3* gene. The studies of Aprile et al., 2009 and 2013 compared wheat cultivars that differed in stress tolerance and water use efficiency and found expression patterns in which higher levels of expression or higher levels of induction paralleled the level of tolerance for the species or genotype. Long term drought treatment showed that *Esi3–1* was more strongly induced in the drought tolerant species *T. aestivum* than in the more sensitive *T. turgidum*. However, the opposite trend was seen for *Esi3–1* when comparing the high water use efficiency *T. turgidum* cultivar, Cappelli, with the low water use efficiency cultivar Ofanto. *Esi3–1* showed decreased expression in Cappelli in response to stress and increased expression in Ofanto (Aprile et al. 2013).

The gene expression datasets explored to characterize *Esi3* gene family members in response to abiotic stresses included a wide range of stress treatments, such as short term and long term osmotic stress, heat, cold treatments and *Fusarium graminearum* inoculation. Plants that were used for these studies were grown under different conditions and analyzed at different stages of growth, including soil-grown plants at flowering stage, seedlings grown in sterile petri dishes and in the case of the Fusarium inoculation, during grain development. Thus the patterns of gene expression were quite diverse; nevertheless, nearly all members of the gene family were shown to be up-regulated in at least one stress condition.

Experiments that were assayed by transcriptome sequencing facilitated the comparison of expression of individual homeologs. In most cases the members of the same homeologous set showed similar gene expression changes, though in some cases these changes were not statistically significant. We point out that most gene expression assays for stress treatments were measured on leaf tissue, whereas studies of tissue-specific expression showed that the *Esi3* gene family members were differentially expressed over a broad range of tissues and developmental stages. If these tissues were evaluated separately a more complex pattern of gene expression in response to stress may be recognized. Indeed, the initial description of *Esi3* differential gene expression was described in the relatively strong induction by salt treatment in the roots of the tolerant species *Lophopyrum elongatum* for the *Esi3–1* gene family member (Gulick et al. 1992).

The *Esi3–9*s had the most unique structural features among the gene family members; they also have the most unique expression pattern. Transcripts for these genes were detected in very few datasets, namely in an RNA-seq datasets from anthers in Triticale and the anthers from the Azhurnaya Spring Wheat (Khalil et al. 2014; Ramírez-González et al. 2018) and in developing seed heads in the experiments that characterized the response to *Fusarium* inoculation of developing spikes.

The widespread differential gene expression of the *Esi3* gene family members in Triticum species in response to abiotic stress suggests that nearly all members of the family may contribute to abiotic stress tolerance. This would merit further investigation through transgenic studies or by comparative expression analysis in genotypes with differing degrees of stress tolerance.

Conclusions

There are twenty-nine *Esi3/RCI2/PMP3* gene family members with ten paralogous groups, each with three homeologous copies in *T. aestivum* except for *Esi3–2* for which no B copy was identified. *Esi3–9*s have an extended N terminal therefore placing it in a group on its own, which has been designated Group III. The other *Esi3*s fall within Group I or II based on amino acid length and properties (Rocha 2015). The gene family members were manually curated and compared to sequences that were annotated automatically and the manually curated sequences were more accurate. This study highlights the importance of manually curating sequences to elucidate gene families and their interrelationships, and for the improvement of automated annotation methods. The *T. aestivum Esi3*s share homology with *Esi3/RCI2/PMP3* genes from *A. thaliana*, *Z. mays*, *O. sativa*, *B. distach- yon*, *Sorghum bicolor*, *Ae. tauschii*, *H. vulgare*, and *Secale cereale*. The ten paralogous *Esi3*s have differential expression in response to a variety of abiotic stresses and in response to infection with *F. graminearum*. The homeologous copies also displayed varied responses to

abiotic and biotic stress, suggesting that the *Esi3* family members play a role in stress tolerance.

Methods

Esi3 gene sequence retrieval

The *Esi3* cDNA sequence from *L. elongatum* (GB Accession U00966.1) and the *Lti6A* and *Lti6B* genes from *Oryza sativa* (Morsy et al. 2005) were used to search the National Center for Biological Information (NCBI) Transcriptome Shotgun Assembly (TSA) databases for *T. aestivum* and *T. monococcum* by Blastn and tBlastn; duplicate hits were eliminated. A total of ten paralogous gene sequences were found, and these were used to search the NCBI EST database and the International Wheat Genome Sequencing Consortium (IWGSC) (IWGSC 2014) wheat survey sequences (WSS) versions 2 and 3 of individual chromosome arms. The sequences were also re-confirmed using the IWGSC whole genome assembly RefSeq v1.0 (Alaux et al. 2018; IWGSC 2018). The latter were used to make chromosomal arm assignments to individual homeologous copies of the gene family mem- bers from the A, B and D genomes of *T. aestivum*. Novel sequences identified in either of these databases were iteratively used to query the TSA and EST data- bases to verify the sequence and delimit exon/intron junctions in the gene sequence. In cases where there was discrepancy between sequences from different databases, contigs were re-assembled with *T. aestivum* EST sequences that shared a minimum of 99% identity using the CAP3 assembly program at prabi (CAP3 assembly). The paralogous set of *Esi3* gene family members were used to identify homologs in other monocotyledonous species, including *Secale cereale, H. vulgare, and Sorghum bicolor* in the GenBank nucleotide collection, TSA and EST databases. *Ae. tauschii* sequences were obtained from the NCBI TSA and nucleotide collection data- bases and from the *Ae. tauschii* Genome release of un- annotated pseudomolecule sequences (*Aegilops tauschii* Genome). *Z. mays* sequences for *Esi3/RCI2/PMP3* genes were taken from those described by Fu et al., 2012 and Zhao et al., 2014; *O. sativa* genes were taken from those re- ported by Morsy et al., 2005 and Medina et al., 2007. Sequences of *Esi3*-like genes for *B. distachyon* were those reported by Rocha 2015 those for Arabidopsis were taken from Capel et al., 1997, and Medina et al., 2007.

Phylogenetic analysis

Phylogenetic trees were constructed using Molecular Evolutionary Genetics Analysis (MEGA) version 7 (Kumar et al. 2007). The *Esi3* homeolog phylogenetic tree was constructed using the nucleotide sequences of the coding regions from all gene family members from *T. aestivum*. The Maximum Likelihood method was used based on the Jukes-Cantor model (Jukes and Cantor 1969) with the same parameters used by Khalil et al., 2014. The analysis involved 29 nucleotide sequences. Codon positions included were 1st+ 2nd+ 3rd+ Noncoding. All positions with less than 95% site coverage were eliminated. That is, fewer than 5% alignment gaps, missing data, and ambiguous bases were allowed at any position. The per- centage of trees in which the associated taxa clustered together is shown next to the branches. There were a total of 165 positions in the final dataset.

The phylogenetic tree and sequence alignment of the *Esi3* homologs in nine species was done using the amino acid sequences. The sequences were aligned using MUSCLE (Edgar 2004) and the phylogenetic tree was constructed using ten paralogous *Esi3* genes from *T. aestivum*, one representative from each homeologous group and the full set of protein sequences from the diploid species *Ae. tauschii, H. vulgare, B. distachyon, Secale cereale, O. sativa, Z. mays, Sorghum bicolor* and *A. thaliana*. The evolutionary history was inferred using the Maximum Likelihood method based on the Whelan And Goldman model (WAG) (Whelan and Goldman 2001). A discrete Gamma distribution was used to model evolutionary rate differences among sites (5 categories (+G, parameter =1.5141)). The analysis in- volved 85 amino acid sequences. All positions containing gaps and missing data were eliminated. There were a total of 54 positions in the final dataset.

Esi3 expression analysis

The *Esi3* gene expression levels in response to abiotic and biotic stresses including drought, heat, combined heat and drought, low temperature and *Fusarium graminearum* infection were determined using Illumina RNA-sequencing libraries listed in the NCBI Sequence Read Archive (SRA) database and then retrieved from the European Nucleotide Archive at EMBL-EBI (Embl-EBI Array) Datasets used for gene expression analysis are listed in Additional file 17: Table S12. The datasets in FASTQ format were converted to FASTA using FASTX Toolkit 0.0.13.2 (Hannonlab.cshl.edu). Due to the high sequence similarity found within the coding region of the *T. aestivum Esi3* sequences, the 3' UTRs from the EST sequences were used to search the datasets using CD-HIT-EST-2D biological sequence clustering algorithm (Fu et al. 2012). The CD-HIT-EST-2D parameters were set to default with the exception of a word size of 5 (n = 5), similarity cut-off of 99% (−c 0.99) and a memory limit of 32G (−M 32000 Mbytes). The expression was normalized to reads per kilobase per million (RPKPM) to normalize for differing library sizes and different 3' UTR lengths among the gene transcripts. The RPKPM was calculated as the number of reads in a library with a minimum of 99% identity to the query sequence/the length of the query sequence/ number of reads in a library/10^6.

Affymetrix microarray 61k RMA normalized datasets (log_2 units) (Schreiber et al 2009) for different wheat tissues at different times of development and to assay gene expression in response to drought, heat, and combined drought and heat stress were retrieved from the PLEXdb database (www.plexdb.org). The differences in fold expression were deduced by comparing the levels of treated samples relative to the levels found within the control measured by fluorescence intensity. The levels of *Esi3* gene expression in response to drought was analyzed using the dataset from Aprile et al., 2009. The effects of drought, heat and combined stress was analyzed using the dataset from Aprile et al., 2013. The *Esi3* expression levels in different tissue types were analyzed using a dataset from Schreiber et al., 2009. Homeologous gene copies in *T. aestivum* cannot be distinguished by the microarray analysis; results were analyzed for the wheat *Esi3* paralogous genes, which represent the combined set of three homeologous genes.

Expression data analysis of the *Esi3* gene family across seventy-one tissue types reported in Ramírez-González et al. 2018 was retrieved from the wheat eFP browser at the University of Toronto BAR (Winter et al. 2007). The identifiers for all *Esi3* gene family members were retrieved from the Ensembl Plants and listed in Additional file 1: Table S1. Data was not avail- able for *Esi3–1-D* as well as for *Esi3–10-A* since the lat- ter has not been identified on Ensembl Plants (https://plants.ensembl.org).

Statistical analysis

The significance of differences in *Esi3* gene expression, in the RNA-seq datasets, was analyzed using a two-way ANOVA to test for significant differences in expression between genotypes in response to treatments and for genotype x treatment interaction effects. Subsequently, the data was analyzed using a one-way ANOVA test with a Duncan's multiple range post hoc test to determine the differences in *Esi3* induction between the A, B, and D copies in response to stress or in differing tissue types. One-way ANOVA was used to test the significance of the differences in *Esi3* gene expression from microarray data. Duncan's multiple range post hoc test was used to determine the significance of differences in gene expression in response to different stress conditions.

Chapter 6: **Characterization and expression of the *Pirin* gene family in *Triticum aestivum*** was first published at Genome *65*(6), 349–362 and can be accessed with the following DOI: https://doi.org/10.1139/gen-2021-0094

Brunetti, S. C., Arseneault, M., and Gulick, P. J. (2022). Characterization and expression of the *Pirin* gene family in *Triticum aestivum*. *Genome*, *65*(6), 349–362. https://doi.org/10.1139/gen-2021-0094

Genome
An International Journal
for Genetics and Genomics

Article

Characterization and expression of the *Pirin* gene family in *Triticum aestivum*

Sabrina C. Brunetti, Michelle K.M. Arseneault, and Patrick J. Gulick

Department of Biology, Concordia University, 7141 Sherbrooke W., Montreal, QC H4B 1R6, Canada

Corresponding author: **Patrick J. Gulick** (email: patrick.gulick@concordia.ca)

Abstract

Pirins are nuclear bicupin proteins, encoded by genes that are one of several gene families that comprise the cupin superfamily in plants. *Pirin* genes have been implicated in stress response pathways studied in Arabidopsis and At-*Pirin1* has been shown to interact with the heterotrimeric G-protein alpha subunit (GPA1). The aim of this study was to identify the members of the *Pirin* gene family in *Triticum aestivum,* to correct their annotations in the whole genome, and gain an insight into their tissue-specific expression as well as their response to abiotic and biotic stresses. The *Pirin* gene family in *T. aestivum* is comprised of 18 genes that represent six paralogous gene copies, each having an A, B, and D homeolog. Expression analysis of the *Pirin* genes in *T. aestivum* Illumina RNA-seq libraries, which included sampling from differing tissue types as well as abiotic and biotic stresses, indicates that the members of the *Pirin* gene family have specialized expression and play a role in stress responses. *Pirin* gene families are also identified in other monocots including *Aegilops tauschii*, *Hordeum vulgare*, *Brachypodium distachyon, Oryza sativa*, *Zea mays*, *Sorghum bicolor*, and the dicot *Arabidopsis thaliana.*

Key words: Cupin superfamily, bicupins, pirins, *Pirin* gene family, *Triticum*

Résumé

Les pirines sont des protéines bicupines nucléaires, codées par des gènes qui appartiennent à l'une de plusieurs familles de gènes que compte la superfamille des cupines chez les plantes. Les gènes *Pirin* ont été impliqués dans les voies de réponse aux stress chez l'Arabidopsis et il a été montré que l'*At-Pirin1* interagit avec la sous-unité alpha de la protéine G hétérotrimérique (GPA1). Le but de cette étude était d'identifier les membres de la famille de gènes *Pirin* chez le *Triticum aestivum*, de corriger leur annotation dans le génome entier et de mieux conprendre leur expression tissulaire ainsi que sur leur réponse aux stress abiotiques et biotiques. La famille de gènes *Pirin* chez le *T. aestivum* comprend 18 gènes, ce qui correspond à six copies paralogues, chacune ayant un homéologue au sein des génomes A, B et D. L'analyse de l'expression des gènes *Pirin* au sein de librairies RNA-seq Illumina du *T. aestivum*, lesquelles étaient préparées à partir de différents tissus de même qu'en conditions de stress abiotiques et biotiques, ont indiqué que les membres de cette famille présentent une expression spécialisée et qu'ils jouent un rôle dans la réponse aux stress. Les familles de gènes *Pirin* sont également identifiées chez d'autres monocoytlédones dont l'*Aegilops tauschii*, l'*Hordeum vulgare*, le *Brachypodium distachyon*, l'*Oryza sativa*, le *Zea mays*, le *Sorghum bicolor* et la dicotylédone *Arabidopsis thaliana*.

Mots-clés : superfamille des cupines, bicupines, pirines, famille de gènes *Pirin*, *Triticum*

Introduction

Gene duplications giving rise to multigene superfamilies are one of the ways that members of the plant kingdom have evolved to adapt to and survive persistent biotic and abiotic pressures. One such superfamily is the cupins, considered to be one of the most functionally diverse supergene families in plants (Dunwell et al. 2004). The cupin superfamily name is based on the conserved β-barrel folds found within the protein sequence; the term "cupa" in Latin refers to a small barrel (Dunwell 1998). The family is characterized by the conserved amino acid sequence (HI/THPRATEI) that is shared between the thermostable wheat protein, germin, and a stress-related protein from the slime mold *Physarum polycephalum* (Dunwell et al. 2004). The members of the cupin superfamily were originally thought to have two highly conserved motifs each with two β-strands separated by an intervening loop (Woo et al. 2000; Dunwell et al. 2004). The conserved motifs were designated as motif 1, $G(X)_5HXH(X)_{3,4}E(X)_6G$ and motif 2, $G(X)_5PXG(X)_2H(X)_3$ N; however, advances in protein sequencing and 3D structuring have recently suggested that the two motifs are less conserved than previously thought (Dunwell et al. 2004). The cupin superfamily is comprised of more than 18 subclasses ranging from, but not limited to enzymes, microbial nonenzymatic

transcription factors, nuclear proteins, hormone-binding proteins, damage repair proteins, and seed storage proteins (Dunwell et al. 2001, 2004). The classification of these subclasses is based on whether the proteins are comprised of a single domain, duplicated (bicupin) domains, or multicupin in which proteins have more than two cupin domains (Dunwell et al. 2004).

Pirins, which are a bicupin subclass within the cupin superfamily, are encoded by small gene families in plants (Dunwell et al. 2004). The Pirin protein can interact with the CCAAT box-binding transcription factor NF1/CTF1 and is an ortholog of the human Pirin (Wendler et al. 1997). The N-terminal half of the human Pirin is believed to be conserved in mammals, plants, fungi, and prokaryotic organisms (Wendler et al. 1997). In humans, roughly 15% of all *Pirin* cDNAs contain short 34-base pair (bp) insertions in the 5^1 untranslated regions (UTR), which indicates an alternate splicing process (Wendler et al. 1997). This 34-bp insertion does not contain a translational start site; however, it does encode an in-frame stop codon, suggesting differences in the 5^1 UTR within the human *Pirin* gene family (Wendler et al. 1997).

Sequence similarity to the human Pirin led to the discovery of the *Arabidopsis thaliana* At-*Pirin1*. The *Pirin* family in Arabidopsis is comprised of four members, designated as At-*Pirin1*–At-*Pirin4*, each containing two cupin motifs, but with At-*Pirin3* and At-*Pirin4* each having a slightly shorter motif 1. At-*Pirin1* was identified as an interactor of the heterotrimeric G*α* subunit, At-*GPA1* (Lapik and Kaufman 2003). The At-*pirin1* mutant phenocopies the *gpa1* mutant for delayed germination and early seedling development, suggesting an increased state of dormancy that is normally alleviated by stratification (Lapik and Kaufman 2003). Similarly, both mutants are hypersensitive to abscisic acid (ABA)-mediated inhibition of seed germination and display delayed cotyledon greening and expansion; according to Lapik and Kaufman (2003), these data suggest that At-*Pirin1* likely functions downstream of *GPA1* in regulating these processes. At-*Pirin1* has been shown to have a five-fold increase in expression in response to ABA and a three-fold increase in expression in response to a single pulse of low-fluence red light (Lapik and Kaufman 2003). At-*Pirin2* was found to play a role in lignin metabolism by suppressing the accumulation of S-type lignin in the stems, since the *prn2* mutant had higher levels of S-type lignin when compared with wild-type (WT) samples (Zhang et al. 2019). At-*Pirin2* was localized to cells adjacent to vessel elements, suggesting a role in noncell-autonomous lignification of xylem vessels (Zhang et al. 2019).

The *Pirin* gene family is found in other dicot species including tomato (*Solanum lycopersicum*), the parasitic plant *Triphysaria versicolor*, and soybean (*Glycine max*) (Bandaranayake et al. 2012). A *Pirin* homolog was also found in the monocot species *Oryza sativa* (rice), and OsPIRIN was found to interact with the Salt-, ABA-, and Drought-Induced RING Finger Protein 1 (OsSADR1), which is an E3 ligase (Park et al. 2018). The interaction between OsADR1 and OsPIRIN mediates the proteolysis activity via the 26S proteasome pathway, resulting in degradation of OsPIRIN (Park et al. 2018). Here, we identified the *Pirin* gene family members in the three highly similar genomes (A, B, and D) of the hexaploid bread wheat, *Triticum aestivum*. The genome of *T. aestivum* developed after two independent polyploidization events, the first involved the A and B genomes' progenitors, the diploid *Triticum urartu* and a species closely related to *Aegilops speltoides*, which gave rise to the tetraploid species *Triticum turgidum*. Approximately 8000 years ago, the second allopolyploidization event involved a cross between *T. turgidum* and the D genome progenitor, *Aegilops tauschii* (Huang et al. 2002; Matsuoka 2011; Khalil et al. 2014).

This study reports all homologous sequences of the *Pirins* in the *T. aestivum* genome as well as their differential expression patterns. The sequence annotations of the *Pirins* in the other monocots, *A. tauschii*, *Brachypodium distachyon*, *Hordeum vulgare*, *O. sativa, Sorghum bicolor*, and *Zea mays*, were also identified and corrected. All sequences were found in both cDNA and genomic DNA sequence sets. The *T. aestivum* Ta-*Pirin* gene expression levels in response to stress treatments were characterized from transcriptome sequence sources. To infer the evolutionary relationships of the homologous plant *Pirins*, the gene sequence similarity was compared between those of other grass species and the dicot *A. thaliana*.

Materials and methods

Pirin sequence retrieval

The Arabidopsis At-Pirin1 amino acid sequence (GB Accession NP_191 481.1) was used to search the National Center for Biotechnology Information (NCBI) Transcriptome Shotgun Assembly (TSA) and NR databases for *Ae. tauschii* genes encoding *Pirin*-like genes. *Aegilops tauschii Pirin*-like sequences were used to search the *T. aestivum* database at Ensembl Plants (http://plants.ensembl.org/index.html) and the International Wheat Genome Sequencing Consortium (IWGSC) databases (IWGSC 2014) for the orthologous *Pirin* genes, each represented by three homeologous copies in the allohexaploid species. The database was also used to assign chromosomal location, chromosome arm, and the intron/exon junction delimitations for the individual homologous gene copies in the A, B, and D genomes. The novel *T. aestivum* sequences were then used to query the TSA and Expressed Sequence Tag (EST) databases for sequence verification. In the case of Ta-*Pirin-2*, there were no EST or TSA sequences to confirm the exon/intron junctions indicated in the whole genome annotations for the three homeologous gene copies; therefore, it was annotated by comparison to *H. vulgare* cDNA (GB accession AK248948.1), *B. distachyon* cDNA (GB accession GFJC01008957.1), and *O. sativa* cDNA (GB accession AK105971.1, BAG97473.1). The *T. aestivum* Pirin amino acid and coding region sequences can be found in File S1.

The *T. aestivum Pirin* genes were also used to identify homologs in the other monocotyledonous species including *H. vulgare*, *B. distachyon, S. bicolor*, *Z. mays*, and *O. sativa* using each species' respective database at Ensembl Plants. All sequences were confirmed using the TSA and EST databases; in some cases, there were differences between gene sequences for the same gene identified in different databases that

suggested misannotation; therefore, contigs were reassembled from EST and TSA sequences at NCBI using the CAP3 assembly program at PRABI (CAP3) (Huang and Madan 1999) (http://doua.prabi.fr/software/cap3). In the cases where multiple gene transcripts were listed for the same gene in the Ensembl Plants database, the TSA and EST databases were used to curate the correct transcript copy. The amino acid sequences for these species can be found in File S2.

Phylogenetic, gene structure, and promoter analysis

The Triticum homeolog phylogenetic tree was created by aligning the coding region nucleotide sequences of the *Pirin* homeologs with MUSCLE using Molecular Evolutionary Genetics Analysis (MEGA) version 7 (Kumar et al. 2007) with the same parameters as Brunetti et al. (2018) using the Maximum Likelihood methods based on the Jukes-Cantor model (Jukes and Cantor 1969). The analysis involved 18 nucleotide sequences, and any positions with less than 95% coverage in the set were eliminated from the analysis, resulting in less than 5% alignment gaps, missing data, and ambiguous bases. There was a total of 975 positions in the final data set. The phylogenetic tree for the Pirin homologs in other species was constructed by aligning the amino acid sequences using MUSCLE as described above and according to Brunetti et al. (2018). The analysis involved 36 amino acid sequences and any position with less than 95% coverage in the set was eliminated. There was a total of 279 positions in the final data set. The bootstrap analysis was set to 100 iterations.

The gene structure was analyzed by comparing the CDS and genomic sequences of the *Pirin* gene family members using the Gene Structure Display Server (GSDS, http://gsds.gao-lab.org/). The promoter analysis was carried out using a 2-kb fragment upstream of the 5^{1} UTR and analyzed using the software on the Plant *cis*-Acting Regulatory Element (CARE) webpage (Lescot et al. 2002) (http://bioinformatics.psb.ugent.be/webtools/plantcare/html/).

Pirin expression analyses

Illumina RNA-sequencing libraries from the NCBI Sequence Read Archive (SRA) database were retrieved and used to measure tissue expression, and responses to abiotic and biotic stresses, which included ABA treatment (25 μm), drought, heat, a combination of heat and drought, low temperature, *Fusarium graminearum* infection, *F. graminearum* coapplied with ABA (1 mM) or gibberellic acid (GA, 1 mM) and infection by powdery mildew (*Blumeria graminis* f. sp. tritici; *Bgt*). The SRA database was used to obtain the identifiers that were then used for the data set retrieval from the European Nucleotide Archive at the European Molecular Biology Laboratory's European Bioinformatics Institute (EMBL-EBI) (EMBL-EBI Array express; https://www.ebi.ac.uk/arrayexpress/). The data set identifiers used in this study can be found in Table S1. The data sets were downloaded, unzipped, converted, and searched using the CD-HIT-EST-2D biological sequencing clustering algorithm according to Brunetti et al. (2018). The nucleotide sequence for each of the *Pirin* genes was used as a query with the CD-HIT-EST-2 D algorithm to search individual RNA-Seq libraries with the stringency requiring a 99% sequence identity to register a hit. The number of hits per library was normalized to reads per kilobase per million (RPKPM) by considering the size of the library and the length of the query sequence. The *Pirin* 3^{1} UTR regions were used in the CD-HIT-EST-2D analysis to ensure distinction between homeologs. The 71-tissue panel in the Triticum spring wheat cultivar Azhurnaya was retrieved from the Wheat eFP Browser (Ramírez-González et al. 2018; Winter et al. 2007) (https://bar.utoronto.ca/efp_wheat/cgi-bin/efpWeb.cgi).

Statistical analysis

The statistical significance of differences in *Pirin* gene expression was calculated using a one-way ANOVA with a Duncan's multiple range post-hoc test. The post-hoc test was used to determine the differences in expression levels of the A, B, and D copies in response to the abiotic and biotic stress conditions analyzed.

Results

Pirin genes in *T. aestivum*

Eighteen *Pirin*-encoding genes were identified in the hexaploid *T. aestivum* genome. These represent six paralogs per haploid genome with a copy from each of the three diploid progenitors of this allohexaploid genome; these copies are referred to as homeologs from the A, B, and D genomes (Table 1). Four of the *Pirin* family members, Ta-*Pirin-1*, Ta-*Pirin-2*, Ta-*Pirin-3*, and Ta-*Pirin-6* are tandemly repeated genes in three clusters on chromosomes 5B, 5D, and 4A (Fig. S1; Table 1). The Ta-*Pirin-4* homeologs are also on chromosomes 5A, 5B, and 5D; however, they are more than 200-Mb distant from the Ta-*Pirin-1*, Ta-*Pirin-2*, Ta-*Pirin-3*, and Ta-*Pirin-6* gene clusters, and were not part of the tandem duplications. Ta-*Pirin-5* is present on chromosomes 1A, 1B, and 1D (Table 1; Fig. S1).

The *Pirin* genes display the trend expected for sequence similarity of wheat homeologous genes; they have nearly identical amino acid sequences and ~97% sequence identity at the nucleotide level. The exceptions are the Ta-*Pirin-2* homeologs; the B and D copies of Ta-*Pirin-2* are 72 and 61 amino acids longer on the N-terminal end than the A copy (Table S2). However, these annotations for the Ta-*Pirin-2* homeologs can be considered to have low confidence, since they cannot be confirmed with transcript sequences and were based on the long open-reading frame (ORF) of the first exon in the genomic sequences. Ta-*Pirin-2-A* and Ta-*Pirin-3-A* do not have corresponding transcript sequences in the EST nor the TSA database at NCBI. Misannotations for the gene family members in the Ensembl Plants database such as truncated or extended N-terminal ends and missing parts of coding regions for the *Pirin* gene family are summarized in Table S2.

The *T. aestivum Pirin* sequences contain two cupin domains, indicative of a bicupin, a characteristic of the *Pirin* gene family (Fig. S2). The members of the *Pirin* gene family are varied in gene structure with the number of exons ranging from four exons in the Ta-*Pirin-4* homeologs to eight

Table 1. *Pirin* genes of *Triticum aestivum*.

Gene	Genome	Chromosome	Start codon*	Alignment	mRNA	CDS	a.a†	Exons	Ensembl Plants identifier	TSA identifier
Ta-*Pirin-1*	A	4AL	619,901,105	+/+	1405	1026	341	6	TraesCS4A02G336200.1	GFFI01048533.1, GILY01013465.1
	B	5BL	693,280,364	+/+	1309	1113	370	5	TraesCS5B02G536000.2	GILY01027417.1
	D	5DL	551,849,778	+/+	1429	1029	342	6	TraesCS5D02G533500.1	GILY01031085.1, GILY01031086.1
Ta-*Pirin-2*	A	4AL	620,011,204	+/+	1225	885	294	5	TraesCS4A02G336000.1	ND
	B	5BL	693,111,750	+/+	1366	1110	369	5	TraesCS5B205535700.3	ND
	D	5DL	551,807,329	+/+	1211	975	324	5	TraesCS5D02G533200.1	ND
Ta-*Pirin-3*	A	4AL	551,764,934	+/−	1252	885	294	5	TraesCS4A02G335900.1	GILY01013453.1
	B	5BL	693,136,332	+/−	1457	1119	372	5	TraesCS5B02G535800.1	GILY01027409.1
	D	5DL	551,765,165	+/−	1398	1134	377	5	TraesCS5D02G533100.1	GILY01031079.1, GILY01031078.1
Ta-*Pirin-4*	A	5AL	476,241,914	+/+	1297	939	312	4	TraesCS5A02G262700.1	GIJS01150985.1
	B	5BL	448,611,465	+/+	1351	918	305	4	TraesCS5B02G261100.1	GILY01025833.1
	D	5DL	376,826,047	+/+	1500	921	306	4	TraesCS5D02G70300.1	GILY01029555.1
Ta-*Pirin-5*	A	1AL	560,606,004	+/+	1467	1089	362	8	TraesCS1A02G391900.1	GILY01006401.1, GIJS01064281.1, GFFI01049354.1
	B	1BL	650,561,417	+/+	1549	1083	360	8	TraesCS1B02G420000.1	GILY01040388.1, GFFI01042348.1
	D	1DL	469,025,797	+/+	1444	1083	360	8	TraesCS1D02G400000.1	GILY01053162.1, GILY01053161.1
Ta-*Pirin-6*	A	4AL	619,965,404	+/+	1221	885	294	5	TraesCS4A02G336100.1	GILY01013459.1, GILY01013458.1
	B	5BL	693,162,656	+/+	1266	885	294	5	TraesCS5B20G535900.1	GILY01027411.1, GILY01027412.1
	D	5DL	551,816,103	+/+	1337	885	294	5	TraesCS5D02G533400.1	IAAL01004437.1, GILY01031080.1

Note: The Ensembl identifier represents the accurate transcript among multiple tentative coding region sequences (CDS). The GenBank TSA identifiers are representative. ND: not detected. Ta-*Pirin*-2 has no TSA sequences and was annotated based on sequence similarity to the barley, Brachypodium, and rice *Pirin* genes.
*ATG location (bp) on the chromosome according to alignments from the IWGSC RefSeq v2.0 database.
†a.a: amino acid.

exons in the Ta-*Pirin-5* homeologs (Fig. 1; Table S3). The coding sequence of Ta-*Pirin-1-B* includes a region that is an intron in the Ta-*Pirin-1-A* and Ta-*Pirin-1-D* copies, which caused the B copy to have one less exon and an insertion of 28 amino acids compared with the Ta-*Pirin-1-A* and Ta-*Pirin-1-D* homeologs (Fig. 1; Table S3). All members of the gene family have ABA response elements (ABRE) in their promoters. The great majority of the *Pirin* genes also have temperature and light responsive *cis* elements as well as MYB and MYC transcription factor binding *cis* elements (Fig. S3). All *Pirin* promoters also share similar phytohormone elements such as methyl jasmonate (MeJA)-responsive *cis*-acting regulatory elements (CGTCA-motif, TGACG-motif) and salicylic acid-responsive *cis*-acting elements (TCA-motif and TGA-motif) (Fig. S3). All *Pirin* family members have CAAT- or CCAAT-box transcription factor binding domains (Fig. S3).

Pirin genes in other monocotyledonous species

The *Pirin* genes were identified in *H. vulgare*, *B. distachyon*, *O. sativa*, *S. bicolor*, and *Z. mays* (Table 2). Like *T. aestivum*, *H. vulgare* (barley) has six *Pirin* gene copies (Hv-*Pirin-1*–Hv-*Pirin6*) with four tandemly duplicated genes on chromosome 5 (Hv-*Pirin-1*, Hv-*Pirin-2*, Hv-*Pirin-3*, and Hv-*Pirin-6*) (Table 2). Hv-*Pirin-4* in *H. vulgare* is also located on chromosome 5, though it is quite distant from the cluster of tandem duplications like the gene locations in *T. aestivum* (Table 2). Similarly, barley also has an Hv-*Pirin-5* gene copy on chromosome 1. The barley gene annotations have little or no confirmation with full-length sequences in the TSA and EST databases and three of the sequences were confirmed by creating contigs using multiple partial-length EST and TSA sequences (Table S4A). The *Pirin* gene copies in *H. vulgare*, *T. aestivum*, and *Ae. tauschii* are present on the phylogenetic tree in clusters (Fig. 2). This evolutionary relationship is not surprising, since the three species are closely related members of the Triticeae tribe and *Ae. tauschii* is the D genome progenitor of *T. aestivum*.

Zea mays has five *Pirin* gene copies (Zm-*Pirin-1*–Zm-*Pirin-5*), with Zm-*Pirin-1* and Zm-*Pirin-4* being present on chromosome 8; however, they are distant from each other (Table 2; Table S4). Three of the genes, Zm-*Pirin-2*, Zm-*Pirin-4*, and Zm-*Pirin-5*, were confirmed by creating contigs using partial-length sequences from the TSA and EST databases (Table S4A). Zm-*Pirin-4* has two alternate transcripts supported by TSA sequences with one appearing to be more abundant,

Fig. 1. Gene structure of the *Triticum aestivum Pirin* gene family. The charcoal-colored boxes depict the 5[1] and 3[1] untranslated regions (UTR), the black boxes represent exons, and the connecting lines represent introns.

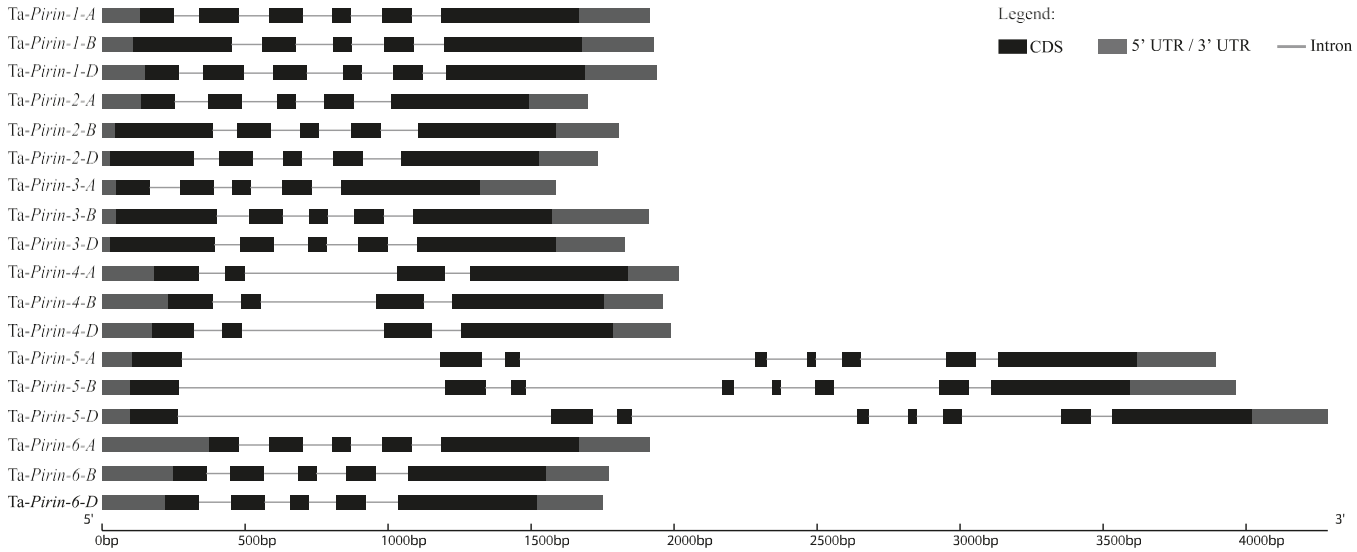

Table 2. *Pirin* homologs in other monocot species and the dicot *Arabidopsis thaliana*.

Species	Annotation	Chromosome	Location	Ensembl accession	NCBI accession
Aegilops tauschii	Aet-*Pirin-1*	5	559,834,378 – 559,836,646	AET5Gv21181500	XP_020150946.1
	Aet-*Pirin-2*	5	559,789,711 – 559,791,968	N/A*	XP_020188087.1
	Aet-*Pirin-3*	5	559,751,530 – 559,753,393	N/A*	XP_020188085.1
	Aet-*Pirin-4*	5	380,704,000 – 380,705,617	AET5Gv20617100	XP_020172933.1
	Aet-*Pirin-5*	1	473,720,038 – 473,722,433	AET1Gv20942800	XP_020170225.1
	Aet-*Pirin-6*	5	559,800,589 – 559,799,299	N/A*	XP_045085302.1
Arabidopsis thaliana	At-*Pirin-1*	3	21,893,417 – 21,896,184	At3G59220	NP_191481.1
	At-*Pirin-2*	2	17,926,790 – 17,929,529	At2G43120	NP_850385.1
	At-*Pirin-3*	3	21,903,569 – 21,905,458	At3g59260	NP_191485.1
	At-*Pirin-4*	1	18,732,014 – 18,734,563	At1g50590	NP_175474.1
Brachypodium distachyon	Bd-*Pirin-1*	1	1,260,773 – 1,262,935	BRADI_1g01870v3	XP_003559150.1
	Bd-*Pirin-2*	4	39,151,499 – 39,153,816	BRADI_4g33540v3	XP_003578320.2
	Bd-*Pirin-3*	3	20,882,141 – 20,885,154	BRADI_3g21730v3	XP_003571689.1
Hordeum vulgare	Hv-*Pirin-1*	5	658,376,982 – 658,378,458	HORVU5Hr1G120800	N/A
	Hv-*Pirin-2*	5	658,362,232 – 658,364,059	HORVU5Hr1G120790	N/A
	Hv-*Pirin-3*	5	658,358,095 – 658,359,987	HORVU5Hr1G120780	N/A
	Hv-*Pirin-4*	5	536,497,645 – 536,497,900	HORVU5Hr1G072760	N/A
	Hv-*Pirin-5*	1	537,502,510 – 537,507,213	HORVU1Hr1G086450	N/A
	Hv-*Pirin-6*	5	658,399,785 – 658,400,880	HORVU5Hr1G120810	N/A
Oryza sativa	Os-*Pirin-1*	3	35,523,859 – 35,526,606	Os03g0845000	XP_015631161.1
	Os-*Pirin-2*	9	18,707,397 – 18,710,800	Os09g0484800	XP_015651432.1
	Os-*Pirin-3*	8	16,891,540 – 16,897,204	Os08g0364900	XP_015650594.1
Sorghum bicolor	Sb-*Pirin-1*	1	1,345,892 – 1,348,378	SORBI_3001G015100	XP_021302996.1
	Sb-*Pirin-2*	2	63,369,191 – 63,372,475	SORBI_3002G245100	XP_002460441.1
	Sb-*Pirin-3*	7	38,615,611 – 38,621,280	SORBI_3007G107000	XP_002445387.1
Zea mays	Zm-*Pirin-1*	8	13,962,715 – 13,964,723	Zm00001d008595	NP_001150652.2
	Zm-*Pirin-2*	7	136,479,777 – 136,482,266	Zm00001d020915	NP_001131616.1
	Zm-*Pirin-3*	1	225,700,320 – 225,701,018	Zm00001eb042780	NP_001137098.1
	Zm-*Pirin-4*	8	68,470,753 – 68,471,912	Zm00001d009514	PWZ04198.1
	Zm-*Pirin-5*	1	303,243,570 – 303,245,421	Zm00001d034829	XP_008647165.1

*The annotation of these Aegilops *Pirin* sequences are deficient at the Ensembl Plant database. N/A: not applicable.

Fig. 2. The phylogenetic relationships of the *Pirin* gene family members among seven grass species, *Triticum aestivum* (Ta), *Aegilops tauschii* (Aet), *Hordeum vulgare* (Hv), *Brachypodium distachyon* (Bd), *Sorghum bicolor* (Sb), *Zea mays* (Zm), and *Oryza sativa* (Os) and the dicot *Arabidopsis thaliana* (At) as an outgroup. Only one homeologous copy from each paralogous group from the hexaploid *T. aestivum* is included to simplify the figure. The phylogeny was developed using the Maximum Likelihood method based on the Whelan and Goldman model (Whelan and Goldman 2001). The tree with the highest log likelihood (−5052.3717) is shown. The values next to the branches represent the bootstrap values. The scale bar units are in substitutions per site.

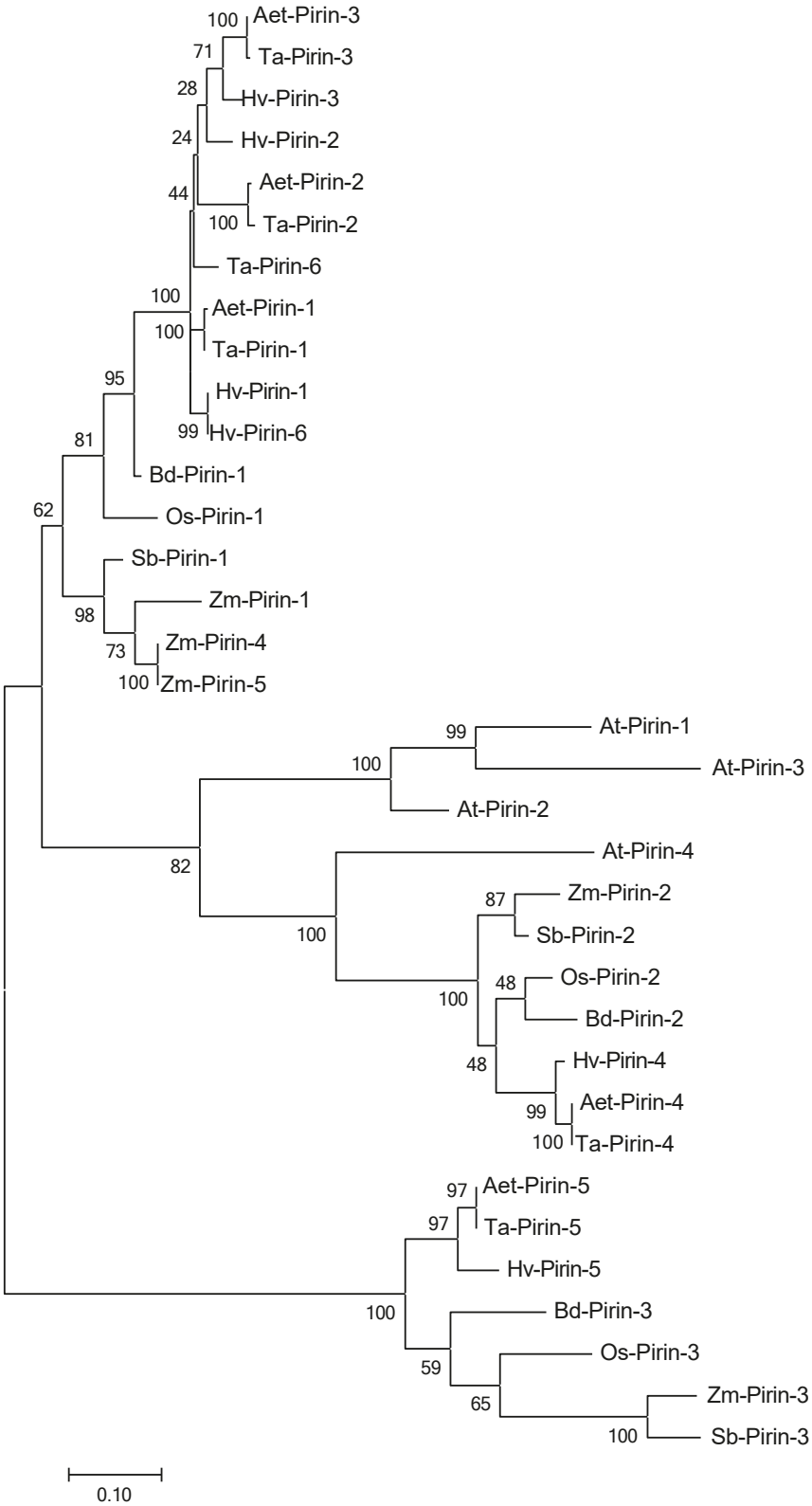

and upon comparison of the two transcripts, the presence of an alternate splice junction for one exon is evident.

Three *Pirin* gene copies are found in *B. distachyon*, and they are annotated as Bd-*Pirin-1*–Bd-*Pirin-3* (Table 2; Table S4). The three genes are located on chromosomes 1, 3, and 4. Bd-*Pirin-3* was confirmed using a contig constructed from available EST sequences (Table S4A). Bd-*Pirin-1* has two transcripts available at Ensembl Plants, the transcript presented in this study has an 87 nucleotide insert compared to the other transcript available. This is considered the transcript with higher confidence, since there are corresponding transcript sequences in the TSA and EST databases at NCBI (Table S4).

Both *O. sativa* and *S. bicolor* have three *Pirin* genes each designated as *Pirin-1*–*Pirin-3*. All three copies in both species are present on different chromosomes. The transcripts were previously reported by Park et al. (2018) and Bandaranayake et al. (2012) and have been confirmed with updated accessions in this study (Table 2; Table S4).

Pirin expression in tissues of *T. aestivum*

To better understand the tissue-specific expression of the *Pirin* gene family, a transcriptome library containing five different tissue types in *T. aestivum* was analyzed (Pingault et al. 2015). The tissue types investigated included the developing seed, stem, inflorescence, leaf, and the root at the cotyledon emergence stage; however, the developing seed data are not graphically represented as the reads per kilobase per million (RPKPM) values are between 0 and 0.79 RPKPM for all *Pirin* gene family members. The expression levels of the *Pirins* in this tissue panel had a range of 14.5 RPKPM to undetected (Table S5). The Ta-*Pirin-1* and Ta-*Pirin-5* homeologs have high levels of expression relative to other members of the gene family with the Ta-*Pirin-5* having the highest levels of expression in the roots and Ta-*Pirin-1* with the highest expression in the roots and stem (Fig. 3). Ta-*Pirin-2*, Ta-*Pirin-3*, Ta-*Pirin-4*, and Ta-*Pirin-6* have low expression levels ranging from 0 to 2 RPKPM in all tissue types assayed (Table S5). Ta-*Pirin-5-A*, Ta-*Pirin-5-B*, and Ta-*Pirin-5-D* have expression levels of 7.4, 11, and 14.5 RPKPM in the roots, respectively (Fig. 3A; Table S5). Ta-*Pirin-1* has relatively high levels of expression in the root and stem with *Pirin-1-B* having 9.2 RPKPM in the root and 12 RPKPM in the stem, and the *Pirin-1-A* and *Pirin-1-D* copies of the gene having approximately two thirds of these levels of expression.

A second panel of 71 tissues from the Azhurnaya cultivar gives a larger scope of the *Pirin* gene family tissue-specific expression (Table S6) (Ramírez-González et al. 2018; Winter et al. 2007). Like the trend previously mentioned, Ta-*Pirin-1* and Ta-*Pirin-5* show the highest relative levels of expression and are widely expressed in many tissues; the Ta-*Pirin-1* copies are most highly expressed in the anthers, peduncle and the first leaf at the seedling stage, and the Ta-*Pirin-5* copies are most highly expressed in the anthers, first leaf at the tillering stage and in the awns at the ear emergence stage (Table S6). Results in the assays of 71 tissues were similar to those of Pingault et al. (2015) mentioned above, in that the Ta-*Pirin*-1 homeologs were found to be expressed in root and stem tissues at levels higher than the median levels of expression over all tissues. However, the larger study included many more tissues and stages of development and found the levels of expression in the anthers, peduncle, and lemma to be two- to five-times higher than those in the roots, depending on the stage of development of the roots. Similarly, the larger 71 tissue studies by Ramírez-González et al. (2018) and Winter et al. (2007) showed relatively high expression of the Ta-*Pirin-5* homeologs in the roots and stems, similar to the initial study by Pingault et al. (2015); however, the larger studies found levels of expression to be ten-times higher in the anther, first leaf, and awns than those of the roots (Table S6). Ta-*Pirin-3*, Ta-*Pirin-4*, and Ta-*Pirin-6* showed more specialized patterns and relatively low levels of expression. The Ta-*Pirin-3* homeologs showed their highest levels of expression in the first leaf at the tillering stage, in the roots and in the lemma. The Ta-*Pirin-4* homeologs had the highest levels of expression in the peduncle and in the lemma. Ta-*Pirin-6* homeologs displayed the highest levels of expression in the first leaf at the tillering stage, in the flag leaf sheath at the grain fill stage and in the internode 2 at the milk grain stage. The Ta-*Pirin-2* homeologs had the lowest levels of expression in the tissues assayed but had their highest levels of expression in the roots (Table S6). For all Ta-*Pirin* genes, there was variance in the level of gene expression among their homeologous copies, indicating a specialized pattern of expression among these tissue types.

Pirin expression in response to abiotic stress

Differential gene expression in response to abiotic stress was analyzed in transcriptome libraries for wheat seedlings developed by Liu et al. (2015). Ta-*Pirin-1-D* is upregulated in response to 1 and 6 h of heat as well as 1 h of combined heat and drought stress treatments (Fig. 4A; Table S7), whereas the A and B homeologous copies of the *Pirin-1* gene did not show significant changes in expression. Ta-*Pirin-1-D* was the only *Pirin* to have a change in expression in response to cold treatment at 4°C, with a 2.6-fold increase (Li et al. 2015) (Fig. 5A; Table S8). The three Ta-*Pirin-5* homeologs are differentially expressed in response to heat, drought, and combined heat and drought stress treatments with both significant increases and decreases in expression (Fig. 4B; Table S7).

To understand the effects of ABA signaling on *Pirin* gene expression, mRNA levels in a transgenic *T. aestivum* line with overexpression of the ABA receptor, Ta-*PYL4,* were compared with the WT for effects of endogenous ABA and drought (Mega et al. 2019) (Fig. 5B; Table S9). Interestingly, Ta-*Pirin-1-A* appears to be significantly upregulated 1.4-fold in the Ta-*PYL4* overexpression line under control conditions (Fig. 5B; Table S9). This indicates that Ta-*Pirin-1-A* is affected by the expression of Ta-*PYL4* and may be downstream in the signaling pathway of this ABA receptor.

Pirin expression in response to *F. graminearum*

The impact of biotic stress was analyzed by transcriptome data comparison of a Fusarium-resistant line, NIL-38, and the susceptible line, NIL-51, whose spikes were inoculated with *F. graminearum* (Steiner et al. 2017). Ta-*Pirin-1* and Ta-*Pirin-5* are the only *Pirin* genes with significant changes in expression

Fig. 3. Tissue expression of the *Triticum aestivum* Ta-*Pirin-1* and Ta-*Pirin-5* across a panel of four tissue types—the stem, inflorescence, leaf, and root at the cotyledon emergence stage. **(A)** Expression levels of Ta-*Pirin-5-A*, Ta-*Pirin-5-B*, and Ta-*Pirin-5-D*. **(B)** Expression levels of Ta-*Pirin-1-A*, Ta-*Pirin-1-B*, and Ta-*Pirin-1-D*. Expression levels are depicted in reads per kilobase per million (RPKPM). The letters represent the significant differences between all homeologs across all tissues as tested by a Duncan's multiple range posthoc test, following a one-way ANOVA. Bars that do not share a common letter are significantly different with a p-value of 0.05 or less.

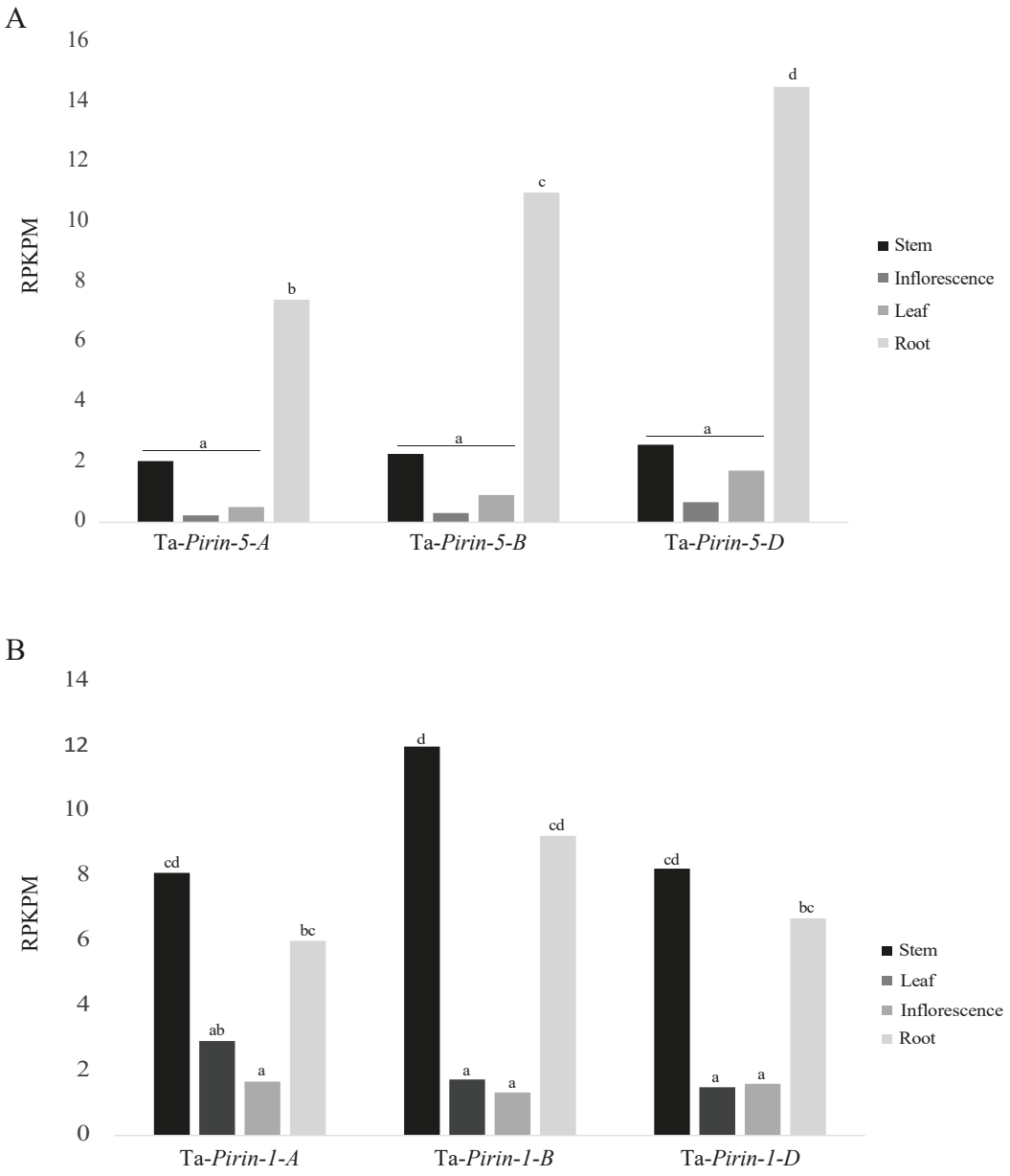

in response to inoculation and only in the susceptible NIL-51 line (Fig. 6; Table S10). Ta-*Pirin-1-A* and Ta-*Pirin-1-D* have 2.0- and 2.6-fold higher levels of expression, respectively, 48 h after inoculation relative to mock treated plants (Fig. 6A; Table S10). Though the resistant NIL-38 line did not show higher levels of expression in response to Fusarium inoculation compared with mock-inoculated plants, the constitutive levels of expression in these plants were similar to those of the NIL-51 line after inoculation (Figs. 6B and 6D). Ta-*Pirin-5-B* is upregulated with a 1.7-fold increase in expression 12 h after inoculation (Table S10), followed by a significant 30% decrease in expression 48 h after inoculation in the NIL-51 line (Fig. 6C). Ta-*Pirin-5-A* was also significantly downregulated 48 h after inoculation (Fig. 6C; Table S10). Ta-*Pirin-5* showed no significant differences in the level of expression between mock- and Fusarium-inoculated plants in the resistant NIL-38 line at any of the time points used in the study (12, 24, and 48 h) (Fig. 6D; Table S10). Taken together these data suggest that both Ta-*Pirin-1* and Ta-*Pirin-5* play roles in pathogen response. A second Fusarium inoculation study carried out in the Fielder cultivar, another Fusarium-susceptible cultivar, showed

Fig. 4. Response to drought, heat, and a combination of heat and drought at 1 and 6 h of treatment. **(A)** Expression profile of Ta-*Pirin-1-D* and **(B)** the expression profile of Ta-*Pirin-5-A*, Ta-*Pirin-5-B*, and Ta-*Pirin-5-D* in response to the treatments. Expression levels are depicted in reads per kilobase per million (RPKPM). The letters represent the significant differences between all homeologs across all treatments as tested by a Duncan's multiple range post-hoc test following a one-way ANOVA. Bars that do not share a common letter are significantly different with a *p*-value of 0.05 or less. Ta-*Pirin-1-D* is the only homeolog depicted in (A); the Ta-*Pirin-1-A* and Ta-*Pirin-1-B* homeologs have nonsignificant changes in expression for these treatments.

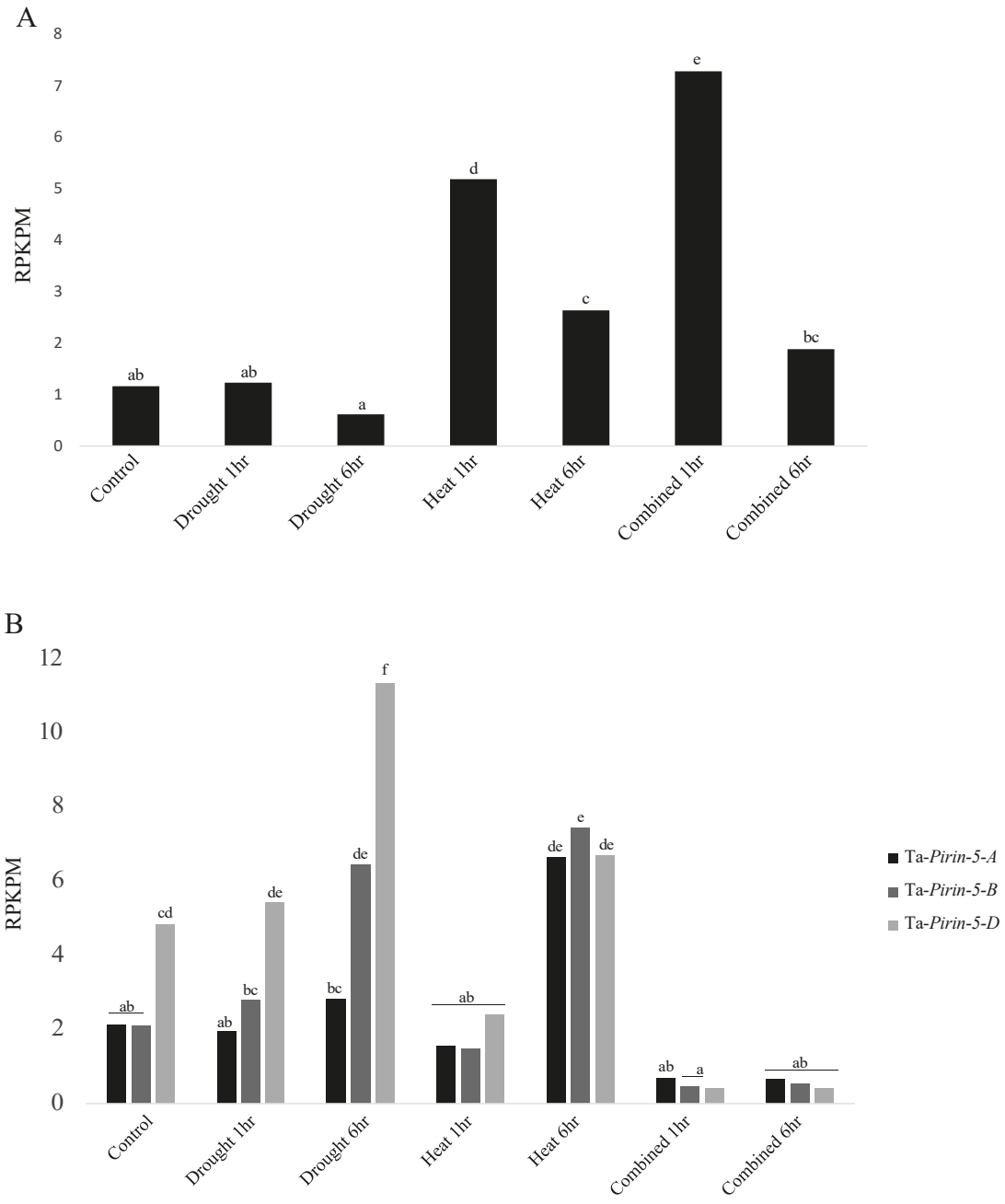

similar results (Buhrow et al. 2021). Ta-*Pirin-5* has a large increase in expression in response to Fusarium, while the Ta-*Pirin-1-B* copy has a significant increase that is mediated by ABA (Table S11). In addition to a Fusarium response, the Ta-*Pirin-5* homeologs are also significantly increased in response to both ABA and GA (Tables S11 and S11A).

The *T. aestivum* winter wheat cultivar N9134, which is resistant to all lines of powdery mildew (*Bgt*), showed a significant increase in Ta-*Pirin-1-B* and Ta-*Pirin-3-B* expression levels one-day post-inoculation with *Bgt* (1 dpi) (Zhang et al. 2014) (Fig. S4). The level of expression of Ta-*Pirin-3-B* increased from 0 to 29.6 RPKPM one-day post-inoculation, while the Ta-*Pirin-3-A* and Ta-*Pirin-3-D* homeologs showed extremely low levels of expression throughout the time course of the experiment and did not show gene induction (Fig. S4; Table S12).

Fig. 5. Differential expression of Ta-*Pirin-1-A*, Ta-*Pirin-1-B*, and Ta-*Pirin-1-D* in **(A)** response to cold treatment at 4°C and control conditions at 23°C and **(B)** Ta-*Pirin-1-A*, Ta-*Pirin-1-B*, and Ta-*Pirin-1-D* expression in response to ABA treatment and drought in the WT and a line overexpressing Ta-PYL4 (oxPYL4). wwc = well-watered control, ABA = 24 h incubation with 25 μm ABA, drought = 24 h without water. The expression levels are depicted in reads per kilobase per million (RPKPM). The letters represent the significant differences between all homeologs under both temperature conditions as tested by a Duncan's multiple range post-hoc test following a one-way ANOVA. Different letters indicate significant differences.

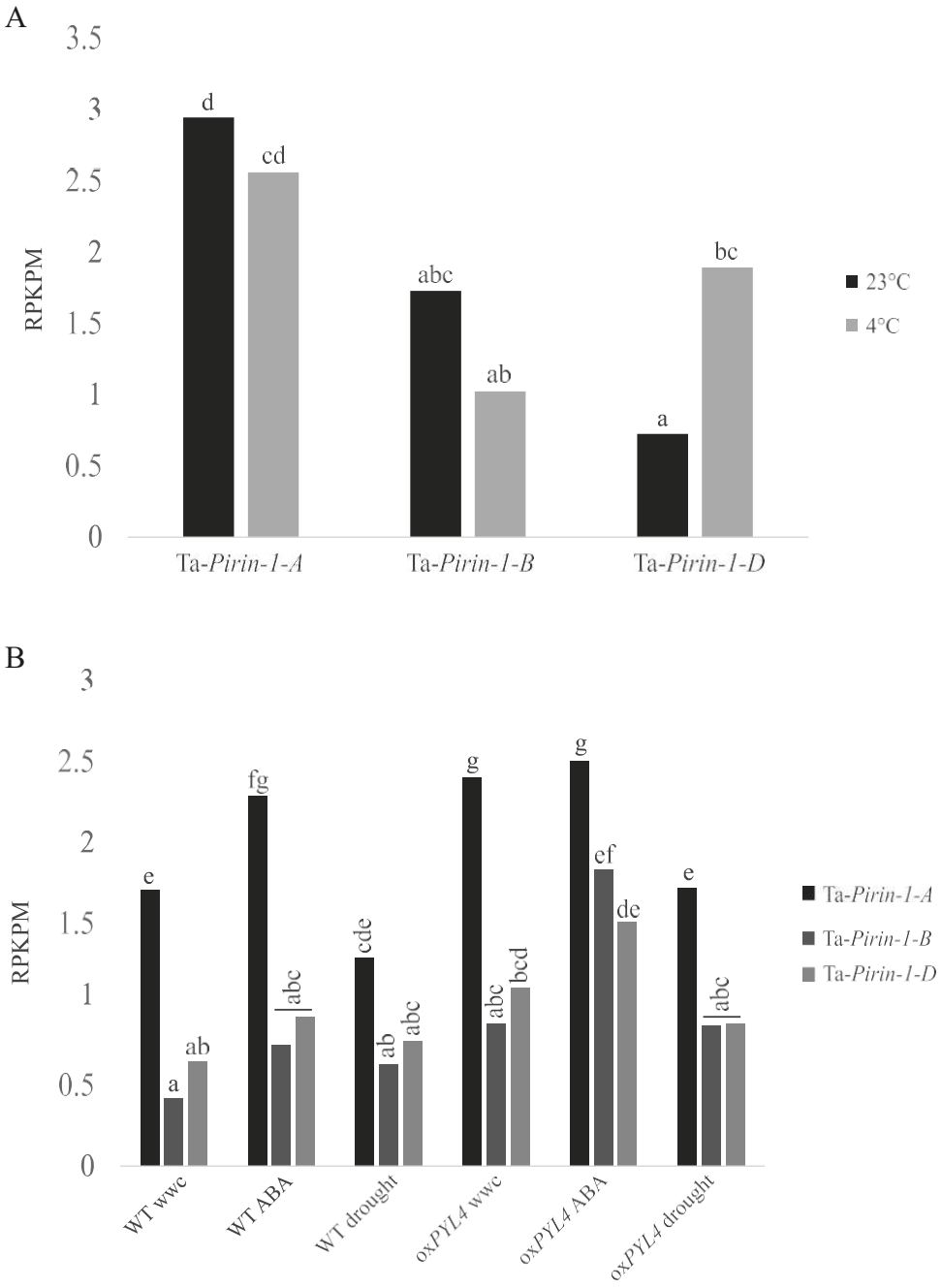

Discussion

The *Pirin* gene family

The *Pirin* gene family in Triticum is comprised of six paralogous gene copies per haploid genome, Ta-*Pirin-1* to Ta-*Pirin-6*; four of the six members are found in tandem duplications on chromosome 5. The tandem duplication cluster is present on the 4A, 5B, and 5D chromosomes (Fig. S1). The presence of these *Pirin* gene duplications on the three subgenomes of *T. aestivum* as well as in *Ae. tauschii* and *H. vulgare* indicates that the gene duplications occurred after the evolutionary separation of the Triticeae and Brachypodium. However, this happened before the speciation of the members of the Triticeae, namely *Ae. tauschii* and the other progenitor species of *T. aestivum* and *H. vulgare* (Fig. 2). The location of the tandemly duplicated genes on chromosome 4A, rather than on 5A, is due

Fig. 6. Ta-*Pirin-1* and Ta-*Pirin-5* expression in response to 48 h of *Fusarium graminearum* infection in the NIL-38 resistant line and the NIL-51 susceptible line. **(A)** Expression of Ta-*Pirin-1-A*, Ta-*Pirin-1-B*, and Ta-*Pirin-1-D* in the susceptible NIL-51 line. **(B)** Expression of Ta-*Pirin-1-A*, Ta-*Pirin-1-B*, and Ta-*Pirin-1-D* in the resistant NIL-38 line. **(C)** Expression of Ta-*Pirin-5-A*, Ta-*Pirin-5-B*, and Ta-*Pirin-5-D* in the susceptible NIL-51 line. **(D)** Expression of Ta-*Pirin-5-A*, Ta-*Pirin-5-B*, and Ta-*Pirin-5-D* in the resistant NIL-38 line. The expression levels are depicted in reads per kilobase per million (RPKPM). The letters represent the significant differences between all homeologs as tested by a Duncan's multiple range post-hoc test, following a one-way ANOVA. Different letters indicate significant differences. Mock = control treatment, Inoculated = Fusarium treatment.

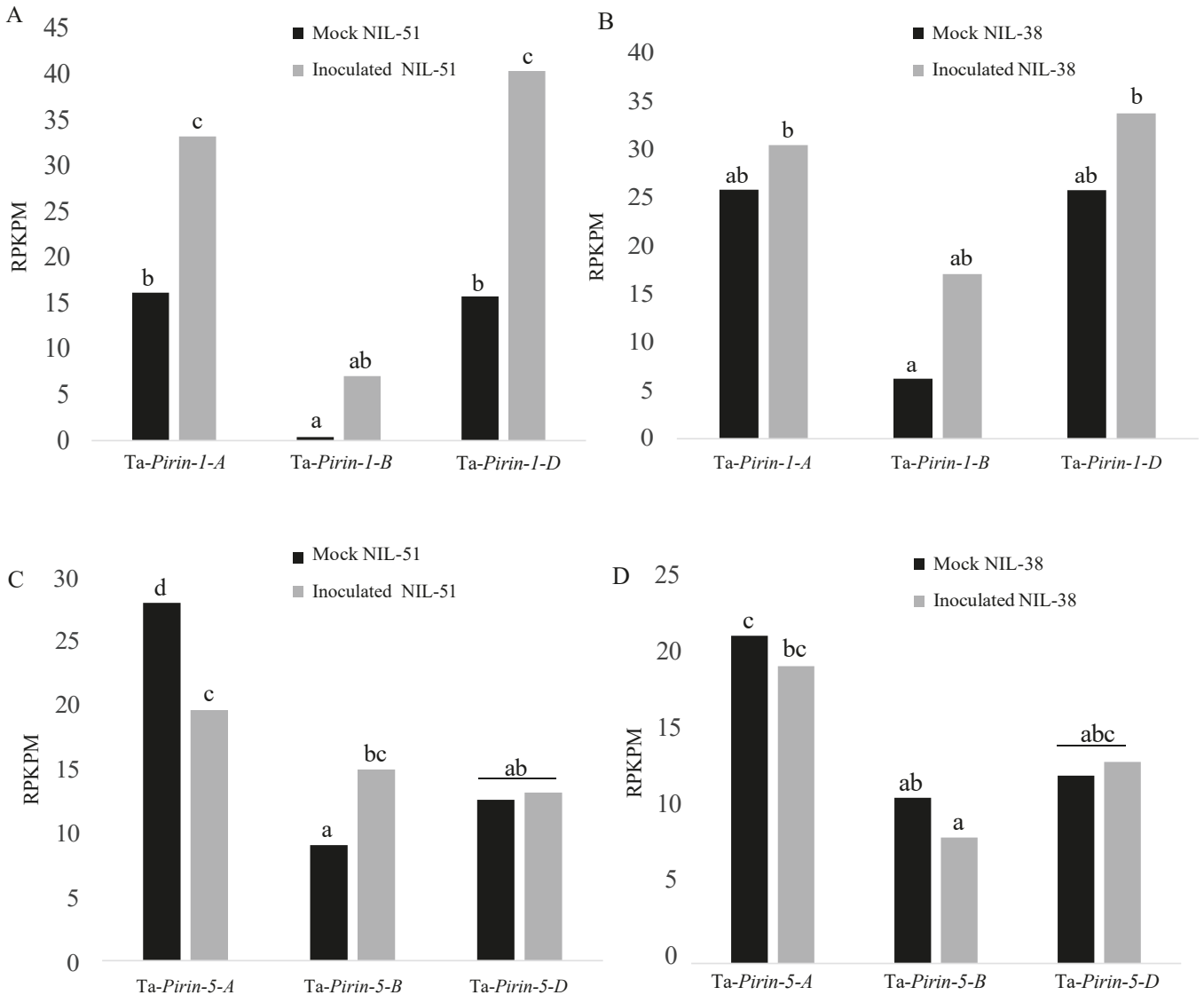

to a reciprocal translocation between the 4AL and 5AL chromosomes in *T. aestivum*, a translocation that has also been recognized in *T. turgidum*, the tetraploid progenitor of *T. aestivum* (Nelson et al. 1995). The phylogenetic analysis suggests that the monocot species shared three ancestral genes corresponding to *T. aestivum* Ta-*Pirin-1*, Ta-*Pirin-4*, and Ta-*Pirin-5* and that the Triticeae lineage underwent a quadruplication of the Ta-*Pirin-1* locus (Fig. S5). *Zea mays* appears to have had an independent triplication of *Pirin1*. The tandemly duplicated *Pirins* in *T. aestivum* have substantial variation in the length of the N-terminals of the proteins encoded by the genes, and the *Pirin* gene family members appear to have specialized expression.

Accuracy of gene annotation

Automation of gene annotation causes some inaccuracies in predicting coding sequences, which underscores the importance of manually curating gene sequences and families. Algorithms that detect ORFs sometimes do not always correctly identify exon/intron junctions; in many cases, multiple candidate transcript variants are listed that do not have confirmation from transcripts of cDNA, EST, or TSA sequences. Many of the transcript variants listed for the *Pirin* genes at the Ensembl Plants database were incorrect due to an incorrect start codon (Table S2). Five of the 18 annotations were incorrect, and an additional three genes had multiple candidate CDS sequences that included incorrect annotations.

Ta-*Pirin-1* and Ta-*Pirin-2* are listed with multiple transcript variants at Ensembl Plants with most of the inaccuracies occurring at the 5[1] end of the gene sequence. Ta-*Pirin-3* and Ta-*Pirin-4* only have one transcript variant at Ensembl Plants; however, these annotations had incorrectly predicted start codons, indicated by comparison of the genomic sequence to transcript sequences in the EST and TSA databases. The errors that lead to discrepancies in protein sequence and length are listed in Table S2.

The *Pirin* gene annotations in the Ensembl Plants database for the other monocot species that were characterized also displayed discrepancies in their annotations between the proposed CDS and sequences available in the transcriptome databases at NCBI. Some of the *Pirin* gene sequences in these species had multiple predicted transcripts, many of which have no transcript support in the NR, EST, or TSA databases and several of the predicted protein sequences have truncated N- and C-terminals. For example, the *Ae. tauschii* sequence for Aet-*Pirin-5* at Ensembl Plants has a predicted transcript that is missing 57 nucleotides of the 5[1] end when compared with the transcripts at NCBI (Table 2; Table S4).

Expression profile

The gene expression profiles of the *Pirin* gene family members have specialized tissue expression patterns. Aside from Ta-*Pirin-1*, which has relatively high levels of expression in numerous tissue types, the other members of the tandemly repeated gene cluster on chromosome 5 have low differential levels of expression in a variety of different tissues (Fig. 3; Tables S5 and S6). Those members of the gene family have long intact ORFs as well as evidence for their corresponding mRNAs, which are both indications that they are functional genes. Some of the Ta-*Pirin* genes have differential expression in response to the abiotic or biotic stress conditions assayed here. However, the different homeologous copies of the Ta-*Pirin* genes appear to have differing roles in response to stress conditions, similar to results observed in other *T. aestivum* gene families (Brunetti et al. 2018). The Ta-*Pirin-1-D* copy has an increase in expression in response to both heat and cold treatment, suggesting that the Ta-*Pirin-1-D* copy plays a role in adaptation to temperature extremes (Figs. 4 and 5A). Additionally, the Ta-*Pirin-5-D* and Ta-*Pirin-5-B* copies have significant changes in expression in response to drought and heat, whereas the Ta-*Pirin-5-A* copy was only significantly affected by heat (Fig. 4B).

The *Arabidopsis* homolog At-*Pirin1* has been implicated in the inhibition of seed germination in response to ABA, with the increase in expression of At-*Pirin1* leading to a decreasing degree of inhibition of germination by ABA treatment (Lapik and Kaufman 2003). ABA binds the PYL/PYR/RCAR receptors, which inhibit Clade A PP2Cs allowing for the activation of protein kinases capable of phosphorylating and activating target proteins involved in the regulation of seed germination (Hauser et al. 2017). The overexpression of Ta-*PYL4* elicits a response like that of an ABA treatment, and an increase in Ta-*Pirin-1-A* expression is observed in such plants (Fig. 5B). It is plausible that Ta-*Pirin-1-A*, like its Arabidopsis homolog At-*Pirin1*, has an effect in the ABA signaling pathway, although the traits it may affect are unclear from the data set studied here. A second study with both ABA and GA treatments corroborates the role of Ta-*Pirin-1* in ABA response, since all homeologs have significant increases in response to both ABA and GA (Tables S11 and S11A). In addition, Ta-*Pirin-5* also shows significant increases in expression after ABA or GA treatment suggesting that other *Pirin* gene family members are responsive to phytohormone stress (Tables S11 and S11A).

The change of expression of Ta-*Pirin-1* and Ta-*Pirin-5* in response to *F. graminearum* infection in the susceptible NIL-51 line suggests that these homeologs may play a role in pathogen response. The Ta-*Pirin-1-A* copy has a significant increase in expression post-inoculation; however, the opposite pattern is observed in Ta-*Pirin-5-A*, indicating that Ta-*Pirin-5-A* and Ta-*Pirin-1-A* do not function redundantly but may be working antagonistically or in synchrony (Figs. 6A and 6C; Table S10). When subjected to powdery mildew (*Bgt*) both the Ta-*Pirin-1* and Ta-*Pirin-3-B* copies have significant increases in expression suggesting an induction in response to this fungus; however, the role of these genes in plant defense is unclear (Table S12).

The low to undetectable expression levels seen with three of the tandemly repeated genes, Ta-*Pirin-2*, Ta-*Pirin-3*, and Ta-*Pirin-6*, suggests that the genes have evolved specialized functions. The intact ORFs of the genes suggest that they are functional, but their low levels of expression suggest that they may be expressed in limited tissues, cell types, developmental stages, and treatment conditions that merit further investigation.

Chapter 7: Conclusion

7.1 Conclusion

Both the caleosins RD20/CLO3 and CLO7 are implicated in G-protein signaling and both interact with the Gα subunit of the Heterotrimeric G protein complex, GPA1 (Chapters 2 and 3). The interaction between the caleosins and GPA1 is affected by both calcium and the nucleotide-bound state of GPA1. Using mutant forms of RD20/CLO3 and CLO7 where critical calcium-binding amino acids were altered, it was observed that when GPA1 is active and bound to GTP ($GPA1^{QL}$), the strength of interaction with either RD20/CLO3 or CLO7 is enhanced by calcium. If GPA1 is GDP-bound, the interaction is calcium-dependent since the interaction between the calcium mutant forms of both the caleosins and GPA1 is abolished (Chapters 2 and 3). A notable difference between the CLO7 and RD20/CLO3 interactions with GPA1 is the cellular localization of the interaction (Chapters 2 and 3). The RD20/CLO3 and GPA1 interaction occurs at the ER whereas the CLO7 and GPA1 interaction occurs at the plasma membrane (PM) (Chapters 2 and 3). Interestingly, when GPA1 is GTP-bound ($GPA1^{QL}$) the interaction with RD20/CLO3 localizes to the PM, indicating a shift in localization from the ER, however the interaction between $GPA1^{QL}$ and CLO7 remains at the PM. Both of the caleosins play a role in stress response phenotypes with GPA1, such as hypocotyl elongation and seed germination (Chapters 2 and 3). RD20/CLO3 is a negative regulator of GPA1 for both hypocotyl elongation in the dark and leaf morphology. The *CLO7* and *GPA1* double mutant cannot be recovered indicating an embryo lethal phenotype. The siliques of the *clo7* +/- *gpa1* had a higher number of aborted seeds as well as seeds with an affected phenotype (Chapter 3). *CLO7* and *GPA1* also play a role in seed germination in response to ABA treatment and osmotic stress and *CLO7* appears to be affecting this trait with *GPA1* (Chapter 3). Both CLO7 and *GPA1* are needed for embryo development and viability, and the synthetic lethal phenotype observed suggests that they share a common pathway for this trait (Chapter 3). In addition to this shared embryo development pathway, the data indicates that each participates in additional pathways that converge to regulate seed germination (Chapter 3). Taken together, these data suggests that the caleosins are involved in the heterotrimeric G-protein stress response pathways, share parallel pathways and have unique roles within these pathways (Chapters 2 and 3).

Although the caleosins are part of a multi-gene family in Arabidopsis comprised of seven members, the roles of RD20/CLO3 and CLO7 are not redundant within G-protein signaling (Chapter 4). RD20/CLO3 and CLO7 appear to play a redundant role in flowering time under long day conditions. When both caleosins are reduced in expression an early flowering phenotype

is observed, suggesting redundancy for this particular trait. Lastly, RD20/CLO3 is a caleosin known to be induced by ABA and it was found to play a role in lateral root development and elongation in response to ABA, a unique characteristic of this caleosin and the caleosins studied to date.

The work presented in Chapters 5 and 6 which characterizes the *Esi3* and *Pirin* gene family in *Triticum aestivum* highlights the importance of curating gene families in Triticum since it is an allohexaploid species. The gene families in this species have three homeologous copies present on the A, B and D genomes, three family members with very high sequence identity. This redundancy as well as a sufficiently rich transcript database that can be used to accurately demark exon/intron junctions can contribute to the accurate annotation of members of gene families in *T. aestivum* and related species. These are resources that have not been fully exploited in the annotations of the whole genome. The *Esi3* gene family is comprised of 10 paralogous groups totalling 29 family members. The *Pirin* gene family is comprised of 6 paralogous groups totalling 18 gene family members. All *Esi3* genes in *T. aestivum* have differential and altered expression in response to the abiotic and biotic stresses tested. It was found that one *Esi3* family member, *Esi3-9*, has a unique N-terminal extension placing this family member into a new group of Esi3/RCI2/PMP3, designated as Group III. Four of the *Pirin* gene family members, Ta-*Pirin-1*, *-2*, *-3* and *-6*, are present in a tandem duplication on chromosome 5. The *Pirin* genes appear to have more specialized functions since only Ta-*Pirin-1* and *-5* have differential expression in response to the biotic and abiotic stress conditions analyzed in this study. However, differences in Ta-*Pirin-3-B* were observed in plants infected with powdery mildew. Changes in gene expression among homoeologous members of both gene families were observed. These data suggests that both the *Pirin* and *Esi3* gene family members play roles in the abiotic and biotic stresses tested in these studies.

7.2 Future Directions

The work presented in Chapters 2 and 3 should be directed towards a better understanding of the mechanisms by which the caleosins, RD20/CLO3 and CLO7, and the G protein, GPA1, regulate the traits that were characterized here. It would be interesting to screen for other genes that play a role in these pathways and test their expression levels in the *rd20/clo3*, *clo7* and *gpa1* mutant backgrounds, and to develop higher order genetic lines with double mutants and over-expression in different mutant backgrounds. For example, an altered leaf morphology phenotype

was observed with *RD20/CLO3* and *GPA1* mutants and OE lines: mutations in *ANGUSTIFOLIA3* (*AN3*) and *ROTUNDIFOLIA3 (ROT3)* give rise to similar phenotypes. These genes affect the leaf width and length, and their expression levels may be affected by *RD20/ CLO3* and *GPA1*. Another example is the *CLO7* and *GPA1* germination phenotype in response to ABA treatment. Since both CLO7 and GPA1 interact with Pirin1 and *Pirin1* has been implicated in ABA seed germination, it would be interesting to further study these interactions by developing double or triple mutant lines. It has been proposed that *GPA1* and *Pirin1* affect germination rates in the ABA signaling pathway through the Pirin1 interaction with Nuclear Factor Y, (NF-Y). The *NF-Y* mutants have delayed germination in response to ABA treatment, a phenotype similar to both the *gpa1* and *pirin1* mutants. Assaying the levels of *NF-Y* expression in the *clo7* mutant would be a reasonable starting point, as well as assaying for a physical interaction between *CLO7* and *NF-Y*. This approach can be carried out on the phenotypes reported in this work, hypocotyl elongation, seed germination, leaf morphology, flowering time and root development, and could place the caleosins and the G proteins into a larger signaling network. This could create larger working models that can be beneficial to developing strategies to increase plant resistance to environmental stresses.

Assaying the remaining caleosins for an interaction with GPA1 as well as testing them for stress-responsive phenotypes would be another investigation worth pursuing. Understanding their expression in response to abiotic or biotic stresses by using the GUS reporter system in combination with *in-situ* analysis results can help answer the question; are other caleosins stress responsive? And what traits in Arabidopsis might they affect?

Chapter 4 reported the early-flowering phenotype observed with the *CLO7*-RNAi/*rd20* and the *RD20/CLO3*-RNAi/*clo7* knock-down lines. Future work could investigate more deeply this phenomena. The Arabidopsis flowering pathway has been studied in-depth and the elaborate network controlling flowering in response to many stimuli has been identified. All stimuli eventually converge on three main genes that control flowering; Flowering Locus T (FT), Suppressor of Overexpression of CO 1 (SOC1) and LEAFY (LFY). These genes are regulated at the transcriptional level, therefore testing the level of expression of any of these three genes in the *RD20:*RNAi/*clo7* and the *CLO7*:RNAi/*rd20* knock-down/mutant background can be the next step in understanding this signaling cascade.

Chapters 5 and 6, which investigated the *Esi3* and *Pirin* gene family in Triticum, could be extended to *in-vitro* and *in-vivo* experiments. The RNA-Seq and microarray analysis has given an understanding of the tissue-specific expression of the genes as well as their response to biotic and abiotic stresses. These data can be used to design experiments in the crop species, namely *Triticum aestivum*, or a closely related monocot like *Brachypodium distachyon*. Brachypodium is easier to manipulate and there are some T-DNA insertional mutants in this species. Therefore, Brachypodium T-DNA mutants may be available for certain *Pirin* or *Esi3* homologs. They can be used to test the response to the biotic and abiotic stresses analysed in these studies. Promising results could direct further work in Triticum to understand some stress-response pathways. For example, *Esi3-4, Ta-Pirin-1* and *-5* are responsive to *Fusarium graminearium* infection, therefore testing mutations or over-expression lines of these genes in Triticum and assaying for resistance could be important. It would also be interesting to test these genes in response to other fungal pathogens in crop species.

7.3 Supplemental Material

Chapter 2: “The stress induced caleosin, RD20/CLO3, acts as a negative regulator of GPA1 in Arabidopsis”

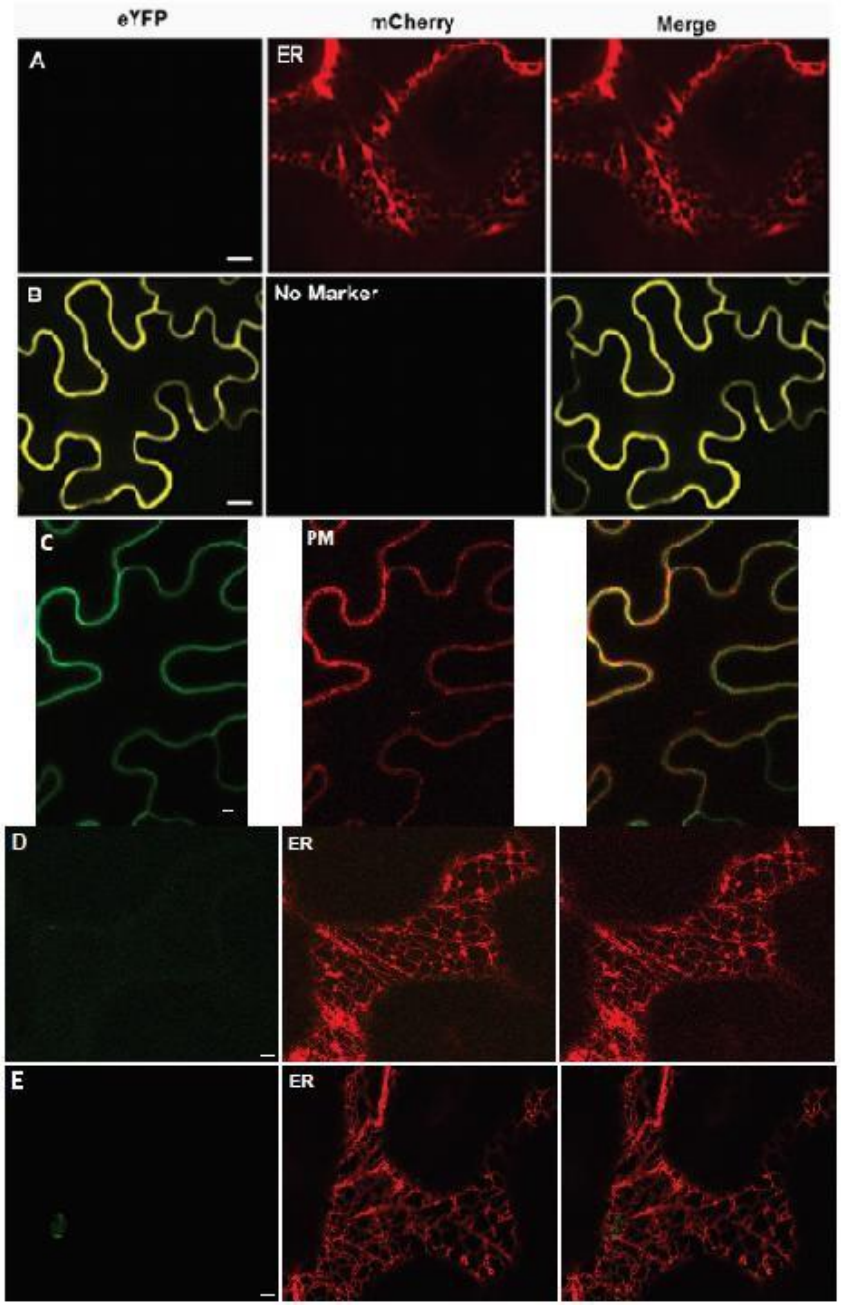
eYFP
mCherry
Merge
A
ER
B
No Marker
C
PM
D
ER
E
ER

Figure S1. Negative and positive control interactions for BiFC assays in tobacco epidermal leaf tissue. **(A)** Lack of interaction between RD20/CLO3-N-YFP and P24B1-C-YFP (type I membrane protein) co-infiltrated with the ER marker, signal peptide of the wall-associated kinase2, AtWAK2:mCherry fusion. **(B)** Positive interaction between GPA1-C-YFP and RGS1-N-YFP (Regulator of G-protein signalling 1). **(C)** Positive interaction between $GPA1^{QL}$-C-YFP and RGS1-N-YFP which is a known interactor of GPA1. **(D)** Lack of interaction between RD20/$CLO3^{D70A}$ and P24B1-C-YFP co-infiltrated with the ER marker. **(E)** Lack of interaction between RD20/$CLO3^{E81R}$ and P24B1-C-YFP co-infiltrated with the ER marker. Scale bar for panel A and B= 50 µm, scale bar for panel C, D and E = 10 µm.

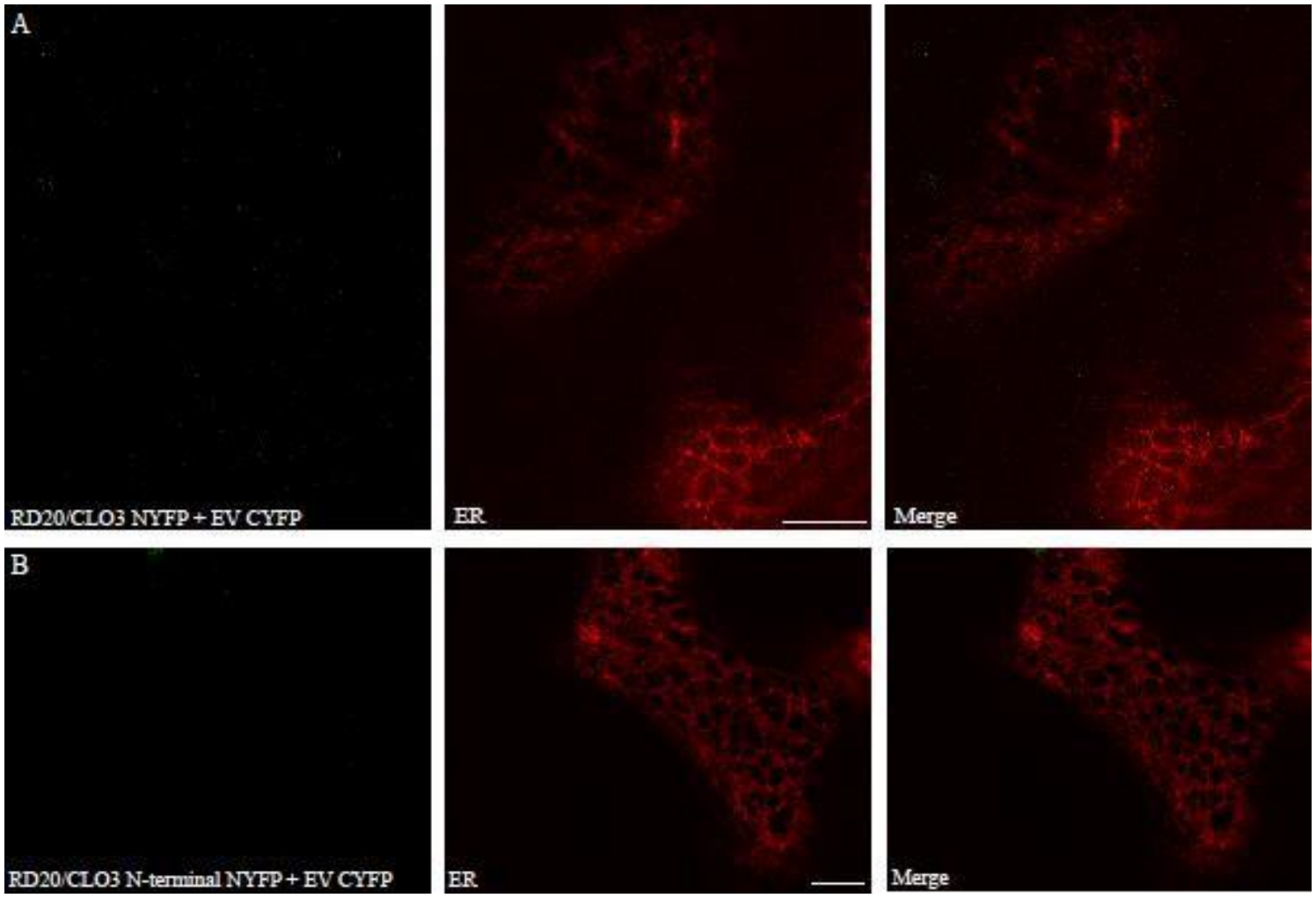
A
RD20/CLO3 NYFP + EV CYFP
ER
Merge
B
RD20/CLO3 N-terminal NYFP + EV CYFP
ER
Merge

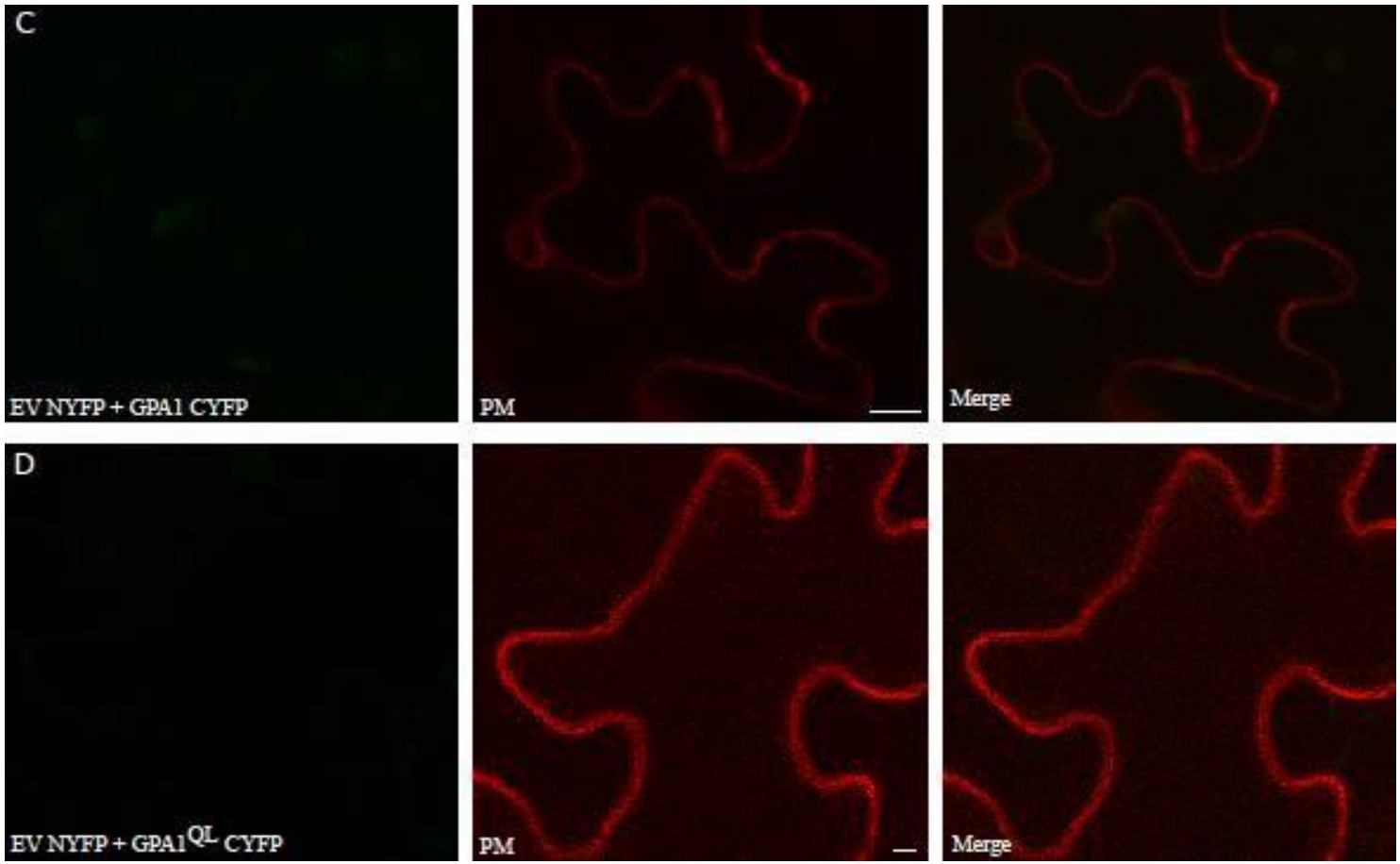

Figure S2. Negative controls for the BiFC assays for RD20/CLO3, GPA1 and GPA1^{QL}. **(A)** Full length RD20/CLO3-N-YFP with an empty C-YFP (EV) vector and the endoplasmic reticulum (ER) mCherry marker. **(B)** RD20/CLO3 N-terminal region-N-YFP with an empty C-YFP vector and the ER mCherry marker. **(C)** GPA1 full length C-YFP with an empty N-YFP vector and the plasma membrane (PM) mCherry marker. **(D)** GPA1^{QL} full length C-YFP with an empty N-YFP vector and the PM mCherry marker Scale bar = 10μm. N-YFP = N-terminal half of the YFP molecule, C-YFP = C-terminal half of the YFP molecule.

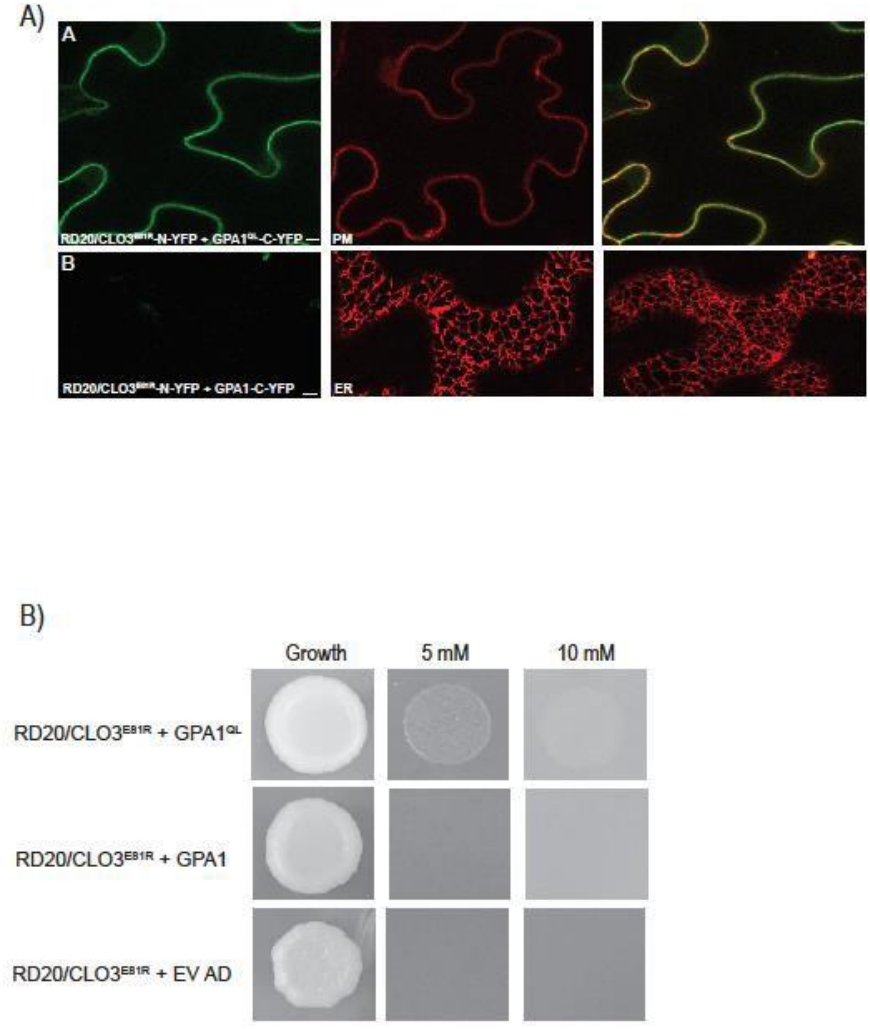

Figure S3. BiFC and Y2H interaction between RD20/CLO3^{E81R} and GPA1 or GPA1^{QL}. **(A-A)** BiFC interaction between RD20/CLO3^{E81R} and GPA1^{QL}-C-YFP localized to the PM. **(A-B)** Lack of BiFC interaction between RD20/CLO3^{E81R} and GPA1-C-YFP, co-transformed with the ER- mCherry marker. Bar =10 µm. **(B)** Y2H assay testing the interaction between GPA1-AD or GPA1^{QL}-AD and the N-terminal half (amino acids 1 to 90) of RD20/CLO3^{E81R}-BD. Yeast growth (Growth) was confirmed on SD-Trp-Leu and the interactions were assayed on SD-Leu-Trp-His supplemented with various 3-AT concentrations (0-5 mM). The lack of growth at elevated levels of 3-AT indicates weak interaction between the two proteins. FL=Full-length, EV=empty vector.

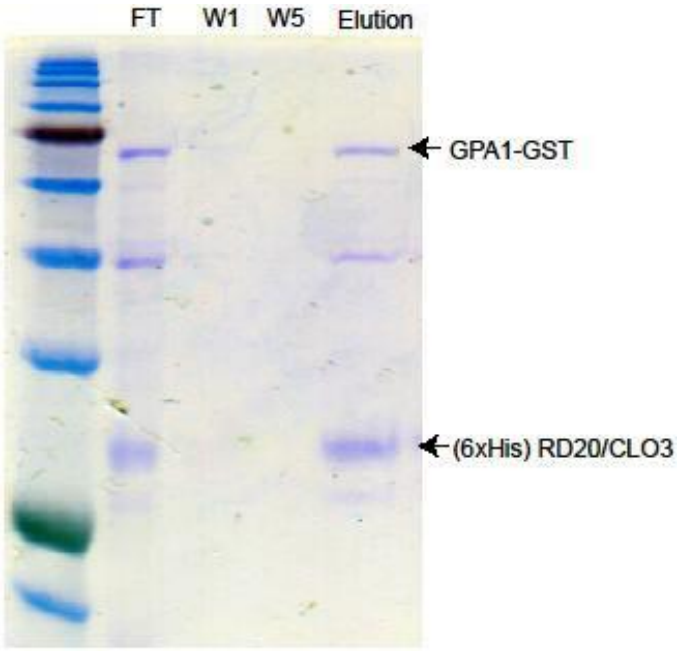

Figure S4. In vitro on column binding of GPA1-GST and (6xHis) RD20/CLO3. FT stands for the flow through, W1 is a fraction of the first wash, W5 is a fraction of the fifth and last wash. The Elution lane shows the presence of GPA1-GST at approximately 72-kDA and the presence of 6xHis-tag RD20/CLO3 at 27-kDa, eluted off of reduced glutathione resin.

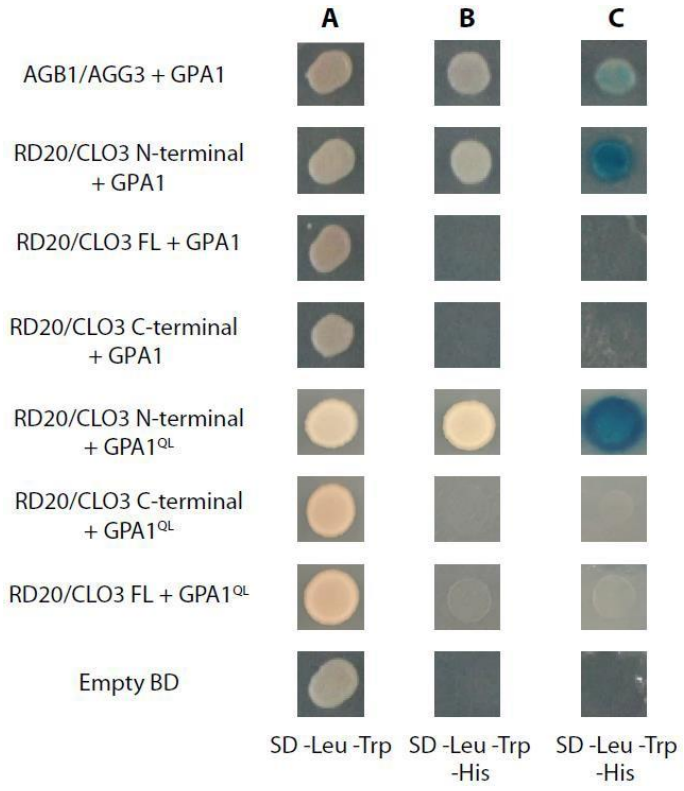

Figure S5. Plate assay for the yeast two-hybrid assay for the interaction between the RD20/CLO3 N-terminal truncation, GPA1 and GPA1^{QL}. **(A)** SD media lacking leucine (Leu) and tryptophan (Trp) showing the presence of the two plasmids to test the following interactions: the positive control of GPA1:AD and AGB1/AGG3(γ):BD; RD20/CLO3 N-terminal region:BD and GPA1:AD; full length RD20/CLO3 (FL):BD and GPA1:AD; RD20/ CLO3 C-terminal region:BD and GPA1:AD; RD20 N-terminal region:BD and GPA1^{QL}:AD; RD20/CLO3 C- terminal region:BD and GPA1^{QL}:AD; RD20/CLO3 FL:BD and GPA1^{QL}:AD; the GPA1:AD with an empty BD vector. **(B)** SD media lacking Leu, Trp and histidine (His) the growth indicates a positive interaction of Y2H partners listed above. **(C)** SD media lacking Leu, Trp and His with the β-galactosidase assay. Blue color indicates positive interaction for Y2H partners. The AGB1/AGG3(γ) construct is a full-length AGB1 with an truncated AGG3 (residues 1 to 112) which maintains the Gγ-like domain (Chakravorty et al., 2015).

Table S1. mCherry protein fusions used as organelle markers in the BiFC assays.

Organelle	Targeting Protein
Plasma membrane	Full length of AtPIP2A, a plasma membrane aquaporin.
Endoplasmic Reticulum	Signal peptide of AtWAK2 (N-terminus of protein), wall-associated kinase2 with an ER retention signal (His-Asp-Glu-Leu) at the C- terminus.

Table S2. Positive and negative controls used in the BiFC assays.

Fusion	**Description**
RGS1-N-YFP	RGS1-N-YFP binary vector for BiFC positive control; Regulator of G-protein signalling 1 (RGS1).
GPA1-C-YFP	GPA1-C-YFP binary vector for BiFC negative control.
P24β1-C-YFP	P24β1-C-YFP binary vector for BiFC negative control, a transmembrane emp24 domain-containing protein (At3g07680).
RD20/CLO3-N-YFP	RD20/CLO3-N-YFP binary vector for BiFC negative control.

Table S3. GTPase activity of GPA1, RD20/CLO3 and GPA1 with RD20/CLO3. GTPase activity was recorded using a coupled enzyme spectrophotometric assay. Activity was subtracted from the background and was linear over 35 minutes. GPA1 and RD20/CLO3 were incubated together at a molar ratio of 1:1.

Protein in assay	GTPase specific activity (nmol min-1 mg-1 protein)	kcat (s-1)
GPA1	4.27	0.0052
GPA1 + RD20/CLO3	5.77*	0.0069
RD20	>0.21**	-

*The specific activity of GPA1 and GPA1 with the addition of RD20/CLO3 is not significantly different.
**GTPase activity of RD20/CLO3 is not significantly different from the background.

Table S4. Gateway primers used to amplify and clone the *RD20/CLO3* promoter::*GUS* expression clones, RNAi constructs, P35S over-expression constructs, BiFC and Y2H clones**,** RD20/CLO3 EF-hand mutants, RT-PCR primers and primers used to screen T-DNA insertional Arabidopsis mutants for the double mutant.

Primer	Sequence (5'-3)[a]	Application
GWPrord20[b]	GGGGACAACTTTGTACAAAAAAGCAGGCTTCTCATGAATATCTTGACAACAA	*RD20/CLO3* promoter for *GUS* construct
GWPrord20[c]	GGGGACCACTTTGTACAAGAAAGCTGGGTATCTCTCTCTCTTACTCTTTTACAATC	*RD20/CLO3* promoter for *GUS* construct
RD20GW[b]	GGGGACAACTTTGTACAAAAAAGCAGGCTTCATGGCAGGAGAGGCAGAGGCTTT	*RD20/CLO3* CDS for BiFC, Y2H, GTPase assay constructs, RNAi and over-expression constructs
RD20GW[c]	GGGGACCACTTTGTACAAGAAAGCTGGGTAGTCTTGTTTGCGAGAATTGGCCCT	*RD20/CLO3* CDS for BiFC, GTPase assay constructs
RD20GW2[c]	GGGGACCACTTTGTACAAGAAAGCTGGGTATTAGTCTTGTTTGCGAGAATTGGCCCT	*RD20/CLO3* CDS for Y2H, RNAi and over-expression constructs

(Continued)

Supplemental Table 4. Continued

Primer	Sequence (5'-3')[a]	Application
GPA1GW[b]	GGGGACAACTTTGTACAAAAAAGCAGGCTTCATGGGCTTACTCTGCAGTAGAAGTCG	*GPA1* CDS for BiFC constructs
GPA1GW[c]	GGGGACCACTTTGTACAAGAAAGCTGGGTATCATAAAAGGCCAGCCTCCAGTAAATTTC	*GPA1* CDS for BiFC constructs, stop codon (bold) added for Y2H
RD20[b]	GGAATGTAACCGAGGGAAAT	*RD20/CLO3* 3' end for RT-PCR
RD20[c]	ACAAATCCCCAAACTGAATAAC	*RD20/CLO3* 3' end for RT-PCR
Actin 2/8[b]	GGTAACATTGTGCTCAGTGGTGG	*Actin 2/8* internal control for RT-PCR
Actin2/8[c]	AACGACCTTAATCTTCATGCTGC	*Actin 2/8* internal control for RT-PCR
GPA1WS LP[b]	GAGTTTGCTCAAAATGAAACAGATTCT	*GPA1* specific primer for double mutant screen
GPA1WS RP1[c]	ACAATCGGTACACTTCACCACTTTT	*GPA1* specific primer for double mutant screen

(Continued)

Supplemental Table 4. Continued

Primer	Sequence (5'-3')[a]	Application
T-DNA RB GPA1WS[c]	GAAAACCTGGCGTTACCCAACTTAAT	*GPA1* T-DNA right border primer to screen for *gpa1*
RD20WS RP[c]	AACAAGCGGGAAATTAAGTGG	*RD20/CLO3* specific primers for double mutant screen
RD20WS LP[b]	ACTAACCATCCAAAAGGATCG	*RD20/CLO3* specific primers for double mutant screen
T-DNA LB1.3[b]	ATTTTGCCGATTTCGGAAC	T-DNA left border primer to screen for *rd20/clo3*

(Continued)

Supplemental Table 4. Continued

Primer	Sequence (5'-3')[a]	Application
RD20^{D70A} FP[b]	TTCTTC**GCC**CAAAACGACGATGGAATC	*RD20/CLO3* primer to create the D70A mutant
RD20^{D70A} RP[c]	GATTCCATCGTCGTTTTG**GGC**GAAGAA	*RD20/CLO3* primer to create the D70A mutant
RD20 EF-mut FP[b]	GGGGACAACTTTGTACAAAAAAGCAGGCTTCATGGCAGGAGAGGCAGAGGCTTTGG	*RD20/CLO3* primer to create the EF-hand mutants
RD20^{E81R} FP[c]	GACGATGGAATCGTCTATCCTTGG**CGC**ACT	*RD20/CLO3* primer to create the E81R mutant

(Continued)

Supplemental Table 4. Continued

Primer	Sequence (5'-3')[a]	Application
RD20^{E81R} RP[c]	AGT**GCG**CCAAGGATAGACGATTCCATCGTC	*RD20/CLO3* primer to create the E81R mutant

[a] Underlined sequences are the attB sites used for Gateway Cloning
[b] Forward primer
[c] Reverse primer
Sequences in bold are the nucleotides changed to create the EF-hand mutants.

Table S5. Expression results for semi-quantitative RT-PCR of the transgenic lines.

Genotype	Quantity[a]	Percent[b]
WS	240	N/A
WS	240	N/A
P35S:*RD20* 4	720	300
P35S:*RD20* 6	480	200
P35S:*RD20* in *gpa1* 8	672	280
P35S:*RD20* in *gpa1* 9	576	240

[a] Quantity of *RD20*/*CLO3* in ng/µl

[b] Percent of *RD20*/*CLO3* increase or decrease in expression relative to WS

7.4 Supplemental Material

Chapter 3: “The caleosin CLO7 and its role in the heterotrimeric G-protein signalling network”

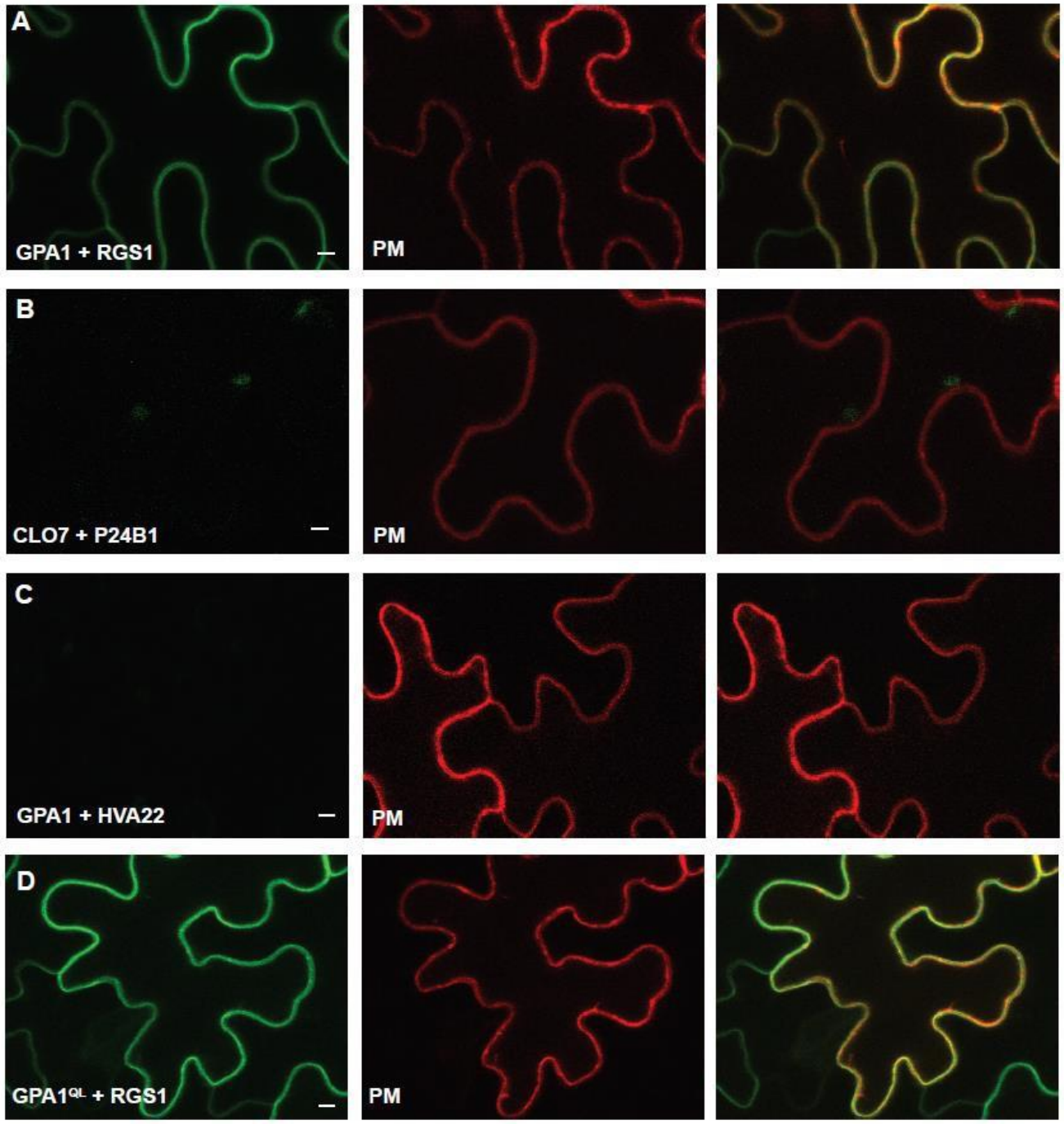
A
GPA1 + RGS1
PM
B
CLO7 + P24B1
PM
C
GPA1 + HVA22
PM
D
GPA1QL + RGS1
PM

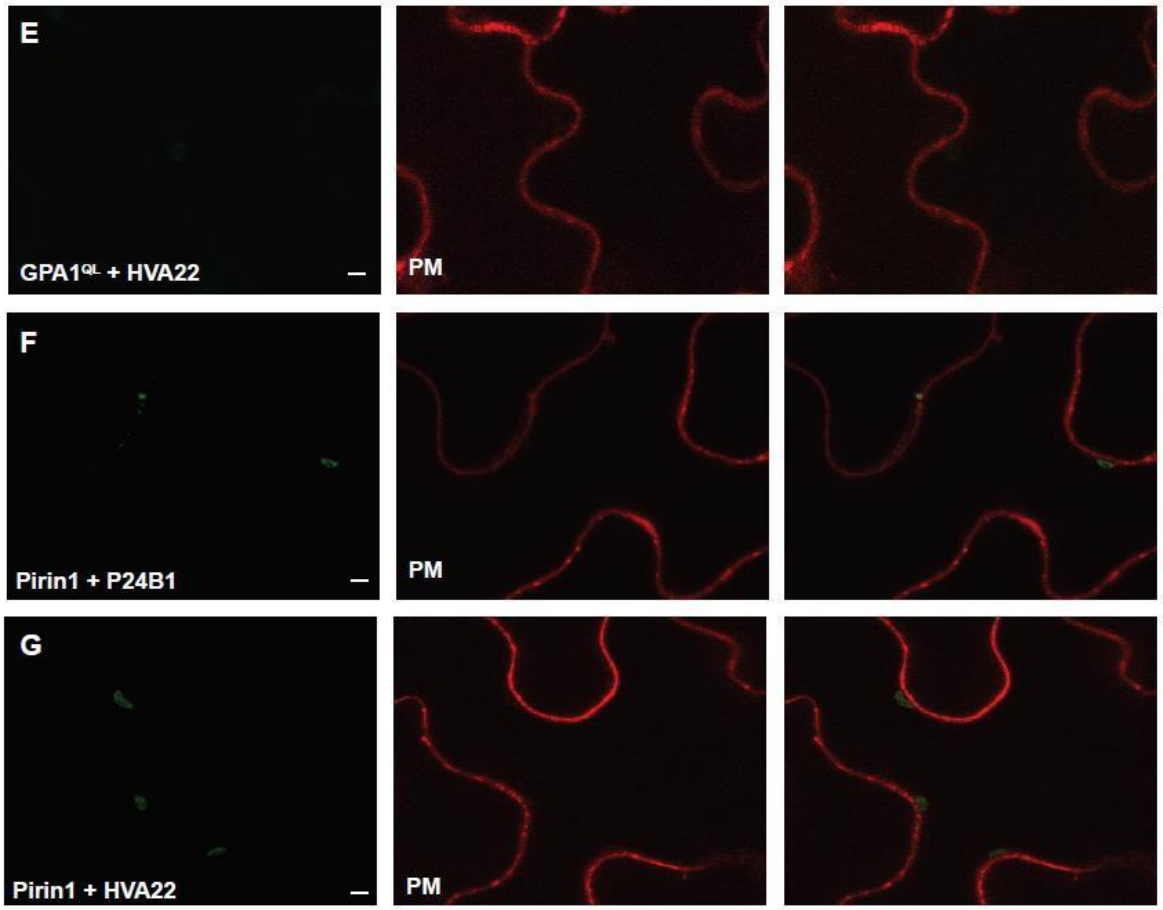

Supplemental Figure 1. BiFC controls for the CLO7, GPA1 and Pirin1 interactions. **(A)** Positive control of GPA1-C-YFP and RGS1-N-YFP (Regulator of G protein Signaling 1) the known GTPase for GPA1 in Arabidopsis, with the plasma membrane (PM) marker fused to mCherry. **(B)** Negative control of the full-length CLO7-N-YFP and P24B1-C-YFP with the PM marker. **(C)** Negative control of GPA1-C-YFP and HVA22-N-YFP with the PM marker. **(D)** Positive control of $GPA1^{QL}$-C-YFP and RGS1-N-YFP with the PM marker. **(E)** Negative control of $GPA1^{QL}$-C-YFP and HVA22-N-YFP with the PM marker. **(F)** Negative control of Pirin1-N-YFP and P24B1-C-YFP with the PM marker. **(G)** Negative control of Pirin1-C-YFP and HVA22-N-YFP with the PM marker. Scale bar = 10 μm.

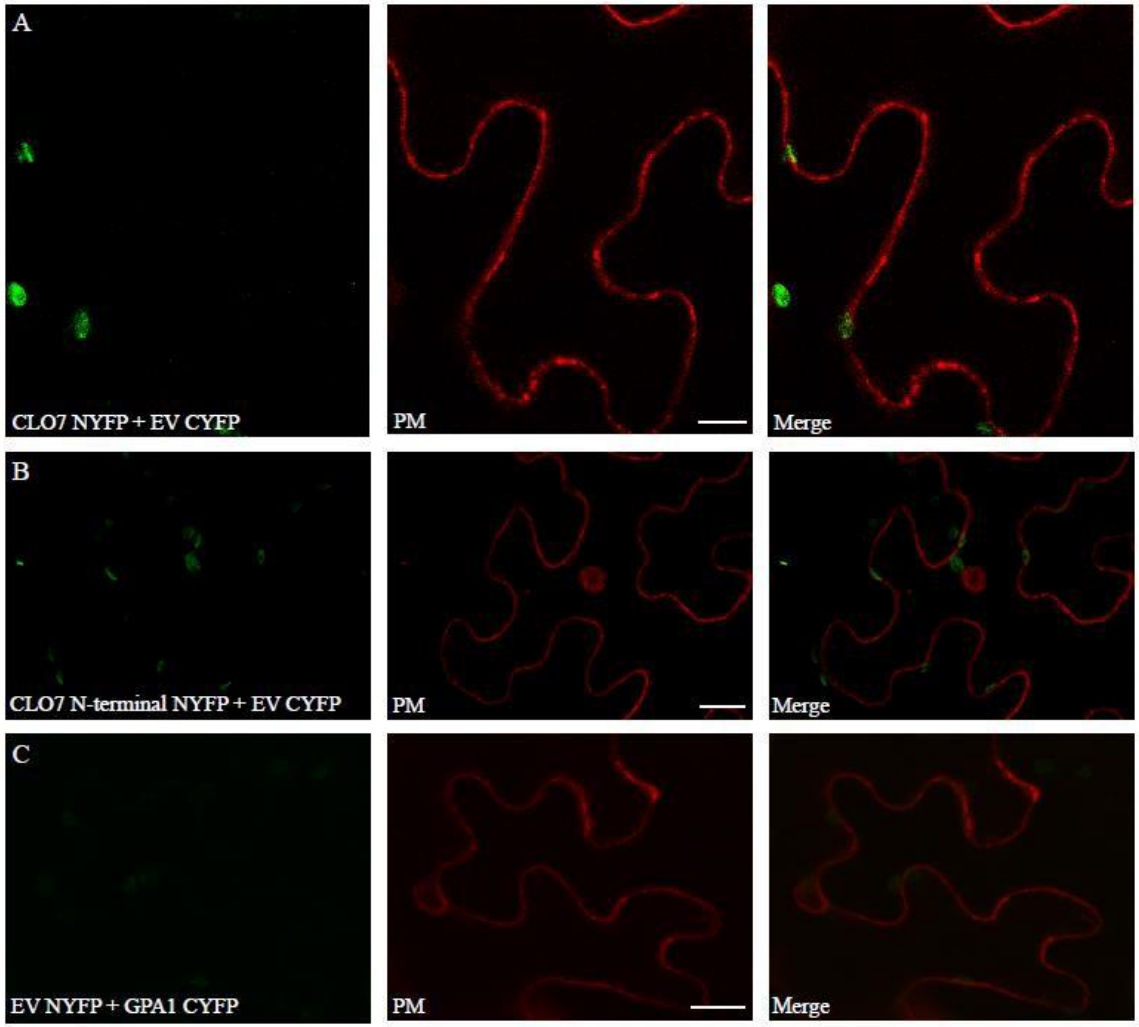

Supplemental Figure 2. Negative BiFC controls for the CLO7 and GPA1 interactions. **(A)** Full-length CLO7-NYFP and an empty CYFP vector with the plasma membrane marker fused to mCherry (PM). **(B)** CLO7 N-terminal truncation (amino acid 1 to 76) NYFP and an empty CYFP vector with the plasma membrane marker. **(C)** An empty NYFP vector with GPA1 CYFP and the plasma membrane marker. Scale bar = 10 μm.

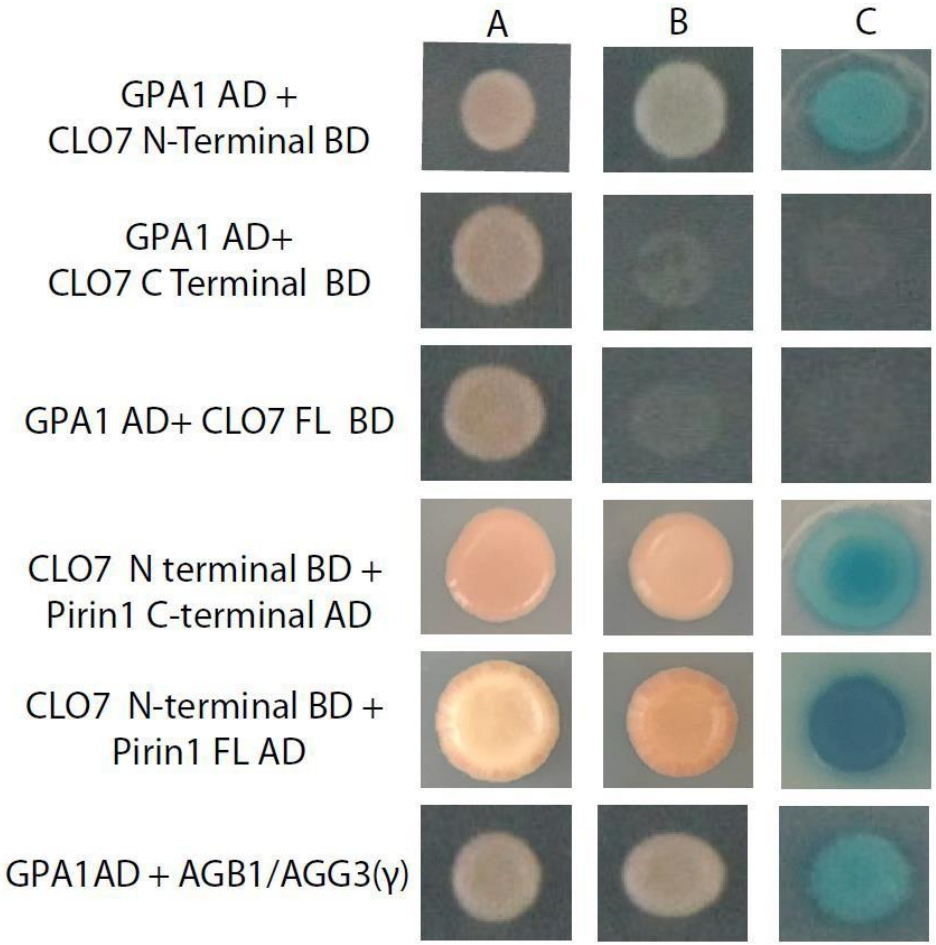
A
B
C
GPA1 AD +
CLO7 N-Terminal BD
GPA1 AD+
CLO7 C Terminal BD
GPA1 AD+ CLO7 FL BD
CLO7 N terminal BD +
Pirin1 C-terminal AD
CLO7 N-terminal BD +
Pirin1 FL AD
GPA1AD + AGB1/AGG3(γ)

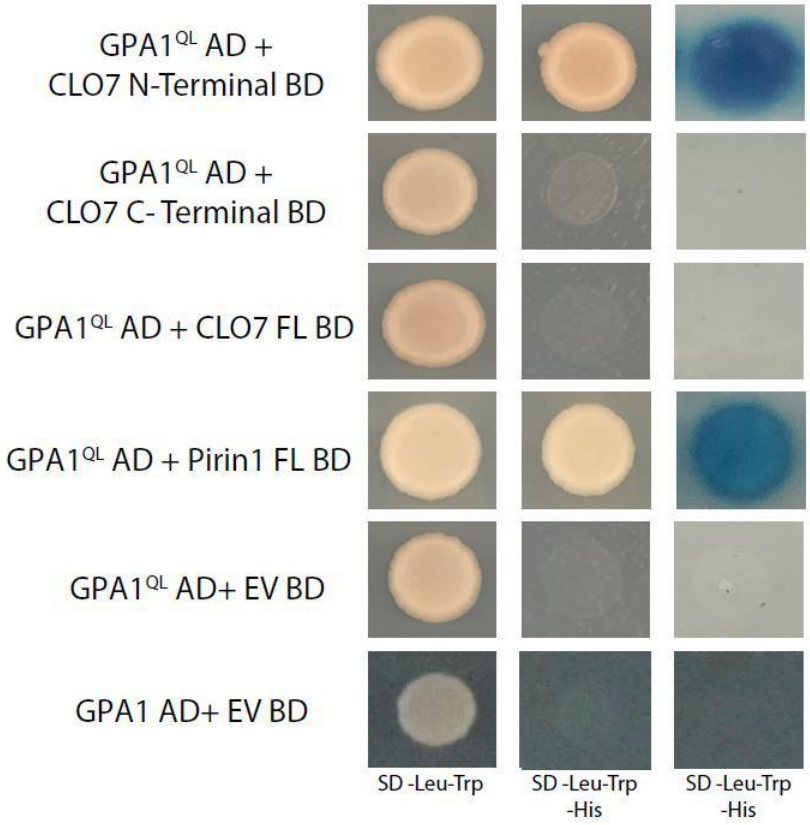

Supplemental Figure 3. CLO7, GPA1, GPA1^{QL} and Pirin1 β-Galactosidase plate assay. **(A)** SD media lacking leucine (Leu) and tryptophan (Trp) indicating that both the GPA1-AD, or GPA1^{QL}-AD, the CLO7-BD fusions, the Pirin1-AD fusions as well as the AGB1/AGG3(γ)-BD and empty-BD are present within the yeast strain. **(B)** SD media lacking leucine, tryptophan and histidine (His) confirming an interaction between GPA1-AD or GPA1^{QL}-AD with the CLO7 N-terminal truncation-BD, the CLO7 N-terminal truncation-BD with the Pirin1 C-terminal truncation-AD (170 a.a) and Pirin1 FL-BD, the GPA1^{QL}-AD and Pirin1 FL-BD and lastly the GPA1-AD and the AGB1/AGG3(γ) positive control. **(C)** SD media lacking leucine, tryptophan and histidine overlay with X-Gal, displaying a blue color indicative of an interaction between GPA1-AD or GPA1^{QL}-AD and the CLO7 N-terminal truncation-BD, the CLO7 N-terminal truncation-BD with the Pirin1 C-terminal-AD and full-length-AD, the GPA1^{QL}-AD with Pirin1 FL-BD and GPA1-AD and the AGB1/AGG3(γ)-BD positive control. FL= full-length, EV= empty vector. The AGB1/AGG(γ) is a BD fusion containing a truncated AGG3 (residues 1-112, Chakravorty et al., 2015).

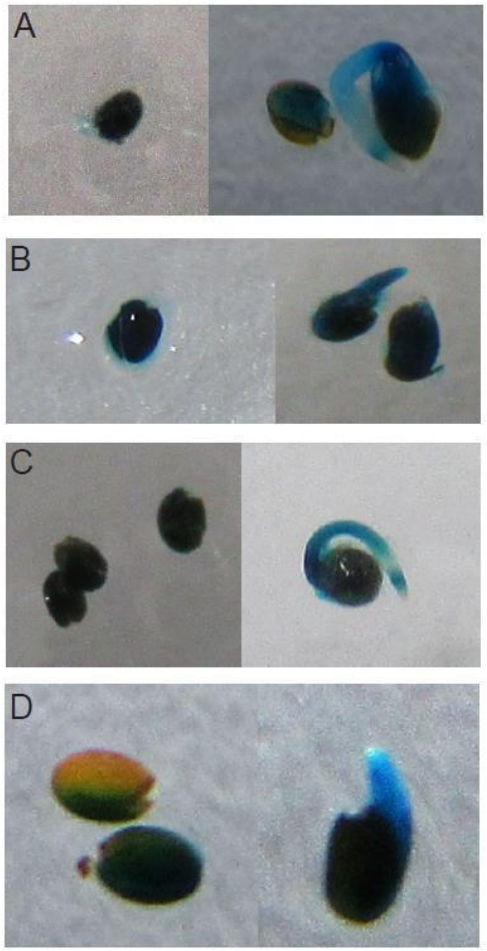

Supplemental Figure 4. β-Glucoronidase assay (GUS) of the promoter*CLO7*:GUS fusion in seed tissue and young radicles of Arabidopsis. **(A)** Germinating seed on ½ MS media with 1% sucrose (control media). **(B)** Germinating seed on ½ MS media with 1% sucrose supplemented with 2 µm abscisic acid (ABA). **(C)** Germinating seed on ½ MS media with 1% sucrose supplemented with 150 mM mannitol. **(D)** Germinating seed on ½ MS media with 1% sucrose supplemented with 200 mM NaCl.

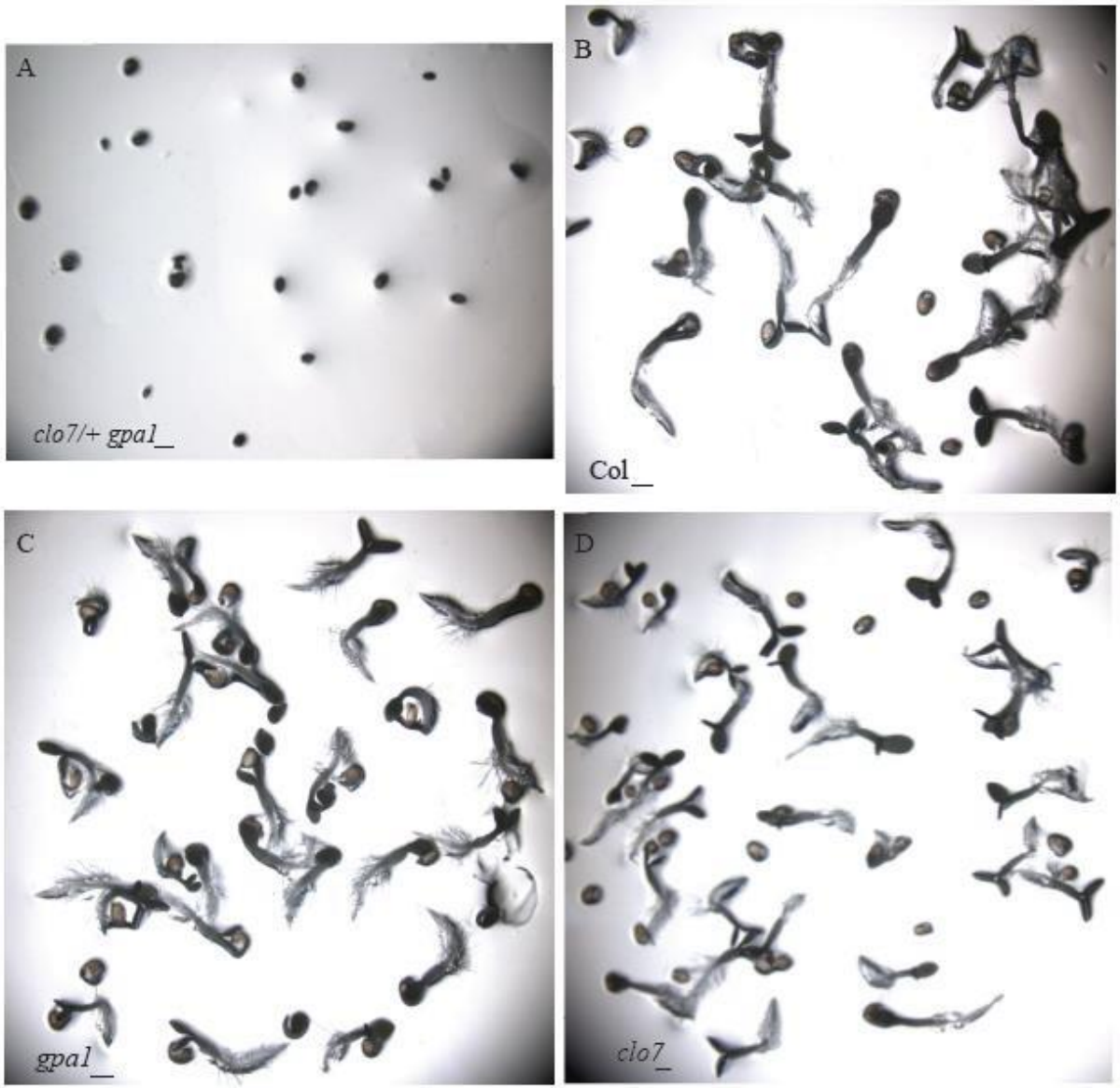

Supplemental Figure 5. Viability test of the abnormal, small shriveled seed from **(A)** the *clo7/+ gpa1* plants, compared to the germination of seed from **(B)** the wild-type Columbia (Col), **(C)** *gpa1*, and **(D)** *clo7*. Bar = 1 mm.

Supplemental Table 1. Primers used to construct promoter *CLO7*:GUS expression clones, RNAi and over-expression (35S) constructs, PCR Gateway primers for BiFC and Y2H**,** RT-PCR primers, primers for the T-DNA mutant screen and primers to create the EF-hand mutants.

Primer	Sequence (5'-3')[a]	Application
GWProCLO7[b]	GGGGACAACTTTGTACAAAAAAGCAGGCTTCTCTTCTTCATCTCGTGGCAAGA	*CLO7* promoter for GUS construct
GWProCLO7[c]	GGGGACCACTTTGTACAAGAAAGCTGGGTAGTTCCTGTCGAAGAAGGAAACATGT	*CLO7* promoter for GUS construct
CLO7GW[b]	GGGGACAACTTTGTACAAAAAAGCAGGCTTCATGTCTCATCAGACAGTAGCGC	*CLO7* CDS for BiFC, Y2H, RNAi and over-expression constructs
CLO7GW[c]	GGGGACCACTTTGTACAAGAAAGCTGGGTATGGTAGTTTTTGTTTCTTGCCA	*CLO7* CDS for BiFC.
CLO7GW2[c]	GGGGACCACTTTGTACAAGAAAGCTGGGTATTATGGTAGTTTTTGTTTCTTGCC	*CLO7* CDS for Y2H, RNAi and over-expression constructs
GPA1GW[b]	GGGGACAACTTTGTACAAAAAAGCAGGCTTCATGGGCTTACTCTGCAGTAGAAGTCG	*GPA1* CDS for BiFC constructs
GPA1GW[c]	GGGGACCACTTTGTACAAGAAAGCTGGGTATAAAAGGCCAGCCTCCAGTAAATTTC	*GPA1* CDS for BiFC constructs
CLO7[b]	GATTTGTGGAATCAAAATTCGA	*CLO7* 5' end for RT-PCR

CLO7[b]	TCATCAACATGGGACTCAGC	*CLO7* 5' end for RT-PCR
CLO7[c]	TGCCACGAGAAGAAGAAGAAG	*CLO7* 3' end for RT-PCR
CLO7[c]	GCTACCATCGTAGATGGCC	*CLO7* 3' end for RT-PCR
CLO7[c]	CAAGAATGTTATGTGATCTCCACATA	*CLO7 3'* UTR for RT-PCR
Actin 2/8[b]	GGTAACATTGTGCTCAGTGGTGG	*Actin 2/8* internal control for RT-PCR
Actin2/8[c]	AACGACCTTAATCTTCATGCTGC	*Actin 2/8* internal control for RT-PCR
CLO7 LP2[c]	TTGTGGAATCAAAATTCGAGG	*CLO7* left primer for T-DNA mutant screen
CLO7 RP[b]	TCAGACAGTAGCGCTAGCCTC	*CLO7* right primer for T-DNA mutant screen
SALK LB1.3[d]	ATTTTGCCGATTTCGGAAC	Salk primer to detect T-DNA
CLO7EFmut1[b]	TTC**GCC**AGGAACAAAGACGGCACCGTTTAT	*CLO7* primer to create *CLO7*^{D37A}

CLO7 EFmut1[c]	ATAAACGGTGCCGTCTTTGTTCCT**GGC**GAA	*CLO7* primer to create *CLO7*^{D37A}
CLO7 EFmut2[b]	TGG**GCC**ACCTACCAAGGATTTAGAGCGCTCG	*CLO7* primer to create *CLO7*^{E48A}
CLO7 EFmut2[c]	GCGCTCTAAATCCTTGGTAGGT**GGC**CCA	*CLO7* primer to create *CLO7*^{E48A}

[a] Underlined sequences are the attB sites used for Gateway Cloning
[b] Forward primer
[c] Reverse primer
[d] SALK Institute (La Jolla, USA)
Bold sequences highlight the point mutation used to create *CLO7*^{D37A} and *CLO7*^{E48A}

Supplemental Table 2. Expression of *CLO7* in the transgenic lines using semi-quantitative RT-PCR.

Genotype	Quantity[a]	Percent [b]
Col	50	N/A
Col	50	N/A
CLO7- RNAi 4 in Col	20	40
CLO7- RNAi 6 in Col	20	40
CLO7- RNAi *gpa1* 4	20	40
CLO7- RNAi *gpa1* 2	20	40
35S:*CLO7* 6	200	400
35S:*CLO7* 4	250	500
35S:*CLO7 gpa1* 1	150	300
35S:*CLO7 gpa1* 6	250	500
35S:*CLO7 clo7* 2	150	300
35S:*CLO7 clo7* 3	150	300
35S:*CLO7 clo7* 1	75	150

[a] Quantity of *CLO7* in ng/µl.
[b] The percent of *CLO7* increase or decrease in expression relative to Col.

Supplemental Table 3. Organelle markers used in bimolecular fluorescence complementation (BiFC).

Organelle	**Targeting Protein**
Plasma membrane	Full-length of AtPIP2A, a plasma membrane aquaporin.
Endoplasmic reticulum	Signal peptide of AtWAK2 (N-terminus of protein), wall-associated kinase2; ER retention signal (His-Asp-Glu-Leu) at the C-terminus.

Supplemental Table 4. Percent germination in repsonse to 2 µm ABA treatment.

Genotype	Day 1 % Germinated	SE	Tukey's *post hoc*	Genotype	Day 2 % Germinated	SE	Tukey's *post hoc*
Col	28	0.4	b	Col	61	0.9	c
gpa1	16	0.5	a	*gpa1*	35	0.8	ab
pirin1	16	0.6	a	*pirin1*	36	0.9	a
clo7	42	0.5	d	*clo7*	95	0.5	de
CLO7- RNAi 6	41	0.2	cd	*CLO7*- RNAi 6	93	0.2	d
CLO7- RNAi 4	39	1.4	c	*CLO7*- RNAi 4	94	0.0	de
CLO7- RNAi/*gpa1* 2	16	1.1	a	*CLO7*- RNAi/*gpa1* 2	34	2.2	a
CLO7- RNAi/*gpa1 4*	17	1.2	a	*CLO7*- RNAi/*gpa1 4*	35	0.9	ab
35S:*CLO7* 6	17	1.2	a	35S:*CLO7* 6	39	0.6	b
35S:*CLO7* 4	17	1.8	a	35S:*CLO7* 4	39	0.1	b
35S:*CLO7*/*gpa1* 1	18	0.6	a	35S:*CLO7*/*gpa1* 1	39	1.4	ab
35S:*CLO7*/*gpa1* 6	18	0.3	a	35S:*CLO7*/*gpa1* 6	37	0.1	ab
35S:*CLO7*/*clo7* 2	28	0	b	35S:*CLO7*/*clo7* 2	59	0.1	c
35S:*CLO7*/*clo7* 1	29	0.2	b	35S:*CLO7*/*clo7* 1	60	0.4	c
35S:*CLO7*/*clo7* 3	28	0.5	b	35S:*CLO7*/*clo7* 3	60	0.7	c

SE = standard error of the mean.

(Continue)

Supplemental Table 4. Continued

Genotype	Day 3 % Germinated	SE	Tukey's *post hoc*	Genotype	Day 4 % Germinated	SE	Tukey's *post hoc*
Col	61	0.9	c	Col	100	0.0	a
gpa1	35	0.8	ab	*gpa1*	100	0.0	a
pirin1	36	0.9	a	*pirin1*	100	0.0	a
clo7	95	0.5	de	*clo7*	100	0.0	a
CLO7- RNAi 6	93	0.2	d	*CLO7*- RNAi 6	100	0.0	a
CLO7- RNAi 4	94	0.0	de	*CLO7*- RNAi 4	100	0.0	a
CLO7- RNAi/*gpa1* 2	34	2.2	a	*CLO7*- RNAi/*gpa1* 2	100	0.0	a
CLO7- RNAi/*gpa1 4*	35	0.9	ab	*CLO7*- RNAi/*gpa1 4*	100	0.0	a
35S:*CLO7* 6	39	0.6	b	35S:*CLO7* 6	100	0.0	a
35S:*CLO7* 4	39	0.1	b	35S:*CLO7* 4	100	0.0	a
35S:*CLO7*/*gpa1* 1	39	1.4	ab	35S:*CLO7*/*gpa1* 1	100	0.0	a
35S:*CLO7*/*gpa1* 6	37	0.1	ab	35S:*CLO7*/*gpa1* 6	100	0.0	a
35S:*CLO7*/*clo7* 2	59	0.1	c	35S:*CLO7*/*clo7* 2	100	0.0	a
35S:*CLO7*/*clo7* 1	60	0.4	c	35S:*CLO7*/*clo7* 1	100	0.0	a
35S:*CLO7*/*clo7* 3	60	0.7	c	35S:*CLO7*/*clo7* 3	100	0.0	a

Supplemental Table 4A. Percent germination on control media (0 µm ABA) on Day

Genotype	Day 1 % Germinated	SE	Tukey's *post hoc*
Col	100	0	a
gpa1	100	0	a
pirin1	100	0	a
clo7	100	0	a
CLO7- RNAi 6	100	0	a
CLO7- RNAi 4	100	0	a
CLO7- RNAi/*gpa1* 2	100	0	a
CLO7- RNAi/*gpa1 4*	100	0	a
35S:*CLO7* 6	100	0	a
35S:*CLO7* 4	100	0	a
35S:*CLO7*/*gpa1* 1	100	0	a
35S:*CLO7*/*gpa1* 6	100	0	a
35S:*CLO7*/*clo7* 2	100	0	a
35S:*CLO7*/*clo7* 1	100	0	a
35S:*CLO7*/*clo7* 3	100	0	a

SE = standard error of the mean.

Supplemental Table 5. Percent germination in repsonse to 400 mM mannitol treatment.

Genotype	Day 1 % Germinated	SE	Tukey's *post hoc*	Genotype	Day 2 % Germinated	SE	Tukey's *post hoc*	Genotype	Day 3 % Germinated	SE	Tukey's *post hoc*
Col	0	N/A	N/A	Col	30	0.2	ef	Col	66	0.2	c
gpa1	0	N/A	N/A	*gpa1*	18	0.4	a	*gpa1*	46	0.5	a
clo7	0	N/A	N/A	*clo7*	34	0.1	g	*clo7*	75	0.4	d
CLO7- RNAi 6	0	N/A	N/A	*CLO7*- RNAi 6	32	0.9	fg	*CLO7*- RNAi 6	73	1.1	d
CLO7- RNAi 4	0	N/A	N/A	*CLO7*- RNAi 4	32	0.6	g	*CLO7*- RNAi 4	73	0.5	d
CLO7- RNAi/*gpa1* 2	0	N/A	N/A	*CLO7*- RNAi/*gpa1* 2	32	0.6	g	*CLO7*- RNAi/*gpa1* 2	73	0.7	d
CLO7- RNAi/*gpa1 4*	0	N/A	N/A	*CLO7*- RNAi/*gpa1 4*	32	0.3	g	*CLO7*- RNAi/*gpa1 4*	73	0.4	d
35S:*CLO7* 6	0	N/A	N/A	35S:*CLO7* 6	24	0.1	bc	35S:*CLO7* 6	59	0.1	b
35S:*CLO7* 4	0	N/A	N/A	35S:*CLO7* 4	24	0.1	b	35S:*CLO7* 4	59	0.4	b
35S:*CLO7*/*gpa1* 1	0	N/A	N/A	35S:*CLO7*/*gpa1* 1	25	0.7	bc	35S:*CLO7*/*gpa1* 1	58	0.4	b
35S:*CLO7*/*gpa1* 6	0	N/A	N/A	35S:*CLO7*/*gpa1* 6	24	0.7	cd	35S:*CLO7*/*gpa1* 6	59	0.2	b
35S:*CLO7*/*clo7* 2	0	N/A	N/A	35S:*CLO7*/*clo7* 2	29	0.3	e	35S:*CLO7*/*clo7* 2	66	0.7	c
35S:*CLO7*/*clo7* 1	0	N/A	N/A	35S:*CLO7*/*clo7* 1	28	0.1	e	35S:*CLO7*/*clo7* 1	65	0.5	c
35S:*CLO7*/*clo7* 3	0	N/A	N/A	35S:*CLO7*/*clo7* 3	28	0.5	de	35S:*CLO7*/*clo7* 3	66	0.2	c

SE = standard error of the mean.

N/A = Not Applicable.

(Continued)

Supplemental Table 5. Continued

Genotype	Day 4 % Germinated	SE	Tukey's *post hoc*	Genotype	Day 5 % Germinated	SE	Tukey's *post hoc*
Col	92	0.3	a	Col	100	0	a
gpa1	94	0.7	abc	*gpa1*	100	0	a
clo7	100	0.0	d	*clo7*	100	0	a
CLO7- RNAi 6	100	0.0	d	*CLO7*- RNAi 6	100	0	a
CLO7- RNAi 4	100	0.0	d	*CLO7*- RNAi 4	100	0	a
CLO7- RNAi/*gpa1* 2	100	0.0	d	*CLO7*- RNAi/*gpa1* 2	100	0	a
CLO7- RNAi/*gpa1 4*	100	0.0	d	*CLO7*- RNAi/*gpa1 4*	100	0	a
35S:*CLO7* 6	94	1.5	bc	35S:*CLO7* 6	100	0	a
35S:*CLO7* 4	93	1.5	abc	35S:*CLO7* 4	100	0	a
35S:*CLO7*/*gpa1* 1	93	0.9	ab	35S:*CLO7*/*gpa1* 1	100	0	a
35S:*CLO7*/*gpa1* 6	96	0.7	bc	35S:*CLO7*/*gpa1* 6	100	0	a
35S:*CLO7*/*clo7* 2	95	0.3	bc	35S:*CLO7*/*clo7* 2	100	0	a
35S:*CLO7*/*clo7* 1	97	0.7	c	35S:*CLO7*/*clo7* 1	100	0	a
35S:*CLO7*/*clo7* 3	95	0.2	abc	35S:*CLO7*/*clo7* 3	100	0	a

Supplemental Table 5A. Percent germination on control media (0 mM mannitol) on Day 1.

	Day 1		
Genotype	% Germinated	SE	Tukey's *post hoc*
Col	100	0	a
gpa1	100	0	a
clo7	100	0	a
CLO7- RNAi 6	100	0	a
CLO7- RNAi 4	100	0	a
CLO7- RNAi/*gpa1* 2	100	0	a
CLO7- RNAi/*gpa1 4*	100	0	a
35S:*CLO7* 6	100	0	a
35S:*CLO7* 4	100	0	a
35S:*CLO7*/*gpa1* 1	100	0	a
35S:*CLO7*/*gpa1* 6	100	0	a
35S:*CLO7*/*clo7* 2	100	0	a
35S:*CLO7*/*clo7* 1	100	0	a
35S:*CLO7*/*clo7* 3	100	0	a

SE = standard error of the mean.

7.5 Supplemental Material

Chapter 4: "The caleosin *RD20/CLO3* regulates abscisic acid affects on lateral root development and in conjunction with the caleosin *CLO7* regulates flowering time"

Supplemental Table 1. Expression levels of *RD20/CLO3* in a *soc ful* double mutant and wild-type *RD20/CLO3* expression

soc ful mutant	62
Col wild-type	137

Supplemental Table 1a. Expression levels of *CLO7* in a *elf6-3 ref6C* double mutant and wild-type *CLO7* expression

elf6-3 ref6C mutant	33
Col wild-type	53

Expression is normalized to fragments per kilobase per million (FPKM)

7.6 Supplemental Material

Chapter 5: “Characterization of the Esi3/RCI2/PMP3 gene family in the Triticeae”

Table S1: Comparison between Esi3/RCI2/PMP3 amino acid sequence and annotations of *Triticum aestivum*				
Gene	Ensembl Plants[a] Identifier	Comparison of NCBI's Translation to Ensembl Plants	Same Protein Translation[b]	Differences Between Translations
Esi3-1-A	TraesCS4A01G107100.1		Yes	
Esi3-1-B	TraesCS4B01G197300.1		Yes	
Esi3-1-D	TraesCS4D01G19770.1		Yes	
Esi3-2-A	TraesCS4A01G107000.1		Yes	
Esi3-2-D	TraesCS4D01G197800.1		Yes	
Esi3-3-A	TraesCS5A01G360000.1		Yes	
Esi3-3-B	TraesCS5B01G362500.1		Yes	
Esi3-3-D	TraesCS5D01G369400.1		Yes	
Esi3-4-A	TraesCS1A01G082500.2		Yes	
Esi3-4-B	TraesCS1B01G100100.1		Yes	
Esi3-4-D	TraesCS1D01G083900.1		Yes	
Esi3-5-A	TraesCS2A01G152000.1		Yes	
Esi3-5-B	TraesCS2B01G177100.1		Yes	
Esi3-5-D	TraesCS2D01G157100.1		Yes	
Esi3-6-A	TraesCS7A01G504000.1		Yes	
Esi3-6-B	TraesCS7B01G411100.1	Coverage 100%; 99% Identity	No	Ensembl Plants has conserved amino acid change at position 47
Esi3-6-D	TraesCS7D01G491100.1	Coverage 100%; 97% Identity	No	Two conserved amino acid differences at positions 43 and 70
Esi3-7-A	TraesCS7A01G149300.1		Yes	
Esi3-7-B	TraesCS7B01G053000.1	Coverage 41%, 100% Identity	No	Ensembl Plants has long N-terminal extension
Esi3-7-D	TraesCS7D01G150900.1		Yes	
Esi3-8-A	TraesCS1A01G062000.1		Yes	
Esi3-8-B	TraesCS1B01G080300.1		Yes	
Esi3-8-D	TraesCS1D01G062900.1		Yes	
Esi3-9-A	TraesCS2A01G582800.1		Yes	
Esi3-9-B	TraesCS2B01G603700.1		Yes	
Esi3-9-D	TraesCS2D01G597300.1		Yes	
Esi3-10-A	Not Annotated	No predicted protein	N/A	Sequence with highest identity not annotated on Ensembl Plants
Esi3-10-B	TraesCS5B01G362400.1		Yes	
Esi3-10-D	TraesCS5D01G369300.1	Coverage 100%; 81% Identity	No	Multiple mismatches from amino acids 15-31
[a] [23] Ensembl Plants database http://plants.ensembl.org/index.html				
[b] Protein coding comparison between NCBI sequences and Ensembl Plants sequences				

Table S2: Nucleic acid and amino acid sequence identity among members of the *Esi3/RCI2/PMP3* gene family in *Triticum aestivum*

	Nucleic Acid Sequence																													
Amino Acid Sequence	*Esi3-1-A*	*Esi3-1-B*	*Esi3-1-D*	*Esi3-2-A*	*Esi3-2-D*	*Esi3-3-A*	*Esi3-3-B*	*Esi3-3-D*	*Esi3-4-A*	*Esi3-4-B*	*Esi3-4-D*	*Esi3-5-A*	*Esi3-5-B*	*Esi3-5-D*	*Esi3-6-A*	*Esi3-6-B*	*Esi3-6-D*	*Esi3-7-A*	*Esi3-7-B*	*Esi3-7-D*	*Esi3-8-A*	*Esi3-8-B*	*Esi3-8-D*	*Esi3-9-A*	*Esi3-9-B*	*Esi3-9-D*	*Esi3-10-A*	*Esi3-10-B*	*Esi3-10-D*	Amino Acid Sequence
Esi3-1-A	100.00	100.00	99.31	92.41	91.72	76.55	76.55	77.93	71.03	71.03	72.41	66.21	66.21	66.21	67.59	66.21	66.21	67.59	68.28	66.9	76.55	75.86	75.86	66.90	68.97	67.59	76.55	77.93	78.62	*Esi3-1-A*
Esi3-1-B	100.00	100.00	99.31	92.41	91.72	76.55	76.55	77.93	71.03	71.03	72.41	66.21	66.21	66.21	67.59	66.21	66.21	67.59	68.28	66.9	76.55	75.86	75.86	66.90	68.97	67.59	76.55	77.93	78.62	*Esi3-1-B*
Esi3-1-D	100.00	100.00	100.00	93.10	92.41	75.86	75.86	77.24	70.34	70.34	71.72	66.21	66.21	66.21	66.90	65.52	66.90	66.90	67.59	66.2	75.86	75.17	75.17	66.90	68.97	67.59	75.86	77.24	77.93	*Esi3-1-D*
Esi3-2-A	89.58	89.58	89.58	100.00	98.62	77.24	76.55	77.24	72.41	72.41	72.41	68.97	68.97	68.97	66.21	64.83	66.21	66.90	67.59	66.2	77.93	77.24	77.24	64.83	65.52	64.14	76.55	77.24	78.62	*Esi3-2-A*
Esi3-2-D	89.58	89.58	89.58	100.00	100.00	76.55	77.24	77.93	72.41	72.41	72.41	68.97	68.97	68.97	66.21	64.83	66.21	67.59	68.28	66.9	78.62	77.93	77.93	64.83	65.52	64.14	77.24	77.93	79.31	*Esi3-2-D*
Esi3-3-A	75.00	75.00	75.00	77.08	77.08	100.00	97.32	97.32	77.93	77.93	75.86	78.62	78.62	78.62	78.52	78.52	77.85	79.87	78.52	80.5	85.52	86.90	86.90	67.59	68.97	67.59	93.96	92.62	93.29	*Esi3-3-A*
Esi3-3-B	77.08	77.08	77.08	79.17	79.17	97.96	100.00	98.66	76.55	76.55	74.48	78.62	78.62	78.62	79.19	79.19	78.52	81.21	79.87	81.9	85.52	86.90	86.90	68.97	68.97	68.97	93.96	93.96	93.29	*Esi3-3-B*
Esi3-3-D	79.17	79.17	79.17	79.17	79.17	95.92	97.96	100.00	77.24	77.24	75.17	79.31	79.31	79.31	80.54	80.54	79.87	82.55	81.21	83.2	85.52	86.90	86.90	68.97	70.34	68.97	95.30	95.30	94.63	*Esi3-3-D*
Esi3-4-A	68.75	68.75	68.75	70.83	70.83	70.83	68.75	68.75	100.00	100.00	97.24	88.28	88.28	88.28	72.41	71.72	71.03	73.79	73.79	73.1	74.48	74.48	74.48	73.10	74.48	73.10	77.93	76.55	77.24	*Esi3-4-A*
Esi3-4-B	68.75	68.75	68.75	70.83	70.83	70.83	68.75	68.75	100.00	100.00	97.24	88.28	88.28	88.28	72.41	71.72	71.03	73.79	73.79	73.1	74.48	74.48	74.48	73.10	74.48	73.10	77.93	76.55	77.24	*Esi3-4-B*
Esi3-4-D	68.75	68.75	68.75	70.83	70.83	70.83	68.75	68.75	100.00	100.00	100.00	86.21	86.21	86.21	72.41	71.72	71.03	71.72	71.72	71.0	72.41	72.41	72.41	73.79	75.17	73.79	75.86	74.48	76.55	*Esi3-4-D*
Esi3-5-A	64.58	64.58	64.58	64.58	64.58	60.42	62.50	62.50	83.33	83.33	83.33	100.00	100.00	100.00	73.79	73.10	73.10	75.17	73.79	74.5	73.79	75.17	75.17	75.17	76.55	75.17	80.00	78.62	79.31	*Esi3-5-A*
Esi3-5-B	64.58	64.58	64.58	64.58	64.58	60.42	62.50	62.50	83.33	83.33	83.33	100.00	100.00	100.00	73.79	73.10	73.10	75.17	73.79	74.5	73.79	75.17	75.17	75.17	76.55	75.17	80.00	78.62	79.31	*Esi3-5-B*
Esi3-5-D	64.58	64.58	64.58	64.58	64.58	60.42	62.50	62.50	83.33	83.33	83.33	100.00	100.00	100.00	73.79	73.10	73.10	75.17	73.79	74.5	73.79	75.17	75.17	75.17	76.55	75.17	80.00	78.62	79.31	*Esi3-5-D*
Esi3-6-A	62.50	62.50	62.50	60.42	60.42	65.31	67.35	69.39	58.33	58.33	58.33	58.33	58.33	58.33	100.00	98.67	98.67	74.50	73.15	73.8	71.03	73.79	73.79	64.83	65.52	64.14	77.18	77.18	77.18	*Esi3-6-A*
Esi3-6-B	58.33	58.33	58.33	58.33	58.33	63.27	65.31	67.35	56.25	56.25	56.25	56.25	56.25	56.25	95.92	100.00	98.67	73.83	72.48	73.8	71.72	74.48	74.48	64.14	64.83	63.45	77.18	77.18	77.18	*Esi3-6-B*
Esi3-6-D	58.33	58.33	58.33	58.33	58.33	63.27	65.31	67.35	56.25	56.25	56.25	56.25	56.25	56.25	95.92	100.00	100.00	73.15	71.81	73.2	70.34	73.10	73.10	64.14	64.83	63.45	76.51	76.51	76.51	*Esi3-6-D*
Esi3-7-A	58.33	58.33	58.33	56.25	56.25	65.31	65.31	67.35	58.33	58.33	58.33	54.17	54.17	54.17	61.22	59.18	59.18	100.00	98.66	99.3	75.17	76.55	75.86	62.76	64.14	62.76	80.54	80.54	79.87	*Esi3-7-A*
Esi3-7-B	58.33	58.33	58.33	56.25	56.25	65.31	65.31	67.35	58.33	58.33	58.33	54.17	54.17	54.17	61.22	59.18	59.18	100.00	100.00	98.0	75.17	75.17	74.48	64.14	65.52	64.14	79.19	79.19	78.52	*Esi3-7-B*
Esi3-7-D	58.33	58.33	58.33	56.25	56.25	67.35	67.35	69.39	58.33	58.33	58.33	54.17	54.17	54.17	61.22	59.18	59.18	97.96	97.96	100.0	75.86	77.24	76.55	62.07	63.45	62.07	81.21	81.21	80.54	*Esi3-7-D*
Esi3-8-A	79.17	79.17	79.17	81.25	81.25	81.25	79.17	77.08	68.75	68.75	68.75	60.42	60.42	60.42	56.25	56.25	56.25	58.33	58.33	60.4	100.00	96.55	95.86	62.07	63.45	62.07	83.45	83.45	82.76	*Esi3-8-A*
Esi3-8-B	79.17	79.17	79.17	81.25	81.25	81.25	79.17	77.08	68.75	68.75	68.75	60.42	60.42	60.42	56.25	56.25	56.25	58.33	58.33	60.4	100.00	100.00	99.31	62.76	64.14	62.76	84.83	84.83	84.14	*Esi3-8-B*
Esi3-8-D	79.17	79.17	79.17	81.25	81.25	81.25	79.17	77.08	68.75	68.75	68.75	60.42	60.42	60.42	56.25	56.25	56.25	58.33	58.33	60.4	100.00	100.00	100.00	63.45	64.83	63.45	84.83	84.83	84.14	*Esi3-8-D*
Esi3-9-A	64.58	64.58	64.58	60.42	60.42	58.33	60.42	62.50	64.58	64.58	64.58	68.75	68.75	68.75	56.25	54.17	54.17	47.92	47.92	47.9	56.25	56.25	56.25	100.00	97.93	99.31	68.97	67.59	69.66	*Esi3-9-A*
Esi3-9-B	66.67	66.67	66.67	62.50	62.50	60.42	62.50	64.58	66.67	66.67	66.67	70.83	70.83	70.83	58.33	56.25	56.25	50.00	50.00	50.0	58.33	58.33	58.33	97.92	100.00	98.62	70.34	68.97	71.03	*Esi3-9-B*
Esi3-9-D	64.58	64.58	64.58	60.42	60.42	58.33	60.42	62.50	64.58	64.58	64.58	68.75	68.75	68.75	56.25	54.17	54.17	47.92	47.92	47.9	56.25	56.25	56.25	100.00	97.92	100.00	68.97	67.59	69.66	*Esi3-9-D*
Esi3-10-A	77.08	77.08	77.08	77.08	77.08	87.76	89.80	91.84	70.83	70.83	70.83	62.50	62.50	62.50	65.31	63.27	63.27	65.31	65.31	67.4	75.00	75.00	75.00	60.42	62.50	60.42	100	96.64	97.32	*Esi3-10-A*
Esi3-10-B	79.17	79.17	79.17	79.17	79.17	89.80	91.84	93.88	70.83	70.83	70.83	64.58	64.58	64.58	67.35	65.31	65.31	67.35	67.35	69.4	77.08	77.08	77.08	62.50	64.58	62.50	97.96	100	96.64	*Esi3-10-B*
Esi3-10-D	79.17	79.17	79.17	79.17	79.17	89.80	91.84	93.88	70.83	70.83	70.83	64.58	64.58	64.58	67.35	65.31	65.31	67.35	67.35	69.4	77.08	77.08	77.08	62.50	64.58	62.50	97.96	100	100	*Esi3-10-D*

Table S3: Homologous *Esi3/RCI2/PMP3* NCBI accession numbers and comparison to Ensembl Plants annotations

Species	Gene	NCBI Accession	Publication	Ensembl Plants Annotation	Same Translation[a]	Translation Comparisons
Hordeum vulgare	*HvEsi3-1*	BAJ85904.1	Unpublished	HORVU4Hr1G057000.3	No	Extended 5' and 3' ends
	HvBlt101-2	BAJ89049.1	Goddard et al., 1993	HORVU4Hr1G057020.2, HORVU4Hr1G057020.3	Yes	
	HvEsi3-4	BAK03378.1	Unpublished	HORVU1Hr1G017700.3	Yes	
	HvEsi3-5	BAJ88867.1	Unpublished	HORVU2Hr1G027430.2, HORVU2Hr1G027430.3	Yes	
	HvEsi3-6	BAK03743.1	Unpublished	HORVU7Hr1G113020.4	Yes	
	HvEsi3-7	DK716258.1	Unpublished	HORVU7Hr1G030530.3	No	Extended 5' end
	HvEsi3-8	BG416092.2	Unpublished	HORVU1Hr1G012710.1	No	Extended 5' and 3' ends
	HvEsi3-9	BAK07288.1	Unpublished	N/A	No	Not annotated as protein coding
	HvEsi3-10	BAJ90014.1	Khurana et al., 2015	HORVU7Hr1G030530.1, HORVU7Hr1G030530.3	No	Extended 5' end
Sorghum bicolor	*SbEsi3-1*	XP_002440508.1	unpublished	SORBI_3009G025500	Yes	
	SbEsi3-2	XP_002465426.1	unpublished	SORBI_3001G409400	Yes	
	SbEsi3-3	XP_002460652.1	Khurana et al., 2015	SORBI_3002G294500	Yes	
	SbEsi3-4	XP_021309366.1	unpublished	SORBI_3002G389400	Yes	
	SbEsi3-5	XP_002437373.1	unpublished	SORBI_3010G211400	Yes	
	SbEsi3-6	XP_002437973.1	unpublished	SORBI_3010G066300	Yes	
	SbEsi3-7	XP_002465219.1	unpublished	SORBI_3001G359601	Yes	
Brachypodium distachyon	*BdRCI2-1*	XP_003563330.1	Rocha, 2015	BRADI_1g31072v3	Yes	
	BdRCI2-2	XP_003568974.1	Rocha, 2015	BRADI_2g36770v3	Yes	
	BdRCI2-3	XP_003557909.1	Rocha, 2015	BRADI_1g61460v3	Yes	
	BdRCI2-4	XP_003558174.1	Rocha, 2015	BRADI_1g65780v3	Yes	
	BdRCI2-5	XP_003578630.1	Rocha, 2015	BRADI_4g37720v3	Yes	
	BdRCI2-6	XP_003564192.1	Rocha, 2015	BRADI_1g47270v3	Yes	
	BdRCI2-7	XP_014752685.1	Unpublished	BRADI_1g20220v3	Yes	
	BdRCI2-8	XP_014754368.1	Unpublished	BRADI_2g11135v3	Yes	
Zea mays	*ZmPMP3-1*	EU364508.1	Fu et al., 2012	Zm00001d024778_T001	No	99% identity, but protein sequence ends in a T vs N
	ZmPMP3-2	EU959002.1	Fu et al., 2012	Zm00001d006329_T001	Yes	
	ZmPMP3-3	EU962407.1	Fu et al., 2012	Zm00001d045096_T001	Yes	
	ZmPMP3-4	EU954642.1	Fu et al., 2012	Zm00001d028718_T001	Yes	
	ZmPMP3-5	EU975274.1	Fu et al., 2012	Zm00001d022264_T001	No	98% identity; FLG vs FFG in translation
	ZmPMP3-6	EU976341.1	Fu et al., 2012	Zm00001d035505_T001	Yes	
	ZmPMP3-7	EU955642.1	Fu et al., 2012	Zm00001d008200_T001	Yes	
	ZmPMP3-8	EU971491.1	Fu et al., 2012	Zm00001d040544_T001	Yes	
	ZmRCI2-3	XP_020404221.1	Zhao et al., 2014	N/A	No	Not annotated as protein coding
	ZmRCI2-8	NP_001151922.1	Zhao et al., 2014	Zm00001d046834_T001	Yes	
	ZmRCI2-9	XP_020399959.1	Zhao et al., 2014	Zm00001d047419_T001	Yes	
Oryza sativa	*OsRCI2-1*	EEE54356.1	Medina et al., 2007	BGIOSGA003302-TA	Yes	
	OsRCI2-2	AP014957.1	Medina et al., 2007	N/A	No	Not annotated as protein coding
	OsRCI2-3	AAG46140.1	Medina et al., 2007	BGIOSGA010660-TA	Yes	co-ordinates 24254–24679
	OsRCI2-4	EAY90184.1	Medina et al., 2007	BGIOSGA010661-TA	Yes	
	OsRCI2-5	XP_015633211.1	Medina et al., 2007	BGIOSGA010954-TA	Yes	
	OsLTI6A	XP_015647973.1	Morsy et al., 2005	OS07T0635900-01	Yes	
	OsLTI6B	XP_015640253.1	Morsy et al., 2005	BGIOSGA018851-TA	No	extended 3' end
	OsRCI2-7	XP_015637682.1	Medina et al., 2007	BGIOSGA018907-TA	Yes	
	OsRCI2-8	XP_015643303.1	Medina et al., 2007	BGIOSGA021772-TA	Yes	
	OsRCI2-9	EAZ01907.1	Medina et al., 2007	BGIOSGA023380-TA	Yes	
	OsRCI2-11	XP_015612003.1	Medina et al., 2007	BGIOSGA031251-TA	Yes	
	OsRCI2-12	BAF24778.1	Medina et al., 2007	OS09T0322400-01	Yes	
Aegilops tauschii	*AetEsi3-1*	XP_020150593.1	Unpublished	EMT15832	Yes	
	AetEsi3-2	XP_020150605.1	Unpublished	EMT15831	No	98.1% identity; RYG vs RSG in translation
	AetEsi3-3	XP_020168538.1	Unpublished	EMT24455	No	96% identity; WGR vs CCS in translation
	AetEsi3-4	XP_020190487.1	Unpublished	N/A	No	Not annotated as protein coding
	AetEsi3-5	XM_020319125.1	Unpublished	EMT07358	Yes	
	AetEsi3-6	XP_020198926.1	Unpublished	EMT12999	Yes	
	AetEsi3-7	XP_020151310.1	Unpublished	EMT01854	Yes	
	AetEsi3-8	XP_020178067.1	Unpublished	EMT05681	Yes	
	AetEsi3-9	XP_020160007.1	Unpublished	N/A	No	Not annotated as protein coding
	AetEsi3-10	XP_020168537.1	Unpublished	EMT25386	Yes	
Arabidopsis thaliana	*AtRCI2A*	NP_187239.1	Capel et al., 1997	AT3G05880.1	Yes	
	AtRCI2B	NP_187240.1	Capel et al., 1997	AT3G05890.1	Yes	
	AtRCI2C	NP_176067.1	Medina et al., 2007	AT1G57550.1	Yes	
	AtRCI2D	NP_179982.1	Medina et al., 2007	AT2G24040.1	Yes	
	AtRCI2E	NP_194794.1	Medina et al., 2007	AT4G30650.1	Yes	
	AtRCI2F	NP_194795.1	Medina et al., 2007	AT4G30660.1, AT4G30660.2	Yes	
	AtRCI2G	NP_974629.1	Medina et al., 2007	AT4G28088.1	Yes	
	AtRCI2H	NP_565897.1	Medina et al., 2007	AT2G38905.1	Yes	
Secale cereale	*ScEsi3-1*	GCJW01020680.1	Unpublished	Genome not annotated	N/A	
	ScEsi3-2	GCJW01023827.1	Unpublished	Genome not annotated	N/A	
	ScEsi3-3	GCJW01020158.1	Unpublished	Genome not annotated	N/A	
	ScEsi3-4	GCJW01019226.1	Unpublished	Genome not annotated	N/A	
	ScEsi3-5	GCJW01023929.1	Unpublished	Genome not annotated	N/A	
	ScEsi3-6	GCJW01020650.1	Unpublished	Genome not annotated	N/A	
	ScEsi3-7	GCJW01023828.1	Unpublished	Genome not annotated	N/A	
	ScEsi3-8	GCJW01021120.1	Unpublished	Genome not annotated	N/A	
	ScEsi3-9	GCJW01018134.1	Unpublished	Genome not annotated	N/A	
	ScEsi3-10	GCJW01020353.1	Unpublished	Genome not annotated	N/A	

[a]Protein coding comparison between NCBI sequences and Ensembl Plants sequences

N/A - not applicable, protein is not annotated

Additional File 4: Sequences S4

Brachypodium distachyon

>*BdRCI2-1*_XP_003563330.1 MSSSGGCSTCLETIFAAVLPPLGVFFRYGCCSSEFFISLLLTALGYVPGIAYSVWVILKTAPEPPGIDGDRPYYILA

>*BdRCI2-2*_XP_003568974.1
MAGTANCIDIILAIILPPLGVFLKFGCGHEFWICLLLTFLGYIPGIIYAIYAITK

>*BdRCI2-3*_XP_003557909.1
MADNTATFIDLILAIILPPLGVFLKYGCEIEFWICLVLSFFGYLPGIIYAVWVIVK

>*BdRCI2-4*_XP_003558174.1
MASATFLEVILAIILPPVGVFLRYGLGVEFWICLLLTILGYIPGIIYAVYVLVA

>*BdRCI2-5*_XP_003578630.1
MASGGCCTFLEILLAIFLPPLGVFLHYGCCSMEFCICLLLTILGYIPGIIYAIYVLVALDSEERHREYYTLA

>*BdRCI2-6*_XP_003564192.1
MGLGSCCCRCLEILCAILLPPLGVCLRHGCCSMEFWISVLLTILGYLPGVLYAAYVILSVDPDRVRRRGHDDDDDYIYVA

>*BdRCI2*-7_XP_014752685.1
MADEGTANCIDIILAIILPPLGVFFKFACGIEFWICLLLTFFGYLPGIIYAVWVITR

>*BdRCI2-8*_XP_014754368.1
MSNSTEKCVSIVLAIILPPLGVLLKFGCQTEFWLCLLLTLFGYLPGIIYAVYVLTK

Hordeum vulgare

>HvEsi3-1_BAJ85904.1
MGSATVLEVILAIILPPVGVFLRYKLGVEFWICLLLTILGYIPGIIYAVYVLVV

>HvBlt101-2_BAJ89049.1
MASATFIEVILAIILPPVGVFLRYGLAVEFWICLLLTLLGYIPGIIYAVYVLVA

>HvEsi3-4_BAK03378.1
MAGTANCIDIILAIILPPLGVFLKFGCGHEFWICLLLTFLGYIPGIIYAIYAITK

>HvEsi3-5_BAJ88867.1
MADEGTANCIDIILAIILPPLGVFFKFACGIEFWICLLLTFFGYLPGIIYAVWVITK

>HvEsi3-6_BAK03743.1

MSSGGCSTCLEIIFAAVLPPLGVFFRYGWCSSEFFISLPLTMLGYVPGIIYSVYVILKTPPELPSIDGDRPYYILA

>HvEsi3-7_DK716258.1
MGMCSCCCRCLEIMCAILLPPLGVCLRHGCCSMEFWISVLLTILGYLPGVLYAAYVICSVDPERVRRRGDSDDDYIYVA

>HvEsi3-8_BG416092.2
MGSETFVEILLAILLPPVGVFLRYGIGMEFWICLLLTLLGYIPGIIYAIFVLVA

>HvEsi3-9_BAK07288.1
MAETAAIAPPPQPMAESATAAPPQPMAGNATTAAVVVVVPPPSPPDNTMTFLCLLIAIFLPPLGVFIKYNCEVEFWI
CLVLTFFGYFPGVIYAIWVIVKP

>HvEsi3-10_ BAJ90014.1
MASRSCTFLEILFAIILPPLGVFLRFGCCSMEFCICLLLTILGYIPGIIYAVYVLVALGSEDRDRDYDTLA

Secale cereale

>ScEsi3-1_GCJW01020680.1
MGSATVLEVILAIILPPVGVFLRYKLGVEFWICLLLTILGYIPGIIYAVYVLVV

>ScEsi3-2_GCJW01023827.1
MASATFIEVILAIILPPVGVFLRYGLAVEFWICLLLTLLGYIPGIIYAVYVLVA

>ScEsi3-3_GCJW01020158.1
MASQGCTFLEILIAVLLPPLGVFLRYGCCSMEFLICLLLTILGYIPGIIYAVYVLVSHGSASQERDYDALA

>ScEsi3-4_GCJW01019226.1
MAGTANCIDIILAIILPPLGVFLKFGCGHEFWICLLLTFLGYIPGIIYAIYAITK

>ScEsi3-5_GCJW01023929.1
MADEGTANCIDIILAIILPPLGVFFKFACGIEFWICLLLTFFGYLPGIIYAVWVITK

>ScEsi3-6_GCJW01020650.1
MSYSGGCSTCLEIVFAAVLPPLGVFFRYGWCSSEFFISLPLTMLGYPGIIYSVYVILKTPPELPSIDGERPYYILA

>ScEsi3-7_GCJW01023828.1
MGMCSCCCRCLEILCAILLPPLGVCLRHGCCSMEFWISVLLTILGYLPGVLYAAYVICSVDPDRVRRRDDDYIYVA

>ScEsi3-8_GCJW01021120.1
MGSETFVEILLAILLPPVGVFLRYGVGVFWICLLLTVLGYIPXIIYAIFVLVA

>ScEsi3-9_GCJW01018134.1

MAESAVIAPPPQPTAPPQPMAESATAPPSQPMAPPQPMAENATAAPPQPMAENATATVVVVVPPPPPDSTTTFLCLILAFFIPPLGVFIKYECEVEFWICLVLTFLA
YAPGIIYAVWVIVKK

>ScEsi3-10_ GCJW01020353.1
MASRSCTFLEILLAIFLPPLGVFLHYGCCSMEFCICLLLTILGYIPGIIYAVYVLVALGSEDRDRDYDNLA

<u>Oryza sativa</u>

>OsRCI2-1_EEE54356.1
MSDGTANCIDILIAIILPPLGVFLKFGCKVEFWLCLLLTFFGYLPGIIYAVYAITK

>OsRCI2-2_ AP014957.1
MTNHHHHHHHHDDDHKVGANFCNILLSIILPPFAIGVVVGCKKEFWICLLLTCLGYLPGIIYAICIISGAHIHD

>OsRCI2-3_AAG46140.1
MADRPPAMADRTATFVDLVIAIILPPLGVFLKVGCEIEFWICLLLTFLGYFPGIIYAVWVIVNH

>OsRCI2-4_EAY90184.1
MADRTATFVDLVIAIILPPLGVFLKVGCEIKFWICLLLSFFGYLPGIIYAVWVIVNH

>OsRCI2-5_XP_015633211.1
MASATFLEVLLAIFLPPVGVFLRYGLGIEFWIDLLLTILGYIPGIIYAVYVLVA

>OsLTI6A_XP_015647973.1
MADSTATCIDIILAIILPPLGVFFKFGCGIEFWICLLLTFFGYLPGIIYAVWVITK

>OsLTI6B_XP_015640253.1
MAGTANCIDILIAIILPPLGVFLKFGCGHEFWICLLLTFLGYIPGIIYAIYAITK

>OsRCI2-7_XP_015637682.1
MGSETFLEILLAILLPPLGVFLRYGIGMEFWIALLLTILGYLPGIIYAVYVLVA

>OsRCI2-8_XP_015643303.1
MGCCCRCLEILCAILLPPLGVCLRHGCCTMEFWISVLLTILGYLPGVLYAVYVIVSVDPDRERRRRVDPDEYIYVA

>OsRCI2-9_EAZ01907.1
MSYSGGCSTCLETIFSVVLPPLGVFFRYGFCSSEFVVSSALTALFYVPGIVYSVWVVILKTPPEPPGIDGERPYYILA

>OsRCI2-11_XP_015612003.1
MASGRCCTFLEILLAIILPPLGVFLRFGCCSMEFCICLLLTILGYVPGIIYAVYVLVALDSDQYQREYHTLA

>OsRCI2-12_BAF24778.1
MGHFMMDDQNIFAWLCTSCVLCCFMGCAYIFYIIVTIILPPLPVFIRHHCEVSQICRFYLVSDVLKRNKLVFISCYSFRCLA

Zea mays

>ZmPMP3-1_EU364508.1
MSEGTANCVDILIAIILPPLGVFLKYGCGHEFWICLLLTFLGYIPGIIYAIYAITKNN

>ZmPMP3-2_EU959002.1
MADGRCCTFLEILFAIILPPLGVFLRFGCCRIEFCICLLLTILGYVPGIIYAIYVLVALDSDQHEREYYTLA

>ZmPMP3-3_EU962407.1
MGLCSCCCRCLELLCSVLLPPLGVCLRHGCCSMEFWISVLLTILGYLPGVLYAVYVICSVDPHRHRDDDDYVYVA

>ZmPMP3-4_EU954642.1
MASATFLEVLLAIFLPPVGVFLRYGCGVEFWIDLLLTVLGYIPGIIYAVYVLVA

>ZmPMP3-5_EU975274.1
MSDGTATCIDIILAIILPPLGVFFKFGCGVEFWICLILTFFGYLPGIIYAVWAITK

>ZmPMP3-6_EU976341.1
MGSETFVEILLAILLPPVGVFLRYGIGVEFWICLLLTILGYIPGIIYAVYVLVA

>ZmPMP3-7_EU955642.1
MKEGTANCIDILIAIILPPLGVFLKFGCKVEFWLCLLLTFLAYLPGIIYAIYVITKD

>ZmPMP3-8_EU971491.1
MKEGTANCVDILIAIILPPLGVFLKFGCKVEFWLCLLLTFLAYLPGIIYAIYAITKD

>ZmRCI2-3_XP_020404221.1
MSDGTATCVDIILAIILPPLGVFFKFGCGAEFWICLILTFFGYLPGIIYAVWVITMFFF

>ZmRCI2-8_NP_001151922.1
MSSGGCSTCLEVIFAAILPPLGVFFRYGCCSSEFFVSLLLTLLCYVPGVAYSLYVILRTPPEPPGIDGERPYDMLA

>ZmRCI2-9_XP_020399959.1
MADNMVTLVRLVLAIILPPLGVFLKHGLKIEFWICLLLCFFGYLPGVIYAVWVIIRKEDD

Arabidopsis thaliana

>AtRCI2A_NP_187239.1
MSTATFVDIIIAILLPPLGVFLRFGCGVEFWICLVLTLLGYIPGIIYAIYVLTK

>AtRCI2B_NP_187240.1
MSTATFVEIILAIILPPLGVFLKFGCKVEFWICLILTLFGYLPGILYALYIITK

>AtRCI2C_NP_176067.1
MGSFLEVLCAIFIPPVGVFLRYGLGLEFWVCLLLTLFAFIPGLIYAIYVLTK

>AtRCI2D_NP_179982.1
MASSCELCCEIFIAILLPPVGVCLRHGCCTVEFFICLILTCLGYLPGIIYAIYAICFLHRDEYFDEYRRPIYYVA

>AtRCI2E_NP_194794.1
MASNMEVFCEILIAILLPPLGVCLKRGCCTVEFLICLVLTILGYIPGIIYALYVIVFQNREGSTELGAPLNSA

>AtRCI2F_NP_194795.1
MPSNCEILCEIIIAILLPPLGVCFRKGCCTVEFLICLVLTILGYVPGIIYAIYVIVFQHREEYFDEYRRPIYSA

>AtRCI2G_NP_974629.1
MANGCEICCEIMIAILIPPLGVCLRHGCCTTEFMICLILTLLGYVPGIIYALYAIVYVDRDQFFDEYRRPLFYAQSP

>AtRCI2H_NP_565897.1
MGSETFLEIILAILLPPVGVFLRYGCGVEFWICLLLTILGYIPGIIYAIYVLVG

Sorghum bicolor

>SbEsi3-1_XP_002440508.1
MGSETFLEILLAILLPPVGVFLRYGIGVEFWICLLLTILGYIPGIIYAVYVLVA

>SbEsi3-2_XP_002465426.1
MASATFLEVLLAIFLPPVGVFLRYGCGVEFWIDLLLTVLGYIPGIIYALYVLVA

>SbEsi3-3_ XP_002460652.1
MADGRCCTFLEILLAIILPPLGVFLRFGCCRIEFCICLLLTILGYIPGMIYAIYVLVALDSDRHEREYYTLA

>SbEsi3-4_XP_021309366.1
MSNSDGTATCIDIILAIILPPLGVFFKFGCGVEFWICLILTFFGYLPGIIYAVWAITK

>SbEsi3-5_XP_002437373.1
MSSGGCSTCLEVIFAVVLPPLGVFFRYGCCSSEFFISLLLTVLCYVPGIVYSLYVILRTPPEPPGIDGERPYDMLA

>SbEsi3-6_XP_002437973.1

MGLCSCCCRCLELLCSVLLPPLGVCLRHGCCSLEFWISVLLTILGYLPGVLYAVYVICSVDPHRHRDPDDDYVYVA

>SbEsi3-7_XP_002465219.1
MADDNTVTLVRLILAIILPPLGVFLKHGLKLEFWICLILSFFAYLPGIIYAVWVIIKKDDD

Aegilops tauschii

>AetEsi3-1_XP_020150593.1
MGSATVLEVILAIILPPVGVFLRYKLGVEFWICLLLTILGYIPGIIYAVYVLVV

>AetEsi3-2_XP_020150605.1
MASATFIEVILAIILPPVGVFLRYGLAVEFWICLLLTLLGYIPGIIYAVYVLVA

>AetEsi3-3_ XP_020168538.1
MASRSCTFLEILLAVILPPLGVFLRYGCCSMEFLICLLLTILGYIPGIIYAVYVLVAHGSASEESGRDYDALA

>AetEsi3-4_XP_020190487.1
MAGTANCIDIILAIILPPLGVFLKFGCGHEFWICLLLTFLGYIPGIIYAIYAITK

>AetEsi3-5_XM_020319125.1
MADEGTANCIDIILAIILPPLGVFFKFACGIEFWICLLLTFFGYLPGIIYAVWVITK

>AetEsi3-6_XP_020198926.1
MSYSGGCSTCLEIVFAAVLPPLGVFFRYGWCSSEFFISLPLTILGYVPGIIYSVYVILKTPPELPSIDGDRPYYILA

>AetEsi3-7_XP_020151310.1
MGLCSCCCRCLEILCAILLPPLGVCLRHGCCSMEFWISVLLTILGYLPGVLYAAYVICSVDPDRVRRRDDDYIYVA

>AetEsi3-8_XP_020178067.1
MGSETFVEILLAILLPPVGVFLRYGIGVEFWICLLLTLLGYIPGIIYAIFVLVA

>AetEsi3-9_XP_020160007.1
MAESAAIAPPPQPMAPPQPVEENATAAPPQPMAPPQPMAENATAAPPQPMAENATVVVVVPPPPPDGTTTFLCLILAFFIPPLGVFLKYKCEIEFWICLILTFLAYA
PGIIYAVWVIVK

>AetEsi3-10_XP_020168537.1
MASRSCTFLEILLAIILPPLGVFLHYGCCSMEFCICLLLTILGYIPGIIYAVYVLVALGSEERDRDYDTLA

Additional File 4: Sequences S4

Additional File 5: Sequences S5

Amino Acid Sequences

>TaEsi3-1-A_JP881209.1
MGSATVLEVILAIILPPVGVFLRYKLGVEFWICLLLTILGYIPGIIYAVYVLVV

>TaEsi3-1-B_JZ888897.1
MGSATVLEVILAIILPPVGVFLRYKLGVEFWICLLLTILGYIPGIIYAVYVLVV

>TaEsi3-1-D_JP881207.1
MGSATVLEVILAIILPPVGVFLRYKLGVEFWICLLLTILGYIPGIIYAVYVLVV

>TaEsi3-2-A_HAAB01071723.1
MASATFIEVILAIILPPVGVFLRYGLAVEFWICLLLTLLGYIPGIIYAVYVLVA

>TaEsi3-2-D_HAAB01071724.1
MASATFIEVILAIILPPVGVFLRYGLAVEFWICLLLTLLGYIPGIIYAVYVLVA

>TaEsi3-3-A_CV767975.1
MASRSCTFVEILLAVILPPLGVFLRYGCCSMEFLICLLLTILGYIPGIIYAIYVLVAHGSASEESGKDYDALA

>TaEsi3-3-B_CJ925039.1
MASRSCTFVEILLAVILPPLGVFLRYGCCSMEFLICLLLTILGYIPGIIYAVYVLVAHGSASEESGRDYDALG

>TaEsi3-3-D_CJ595273.1 CJ591008.1 CJ615800.1
MASRSCTFLEILLAVILPPLGVFLRYGCCSMEFLICLLLTILGYIPGIIYAVYVLVAHGSASEESGRDYDALA-

>TaEsi3-4-A_CA665474.1
MAGTANCIDIILAIILPPLGVFLKFGCGHEFWICLLLTFLGYIPGIIYAIYAITK

>TaEsi3-4-B_CJ901293.1
MAGTANCIDIILAIILPPLGVFLKFGCGHEFWICLLLTFLGYIPGIIYAIYAITK

>TaEsi3-4-D_JV989019.1
MAGTANCIDIILAIILPPLGVFLKFGCGHEFWICLLLTFLGYIPGIIYAIYAITK

>TaEsi3-5-A_HAAB01033003.1
MADEGTANCIDIILAIILPPLGVFFKFACGIEFWICLLLTFFGYLPGIIYAVWVITK

>TaEsi3-5-B_JV846264.1
MADEGTANCIDIILAIILPPLGVFFKFACGIEFWICLLLTFFGYLPGIIYAVWVITK

>TaEsi3-5-D_HP629889.1
MADEGTANCIDIILAIILPPLGVFFKFACGIEFWICLLLTFFGYLPGIIYAVWVITK

>TaEsi3-6-A_CJ671046.1
MSSGGCSTCLEIIFAAVLPPLGVFFRYGWCSSEFFISLPLTILGYVPGIIYSVYVILKTPPELPSIDGERPYYILA

>TaEsi3-6-B_CJ562290.1
MSYSGGCSTCLEIVFAAVLPPLGVFFRYGWCSSEFFISLPLTMLGYVPGIIYSVYVILKTPPELPSIDGERPYYILA

>TaEsi3-6-D_CJ559253.1
MSYSGGCSTCLEIVFAAVLPPLGVFFRYGWCSSEFFISLPLTILGYVPGIIYSVYVILKTPPELPSIDGDRPYYILA

>TaEsi3-7-A_BJ261574.1
MGLCSCCCRCLEIMCAILLPPLGVCLRHGCCSMEFWISVLLTILGYLPGVLYAAYVICSVDPDRVRRHDDDYIYVA

>TaEsi3-7-B_CJ725702.1
MGLCSCCCRCLEIMCAILLPPLGVCLRHGCCSMEFWISVLLTILGYLPGVLYAAYVICSVDPDRVRRRGDSDDDYIYVA

>TaEsi3-7-D_CJ825516.1
MGLCSCCCRCLEILCAILLPPLGVCLRHGCCSMEFWISVLLTILGYLPGVLYAAYVICSVDPDRVRRRDDDYIYVA

>TaEsi3-8-A_CD909025.1
MGSETFVEILLAILLPPVGVFLRYGIGVEFWICLLLTVLGYIPGIIYAIFVLVA

>TaEsi3-8-B_HAAB01084472.1
MGSETFVEILLAILLPPVGVFLRYGIGVEFWICLLLTVLGYIPGIIYAIFVLVA

>TaEsi3-8-D_CJ648786.1
MGSETFVEILLAILLPPVGVFLRYGIGVEFWICLLLTVLGYIPGIIYAIFVLVA

>TaEsi3-9-A_HAAB01083453.1

MAETAAIAPPPQPMAPPQPVEENATAAPSQPMAPLQPMAESATVVVVVPPPPPDGTTTFLCLILAFFIPPLGVFLKYKCEIEFWICLILTFLAYAPGI
IYAVWVIVK

>TaEsi3-9-B_BJ243843
MAESAVIAPPLQPMTPPQPMAENATEAPPQPMAPPQQMAENATAAPPPQPMAENATAAPPPQPMVENATVVVVVPPPPPDSTTTFLCLILAFFLPPLG
VFLKYKCEIEFWICLILTFLAYAPGIIYAVWVIVK

>TaEsi3-9-D_BJ243706.1
MAESTAIAPPPQPMAPPQPVEENATAAPPQPMAPPQPMAENATAAPPQPMAENATVVVVVPPPPPDGTTTFLCLILAFFIPPLGVFLKYKCEIEFWIC
LILTFLAYAPGIIYAVWVIVK

>TaEsi3-10-A_HX161660.1 HX161634.1 CJ823027.1 CA645450.1
MASRSCTFLEILLAIILPPLGVFLHYGCCSMEFCICLLLTILGYIPGIIYAVYMLVALGSEERDRDYNTLA-

>TaEsi3-10-B_CA611646.1
MASRSCTFLEILLAIILPPLGVFLHYGCCSMEFCICLLLTILGYIPGIIYAVYVLVALGSEERDRDYDTLA-

>TaEsi3-10-D_BJ278420.1
MASRSCTFLEILLAIILPPLGVFLHYGCCSMEFCICLLLTILGYIPGIIYAVYVLVALGSEERDRDYDTLA-

Coding Sequences

>TaEsi3-1-A_JP881209.1
ATGGGCTCGGCAACAGTCCTGGAGGTGATCCTCGCCATCATCCTGCCTCCCGTCGGCGTCTTCCTGCGCTACAAACTCGGCGTGGAGTTCTGGATCTG
TCTCTTGCTGACCATACTGGGGTACATACCGGGGATCATCTACGCGGTGTACGTGCTGGTAGTTTAA

>TaEsi3-1-B_JZ888897.1
ATGGGCTCGGCAACAGTCCTGGAGGTGATCCTCGCCATCATCCTGCCTCCCGTCGGCGTCTTCCTGCGCTACAAACTCGGCGTGGAGTTCTGGATCTG
TCTCTTGCTGACCATACTGGGGTACATACCGGGGATCATCTACGCGGTGTACGTGCTGGTAGTTTAA

>TaEsi3-1-D_JP881207.1
ATGGGCTCGGCAACAGTCCTGGAGGTGATCCTCGCCATCATCCTGCCTCCCGTCGGCGTCTTCCTGCGCTACAAACTCGGCGTGGAGTTCTGGATCTG
TCTCTTGCTGACCATACTGGGGTACATACCGGGGATCATCTACGCGGTGTATGTGCTGGTAGTTTAA

>TaEsi3-2-A_HAAB01071723.1

ATGGCCTCAGCAACGTTCATAGAGGTGATCCTCGCCATCATCCTGCCTCCGGTCGGCGTCTTCCTGCGCTACGGCCTCGCCGTGGAGTTCTGGATCTG
TCTCTTGCTGACCTTACTGGGGTACATACCGGGGATCATCTACGCGGTGTATGTGCTGGTGGCTTAA

>TaEsi3-2-D_HAAB01071724.1
ATGGCCTCAGCAACGTTCATAGAGGTGATCCTCGCCATCATCCTGCCTCCGGTCGGCGTCTTCCTGCGCTACGGCCTCGCCGTGGAGTTCTGGATCTG
CCTCTTGCTGACCCTACTGGGGTACATACCGGGGATCATCTACGCGGTGTATGTGCTGGTGGCTTAA

>TaEsi3-3-A_CV767975.1
ATGGCGTCCCGAAGCTGCACCTTCGTCGAGATCCTGCTCGCCGTCATCCTGCCGCCGCTCGGCGTCTTCCTCCGCTACGGCTGCTGCAGCATGGAGTT
CTTGATCTGTCTGCTGCTCACCATCCTGGGCTACATCCCCGGCATCATCTACGCCATCTACGTGCTCGTCGCGCATGGCTCGGCCTCGGAGGAGAGCG
GCAAGGACTACGACGCCCTTGCTTGA

>TaEsi3-3-B_CJ925039.1
ATGGCGTCCCGGAGCTGCACCTTCGTGGAGATCCTGCTCGCCGTCATCCTGCCGCCGCTCGGCGTCTTCCTCCGCTACGGCTGCTGTAGCATGGAGTT
CTTGATCTGCCTGCTGCTCACCATCCTGGGCTACATCCCCGGCATCATCTACGCCGTCTACGTGCTCGTCGCGCATGGCTCTGCCTCGGAGGAGAGCG
GCAGGGACTACGACGCCCTTGGTTGA

>TaEsi3-3-D_CJ595273.1 CJ591008.1 CJ615800.1
ATGGCGTCCCGGAGCTGCACCTTCCTGGAGATCCTGCTCGCCGTCATCCTGCCGCCGCTCGGCGTCTTCCTCCGCTACGGCTGCTGCAGCATGGAGTT
CTTGATCTGCCTGCTGCTCACCATCCTGGGCTACATCCCCGGCATCATCTACGCCGTCTACGTGCTCGTCGCGCATGGCTCCGCCTCGGAGGAGAGCG
GCAGGGACTACGACGCCCTTGCTTGA

>TaEsi3-4-A_CA665474.1
ATGGCGGGCACGGCCAACTGCATCGACATCATCCTCGCCATCATCCTCCCGCCCCTCGGCGTCTTCCTCAAGTTCGGCTGCGGGCACGAGTTCTGGAT
CTGCCTCCTGCTCACCTTCCTCGGGTACATCCCGGGGATCATCTACGCCATCTACGCCATCACCAAGTAA

>TaEsi3-4-B_CJ901293.1
ATGGCGGGCACGGCCAACTGCATCGACATCATCCTCGCCATCATCCTCCCGCCCCTCGGCGTCTTCCTCAAGTTCGGCTGCGGGCACGAGTTCTGGAT
CTGCCTCCTGCTCACCTTCCTCGGGTACATCCCGGGGATCATCTACGCCATCTACGCCATCACCAAGTAA

>TaESI3-4-D_JV989019.1
ATGGCGGGCACGGCCAACTGCATCGACATCATCCTCGCCATCATCCTCCCGCCCCTCGGCGTCTTCCTCAAGTTCGGATGCGGGCACGAGTTCTGGAT
CTGCCTCTTGCTGACCTTCCTCGGGTACATCCCGGGTATCATCTACGCCATCTACGCCATCACCAAGTAA

>TaEsi3-5-A_HAAB01033003.1
ATGGCGGACGAGGGGACGGCCAACTGCATCGACATCATCCTCGCCATCATCCTGCCGCCGCTCGGCGTCTTCTTCAAGTTCGCCTGCGGGATCGAGTT
CTGGATCTGCTTGCTGCTCACCTTCTTCGGCTACCTCCCCGGCATCATCTACGCCGTCTGGGTCATCACCAAGTAG

>TaEsi3-5-B_JV846264.1
ATGGCGGACGAGGGGACCGCCAACTGCATCGACATCATCCTCGCCATCATCCTGCCGCCGCTCGGCGTCTTCTTCAAGTTCGCCTGCGGGATCGAGTT
CTGGATCTGCTTGCTGCTCACCTTCTTCGGCTACCTCCCCGGCATCATCTACGCCGTCTGGGTCATCACCAAGTAG

>TaEsi3-5-D_CJ854183.1
ATGGCGGACGAGGGGACGGCCAACTGCATCGACATCATCCTCGCCATCATCCTGCCGCCGCTCGGCGTCTTCTTCAAGTTCGCCTGCGGGATCGAGTT
CTGGATCTGCTTGCTGCTCACCTTCTTCGGCTACCTCCCCGGCATCATCTACGCCGTCTGGGTCATCACCAAGTAG

>TaEsi3-6-A_CJ671046.1
ATGAGCTCCGGCGGCTGCTCGACGTGCCTGGAGATCATCTTCGCCGCCGTGCTCCCGCCGCTCGGCGTCTTCTTCCGGTACGGCTGGTGCAGCTCGGA
GTTCTTCATCTCGCTGCCGCTGACGATACTCGGCTACGTCCCCGGCATCATCTACTCCGTCTACGTCATCCTGAAGACGCCGCCGGAGCTGCCGAGCA
TCGACGGCGAGCGGCCCTACTACATCCTCGCCTGA

>TaEsi3-6-B_CJ562290.1
ATGAGCTACTCCGGCGGCTGCTCGACGTGCCTGGAGATCGTCTTCGCCGCCGTGCTCCCGCCGCTCGGCGTCTTCTTCCGGTACGGCTGGTGCAGCTC
GGAGTTCTTCATCTCGCTGCCGCTGACGATGCTCGGCTACGTCCCCGGCATCATCTACTCCGTCTACGTCATCCTGAAGACGCCGCCGGAGCTGCCGA
GCATCGACGGCGAGCGGCCCTACTACATCCTCGCCTGA

>TaEsi3-6-D_CJ559253.1
ATGAGCTACTCCGGCGGCTGCTCGACGTGCCTGGAGATCGTCTTCGCCGCCGTGCTCCCGCCGCTCGGCGTCTTCTTCCGGTACGGCTGGTGCAGCTC
GGAGTTCTTCATCTCGCTGCCGCTGACGATACTCGGCTACGTCCCCGGCATCATCTACTCCGTCTATGTCATCCTGAAGACGCCGCCGGAGCTGCCGA
GCATCGACGGCGACCGGCCATACTACATCCTCGCCTAA

>TaEsi3-7-A_BJ261574.1
ATGGGGCTGTGCTCGTGCTGCTGCCGGTGCCTGGAGATCATGTGCGCCATCCTCCTCCCGCCCCTCGGCGTCTGCCTCCGCCACGGCTGCTGCTCCAT
GGAGTTCTGGATCAGCGTGCTGCTCACCATCCTCGGCTACCTCCCCGGCGTCCTCTACGCCGCCTACGTCATCTGCTCCGTCGACCCCGACCGCGTCC
GCCGCCACGACGACGACTACATCTACGTCGCCTGA

>TaEsi3-7-B_CJ725702.1
ATGGGGCTGTGCTCGTGCTGCTGCCGGTGCCTGGAGATCATGTGCGCCATCCTCCTCCCGCCCCTCGGCGTCTGCCTCCGCCACGGCTGCTGCTCCAT
GGAGTTCTGGATCAGCGTGCTGCTCACCATCCTCGGCTACCTGCCGGGCGTCCTCTACGCCGCCTACGTCATCTGCTCCGTCGACCCCGACCGCGTCC
GCCGCCGCGGCGACAGCGACGACGACTACATCTACGTCGCCTGA

>TaEsi3-7-D_CJ825516.1

ATGGGGCTGTGCTCGTGCTGCTGCCGGTGCCTGGAGATCCTGTGCGCCATCCTCCTCCCGCCCCTCGGCGTCTGCCTCCGCCACGGCTGCTGCTCCAT
GGAGTTCTGGATCAGCGTGCTGCTCACCATCCTCGGCTACCTCCCCGGCGTCCTCTACGCCGCCTACGTCATCTGCTCCGTCGACCCCGACCGCGTCC
GCCGCCGCGACGACGACTACATCTACGTCGCCTGA

>TaEsi3-8-A_CD909025.1
ATGGGCTCGGAGACGTTCGTGGAGATCCTGCTGGCCATACTGCTGCCGCCGGTCGGCGTCTTCCTCCGCTACGGCATCGGCGTGGAGTTCTGGATATG
CCTGCTGCTCACCGTGCTGGGCTACATCCCGGGCATCATCTACGCCATCTTCGTCCTCGTCGCTTAG

>TaEsi3-8-B_HAAB01084472.1
ATGGGTTCGGAGACGTTCGTGGAGATCCTGCTGGCCATCCTGCTGCCGCCGGTCGGCGTCTTCCTCCGCTACGGCATCGGCGTGGAGTTCTGGATCTG
CCTGCTGCTCACGGTGCTGGGCTACATCCCCGGCATCATCTACGCCATCTTCGTCCTCGTCGCATAG

>TaEsi3-8-D_CJ648786.1
ATGGGTTCGGAGACGTTCGTGGAGATCCTGCTGGCCATCTTGCTGCCGCCGGTCGGCGTCTTCCTCCGCTACGGCATCGGCGTGGAGTTCTGGATCTG
CCTGCTGCTCACGGTGCTGGGCTACATCCCCGGCATCATCTACGCCATCTTCGTCCTCGTCGCATAG

>TaEsi3-9-A_HAAB01083453.1
ATGGCAGAAACCGCAGCGATAGCACCACCACCACAACCAATGGCACCACCGCAACCAGTGGAGGAAAACGCAACGGCGGCACCGTCACAACCAATGGC
ACCACTGCAACCAATGGCGGAAAGCGCAACTGTCGTTGTGGTGGTGCCACCACCACCGCCAGACGGCACCACGACATTCCTCTGCCTCATCCTCGCCT
TCTTCATCCCTCCCCTCGGCGTTTTCCTCAAGTACAAATGTGAGATTGAATTCTGGATCTGCCTCATCCTAACATTCTTGGCCTACGCGCCGGGCATC
ATCTACGCCGTCTGGGTGATCGTGAAGTAG

>TaEsi3-9-B_BJ243843
ATGGCAGAAAGCGCAGTGATAGCACCACCACTACAACCAATGACACCACCGCAACCAATGGCAGAAAACGCAACGGAGGCACCACCACAACCAATGGC
ACCACCGCAACAAATGGCGGAAAACGCAACGGCCGCACCACCACCACAACCAATGGCGGAAAACGCAACGGCGGCACCACCACCACAACCAATGGTGG
AAAACGCAACGGTGGTTGTGGTGGTGCCACCACCACCGCCAGACAGCACCACAACATTCCTCTGCCTCATCCTCGCCTTCTTCCTCCCTCCCCTCGGC
GTTTTCCTCAAGTACAAATGCGAGATTGAATTCTGGATCTGCCTCATCCTAACATTCTTGGCCTACGCGCCGGGCATCATCTACGCCGTCTGGGTGAT
CGTAAAGTAG

>TaEsi3-9-D_BJ243706.1
ATGGCAGAAAGCACAGCAATAGCACCACCACCACAACCAATGGCACCACCGCAACCAGTGGAGGAAAACGCAACGGCGGCACCGCCGCAACCAATGGC
ACCACCGCAACCAATGGCGGAAAACGCAACGGCGGCACCACCGCAACCAATGGCGGAAAACGCAACTGTCGTTGTGGTGGTGCCACCACCACCGCCAG
ACGGCACCACGACATTCCTCTGCCTCATCCTCGCCTTCTTCATCCCTCCCCTCGGCGTTTTCCTCAAGTACAAATGTGAGATTGAATTCTGGATCTGC
CTCATCCTAACATTCTTGGCCTACGCGCCGGGCATCATCTACGCCGTCTGGGTGATCGTAAAGTAG

>TaEsi3-10-A_HX161660.1 HX161634.1 CJ823027.1 CA645450.1

ATGGCGTCCCGGAGCTGCACCTTCCTCGAGATCCTGCTCGCCATCATCCTGCCGCCGCTCGGCGTCTTCCTCCACTACGGCTGCTGCAGCATGGAGTT
CTGCATCTGCCTGCTGCTCACCATCCTGGGCTACATCCCCGGCATCATCTACGCTGTCTACATGCTCGTCGCGCTCGGCTCGGAGGAGCGTGATAGGG
ACTACAACACACTTGCTTAA
>TaEsi3-10-B_CA611646.1
ATGGCGTCCCGGAGCTGCACCTTCCTGGAGATCCTGCTCGCCATCATCCTGCCGCCGCTCGGTGTCTTCCTCCACTACGGCTGCTGCAGCATGGAGTT
CTGCATCTGCCTGCTGCTCACCATCCTGGGCTACATCCCCGGCATCATCTACGCGGTCTACGTGCTTGTCGCGCTCGGCTCGGAGGAGCGGGATCGGG
ACTACGACACCCTTGCTTAA

>TaEsi3-10-D_BJ278420.1
ATGGCGTCCCGGAGCTGCACCTTCCTCGAGATCCTGCTCGCCATCATCCTGCCGCCGCTCGGCGTCTTCCTCCACTACGGCTGCTGCAGCATGGAGTT
CTGCATCTGCCTGTTGCTCACCATCCTGGGCTACATCCCCGGCATCATCTACGCGGTCTACGTGCTCGTTGCGCTCGGCTCAGAGGAGCGTGATCGGG
ACTACGACACCCTTGCTTAA

Table S4 A: *Esi3/RCI2/PMP3* gene expression in tissues of *T. aestivum* (RPKPM)

	Leaf[a]	Seed[b]	Root[c]	Stem[d]	Inflorescence[e]
Esi3-1-A	5.02	0.90	32.54	35.66	6.21
Esi3-1-B	0.78	0.05	16.65	27.47	3.42
Esi3-1-D	0.79	0.00	24.54	13.11	0.24
Esi3-2-A	0.79	0.00	5.19	3.84	6.61
Esi3-2-D	0.11	0.00	1.90	1.33	0.45
Esi3-3-A	1.05	0.15	0.38	0.57	0.10
Esi3-3-B	15.68	8.31	4.35	15.88	0.98
Esi3-3-D	5.28	5.44	3.08	14.56	2.77
Esi3-4-A	3.92	4.87	37.43	23.86	8.48
Esi3-4-B	17.70	38.89	102.39	40.78	21.20
Esi3-4-D	34.82	31.11	78.78	60.85	36.66
Esi3-5-A	112.03	11.59	43.53	51.85	28.49
Esi3-5-B	87.93	2.35	151.88	89.51	34.14
Esi3-5-D	104.50	4.46	65.03	43.50	50.07
Esi3-6-A	0.05	0.00	0.00	0.00	0.03
Esi3-6-B	0.30	0.00	0.15	0.00	0.07
Esi3-6-D	0.30	0.00	0.15	0.00	0.07
Esi3-7-A	3.38	0.08	1.61	1.54	1.62
Esi3-7-B	1.76	0.62	0.95	1.94	1.03
Esi3-7-D	3.56	0.30	1.84	4.56	0.94
Esi3-8-A	0.00	1.21	0.00	0.00	0.00
Esi3-8-B	0.23	6.70	0.06	0.52	0.09
Esi3-8-D	0.00	40.80	0.00	0.00	0.03
Esi3-9-A	0.00	0.00	0.00	0.00	0.00
Esi3-9-B	0.00	0.00	0.00	0.00	0.00
Esi3-9-D	0.00	0.00	0.00	0.00	0.00
Esi3-10-A	0.00	0.00	0.00	0.00	0.00
Esi3-10-B	24.46	7.03	21.34	27.39	21.71
Esi3-10-D	66.61	2.74	89.05	84.73	59.72

Note: Data from Pingault et al., 2015 [27].

[a] whole plant fruit formation stage 30 to 50%

[b] whole plant at the ripening stage

[c] cotyledon emergence stage

[d] two nodes or internodes visible stage

[e] maximum stem length reached stage

Table S5 A: *Esi3/RCI2/PMP3* expression across seventy tissue types.

	Esi3-1-A		*Esi3-1-B*		*Esi3-2-A*		*Esi3-2-D*		*Esi3-3-A*		*Esi3-3-B*		*Esi3-3-D*	
Tissue Type	Expression Level	Standard Deviation	Expression Level	Standard Deviation	Expression Level	Standard Deviation	Expression Level	Standard Deviation	Expression Level	Standard Deviation	Expression Level	Standard Deviation	Expression Level	Standard Deviation
First leaf sheath - Tillering stage	274.47	152.87	118.6	47.04	19.49	3.53	3.35	1.64	11.51	5.41	14.69	6.13	20.42	10.31
Internode #2 - Milk grain stage	37.13	2.54	25.72	9.89	3.01	0.08	0	0	3.9	2.54	34.83	13.83	12.13	5.48
Shoot apical meristem - Seedling stage	27.26	10.73	11.34	5.51	8.16	1.6	5.61	1.6	1.39	0.4	2.56	0.26	1.99	0.55
Grain - Milk grain stage	11.19	0.74	3.85	1.16	30.91	12.33	3.49	1.78	1.33	0.98	1.38	0.4	1	0.34
First leaf blade - Seedling stage	63.53	33.62	32.32	18.06	16.81	10.04	4.11	3.6	6.75	3.72	6.12	4.88	5.44	3.19
Flag leaf blade - Full boot	14.19	4.11	2.96	0.87	1.3	0.15	0.23	0.21	8.47	1.67	5.82	1.65	1.85	0.45
Awn - 50 percent spike	31.17	8.93	16.59	4.11	21.93	5.33	1.01	0.42	4.9	1.52	1.64	0.67	3.82	0.66
flag leaf blade night (-0.25h) 06:45	1.65	0.81	0.59	0.37	0.91	0.32	0.06	0.08	7.87	1.77	2.03	0.75	2.4	0.82
Shoot axis - Flag leaf stage	143.25	66.72	85.15	35.17	7.74	1.44	3.73	1.33	1.67	0.76	9.65	3.46	5.95	2.19
Fifth leaf blade - Flag leaf stage	66.79	72.62	40.82	52.04	3.47	3.14	0.05	0.07	6.78	3	12.47	7.44	5.3	4.99
Third leaf sheath - Three leaf stage	54.54	59.45	29.45	32.92	25	15.56	12.14	7.08	6.15	4.43	2.86	2	5.6	1.51
Internode #2 - Ear emergence	52.58	26.9	21.39	5.99	2.16	1.29	0.24	0.12	3.46	2.65	97.71	61.91	8.32	5.19
Anther	239.04	117.58	12.55	7.22	12.9	2.92	14.41	4.94	1.1	0.47	1.7	1.19	7.39	1.27
Spike	78.86	11.16	51.73	8.43	28.41	6.52	1.47	0.66	2.83	0.95	1.19	0.34	7.39	0.62
Coleoptile	101.24	24.39	72.65	12.91	25.74	6.77	11.54	3.15	8.91	1.52	9.14	1.06	10.78	5.27
Stigma and Ovary	52.85	13.72	13.89	5.34	9.69	1.19	0.62	0.57	0.47	0.36	0.47	0.08	1.78	0.43
Roots - Flag leaf stage	52.86	17.22	23.97	7.03	19.14	4.02	11.37	1.77	0.16	0.23	1.91	1.18	2.3	0.72
Fifth leaf sheath - Flag leaf stage	341.75	176.91	233.81	102.45	38.41	21.83	17.74	11.62	1.77	0.76	18.4	6.93	9.84	1.89
Root apical meristem - Three leaf stage	33.2	15.82	62.65	12.66	3.82	2.57	4.76	2.07	1	0.4	2.71	0.15	0.86	0.22
Flag leaf sheath - Ear emergence	33.15	8.04	18.76	6.31	1.21	0.31	0.18	0.13	6.76	3.46	3.53	0.95	3.17	0.8
Roots - Three leaf stage	61.75	21.71	25.33	3.33	10.68	0.81	17.89	9.64	1.74	1.67	1.43	0.89	2.77	2.65
Axillary roots - Three leaf stage	104	8.3	153.76	2.03	18.14	4.27	9.43	6.13	0.75	1.06	4.85	3.92	0.9	0.21
Flag leaf sheath - 50 percent spike	52.55	8.24	30.84	8.21	1.05	0.49	0.05	0.07	9.52	2.56	8.16	2.35	5.65	0.95
Radicle - Seedling stage	143.48	89.75	125.8	46.23	18.9	1.58	7.7	4.04	7.17	5.26	22.99	22.21	8.34	8.9
Roots - 50 percent spike	35.13	38.61	41.11	54.84	11	8.34	9.37	0.86	0.51	0.36	0.94	1.22	1.45	0.26
Third leaf blade - Three leaf stage	92.46	71.26	47.51	43.92	15.57	20.98	6.81	9.64	5.76	2.67	8.88	2.22	5.06	2.71
Spikelets - 50 percent spike	27.54	8.12	15.3	4.08	20.56	2.39	1.32	0.6	3.77	1.09	0.94	0.11	2.85	0.65
Root apical meristem - Tillering stage	55.96	26.47	52.9	13.12	6.91	4	3.5	1.5	3.33	2.44	16.37	12.51	2.76	2.95
Grain - Ripening stage	12.98	16.84	1.03	1.46	0	0.06	0.21	0.08	3.67	1.45	18.4	1.04	10.53	1.2
Awns - Ear emergence	50	22.86	20.08	11.18	2.22	0.78	1.48	1.57	6.42	2.82	2.91	1.22	2.94	0.91
Glumes	14.48	3.62	2.68	1.42	2.29	0.48	0.15	0.22	0.88	0.89	0.21	0.24	1.23	0.52
Glumes - Ear emergence	34.22	2.22	7.93	0.71	6.94	1.11	0.07	0.1	1.79	0.98	1.93	0.15	2.54	0.56
Leaf ligule	142.47	55.57	101.68	30.48	13.18	2.37	1.49	0.87	5.98	1.46	6.23	0.25	12.38	3.88
Flag leaf blade - 50 percent spike	3.63	1.59	0.31	0.26	0.52	0.09	0.24	0.2	4.89	2.13	2.59	1.16	1.03	0.3
Internode #2 - 50 percent spike	160.86	62.62	41.51	1.09	4.73	0.38	0.06	0.09	1.49	1.78	116.07	81.26	9.61	5.82
Fifth leaf sheath - Fifth leaf stage	50.73	13.46	25.5	5.83	15.66	1.52	11.77	4.27	6.86	2.73	2.55	0.11	7.11	1.07
fifth leaf blade night (-0.25h) 21:45	132.67	88.76	79.22	64.43	3.82	2.98	0.06	0.09	4.23	3.99	4.23	0.53	7.38	2.89
Grain - Soft dough	31.95	13.29	9.34	3.41	20.76	7.39	9.29	3.79	2.81	0.98	3.77	1.06	1.4	0.5
Flag leaf blade (senescence) - Dough stage	3.01	2.28	1.96	1.66	1.1	0.54	0.08	0.11	7.59	2.89	0.24	0.05	1.08	0.37
Flag leaf blade night (-0.25h) 06:45 - Flag leaf stage	31.86	18.35	44.99	42.33	6.52	3.7	0.59	0.48	4.69	1.54	3.03	1.75	7.54	2.79
Flag leaf blade (senescence) - Ripening stage	105.92	6.08	7.12	2.12	10.16	4.36	0.82	0.2	3.17	0.7	2.17	1.69	1.48	1.17
First leaf blade - Tillering stage	153.15	87.57	21.46	4.81	2.53	0.68	0.19	0.16	16.57	5.62	9.74	3.31	6.65	4.4
Shoot apical meristem - Tillering stage	172.49	84.75	91.38	55.66	10.09	3.8	8.06	1.87	1.29	1.08	11.21	3.95	7.07	1.53
Shoot axis - First leaf stage	202.18	86.74	123.4	51.87	50.31	4.46	21.2	0.89	6.88	0.79	4.93	2.71	5.85	1.81
Roots - Seedling stage	105.85	8.6	150.69	22.98	18.12	8.73	6.39	1.17	3.82	2.19	6.73	1.81	0.8	0.07
Shoot axis - Milk grain stage	150.2	106.88	90	71.52	15.76	5.77	0.98	0.55	0.35	0.24	39.06	10.54	4.87	4.34
Fifth leaf blade - Fifth leaf stage	40.72	22.02	17.9	10.37	9.43	9.91	3.47	4.92	2.43	0.12	3.21	0.96	3.97	0.77
Flag leaf blade - Ear emergence	1.31	0.45	0.1	0.15	0.34	0.08	0	0	6.4	1.11	0.8	0.14	0.91	0.37
flag leaf blade night (+0.25h) 07:15	21.75	4.45	43.47	3.49	12.33	1.97	0.6	0.19	5.47	1.91	1.8	0.07	8.9	2.43
Fifth leaf blade night (-0.25h) 21:45	17.6	16.24	4.86	3.54	3.61	1.86	0.08	0.11	5.39	1.92	0.99	0.43	1.64	1.09
Shoot axis - Tillering stage	151.86	94.22	62.26	34.85	9.74	5.48	7.19	3.63	1.37	1.15	6.72	3.2	4.47	2.24
Stem axis - First leaf stage	202.18	86.74	123.4	51.87	50.31	4.46	21.2	0.89	6.88	0.79	4.93	2.71	5.85	1.81
Endosperm	76.78	24.21	14.48	5.77	1.63	0.55	6.54	0.81	5.36	3.39	27.82	9.72	7.98	4.02
Peduncle	5.56	1.2	4.19	1	1.85	0.97	0.37	0.28	0.94	1.33	5.83	1.8	2.32	1.05
Peduncle - 50 percent spike	41.82	42.3	41.34	43.4	16.22	8.89	1.97	0.56	0	0	5.03	0.23	1.92	1.67
Peduncle - Ear emergence	15.01	1.55	12.23	2.04	11	3.37	1.24	0.41	0.16	0.23	9.94	1.02	1.57	0.41
Flag leaf sheath - Full boot	71.57	21.86	64.06	2.65	8.19	0.41	0.91	0.8	5.27	3.53	13.34	6.42	6.27	3.19
Flag leaf blade - Flag leaf stage	40.15	8.9	19.13	5.25	4.62	3.62	0.62	0.88	3.94	0.21	4.07	2.18	5.06	0.32
Lemma	10.6	1.99	1.32	0.25	1.92	0.33	0	0	2.35	0.65	0.22	0.1	2.26	1.06
Lemma - Ear emergence	38.3	8.32	13.02	3.06	12.2	2.84	0.07	0.1	1.57	1.11	2.12	0.5	2.28	0.09
Awns - Milk grain stage	50.46	4.46	13.61	2.52	1.45	0.38	0.08	0.11	5.09	0.91	0.31	0.18	2.13	0.95
fifth leaf blade night (+0.25h) 22:15	302.87	139.96	188.27	108.01	7.62	7	0.69	0.61	15.73	13.68	35.39	38.75	21.5	16.5
Flag leaf blade - Milk grain stage	5.7	2.7	2.09	2.21	1.67	0.71	0.1	0.14	6.37	4.39	0.92	0.65	1.34	0.97
Grain - Hard dough	42.05	3.55	9.81	1.93	8.39	6.36	3.14	1.56	5.89	4.2	29.49	5.75	12.14	3
Flag leaf sheath - Milk grain stage	16.93	5.92	8.96	5.36	1.41	0.52	0.24	0.23	4.84	0.77	1.86	0.5	1.75	0.29
Embryo proper	60.69	4.13	17.49	3.2	1.17	0.4	2.65	1.01	9.47	0.24	67.37	5.66	28.72	4.24
Fifth leaf blade (senescence) - Milk grain stage	16.9	14.02	5.73	3.92	1.42	0.34	0	0	4.05	2.01	0.73	0.4	1.65	0.72
Roots - Tillering stage	70.88	29.86	61.76	21.61	18.55	5.48	8.01	1.34	2.17	1.26	4.28	2.83	1.88	0.74
Shoot axis - Full boot	138.36	41.37	86.13	31.6	8.88	2.21	3.84	0.32	3.21	0.3	15.02	2.73	5.93	1.62
Fifth leaf blade - Ear emergence	4.56	2.19	2.2	1.51	0.74	0.15	0	0	5.58	1.86	0.83	0.62	1.37	0.34
First leaf sheath - Seedling stage	202.7	74.94	152.52	55.55	48.68	17.25	30.36	20.01	5.45	1.11	6.62	2.2	5.65	2.32

Expression levels are represented in TPM (Transcripts Per Kilobase Million) [28,49]

In brief, wheat cultivar Azhurnaya were grown 16:8 hours day:night at 25°C:15°C. Tissues were harvested between 7.5 and 8.5h into the day, dataset from Winter at al., 2007.

Continued…..

Esi3-4-A		*Esi3-4-B*		*Esi3-4-D*		*Esi3-5-A*		*Esi3-5-B*		*Esi3-5-D*		*Esi3-6-A*		*Esi3-6-E*		*Esi3-6-I*	
Expression Level	Standard Deviation	Expression Level	Standard Deviation	Expression Level	Standard Deviation	Expression Level	Standard Deviation	Expression Level	Standard Deviation	Expression Level	Standard Deviation	Expression Level	Standard Deviation	Expression Level	Standard Deviation	Expression Level	Standard Deviation
181.03	13.1	282.48	18.96	260.92	33.2	204.22	46.66	101.44	6.65	214.99	39.54	0.43	0.32	0.26	0.18	0.24	0.17
27.71	11.45	19.08	14.78	50.4	17.63	292.07	16.3	342.2	4.07	420.17	19.61	0.4	0.09	0.22	0.14	0	0
14.21	5.77	20.07	7.75	33.74	17.87	53	42.74	60.58	50.32	90.59	60.3	0.11	0.06	0.14	0.08	0.23	0.33
9.99	3.64	32.13	6.53	38.76	5.28	122.05	7.33	26.93	11.06	162.53	9.43	0.13	0.1	0.32	0.3	0.87	1.23
46.43	43.28	109.23	77.91	104.21	91.82	124.97	94.9	55.82	25.24	106.7	67.4	0.95	0.2	1.05	0.16	0.48	0.18
3.85	1.41	4.03	1.69	10.47	4.73	52.9	11.32	23.77	1.97	27.18	3.86	0.17	0.07	1.93	0.3	0.39	0.35
11.19	4.29	9.99	3.83	22.75	10.46	84.48	5.04	44.87	7.47	134.14	6.62	0.9	0.19	0.44	0.04	0.17	0.19
0.99	0.29	5.35	2.93	12.9	8.59	52.33	13.24	15.08	1.98	87.92	11.72	0.2	0.21	3.16	0.83	1.3	1
32.81	17.05	21.14	7.39	54.72	18.33	85.55	15.61	131.3	17.43	183.11	21.74	0.44	0.21	0.29	0.14	0.19	0.27
3.63	1.76	5.9	2.75	10.48	8.24	64.58	41.02	27.18	1.13	31.29	10.19	0.32	0.26	1.88	1.01	1	0.71
17.06	4.52	40.1	19.24	34.03	14.38	54.51	43.71	8.83	8.41	45.3	27.83	0.11	0.15	0.08	0.06	0	0
7.48	3.96	8.59	5.9	19.35	9.69	190.37	8.77	194.97	8.11	293.49	57.63	0.5	0.56	0.58	0.37	0.2	0.16
166.99	22.87	275.56	67.05	272.01	38.86	157.22	19.69	62.53	8.52	131.05	10.13	0	0	0	0	0	0
20.44	13.04	37.87	12.85	66.49	26.31	154.8	9.53	54.74	12.98	180.3	24.97	0.6	0.19	0.6	0.44	0	0
69.63	73.4	150.84	114.46	148.06	109.67	120.21	54.39	59.76	27.77	171.6	55.26	1.15	0.54	0.45	0.34	0	0
23.64	10.37	42.06	15.52	73.73	31.11	122.03	18.79	37.69	7.04	320.91	33.59	0	0.06	0.27	0.33	0	0
62.3	19.67	125.41	23.54	148.83	23.92	118.09	12.21	143.76	31.66	165.05	15.6	0.45	0.02	0.37	0.22	0.14	0.2
13.78	13.76	87.32	16.13	42.06	20.55	85.25	25.66	51.97	10	42.16	14.8	3.41	1.65	1.12	0.2	0.39	0.29
7.39	4.09	58.65	18.37	118.73	18.64	224.11	30.21	165.38	33.94	371.92	60.37	1.15	0.48	0.78	0.3	0.33	0.26
2.7	0.67	11.85	1.22	34.96	7.88	122.39	17.52	47.28	3.95	162.14	5.45	0.57	0.22	1.15	0.12	0.26	0.21
39.57	10.87	112.03	47.05	123.07	45.5	57.86	3.97	73.59	21.13	80.21	5.52	0.2	0.04	0.23	0.24	0.11	0.16
8.7	2.13	80.94	21.7	150.63	49.04	339.68	85.26	229.41	22.51	424	68.8	1.3	0.21	0.84	0.44	0.14	0.2
10.53	7.06	23.13	20.68	55.46	43.1	114.65	23.44	38.76	9.92	121.38	19.47	0.44	0.09	0.84	0.13	0.23	0.32
37.99	13.94	181.59	31.94	205.42	38.79	371.45	86.31	335.15	78.73	480.66	107.42	1.43	0.4	0.63	0.31	0.14	0.2
81.24	29.39	164.68	64.65	199.22	84.91	109.75	82.93	149.06	136.41	170.37	116.91	0.24	0.18	0.16	0.11	0	0
10.89	11.59	37.21	30.41	24.55	20.55	51.34	32.2	27.89	7.54	36.89	25.61	0.48	0.26	0.37	0.1	0.16	0.22
10.16	5.37	9.84	5.9	23.71	10.27	78.69	2.81	43.29	0.97	111.58	12.79	0.67	0.23	0.63	0.07	0.13	0.18
6.35	1.7	63.86	30.52	95.65	35.04	150.09	33.35	146.82	17.55	195.92	29.12	0.84	0.32	0.51	0.21	0.12	0.17
15.95	3.09	81.18	28.9	97.22	41.15	21.48	11.65	4.54	0.94	9.43	2.77	0	0	0	0	0	0
1.13	0.22	6.28	3.57	4.94	2	58.36	17.19	29.34	10.13	49.47	8.75	0.11	0.05	0.49	0.21	0.28	0.4
27.3	4.1	57	23.98	102.65	39.02	153.46	35.95	76.59	15.23	186.4	23.01	0	0.03	0.82	0.37	0	0
21.55	10.55	31.61	16	57.86	31.51	73.39	9.42	41.33	4.55	59.81	6.72	0.38	0.12	1.17	0.29	0.77	0.55
7.3	4.12	4.74	3.05	25.66	18.17	119.54	27.46	42.47	4.39	98.36	13.42	0.2	0.14	0.89	0.01	0.38	0.29
2.45	1.73	8.97	8.07	31.1	28.91	99.35	24.6	32.7	2.4	62.21	15.14	0.38	0.11	1.22	0.38	0.42	0.36
9.37	6.52	10.43	7.91	27.99	21.52	156.84	18.49	211.06	48.41	300.21	21.75	0.45	0.29	0.51	0.13	0.42	0.35
23.25	10.26	36.14	11.79	41.11	13.9	49.31	9.78	11.7	4.52	45.91	2.7	0.09	0.06	0.06	0.05	0.11	0.15
5.44	3.26	18.62	16.15	15.24	10.77	29.4	12.18	17.57	6.21	24.17	10.32	0.31	0.39	0.48	0.39	0.1	0.14
4.43	1.34	23.4	5.52	26.4	11.39	88.25	15.57	15.14	0.55	66.32	37.57	0	0	0.06	0.08	0	0
2.68	1.83	11.85	5.05	29.68	11.49	168.83	16.43	47.06	4.64	181.51	11.38	0.24	0.2	1.04	0.34	0.27	0.18
1.96	0.6	1.64	0.59	1.8	0.94	9.4	3.1	10.52	2.74	11.35	3.99	0.18	0.15	0.65	0.37	0	0
16.29	6.45	45.39	21.75	62.29	30.54	347.09	27.51	112.57	23.87	263.06	4.6	0.53	0.37	2.56	0.66	1.67	0.54
46.11	44.13	150.96	118.82	129.19	83.99	282.72	69.05	48.82	20.9	135.11	54.61	1.07	0.47	2.45	0.2	0.72	0.51
65.56	30.51	55.2	24.78	99.46	37.12	103.25	27.26	156.57	45.55	220.74	57.76	0.17	0.05	0.19	0.05	0.33	0.46
54.33	3.32	162.91	9.68	120.73	5.16	90.74	24.62	50.44	10.76	79.65	18.49	1.4	0.63	0.52	0.13	0.36	0.51
22.65	20.05	145.76	76.51	182.24	71.62	490.72	117.84	349.8	55.94	604.55	86.75	1.42	0.28	0.84	0.05	0.14	0.21
106.49	104.31	31.88	21.53	107.04	95.63	144.04	34.92	333.94	38.42	266.35	11.43	0	0	0.06	0.08	0	0
11.87	8.92	24.22	25.77	20.05	19.18	33.11	13.41	18.98	1.94	27.88	13.94	0.18	0.04	0.56	0.3	0.57	0.41
0.78	0.23	4.11	1.1	14.73	4.24	97.91	9.78	25.64	7.9	83.22	7.26	0.41	0.12	1.38	0.26	0.73	0.76
4.68	2.15	3.77	1.07	3.2	1.9	8.69	2.11	12.56	1.65	12.89	1.5	0.22	0.14	0.49	0.04	0	0
2.69	1.12	11.33	4.52	16.81	3.93	53.27	1.47	15.17	2.51	54.89	4.92	0.07	0.1	1.54	0.39	0.82	0.61
34.33	12.1	40.01	7.73	88.12	26.07	91.74	32.25	182.28	93.72	220.99	98.23	0.11	0.07	0.06	0.05	0.2	0.15
54.33	3.32	162.91	9.68	120.73	5.16	90.74	24.62	50.44	10.76	79.65	18.49	1.4	0.63	0.52	0.13	0.36	0.51
9.77	5.38	33.69	14.47	34.24	15.9	92.26	21.49	6.87	1.76	10.1	4.76	0	0	0	0	0	0
2.42	1.7	3.52	1.43	10.76	6.99	259.29	112.58	324.23	111.82	300.97	72.92	0	0	0.06	0.04	0.21	0.29
14.94	17.32	58.36	69.39	46	56.27	193.54	167.1	144.56	78.92	149.49	150.03	0.47	0.2	0.82	0.35	0.09	0.13
5.29	3.23	19.89	8.57	13.86	8.67	157.46	46.81	149.73	12.36	69.88	30.59	0.68	0.58	1.08	0.66	0.18	0.25
9.55	6.13	14.16	7.53	23.62	14.39	68.03	22.54	25.51	5.59	46.97	19.11	1.35	1.11	0.58	0.35	0.23	0.33
2.28	2	2.56	2.55	2.12	1.44	21.83	1.89	24.95	6.36	16.59	2.77	0.28	0.26	0.85	0.39	0.2	0.14
47.1	11.62	97.5	26.26	188.65	33.57	249.84	27.95	97.04	11.38	261.27	18.88	0.33	0.13	1.17	0.51	0.59	0.42
41.05	11.53	49.68	21.11	102.87	37.31	88.93	18.63	47.56	6.53	70.66	14.78	0.26	0.14	1.16	0.59	0	0
7.49	1.72	33.08	3.78	49	5.86	185.19	29.53	58.01	4.69	145.9	0.71	0.39	0.11	1.22	0.46	0.54	0.38
1.89	0.46	2.31	1.02	3.22	0.96	29.07	4.05	18.41	6.08	16.56	3.25	0.09	0.08	0.68	0.49	0.33	0.26
2.36	0.57	19.84	9.07	46.14	11.49	178.08	88.13	60.4	33.19	165.87	47.78	0.31	0.18	1.24	0.07	0.35	0.5
12.95	4.47	32.53	5.24	41.7	12.74	69.29	4.17	22.92	16.07	46.24	32.3	0	0	0.07	0.05	0	0
4.3	1.78	10.08	3.32	40.97	19.81	178.89	50.07	117.06	51.98	258.27	52.56	0.1	0.08	0.66	0.38	0	0
6.77	2.2	15.03	2.59	22.15	2.52	6.28	1.27	2.64	1.14	8.12	0.8	0	0	0	0	0	0
4.68	2.92	27.83	12.03	57.06	18.75	133.15	29.12	35.21	6.1	133.49	12.66	0.3	0.17	2.09	0.52	0.12	0.18
79.92	14.49	178.02	31.12	228.58	27.46	191.06	78.25	242.86	74.52	232.9	92.19	0.96	0.82	0.3	0.14	0	0
41.1	31.13	29.79	19.95	89.69	32.02	137.68	10.27	217.72	77.09	284.68	68.92	0.1	0.07	0.18	0.22	0	0
2.4	2.26	13.5	7.87	45.24	34.48	113.38	32.05	22.76	8.41	77.58	9.06	0.56	0.07	2.12	0.31	0.72	1.02
39.51	9.16	133.26	10.36	106.9	11.7	103.43	30.18	75.98	31.85	116.09	22.45	4.1	3.27	0.76	0.47	0.48	0.68

In brief, wheat cultivar Azhurnaya were grown 16:8 hours day:night at 25°C:15°C. Tissues were harvested between 7.5 and 8.5h into the day, dataset from Winter at al., 2007.

Continued…..

Esi3-7-A		*Esi3-7-B*		*Esi3-7-D*		*Esi3-8-A*		*Esi3-8-B*		*Esi3-8-D*	
Expression Level	Standard Deviation	Expression Level	Standard Deviation	Expression Level	Standard Deviation	Expression Level	Standard Deviation	Expression Level	tandard Deviatio	Expression Level	Standard Deviation
3.41	0.98	9.31	0.34	12.87	0.65	0	0	0	0	0.44	0.21
2.32	0.26	9.55	0.5	9.66	2.44	0	0	0	0	0.37	0.02
2.1	0.9	5.52	0.33	3.15	0.66	0.24	0.34	0	0	0.09	0.09
1.38	1.51	5.33	1.07	4.72	0.82	0	0	1.12	1.07	4.1	1.72
2.29	0.6	7.21	2.02	4.69	2.04	0	0	1.57	1.7	0.71	0.49
1.01	1.44	4.74	0.23	4.55	0.71	0	0	0	0	0.18	0
1.66	0.42	5.44	0.57	3.91	0.35	0	0	0	0	0.32	0.17
9.05	3.27	9.22	1.01	7.65	1.11	0	0	0	0	0.28	0.16
2.2	1.13	4.85	0.34	3.95	0.39	0	0	0.21	0.3	0.36	0.15
1.9	0.57	4.49	1.37	5.26	2.02	0	0	0.23	0.33	0.08	0.06
1.36	0.64	5.96	0.44	2.16	0.24	0	0	0	0	0	0.05
3.98	1.61	9.1	1.07	6.67	1.79	0	0	0.57	0.4	0.34	0.2
0.5	0.7	4.42	0.82	5.03	1.59	0	0	0.68	0.5	0.84	0.19
1.77	0.82	4.67	0.34	3.53	0.79	0	0	0.42	0.59	0.14	0.02
3.48	1.15	7.45	0.8	4.86	2.25	0	0	1.73	1.41	0.45	0.18
1.06	1.07	6.7	1.06	4.49	0.99	0	0	0	0	0.35	0.11
2.58	0.68	3.95	0.34	4.1	0.8	0	0	0	0	0.26	0.25
2.53	1.04	4.73	0.48	5.28	3.62	0	0	0.05	0.08	0.19	0.27
3.26	0.84	6.82	0.4	4.14	0.61	0	0	0	0	0.2	0.28
2.05	0.83	8.12	1.28	9.86	1.71	0	0	0.2	0.29	0.19	0.05
1.95	0.99	4.61	0.58	3.44	0.9	0	0	0.23	0.33	0.34	0.31
4.22	2.49	8.13	1.12	6.66	0.87	0	0	0.43	0.61	0.93	0.25
2.45	1.4	5.61	0.98	5.41	1.34	0	0	0.56	0.79	0.14	0.1
2.25	0.2	7.4	0.83	5.07	0.84	22.32	31.56	2.81	3.29	11.49	15.18
2.67	2.23	4.67	0.27	3.21	0.87	0	0	1.05	0.74	0.28	0.2
0.78	0.21	5.4	2.12	4.37	2.25	0	0	0.26	0.37	0.07	0.07
1.93	1.75	4.61	0.17	2.93	0.36	0.1	0.14	0.21	0.29	0.1	0
2.36	1.99	5.3	0.36	3.23	0.72	0	0	0.72	1.02	0.1	0.14
0	0	2.94	1.2	1.66	1.67	91.09	44.79	8.71	6.76	121.29	6.08
4.82	0.9	5.93	1.32	4.81	1.31	0	0	0.61	0.51	0.26	0.12
1.28	1.15	5.88	0.72	8.88	2.34	0	0	0	0	0.13	0.09
3.86	1.27	6.06	0.78	7.11	2.04	0	0	0.35	0.5	0.4	0.21
4.04	1.23	7.35	0.46	6.96	0.76	0	0	0.26	0.37	0.44	0.23
1.97	0.95	6.8	0.61	6.04	1.09	0	0	0.16	0.23	0.19	0.13
1.37	0.98	8.85	0.91	6.04	0.52	0	0	0	0	0.67	0.21
2.08	0.93	5.92	0.6	2.54	0.58	0	0	0	0	0.09	0.08
3.17	1.54	6.11	1.08	4.22	0.95	0	0	0.61	0.43	0.2	0.16
1.47	0.79	5.06	0.52	5.54	1.69	14.79	12.55	8.4	6.83	27.91	19.43
1.14	0.8	7.23	1.09	6.78	0.91	0	0	0.91	1.29	0.85	0.44
5.96	2.82	5.39	2.36	4.4	1.99	0	0	0	0	0	0.04
1.86	1.86	10.22	1.13	14.09	1.15	0	0	3.4	3.4	1.85	0.48
3.7	0.99	10.96	0.68	10.54	1.32	0.26	0.38	1.48	1.16	0.21	0.18
1.15	1.63	6.53	0.63	5.82	1.5	0	0	0	0	0.3	0.24
1.88	0.99	5.38	0.88	3.01	0.86	0	0	0	0	0.12	0.11
2.82	1.68	9.2	1.53	5.63	0.81	0	0	1.24	1.15	0.47	0.12
1.17	0.84	6.41	1	5.24	1.52	0	0	0.58	0.42	0.53	0.2
2.79	0.78	5.59	0.29	2.75	0.5	0	0	0	0	0	0.03
2.06	0.87	7.26	0.15	7.15	1.34	0	0	0.25	0.36	0.31	0.21
8.27	2.42	5.87	0.53	3.38	0.53	0	0	0	0	0	0.04
3.25	2.54	8.23	1.75	5.91	0.28	0	0	0.67	0.96	0.46	0.23
1.11	0.83	5.75	0.4	4.46	1.68	0	0	0	0	0.22	0.28
1.88	0.99	5.38	0.88	3.01	0.86	0	0	0	0	0.12	0.11
2.58	1.48	7.76	2.07	9.85	2.01	72.92	27.48	12.21	3.03	75.42	23.65
1.61	1.34	9.48	2.43	5.22	2.34	0	0	0	0	0.17	0.25
1.73	1.31	5.63	0.33	3.18	0.91	0.2	0.29	0	0	0.24	0.17
3.61	2.51	5.35	1.54	4.16	0.71	0	0	0.44	0.63	0.14	0.14
3.86	0.74	4.83	1.64	5.44	2.66	0	0	0	0	0.14	0.13
3.41	1.82	3.04	0.81	3.12	1.34	0	0	0.45	0.64	0.16	0.06
1	0.78	4.92	0.52	9.4	0.31	0	0	0.35	0.49	0.45	0.18
0.96	0.62	5.68	0.79	7.48	2.29	0	0	0.3	0.43	0.3	0.32
3.49	0.82	6.09	0.61	6.17	0.61	0	0	0.34	0.48	0.59	0.42
4.25	1.69	7.36	0.09	5.03	0.73	0	0	0	0	0.13	0.06
0.57	0.44	10.67	5.02	9.79	1.95	0	0	0	0	1.22	0.8
2.89	2.07	7.25	1.81	7.1	0.93	101.95	41.27	20.56	7.01	134.32	42.71
1.16	0.71	7.28	0.58	6.7	1.97	0	0	0	0	0.32	0.27
0	0	3.31	1.23	0.57	0.2	269.99	6.74	29.34	4.64	346.95	17.14
2.49	1.15	6.08	1.89	7.8	2.04	0	0	0.38	0.54	0.29	0.34
2.58	0.85	5.48	1.29	4.87	0.96	0	0	0	0	0.45	0.44
2.27	0.93	6.29	0.69	3.45	1.77	0	0	0	0	0.38	0.12
2.23	0.75	5.6	1.51	7.83	2.86	0	0	0	0	0.26	0.15
1.42	0.33	7.22	1.21	4.21	1.74	0	0	0	0	0.17	0.13

In brief, wheat cultivar Azhurnaya were grown 16:8 hours day:night at 25°C:15°C. Tissues were harvested between 7.5 and 8.5h into the day, dataset from Winter at al., 2007.

Continued…..

Esi3-9-A		*Esi3-9-B*		*Esi3-9-D*		*Esi3-10-B*		*Esi3-10-D*		
Expression Level	Standard Deviation	Expression Level	Standard Deviation	Expression Level	Standard Deviation	Expression Level	Standard Deviation	Expression Level	Standard Deviation	Tissue Type
0	0	0	0	0	0	37.68	2.7	5.05	1.56	First leaf sheath - Tillering stage
0.06	0.06	0.12	0.12	0	0	35.43	1.21	3.69	1.82	Internode #2 - Milk grain stage
0	0.06	0	0	0	0	25.72	4.11	1.84	0.27	Shoot apical meristem - Seedling stage
0	0	0	0	0	0	27.41	2.4	2.68	1.13	Grain - Milk grain stage
0	0.02	0	0	0	0	15.49	3.27	1.26	1.24	First leaf blade - Seedling stage
0	0	0	0	0	0	16.83	0.82	0.64	0.61	Flag leaf blade - Full boot
3.04	3.52	0.32	0.45	0.05	0.07	34.51	2.02	3.05	0.66	Awn - 50 percent spike
0	0.03	0	0	0	0	22.06	2.24	1.73	0.68	flag leaf blade night (-0.25h) 06:45
0	0	0	0	0	0	29.1	2.03	2.88	1.37	Shoot axis - Flag leaf stage
0	0	0	0	0	0	17.69	4.68	1.54	0.15	Fifth leaf blade - Flag leaf stage
0	0	0	0	0	0	30.72	6.67	2.6	1.54	Third leaf sheath - Three leaf stage
0	0	0	0.02	0	0	40.11	8.16	4.99	3.34	Internode #2 - Ear emergence
689.07	246.22	225.61	79.48	8.17	2.71	13.27	0.34	3.17	1.19	Anther
0	0	0	0	0	0	49.99	1.06	6.47	4.54	Spike
0	0.06	0	0	0	0	28.9	3.06	4.56	4.08	Coleoptile
1.16	0.3	0.3	0.11	0	0.03	35.44	1.83	5.96	3.32	Stigma and Ovary
0	0	0	0	0	0	28.09	1.36	5.64	2.96	Roots - Flag leaf stage
0	0	0	0	0	0	26.43	2.74	3.38	1.62	Fifth leaf sheath - Flag leaf stage
0	0	0	0	0	0	40.44	9.57	3.98	0.27	Root apical meristem - Three leaf stage
0.14	0.19	0	0	0	0	30.45	3.48	1.62	0.8	Flag leaf sheath - Ear emergence
0	0	0	0	0	0	31.56	1	3.66	1.4	Roots - Three leaf stage
0	0	0	0	0	0	36.24	2.37	2.85	0.74	Axillary roots - Three leaf stage
0	0	0	0	0	0	25.46	1.7	5.06	3.83	Flag leaf sheath - 50 percent spike
0.08	0.12	0.05	0.07	0	0	40.36	3.41	3.53	1.45	Radicle - Seedling stage
0.05	0.04	0.06	0.09	0	0	27.48	6.4	8.62	6.19	Roots - 50 percent spike
0	0	0	0	0	0	17.77	8.32	1.39	1.22	Third leaf blade - Three leaf stage
4.05	3.23	0.7	0.78	0.15	0.22	30.2	2.12	4.34	2.34	Spikelets - 50 percent spike
0	0	0	0	0	0	43.86	1.59	4.94	0.52	Root apical meristem - Tillering stage
0	0	0	0	0	0	8.59	5.31	0	0	Grain - Ripening stage
0.14	0.13	0	0	0	0	15.5	3.55	2.07	1.27	Awns - Ear emergence
0.07	0.05	0	0	0	0	24.62	3.65	8.73	3.16	Glumes
0.11	0.08	0.07	0.05	0	0.02	28.61	1.03	7.81	2.35	Glumes - Ear emergence
0	0	0	0	0	0	26.94	0.61	2.51	2.05	Leaf ligule
0	0	0.06	0.09	0	0	18.9	2.18	1.9	0.8	Flag leaf blade - 50 percent spike
0.16	0.23	0	0.03	0	0	41.3	8.32	5.56	2.23	Internode #2 - 50 percent spike
0	0	0	0	0	0	33.08	3.12	4.88	3.28	Fifth leaf sheath - Fifth leaf stage
0	0	0	0	0	0	14.38	1.55	3.02	0.48	fifth leaf blade night (-0.25h) 21:45
0	0.03	0	0	0	0	20.75	4.45	0.96	0.78	Grain - Soft dough
0	0	0	0	0	0	25.78	1.86	2.05	1.27	Flag leaf blade (senescence) - Dough stage
0	0	0	0	0	0	14.1	4.25	1.85	1.35	Flag leaf blade night (-0.25h) 06:45 - Flag leaf stage
0	0.02	0	0	0	0	43.28	5.8	2.01	0.75	Flag leaf blade (senescence) - Ripening stage
0	0	0	0	0	0	37.39	7.9	2.49	1.2	First leaf blade - Tillering stage
0	0.01	0	0	0	0	37.52	7.61	5.65	3.51	Shoot apical meristem - Tillering stage
0	0.05	0	0.02	0	0	27.19	1.28	2.37	1.46	Shoot axis - First leaf stage
0	0	0	0	0	0	41.59	3.29	2.53	1.45	Roots - Seedling stage
0	0	0	0	0	0	30.18	4.17	4.84	4.45	Shoot axis - Milk grain stage
0	0	0	0	0	0	14.2	5.69	1.29	0.11	Fifth leaf blade - Fifth leaf stage
0	0	0	0	0	0	24.26	1.83	2.26	0.59	Flag leaf blade - Ear emergence
0	0	0	0	0	0	13.38	0.05	0.62	0.33	flag leaf blade night (+0.25h) 07:15
0	0.04	0	0	0	0	26.31	2.34	3.01	0.64	Fifth leaf blade night (-0.25h) 21:45
0	0	0	0	0	0	31.64	3.46	3.17	0.84	Shoot axis - Tillering stage
0	0.05	0	0.02	0	0	27.19	1.28	2.37	1.46	Stem axis - First leaf stage
0	0.02	0	0	0	0	26.95	4.48	1.89	0.13	Endosperm
0.1	0.11	0.06	0.08	0	0	23.15	5.51	0.84	0.6	Peduncle
0	0	0.05	0.08	0	0	24.2	5.79	4.26	4.56	Peduncle - 50 percent spike
0	0.05	0	0	0	0	25.18	5.72	3.43	0.93	Peduncle - Ear emergence
0	0	0	0	0	0	22.47	4.7	3.12	1.58	Flag leaf sheath - Full boot
0	0	0	0	0	0	14.97	1.54	1.53	0.94	Flag leaf blade - Flag leaf stage
0	0	0	0	0	0	26.65	1.23	11.04	2.37	Lemma
4.21	2.18	2.41	1.15	0.12	0.11	27.32	1.63	9.26	3.37	Lemma - Ear emergence
0.29	0.41	0	0.06	0	0	21.31	2.14	3.69	1.45	Awns - Milk grain stage
0	0	0	0	0	0	16.71	3.2	1.09	1	fifth leaf blade night (+0.25h) 22:15
0	0	0	0.04	0	0	37.43	9.6	3.33	2.16	Flag leaf blade - Milk grain stage
0	0.06	0	0	0	0	22.32	4.98	1.8	1.01	Grain - Hard dough
0.13	0.1	0	0.05	0	0	26.37	1.53	1.57	1.26	Flag leaf sheath - Milk grain stage
0	0	0	0	0	0	11.04	0.73	0.45	0.35	Embryo proper
0.11	0.16	0	0	0	0	28.66	5.52	1.94	1.64	Fifth leaf blade (senescence) - Milk grain stage
0	0.03	0	0	0	0.03	41.61	3.93	9.77	2.27	Roots - Tillering stage
0	0.02	0	0	0	0	37.31	1.41	2.68	2.19	Shoot axis - Full boot
0	0.01	0	0	0	0	24.59	5.3	1.98	1.39	Fifth leaf blade - Ear emergence
0	0	0	0.02	0	0	25.45	5.51	3.06	1.21	First leaf sheath - Seedling stage

In brief, wheat cultivar Azhurnaya were grown 16:8 hours day:night at 25°C:15°C. Tissues were harvested between 7.5 and 8.5h into the day, dataset from Winter at al., 2007.

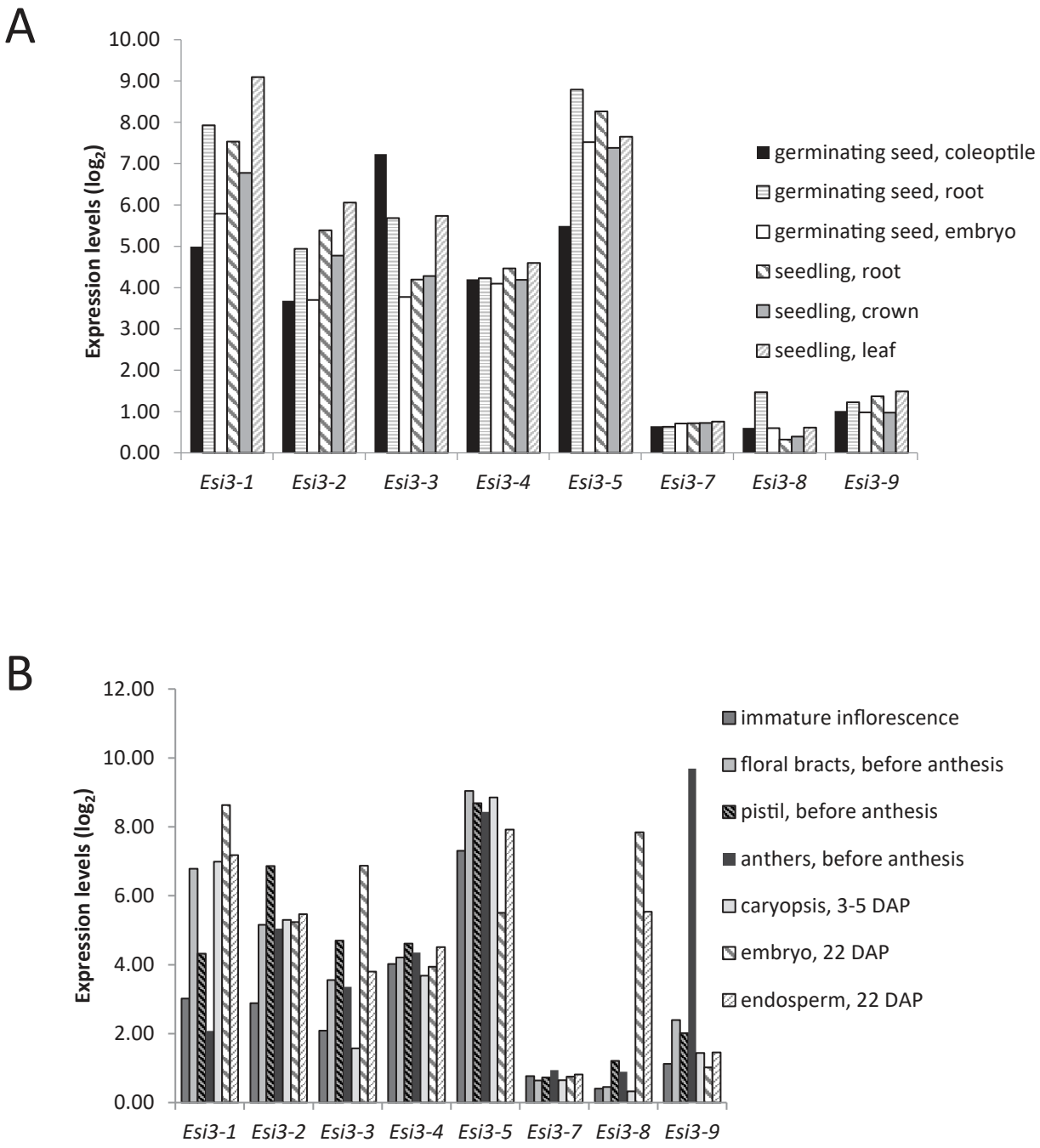

Additional Figure 1: Tissue specific expression of the *Esi3* genes across thirteen *T. aestivum* tissue types assayed by microarray dataset by Schreiber et al., 2009. **(A)** Young tissue types ranging from germinating seed to seedling stages. **(B)** Mature tissue types before anthesis, 3-5 and 22 days after pollination (DAP). Values are RMA normal-ized and are in $\log_2$ units. All microarray values had 4 subtracted, this was treated as background.

Table S6 A. *Esi3/RCI2/PMP3* tissue-specific expression assayed by microarray analysis (log_2)

Tissue	*Esi3-1*	*Esi3-2*	*Esi3-3*	*Esi3-4*	*Esi3-5*	*Esi3-7*	*Esi3-8*	*Esi3-9*	*Esi3-10*
Germinating seed, coleoptile	4.99	3.68	7.23	4.20	5.50	0.65	0.61	1.01	0.53
Germinating seed, root	7.93	4.94	5.68	4.23	8.79	0.63	1.47	1.23	0.53
Germinating seed, embryo	5.79	3.70	3.78	4.10	7.52	0.71	0.60	0.98	0.57
Seedling, root	7.53	5.39	4.19	4.46	8.27	0.72	0.32	1.37	0.33
Seedling, crown	6.77	4.77	4.28	4.19	7.38	0.72	0.40	0.98	0.33
Seedling, leaf	9.09	6.06	5.73	4.59	7.65	0.75	0.61	1.49	0.51
Immature inflorescence	3.02	2.89	2.08	4.02	7.31	0.77	0.40	1.12	0.71
Floral bracts, before anthesis	6.78	5.16	3.55	4.21	9.04	0.64	0.45	2.39	0.36
Pistil, before anthesis	4.32	6.86	4.70	4.62	8.69	0.73	1.21	2.02	0.22
Anthers, before anthesis	2.08	5.05	3.36	4.36	8.44	0.94	0.90	9.69	0.64
Caryopsis, 3-5 DAP[a]	6.99	5.30	1.58	3.68	8.85	0.65	0.32	1.44	0.35
Embryo, 22 DAP[a]	8.63	5.23	6.87	3.94	5.51	0.76	7.85	1.02	0.41
Endosperm, 22 DAP[a]	7.18	5.47	3.80	4.51	7.93	0.81	5.54	1.46	0.42

Affymetrix microarray data from Schreiber et al., 2009 [29].

Values are in log2 units and all values had 4 subtracted as background.

[a]DAP - Days After Pollination

Table S6 B. *Esi3/RCI2/PMP3* fold differences in tissue-specific expression compared to the caryopsis 3-5 DAP

Tissue	*Esi3-1*	*Esi3-2*	*Esi3-3*	*Esi3-4*	*Esi3-5*	*Esi3-7*	*Esi3-8*	*Esi3-9*	*Esi3-10*
Germinating seed, coleoptile	0.06	0.19	2.83	0.76	0.22	0.93	1.00	0.72	1.02
Germinating seed, root	0.45	0.46	0.96	0.77	2.20	0.92	1.81	0.83	1.02
Germinating seed, embryo	0.10	0.20	0.26	0.71	0.91	0.97	0.99	0.70	1.05
Seedling, root	0.34	0.63	0.34	0.91	1.53	0.97	0.82	0.92	0.88
Seedling, crown	0.20	0.41	0.37	0.75	0.83	0.98	0.86	0.70	0.89
Seedling, leaf	1	1	1	1	1	1	1	1	1
Immature inflorescence	0.01	0.11	0.08	0.67	0.79	1.01	0.87	0.78	1.15
Floral bracts, before anthesis	0.20	0.54	0.22	0.77	2.62	0.93	0.89	1.87	0.90
Pistil, before anthesis	0.04	1.75	0.49	1.01	2.05	0.98	1.52	1.44	0.82
Anthers, before anthesis	0.01	0.50	0.19	0.85	1.72	1.14	1.22	293.64	1.10
Caryopsis, 3-5 DAP[a]	0.23	0.59	0.06	0.53	2.30	0.93	0.82	0.96	0.90
Embryo, 22 DAP[a]	0.72	0.57	2.20	0.64	0.23	1.00	150.77	0.72	0.94
Endosperm, 22 DAP[a]	0.27	0.67	0.26	0.94	1.21	1.04	30.47	0.98	0.94

Affymetrix microarray data from Schreiber et al., 2009 [29].

Values are in log2 units and all values had 4 subtracted as background.

[a]DAP - Days After Pollination

Note: This is the same data as in Table S6 A, but the values are expressed as fold differences and are non-logarithmic

Table S7A. *Esi3/RCI2/PMP3* gene expression in response to drought and heat stress

	Control	Drought 1 hr	Drought 6 hr	Heat 1 hr	Heat 6 hr	Mixed 1 hr	Mixed 6 hr
Esi3-1-A	26.83	98.85	546.84	10.76	7.61	9.32	54.87
Esi3-1-B	2.69	6.68	119.54	0.62	0.23	0.99	2.46
Esi3-1-D	2.20	12.18	196.01	0.79	0.36	0.45	2.50
Esi3-2-A	3.41	3.36	32.89	1.41	2.49	2.78	6.18
Esi3-2-D	0.03	0.53	29.39	0.08	0.00	0.08	0.70
Esi3-3-A	19.99	37.60	120.09	17.66	4.79	6.23	3.88
Esi3-3-B	18.99	76.23	416.37	22.12	6.03	19.48	19.91
Esi3-3-D	15.19	54.42	276.52	11.87	8.53	10.38	7.99
Esi3-4-A	0.00	0.00	0.00	0.00	0.00	0.00	0.00
Esi3-4-B	28.28	67.56	76.16	38.51	76.17	25.66	63.84
Esi3-4-D	20.52	56.20	48.36	30.12	62.85	31.19	78.15
Esi3-5-A	92.03	83.50	43.55	226.10	579.36	288.85	571.86
Esi3-5-B	46.54	42.85	31.13	39.97	99.35	17.40	70.88
Esi3-5-D	52.61	52.00	18.25	83.32	372.44	84.53	424.07
Esi3-6-A	0.04	0.04	0.02	0.00	0.00	0.00	0.00
Esi3-6-B	0.07	0.00	0.00	0.07	0.00	0.00	0.00
Esi3-6-D	0.07	0.00	0.00	0.07	0.00	0.00	0.00
Esi3-7-A	1.47	1.97	3.51	2.46	4.13	1.20	4.96
Esi3-7-B	1.73	2.38	4.42	1.72	4.89	0.92	3.07
Esi3-7-D	2.60	3.84	6.04	2.81	5.11	2.40	5.16
Esi3-8-A	0.00	0.00	0.00	0.00	0.00	0.00	0.00
Esi3-8-B	0.23	0.21	0.79	0.05	0.20	0.11	0.38
Esi3-8-D	0.00	0.00	0.20	0.00	0.00	0.00	0.00
Esi3-9-A	0.00	0.00	0.00	0.00	0.00	0.00	0.00
Esi3-9-B	0.00	0.00	0.00	0.00	0.00	0.00	0.00
Esi3-9-D	0.00	0.00	0.00	0.00	0.00	0.00	0.00
ESI3-10-A	3.42	5.25	5.47	3.79	1.14	1.14	2.10
ESI3-10-B	18.06	22.18	28.89	13.56	19.82	13.31	32.67
ESI3-10-D	10.57	15.59	15.27	12.24	24.55	13.78	53.21

Note: Microarray dataset by Liu et al., 2015 and stress conditions are described as seedlings grown on filter paper and treated with 20% PEG, 40°C or both heat and PEG, RNA was extracted from leaves.

Units are RPKPM. Values are averages from two transcriptome libraries.

Mixed refers to combined drought and heat treatment.

Table S7 B. *Esi3/RCI2/PMP3* fold change in gene expression in response to drought and heat

	Control	Drought 1 hr	Drought 6 hr	Heat 1 hr	Heat 6 hr	Mixed 1 hr	Mixed 6 hr
Esi3-1-A	1.00	3.68	20.38	0.40	0.28	0.35	2.04
Esi3-1-B	1.00	2.49	44.51	0.23	0.08	0.37	0.92
Esi3-1-D	1.00	5.53	88.94	0.36	0.16	0.20	1.13
Esi3-2-A	1.00	0.99	9.65	0.41	0.73	0.82	1.82
Esi3-2-D	1.00	20.18	1121.01	3.14	0.00	3.02	26.58
Esi3-3-A	1.00	1.88	6.01	0.88	0.24	0.31	0.19
Esi3-3-B	1.00	4.01	21.92	1.16	0.32	1.03	1.05
Esi3-3-D	1.00	3.58	18.20	0.78	0.56	0.68	0.53
Esi3-4-A	1.00	0.00	0.00	0.00	0.00	0.00	0.00
Esi3-4-B	1.00	2.39	2.69	1.36	2.69	0.91	2.26
Esi3-4-D	1.00	2.74	2.36	1.47	3.06	1.52	3.81
Esi3-5-A	1.00	0.91	0.47	2.46	6.30	3.14	6.21
Esi3-5-B	1.00	0.92	0.67	0.86	2.13	0.37	1.52
Esi3-5-D	1.00	0.99	0.35	1.58	7.08	1.61	8.06
Esi3-6-A	1.00	1.13	0.64	0.00	0.00	0.00	0.00
Esi3-6-B	1.00	0.00	0.00	1.05	0.00	0.00	0.00
Esi3-6-D	1.00	0.00	0.00	1.05	0.00	0.00	0.00
Esi3-7-A	1.00	1.34	2.39	1.67	2.81	0.82	3.38
Esi3-7-B	1.00	1.38	2.55	1.00	2.82	0.53	1.77
Esi3-7-D	1.00	1.48	2.33	1.08	1.97	0.92	1.99
Esi3-8-A	1.00	0.00	0.00	0.00	0.00	0.00	0.00
Esi3-8-B	1.00	0.92	3.51	0.20	0.88	0.49	1.69
Esi3-8-D	1.00	0.00	0.00	0.00	0.00	0.00	0.00
Esi3-9-A	1.00	0.00	0.00	0.00	0.00	0.00	0.00
Esi3-9-B	1.00	0.00	0.00	0.00	0.00	0.00	0.00
Esi3-9-D	1.00	0.00	0.00	0.00	0.00	0.00	0.00
ESI3-10-A	1.00	1.54	1.60	1.11	0.33	0.33	0.61
ESI3-10-B	1.00	1.23	1.60	0.75	1.10	0.74	1.81
ESI3-10-D	1.00	1.47	1.44	1.16	2.32	1.30	5.03

Note: This is the same data as Table S7 A however the data is represented in fold change and is non-logarithmic.

Table S8 A. *Esi3/RCI2/PMP3* expression in response to drought in Cappelli, a water use efficient line, and Ofanto, a water use inefficient line (log_2)

	Esi3-1	*Esi3-2*	*Esi3-3*	*Esi3-4*	*Esi3-5*	*Esi3-7*	*Esi3-8*	*Esi3-9*	*Esi3-10*
Cappelli, control	5.89	3.14	6.21	3.28	6.81	0.14	1.58	0.37	5.77
Cappelli, drought	4.11	2.90	6.58	3.20	6.66	0.07	1.67	0.31	5.89
Cappelli, heat	5.11	4.63	4.93	3.36	9.65	0.36	2.20	0.20	5.32
Cappelli, drought + heat	4.61	4.39	5.11	3.33	9.14	0.14	2.64	0.31	5.29
Ofanto, control	5.94	2.55	4.74	3.68	6.40	0.27	0.90	0.56	5.03
Ofanto, drought	7.34	3.37	6.12	3.46	6.30	0.11	1.12	0.35	5.38
Ofanto, heat	5.63	3.01	5.08	3.16	7.85	0.13	1.22	0.17	4.56
Ofanto, drought + heat	6.37	4.11	5.23	3.43	9.17	0.26	2.94	0.43	5.36

Note: *Esi3/RCI2/PMP3* expression was quantified with an Affymetrix microarray by Aprile et al., 2013. Conditions were those described in Aprile et al., 2013 [31]; in brief, plants were stressed at booting stage by withholding water to 12.5% soil water content. Heat treatment was by incremental increases to 40°C, combined treatment used the same two conditions. Measurements are on the log_2 scale Background of 3.4 subtracted from all values.

Table S8 B. *Esi3/RCI2/PMP3* fold change in expression in response to drought in Cappelli, a water use efficient line, and Ofanto, a water use inefficient line

	Esi3-1	*Esi3-2*	*Esi3-3*	*Esi3-4*	*Esi3-5*	*Esi3-7*	*Esi3-8*	*Esi3-9*	*Esi3-10*
Cappelli, control	1	1	1	1	1	1	1	1	1
Cappelli, drought	0.29	0.85	1.30	0.94	0.90	0.95	1.06	0.96	1.09
Cappelli, heat	0.58	2.81	0.41	1.06	7.16	1.17	1.54	0.89	0.74
Cappelli, drought + heat	0.41	2.38	0.47	1.04	5.03	1.01	2.09	0.96	0.72
Ofanto, control	1	1	1	1	1	1	1	1	1
Ofanto, drought	2.65	1.77	2.60	0.85	0.93	0.90	1.17	0.87	1.28
Ofanto, heat	0.81	1.37	1.26	0.70	2.73	0.91	1.25	0.77	0.72
Ofanto, drought + heat	1.35	2.95	1.41	0.84	6.82	0.99	4.12	0.92	1.26

Note: This is the same data as in Table S8 A, but the values are expressed as fold change compared to the controls and are non-logarithmic

Table S9 A. *Esi3/RCI2/PMP3* response to drought in the hexaploid Chinese Spring, the tetraploid Creso, and a Chinese Spring chromosome deletion line ($\log_2$)

	Esi3-1	*Esi3-2*	*Esi3-3*	*Esi3-4*	*Esi3-5*	*Esi3-7*	*Esi3-8*	*Esi3-9*	*Esi3-10*
Creso Control	5.79	3.73	4.25	2.37	7.40	0.37	0.32	3.26	5.73
Creso Mild stress	5.48	4.28	4.75	2.29	7.62	0.70	1.23	3.23	5.66
Creso Severe stress	5.16	4.51	5.22	2.36	7.82	0.70	2.33	3.84	5.82
Chinese Spring Control	3.79	4.02	2.17	2.02	8.07	0.34	0.68	3.20	0.00
Chinese Spring mild stress	5.46	4.43	3.46	2.15	8.15	0.26	1.18	3.27	0.00
Chinese Spring severe stress	5.26	3.82	3.26	2.31	8.14	0.40	1.08	3.53	0.00
Chinese Spring-5AL Control	4.42	3.93	0.01	2.12	8.19	0.29	0.87	3.95	0.00
Chinese Spring-5AL Mild stress	6.62	4.79	0.29	2.12	8.32	0.60	1.54	4.44	0.00
Chinese Spring-5AL Severe stress	5.38	4.33	0.09	2.17	8.49	0.53	1.84	4.26	0.00

Note: *Esi3/RCI2/PMP3* expression was quantified with an Affymetrix microarray by Aprile et al., 2009. Plants were grown as described by Aprile et al., 2009 [32]; briefly, soil grown plants were treated at anthesis at the following levels of stress: Control field capacity 28% water content, mild stress 18% water content or severe stress at 12.5% water content. Background of 3.3 subtracted from all values, values are in $\log_2$ units.

Table S9 B. *Esi3/RCI2/PMP3* fold change in response to drought in the hexaploid Chinese Spring, the tetraploid Creso, and a Chinese Spring chromosome deletion line

	Esi3-1	*Esi3-2*	*Esi3-3*	*Esi3-4*	*Esi3-5*	*Esi3-7*	*Esi3-8*	*Esi3-9*	*Esi3-10*
Creso Control	1	1	1	1	1	1	1	1	1
Creso Mild stress	0.81	1.47	1.41	0.95	1.17	1.25	1.88	0.98	0.95
Creso Severe stress	0.64	1.71	1.97	0.99	1.34	1.26	4.04	1.49	1.06
Chinese Spring Control	1	1	1	1	1	1	1	1	1
Chinese Spring mild stress	3.18	1.32	2.45	1.09	1.06	0.95	1.41	1.05	1.00
Chinese Spring severe stress	2.77	0.87	2.14	1.22	1.05	1.04	1.32	1.25	1.00
Chinese Spring-5AL Control	1	1	1	1	1	1	1	1	1
Chinese Spring-5AL Mild stress	4.60	1.81	1.22	1.00	1.09	1.24	1.59	1.40	1.00
Chinese Spring-5AL Severe stress	1.95	1.31	1.06	1.04	1.22	1.18	1.96	1.24	1.00

Note: This is the same data as in Table S9 A, but the values are expressed as fold change relative to the non-stressed controls and are non-logarithmic.

Table S10. *Esi3/RCI2/PMP3* gene expression in cold treated seedlings

		Duncan's		Duncan's	
	23°C	MR[a]	4°C	MR[a]	Fold change
Esi3-1-A	39.89	b	256.62	e	6.43
Esi3-1-B	8.58	a	112.26	d	13.09
Esi3-1-D	1.72	a	59.21	c	34.38
Esi3-2-A	1.91	b	10.29	c	5.40
Esi3-2-D	0.04	a	0.68	a	15.70
Esi3-3-A	0.14	a	0.80	a	5.74
Esi3-3-B	1.84	a	54.33	b	29.55
Esi3-3-D	3.63	a	59.31	b	16.33
Esi3-4-A	1.20	a	0.40	a	0.33
Esi3-4-B	37.25	c	5.75	a	0.15
Esi3-4-D	20.90	b	4.95	a	0.24
Esi3-5-A	25.13	c	3.07	a	0.12
Esi3-5-B	7.77	b	1.33	a	0.17
Esi3-5-D	8.92	b	2.27	a	0.25
Esi3-6-A	0.12		0.03		0.21
Esi3-6-B	0.06		0.11		1.93
Esi3-6-D	0.06		0.11		1.93
Esi3-7-A	1.43	a	2.35	b	1.64
Esi3-7-B	1.40	a	0.76	a	0.54
Esi3-7-D	1.35	a	0.88	a	0.65
Esi3-8-A	0.00	a	0.00	a	0.00
Esi3-8-B	0.00	a	0.06	b	0.00
Esi3-8-D	0.00	a	0.00	a	0.00
Esi3-9-A	0.00		0.00		0.00
Esi3-9-B	0.00		0.00		0.00
Esi3-9-D	0.00		0.00		0.00
Esi3-10-A	0.00	a	0.00	a	0.00
Esi3-10-B	10.37	bc	12.76	c	1.23
Esi3-10-D	9.29	b	13.32	c	1.43

Note: Microarray dataset by Li et al., 2015. Plants were grown as described in Li et al., 2015, in brief, seedlings were grown in soil for 2 weeks at 23 °C, moved to 4°C for 2 weeks. RNA samples were from the leaf. Values are in RPKPM, and represent the average of three replicates.

[a] Duncan's multiple range (MR) *post hoc* test

Table S11. *Esi3/RCI2/PMP3* gene expression in wheat spikes in response to *Fusarium graminearum* inoculation in the disease susceptible NIL 51 and disease resistant NIL 38 [+].

	24 hr Moc NIL 51		24 hr Fus NIL 51		24 hr Moc NIL 38		24 hr Fus NIL 38		48 hr Moc NIL 51		48 hr Fus NIL 51		48 hr Moc NIL 38		48 hr Fus NIL 38	
Esi3-1-A	4.22		4.06		5.06		3.73		7.53		4.04		5.57		3.74	
Esi3-1-B	0.54		0.69		0.56		0.82		1.09		0.69		0.87		0.41	
Esi3-1-D	0.00		0.26		0.16		0.08		0.17		0.03		0.07		0.08	
Esi3-2-A	2.02		1.20		1.68		2.38		2.13		1.09		2.09		1.36	
Esi3-2-D	0.00		0.00		0.00		0.00		0.11		0.00		0.15		0.00	
Esi3-3-A	0.93		0.57		0.22		0.73		1.10		0.64		0.44		0.61	
Esi3-3-B	0.41		0.38		0.38		0.76		0.42		0.55		0.53		0.43	
Esi3-3-D	0.17	a	1.10	c	0.69		0.79		0.18		0.40		0.31		0.00	
Esi3-4-A	1.84	ab	3.51	ab	1.82	ab	5.34	bc	0.69	a	10.40	d	3.45	ab	8.17	cd
Esi3-4-B	0.00		0.00		0.00		0.00		0.00		0.00		0.00		0.00	
Esi3-4-D	4.32	a	7.85	a	4.50	a	11.12	a	3.94	a	33.52	b	7.20	a	32.06	b
Esi3-5-A	63.61		65.13		70.85		54.13		63.23		69.21		76.12		54.45	
Esi3-5-B	63.49		61.44		61.33		56.93		46.00		57.11		54.63		50.09	
Esi3-5-D	69.17		72.72		71.78		60.64		67.13		80.20		75.53		68.38	
Esi3-6-A	0.00		0.00		0.00		0.11		0.00		0.00		0.00		0.00	
Esi3-6-B	0.11		0.00		0.05		0.04		0.26		0.05		0.05		0.14	
Esi3-6-D	0.11		0.14		0.05		0.04		0.26		0.05		0.05		0.14	
Esi3-7-A	1.05		1.01		0.73		0.94		0.71		0.47		0.88		1.15	
Esi3-7-B	1.51		1.50		1.65		1.87		1.45		1.66		1.32		1.92	
Esi3-7-D	1.01		0.97		2.04		0.73		0.76		2.08		0.47		1.35	
Esi3-8-A	0.00		0.00		0.00		0.00		0.00		0.00		0.00		0.00	
Esi3-8-B	0.00		0.00		0.00		0.00		0.00		0.00		0.00		0.00	
Esi3-8-D	0.00		0.00		0.00		0.00		0.00		0.00		0.00		0.00	
Esi3-9-A	23.74		22.60		21.91		24.27		6.59		5.29		5.32		5.56	
Esi3-9-B	10.21		8.48		10.74		10.39		2.40		2.46		2.18		1.89	
Esi3-9-D	0.00		0.00		0.00		0.00		0.00		0.00		0.00		0.06	
Esi3-10-A	2.20		2.27		3.26		2.48		2.31		4.31		2.86		2.44	
Esi3-10-B	13.23		14.01		13.88		13.97		16.64		14.14		17.93		10.99	
Esi3-10-D	6.60		6.15		7.61		5.00		5.83		7.13		8.49		5.89	

	Fold Change			
	24 hr NIL 51	24 hr NIL 38	48 hr NIL 51	48 hr NIL 38
Esi3-1-A	0.96	0.74	0.54	0.67
Esi3-1-B	1.28	1.46	0.64	0.47
Esi3-1-D		0.49	0.19	1.14
Esi3-2-A	0.59	1.41	0.51	0.65
Esi3-2-D			0.00	0.00
Esi3-3-A	0.62	3.30	0.58	1.39
Esi3-3-B	0.93	1.99	1.30	0.81
Esi3-3-D	6.56 *	1.14	2.19	
Esi3-4-A	1.91 *	2.93 *	15.02 *	2.37
Esi3-4-B				
Esi3-4-D	1.82 *	2.47 *	8.52 *	4.45
Esi3-5-A	1.02	0.76	1.09	0.72
Esi3-5-B	0.97	0.93	1.24	0.92
Esi3-5-D	1.05	0.84	1.19	0.91
Esi3-6-A				
Esi3-6-B	0.00	0.76	0.18	2.96
Esi3-6-D	1.26	0.76	0.18	2.96
Esi3-7-A	0.96	1.29	0.67	1.31
Esi3-7-B	1.00	1.13	1.14	1.46
Esi3-7-D	0.96	0.36	2.71 *	2.88
Esi3-8-A				
Esi3-8-B				
Esi3-8-D				
Esi3-9-A	0.95	1.11	0.80	1.05
Esi3-9-B	0.83	0.97	1.03	0.87
Esi3-9-D				
Esi3-10-A	1.03	0.76	1.86	0.85
Esi3-10-B	1.06	1.01	0.85	0.61
Esi3-10-D	0.93	0.66	1.22	0.69

[+] Data is from Steiner et al., 2017 [36]; from the Bioproject PRJEB12358 deposited in the GenBank SRA database.

The data, expressed in RPKPM, is from spikes that were either mock innoculated (Moc) with water or innoculated with a suspension of *Fusarium graminearum* spores (Fus).

*Fold change values greater than 1.8 fold and a P value less than 0.05 are marked.

Duncan's multiple range value applies to each row for the given *Esi3-3-D*, *Esi3-4-A or Esi3-4-D*

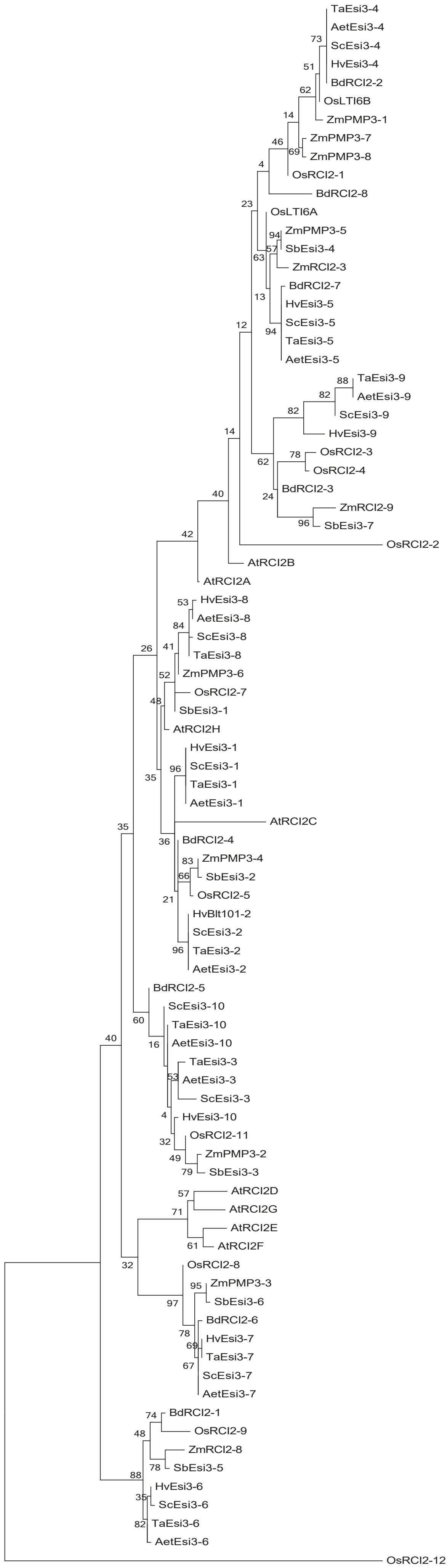

Additional Figure 2: Molecular Phylogenetic analysis of the Esi3/RCI2/PMP3 protein sequences from nine species. The evolutionary history was inferred by using the Maximum Likelihood method based on the Whelan And Goldman model [44]. The tree with the highest log likelihood (-2067.2128) is shown. The tree is drawn to scale, with branch lengths mea sured in the number of substitutions per site. The analysis involved 85 amino acid sequences. All positions containing gaps and missing data were eliminated. There were a total of 54 positions in the final dataset. The percentage of trees in which the associated taxa clustered together is shown next to the branches. The species abbreviatons are as follows; Ta- *Triticum aestivum*, Hv - *Hordeum vulgare*, At- *Arabidopsis thaliana*, Sb - S*orghum bicolor*, Aet - *Aegilops tauschii*, Sc- *Secale cereale*, Zm- *Zea mays*, Os- *Oryza sativa*, Bd- *Brachypodium distachyon*.

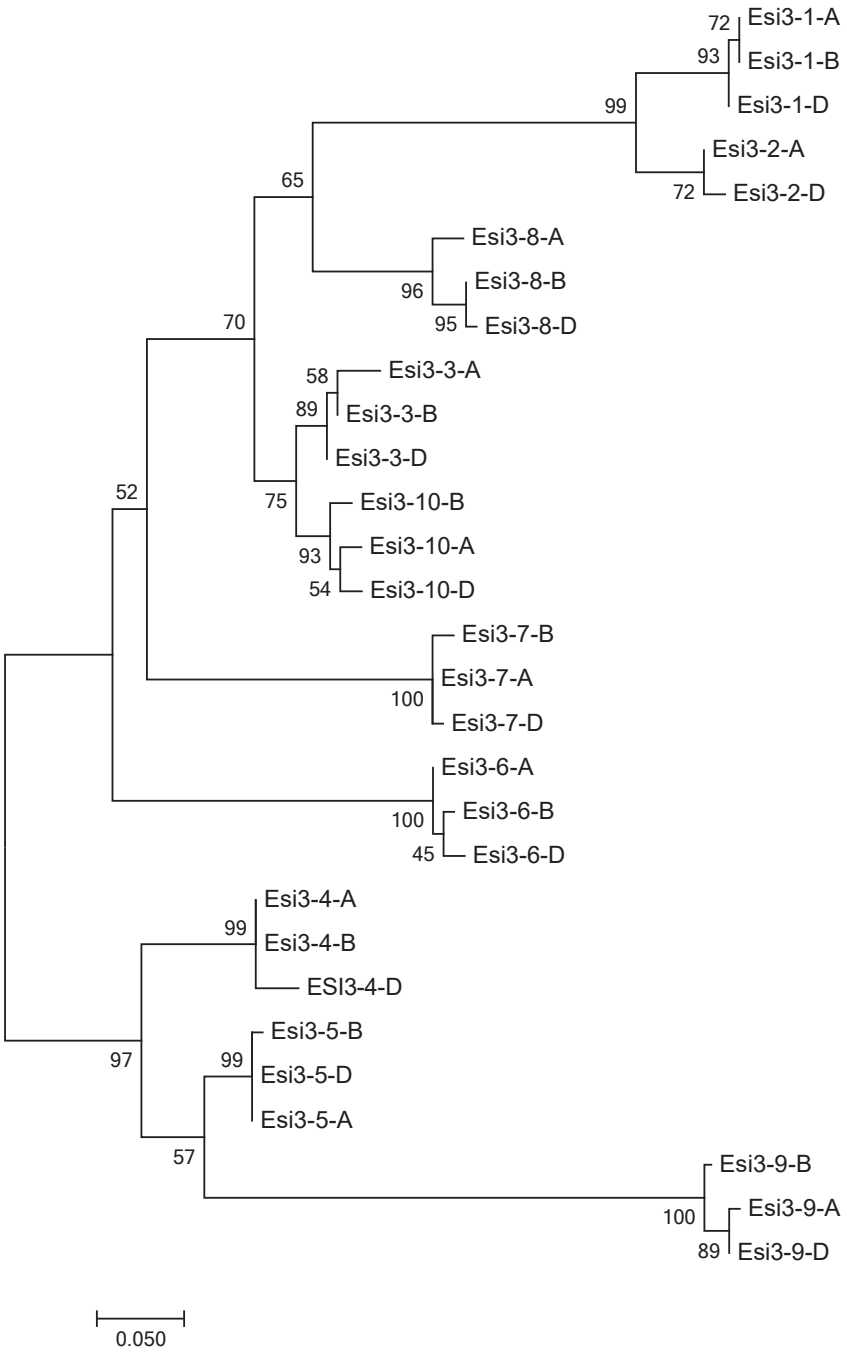

Additional Figure 3: Molecular phylogenetic analysis of the *Esi3* genes from *T. aestivum* by Maximum Likelihood method based on the Jukes-Cantor model [42]. The tree with the highest log likelihood (-1283.8239) is shown. The percentage of tress in which the associated taxa clustered together is shown next to the branches. A discrete Gamma distribution was used to model evolutionary rate differences among sites (5 categories (+G, parameter = 1.1637)). The tree is drawn to scale, with branch lengths measured in the number of sustitutions per site. The analysis involved 29 nucleotide sequences.

Table S12: *Triticum aestivum* RNA-seq datasets used to compare *Esi3/RCI2/PMP3* gene expression levels

Tissue Specific Expression Data[a]			
Details	**Experiment ID (ENA SRA ID)**	**Total Reads**	**Number of replicates**
Fruit whole plant ripening stage	ERX391046 (ERR424721_2)	49053093	2
	ERX391050 (ERR424750_2)	30038860	
Cotyledon emergence root	ERX391071 (ERR424737_2)	45116709	2
	ERX391061(ERR424770_2)	51833599	
Leaf at whole plant fruit formation stage 30 to 50%	ERX391062 (ERR424749_2)	47106971	2
	ERX391021 (ERR424763_2)	33655313	
Stem at two nodes or internodes visible stage	ERX391032 (ERR424733_2)	40953211	2
	ERX391016 (ERR424767_2)	55483346	
Inflorescence maximum stem length reached stage	ERX391052 (ERR424735_2)	52120581	2
	ERX391070 (ERR424753_2)	45271806	
Cold Stress[b]			
Details	**Experiment ID (ENA SRA ID)**	**Total Reads**	**Number of replicates**
Control (23°C)	SRX625519 (SRR1460549)	32616607	3
	SRX625520 (SRR1460550)	77577791	
	SRX625521 (SRR1460551)	28872198	
Colds stress (4°C)	SRX625522 (SRR1460552)	40138740	3
	SRX625523 (SRR1460553)	25425859	
	SRX625524 (SRR1460554)	19047190	
Drought, Heat and Combined Stress[c]			
Details	**SRA database accession (ENA SRA ID)**	**Total Reads**	**Number of replicates**
Control	SRX673834 (SRR1542404_2)	81155853	2
	SRX673835 (SRR1542405_2)	75969741	
Drought stress 1hr	SRX673836 (SRR1542406_2)	68467921	2
	SRX673838 (SRR1542407_2)	75864652	
Drought stress 6hr	SRX673839 (SRR1542408_2)	63320064	2
	SRX673840 (SRR1542409_2)	73614455	
Heat stress 1hr	SRX673841 (SRR1542410_2)	66035008	2
	SRX673843 (SRR1542411_2)	51618473	
Heat stress 6hr	SRX673844 (SRR1542412_2)	76623839	2
	SRX673845 (SRR1542413_2)	67378274	
Combined stress 1hr	SRX673846 (SRR1542414_2)	53762767	2
	SRX673847 (SRR1542415_2)	55585647	
Combied stress 6hr	SRX673848 (SRR1542416_2)	53901424	2
	SRX673849 (SRR1542417_2)	56318014	

Fusarium graminearum Infection[d]			
Details	**Experiment ID (ENA SRA ID)**	**Total Reads**	**Number of replicates**
NIL51 Mock 6hr	ERX1274043 (ERR1201818_2)	38595486	3
	ERX1274044 (ERR1201819_2)	24236679	
	ERX1274045 (ERR1201820_2)	42159031	
NIL51 *F. graminearum* 6hr	ERX1274025 (ERR1201800_2)	25871100	3
	ERX1274026 (ERR1201801_2)	20072367	
	ERX1274027 (ERR1201802_2)	25871100	
NIL51 Mock 12hr	ERX1274028 (ERR1201803_2)	29301258	3
	ERX1274029 (ERR1201804_2)	25869265	
	ERX1274030 (ERR1201805_2)	33058978	
NIL51 *F. graminearum* 12hr	ERX1274010 (ERR1201785_2	25418710	3
	ERX1274011 (ERR1201786_2)	38234787	
	ERX1274012 (ERR1201787_2)	40831345	
NIL51 Mock 24hr	ERX1274031 (ERR1201806_2)	22984326	3
	ERX1274032 (ERR1201807_2)	27832536	
	ERX1274033 (ERR1201808_2)	20840051	
NIL51 *F. graminearum* 24hr	ERX1274013 (ERR1201788_2)	27578418	3
	ERX1274014 (ERR1201789_2)	34713400	
	ERX1274015 (ERR1201790_2)	31343655	
NIL51 Mock 48hr	ERX1274040 (ERR1201815_2)	34787468	3
	ERX1274041 (ERR1201816_2)	20013677	
	ERX1274042 (ERR1201817_2)	23404211	
NIL51 *F. graminearum* 48hr	ERX1274022 (ERR1201797_2)	24045575	3
	ERX1274023 (ERR1201798_2)	32710023	
	ERX1274024 (ERR1201799_2)	25984652	
NIL38 Mock 6hr	ERX1274022 (ERR1201782_2)	32065126	3
	ERX1274023 (ERR1201783_2)	31408636	
	ERX1274024 (ERR1201784_2)	28365364	
NIL38 *F. graminearum* 6hr	ERX1273989 (ERR1201764_2)	30075553	3
	ERX1273990 (ERR1201765_2)	34903902	
	ERX1273991 (ERR1201766_2)	21031798	
NIL38 Mock 12hr	ERX1273992 (ERR1201767_2)	34997985	3
	ERX1273993 (ERR1201768_2)	23599332	
	ERX1273994 (ERR1201769_2)	40003384	
NIL38 *F. graminearum* 12hr	ERR1201749 (ERR1201749_2)	27620906	3
	ERR1201750 (ERR1201750_2)	19449433	
	ERR1201751 (ERR1201751_2)	32223388	
NIL38 Mock 24hr	ERX1273995 (ERR1201770_2)	25917089	3
	ERX1273996 (ERR1201771_2)	29732769	
	ERX1273997 (ERR1201772_2)	24822761	
NIL38 *F. graminearum* 24hr	ERX1273977 (ERR1201752_2)	25747899	3
	ERX1273978 (ERR1201753_2)	32609188	
	ERX1273979 (ERR1201754_2)	27776756	
NIL38 Mock 48hr	ERX1274004 (ERR1201779_2)	25760916	3
	ERX1274005 (ERR1201780_2)	38829518	
	ERX1274006 (ERR1201781_2)	25218505	
NIL38 *F. graminearum* 48hr	ERX1273986 (ERR1201761_2)	22760086	3
	ERX1273987 (ERR1201762_2)	37353756	
	ERX1273988 (ERR1201763_2)	26837655	
Note: All data retrieved from Array Express at EMBL-EBI			
[a] Ramírez-González et al., 2018; Bioproject PRJEB5314			
[b] Li et al., 2015; NCBI Bioproject PRJNA253535			
[c] Liu et al., 2015; NCBI Bioproject PRJNA257938			
[d] Steiner et al., 2017; NCBI Bioproject PRJEB12358			

7.7 Supplemental Material

Chapter 6: “Characterization and Expression of the *Pirin* Gene Family in *Triticum aestivum*”

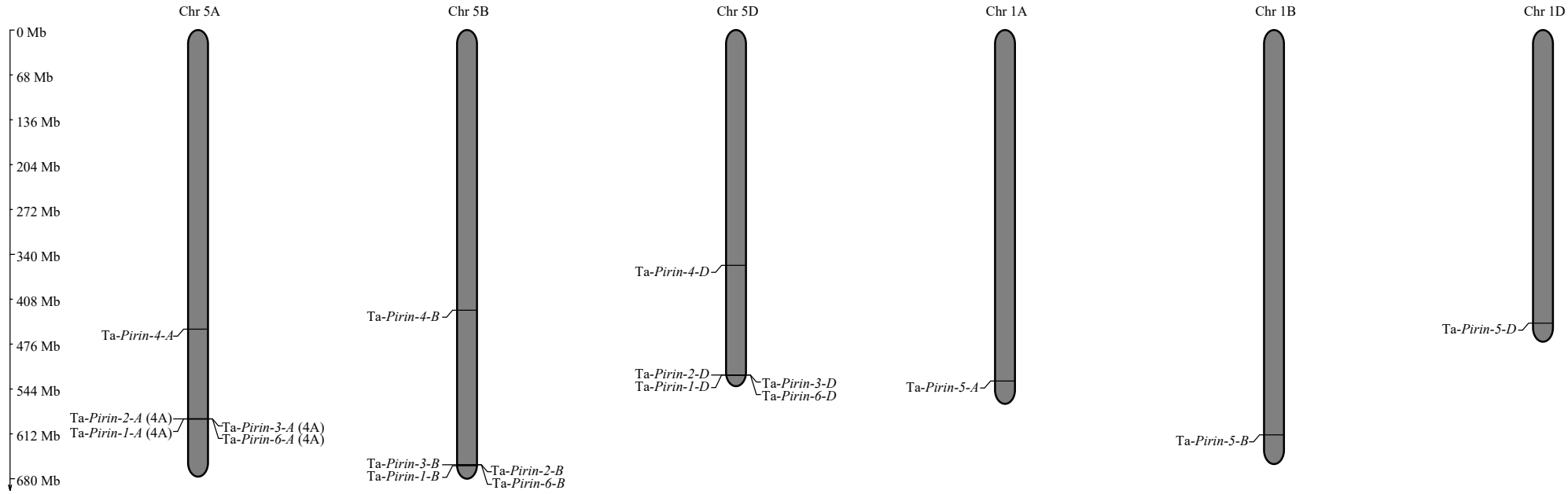

Fig S1. Schematic of the Ta-*Pirin* homeolog chromosome locations. The tandemly duplicated cluster of Ta-*Pirin-1, -2, -3* and *-6* is illustrated on chromosomes 5A, 5B and 5D, as well as the location of the Ta-*Pirin-4-A*, *-B* and *-D* homeologs. The A copies of Ta-*Pirin-1, -2, -3* and *-6* are the result of a translocation event between chromosomes 4A and 5A. The Ta-*Pirin-5-A*, *-B* and *-D* homeologs are depicted on chromsomes 1A, 1B and 1D. Mb = megabases, Chr = chromosome.

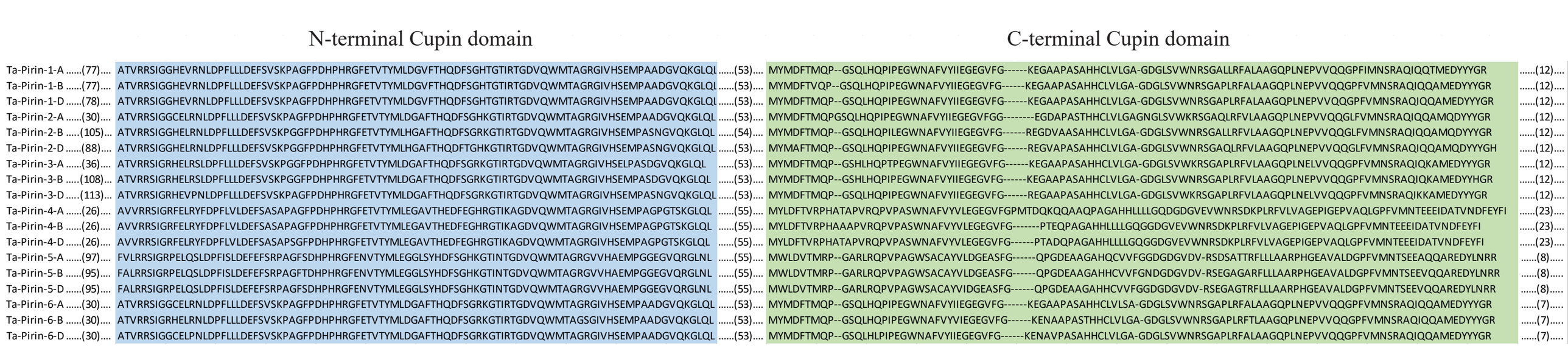

Fig S2. Ta-Pirin Cupin domain locations and amino acid sequences. Blue depicts the N-terminal Cupin domain and green depicts the C-terminal Cupin domain.

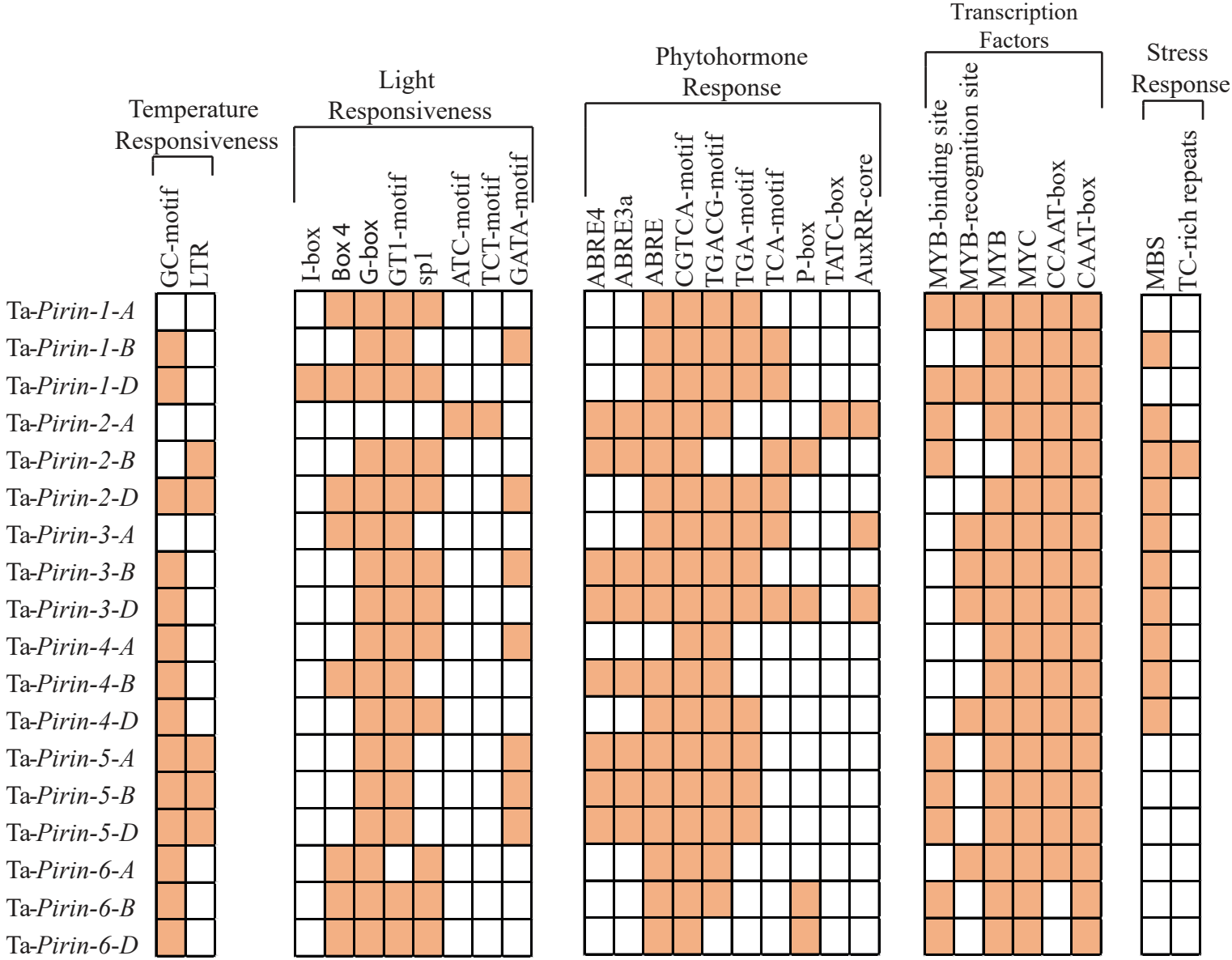

Fig. S3. Promoter analysis of the *Pirin* gene family using a 2-kb fragment upstream of the 5' UTR. The analysis was carried out using the Plant Cis-Acting Regulatory Element (CARE) webpage (Lescot et al., 2002). If the *Pirin* copy had a particular promoter element the box will be colored in therefore the non-colored boxes indicate the lack of that promoter element.

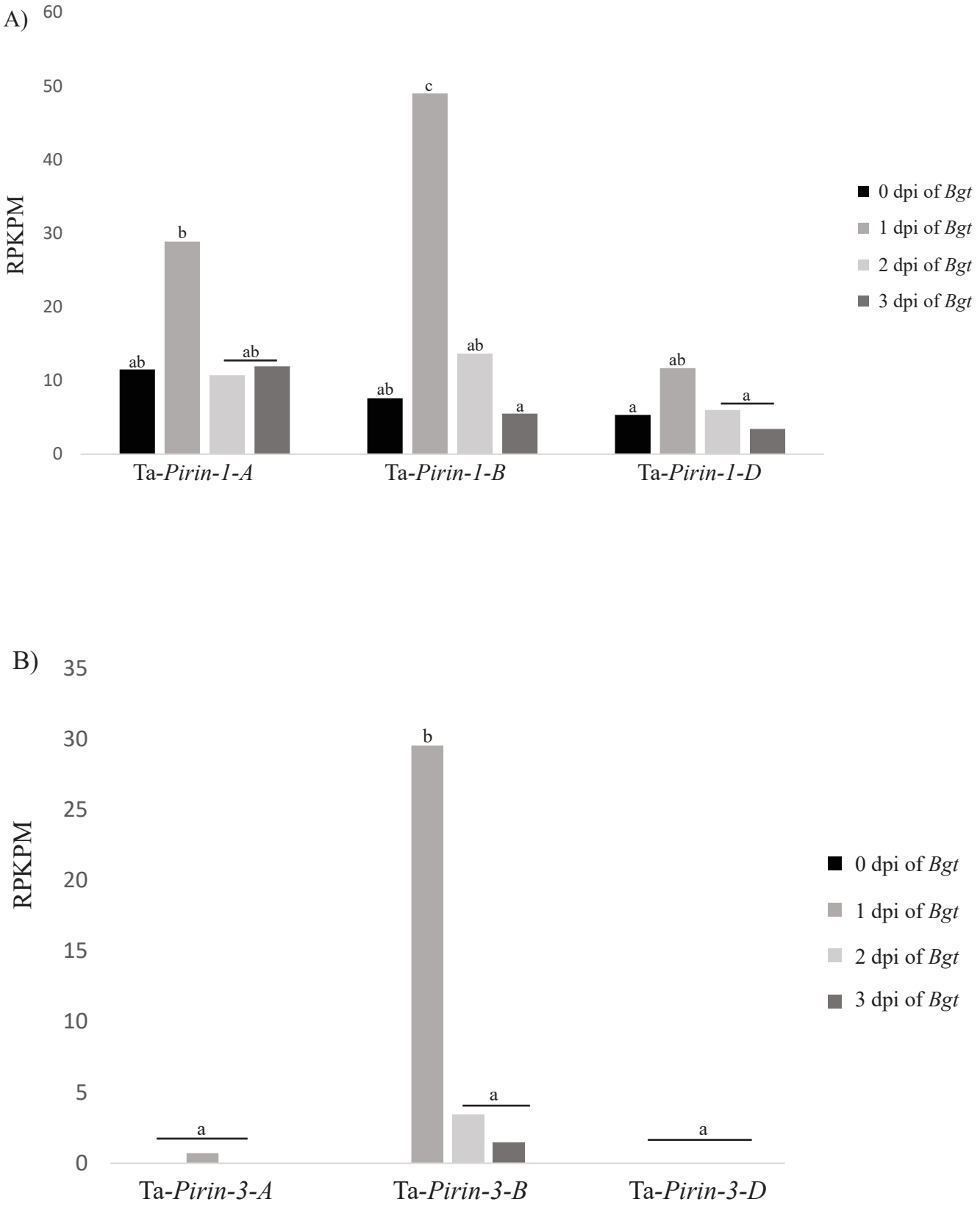

Fig. S4. Expression of Ta-*Pirin-1* and Ta-*Pirin-3* 0, 1, 2 and 3 days post-inoculation (dpi) with mildew (*Bgt*). **(A)** Expression of Ta-*Pirin-1-A*, *-B* and *-D* in control (0 dpi) and post-inoculation. **(B)** Expression of Ta-*Pirin-3-A*, *-B* and *-D* in control (0 dpi) and post-inoculation. Expression is normalized to reads per kilobase per million (RPKPM). The letters represent the significant differences between homeologs as tested by a Duncan's multiple range *post-hoc* test following a one-way ANOVA. Bars that do not share a common letter are significantly different with a p-value of 0.05 or less.

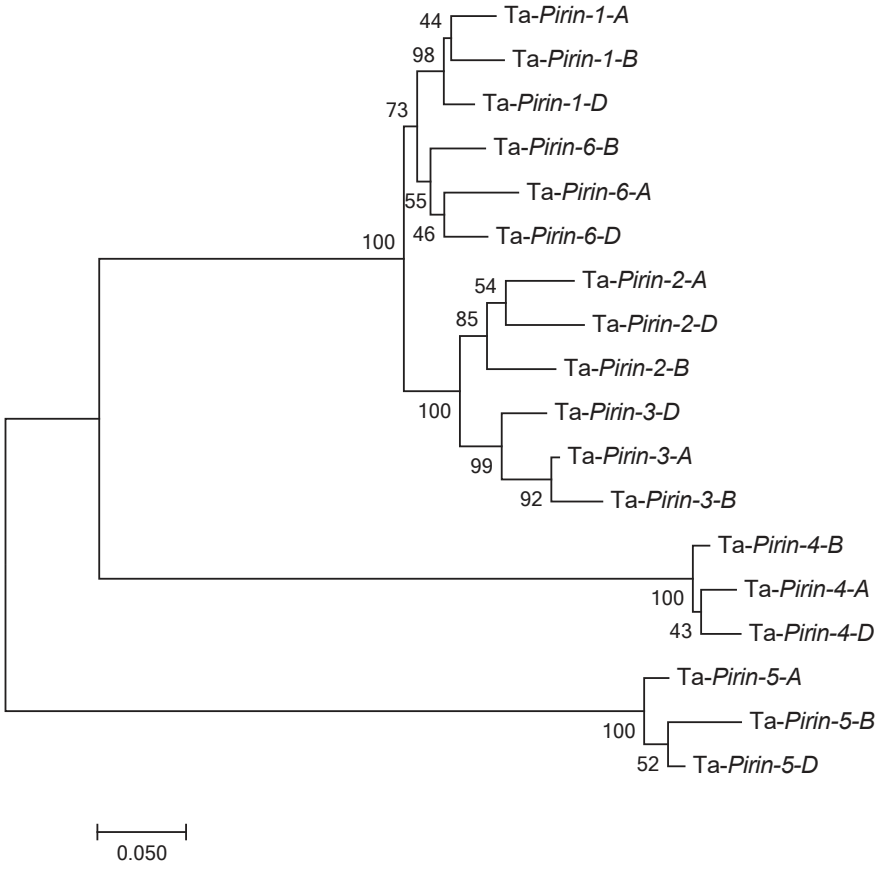

Fig. S5. The evolutionary history was inferred by using the Maximum Likelihood method based on the Jukes-Cantor model (Jukes and Cantor, 1969). A discrete Gamma distribution was used to model evolutionary rate differences among sites (5 categories (+G, parameter = 0.7176)). The tree is drawn to scale, with branch lengths measured in the number of substitutions per site. The analysis involved 18 nucleotide sequences. Codon positions included were 1st+2nd+3rd+Noncoding. All positions with less than 95% site coverage were eliminated. There were a total of 975 positions in the final dataset. Evolutionary analyses were conducted in MEGA7 (Kumar et al., 2016).

Supplementary File S1
The amino acid and nucleotide sequences of the *Triticum aestivum Pirin* gene family members

>Ta-Pirin-1-A_TraesCS4A02G336200.1
MPRHSAASPIYTALARLANFNSGRRVLLASRKTSSSSARTIMSSSSSSSAAAASVPFQSPRKVVKKVLSLSQSEGQGATVRRSIGGHEVRNLDPFLLL
DEFSVSKPAGFPDHPHRGFETVTYMLDGVFTHQDFSGHTGTIRTGDVQWMTAGRGIVHSEMPAADGVQKGLQLWINLASKDKMIEPRYQELESKDISQ
AEKDGVAVRIIAGEAFGVRSPVYTRTPTMYMDFTMQPGSQLHQPIPEGWNAFVYIIEGEGVFGKEGAAPASAHHCLVLGAGDGLSVWNRSGALLRFAL
AAGQPLNEPVVQQGPFIMNSRAQIQQTMEDYYYGRNGFEKASQWSSA

>Ta-Pirin-1-B_TraesCS5B02G536000.2
MPRHSAASPIYTALARLANFNSGRRVLLASRNTSSSSARSSAKTRPFLCLSVLLLLILVVTAVFLFPPAIMSSSSSSAATAASVPFQSPRKVVKKVLS
LSQSEGQGATVRRSIGGHEVRNLDPFLLLDEFSVSKPAGFPDHPHRGFETVTYMLDGVFTHQDFSGHTGTIRTGDVQWMTAGRGIVHSEMPAADGVQK
GLQLWINLASKDKMIEPRYQELESKDISQAEKDGVAVRIIAGEAFGVRSPVYTRTPTMYMDFTVQPGSQLHQPIPEGWNAFVYIIEGEGVFGKEGAAP
ASAHHCLVLGAGDGLSVWNRSGAPLRFALAAGQPLNEPVVQQGPFVMNSRAQIQQAMEDYYYGRNGFEKASQWSSA

>Ta-Pirin-1-D_TraesCS5D02G533500.1
MPRHSAASPIYTALARLANFNSGRRVLLASRKTSSSSARTIMSSSSSSSSAAAASVPFQSPRKVVKKVLSLSQSEGQGATVRRSIGGHEVRNLDPFLL
LDEFSVSKPAGFPDHPHRGFETVTYMLDGVFTHQDFSGHTGTIRTGDVQWMTAGRGIVHSEMPAADGVQKGLQLWINLASKDKMIEPRYQELESKDIS
QAEKDGVAVRIIAGEAFGVRSPVYTQTPTMYMDFTMQPGSQLHQPIPEGWNAFVYIIEGEGVFGKEGAAPASAHHCLVLGAGDGLSVWNRSGAPLRFA
LAAGQPLNEPVVQQGPFVMNSRAQIQQAMEDYYYGRNGFEKASQWSSA

>Ta-Pirin-2-A_TraesCS4A02G336000.1
MSSSSTPVTFENPRKVVKKVLSLSQSEGDGATVRRSIGGCELRNLDPFLLLDEFSVSKPAGFPDHPHRGFETVTYMLDGAFTHQDFSGHKGTIRTGDV
QWMTAGRGIVHSEMPAADGVQKGLQLWINLASKDKMIEPRYQELKSKDISQAEKHGVKVRIIAGEAFGVQSPVYTRTPTMYMDFTMQPGSQLHQPIPE
GWNAFVYIIEGEGVFGGEGDAPASTHHCLVLGAGNGLSVWKRSGAQLRFVLAAGQPLNEPVVQQGLFVMNSRAQIQQAMQDYYYGRNGFEKASQWSSA

>Ta-Pirin-2-B_TraesCS5B02G535700.3
MLRQHLPLFSSSSYSPIYMALSRLTRQNSHRLPPASTKTSSRSSAKTKPLLFLLLLIVILVVTAVFLFPPAIMSSSSPSAASVPFESPRKVVKKVLSL
SQSEGDGATVRRSIGGHELRNLDPFLLLDEFSVSKPGGFPDHPHRGFETVTYMLHGAFTHQDFSGRKGTIRTGDVQWMTAGRGIVHSEMPASNGVQKG
LQLWINLASKDKMIEPRYQELKSKDISQAEKHGVKVRIIAGEAFGVRSPVYTRTPTMYMDFTMQPGSQLHQPILEGWNAFVYIIEGEGVFGREGDVAA
SAHHCLVLGAGDGLSVWNRSGALLRFVLAAGQPLNEPVVQQGLFVMNSRAQIQQAMQDYYYGRNGFEKASQWSSA

>Ta-Pirin-2-D_TraesCS5D02G533200.1
MLRQHLPLFSSSSSSPIHMALARLTRKTSSRSSAKTKPLLFLLLLIVILVVTAVFLFPPATMSSSSSFENPRKVVKKVMSLSQAEGDGATVRRSIGGH
ELRNLDPFLLLDEFSVSKPGGFPDHPHRGFETVTYMLHGAFTHQDFTGHKGTIRTGDVQWMTAGRGIVHSEMPASNGVQKGLQLWINLASKDKMIEPR
YQELKSKDISQAEKHGVKVRIIAGEAFGVRSPVYARTPTMYMAFTMQPGSQLHQPIPEGWNAFVYIIEGEGVFGREGVAPASAHHCLVLGAGDGLSVW
NRSGAQLRFVLAAGQPLNEPVVQQGLFVMNSRAQIQQAMQDYYYGHNGFEKASQWSSA

>Ta-Pirin-3-A_TraesCS4A02G335900.1
MSSSSSSVSFQTPRKVVKKVLSLSQSEADGATVRRSIGRHEVPNLDPFLLLDEFSVSKSEMECSASSISCSVPFCLHHGAFTHQDFSGRKGTIRTGDV
QWMTAGRGIVHSEMPASDGVQKGLQLWINLASKDKMIKPRYQELESKDISQAEKDGVKVRIIAGEAFGVRSPVYTRTPTMYMDFTMQPGSQLHQPIPK
GWNAFVYIIKGEGVFGREAAASASAHHCLVLGTGDGLSVWNRSGARLRFMLAAGQPLNELVVQQGPFVMNSRAQIQKAMEDYYYGRNGFEKASQWSST

>Ta-Pirin-3-B_TraesCS5B02G535800.1
MIQHLTSPDLTATKMLRQHLPYFNSSRRVPVASRKTSSSSRSSANTRPFLCLALFLLLILVVAAVFLFPPAIMSSSSSSSSSAAAVPFQSPRKVVKKV
LSLSQSEGDGATVRRSIGRHELRSLDPFLLLDEFSVSKPGGFPDHPHRGFETVTYMLDGAFTHQDFSGRKGTIRTGDVQWMTAGRGIVHSEMPASDGV
QKGLQLWINLASKDKMIKPRYQELESKDISQAEKHGVKVRIIAGEAFGVRSPVYTRTPTMYMDFTMQPGSHLHQPIPEGWNAFVYIIEGEGVFGKEGA
APASAHHCLVLGAGDGLSVWNRSGAPLRFVLAAGQPLNEPVVQQGPFVMNSRAQIQKAMEDYYHGRNGFKKASQWSST

>Ta-Pirin-3-D_TraesCS5D02G533100.1
MLRQLLPHFSSSSSSSSPIYSLARLTRQSSSRRVPLASRKTSSSSRSSASTRPFLCLALFLLLILVVTALFLFPPAIMSSSSSSSSAASVPFERPRK
VVKKVLSLSQSEGDGATVRRSIGRHEVPNLDPFLLLDEFSVSKPAGFPDHPHRGFETVTYMLDGAFTHQDFSGRKGTIRTGDVQWMTAGRGIVHSEMP
ASNGVQKGLQLWINLASKDKMIKPRYQELESKDISQAEKHGVKVRIIAGEAFGVRSPVYTRTPTMYMDFTMQPGSQLHQPIPEGWNAFVYIIEGEGVF
GREGAAPASAHHCLVLGAGDGLSVWKRSGAPLRFVLAAGQPLNELVVQQGPFVMNSRAQIKKAMEDYYYGRNGFEKASQWSST

>Ta-Pirin-4-A_TraesCS5A02G262700.1
MSTMEVAKPRQVARRFQARPQHEGAGAVVRRSIGRFELRYFDPFLVLDEFSASAPAGFPDHPHRGFETVTYMLEGAVTHEDFEGHRGTIKAGDVQWMT
AGRGIVHSEMPAGPGTSKGLQLWVNLASKNKMVEPGYQEFQSKDIASTTSADGDVTVRVIAGEAMGARSPVRTRTPTMYLDFTVRPHATAPVRQPVPA
SWNAFVYVLEGEGVFGPMTDQKQQAAQPAGAHHLLLLGQDGDGVEVWNRSDKPLRFVLVAGEPIGEPVAQLGPFVMNTEEEIDATVNDFEYFINGFEK
AKHWKSQAMIALELEYVG-

>Ta-Pirin-4-B_TraesCS5B02G261100.1

MSTMEVTKPRQVVRRFLARPQHEGAGAVVRRSIGRFELRYFDPFLVLDEFSASAPAGFPDHPHRGFETVTYMLEGAVTHEDFEGHRGTIKAGDVQWMT
AGRGIVHSEMPAGPGTSKGLQLWVNLASKNKMVEPGYQEFQSKDIASTTSADGDVTVRVIAGESMGARSPVRTRTPTMYLDFTVRPHAAAPVRQPVPA
SWNAFVYVLEGEGVFGPTEQPAGAHHLLLLGQGGDGVEVWNRSDKPLRFVLVAGEPIGEPVAQLGPFVMNTEEEIDATVNDFEYFINGFEKAKHWKSQ
AMIALELEYVG

>Ta-Pirin-4-D_TraesCS5D02G270300.1
MSTMEVKKPRQVARRFLARPQHEGAGAVVRRSIGRFELRYFDPFLVLDEFSASAPSGFPDHPHRGFETVTYMLEGAVTHEDFEGHRGTIKAGDVQWMT
AGRGIVHSEMPAGPGTSKGLQLWVNLASKNKMVEPGYQEFQSKDIASTTSADGDVTVRVIAGEAMGARSPVRTRTPTMYLDFTVRPHATAPVRQPVPA
SWNAFVYVLEGEGVFGPTADQPAGAHHLLLLGQGGDGVEVWNRSDKPLRFVLVAGEPIGEPVAQLGPFVMNTEEEIDATVNDFEYFINGFEKAKHWKS
QAMIALELEYVG

>Ta-Pirin-5-A_TraesCS1A02G391900.1
MSAAACVSFCPSPASSRHGAGPIVDVVGLPPAVEEAEERGAERDLLEFGADGMISASSDSDEDAAAAEIDDEEEHSVRRPRAVVQKFMCERKAVGDGF
VLRRSIGRPELQSLDPFISLDEFEFSRPAGFSDHPHRGFENVTYMLEGGLSYHDFSGHKGTINTGDVQWMTAGRGVVHAEMPGGEGVQRGLNLWLNLS
SKDKMVAPRYQDLRSHDVPTAEKDGVSIKVIAGEALGARSPIQTRTPAMWLDVTMRPGARLRQPVPAGWSACAYVLDGEASFGQPGDEAAGAHQCVVF
GGDGDGVDVRSDSATTRFLLLAARPHGEAVALDGPFVMNTSEEAQQAREDYLNRRNGFEMAAGWTSSQ

>Ta-Pirin-5-B_TraesCS1B02G420000.1
MSAAACVPFCPSPASSRHGAGPIVDVAGLPPATEAEEHGAGRDLLEFGVNGVIGANSDSDDAAAAEIDDEEEHSVRRPRAVVQKFMCERKAVGDGFAL
RRSIGRPELQSLDPFISLDEFEFSRPAGFTDHPHRGFENVTYMLEGGLSYHDFSGHKGTINTGDVQWMTAGRGVVHAEMPGGEGVQRGLNLWLNLSSK
DKMVAPRYQELRSRDIPTAEKDGVSVKVIAGEALGARSPIQTRTPAMWLDVTMRPGARLRQPVPAGWSACAYVLDGEASFGQPGDEAAGAHHCVVFGN
DGDGVDVRSEGAGARFLLLAARPHGEAVALDGPFVMNTSEEVQQAREDYLNRRNGFEMAAGWTSGQ

>Ta-Pirin-5-D_TraesCS1D02G400000.1
MSAAACVSFCPSPASSRHGGPIVDLAGLPPATEAEERGAQRDLLEFGVNGTIGANSDSDEDAAAAEIDDEEEHSVRRPRAVVQKFMCERKAVGDGFAL
RRSIGRPELQSLDPFISLDEFEFSRPAGFSDHPHRGFENVTYMLEGGLSYHDFSGHKGTINTGDVQWMTAGRGVVHAEMPGGEGVQRGLNLWLNLSST
DKMVAPRYQELRSRDVPTAEKDGASIKVIAGEALGARSPIQTRTPAMWLDVTMRPGARLRQPVPAGWSACAYVIDGEASFGQPGDEAAGAHHCVVFGG
DGDGVDVRSEGAGTRFLLLAARPHGEAVALDGPFVMNTSEEVQQAREDYLNRRNGFEMAAGWTSGQ

>Ta-Pirin-6-A_TraesCS4A02G336100.1

MSSSSTPVPFENPRKVVKKVLSLSQSEGDGATVRRSIGGCELRNLDPFLLLDEFSVSKPAGFPDHPHRGFETVTYMLDGAFTHQDFSGRKGTIRTGDV
QWMTAGRGIVHSEMPAADGVQKGLQLWINLASKDKMIEPRYQELESKDISQAEKDGVAVRIIAGEAFGVRSPVYTQTPTMYMDFTMQPGSQLHQPIPE
GWNAFVYIIEGEGVFGKEGAAPASAHHCLVLSAGDGLSVWNRSGAPLRFALAAGQPLNEPVVQQGPFVMNSRAQIQQAMEDYYYGRNGFEKASQWSSA

>Ta-Pirin-6-B_TraesCS5B02G535900.1
MSSSSSSVTFENPRKVVKKVLSLSQSEGDGATVRRSIGRHELRNLDPFLLLDEFSVSKPAGFPDHPHRGFETVTYMLDGAFTHQDFSGRKGTIRTGDV
QWMTAGSGIVHSEMPAADGVQKGLQLWINLASKDKMIEPRYQELESKDISQAEKDGVAVRIIAGEAFGVRSPVYTRTPTMYMDFTMQPGSQLHQPIPE
GWNAFVYVIEGEGVFGKENAAPASTHHCLVLGAGDGLSVWNRSGAPLRFTLAAGQPLNEPVVQQGPFVMNSRAQIQQAMEDYYYGRNGFEKASQWSSA

>Ta-Pirin-6-D_TraesCS5D02G533400.1
MSSSSTPVTFENPRKVMKKVLSLSQSEGDGATVRRSIGGCELPNLDPFLLLDEFSVSKPAGFPDHPHRGFETVTYMLDGAFTHQDFSGRKGTIRTGDV
QWMTAGRGIVHSEMPAADGVQKGLQLWINLASKDKMIEPRYQEIESKDISQAEKDGVAVRIIAGEAFGVRSPVYTRTPTMYMDFTMQPGSQLHLPIPE
GWNAFVYIIEGEGVFGKENAVPASAHHCLVLGAGDGLSVWNRSGAPLRFALAAGQPLNEPVVQQGPFVMNSRAQIQQAMEDYYYGRNGFEKASQWSSA

The nucleotide coding sequences of the *Triticum aestivum Pirin* gene family members

>Ta-Pirin-1-A_TraesCS4A02G336200.1
ATGCCAAGGCACTCTGCGGCTTCCCCTATTTATACGGCACTCGCTCGCCTCGCCAATTTCAACAGCGGCCGCCGCGTCCTCCTCGCCTCCAGAAAGAC
GAGCTCCAGCTCTGCTAGAACCATCATGTCTTCGTCTTCCTCGTCGTCGGCGGCGGCCGCGTCCGTGCCGTTTCAGAGCCCGAGGAAGGTGGTGAAGA
AGGTGCTGTCCTTGTCCCAGTCCGAGGGCCAGGGCGCCACCGTCCGCCGGAGCATCGGCGGGCACGAGGTCCGGAACCTGGACCCGTTCCTCCTGCTC
GACGAGTTCTCCGTCTCCAAGCCCGCTGGATTCCCCGACCACCCCCACCGGGGCTTCGAGACCGTCACCTACATGCTCGATGGGGTGTTCACCCACCA
GGACTTCTCCGGACACACGGGCACCATCAGGACCGGAGATGTGCAGTGGATGACGGCGGGGCGCGGCATCGTGCACTCAGAGATGCCTGCGGCGGACG
GAGTGCAGAAGGGCCTGCAGCTCTGGATCAACCTTGCCTCCAAGGACAAGATGATCGAGCCACGGTACCAGGAGCTCGAGAGCAAGGACATCAGCCAG
GCCGAGAAGGACGGCGTGGCGGTGCGGATCATTGCTGGGGAGGCCTTCGGGGTACGGTCACCGGTCTACACGCGGACGCCAACCATGTACATGGACTT
CACAATGCAACCAGGGTCGCAGCTCCACCAGCCAATCCCTGAGGGCTGGAACGCCTTCGTGTACATCATCGAGGGGGAGGGCGTGTTCGGTAAGGAGG
GTGCAGCGCCGGCGAGCGCGCACCACTGCCTCGTGCTTGGCGCGGGGGATGGGCTCAGCGTCTGGAATCGGTCCGGCGCACTGCTGCGGTTCGCGCTG
GCGGCAGGGCAGCCGCTGAACGAGCCGGTGGTGCAGCAGGGGCCCTTCATCATGAACTCGCGTGCCCAGATCCAGCAGACCATGGAGGACTACTACTA
CGGCCGCAACGGTTTCGAGAAGGCCAGCCAGTGGAGCTCCGCCTGA

>Ta-Pirin-1-B_TraesCS5B02G536000.2

ATGCCGAGGCACTCCGCGGCTTCCCCTATTTATACGGCACTCGCGCGCCTCGCCAATTTCAACAGCGGCCGCCGCGTCCTCCTCGCCTCCAGAAACAC
GAGCTCCAGCTCTGCTAGAAGTAGCGCCAAGACCAGACCTTTTCTGTGCCTATCCGTGTTGCTCCTCCTGATTCTTGTTGTGACCGCCGTCTTCTTGT
TCCCGCCAGCGATCATGTCTTCCTCTTCCTCGTCGGCGGCGACGGCTGCGTCCGTGCCGTTCCAGAGCCCGAGGAAGGTGGTCAAGAAGGTGCTGTCC
TTGTCCCAGTCCGAGGGCCAGGGCGCCACCGTCCGCCGGAGCATCGGCGGGCACGAGGTCCGGAACCTGGACCCGTTCCTCCTGCTCGACGAGTTCTC
CGTCTCCAAGCCCGCCGGATTCCCCGACCACCCTCACCGGGGCTTCGAGACCGTCACCTACATGCTAGACGGGGTGTTCACCCACCAGGACTTCTCCG
GACACACTGGCACCATCAGGACCGGAGATGTGCAGTGGATGACGGCCGGGCGCGGCATCGTGCACTCGGAGATGCCGGCGGCCGACGGTGTGCAGAAG
GGCCTGCAGCTTTGGATCAACCTCGCCTCCAAGGACAAGATGATCGAGCCCCGGTACCAGGAGCTCGAGAGCAAGGACATCAGCCAGGCCGAGAAGGA
CGGTGTGGCGGTGCGAATCATCGCCGGGGAGGCATTCGGGGTGCGGTCGCCGGTCTACACGCGGACGCCGACCATGTACATGGACTTCACAGTGCAAC
CAGGTTCGCAGCTCCACCAGCCAATCCCAGAGGGCTGGAACGCCTTCGTGTACATCATCGAGGGGGAGGGCGTGTTCGGCAAGGAGGGTGCAGCGCCG
GCGAGTGCACACCACTGCCTCGTGCTCGGCGCAGGGGATGGGCTCAGCGTGTGGAACCGGTCTGGCGCACCGCTACGGTTCGCCCTTGCGGCAGGGCA
GCCGCTGAACGAGCCGGTGGTGCAGCAGGGGCCCTTCGTCATGAACTCACGTGCCCAGATCCAGCAGGCCATGGAGGATTACTACTATGGCCGCAACG
GCTTCGAGAAGGCCAGCCAGTGGAGCTCCGCCTGA

>Ta-Pirin-1-D_TraesCS5D02G533500.1
ATGCCAAGGCACTCTGCGGCTTCCCCTATTTATACGGCACTCGCGCGCCTCGCCAATTTCAACAGCGGCCGCCGCGTCCTCCTCGCTTCCAGAAAGAC
GAGCTCCAGCTCTGCTAGAACGATCATGTCTTCGTCTTCCTCCTCGTCGTCGGCGGCGGCCGCGTCCGTGCCGTTTCAGAGCCCGAGGAAGGTGGTCA
AGAAGGTGCTGTCCTTGTCCCAGTCCGAGGGGCAGGGCGCCACCGTCCGCCGGAGCATCGGCGGGCACGAGGTCCGGAACCTGGACCCGTTCCTCCTG
CTCGACGAGTTCTCCGTCTCAAAGCCCGCCGGCTTCCCCGACCACCCGCACCGGGGCTTCGAGACCGTCACCTACATGCTCGACGGGGTGTTCACCCA
CCAGGACTTCTCCGGACACACGGGCACCATCAGGACCGGAGATGTGCAGTGGATGACGGCGGGGCGCGGCATCGTGCACTCGGAGATGCCTGCGGCCG
ACGGAGTGCAGAAGGGCCTGCAGCTCTGGATCAACCTCGCCTCCAAGGACAAGATGATCGAGCCCCGGTACCAGGAGCTCGAGAGCAAGGACATCAGC
CAGGCCGAGAAGGATGGCGTGGCGGTGCGGATCATCGCCGGGGAGGCCTTCGGGGTGCGGTCGCCAGTCTACACACAGACGCCGACCATGTACATGGA
CTTCACAATGCAACCAGGTTCGCAGCTCCACCAGCCAATCCCGGAGGGCTGGAACGCCTTCGTGTACATCATCGAGGGGGAGGGCGTGTTCGGCAAGG
AGGGTGCAGCGCCGGCGAGCGCGCACCACTGCCTCGTGCTTGGCGCGGGGGACGGGCTCAGCGTGTGGAATCGGTCTGGCGCACCGCTGCGGTTCGCG
CTGGCGGCGGGGCAGCCGCTGAACGAGCCAGTGGTGCAGCAGGGTCCATTCGTCATGAACTCGCGTGCCCAGATCCAGCAGGCCATGGAGGACTATTA
CTACGGCCGCAACGGCTTCGAGAAGGCCAGCCAGTGGAGCTCGGCCTGA

>Ta-Pirin-2-A_TraesCS4A02G336000.1
ATGTCTTCCTCTTCCACGCCCGTGACGTTTGAGAATCCGAGGAAGGTGGTGAAGAAGGTGCTGTCCTTGTCCCAGTCCGAGGGGGACGGCGCCACCGT
CCGCCGGAGCATCGGCGGTTGCGAGCTCCGGAACCTGGACCCGTTTCTCCTGCTCGACGAGTTCTCCGTCTCCAAGCCCGCCGGATTCCCCGACCACC
CCCACCGGGGCTTCGAGACCGTCACCTACATGCTCGACGGGGCCTTCACCCACCAGGACTTCTCGGGGCACAAGGGCACCATCAGGACAGGAGATGTC
CAGGTCCGATCTACTCATCCAATTCTTCAGACAAACCACTTGACCCATTCCATTTTTGACTTGAGAACCAACAATGCATCTGAATGCTCTGTTCCTCA
ACAATGGATGACGGCAGGGCGCGGCATCGTGCACTCGGAGATGCCGGCGGCCGACGGCGTGCAGAAGGGCCTGCAGCTCTGGATCAACCTCGCCTCCA
AGGACAAGATGATCGAGCCACGGTACCAGGAGCTCAAGAGCAAGGACATTAGCCAGGCTGAGAAGCATGGTGTGAAGGTGCGGATCATCGCAGGGGAG
GCCTTCGGGGTGCAGTCGCCAGTCTACACACGCACACCAACAATGTACATGGACTTCACAATGCAACCAGGGTCGCAGCTCCACCAGCCGATCCCCGA
GGGCTGGAACGCTTTCGTGTACATCATCGAGGGGGAGGGTGTATTTGGTGGGGAGGGCGATGCACCGGCGAGCACGCACCATTGCCTCGTGCTTGGTG

CCGGCAACGGGCTTAGCGTGTGGAAACGGTCTGGCGCGCAGCTGCGGTTCGTGCTGGCGGCAGGGCAGCCGTTGAATGAGCCAGTGGTGCAGCAGGGG
CTCTTCGTCATGAACTCTCGTGCCCAGATCCAGCAGGCCATGCAGGACTATTACTACGGACGCAACGGCTTCGAGAAGGCCAGCCAGTGGAGCTCCGC
CTGA

>Ta-Pirin-2-B_TraesCS5B02G535700.3
ATGCTGAGGCAGCACCTCCCCCTCTTCTCCTCTTCCTCTTATTCCCCTATTTACATGGCACTCTCGCGCCTCACCAGACAGAATAGCCATCGTCTTCC
TCCTGCGTCCACAAAGACCAGCTCTAGAAGTAGTGCGAAGACCAAACCTCTCCTCTTCCTGCTACTCCTAATTGTGATTCTTGTTGTGACGGCTGTCT
TCTTGTTCCCACCAGCGATCATGTCTTCTTCGTCGCCGTCGGCCGCGTCCGTGCCGTTCGAGAGCCCGAGGAAAGTGGTGAAGAAGGTGCTGTCCTTG
TCCCAGTCCGAGGGGGACGGCGCCACCGTCCGCCGGAGCATCGGCGGGCACGAGCTCCGGAACCTGGACCCGTTCCTCCTGCTCGACGAGTTCTCCGT
CTCCAAGCCCGGCGGATTCCCTGACCAT
CCTCACCGGGGCTTCGAGACCGTCACCTACATGCTCCACGGAGCATTTACCCACCAGGACTTCTCGGGGCGCAAGGGCACCATCAGGACCGGAGATGT
GCAGTGGATGACGGCTGGCCGCGGCATCGTGCACTCGGAGATGCCGGCTTCCAACGGCGTGCAGAAGGGCCTGCAGCTCTGGATCAACCTCGCCTCCA
AGGACAAGATGATCGAGCCACGGTACCAGGAGCTCAAGAGCAAGGACATCAGCCAGGCTGAGAAGCATGGTGTGAAGGTGCGGATCATCGCCGGGGAG
GCCTTCGGGGTGCGGTCGCCAGTCTACACGCGGACGCCAACCATGTACATGGACTTCACAATGCAACCAGGGTCACAGCTTCACCAACCGATCCTCGA
GGGCTGGAACGCTTTCGTGTACATCATC
GAGGGGGAGGGTGTATTTGGTAGGGAGGGCGATGTGGCGGCGAGCGCGCACCATTGCCTCGTGCTTGGCGCCGGCGATGGGCTCAGCGTGTGGAACCG
GTCCGGCGCCCTGCTGCGGTTTGTGCTGGCGGCAGGGCAGCCGTTGAACGAGCCAGTGGTGCAGCAGGGGCTCTTCGTCATGAACTCTCGTGCCCAGA
TCCAGCAGGCCATGCAGGACTATTACTACGGGCGCAACGGCTTCGAGAAGGCCAGCCAGTGGAGCTCCGCCTGA

>Ta-Pirin-2-D_TraesCS5D02G533200.1
ATGCTGAGGCAGCACCTCCCCCTCTTCTCATCTTCCTCTTCTTCCCCTATTCATATGGCACTCGCGCGCCTCACCAGAAAGACAAGCTCTAGAACGAC
CATGTCTTCTTCATCGTCGTTCGAGAATCCAAGGAAGGTGGTGAAGAAGGTGATGTCGCTATCCCAAGCCGAGGGGGACGGCGCCACCGTCCGCCGGA
GCATCGGCGGGCACGAGCTCCGGAACCTGGACCCGTTCCTCCTGCTCGACGAGTTCTCCGTCTCCAAGCCCGGCGGCTTCCCCGACCACCCGCACCGG
GGCTTCGAGACCGTCACCTACATGCTCCACGGGGCCTTCACCCACCAGGACTTCACAGGGCACAAGGGCACCATCAGGACAGGAGATGTGCAGTGGAT
GACGGCTGGCCGCGGCATCGTGCACTCGGAGATGCCGGCATCCAACGGCGTGCAGAAGGGCCTGCAGCTCTGGATCAACCTCGCCTCCAAGGACAAGA
TGATCGAGCCACGGTACCAGGAGCTCAAGAGCAAGGACATCAGCCAGGCCGAGAAGCATGGTGTGAAGGTGCGGATCATCGCAGGGGAGGCCTTCGGG
GTGCGGTCACCAGTCTACGCACGGACACCAACCATGTACATGGCCTTCACAATGCAACCAGGGTCGCAGCTCCACCAGCCGATCCCCGAGGGTTGGAA
CGCTTTCGTGTACATCATTGAGGGGGAGGGTGTATTTGGCAGGGAGGGCGTTGCGCCGGCGAGTGCGCACCATTGCCTCGTGCTTGGCGCCGGTGACG
GGCTCAGCGTGTGGAACCGGTCTGGTGCGCAACTACGGTTCGTGCTGGCAGCAGGGCAGCCGTTGAACGAGCCAGTGGTGCAGCAGGGGCTCTTCGTC
ATGAACTCTCGTGCCCAGATCCAGCAGGCCATGCAGGACTATTACTACGGACACAACGGCTTCGAGAAGGCCAGCCAGTGGAGCTCCGCGTGA

>Ta-Pirin-3-A_TraesCS4A02G335900.1

ATGTCTTCCTCTTCCTCGTCCGTCTCGTTCCAGACTCCGAGGAAGGTGGTGAAGAAGGTGCTCTCGTTGTCCCAGTCCGAGGCGGACGGCGCCACCGT
CCGCCGGAGCATCGGCCGGCACGAGGTCCCGAACCTGGACCCGTTCCTCCTGCTGGACGAGTTCTCCGTCTCCAAGTCCGAGATGGAATGCTCTGCTT
CTTCCATCTCGTGCTCTGTTCCCTTCTGCCTGCACCATGGGGCCTTCACCCACCAGGACTTCTCGGGGCGCAAGGGCACCATCAGGACCGGAGATGTG
CAGTGGATGACGGCTGGCCGCGGCATCGTGCACTCGGAGATGCCGGCATCTGACGGCGTGCAGAAGGGCCTGCAGCTCTGGATCAACCTCGCCTCCAA
GGACAAGATGATCAAGCCGCGGTACCAGGAGCTCGAGAGCAAGGACATCAGCCAGGCCGAGAAGGACGGTGTGAAGGTGCGGATCATCGCCGGGGAGG
CCTTTGGGGTGCGGTCGCCGGTCTACACACGGACGCCAACCATGTACATGGACTTCACAATGCAACCAGGGTCGCAACTCCACCAGCCAATCCCCAAG
GGCTGGAACGCTTTCGTGTACATCATCAAAGGGGAGGGTGTATTTGGCAGGGAGGCCGCGGCGTCGGCGAGCGCCCACCATTGCCTTGTGCTCGGCAC
TGGCGATGGGCTCAGTGTGTGGAACCGGTCCGGTGCGCGGCTGCGGTTCATGCTGGCGGCAGGTCAGCCCTTGAACGAGCTAGTGGTGCAGCAGGGGC
CCTTCGTCATGAACTCTCGTGCCCAGATCCAGAAGGCCATGGAGGACTATTACTACGGCCGCAACGGCTTCGAGAAGGCCAGCCAGTGGAGCTCCACT
TGA

>Ta-Pirin-3-B_TraesCS5B02G535800.1
ATGATCCAGCACCTCACCTCACCTGACCTCACAGCGACGAAGATGCTGAGGCAGCACCTCCCCTATTTCAACAGCAGCCGTCGTGTTCCTGTTGCGTC
TAGAAAGACAAGCTCAAGCTCTAGAAGTAGCGCCAACACCAGACCTTTTCTGTGCCTAGCCCTCTTCCTCCTCCTGATTCTTGTTGTGGCCGCCGTCT
TCTTGTTCCCACCAGCGATCATGTCTTCCTCTTCCTCGTCGTCGTCGTCGGCCGCGGCCGTGCCGTTTCAGAGCCCGAGGAAGGTGGTGAAGAAGGTG
CTCTCGTTGTCCCAGTCCGAGGGCGACGGCGCCACCGTCCGCCGGAGCATCGGCCGTCATGAGCTGCGGAGCCTGGACCCGTTCCTCCTGCTCGACGA
GTTCTCCGTCTCCAAGCCCGGCGGATTCCCGGACCATCCGCACCGAGGCTTCGAGACCGTCACCTACATGCTCGATGGGGCCTTCACCCACCAGGACT
TCTCTGGCCGCAAGGGCACCATCAGGACAGGAGATGTGCAGTGGATGACTGCGGGGCGTGGCATCGTGCACTCGGAGATGCCGGCATCCGACGGCGTG
CAGAAGGGCCTGCAGCTGTGGATCAACCTCGCTTCCAAGGACAAGATGATCAAGCCGCGGTACCAGGAGCTCGAGAGCAAGGACATCAGCCAGGCCGA
GAAGCACGGTGTGAAGGTGCGGATCATCGCCGGGGAGGCCTTCGGGGTGCGGTCGCCGGTCTACACACGAACACCGACCATGTACATGGACTTCACAA
TGCAACCAGGGTCGCATCTCCACCAGCCAATCCCTGAGGGCTGGAATGCTTTCGTGTACATCATCGAGGGGGAGGGTGTATTTGGCAAGGAGGGGGCC
GCGCCGGCGAGCGCGCACCATTGCCTTGTGCTCGGCGCCGGCGATGGGCTCAGTGTGTGGAACCGGTCTGGCGCGCCGCTGCGCTTCGTGTTGGCTGC
AGGTCAGCCGTTGAATGAGCCAGTGGTGCAGCAGGGGCCCTTCGTCATGAACTCTCGTGCCCAGATCCAGAAGGCCATGGAGGACTATTACCACGGCC
GCAACGGCTTCAAGAAGGCCAGCCAGTGGAGCTCCACTTGA

>Ta-Pirin-3-D_TraesCS5D02G533100.1
ATGCTGAGGCAGCTCCTCCCCCACTTCTCCTCCTCATCTTCTTCTTCCTCCCCTATTTATTCACTCGCGCGGCTCACCAGGCAGAGCAGCAGCCGTCG
TGTCCCTCTTGCGTCCAGGAAGACAAGCTCAAGCTCTAGAAGTAGCGCCAGCACCAGACCTTTTCTGTGCCTAGCCCTCTTCCTCCTCCTGATTCTTG
TTGTGACCGCCCTCTTCTTGTTCCCACCAGCGATCATGTCTTCCTCTTCCTCGTCGTCGTCGTCGGCCGCGTCCGTGCCGTTCGAGAGACCGAGGAAG
GTGGTGAAGAAGGTGCTGTCCTTGTCCCAGTCCGAGGGGGACGGCGCGACCGTCCGCCGGAGCATCGGCAGGCACGAGGTCCCGAACCTGGACCCATT
CCTCCTGCTCGACGAGTTCTCTGTATCCAAGCCCGCCGGCTTCCCTGACCACCCTCACCGAGGCTTCGAGACCGTCACCTACATGCTCGATGGGGCGT
TCACCCACCAGGACTTCTCGGGGCGCAAGGGAACCATCAGGACCGGAGATGTGCAGTGGATGACGGCTGGCCGCGGCATCGTCCACTCGGAGATGCCG
GCATCTAACGGCGTGCAGAAGGGCCTGCAGCTCTGGATCAACCTCGCCTCCAAGGACAAGATGATCAAGCCGCGGTACCAGGAGCTCGAGAGCAAGGA
CATCAGCCAGGCCGAGAAGCACGGTGTGAAGGTGCGGATCATCGCTGGGGAGGCCTTCGGGGTGCGGTCGCCGGTCTACACACGGACACCGACCATGT

ACATGGACTTCACAATGCAACCAGGGTCGCAGCTCCACCAGCCAATCCCCGAGGGCTGGAACGCTTTCGTGTACATCATCGAGGGGGAGGGTGTCTTT
GGCAGGGAGGGCGCCGCGCCGGCGAGCGCGCACCATTGCCTTGTGCTTGGCGCCGGCGATGGGCTCAGTGTGTGGAAGCGGTCCGGTGCGCCGCTGCG
GTTCGTGCTGGCGGCAGGTCAGCCCTTGAACGAGCTAGTGGTGCAGCAGGGGCCCTTCGTCATGAACTCTCGTGCCCAGATCAAGAAGGCCATGGAGG
ACTATTACTACGGCCGCAACGGCTTCGAGAAGGCCAGCCAGTGGAGCTCCACTTGA

>Ta-Pirin-4-A_TraesCS5A02G262700.1
ATGTCGACAATGGAGGTGGCGAAGCCCCGGCAGGTGGCGCGGAGGTTCCAGGCGCGGCCGCAGCACGAGGGCGCCGGCGCCGTCGTCCGCCGCAGCAT
CGGCAGGTTCGAGCTGAGGTATTTCGATCCGTTCCTCGTCCTGGACGAGTTCTCAGCTTCTGCGCCGGCCGGGTTCCCTGACCATCCACACCGGGGCT
TCGAGACCGTCACCTACATGCTCGAGGGGGCGGTGACGCACGAGGACTTCGAGGGCCACCGTGGCACGATCAAGGCCGGCGACGTGCAGTGGATGACG
GCCGGCCGCGGCATCGTGCACTCCGAGATGCCGGCCGGCCCCGGCACCTCCAAGGGCCTCCAGCTCTGGGTCAACCTCGCCTCCAAGAACAAAATGGT
CGAGCCCGGGTACCAGGAGTTCCAGAGCAAGGACATCGCGTCCACCACGTCGGCGGACGGCGACGTGACGGTGCGCGTCATCGCGGGGGAGGCCATGG
GCGCCCGGTCGCCGGTGCGCACGCGGACGCCGACCATGTACCTCGACTTCACGGTGCGCCCGCACGCCACCGCGCCCGTGCGGCAGCCGGTGCCGGCC
TCGTGGAACGCCTTCGTGTACGTGCTCGAGGGCGAGGGCGTGTTCGGGCCGATGACAGACCAGAAGCAGCAGGCGGCGCAGCCGGCGGGGGCGCACCA
CCTGCTGTTGTTGGGGCAGGACGGCGACGGCGTGGAGGTTTGGAACAGGTCGGACAAGCCGCTCCGGTTCGTGCTCGTGGCCGGCGAGCCCATCGGCG
AGCCCGTGGCGCAGCTGGGCCCGTTCGTGATGAACACCGAGGAGGAGATCGACGCCACCGTCAACGACTTCGAGTACTTCATCAACGGGTTCGAGAAG
GCCAAGCATTGGAAGTCGCAGGCCATGATCGCGCTAGAGCTAGAATACGTAGGGTGA

>Ta-Pirin-4-B_TraesCS5B02G261100.1
ATGTCGACAATGGAGGTGACGAAGCCCCGGCAGGTGGTGAGGAGGTTCCTGGCGCGGCCGCAGCACGAGGGCGCCGGCGCCGTCGTCCGCCGCAGCAT
CGGCAGGTTCGAGCTGAGGTACTTCGACCCGTTCCTCGTCCTGGACGAGTTCTCAGCTTCTGCTCCGGCTGGGTTCCCTGATCATCCACACCGGGGCT
TCGAGACCGTCACCTACATGCTCGAGGGAGCGGTGACGCACGAGGACTTCGAGGGCCACCGTGGCACGATCAAGGCCGGCGACGTGCAGTGGATGACG
GCCGGCCGCGGCATCGTGCACTCCGAGATGCCCGCCGGCCCCGGCACCTCCAAGGGCCTCCAGCTCTGGGTCAACCTCGCATCCAAGAACAAAATGGT
CGAGCCGGGGTACCAGGAGTTCCAGAGCAAGGACATCGCGTCCACCACGTCGGCGGACGGCGACGTGACGGTGCGCGTCATCGCGGGGGAGTCCATGG
GCGCCCGGTCGCCGGTGCGCACGCGGACTCCGACCATGTACCTTGACTTCACGGTGCGCCCGCACGCCGCCGCGCCCGTGCGGCAGCCGGTGCCGGCG
TCGTGGAACGCGTTCGTGTACGTGCTCGAGGGCGAGGGCGTGTTCGGGCCGACGGAGCAGCCGGCGGGGGCGCACCACCTGCTGCTGCTCGGGCAGGG
CGGCGACGGCGTGGAGGTTTGGAACAGGTCGGACAAGCCGCTCCGGTTCGTGCTCGTGGCCGGCGAGCCCATCGGCGAGCCCGTGGCGCAGCTGGGCC
CGTTCGTGATGAACACCGAGGAGGAGATCGACGCCACCGTCAACGACTTCGAGTACTTCATCAACGGGTTCGAGAAGGCCAAGCATTGGAAGTCGCAG
GCGATGATCGCGCTAGAGCTAGAGTACGTAGGGTGA

>Ta-Pirin-4-D_TraesCS5D02G270300.1
ATGTCGACAATGGAGGTGAAGAAGCCCCGGCAGGTGGCGAGGCGGTTCCTGGCGCGGCCGCAGCACGAGGGCGCCGGCGCCGTCGTCCGCCGCAGCAT
CGGCAGGTTCGAGCTGAGGTACTTCGACCCGTTCCTCGTCCTGGACGAGTTCTCAGCTTCTGCGCCGTCTGGGTTCCCCGACCATCCGCACCGAGGCT
TCGAGACCGTCACCTACATGCTCGAGGGAGCGGTGACGCACGAGGACTTCGAGGGCCACCGTGGCACGATCAAGGCCGGCGACGTGCAGTGGATGACG
GCCGGCCGCGGCATCGTGCACTCCGAGATGCCCGCCGGCCCCGGCACCTCCAAGGGCCTCCAGCTCTGGGTCAACCTCGCCTCCAAGAACAAAATGGT
CGAGCCGGGGTACCAGGAGTTCCAGAGCAAGGACATCGCGTCCACGACGTCGGCGGACGGCGACGTGACGGTGCGCGTCATCGCGGGGGAGGCCATGG

GCGCCCGGTCGCCGGTGCGCACGCGGACGCCGACCATGTACCTCGACTTCACGGTGCGCCCGCACGCCACCGCGCCCGTGCGGCAGCCGGTGCCGGCC
TCGTGGAACGCGTTCGTGTACGTGCTCGAGGGCGAGGGCGTGTTCGGGCCGACGGCGGACCAGCCGGCGGGGGCGCACCACCTGCTGCTGCTCGGGCA
GGGCGGCGACGGCGTGGAGGTTTGGAACAGGTCGGACAAGCCGCTCCGGTTCGTGCTCGTCGCCGGCGAGCCCATCGGGGAGCCCGTGGCGCAGCTGG
GCCCATTCGTGATGAACACCGAGGAGGAGATCGACGCCACCGTCAACGACTTTGAGTACTTCATCAATGGGTTCGAGAAGGCCAAGCATTGGAAGTCG
CAGGCCATGATCGCGCTAGAGCTAGAGTACGTAGGGTGA

>Ta-Pirin-5-A_TraesCS1A02G391900.1
ATGTCTGCCGCCGCCTGCGTCTCCTTCTGCCCCTCCCCCGCGTCCTCTCGCCACGGCGCCGGGCCGATCGTCGACGTCGTCGGGCTGCCGCCGGCTGT
GGAGGAGGCGGAGGAGCGCGGCGCCGAGAGGGACCTCCTGGAGTTCGGCGCCGACGGGATGATCAGCGCCAGCAGTGACAGTGACGAAGATGCTGCTG
CTGCTGAGATCGATGACGAGGAGGAGCACTCGGTGAGGAGGCCACGGGCGGTGGTTCAGAAGTTCATGTGCGAACGCAAGGCTGTCGGCGACGGCTTC
GTTCTCCGGAGGAGCATTGGCAGGCCTGAGTTGCAGAGCTTGGATCCTTTCATCTCCCTGGACGAGTTTGAATTTTCTCGTCCAGCTGGCTTTTCCGA
TCATCCACACCGAGGATTCGAGAATGTTACCTACATGCTTGAGGGAGGCTTGAGTTACCATGACTTTTCAGGCCACAAGGGCACGATCAACACCGGGG
ATGTTCAGTGGATGACGGCCGGGCGTGGTGTGGTGCACGCAGAGATGCCGGGCGGTGAGGGGGTGCAGAGGGGCCTCAACCTCTGGCTCAACCTCTCC
TCAAAGGACAAGATGGTGGCGCCGAGGTACCAGGACCTGAGGAGCCACGACGTCCCCACGGCGGAGAAGGACGGCGTGTCCATCAAGGTCATCGCCGG
CGAGGCCCTGGGCGCGCGCTCGCCGATCCAGACGCGCACCCCGGCCATGTGGCTCGACGTCACCATGCGGCCCGGCGCGCGCCTGCGCCAGCCCGTCC
CGGCCGGCTGGAGCGCGTGCGCCTACGTCCTCGACGGCGAGGCCAGCTTCGGCCAGCCAGGGGACGAGGCGGCCGGCGCGCACCAGTGCGTCGTGTTC
GGCGGCGACGGCGATGGCGTGGACGTGCGGAGCGACAGCGCGACGACGCGTTTCTTGTTGCTGGCGGCGCGGCCGCACGGCGAGGCGGTGGCGCTGGA
CGGGCCCTTCGTGATGAACACGAGCGAGGAGGCGCAACAGGCCAGGGAGGACTACCTGAACCGCCGCAACGGCTTCGAGATGGCCGCCGGCTGGACCT
CTAGCCAGTGA

>Ta-Pirin-5-B_TraesCS1B02G420000.1
ATGTCTGCCGCCGCGTGCGTCCCCTTCTGCCCCTCCCCCGCGTCTTCTCGCCACGGCGCCGGGCCGATCGTTGACGTCGCTGGGCTGCCGCCGGCCAC
CGAGGCGGAGGAGCACGGCGCCGGGAGGGACCTCCTGGAGTTCGGGGTCAACGGGGTGATCGGCGCCAACAGTGACAGTGACGATGCTGCTGCTGCTG
AGATCGATGACGAGGAGGAGCACTCGGTGAGGAGGCCACGGGCGGTGGTTCAGAAGTTCATGTGCGAACGCAAGGCTGTCGGCGACGGCTTCGCTCTC
CGGAGGAGCATTGGCAGGCCCGAGTTGCAGAGCTTGGATCCTTTCATCTCCTTGGATGAGTTTGAATTTTCTCGTCCAGCCGGCTTTACTGATCATCC
ACACCGAGGATTCGAGAATGTTACCTACATGCTTGAGGGAGGCTTGAGTTACCATGACTTTTCAGGCCACAAGGGCACGATCAACACCGGAGATGTTC
AGTGGATGACGGCCGGGCGTGGTGTGGTGCACGCAGAGATGCCGGGTGGTGAGGGGGTGCAGAGGGGCCTCAACCTCTGGCTCAACCTCTCCTCAAAA
GACAAGATGGTGGCGCCGAGGTACCAGGAGCTGAGGAGCCGCGACATCCCCACGGCGGAGAAGGACGGCGTGTCCGTCAAGGTCATCGCCGGCGAGGC
CCTGGGCGCGCGCTCGCCGATCCAGACGCGCACCCCGGCCATGTGGCTCGACGTGACCATGCGGCCCGGCGCGCGCCTGCGCCAGCCCGTCCCGGCCG
GCTGGAGCGCGTGCGCCTACGTCCTCGACGGCGAGGCCAGCTTCGGCCAGCCAGGGGACGAGGCGGCCGGCGCGCATCACTGCGTCGTGTTCGGCAAC
GACGGCGATGGCGTGGACGTGCGGAGCGAAGGCGCGGGGGCCCGGTTCTTGCTGCTGGCGGCGCGGCCGCACGGCGAGGCGGTGGCGCTGGACGGGCC
CTTCGTGATGAACACGAGCGAGGAGGTGCAGCAGGCCAGGGAGGATTACCTGAACCGCCGTAACGGCTTCGAGATGGCCGCCGGCTGGACCTCTGGCC
AGTGA

>Ta-Pirin-5-D_TraesCS1D02G400000.1

ATGTCTGCCGCCGCATGCGTCTCCTTCTGCCCCTCCCCCGCGTCCTCTCGCCACGGCGGGCCGATCGTCGACTTGGCCGGGCTGCCGCCGGCTACGGA
GGCGGAGGAGCGCGGCGCCCAGAGGGACCTCCTGGAGTTCGGGGTCAACGGAACGATCGGCGCCAACAGTGACAGTGACGAAGATGCTGCTGCTGCTG
AGATCGATGACGAGGAGGAGCACTCGGTGAGGAGGCCACGGGCGGTGGTTCAGAAGTTCATGTGCGAACGCAAGGCTGTCGGCGACGGCTTCGCTCTC
CGGAGGAGCATTGGCAGGCCTGAGTTGCAGAGCTTGGATCCTTTCATCTCCTTGGATGAGTTTGAATTTTCTCGTCCAGCTGGCTTTTCTGATCATCC
ACACCGAGGATTCGAGAATGTTACCTACATGCTTGAGGGAGGCTTGAGTTACCATGACTTTTCAGGCCACAAGGGCACGATCAACACCGGAGATGTTC
AGTGGATGACGGCCGGGCGTGGTGTGGTGCACGCAGAGATGCCGGGTGGTGAGGGGGTGCAGAGGGGCCTCAACCTCTGGCTCAACCTCTCCTCAACA
GACAAGATGGTGGCGCCGAGGTACCAGGAGCTGAGGAGCCGCGACGTCCCCACGGCGGAGAAGGACGGCGCGTCCATCAAGGTCATCGCCGGCGAGGC
CCTGGGCGCGCGCTCGCCGATCCAGACGCGCACCCCGGCCATGTGGCTCGACGTGACCATGCGGCCCGGCGCGCGCCTGCGCCAGCCCGTCCCAGCCG
GCTGGAGCGCGTGCGCCTACGTCATCGACGGCGAGGCCAGCTTCGGCCAGCCAGGGGACGAGGCGGCCGGCGCGCATCACTGCGTCGTGTTTGGCGGC
GACGGCGATGGCGTGGACGTGCGGAGCGAAGGCGCGGGGACCCGGTTCTTGCTGCTGGCGGCGCGGCCGCATGGCGAGGCGGTGGCGCTGGACGGGCC
CTTCGTGATGAACACGAGCGAGGAGGTGCAACAGGCCAGGGAGGACTACCTGAACCGCCGCAACGGCTTCGAGATGGCCGCCGGCTGGACCTCTGGCC
AGTGA

>Ta-Pirin-6-A_TraesCS4A02G336100.1
ATGTCTTCCTCTTCCACGCCCGTCCCGTTCGAGAATCCGAGGAAGGTAGTGAAGAAGGTGCTGTCCTTGTCCCAGTCCGAGGGGGACGGCGCCACCGT
CCGCCGGAGCATCGGCGGTTGCGAGCTCCGGAACCTGGACCCGTTTCTCCTGCTCGACGAGTTCTCCGTCTCCAAGCCCGCCGGATTCCCCGACCACC
CCCACCGGGGCTTCGAGACCGTCACCTACATGCTAGACGGGGCCTTCACCCACCAGGACTTCTCTGGCCGCAAGGGCACCATCAGGACAGGAGATGTC
CAGTGGATGACGGCAGGGCGCGGCATCGTGCACTCGGAGATGCCGGCAGCCGACGGCGTGCAGAAGGGCCTGCAGCTCTGGATCAACCTCGCCTCCAA
AGACAAGATGATTGAGCCAAGGTACCAGGAGCTCGAGAGCAAGGACATCAGCCAGGCCGAGAAAGACGGCGTGGCGGTGCGGATCATTGCGGGGGAAG
CCTTCGGGGTGCGGTCGCCGGTCTACACACAGACGCCCACCATGTACATGGACTTCACAATGCAACCAGGGTCGCAGCTCCACCAGCCGATCCCCGAG
GGCTGGAACGCCTTCGTGTACATCATTGAGGGGGAGGGCGTGTTCGGCAAGGAGGGTGCAGCTCCGGCGAGCGCGCACCACTGCCTCGTCCTCAGCGC
AGGGGACGGGCTCAGCGTGTGGAACCGGTCCGGCGCGCCGCTGCGGTTTGCATTAGCAGCGGGACAGCCGCTCAATGAGCCGGTGGTGCAGCAGGGGC
CCTTCGTCATGAACTCACGTGCCCAAATCCAGCAGGCCATGGAGGACTACTACTACGGCCGCAACGGCTTTGAGAAGGCCAGCCAGTGGAGCTCCGCC
TGA

>Ta-Pirin-6-B_TraesCS5B02G535900.1
ATGTCTTCGTCTTCCTCCTCCGTGACGTTCGAGAATCCGAGGAAGGTGGTGAAGAAGGTGCTGTCATTGTCCCAGTCCGAGGGGGACGGCGCCACCGT
CCGCCGGAGCATCGGCCGGCACGAGCTCCGGAACCTGGACCCGTTCCTCCTGCTCGACGAGTTCTCCGTCTCCAAGCCCGCCGGCTTCCCCGACCACC
CTCACCGTGGCTTCGAGACCGTCACCTACATGCTCGATGGGGCCTTCACCCACCAGGACTTCTCTGGCCGCAAGGGCACCATCAGGACCGGAGATGTG
CAGTGGATGACGGCGGGGAGTGGCATCGTGCACTCAGAGATGCCGGCAGCAGACGGAGTGCAGAAAGGCCTGCAGCTCTGGATCAACCTCGCCTCCAA
AGACAAGATGATCGAGCCGCGGTACCAGGAGCTCGAGAGCAAGGACATTAGCCAGGCCGAGAAGGACGGCGTGGCGGTGCGGATCATCGCTGGGGAAG
CATTTGGGGTGCGGTCGCCGGTCTACACGCGGACGCCAACCATGTACATGGACTTCACAATGCAACCAGGTTCGCAGCTCCACCAGCCAATCCCCGAG
GGCTGGAACGCCTTCGTGTACGTCATCGAGGGGGAGGGCGTGTTCGGCAAGGAGAATGCAGCGCCGGCGAGCACGCACCACTGCCTTGTGCTTGGCGC
GGGGGACGGGCTCAGCGTGTGGAATAGGTCAGGCGCACCGCTGCGGTTCACCCTTGCGGCGGGGCAGCCGCTGAACGAGCCGGTGGTGCAGCAGGGGC

CCTTTGTCATGAACTCGCGTGCCCAGATCCAGCAGGCCATGGAGGACTACTACTACGGCCGCAACGGCTTCGAGAAGGCCAGCCAGTGGAGCTCCGCC
TGA

>Ta-Pirin-6-D_TraesCS5D02G533400.1
ATGTCTTCGTCTTCCACGCCCGTGACGTTCGAGAATCCGAGGAAGGTGATGAAGAAGGTGCTGTCCTTGTCCCAGTCCGAGGGGGACGGCGCCACCGT
CCGCCGGAGCATCGGCGGTTGCGAGCTCCCGAACCTGGACCCGTTCCTCCTGCTCGACGAGTTCTCTGTCTCCAAGCCCGCCGGCTTCCCCGACCACC
CCCACCGGGGCTTCGAGACCGTCACCTACATGCTAGACGGGGCCTTCACCCACCAGGATTTCTCTGGCCGCAAGGGCACCATCAGGACAGGAGATGTG
CAGTGGATGACGGCGGGGCGCGGCATCGTGCACTCGGAGATGCCGGCGGCCGACGGAGTGCAGAAGGGCCTGCAGCTCTGGATCAACCTCGCCTCCAA
AGACAAGATGATCGAGCCGCGGTACCAGGAGATTGAGAGCAAGGACATCAGCCAGGCCGAGAAGGACGGCGTGGCGGTGCGGATCATTGCGGGGGAAG
CCTTTGGGGTGCGGTCGCCGGTCTACACACGGACGCCGACCATGTACATGGACTTCACAATGCAACCAGGTTCGCAGCTCCACCTGCCAATCCCAGAG
GGCTGGAACGCCTTCGTGTACATCATCGAGGGGGAGGGCGTGTTCGGCAAGGAGAATGCAGTGCCGGCGAGCGCGCACCACTGCCTTGTGCTTGGCGC
GGGGGACGGGCTCAGCGTGTGGAATCGGTCAGGCGCACCGCTGCGGTTCGCGCTGGCGGCGGGGCAGCCGCTGAACGAGCCAGTGGTGCAGCAGGGGC
CCTTCGTCATGAACTCGCGGGCCCAGATCCAGCAGGCCATGGAGGATTACTACTACGGCCGCAACGGCTTCGAGAAGGCCAGCCAGTGGAGCTCCGCC
TGA

Supplementary File S2
Pirin gene family members' amino acid sequence in seven species

Aegilops tauschii

>Aet-Pirin-1
MPRHSAASPIYTALARLANFNSGRRVLLASRKTSSSSARSSAKTRPFLCLALFRILVVVTAVFLFPPAIMSSSSSSSSAAAASVPFQSPRKVVKKVLSLSQSEGQGATVRRSIG
GHEVRNLDPFLLLDEFSVSKPAGFPDHPHRGFETVTYMLDGVFTHQDFSGHTGTIRTGDVQWMTAGRGIVHSEMPAADGVQKGLQLWINLASKDKMIEPRYQELESK

DISQAEKDGVAVRIIAGEAFGVRSPVYTQTPTMYMDFTMQPGSQLHQPIPEGWNSFVYIIEGEGVFGKEGAAPASAHHCLVLGAGDGLSVWNRSGAPLRFALAAGQP
LNEPVVQQGPFVMNSRAQIQQAMEDYYYGRNGFEKASQWSSA

>Aet-Pirin-2
MLRQHLPLFSSSSSSPIHMALARLTRKTSSRSSAKTKPLLFLLLLIVILVVTAVFLFPPATMSSSSSFENPRKVVKKVMSLSQAEGDGATVRRSIGGHELRNLDPFLLLDEFSVS
KPGGFPDHPHRGFETVTYMLHGAFTHQDFTGHKGTIRTGDVQWMTAGRGIVHSEMPASDGVQKGLQLWINLASKDKMIEPRYQELKSKDISQAEKHGVKVRIIAGEA
FGVRSPVYARTPTMYMDFTMQPGSQLHQPIPEGWNAFVYIIEGEGVFGREGVAPASAHHCLVLGAGDGLSVWNRSSAQLRFVLAAGQPLNEPVVQQGLFVMNSRA
QIQQAMQDYYYGHNGFEKASQWSSA

>Aet-Pirin-3
MLRQLLPHFSSSSSSSSPIYSLARLTRQSSSRRVPLASRKTSSSSRSSASTRPFLCLALFLLLILVVTALFLFPPAIMSSSSSSSSSAASVPFERPRKVVKKVLSLSQSEGDGATVR
RSIGRHEVPNLDPFLLLDEFSVSKPAGFPDHPHRGFETVTYMLDGAFTHQDFSGRKGTIRTGDVQWMTAGRGIVHSEMPAADGVQKGLQLWINLASKDKMIKPRYQE
LESKDISQAEKHGVKVRIIAGEAFGVRSPVYTRTPTMYMDFTMQPGSQLHQPIPEGWNAFVYIIEGEGVFGREGAAPASAHHCLVLGAGDGLSVWKRSGAPLRFVLAA
GQPLNELVVQQGPFVMNSRAQIKKAMEDYYYGRNGFEKASQWSST

>Aet-Pirin-4
MSTMEVKQPRQVARRFLARPQHEGAGAVVRRSIGRFELRYFDPFLVLDEFSASAPSGFPDHPHRGFETVTYMLEGAVTHEDFEGHRGTIKAGDVQWMTAGRGIVHSE
MPAGPGTSKGLQLWVNLASKNKMVEPGYQEFQSKDIASTTSADGDVTVRVIAGEAMGARSPVRTRTPTMYLDFTVRPHATAPVRQPVPASWNAFVYVLEGEGVFGP
TADQPAGAHHLLLLGQGGDGVEVWNRSDKPLRFVLVAGEPIGEPVAQLGPFVMNTEEEIDATVNDFEYFINGFEKAKHWKSQAMIALELEYVG

>Aet-Pirin-5
MSAAACVSFCPSPASSRHGGPIVDLAGLPPATEAEERGAQRDLLEFGVNGTIGANSDSDEDAAAAEIDDEEEHSVRRPRAVVQKFMCERKAVGDGFALRRSIGRPELQS
LDPFISLDEFEFSRPAGFSDHPHRGFENVTYMLEGGLSYHDFSGHKGTINTGDVQWMTAGRGVVHAEMPGGEGVQRGLNLWLNLSSTDKMVAPRYQELRSRDVPTA
EKDGASIKVIAGEALGARSPIQTRTPAMWLDVTMRPGARLRQPVPAGWSACAYVIDGEASFGQPGDEAAGAHHCVVFGGDGDGVDVRSEGAGTRFLLLAARPHGEA
VALDGPFVMNTSEEVQQAREDYLNRRNGFEMAAGWTSGQ

>Aet-Pirin-6
MSSSSTPVTFENPRKVMKKVLSLSQSEGDGATVRRSIGGCELRNVDPFLLLDEFSVSKPAGFPDHPHRGFETVTYMLDGAFTHQDFSGRKGTIRTGDVQWMMAGRGI
VHSEMPAADGVQKGLQLWINLASKDKMIEPRYQEIESKDISQAEKDGVAVRIIVGEAFGVRSPVYTRTPTMYMDFTMQPGSQLHQPIPEGWNAFVYIIEGEGVFGKEN
AVPASAHHCVVLGAGDGLSVWNRSGAPLRFALAAGQPLNEPVVQQGPFVMNSRAQIQQAMEDYYYGRNGFEKASQWSSA

Arabidopsis thaliana

>At-Pirin-1
MTYENNSVPRIVIKKVLAKLEKEGEGAVVRNGITKIDQKLLDPFVLLVEFSFSLSAGFPDHPHRGFESVTYMLQGGIIHKDPKGHKGTIQAGDVQWMTAGRGIIHSEFPEE
EVNNGLQLWINLPSTEKMTEPKYKELSSLDIPRAEENGVEVKVIAGDSMGIKSPVYTRTPTMFLDFTLKPGSQTHQTVPESWTAFAYIIEGDEGVFGSLNSSAISAHHVVV
FGPGDLVSVWNKSTSRSLRFLLIAGEPIGEPVVQCGPFVMNSQAEIDMAFDDYQNAKNGFEMAKC

>At-Pirin-2
MRAAINRANSLGGLFSFRFIRNIKSMSSSTSQDFVSRPVIKKVFAKLQKEGDGAVVRRGISRSEQKLLDPFLMLDEFSVSPPAGFPDHPHRGFETVTYVLEGGITHQDFKG
HKGTIYAGDVQWMTAGRGIIHSEMPEEEVNKGLQLWINLSSNEKMIEPNYQELSHSDIPKAEQNGVEVKVIAGESMGIQSPVYTRTPTMFLDFTLQPGAQIHQNVPES
WNAFAYILESGEGGGVFSSSNSSPIPAHSVVVFGPGNDGVSVWNKSSSKQLRFVLIAGEPIGEPVVQYGPFVMNTQAEIDMTIEDYHYGKNGFEMAKYWRSQ

>At-Pirin-3
MKVMVLSLGKASPSKSDHELLDPFVSLVEFSVSPPGGFKDHPHRGFESVTYMFQGGIIHQDCNGNKGTIHEGDVQWMTAGRGIIHSEMPEEQVNKGLQLWINLPSSA
KMIEPKNIEISSSEIPSADDYGVEVKVIAGESM
GVKSPFYTKTPIMFLDFTLDPKAQTHQAVPESWTAFAYIVEGDEGVFSSSDSSTVQAHNVVVFGTGDEVS
VWNTSNSRPLRFLLIAGEPIGEPVVQHGPFVMNSQDEIEMTIGDYRNGMNGFEMAKHWRSE

>At-Pirin-4
MPISEKSSATNTRLVVKKLFARQLHEGFGAVVRRSIGRFEFRYFDPFLVLDEFSVSAPAGFPDHPHRGFE
TVTYMLEGEILHEDCEGHKGVIREGGLQWMTAGKGIVHSEMPSSNSNGITHNKGLQLWINLSSRQKLVEP
SYQEIESKDIAETEKDGVRVRVIAGEWNGVKSKICTRTPTMYLDFTLSPGSRISQPIPLHWNAFVYVLQG
HGHFGDSKLQHSAAAAHHLLVLGLGGDMLEAWNGSDSGLPLRFILVAGEPIGEPMVQFGPFVMNTQEEIDETIDDFENFRNGFEKARHWKSQAASALGLF

Brachypodium distachyon

>Bd-Pirin-1
MAQKVLAATTRLRPSSSSSSPIYTALARLTKRNSSHRLLSSSSRNTTSKAKSKPILLLLILFLLVVAVVVTVLLFPALAMSSSSASSAVAAGPLENPRAVVKKVLAESQPEGQG
ATVRRSIGRHELRNLDPFLMLDEFSVSKPAGFPDHPHRGFETVTYMLDGAFTHQDFSGHKGTIRTGDVQWMTAGRGIVHSEMPASDGVQKGLQLWINLSSKDKMIEP

RYQELQSKDISRAEKDGVEVRIIAGEAFGVRSPVYTRTPTMYMDFTMQPGSQLHQPIPEGWNAFVYIIEGEGVFGSEKAAPASAHHCLVLGASGDGLSVWNKSGAPLR
FALAAGQPLKEPVVQQGPFVMNTRAEIQQAMEDYYYGKNGFEKASQWSSST

>Bd-Pirin-2
MEKPRQVVRKFLARPQHEGAGAVVRRSIGRFELRYFDPFLVLDEFSVSAPAGFPDHPHRGFETVTYMLEGAVTHEDFEGHRGTIKAGDVQWMTAGRGIVHSEMPAAP
GTSRGLQLWVNLSSQNKMIEPRYQEMQSKDIASTTSSDGVTVRVVAGHSMGARSPVCTRTPTMYLDFTVRPHAAARQPVPASWNAFAYVLEGEGVFAGGGAAEAA
DSSSSSKAGPHHLLLLGLQGDGVEVWNKSDKPLPXFLLIAGEPIGEPVVQLGPFVMNTEEEIDAAVNDFEYCVNGFEKAKHWKSQAMVALEVE

>Bd-Pirin-3
MSAAACVALCPTASSRHGGSPAVVGTPPAAMAAEKEAEQKHLFSGSTEINANGSINGKCDEDGDAAAGVDDVAEHYRDPAVTKPRAVVQRFTCERKPFVDGFALRRS
IGSPELESLDPFLSLDEFEFSPPAGFSDHPHRGFENVTYMLEGGLSYHDFSGHKGTINKGDVQWMTAGRGVVHAEMPGGQGVQRGINLWINLSSKDKMVAPRYQDL
ASVEIPTAEKDGVTIKVIAGSALGARSPLETRTPAMFLDVAMRPGARLRQPVPPGWTACAYVIDGEAGFFFGSGSGSQDAEAGAHECVVFGGDGDGDGVDVRSEGGG
RILLLAARPHGEAVVRDGPFVMNTREEVEQAREDYLNRRNGFEMAAGWASAHAPTAVPR

Hordeum vulgare

>Hv-Pirin-1
MPAHSAASPIYTALARLTNFSSSRRALLASRKTSSSSARSSAKAKAFLFLLLILVVVTAVFLFPPAIMSSSSSSSSSAAAASVPFQSPRKVVKKVLSLSQSEGQGATVRRSIGGH
ELRNLDPFLLLDEFSVSKPAGFPDHPHRGFETVTYMLDGAFTHQDFSGHKGTIRTGDVQWMTAGRGIVHSEMPAADGVQKGLQLWINLASKDKMIEPGYQELESKDIS
QAEKDGVAVRIIAGEAFGVRSPVYTRTPTMYMDFTMQPGSQLHQPIPEGWNAFVYIIEGEGVFGKEGMAPVSAHHCLVLGPGDGLSVWNRSGAPLRFALVAGQPLN
EPVVQQGPFVMNSRAQIQQAMEDYYYGRNGFEKASQWSST

>Hv-Pirin-2
MASSSSSITFENPRKVVKKVMSLSQSEGDGATVRRSIGGVRNLDPFLLLDEFSVSKPAGFPDHPHRGFETVTYMLDGAFTHQDFSGHKGTIRTGDVQWMTAGRGIVHS
EMPAADGVHKGLQLWINLASKDKMIEPRYQELESKDVSQAEKDGVAVRIIAGEAFGVRSPVYTRTPTMYMDFTMQPGSQLHQPIPEGWNAFVYIIEGEGVFGKEGTA
PASAHNCLVLGAGDGLSVWNRSGAPLRFVLAAGQPLKESVVQQGPFVMNSRAQIQKAMEDYYYGRNGFEKASQWSST

>Hv-Pirin-3
MLRQHLSLFSFSSSSSPIYTALARLAKRNSSHRVHLASRNTSSSSRSSANNRPLLFLVLFLLILAVTAVFLFPPAIMSSSSSSVPFESPRKVVKKVLSLSQSEGDGATVRRSIGRH
ELPNLDPFLLLDEFSVSKPAGFPDHPHRGFETVTYMLDGAFTHQDFSGRKGTIRTGDVQWMTAGRGIVHSEMPASDGVHKGLQLWINLASKDKMIKPRYQELESKDIS
QAEKDGVAVRIIAGEAFWVRSPVYTRTPTMYMDFTMQPGSQFHQPIPEGWNAFVYIIEGEGVFGKEGAAPASEHHCLVLGAGDGLIVWNRSGAPLRFVLAAGQPLNE
TVVQQGPFVMNSRAQIQKAMEDYYYGRNGFEKASQWSSA

>Hv-Pirin-4
MSTMEVRKPRQVARRFLARPQHEGAGAVVRRSIGRFELRYFDPFLVLDEFSGSAPAGFPDHPHRGFETVTYMLEGAVTHEDFEGHRGTIKAGDVQWMTAGRGIVHSE
MPAGPGTSKGLQLWVNLASKNKMVEPGYQEFQSKDIASTASADGDVTVRVIAGQAMGARSPVRTRTPTMYLDFTVRPHAAAPVRQPVPASWNAFVYVLEGEGVFG
ATADQAAGAHHLLLLGQGGDGVEAWNRSDKPLRFVLVAGEPIGEPVAQLGPFVMNTEEEIDATVNDFEYFINGFEKAKHWKSQAMIALELD

>Hv-Pirin-5
MSAAACVSFCPSPASSRHGAGPIVDVVVGLPPATEAEEERGAGRDLLEFGADGMIGASSDSDQDAAAAAEIDDEEKHPVRRPRAVVQKFMCERKVVGDGFALRRSIGR
PELQSLDPFISLDEFEFSRPAGFSDHPHRGFENVTYMLEGGLSYHDFSGHKGTVNTGDVQWMTAGRGVVHAEMPGGEGVQRGLNLWLNLSSKDKMVAPRYQDLRS
RDVPSAEKDGVSVKVIAGEALGARSPIQTRTPAMWLDVTMQPGACLRQPVPAGWTACAYVLDGEASFGQPGDEAAGAHQCVVFGGDGDGVDVRTGGARARFLLL
AARPHGEAVAMDGPFVMNTSEEVQQAREDYLNRRNGFELAAGWSSGQ-

>Hv-Pirin-6
MPAHSAASPIYTALARLTNFSSSRRALLASRKTSSSSARSSAKAKAFLFLLLILVVVTAVFLFPPAIMSSSSSSSSSAAAASVPFQSPRKVVKKVLSLSQSEGQGATVRRSIGGH
ELRNLDPFLLLDEFSVSKPAGFPDHPHRGFETVTYMLDGAFTHQDFSGHKGTIRTGDVQWMTAGRGIVHSEMPAADGVQKGLQLWINLASKDKMIEPGYQELESKDIS
QAEKDGVAVRIIAGEAFGVRSPVYTRTPTMYMDFTMQPGSQLHQPIPEGWNAFVYIIEGEGVFGKEGMAPVSAHHCLVLGPGDGLSVWNRSGAPLRFALVAGQPLN
EPVVQQGPFVMNSRAQIQQAMEDYYYGRNGFEKASQWSST-

Oryza Sativa

>Os-Pirin-1
MMTRSMMKFFSPSSSAIYTTLSSRLARINATRHTPPPPPKSSRAARSLTSFLLIRATMSSSSSSSDAVAAAAAATFEKPRTVVKKLLAESQPEGDGATVRRSIGRYELRNLD
PFLMLDEFSVSKPAGFPDHPHRGFETVTYMLEGAFTHQDFAGHKGTIGTGDVQWMTAGRGIVHSEMPAADGVQKGLQLWINLSSKDKMIEPRYQELMSKDISCAEK
DGVEVKIIAGEAFGVRSPVYTRTPTMYMDFTMQPGSQLHQPIPEAWNAFVYIIDGEGVFGREKASPATAHHCLVLGPGDGLSVWNKSGEPLRFALVGGQPLNEPVVQ
HGPFVMNTRAEIQQAMEDYYYGRNGFEKARHWSSTA

>Os-Pirin-3
MSAAACISSFPPPPMAAAAAPAPETTIDVFVVANHTPVTAAADKSSCEGDVVAGGGRTVRRPRAVARTLECERRVVGEGFAVRRGIGRKELDSLDPFISLDEFEFSPPAG
FHDHPHRGFENVTYMLEGGFSYHDFSGHKGTINTGDVQWMTAGRGVVHAEMPGGHGVQRGINLWINLSSKDKMVEPRYQELASHDIPAAERDGVSVKVIAGEALG
ARSPLQTRTPALCLDVAMRPGARLRAPVPPGWSACSYVIDGEAVFGDEAAAAGAHTCVVFGGGGDGVAARATERSAARFLLVAARPHGEAVVKDGPFVMNTREEVE
QAREDYRNRRNGFEMAAGWSSDHVATAAAAH

>Os-Pirin-2
MTTSMEKPRQVVRKFLARPQHEGVGAVVRRSIGRFELRYFDPFLVLDEFSVSAPAGFPDHPHRGFETVTYMLEGAVTHEDFEGHRGTIKAGDVQWMTAGRGIVHSE
MPAGPGTSRGLQLWVNLSSHNKMIEPGYQEIQSKDIASTTSDGVTVRVIAGQSMGARSPVRTRTPTMYLDFTVRPHAAARQPVCATWNAFAYVLEGEGVFGGGGGD
KAGAHHLLLLGQGDGVEVWNRSDKPLRFLLIAGEPIGEPVAQLGPFVMNTEEEIDMTINDFEFSINGFEKAKHWKSQALVALGLE

Sorghum bicolor

>SbPirin-1
MSSSASDSASSAAPFEKPRAVVKKLLAESQPEGQGATVRRSIGRHELRNLDPFLMLDEFSVSKPAGFPDHPHRGFETVTYMLEGAFTHQDFAGHKGTIKTGDVQWMT
AGRGIVHSEMPAGDGVQKGLQLWINLSAKDKMIEPRYQELESKDISRGERDGVEARVIAGEALGAASPVYTRTPTMYVDFTMRPGSRLHQPVPEGWNAFVYVVDGE
GVFGRDKAAPTAAHHCLVLGPGDGLSVWNRSDRPLRFVLVAGKPLGEPVVQHGPFVMNSRAEIQQAMEDYYYGKNGFERASQWSSSSA

>SbPirin-2
MEKPRQVVRKFLARPQHEGVGAVVRRSIGRFELRYFDPFLVLDEFSVSAPAGFPDHPHRGFETVTYMLEGAVTHEDFEGHRGTIKAGDVQWMTAGRGIVHSEMPAGP
GTSKGLQLWVNLSSGNKMVEPGYQEIQSKDIACTSADGVTVRVIAGHAMGVRSPVCTRTPTMYLDFTVRPRGVVRQPVLASWNAFAYVLEGEGVFGAERGAPVGAH
HLLLLGQGDGVEVWNRSDDRPLRFLLIAGEPIGEPVAQLGPFVMNTEEEIDMTVNDFECYANGFEKARHWKSQAMVALGVE

>SbPirin-3
MSAATACMPLVPPSPLHGSSAAMAAAVERRQQPGAMETTKTAGSEGTVVVKSHGNDQDCAGDDDGDVTMSRPRAVVQTLTCERKPFSEGFALWRSIGRPELPELD
PILSFDEFEFSAPAGFPDHPHRGFENVTYMLEGGISYHDFSGHKGTINTGDVQWLTAGRGVVHAEMPAGEGVQRGINIWINLSAADKMVEPRYQDLASHDIPTAVTA
DGVSVKVIAGECLGTRSLLRPRTPALCLDVALRPRARLRQPIPRGWSACAYVIHGEAAFFGGSASDGGATTVTTAAARTLVVFGNEGDGDCVEVRGADASAGQQDGAR
VMLVAARPHNEAVVRDGPFVMNTREEVEQAREDYRRRRNGFEMADGWTSDHASTVATH

Zea mays

>Zm-Pirin-1
MMRLKQHMGLVSSPTPAIVVRLGNNTPHRRRATRSRIVSSSASDAAPFEKPRAVVKKVLAQSQPEGQGATVRRSIGRHELRNLDPFLQLDEFTVSKPAGFPDHPHRGFE
TVTHMFEGAITHQDFAGHKGTIRTGDVQWMTAGRGIVHSEMPAGDGVSEGLQLWINLSSKDKMIEPRYQELERKDISRAETEDGVEARVIAGEAFGVASPVYTRTPI
MYVDFTMRPGSRLHQPVPEGWNAFVYVVDGEGVFGRETATAHHCLVLGSGDGVSVWNRSARPLRFVLAAGQPLGEPVVQHGPFVMNSHAEIQQAMEDYSYGKN
GFERAGQWSSSA

>Zm-Pirin-3
MSAATACMPLVLDPSPLHGSAAMADAVERRQPGGMETTKTGSEGTLGRVVRSQVFGNEDDDRAGHGDGDE
VSKPRAVVHTLTCERKPLFEGFALWRSIGRPELPELDPILSFDEFEFSAPAGFLDHPHRGFENVTYMLEG
GISYHDFSGHKGTINPGDVQWLTAGRGVVHAEMPAAGQGVQRGINIWINLSAADKMVEPRYQDLASHDIP
AAAADAAGGVSVKVIAGECLGARSPLRPRTPALCLDVALRPGARLRQPVPRGWSACAYVIHGEAAFGTAS
GEGNGASTATARTLVVFGGDGDGVELRGDAAGQGARVMLVAARSHGEAVARDGPFVMNTREEVDQAREDY
RHRRNGFEMADGWTSDHASAAEKHS

>Zm-Pirin-2
MEKPRQVARKFLARPQHEGAGAVVRRSIGRFELRYFDPFLVLDEFTVSAPAGFPDHPHRGFETVTYMLEGAVTHEDFEGHRGTIKAGDVQWMTAGRGIVHSEMPAG
PGTSRGLQLWVNLSSANKMVEPGYQEIQSKDIACTSDGDGGVTVRVIAGHAMGVRSPVRTRTPTMYLDFTVRPRGAVRQPVRASWNAFAYVLEGEGVFGAERCAPV
GAHHLLLLGHGDGLEVWNKLPDRPLRFLLVAGEPIGEPVAQLGPFVMNTEEEIDMTVNDFECYANGFEKARHWKSQAMLALGVE

>Zm-Pirin-4
MTTTMMRLRQHLGLVSSPSIYTSAIARFGNNTPHRRRTSTSTTTHITQKQFLLLVILLLLLLLLLFSVVFLIPTVSLPPARSRTMSSSASDAAPFEKPRAVVKKVLAESQPEGQ
GATVRRSIGRHELRNLDPFLLLDEFTVYKPAGFPDHPHRGFETVTYMLEGAFTHQDFAGHKGTIKTGDVQWMTAGRGIVHSEMPAGDGVHKGLQLWINLSSKDKMIE
PRYQELESKDISRGESEDGGVEARVIAGEALGAASPVYTRTPTMYVDFTMRPGSRLHQPVPEGWNAFVYVVDGEGVFGRETATAHYCLVLGPGDGVSVWNRSTRPLR
FVLVAGQPLGEPVVQHGPFVMNSRAQIQKAMEDYYYGKNGFERAGQWSSSA

>Zm-Pirin-5
MTTTMMRLRQHLGLVSSPSIYTSAIARFGNNTPHRRRTSTSTTTHITQKQFLLLVILLLLLLLLLFSVVFLIPTVSLPPARSRTMSSSASDAAPFEKPRAVVKKVLAESQPEGQ
GATVRRSIGRHELRNLDPFLLLDEFTVYKPAGFPDHPHRGFETVTYMLEGAFTHQDFAGHKGTIKTGDVQWMTAGRGIVHSEMPAGDGVHKGLQLWINLSSKDKMIE
PRYQELESKDISRGESEDGGVEARVIAGEALGAASPVYTRTPTMYVDFTMRPGSRLHQPVPEGWNAFVYVVDGEGVFGRETATAHYCLVLGPGDGVSVWNRSTRPLR
FVLVAGQPLGEPVVQHGPFVMNSRAQIQKAMEDYYYGKNGFERAGQWSSSA

Table S1: *Triticum aestivum* RNA-Seq datasets used to compare *Pirin* gene expression levels.

Tissue-specific Expression Data[a]			
Details	**Experiment ID (ENA SRA ID)**	**Total reads**	**Number of replicates**
Fruit at the whole plant ripening stage	ERX391046 (ERR414721_2)	49053093	2
	ERX391050 (ERR414750_2)	30038860	
Cotyledon emergence root	ERX391071 (ERR424737_2)	45116709	2
	ERX391061 (ERR424770_2)	51833599	
Leaf at the whole plant fruit formation stage (30 to 50%)	ERX391062 (ERR414749_2)	47106971	2
	ERX391021 (ERR414763_2)	33655313	
Stem at the two nodes or internodes visible stage	ERX391032 (ERR414733_2)	40953211	2
	ERX391016 (ERR414767_2)	55483346	
Inflorescence maximum stem length reached stage	ERX391052 (ERR414735_2)	52120581	2
	ERX391070 (ERR414753_2)	45271806	
Drought, Heat and Combined Stress[b]			
Details	**Experiment ID (ENA SRA ID)**	**Total reads**	**Number of replicates**
Control	SRX673834 (SRR1542404_2)	81155853	2
	SRX673835 (SRR1542405_2)	75969741	
Drought stress 1 hr	SRX673836 (SRR1542406_2)	68467921	2
	SRX673838 (SRR1542407_2)	75864652	
Drought stress 6 hr	SRX673839 (SRR1542408_2)	63320064	2
	SRX673840 (SRR1542409_2)	73614455	
Heat stress 1 hr	SRX673841 (SRR1542410_2)	66035008	2
	SRX673843 (SRR1542411_2)	51618473	
Heat stress 6 hr	SRX673844 (SRR1542412_2)	76623839	2
	SRX673845 (SRR1542413_2)	67378274	
Combined stress 1 hr	SRX673846 (SRR1542414_2)	53762767	2
	SRX673847 (SRR1542415_2)	55585647	
Combined stress 6 hr	SRX673848 (SRR1542416_2)	53901424	2
	SRX673849 (SRR1542417_2)	56318014	
Cold Stress[c]			
Details	**Experiment ID (ENA SRA ID)**	**Total reads**	**Number of replicates**
Control (23°C)	SRX625519 (SRR1460549)	32616607	3
	SRX625520 (SRR1460550)	77577791	
	SRX625521 (SRR1460551)	28872198	
Cold stress (4°C)	SRX625522 (SRR1460552)	40138740	3
	SRX625523 (SRR1460553)	25425859	
	SRX625524 (SRR1460554)	19047190	

ABA analysis of Ta-*PYL4* overexpressor[d]			
Details	**Experiment ID (ENA SRA ID)**	**Total reads**	**Number of replicates**
Wild-type well-watered control (wwc)	SRX1656399 (SRR3285552_2)	49583197	3
	SRX1656400 (SRR3285553_2)	49111104	
	SRX1656401 (SRR3285554_2)	45609722	
Wild-type ABA treated for 24 hr	SRX1656402 (SRR3285555_2)	43270907	3
	SRX1656403 (SRR3285556_2)	41352264	
	SRX1656404 (SRR3285557_2)	48601309	
Wild-type subjected to drought - 24 hr without water	SRX1656405 (SRR3285558_2)	49129226	3
	SRX1656406 (SRR3285559_2)	49229707	
	SRX1656407 (SRR3285560_2)	47298837	
Over-expressor of Ta-*PYL4* well-watered control (wwc)	SRX1656408 (SRR3285561_2)	46625977	3
	SRX1656409 (SRR3285562_2)	41766695	
	SRX1656410 (SRR3285563_2)	44761537	
Over-expressor of Ta-*PYL4* ABA treated for 24h	SRX1656411 (SRR3285564_2)	39919073	3
	SRX1656412 (SRR3285565_2)	47019575	
	SRX1656413 (SRR3285566_2)	48063424	
Over-expressor of Ta-*PYL4* subjected to drought - 24 hr without water	SRX1656414 (SRR3285567_2)	42714124	3
	SRX1656415 (SRR3285568_2)	43040299	
	SRX1656416 (SRR3285569_2)	39738613	
***Fusarium graminearum* Infection[e]**			
Details	**Experiment ID (ENA SRA ID)**	**Total reads**	**Number of replicates**
NIL-51 *F. graminearum* 48 hr	ERX1274022 (ERR1201797_2)	24045575	3
	ERX1274023 (ERR1201798_2)	32710023	
	ERX1274024 (ERR1201799_2)	25984652	
NIL-51 Mock 48 hr	ERX1274040 (ERR1201815_2)	34787468	3
	ERX1274041 (ERR1201816_2)	20013677	
	ERX1274042 (ERR1201817_2)	23404211	
NIL-51 Mock 12 hr	ERX1274028 (ERR1201803_2)	29301258	3
	ERX1274029 (ERR1201804_2)	25869265	
	ERX1274030 (ERR1201805_2)	33058978	
NIL-51 *F. graminearum* 12 hr	ERX1274010 (ERR1201785_2	25418710	3
	ERX1274011 (ERR1201786_2)	38234787	
	ERX1274012 (ERR1201787_2)	40831345	
NIL-51 Mock 24 hr	ERX1274031 (ERR1201806_2)	22984326	3
	ERX1274032 (ERR1201807_2)	27832536	
	ERX1274033 (ERR1201808_2)	20840051	
NIL-51 *F. graminearum* 24 hr	ERX1274013 (ERR1201788_2)	27578418	3
	ERX1274014 (ERR1201789_2)	34713400	
	ERX1274015 (ERR1201790_2)	31343655	
NIL-38 Mock 12 hr	ERX1273992 (ERR1201767_2)	34997985	3
	ERX1273993 (ERR1201768_2)	23599332	
	ERX1273994 (ERR1201769_2)	40003384	

NIL-38 *F. graminearum* 12 hr	ERR1201749 (ERR1201749_2)	27620906	3
	ERR1201750 (ERR1201750_2)	19449433	
	ERR1201751 (ERR1201751_2)	32223388	
NIL-38 Mock 24 hr	ERX1273995 (ERR1201770_2)	25917089	3
	ERX1273996 (ERR1201771_2)	29732769	
	ERX1273997 (ERR1201772_2)	24822761	
NIL-38 *F. graminearum* 24 hr	ERX1273977 (ERR1201752_2)	25747899	3
	ERX1273978 (ERR1201753_2)	32609188	
	ERX1273979 (ERR1201754_2)	27776756	
NIL-38 Mock 48 hr	ERX1274004 (ERR1201779_2)	25760916	3
	ERX1274005 (ERR1201780_2)	38829518	
	ERX1274006 (ERR1201781_2)	25218505	
NIL-38 *F. graminearum* 48 hr	ERX1273986 (ERR1201761_2)	22760086	3
	ERX1273987 (ERR1201762_2)	37353756	
	ERX1273988 (ERR1201763_2)	26837655	
Powdery Mildew (Bgt - *Blumeria graminis*) Inoculation[f]			
Details	**Experiment ID (ENA SRA ID)**	**Total reads**	**Number of replicates**
0 days post-inoculation (dpi)	SRX514154 (SRR1228254_2)	18059507	3
	SRX514155 (SRR1228255_2)	17854242	
	SRX514156 (SRR1228256_2)	17144705	
1 day post-inoculation (dpi)	SRX514157 (SRR1228257_2)	18532311	3
	SRX514158 (SRR1228258_2)	18296908	
	SRX514159 (SRR1228259_2)	18203334	
2 days post-inoculation (dpi)	SRX514160 (SRR1228260_2)	19818606	3
	SRX514161 (SRR1228261_2)	20122608	
	SRX514162 (SRR1228262_2)	21845331	
3 days post-inoculation (dpi)	SRX514163 (SRR1228263_2)	18738238	3
	SRX514164 (SRR1228264_2)	20259942	
	SRX514164 (SRR1228264_2)	19300558	

Fusarium graminearum Infection Combined with ABA or GA[g]			
Details	**Experiment ID (ENA SRA ID)**	**Total reads**	**Number of replicates**
Water Treatment - Control	SRX6891182 (SRR10166415_2)	42321500	5
	SRX6891186 (SRR10166416_2)	43072768	
	SRX6891187 (SRR10166417_2)	41150383	
	SRX6891188 (SRR10166418_2)	37415527	
	SRX6891189 (SRR10166419_2)	43180561	
Fusarium-challenged 1 day post-inoculation (dpi)	SRX6891190 (SRR10166420_2)	46206887	5
	SRX6891191 (SRR10166421_2)	44390773	
	SRX6891192 (SRR10166422_2)	52339381	
	SRX6891193 (SRR10166423_2)	36888430	
	SRX6891194 (SRR10166424_2)	40072043	
GA-primed; Fusarium-challenged (1 dpi)	SRX6891195 (SRR10166425_2)	42505271	5
	SRX6891196 (SRR10166426_2)	28866105	
	SRX6891197 (SRR10166427_2)	43114476	
	SRX6891198 (SRR10166428_2)	42556091	
	SRX6891199 (SRR10166429_2)	46742428	
1mM (+)-Abscisic acid (ABA)	SRX6891200 (SRR10166430_2)	32125366	5
	SRX6891201 (SRR10166431_2)	33468068	
	SRX6891183 (SRR10166432_2)	27559871	
	SRX6891184 (SRR10166433_2)	37040495	
	SRX6891185 (SRR10166434_2)	16436795	
ABA-primed; Fusarium-challenged (1 dpi)	SRX6891167 (SRR10166400_2)	27562778	5
	SRX6891168 (SRR10166401_2)	32546973	
	SRX6891169 (SRR10166402_2)	36438469	
	SRX6891170 (SRR10166403_2)	43190266	
	SRX6891171 (SRR10166404_2)	32026563	
1mM(+)-Gibberellic acid (GA)	SRX6891172 (SRR10166405_2)	57942903	5
	SRX6891173 (SRR10166406_2)	17522309	
	SRX6891174 (SRR10166407_2)	18097151	
	SRX6891175 (SRR10166408_2)	26190073	
	SRX6891176 (SRR10166409_2)	34981271	
ABA-signaling inhibitor-primed (AS6); Fusarium-challenged (1 dpi)	SRX6891177 (SRR10166410_2)	26015115	5
	SRX6891178 (SRR10166411_2)	36003314	
	SRX6891179 (SRR10166412_2)	17945892	
	SRX6891180 (SRR10166413_2)	30121702	
	SRX6891181 (SRR10166414_2)	21462353	
Note: All data retrieved from Array Express at EMBL-EBI			
[a] Pingault et al., 2015; Bioproject PRJEB5314			
[b] Liu et al., 2015; NCBI Bioproject PRJNA257938			
[c] Li et al., 2015; NCBI Bioproject PRJNA253535			
[d] Mega et al., 2019; NCBI Bioproject PRJNA316081			
[e] Steiner et al., 2017; NCBI Bioproject PRJEB12358			
[f] Zhang et al., 2014; NCBI Bioproject PRJNA243835			
[g] Buhrow et al., 2021; NCBI Bioproject PRJNA573726			

Table S2. *Triticum aestivum Pirin* gene annotation accuracy table.

Gene	Homeolog	Ensembl Plants Accession	Annotation Accuracy	TSA Accessions	Nucleotide Sequence Comparison
Ta-*Pirin-1*	A	TraesCS4A02G336200.1*	Supported by TSA entries and the D homeolog copy.	GFFI01048533.1	100% coverage; 100% identity
				GILY01013465.1	100% coverage; 100% identity
		TraesCS4A02G336200.2	Incorrect sequence; has an extra 29 a.a in the N-terminal compared to the D copy.		
	B	TraesCS5B02G536000.2*	EST support for the extra 29 a.a; these are part of an exon in this copy whereas in the A copy they are an intron.	GILY01027417.1	100% coverage; 100% identity
		TraesCS5B02G536000.1	Incorrect sequence; lacks 29 a.a that are known to be part of the expressed sequence.		
	D	TraesCS5D02G533500	Ensembl-curated start codon of TraesCS5D02G533500.1 is incorrect. TSA support shows protein starts further upstream and is further supported by homeologous sequences.	GILY01031085.1	100% coverage; 100% identity
				GILY01031086.1	100% coverage; 100% identity
Ta-*Pirin-2*	A	TraesCS4A02G336000.1*	Used ESTs and TSAs from *H. vulgare* , *B. distachyon* and *O. sativa* to find and verify. The B and D copies both begin with MLRQ compared to the MSSS in the A copy, and have 72 and 61 more amino acids, respectively, at the beginning of their N-terminal domains.	AK248948.1 (Barley EST), GFJC01008957.1 and GFJB01016295.1 (Brachypodium TSA), AK105971.1 and BAG97473.1 (*Oryza sativa* OS-PIRIN2 ESTs)	
		TraesCS4A02G336000.2	Incorrect sequence; only 82% a.a identity with the curated A copy.		
	B	TraesCS5B02G535700.3*	Used ESTs and TSAs from *H. vulgare* , *B. distachyon* and *O. sativa* to find and verify. Protein sequence matches the curated sequence with 100% identity.		
		TraesCS5B02G535700.1	Incorrect sequence; large gap in a.a alignment resulting in 92% identity.		
		TraesCS5B02G535700.2	Incorrect sequence; large gap in a.a alignment resulting in 92% identity.		
	D	TraesCS5D02G533200	Ensembl-curated start codon of TraesCS5D02G533200.1 is incorrect. Comparison of the protein length to the homeologous B copy suggests the start codon is further upstream, starting with MLRQ.		
Ta-*Pirin-3*	A	TraesCS4A02G335900.1*	Has a TSA sequence to support gene expression; the B and D homeologous copies display longer and more accurate N-terminals.	GILY01013453.1	100% coverage; 99% identity
	B	TraesCS5B02G535800.1	Supported by a TSA entry. Gene structure similar to homeologous D copy.	GILY01027409.1	97% coverage; 99% identity
	D	TraesCS5D02G533100.1*	Supported by TSA entries.	GILY01031079.1	100% coverage; 100% identity
				GILY01031078.1	94% coverage; 100% identity
Ta-*Pirin-4*	A	TraesCS5A02G262700	Ensembl-curated start codon of TraesCS5A02G262700.1 is incorrect. TSA support shows the protein starts further downstream, with the same 6 beginning codons.	GIJS01150985.1	88% coverage; 96% identity
	B	TraesCS5B02G261100.1*	Supported by TSA entry. Consistent with homeologous D copy.	GILY01025833.1	100% coverage; 100% identity
	D	TraesCS5D02G270300	Ensembl-curated start codon of TraesCS5D02G270300.1 is incorrect. TSA support shows the protein starts further upstream, similar to the homeologous B copy.	GILY01029555.1	100% coverage; 100% identity
Ta-*Pirin-5*	A	TraesCS1A02G391900.1*	Supported by TSA entries.	GILY01006401.1	100% coverage; 100% identity
				GIJS01064281.1	100% coverage; 100% identity
				GFFI01049354.1	100% coverage; 100% identity
	B	TraesCS1B02G420000.1*	Supported by TSA entries.	GILY01040388.1	100% coverage; 100% identity
				GFFI01042348.1	100% coverage; 100% identity
	D	TraesCS1D02G400000.1*	Supported by TSA entries.	GILY01053162.1	100% coverage; 100% identity
				GILY01053161.1	100% coverage; 100% identity
Ta-*Pirin-6*	A	TraesCS4A02G336100.1*	Supported by TSA entries.	GILY01013459.1	100% coverage; 100% identity
				GILY01013458.1	100% coverage; 100% identity
	B	TraesCS5B02G535900.1*	Supported by TSA entries.	GILY01027411.1	100% coverage; 100% identity
				GILY01027412.1	100% coverage; 100% identity
	D	TraesCS5D02G533400.1*	Supported by TSA entries.	IAAL01004437.1	100% coverage; 100% identity
				GILY01031080.1	100% coverage; 100% identity

* Correctly curated homeolog sequence

a.a = amino acid

Note - Annotation accuracy refers to TSA and EST support, as well as consistencies in amino acid sequences between homeologs. Nucleotide sequence comparison is the identity and coverage between the Ensembl Plants accession and the TSA accessions.

Table S3. *Pirin* exon and intron lengths.

																	Position	
Gene	**Genome**	**Ensembl ID**	**Exon 1**	**Intron 1**	**Exon 2**	**Intron 2**	**Exon 3**	**Intron 3**	**Exon 4**	**Intron 4**	**Exon 5**	**Intron 5**	**Exon 6**	**Intron 6**	**Exon 7**	**Intron 7**	**Exon 8**	**Start**	**End**
Ta-*Pirin-1*	A	TraesCS4A02G336200.1	252	87	139	106	118	104	63	109	104	103	729					618528278	618530191
	B	TraesCS5B02G536000.1	452	106	118	132	63	113	104	107	735							691941430	691943360
	D	TraesCS5D02G533500.1	270	84	142	101	118	128	63	110	104	84	732					547924781	547926716
Ta-*Pirin-2*	A	TraesCS4A02G336000.1	253	119	118	124	63	99	104	132	687							618417529	618419227
	B	TraesCS5B02G535700.3	386	87	118	104	63	111	104	132	704							691772250	691774058
	D	TraesCS5D02G533200.1	321	88	118	108	63	111	104	132	689							547882596	547884329
Ta-*Pirin-3*	A	TraesCS4A02G335900.1	166	106	118	65	63	111	104	104	734							618411671	618412941
	B	TraesCS5B02G535800.1	400	113	118	94	63	92	104	104	822							691796890	691798749
	D	TraesCS5D02G533100.1	392	92	118	118	63	111	104	105	721							547839680	547841503
Ta-*Pirin-4*	A	TraesCS5A02G262700.1	338	93	68	534	167	89	724									475749396	475751408
	B	TraesCS5B02G261100.1	385	101	68	403	167	102	731									445593654	445595610
	D	TraesCS5D02G270300.1	321	101	68	497	167	102	732									373950987	373952974
Ta-*Pirin-5*	A	TraesCS1A02G391900.1	278	906	144	82	50	824	39	142	29	93	63	302	104	77	760	558550095	558553987
	B	TraesCS1B02G420000.1	269	930	141	90	50	691	39	132	29	125	63	368	104	77	854	643174307	643178268
	D	TraesCS1D02G400000.1	264	1308	144	85	50	790	39	139	29	95	63	347	104	77	751	466425820	466430104
Ta-*Pirin-6*	A	TraesCS4A02G336100.1	227	119	118	92	63	106	104	95	709							618463055	618464687
	B	TraesCS5B02G535900.1	364	85	118	118	63	106	104	112	704							691823839	691825612
	D	TraesCS5D02G533400.1	339	111	118	92	63	97	104	112	713							547891364	547893112

Note: For the Ta-*Pirin-3-A* copy 50 nucleotides *(*nt) upstream of the start codon and 250 nt downstream of the stop codon were taken as a UTR based on the similarity to the 3D copy.

For the Ta-*Pirin-3-B copy* 50 nt upstream of start codon were taken as a UTR based on similarity to the 3D copy.

Position refers to the co-ordinates of the *Pirin* on the chromosome according to Ensembl Plants.

The first and last exon lengths include the 5' and 3' UTR.

Table S4. More information on the *Pirin* homologs in other species.

Species	Annotation	Ensembl Transcript	NCBI mRNA accession	Contig created for verification	Published	Translation Consistency between Ensembl and NCBI
Aegilops tauschii	Aet-*Pirin-1*	AET5Gv21181500.2	XM_020295357.2	No	Unpublished	Same translation
	Aet-*Pirin-2*	N/A[a]	XM_020332498.2	No	Unpublished	N/A
	Aet-*Pirin-3*	N/A[a]	XM_020332496.1	No	Unpublished	N/A
	Aet-*Pirin-4*	AET5Gv20617100.1	XM_020317344.2	No	Unpublished	Same translation
	Aet-*Pirin-5*	AET1Gv20942800.8	XM_020314636.2	No	Unpublished	First 57 nucleotide missing on Ensembl Plant transcript
	Aet-*Pirin-6*	N/A[a]	XM_045229367.1	No	Unpublished	N/A
Arabidopsis thaliana	At-*Pirin-1*	At3G59220.1	NM_115784	No	Lapik and Kaufman, 2003	Same translation
	At-*Pirin-2*	At2G43120.1	NM_180054.2	No	Lapik and Kaufman, 2003	Same translation
	At-*Pirin-3*	At3g59260.1	NM_115788	No	Lapik and Kaufman, 2003	Same translation
	At-*Pirin-4*	At1g50590.1	NM_103941	No	Lapik and Kaufman, 2003	Same translation
Brachypodium distachyon	Bd-*Pirin-1*	KQK12152*	XM_003559102.4	No	Bandaranayake et al., 2012 (Brachypodium distachyon 27723)[b]	Same translation
	Bd-*Pirin-2*	KQJ90728	XM_003578272.4	No	Bandaranayake et al., 2012 (Brachypodium distachyon 19468)[b]	Same translation
	Bd-*Pirin-3*	KQJ96236	XM_003571641.4	Yes	Bandaranayake et al., 2012 (Brachypodium distachyon 251)[b]	Same translation
Hordeum vulgare	Hv-*Pirin-1*	HORVU5Hr1G120800.6	N/A	Yes	Unpublished	N/A
	Hv-*Pirin-2*	HORVU5Hr1G120790.2	N/A	No	Unpublished	N/A
	Hv-*Pirin-3*	HORVU5Hr1G120780.2 HORVU5Hr1G120780.3	N/A	No	Unpublished	N/A
	Hv-*Pirin-4*	HORVU5Hr1G072760.2	N/A	Yes	Unpublished	N/A
	Hv-*Pirin-5*	HORVU1Hr1G086450.9	N/A	Yes	Unpublished	N/A
	Hv-*Pirin-6*	HORVU5Hr1G120810.1	N/A	No	Unpublished	N/A
Oryza Sativa	Os-*Pirin-1*	N/A	XM_015775675.2	No	Park et al.,2018 (Os03g62790)	Same translation
	Os-*Pirin-2*	N/A	XM_015795946.2	No	Bandaranayake et al., 2012 (Os09g31120)	Same translation
	Os-*Pirin-3*	N/A	XM_015795108.2	No	Bandaranayake et al., 2012 (Os08g27720)	Same translation
Sorghum bicolor	Sb-*Pirin-1*	N/A	XM_021447321.1	No	Bandaranayake et al., 2012 (sb01g0014701)	Same translation
	Sb-*Pirin-2*	N/A	XM_002460396.2	No	Bandaranayake et al., 2012 (sb02g0281801)	Same translation
	Sb-*Pirin-3*	N/A	XM_002445342.2	No	Bandaranayake et al., 2012 (sb07g0150301)	Same translation
Zea mays	Zm-*Pirin-1*	T001	NM_001157180.2	No	Bandaranayake et al., 2012 (Zea mays 16282)[b]	Same translation
	Zm-*Pirin-2*	T002	NM_001138144.1	Yes	Bandaranayake et al., 2012 (Zea mays 39858)[b]	Same translation
	Zm-*Pirin-3*	T001	BT038257.1	No	Unpublished	Same translation
	Zm-*Pirin-4*	N/A	PWZ04198.1	Yes	Bandaranayake et al., 2012 (Zea mays 8062)[b]	Y to S at amino acid position 142
	Zm-*Pirin-5*	T001	XM_008648943.1	Yes	Bandaranayake et al., 2012 (Zea mays 26059)[b]	Same translation

[a] The annotation of these Aegilops *Pirin* sequences are deficient at the Ensembl Plant database.

[b] The database for these *Pirin* accession numbers remains unknown and therefore assignment to the *Pirin* sequences within this table is uncertain.

* This transcript has an 87 nucleotide insertion relative to transcript KQK12151, however it is the transcript with the highest confidence since it has both EST and TSA support.

N/A = not applicable

Table S4A. EST and TSA sequences used to build contigs.

Species	Ensembl Accession	EST Sequence ID	TSA Sequence ID
Brachypodium distachyon	BRADI_3g21730v3	HX819382.1, HX808969.1, HX827411.1, HX852625.1, HX858288.1, HX838106.1, HX848065.1	
Hordeum vulgare	HORVU5Hr1G120800	DK808076.1, DK781130.1, DN189147.1, DK772747.1, CB860040.1, CK568981.1, DK800690.1, DN188566.1, FD527179.1, DK799029.1, DN183035.1, CK568752.1, DK838562.1, CK565707.1, CD056301.1, CD054481.1, DN182228.1, DK678585.1, DK642715.1, DK689212.1, DK690123.1, DK616542.1, DK655444.1, CA021125.1, CB879285.1	
	HORVU1Hr1G086450	GGCM01054308.1, BU996108.1, DK603040.1, BM370560.2, DK783118.1, DK781469.1	GGCM01054308.1, GGCT01067731.1
	HORVU5Hr1G072760	DK681405.1, DK831992.1, DK678585.1, DN182228.1	GGCO01028087.1, GGDP01011155.1, GFJO01075144.1, GGCT01061186.1, GGDG01043445.1
Zea mays	Zm00001d009514	CF059539.1, DV529331.1, DR793224.1, EB639592.1, EB401161.1, EB158377.1, DY540079.1, CO529753.1, DV541421.1, DV024050.1, DT945966.1, DT644257.1, DV536465.1, FK972847.1, CK367875.1, FK958663.1, FK958665.1, FK958664.1, FL033315.1, DR820283.1, FL033316.1, EB160746.1, FK958662.1, FK958661.1, FK972846.1, DY236829.1, DR957974.1	
	Zm00001d009514	EB160746.1, GECR01000700.1, GECS01001584.1	GGGX01014931.1, GGGU01022649.1, GECS01001502.1, GECR01000700.1, GECS01001584.1
	Zm00001d020915	GECR01015888.1, GECS01018354.1, CO526041.1, GGGX01033021.1, CK986123.1, CK986289.1, BM337874.1, DR811423.1, CO526042.1, GGGX01009559.1, DR811424.1	
	Zm00001d034829	EB401161.1, FK958665.1, FK972847.1, FK958664.1, DV529331.1, DV024050.1, DT644257.1, DV541421.1, DY236829.1, DT945966.1, DR793224.1, DR793223.1, CF635726.1	

Table S5. *Pirin* gene expression in tissues of *T. aestivum* in reads per kilobase per million (RPKPM).

	Leaf[a]	Seed[b]	Root[c]	Stem[d]	Inflorescence[e]
Ta-*Pirin-1-A*	2.90	0.51	5.98	8.08	1.65
Ta-*Pirin-1-B*	1.72	0.79	9.21	11.96	1.32
Ta-*Pirin-1-D*	1.48	0.53	6.67	8.21	1.59
Ta-*Pirin-2-A*	0.00	0.08	0.16	0.00	0.05
Ta-*Pirin-2-B*	0.05	0.00	0.42	0.00	0.00
Ta-*Pirin-2-D*	0.05	0.00	1.20	0.04	0.00
Ta-*Pirin-3-A*	0.00	0.00	0.00	0.00	0.00
Ta-*Pirin-3-B*	0.35	0.03	1.91	0.33	0.07
Ta-*Pirin-3-D*	0.04	0.00	0.78	0.22	0.00
Ta-*Pirin-4-A*	0.06	0.00	0.70	0.89	0.11
Ta-*Pirin-4-B*	0.16	0.00	1.00	1.99	0.00
Ta-*Pirin-4-D*	0.04	0.00	0.45	0.80	0.03
Ta-*Pirin-5-A*	0.51	0.00	7.43	2.05	0.24
Ta-*Pirin-5-B*	0.91	0.00	11.01	2.29	0.32
Ta-*Pirin-5-D*	1.73	0.00	14.53	2.59	0.68
Ta-*Pirin-6-A*	0.00	0.07	0.24	0.08	0.00
Ta-*Pirin-6-B*	0.00	0.12	0.51	0.06	0.00
Ta-*Pirin-6-D*	0.09	0.00	0.60	0.97	0.14

Note: Data from Pingault et al., 2015.

[a] whole plant fruit formation stage 30 to 50%

[b] whole plant at the ripening stage

[c] cotyledon emergence stage

[d] two nodes or internodes visible stage

[e] maximum stem length reached stage

Table S6. Tissue-specific expression of the *Pirin* gene family in 71 tissues of the *Triticum aestivum* cultivar Azhurnaya.

	Ta-*Pirin*-1-A		Ta-*Pirin*-1-B		Ta-*Pirin*-1-D		Ta-*Pirin*-2-A		Ta-*Pirin*-2-B		Ta-*Pirin*-2-D		Ta-*Pirin*-3-A		Ta-*Pirin*-3-B		Ta-*Pirin*-3-D		Ta-*Pirin*-4-A	
Tissue Type	Expression	SD	Expression	SD	Expression	SD	Expression	SD	Expression	SD	Expression	SD	Expression	SD	Expression	SD	Expression	SD	Expression	SD
First leaf sheath - Tillering stage	10.09	1.27	13.82	2.24	10.05	1.26	0.51	0.53	0.23	0.24	0.16	0.05	1.28	1.12	3.56	1.76	0.38	0.32	2.75	0.55
Internode #2 - Milk grain stage	7.55	0.74	7.57	1.46	9.63	0.97	0.26	0.03	0.02	0.02	0.18	0.03	1.15	0.16	2.71	0.01	0.45	0.17	2.05	1.71
Shoot apical meristem - Seedling stage	2.12	0.21	2.91	0.15	3.11	0.17	0.15	0.05	0.05	0.02	0	0	0.18	0.08	0.68	0.09	0.13	0.06	0.08	0.06
Grain - Milk grain stage	1.14	0.35	2.12	0.34	1.53	0.38	0.02	0.03	0.01	0.02	0.06	0.04	0.02	0.03	0.1	0.02	0.02	0.03	0.14	0.06
First leaf blade - Seedling stage	4.75	1.59	4.92	1.86	5.17	1.9	0.09	0.11	0.05	0.03	0.13	0.04	0.31	0.11	0.63	0.07	0.18	0.16	1.63	0.98
Flag leaf blade - Full boot	2.62	0.34	0.96	0.25	1.37	0.32	0.04	0.04	0	0	0.02	0.02	0.07	0.06	0.2	0.2	0.07	0.07	0.09	0.07
Awn - 50 percent spike	7.6	2.27	7.61	2.09	6.43	1.6	0	0	0	0	0.09	0.01	0.36	0.11	0.24	0.2	0.21	0.03	1.52	0.56
flag leaf blade night (-0.25h) 06:45	3.55	0.66	2.41	0.71	2.7	0.15	0.05	0.03	0.03	0.03	0.02	0.02	0.15	0.08	0.61	0.27	0.08	0.03	0	0
Shoot axis - Flag leaf stage	1.97	0.11	3.16	0.08	2.79	0.37	0.16	0.08	0.1	0.07	0.04	0.05	0.22	0.08	1.52	0.66	0.03	0.01	0.17	0.1
Fifth leaf blade - Flag leaf stage	2.94	0.21	1.21	0.37	1.19	0.58	0	0	0	0	0	0	0.02	0.02	0.21	0.04	0.01	0.01	0.37	0.53
Third leaf sheath - Three leaf stage	2.85	0.25	3.83	1.05	5.31	1.59	0.07	0.04	0.06	0.02	0.03	0	0.16	0.05	0.56	0.19	0.1	0.05	0.14	0.1
Internode #2 - Ear emergence	6.04	0.67	5.15	0.62	7.27	3.89	0.18	0.09	0.06	0.05	0.11	0.08	0.75	0.47	2.15	0.93	0.41	0.28	2.12	2.52
Anther	13.59	4.15	20.55	5.9	30.68	6.72	0.12	0.09	0.01	0.01	0.02	0.02	0.02	0.03	0.42	0.21	0.32	0.07	3.77	1.01
Spike	1.65	0.68	1.15	0.27	1.96	0.73	0.05	0.03	0	0	0.03	0.02	0.3	0.13	0.08	0.02	0.06	0.02	0.16	0.11
Coleoptile	3.63	0.94	4.82	2.17	5.28	2.07	0.08	0.01	0.03	0.03	0.06	0.07	0.14	0.1	0.47	0.36	0.18	0.06	0.67	0.5
Stigma and Ovary	2.07	0.75	2	0.4	2.76	0.69	0.08	0.06	0.07	0.05	0.12	0.1	0.03	0.05	0.1	0.04	0.12	0.08	0.1	0.07
Roots - Flag leaf stage	4.06	0.45	5.14	0.23	3.92	0.25	0.51	0.08	0.07	0.05	0.41	0.33	0.64	0.15	3.37	0.33	0.18	0.07	1.16	0.29
Fifth leaf sheath - Flag leaf stage	9.57	2.95	9.03	2.27	11.39	4.85	0.03	0.04	0.02	0.03	0	0	0.24	0.17	0.55	0.29	0.03	0.02	2.91	0.87
Root apical meristem - Three leaf stage	1.61	0.8	3.75	1.21	4.48	1.54	0.23	0.05	0.05	0.05	0.07	0.03	0.25	0.15	0.66	0.2	0.17	0.11	0.1	0.07
Flag leaf sheath - Ear emergence	4.58	0.25	3.46	0.34	3.78	0.48	0.01	0.01	0.02	0.02	0.05	0.06	0.15	0.06	0.58	0.13	0.11	0.03	0.11	0.13
Roots - Three leaf stage	3.36	1.11	4.42	1.25	3.82	0.61	0.34	0.22	0.07	0.02	0.4	0.36	0.62	0.32	1.9	0.96	0.13	0.02	0.37	0.19
Axillary roots - Three leaf stage	3.32	0.82	6.9	2.09	7.99	1.89	0.11	0.04	0.06	0.07	0.06	0.02	0.48	0.27	2	1.23	0.11	0.03	0.19	0.08
Flag leaf sheath - 50 percent spike	4.04	0.21	2.29	0.28	2.44	0.39	0.03	0.04	0.03	0	0.04	0.04	0.08	0.06	0.54	0.13	0	0	0.16	0.06
Radicle - Seedling stage	4.8	1.44	8.09	2.18	9.11	2.35	0.33	0.21	0.13	0.07	0.12	0.06	0.78	0.68	1.37	0.89	0.57	0.18	0.93	0.28
Roots - 50 percent spike	3.32	0.33	6.23	1.8	4.92	1.23	0.84	0.46	0.08	0.02	0.81	0.6	0.74	0.25	3.87	0.75	0.73	0.6	1.28	0.29
Third leaf blade - Three leaf stage	2.58	1.72	2.72	2.2	3.03	3.36	0.04	0.04	0	0	0.02	0.01	0.08	0.06	0.34	0.26	0.06	0.06	0.42	0.56
Spikelets - 50 percent spike	8.52	2.25	8.54	2.12	7.34	1.9	0.04	0.04	0.05	0.01	0.01	0.02	0.34	0.02	0.13	0.04	0.31	0.08	1.42	0.91
Root apical meristem - Tillering stage	2.26	0.82	2.85	0.55	4.57	0.79	0.22	0.2	0	0	0.07	0.05	0.22	0.1	0.76	0.28	0.21	0.06	0.22	0.07
Grain - Ripening stage	1.31	0.12	1.01	0.21	1.06	0.55	0.03	0.04	0	0	0.05	0.07	0.23	0.07	0.14	0.1	0.07	0.05	0.18	0.26
Awns - Ear emergence	3.09	0.66	1.73	0.46	2.21	0.02	0.04	0.03	0.04	0.06	0.05	0.04	0.03	0.03	0.36	0.12	0.14	0.06	0.17	0.06
Glumes	8.61	1.11	7.37	1.97	6.92	1.79	0.21	0.05	0.1	0.06	0.09	0.13	1.07	0.48	0.85	0.32	0.73	0.31	2.58	0.76
Glumes - Ear emergence	9.09	0.83	7.12	1.8	6.22	1.27	0.1	0.05	0.11	0.06	0.06	0.03	0.64	0.44	0.95	0.41	0.61	0.25	3.38	1.23
Leaf ligule	4.31	0.43	2.53	0.46	2.83	0.54	0	0	0.04	0.03	0	0	0.08	0.08	0.34	0.1	0	0	0.12	0.05
Flag leaf blade - 50 percent spike	2.63	0.25	1.3	0.32	1.34	0.11	0.04	0.03	0.01	0.01	0.06	0.03	0.29	0.2	0.19	0.04	0.08	0.09	0.06	0.04
Internode #2 - 50 percent spike	5.83	1.29	6.03	1.09	7.16	1.51	0.22	0.04	0.07	0.03	0.21	0.12	0.31	0.02	1.75	0.14	0.27	0.19	0.88	0.21
Fifth leaf sheath - Fifth leaf stage	2.15	0.31	2.41	0.33	3.4	0.47	0.08	0.04	0.05	0.01	0.04	0.01	0.27	0.05	0.56	0.17	0.03	0.05	0.11	0.03
fifth leaf blade night (-0.25h) 21:45	5.78	0.82	1.67	0.4	2.24	0.16	0	0	0	0	0	0	0.32	0.11	0.62	0.14	0.11	0.13	0.06	0.06
Grain - Soft dough	0.52	0.07	1.73	0.74	1.2	0.53	0	0	0	0	0.03	0.03	0.03	0.02	0.1	0.09	0.01	0.01	0.38	0.38
Flag leaf blade (senescence) - Dough stage	3.32	0.3	1.8	0.24	2.22	0.45	0.01	0.02	0.03	0.03	0.15	0.05	0.09	0.07	0.57	0.03	0.05	0.03	0.05	0.01
Flag leaf blade night (-0.25h) 06:45 - Flag leaf stage	5.06	0.91	3.48	0.96	6.08	2.47	0.07	0.09	0.02	0.01	0.01	0.02	0.16	0.07	0.21	0.08	0.08	0.05	1.18	0.89
Flag leaf blade (senescence) - Ripening stage	4.87	0.64	4.01	0.06	3.8	0.24	0.1	0.06	0.06	0.01	0.06	0.01	0.14	0.14	0.28	0.04	0	0	0.56	0.03
First leaf blade - Tillering stage	8.48	4.21	4.49	1.98	3.08	1.83	0.04	0.03	0.18	0.13	0.15	0.12	0.12	0.11	0.82	0.4	0.11	0.09	0.28	0.4
Shoot apical meristem - Tillering stage	2.38	0.55	4.35	0.69	3.93	0.14	0.17	0.11	0	0	0.04	0.03	0.61	0.24	1.14	0.55	0.33	0.11	0.84	0.93
Shoot axis - First leaf stage	4.89	1.3	7.62	2.37	8.78	3.32	0.08	0.04	0.01	0.02	0.07	0.03	0.1	0.07	0.39	0.11	0.13	0.03	1.45	0.49
Roots - Seedling stage	3.13	0.81	6.78	1.82	7.82	2.44	0.08	0.08	0.08	0.1	0.09	0.07	0.42	0.37	1.24	0.39	0.27	0.19	0.61	0.52
Shoot axis - Milk grain stage	6.22	0.99	7.43	1.62	7.05	1.23	0.33	0.06	0.03	0.04	0.07	0.05	0.8	0.46	2.13	0.74	0.42	0.41	0.56	0.23
Fifth leaf blade - Fifth leaf stage	2.93	0.6	2.3	0.59	2.53	1.31	0.03	0.04	0	0	0.06	0.09	0.03	0.02	0.44	0.07	0.04	0.03	0.76	0.51
Flag leaf blade - Ear emergence	3.47	0.08	1.93	0.36	2.33	0.27	0.05	0.05	0.06	0.06	0.1	0.07	0.12	0.05	0.4	0.03	0.03	0.03	0	0
flag leaf blade night (+0.25h) 07:15	6.38	0.35	6.56	0.39	10	1.07	0.05	0.02	0.04	0.03	0	0	0.28	0.14	0.46	0.1	0.08	0.01	2.56	0.1
Fifth leaf blade night (-0.25h) 21:45	6.43	0.11	2.05	0.23	2.86	0.62	0.03	0.03	0	0	0.03	0.04	0.13	0.09	0.69	0.11	0.05	0.01	0.08	0.07
Shoot axis - Tillering stage	2.24	0.59	3.12	1.26	3.17	0.32	0.21	0.09	0.05	0.04	0.07	0.04	0.39	0.15	1.06	0.54	0.13	0.03	0.31	0.17
Stem axis - First leaf stage	4.89	1.3	7.62	2.37	8.78	3.32	0.08	0.04	0.01	0.02	0.07	0.03	0.1	0.07	0.39	0.11	0.13	0.03	1.45	0.49
Endosperm	0.53	0.29	0.74	0.25	0.85	0.49	0.01	0.01	0	0	0	0	0.05	0.07	0.21	0.04	0	0	0.24	0.22
Peduncle	4.55	0.34	2.24	0.61	5.62	1.12	0.12	0.09	0	0	0.09	0.08	0.19	0.14	0.49	0.26	0.07	0.08	0.2	0.14
Peduncle - 50 percent spike	7.65	2.43	5.48	1.77	10.46	3.85	0.04	0.04	0.01	0.01	0.08	0.02	0.2	0.15	0.12	0.03	0.13	0.18	4.29	1.32
Peduncle - Ear emergence	13.66	2.96	10.62	3.34	19.2	3.5	0	0	0.01	0.01	0.05	0.04	0.21	0.2	0.2	0.12	0.06	0.05	10.73	6.27
Flag leaf sheath - Full boot	4.35	0.87	3.49	0.67	3.59	0.93	0.01	0.02	0.01	0.02	0.02	0.03	0.09	0.12	0.34	0.21	0.09	0.08	1.76	1.07
Flag leaf blade - Flag leaf stage	2.98	1.02	2.37	1.48	2.91	2.19	0.03	0.03	0	0	0.03	0.02	0.09	0.07	0.23	0.03	0.02	0.03	0.61	0.69
Lemma	11.35	2.29	11.96	2.67	8.82	1.95	0.78	0.28	0.04	0.05	0.16	0.03	2.91	1.41	1.52	0.41	1.18	0.27	4.99	2.06
Lemma - Ear emergence	11.14	1.41	10.93	2.58	7.82	1.2	0.39	0.19	0.03	0.02	0.03	0.03	0.89	0.12	1.35	0.13	0.99	0.27	4.34	1.69
Awns - Milk grain stage	4.94	0.64	4.08	0.66	4.31	0.59	0.07	0.03	0.14	0.08	0.06	0.06	0.32	0.19	0.61	0.13	0.35	0.14	0.5	0.21
fifth leaf blade night (+0.25h) 22:15	7.31	0.94	2.2	0.58	2.74	0.52	0	0	0.01	0.01	0.03	0.02	0.15	0.08	0.45	0.22	0.07	0.08	0.17	0.15
Flag leaf blade - Milk grain stage	3.41	0.75	2.63	0.4	3.36	0.29	0.01	0.02	0.07	0.08	0.08	0.04	0.13	0.01	0.41	0.2	0.07	0.06	0	0
Grain - Hard dough	3.47	3.78	8.89	9.71	4.77	4.79	0.11	0.09	0.06	0.09	0.01	0.02	0.49	0.21	0.15	0.15	0.16	0.18	2.13	2.15
Flag leaf sheath - Milk grain stage	3.95	0.07	3.72	0.7	3.58	0.82	0.06	0.02	0.02	0.03	0.06	0.04	0.43	0.21	0.71	0.1	0.07	0.01	0.09	0.08
Embryo proper	0.58	0.1	0.87	0.25	0.71	0.17	0.17	0.04	0.02	0.04	0	0	0.32	0.11	0.03	0.05	0.06	0.06	0.44	0.24
Fifth leaf blade (senescence) - Milk grain stage	5.09	0.99	3.31	0.63	3.14	0.97	0.15	0.02	0.09	0.06	0.05	0.04	0.17	0.02	1.06	0.44	0.09	0.02	0.06	0.04
Roots - Tillering stage	3.95	0.48	6.79	0.52	6.86	0.39	0.47	0.16	0.12	0.06	0.28	0.13	0.73	0.13	1.56	0.34	0.58	0.12	3.07	0.52
Shoot axis - Full boot	2.12	0.31	3.6	1.49	3.42	0.97	0.33	0.18	0.09	0.12	0.09	0.06	0.55	0.54	1.65	1.44	0.03	0.02	0.55	0.4
Fifth leaf blade - Ear emergence	4.13	1.19	2.46	0.87	2.24	1.24	0.06	0.07	0.08	0.08	0.11	0.09	0.15	0.1	0.46	0.06	0.04	0.03	0.03	0.03
First leaf sheath - Seedling stage	7.81	4.52	16.11	14.78	16.23	11.55	0.06	0.02	0.01	0.02	0.03	0.04	0.4	0.36	0.85	0.54	0.15	0.1	2.83	2.17

Triticum aestivum Pirin expression from the wheat cultivar Azhurnaya grown in cabinets with 16:8 hours day:night length at 25:15℃. There are three biological replicates with five individual plants each. Expression is represented in Transcripts per Million (TPM) (Ramírez-González et al., 2018; Winter et al., 2007)
SD = standard deviation.

Ta-*Pirin-4 -B*		Ta-*Pirin-4 -D*		Ta-*Pirin-5 -A*		Ta-*Pirin-5 -B*		Ta-*Pirin-5 -D*		Ta-*Pirin-6 -A*		Ta-*Pirin-6-B*		Ta-*Pirin-6 -D*	
Expression	SD	Expression	SD	Expression	SD	Expression	SD	Expression	SD	Expression	SD	Expression	SD	Expression	SD
2.71	0.51	3.71	0.62	5.05	6	7.13	8.98	7.3	8.94	0.58	0.41	0.33	0.24	1.31	0.26
3.08	2.72	2.26	1.91	0.25	0.01	0.2	0.12	0.24	0.15	0.26	0.01	0.37	0.13	2.28	0.19
0.21	0.04	0.19	0.13	1.44	0.44	0.77	0.07	1.09	0.16	0.49	0.11	0.14	0.04	0.57	0.12
0.12	0.07	0.75	0.07	0.05	0.04	0.05	0.03	0.53	0.35	0.11	0.02	0.09	0.06	0.39	0.12
0.96	0.51	1.55	0.25	7.56	6.87	6.25	5.89	10.74	11.59	0.15	0.07	0.08	0.06	0.38	0.12
0.3	0.13	0.21	0.08	2.14	0.31	0.95	0.31	1.34	0.67	0.02	0.03	0.03	0.03	0.69	0.28
0.77	0.49	2.97	1.22	0.79	0.34	0.49	0.37	1.67	0.93	0.11	0.05	0.1	0.07	0.21	0.04
0.05	0.05	0	0	0.68	0.21	0.53	0.33	0.46	0.08	0.2	0.07	0.08	0.06	1.11	0.16
0.21	0.01	0.18	0.04	1.43	0.76	0.86	0.36	0.73	0.34	0.46	0.15	0.3	0.2	0.5	0.22
0.37	0.5	0.66	0.89	1.22	0.69	0.96	0.65	1.01	0.84	0.14	0.06	0.01	0.02	0.6	0.19
0.28	0.11	0.32	0.24	0.6	0.21	0.51	0.29	0.9	0.47	1.01	0.27	0.18	0.14	0.92	0.13
1.72	1.51	1.51	1.86	1.74	1.17	1.35	1.28	1.6	1.46	0.14	0.11	0.18	0.09	1.99	0.46
6.77	2.12	7.36	2.41	23.06	9.56	20.57	8.62	45.21	13.59	0.25	0.15	0.15	0.08	0.35	0.16
0.15	0.03	0.16	0.07	0.48	0.04	0.4	0.24	0.2	0.13	0.13	0.07	0.1	0.08	0.35	0.11
0.47	0.36	0.77	0.54	1.1	1.16	0.93	0.67	1.53	0.9	0.23	0.09	0.26	0.25	0.21	0.11
0.07	0.07	0.12	0.08	0.47	0.16	0.62	0.47	0.72	0.15	0.24	0.17	0.06	0.05	0.2	0.01
0.46	0.17	0.81	0.06	0.33	0.1	0.41	0.16	0.43	0.08	0.53	0.17	0.24	0.07	2.17	0.43
2.77	1.04	3.65	2.24	8.79	4.75	5.84	3.04	7.12	2.76	0.17	0.11	0.08	0.02	0.67	0.14
0.16	0.14	0.05	0.08	3.46	2.23	2.34	1.35	2.49	1.81	0.33	0.28	0.2	0.12	0.2	0.08
0.28	0.06	0.08	0.03	1.43	0.13	1.83	0.39	1.28	0.24	0.08	0.04	0.02	0.02	1.1	0.39
0.42	0.18	0.47	0.26	0.38	0.12	0.78	0.48	0.38	0.19	0.4	0.29	0.3	0.14	1.18	0.24
0.43	0.14	0.27	0.11	3.49	3.37	1.85	1.66	2.59	3.22	0.44	0.16	0.5	0.14	0.74	0.42
0.86	0.36	0.37	0.13	1.93	0.77	3.36	1.19	3.64	1.47	0.01	0.02	0.1	0.09	0.88	0.24
1.05	0.58	0.81	0.15	3.52	0.89	1.82	0.33	1.8	0.22	0.96	0.34	0.72	0.48	0.6	0.2
1.05	0.51	1.18	0.18	1.87	0.56	2.33	0.16	2.1	0.18	0.57	0.23	0.23	0.05	1.53	0.49
0.18	0.21	0.73	0.83	1.07	0.12	0.75	0.14	1.19	0.04	0.28	0.34	0.06	0.03	0.51	0.15
1.13	0.48	4	1.44	1	0.19	0.84	0.15	1.85	0.37	0.17	0.14	0.11	0.04	0.3	0.15
0.37	0.24	0.32	0.13	5.96	0.75	4.16	1.43	3.83	1.3	0.24	0.15	0.34	0.27	0.23	0.23
0.44	0.61	0.02	0.03	0.18	0.25	0.23	0.3	0.11	0.16	0.12	0.1	0.1	0.07	0.35	0.13
0.74	0.22	0.7	0.16	10.49	3.83	11.69	4.39	14.28	5.74	0.21	0.07	0.18	0.06	1.02	0.41
4.7	1.27	5.07	1.39	0.85	0.22	0.98	0.08	1.31	0.29	0.06	0.05	0.07	0.05	0.77	0.31
3.92	0.99	8.68	3.48	2.53	0.7	1.83	0.56	2.54	0.42	0.2	0.08	0.21	0.14	1.03	0.11
0.22	0.07	0.28	0.06	2.3	1	2.02	1.77	3.58	1.96	0.05	0.05	0	0	0.47	0.07
0.12	0.16	0.08	0.08	1.15	0.15	0.61	0.24	1.03	0.28	0.08	0.06	0.02	0.02	0.57	0.14
0.75	0.4	0.45	0.22	1.08	1.41	0.38	0.43	0.61	0.55	0.19	0.1	0.17	0.07	1.75	0.49
0.16	0.1	0.13	0.04	0.27	0.07	0.14	0.13	0.24	0.19	0.84	0.16	0.17	0.06	0.83	0.16
0.38	0.29	0.14	0.17	3.61	0.82	2.41	0.72	2.21	0.86	0.11	0.05	0.13	0.09	0.72	0.33
0.37	0.13	0.6	0.18	0.02	0.03	0.03	0.02	0.14	0.04	0.04	0.03	0.06	0.04	0.37	0.26
0.09	0.11	0.05	0.05	1.06	0.7	0.45	0.13	0.97	0.49	0.05	0.07	0.02	0.02	1.02	0.32
1.28	0.92	2.15	1.65	2.92	1.3	2.17	0.79	2.37	1.16	0.12	0.02	0.05	0.04	0.52	0.3
0.28	0.06	0.31	0.26	8.71	3.98	9.54	1.85	16.8	5.81	0.06	0.06	0.08	0.06	1.17	0.1
0.29	0.26	0.16	0.16	32.81	24.98	42.7	33.49	38.74	29	0.27	0.08	0.21	0.06	2.38	0.25
0.72	0.37	0.5	0.5	2.8	1.07	2.14	0.83	2.26	0.81	0.4	0.24	0.19	0.09	0.29	0.03
0.69	0.3	1.62	0.84	1.44	0.83	0.81	0.38	1.51	0.79	0.29	0.11	0.09	0.01	0.42	0.05
0.67	0.58	0.66	0.54	4.13	0.52	1.96	0.56	2.47	0.75	0.68	0.09	0.42	0.22	0.44	0.09
1.23	0.94	0.92	0.29	0.11	0.06	0.14	0.2	0.07	0.06	0.47	0.11	0.19	0.03	1.32	0.46
0.95	0.57	1.64	0.91	1.67	0.44	1.47	0.65	1.2	0.27	0.28	0.2	0.02	0.03	0.52	0.1
0.08	0.08	0.01	0.02	0.68	0.18	0.27	0.16	0.45	0.19	0.13	0.08	0.05	0.07	0.96	0.33
2.53	0.18	5.01	0.53	3.09	0.45	2.94	0.4	4.44	0.75	0.15	0.15	0.04	0.04	0.27	0.19
0.35	0.09	0	0	1.08	0.44	0.34	0.08	0.96	0.21	0.09	0.07	0.14	0.1	0.85	0.21
0.48	0.08	0.29	0.14	2.4	1.29	1.83	1.05	1.75	0.99	0.43	0.12	0.21	0.13	0.22	0.13
0.69	0.3	1.62	0.84	1.44	0.83	0.81	0.38	1.51	0.79	0.29	0.11	0.09	0.01	0.42	0.05
0.02	0.03	0.57	0.28	0.06	0.08	0	0	0	0	0	0	0	0	0.05	0.04
0.61	0.39	0.17	0.12	0.72	0.21	0.17	0.05	0.39	0.11	0.14	0.07	0.04	0.03	0.79	0.19
2.16	0.2	4.96	1.04	1.78	0.85	0.74	0.09	2.58	0.73	0.15	0.09	0.04	0.02	0.18	0.03
4.44	2.65	8.01	5.62	1.67	0.55	0.6	0.11	3.57	1.19	0.05	0.01	0.18	0.04	0.43	0.12
1.86	1.01	2.04	1.27	2.22	1.05	2.69	0.6	4.78	1.72	0.07	0.05	0	0	0.48	0.19
1.06	0.98	2.98	3.04	2.92	0.76	1.75	0.84	2.45	1.41	0.04	0.03	0.06	0.03	0.37	0.16
7.1	2.73	8.33	3.04	2.33	0.42	1.87	0.15	2.33	0.33	0.11	0.04	0.07	0.07	1.68	0.17
3.67	1.56	8.65	1.78	4.6	1.05	3.95	1.23	4.76	0.52	0.15	0.04	0.02	0.03	0.93	0.2
0.97	0.21	0.66	0.25	3.16	0.17	2.34	0.12	4.28	0.31	0.25	0.09	0.1	0.02	1.69	0.05
0.38	0.28	0.21	0.14	4.87	1.63	2.54	0.9	3.27	1.14	0.14	0.05	0.04	0.02	0.55	0.13
0.22	0.2	0.01	0.02	0.8	0.45	0.36	0.2	0.8	0.32	0.13	0.07	0.08	0.08	0.86	0.24
1.41	1.09	1.9	2.01	0.16	0.2	0.34	0.48	0.97	1.22	0.16	0.2	0.17	0.18	1.24	1.36
0.32	0.3	0.11	0.08	0.31	0.06	0.23	0.19	0.37	0.2	0.09	0.01	0.04	0.04	1.13	0.26
0.47	0.01	0.19	0.11	0	0	0.01	0.01	0	0	0.06	0.04	0.09	0.05	0.16	0.01
0.21	0.12	0.06	0.04	0.81	0.15	0.38	0.15	0.93	0.27	0.18	0.18	0.1	0.09	1.52	0.32
1.56	0.71	2.09	0.09	3.63	1.52	3.2	1	3.24	0.52	0.48	0.1	0.33	0.02	1.18	0.53
0.38	0.27	0.54	0.5	0.41	0.07	0.39	0.21	0.26	0.04	0.3	0.22	0.18	0.05	0.36	0.36
0.1	0.09	0.11	0.08	0.83	0.38	0.7	0.4	0.54	0.53	0.13	0.17	0.22	0.03	1.23	0.22
1.26	0.77	3.35	2.95	6.29	7.08	4.08	4.51	10.02	12.12	0.28	0.1	0.11	0.05	0.64	0.27

Triticum aestivum Pirin expression from the wheat cultivar Azhurnaya grown in cabinets with 16:8 hours day:night length at 25:15℃. There are three biological replicates with five individual plants each. Expression is represented in Transcripts per Million (TPM) (Ramírez-González et al., 2018; Winter et al., 2007)
SD = standard deviation.

Table S7. *Pirin* gene expression in response to drought, heat and a combination of both.

	Control	Drought 1 hr	Drought 6 hr	Heat 1 hr	Heat 6 hr	Mixed 1 hr	Mixed 6 hr
Ta-*Pirin-1-A*	2.19	2.77	1.38	1.03	0.98	1.82	1.48
Ta-*Pirin-1-B*	1.96	2.34	0.79	0.89	1.61	1.56	1.19
Ta-*Pirin-1-D*	1.16	1.23	0.62	5.18	2.64	7.28	1.88
Ta-*Pirin-2-A*	0.03	0.00	0.00	0.00	0.00	0.00	0.00
Ta-*Pirin-2-B*	0.11	0.00	0.00	0.00	0.00	0.00	0.00
Ta-*Pirin-2-D*	0.00	0.00	0.00	0.00	0.00	0.00	0.00
Ta-*Pirin-3-A*	0.00	0.00	0.00	0.00	0.00	0.00	0.00
Ta-*Pirin-3-B*	0.15	0.18	0.00	0.10	0.00	0.22	0.11
Ta-*Pirin-3-D*	0.03	0.00	0.00	0.00	0.00	0.00	0.00
Ta-*Pirin-4-A*	0.00	0.00	0.00	0.00	0.00	0.00	0.00
Ta-*Pirin-4-B*	0.46	0.40	0.21	0.28	0.04	0.09	0.04
Ta-*Pirin-4-D*	0.11	0.16	0.03	0.05	0.14	0.00	0.00
Ta-*Pirin-5-A*	2.12	1.96	2.83	1.55	6.63	0.68	1.22
Ta-*Pirin-5-B*	2.11	2.80	6.43	1.48	7.43	0.46	2.30
Ta-*Pirin-5-D*	4.83	5.42	11.32	2.40	6.69	0.42	1.92
Ta-*Pirin-6-A*	0.00	0.00	0.00	0.00	0.00	0.00	0.00
Ta-*Pirin-6-B*	0.11	0.00	0.00	0.00	0.00	0.00	0.00
Ta-*Pirin-6-D*	0.03	0.06	0.00	0.00	0.00	0.00	0.04

Note: Stress conditions are described in Liu et al., 2015 and microarray data from Liu et al., 2015, briefly, RNA was extracted from leaves of seedlings which were grown on filter paper and treated with 20% PEG (drought/ionic stress), 40°C or both high temperature and PEG.

The values are averages from two transcriptome libraries represented as reads per kilobase per million (RPKPM).

The Mixed column refers to a combination of drought and heat treatment.

Table S8. *Pirin* gene expression in cold-treated seedlings.

	23°C	Duncan's MR[a]	4°C	Duncan's MR[a]
Ta-*Pirin-1-A*	2.95	d	2.56	cd
Ta-*Pirin-1-B*	1.73	abc	1.02	ab
Ta-*Pirin-1-D*	0.72	a	1.89	bc
Ta-*Pirin-2-A*	0.00		0.00	
Ta-*Pirin-2-B*	0.00		0.00	
Ta-*Pirin-2-D*	0.02		0.04	
Ta-*Pirin-3-A*	0.00		0.00	
Ta-*Pirin-3-B*	0.07		0.02	
Ta-*Pirin-3-D*	0.09		0.07	
Ta-*Pirin-4-A*	0.00		0.00	
Ta-*Pirin-4-B*	0.15		0.15	
Ta-*Pirin-4-D*	0.05		0.00	
Ta-*Pirin-5-A*	1.53	ab	1.25	a
Ta-*Pirin-5-B*	1.23	a	1.43	ab
Ta-*Pirin-5-D*	2.10	b	2.08	b
Ta-*Pirin-6-A*	0.00		0.04	
Ta-*Pirin-6-B*	0.00		0.00	
Ta-*Pirin-6-D*	0.00		0.00	

Note: Plants were grown as described in the dataset from Li et al., 2015, briefly, RNA is extracted from the leaves of seedlings grown in soil for 2 weeks at 23 °C, moved to 4°C for 2 weeks. The values are an average of three replicates and are represented in reads per kilobase per million (RPKPM).

[a] Duncan's multiple range (MR) *post-hoc* test

Table S9. *Pirin* gene expression in response to drought and abscisic acid (ABA) treatment in a non-transgenic wild-type and an overexpression (ox) Triticum line.

	WT wwc	WT ABA	WT drought	ox wwc	ox ABA	ox drought
Ta-*Pirin-1-A*	1.70	2.29	1.29	2.40	2.50	1.72
Ta-*Pirin-1-B*	0.41	0.75	0.63	0.88	1.83	0.87
Ta-*Pirin-1-D*	0.65	0.92	0.77	1.10	1.51	0.88
Ta-*Pirin-2-A*	0.00	0.00	0.00	0.00	0.00	0.00
Ta-*Pirin-2-B*	0.00	0.04	0.00	0.00	0.00	0.00
Ta-*Pirin-2-D*	0.00	0.00	0.00	0.00	0.00	0.00
Ta-*Pirin-3-A*	0.00	0.00	0.00	0.00	0.00	0.00
Ta-*Pirin-3-B*	0.00	0.00	0.00	0.02	0.00	0.00
Ta-*Pirin-3-D*	0.00	0.00	0.00	0.00	0.00	0.03
Ta-*Pirin-4-A*	0.16	0.00	0.12	0.09	0.00	0.13
Ta-*Pirin-4-B*	0.00	0.00	0.00	0.07	0.04	0.00
Ta-*Pirin-4-D*	0.02	0.00	0.07	0.00	0.00	0.05
Ta-*Pirin-5-A*	0.55	0.39	0.07	0.39	0.53	0.20
Ta-*Pirin-5-B*	0.06	0.23	0.08	0.28	0.55	0.21
Ta-*Pirin-5-D*	0.26	0.26	0.31	0.49	0.58	0.35
Ta-*Pirin-6-A*	0.00	0.03	0.00	0.00	0.00	0.00
Ta-*Pirin-6-B*	0.00	0.00	0.00	0.00	0.00	0.00
Ta-*Pirin-6-D*	0.00	0.07	0.03	0.13	0.00	0.07

Note: Stress conditions are described in the dataset from Mega et al., 2019 , briefly, RNA was extracted from leaves of 40-day-old plants grown under normal conditions (wwc), 24 hr after 25 µm ABA treatment (ABA), and 24 hr after witholding water (drought).

The values are averages from three biological replicates and represented in reads per kilobase per million (RPKPM).

The ox refers to a transgenic line overexpressing Ta-*PYL4* and WT refers to the wild-type.

Table S10. *Pirin* gene expression in the disease-susceptible NIL-51 and disease-resistant NIL-38 spikes in response to *Fusarium graminearum* inoculation[+].

	12 hr Mock		12 hr Fus		12 hr Mock		12 hr Fus			24 hr Mock		24 hr Fus		24 hr Mock		24 hr Fus			48 hr Mock		48 hr Fus		48 hr Mock		48 hr Fus	
	NIL-51		NIL-51		NIL-38		NIL-38			NIL-51		NIL-51		NIL-38		NIL-38			NIL-51		NIL-51		NIL-38		NIL-38	
Ta-*Pirin-1-A*	18.72		18.52		15.98		14.74		Ta-*Pirin-1-A*	9.50	abc	17.44	bc	20.36	b	14.24	ab	Ta-*Pirin-1-A*	16.14	b	33.21	c	25.81	ab	30.46	b
Ta-*Pirin-1-B*	4.73		7.04		7.92		8.02		Ta-*Pirin-1-B*	5.16	abc	4.11	a	5.95	a	7.73	a	Ta-*Pirin-1-B*	0.38	a	7.03	ab	6.22	ab	17.07	ab
Ta-*Pirin-1-D*	17.40		21.56		12.63		15.24		Ta-*Pirin-1-D*	19.60	c	19.09	c	25.25	b	20.27	b	Ta-*Pirin-1-D*	15.74	b	40.34	c	25.77	ab	33.73	b
Ta-*Pirin-2-A*	0.00		0.00		0.41		0.00		Ta-*Pirin-2-A*	0.00		0.60		0.00		0.00		Ta-*Pirin-2-A*	0.00		6.67		0.00		9.41	
Ta-*Pirin-2-B*	0.00		0.00		0.00		0.00		Ta-*Pirin-2-B*	0.00		0.00		0.00		0.00		Ta-*Pirin-2-B*	0.00		0.00		0.00		0.00	
Ta-*Pirin-2-D*	0.00		0.00		0.00		0.00		Ta-*Pirin-2-D*	0.00		0.00		0.00		0.00		Ta-*Pirin-2-D*	0.47		0.00		1.26		0.00	
Ta-*Pirin-3-A*	0.00		0.00		0.00		0.00		Ta-*Pirin-3-A*	0.00		0.00		0.00		0.00		Ta-*Pirin-3-A*	0.00		0.00		0.00		0.00	
Ta-*Pirin-3-B*	1.53		0.39		0.00		0.00		Ta-*Pirin-3-B*	0.00		0.00		0.00		0.00		Ta-*Pirin-3-B*	1.84		2.34		0.76		0.43	
Ta-*Pirin-3-D*	0.00		0.92		1.70		0.00		Ta-*Pirin-3-D*	1.12		1.26		0.95		1.01		Ta-*Pirin-3-D*	0.81		3.16		0.72		5.23	
Ta-*Pirin-4-A*	2.05		2.63		0.00		0.69		Ta-*Pirin-4-A*	0.69		0.55		3.70		2.76		Ta-*Pirin-4-A*	4.24		7.00		1.97		1.54	
Ta-*Pirin-4-B*	0.00		4.64		1.52		0.00		Ta-*Pirin-4-B*	6.23		0.48		0.64		2.38		Ta-*Pirin-4-B*	1.18		2.15		1.27		5.58	
Ta-*Pirin-4-D*	3.48		2.92		3.21		2.52		Ta-*Pirin-4-D*	0.00		2.75		3.68		2.56		Ta-*Pirin-4-D*	2.53		4.10		1.88		7.23	
Ta-*Pirin-5-A*	48.03	b	44.91	b	44.16	a	41.26	a	Ta-*Pirin-5-A*	46.20	b	21.94	a	44.86	a	31.09	a	Ta-*Pirin-5-A*	27.76	d	19.43	c	21.51	c	19.52	bc
Ta-*Pirin-5-B*	34.74	a	49.62	b	31.94	a	48.48	a	Ta-*Pirin-5-B*	21.12	a	24.57	a	24.88	a	29.00	a	Ta-*Pirin-5-B*	8.96	a	14.82	bc	10.87	ab	8.27	ab
Ta-*Pirin-5-D*	45.31	b	48.92	b	44.92	a	58.13	a	Ta-*Pirin-5-D*	32.57	ab	28.13	ab	32.74	a	26.42	a	Ta-*Pirin-5-D*	12.47	ab	13.03	ab	12.32	abc	13.24	abc
Ta-*Pirin-6-A*	0.00		0.00		0.00		0.00		Ta-*Pirin-6-A*	0.00		0.00		0.00		0.00		Ta-*Pirin-6-A*	0.00		2.83		0.76		3.97	
Ta-*Pirin-6-B*	0.00		0.00		0.00		0.00		Ta-*Pirin-6-B*	0.00		0.00		0.00		0.00		Ta-*Pirin-6-B*	0.00		0.00		0.00		0.00	
Ta-*Pirin-6-D*	1.76		0.36		0.42		0.00		Ta-*Pirin-6-D*	0.70		0.00		1.47		2.58		Ta-*Pirin-6-D*	0.73		4.51		1.53		0.39	

[+] Data is from Steiner et al., 2017.

The data is expressed in reads per kilobase per million (RPKPM) from spike tissue that was inoculated with water as a mock treatment (Mock) or inoculated with a suspension of *Fusarium graminearum* spores (Fus).

Duncan's multiple range value applies to each row for the *Pirin* with significant changes.

Table S11. *Pirin* gene expression in response to *Fusarium graminearum* and abscisic acid (ABA).

	Control		Fusarium 1 dpi		Fusarium 1 dpi + ABA		Fusarium 1 dpi + AS6		1 mM ABA	
Ta-*Pirin-1-A*	3.0	c	2.5		2.5		2.4		4.2	d
Ta-*Pirin-1-B*	1.9	ab	2.7		2.9	c	2.0		3.1	c
Ta-*Pirin-1-D*	1.4	a	2.1		2.1		2.0		3.0	bc
Ta-*Pirin-2-A*	0.0		0.0		0.0		0.1		0.0	
Ta-*Pirin-2-B*	0.0		0.0		0.0		0.0		0.0	
Ta-*Pirin-2-D*	0.0		0.1		0.1		0.1		0.1	
Ta-*Pirin-3-A*	0.0		0.0		0.0		0.0		0.0	
Ta-*Pirin-3-B*	0.1		0.0		0.1		0.0		0.0	
Ta-*Pirin-3-D*	0.1		0.1		0.0		0.1		0.2	
Ta-*Pirin-4-A*	0.2		0.1		0.0		0.1		0.1	
Ta-*Pirin-4-B*	0.3		0.0		0.1		0.1		0.2	
Ta-*Pirin-4-D*	0.5		0.0		0.1		0.1		0.4	
Ta-*Pirin-5-A*	0.4	a	2.0	bc	1.5	b	1.6	bc	3.8	e
Ta-*Pirin-5-B*	0.2	a	1.7	bc	1.4	b	1.9	bc	2.9	d
Ta-*Pirin-5-D*	1.3	b	2.2	c	2.3	c	1.9	a	4.4	f
Ta-*Pirin-6-A*	0.0		0.0		0.0		0.0		0.0	
Ta-*Pirin-6-B*	0.0		0.0		0.0		0.0		0.0	
Ta-*Pirin-6-D*	0.2		0.2		0.0		0.1		0.1	

Fusarium-suceptible *T. aestivum* variant, Fielder, treated with Fusarium and a co-application of abscisic acid (ABA) or the ABA-signaling inhibitor AS6.

Samples are taken 1-day post-inoculation (dpi). The control is a water treatment. Values are in reads per kilobase per million (RPKPM). Dataset from Buhrow et al., 2021.

The letters represent the significant differences between homeologs as tested by a Duncan's multiple range *post-hoc* test following a one-way ANOVA.

Different letters indicate significant differences.

Table S11A. *Pirin* gene expression in response to *Fusarium graminearum* and gibberellic acid (GA)**.**

	Control		Fusarium 1 dpi		Fusarium 1 dpi + GA		1 mM GA	
Ta-*Pirin-1-A*	3.0	bcd	2.5		2.3		5.6	e
Ta-*Pirin-1-B*	1.9	ab	2.7		2.1		3.7	cd
Ta-*Pirin-1-D*	1.4	a	2.1		1.5		3.9	d
Ta-*Pirin-2-A*	0.0		0.0		0.1		0.1	
Ta-*Pirin-2-B*	0.0		0.0		0.0		0.0	
Ta-*Pirin-2-D*	0.0		0.1		0.1		0.0	
Ta-*Pirin-3-A*	0.0		0.0		0.0		0.0	
Ta-*Pirin-3-B*	0.1		0.0		0.1		0.0	
Ta-*Pirin-3-D*	0.1		0.1		0.1		0.1	
Ta-*Pirin-4-A*	0.2		0.1		0.0		0.1	
Ta-*Pirin-4-B*	0.3		0.0		0.0		0.3	
Ta-*Pirin-4-D*	0.5		0.0		0.1		0.3	
Ta-*Pirin-5-A*	0.4	ab	2.0	cde	2.5	de	4.3	f
Ta-*Pirin-5-B*	0.2	a	1.7	cd	1.7	cde	2.2	cde
Ta-*Pirin-5-D*	1.3	bc	2.2		2.0		2.8	e
Ta-*Pirin-6-A*	0.0		0.0		0.0		0.0	
Ta-*Pirin-6-B*	0.0		0.0		0.0		0.0	
Ta-*Pirin-6-D*	0.2		0.2		0.1		0.6	

Fusarium-suceptible *T. aestivum* variant, Fielder, treated with Fusarium and a co-application of gibberellic acid (GA).

Samples are taken 1-day post-inoculation (dpi). The control is a water treatment. Values are in reads per kilobase per million (RPKPM). Dataset from Buhrow et al., 2021.

The letters represent the significant differences between homeologs as tested by a Duncan's multiple range *post-hoc* test following a one-way ANOVA. Different letters indicate significant differences.

Table S8. *Pirin* gene expression in cold-treated seedlings.

	23°C	Duncan's MR[a]	4°C	Duncan's MR[a]
Ta-*Pirin-1-A*	2.95	d	2.56	cd
Ta-*Pirin-1-B*	1.73	abc	1.02	ab
Ta-*Pirin-1-D*	0.72	a	1.89	bc
Ta-*Pirin-2-A*	0.00		0.00	
Ta-*Pirin-2-B*	0.00		0.00	
Ta-*Pirin-2-D*	0.02		0.04	
Ta-*Pirin-3-A*	0.00		0.00	
Ta-*Pirin-3-B*	0.07		0.02	
Ta-*Pirin-3-D*	0.09		0.07	
Ta-*Pirin-4-A*	0.00		0.00	
Ta-*Pirin-4-B*	0.15		0.15	
Ta-*Pirin-4-D*	0.05		0.00	
Ta-*Pirin-5-A*	1.53	ab	1.25	a
Ta-*Pirin-5-B*	1.23	a	1.43	ab
Ta-*Pirin-5-D*	2.10	b	2.08	b
Ta-*Pirin-6-A*	0.00		0.04	
Ta-*Pirin-6-B*	0.00		0.00	
Ta-*Pirin-6-D*	0.00		0.00	

Note: Plants were grown as described in from Li et al., 2015, briefly, RNA is extracted from the leaves of seedlings grown in soil for 2 weeks at 23 °C, moved to 4°C for 2 weeks. The RNA-Seq dataset is from Li et al., 2015. The values are an average of three replicates and are represented in reads per kilobase per million (RPKPM).

[a] Duncan's multiple range (MR) *post-hoc* test

References:

Abell, B.M., Holbrook, L.A., Abenes, M., Murphy, D.J., Hills, M.J. and Moloney, M.M. (1997). Role of the proline knot motif in oleosin endoplasmic reticulum topology and oil body targeting. Plant Cell. 9:1481 – 1493.

Adams, M., and Jia, Z.C. (2005). Structural and biochemical analysis reveal pirins to possess quercetinase activity. J. Biol. Chem. 280: 28675–28682.

Aharon, G.S., Gelli, A., Snedden, W.A., and Blumwald, E. (1998) Activation of a plant plasma membrane Ca2+ channel by TG alpha1, a heterotrimeric G protein alpha-subunit homologue. FEBS Lett 424:17–21.

Agati, G., Azzarello, E., Pollastri, S., and Tattini, M. (2012). Flavonoids as antioxidants in plants: Location and functional significance. Plant Sci. 196: 67–76.

Alaux, M., Rogers, J., Letellier, T., Flores, R., Alfama, F., Pommier, C., Mohellibi, N., Durand, S., Kimmel, E., Michotey, C., Guerche, C., Loaec, M., Lainé, M., Steinbach, D., Choulet, F., Rimbert, H., Leroy, P., Guilhot, N., Salse, J., Feuillet, C., International Wheat Genome Sequencing Consortium, Paux, E., Eversole, K., Adam-Blondon, A-F., and Quesneville, H. (2018). Linking the international wheat genome sequencing consortium bread wheat reference genome sequence to wheat genetic and phenomic data. Genome Biol. 19:111. https://doi.org/10.1186/ s13059-018-1491-4.

Aprile, A., Havlickova, L., Panna, R., Marè, C., Borrelli,G.M., Marone, D., Perrotta, C., Rampino, P., De Bellis, L., Curn, V., Mastrangelo, A.M., Rizza, F., and Cattivelli, L. (2013). Different stress responsive strategies to drought and heat in two durum wheat cultivars with contrasting water use efficiency. BMC Genomics. 14:821.

Aprile, A., Mastrangelo, A.M., De Leonardis, A.M., Galiba, G., Roncaglia, E., Ferrari, F., De Bellis, L., Turchi, L., Giuliano, G., and Cattivelli, L. (2009). Transcriptional profiling in response to terminal drought stress reveals differential responses along the wheat genome. BMC Genomics. 10:279. https://doi.org/10.1186/1471- 2164-10-279.

Aubert, Y., Vile, D., Pervent, M., Aldon, D., Ranty, B., Simonneau, T., Vavasseur, A., and Galaud, J.P. (2010). *RD20*, a stress-inducible caleosin, participates in stomatal control, transpiration and drought tolerance in *Arabidopsis thaliana*. Plant Cell Physiol. 51: 1975-1987.

Aubert, Y., Vile, D., Pervent, M., Aldon, D., Ranty, B., Simonneau, T., Vavasseur, A., and Galaud, J.P. (2011). Involvement of *RD20*, a member of caleosin family, in ABA-mediated regulation of germination in *Arabidopsis thaliana*. Plant Signal Behav. 6 (4): 538–540.

Auslender, E.L., Dorion, S., Dumont, S., and Rivoal, J. (2015). Expression, purification and characterization of Solanum recombinant cytosolic pyruvate kinase. Protein Expr Purif. 110:7–13.

Ashikari, M., Wu, J., Yano, M., Sasaki. T., and Yoshimura, A. (1999). Rice gibberellin-insensitive dwarf mutant gene *D arf 1* encodes the α-subunit of GTP-binding protein. Proc. Natl. Acad. Sci. 96:10284-10289.

Baldwin, M. W., Toda, Y., Nakagita, T., O'Connell, M. J., Klasing, K. C., Misaka, T., Edwards, S. V., and Liberles, S. D. (2014). Sensory biology. Evolution of sweet taste perception in hummingbirds by transformation of the ancestral umami receptor. Science. 345: 929–933.

Bandaranayake, P.C.G., Tomilov, A., Tomilova, N.B., Ngo, Q.A., Wickett, N., dePamphilis, C.W., and Yoder. J.I. (2012). The Tv*Pirin* Gene Is Necessary for Haustorium Development in the Parasitic Plant *Triphysaria versicolor*. Plant Physiol. 158(2): 1046–1053.

Blázquez, M.A., Green, R., Nilsson, O., Sussman, M.R. and Weigel, D. (1998) Gibberellins promote flowering of Arabidopsis by activating the L*EAFY* promoter. Plant Cell. 10: 791–800.

Blázquez, M.A. and Weigel, D. (2000). Integration of floral inductive signals in Arabidopsis. Nature. 404: 889–892.

Blée, E., Boachon, B., Burcklen, M., Le Guédard, M., Hanano, D.H., Ehlting, J., Herrfurth, C., Feussner, I., and Bessoule, J.J. (2014). The Reductase Activity of the Arabidopsis Caleosin RESPONSIVE TO DESSICATION 20 Mediates Gibberellin-Dependent Flowering Time, Abscisic Acid Sensitivity, and Tolerance to Oxidative Stress. Plant physiol.166: 109-124.

Blée, E., Flenet, M., Boachon, B., and Fauconnier, M. L. (2012). A non-canonical caleosin from Arabidopsis efficiently epoxidizes physiological unsaturated fatty acids with complete stereoselectivity. FEBS J. 279(20): 3981–3995.

Brunetti, S.C., Arseneault, M.K.M., and Gulick, P.J. (2018). Characterization of the *Esi3*/*RCI2*/*PMP3* gene family in the Triticeae. BMC Genom. 19: 898.

Brunetti, S. C., Arseneault, M.K.M., Wright, J. A., Wang, Z., Ehdaeivand, M. R., Lowden, M. J., Rivoal, J., Khalil, H. B., Garg, G., and Gulick, P. J. (2021). The stress induced caleosin, *RD20/CLO3*, acts as a negative regulator of *GPA1* in Arabidopsis. Plant Mol. Biol.

Busk, P.K., and Pages, M. (1998). Regulation of abscisic acid-induced transcription. Plant Mol. Biol. 37, 425–435.

Buhrow, L.M., Liu, Z., Cram, D., Sharma, T., Foroud, N.A., and Pan, Y. (2021). Wheat transcriptome profiling reveals abscisic and gibberellic acid treatments regulate early-stage phytohormone defense signaling, cell wall fortification, and metabolic switches following *Fusarium graminearum*-challenge. BMC Genomics, 22(1), 798.

Capel, J., Jarillo, J.A., Salinas, J., and Martinez-Zapater, J.M. (1997). Two homologous low- temperature-inducible genes from Arabidopsis encode highly hydrophobic proteins. Plant Physiol. 115:569–76.

CAP3 Sequence Assembly Program; http://doua.prabi.fr/software/cap3

Casimiro, I., Beeckman, T., Graham, N., Bhalerao, R., Zhang, H., Casero, P, Sandberg, G., and Bennett, M.J. (2003). Dissecting Arabidopsis lateral root development. Trends Plant Sci. 8: 165–171.

Chandrashekar, J., Hoon, M.A., Ryba, N.J., and Zuker C.S. (2006). The receptors and cells for mammalian taste. Nature. 444:288–294.

Cattivell, L., Baldi, P., Crosatti, C., Di Fonzo, N., Faccioli, P., Grossi, M., Mastrangelo, A.M., Pecchioni, N., and Stanca, A.M. (2002). Chromosome regions and stress-related sequences involved in resistance to abiotic stress in Triticeae. Plant Mol Biol 48:649–665.

Chakravorty, D., Gookin, T.E., Milner, M.J., Yu, Y., and Assmann, S.M. (2015). Extra-large G proteins (XLGs) expand the repertoire of subunits in Arabidopsis heterotrimeric G protein signaling. Plant Physiol 169(1):512–529.

Chakravorty, D., Trusov, Y., Zhang, W., Acharya., B.R., Sheahan M.B., McCurdy, D.W., Assmann, S.M., and Botella, J.R. (2011). An atypical heterotrimeric G-protein γ-subunit is involved in guard cell K^+-channel regulation and morphological development in *Arabidopsis thaliana*. Plant J. 67(5):840-851.

Chapman, K.D., Dyer, J.M., and Mullen, R.T. (2012) Biogenesis and functions of lipid droplets in plants: thematic review series: lipid drop- let synthesis and metabolism: from yeast to Man. J Lipid Res. 53(2):215–226.

Chater, C.C., Oliver, J., Casson, S., and Gray, J.E. (2014). Putting the brakes on: abscisic acid as a central environmental regulator of stomatal development. New Phytol. 202:376–391.

Chen, J.G., Gao, Y., and Jones, A.M. (2006). Differential roles of Arabidopsis heterotrimeric G-protein subunits in modulating cell division in roots. Plant Physiol. 141: 887-897.

Chen, J.G., Pandey, S., Huang, J., Alonso, J.M., Ecker, J.R, Assmann, S.M., and Jones, A.M. (2004). GCR1 can act independently of heterotrimeric G-protein in response to brassinosteroids and gibberellins in Arabidopsis seed germination. Plant Physiol.135: 907-915.

Chen, J.C.F., Tsai, C.C.Y., and Tzen, J.T.C. (1999). Cloning and Secondary Structure Analysis of Caleosin, a Unique Calcium Binding Protein in Oil Bodies of Plant Seeds. Plant Cell Physiol. 40(10): 1079-1086.

Chen, J.C.F. and Tzen, J.T.C. (2001). An in vitro system to examine the effective phospholipids and structural domain for protein targeting to seed oil bodies. Plant Cell Physiol. 42:1245 –1252.

Chen, J.G., Ullah, H., Temple, B., Liang, J., Guo, J., Alonso, J.M., Ecker, J.R., and Jones, A.M. (2006). RACK1 mediates multiple hormone responsiveness and developmental processes in Arabidopsis. J. Exp. Bot. 57(11): 2697–2708.

Chen, J.G., Willard, F.S., Huang, J., Liang, J., Chasse, S.A., Jones, A.M., and Siderovski, D.P. (2003) A seven-transmembrane RGS protein that modulates plant cell proliferation. Science. 301:1728–1731.

Clough, S.J., and Bent, A.F. (1998) Floral dip: a simplified method for Agrobacterium-mediated transformation of Arabidopsis thaliana. Plant J. 16:736–743.

Corbesier, L., and Coupland, G. (2006). The quest for florigen: a review of recent progress. J. Exp.Bot. 57(13): 3395–3403.

Davin, N., Edger, P. P., Hefer, C. A., Mizrachi, E., Schuetz, M., Smets, E., Myburg, A. A., Douglas, C. J., Schranz, M. E., and Lens, F. (2016). Functional network analysis of genes differentially expressed during xylogenesis in soc1ful woody Arabidopsis plants. Plant J. 86(5): 376–390.

De Block, J., Szopinska, A., Guerriat, B., Dodzian, J., Villers, J., Hochstenbach, J.F., and Morsomme, P. (2015). Yeast Pmp3p has an important role in plasma membrane organization. J Cell Sci. 128:3646–59.

De Domenico, S., Bonsegna, S., Lenuccci, M.S., Poltronieri, P., Di Sansebastiano, G. P., and Santino, A. (2011). Localization of Seed Oil Body Proteins in Tobacco Protoplasts Reveals Specific Mechanisms of Protein Targeting to Leaf Lipid Droplets. J. Integr. Plant Biol. 53(11): 858–868.

de Mendoza, A., Sebé-Pedrós, A., and Ruiz-Trillo, I. (2014). The evolution of the GPCR signaling system in eukaryotes: modularity, conservation, and the transition to metazoan multicellularity. Genome Biol. Evol. 6(3): 606–619.

De Vendittis, E., Adinolfi, B.S., Amatruda, M.R., Raimo, G., Masullo, M., and Bocchini, V. (1999). The A26G replacement in the consensus sequence A-X-X-X-X-G-K-[T, S] of the guanine nucleotide binding site activates the intrinsic GTPase of the elongation fac- tor 2 from the archaeon *Sulfolobus solfataricus*. Eur J Biochem. 262:600–605.

Dell, E.J., Connor, J., Chen, S., Stebbins, E.G., Skiba, N.P., Mochly-Rosen, D., and Hamm, H.E. (2002). The βγ subunit of heterotrimeric G proteins interacts with RACK1 and two other WD repeat proteins. J. Biol. Chem. 277: 49888–49895.

De Smet I., Signora L., Beeckman T., Inzé D., Foyer C.H., Zhang H. (2003). An abscisic acid-sensitive checkpoint in lateral root development of Arabidopsis. Plant J. 33: 543–555

Dorion, S., and Rivoal, J. (2003). Quantification of uridine 5'-diphosphate (UDP)-glucose by high-performance liquid chromatography and its application to a nonradioactive assay for nucleoside diphos- phate kinase using UDP-glucose pyrophosphorylase as a coupling enzyme. Anal Biochem. 323:188–196.

Dunwell, J.M., and Gane, P.J. (1998). Microbial relatives of seed storage proteins: conservation of motifs in a functionally diverse superfamily of enzymes. J. Mol. Evol. 46: 147–154.

Dunwell, J.M., Culham, A., Carter, C.E., Sosa-Aguirre, C.R., and Goodenough, P.W. (2001). Evolution of functional diversity in the cupin superfamily. Trends Biochem. Sci. 26: 740–745.

Dunwell, J.M., Khuri, S., and Gane, P.J. (2000). Microbial relatives of the seed storage proteins of higher plants: conservation of structure, and diversification of function during evolution of the cupin superfamily. Microbiol. Mol. Biol. Rev. 64: 153–179.

Dunwell, J.M., Purvis, A., and Khuri, S. (2004). Cupins: the most functionally diverse protein superfamily?

Phytochem. 65: 7–17.

Edgar, R.C. (2004). MUSCLE: multiple sequence alignment with high accuracy and high throughput. Nucleic Acid Res. 32(5):1792–7.

Edwards, K., Johnstone, C., and Thompson, C. (1991). A simple and rapid method for the preparation of plant

genomic DNA for PCR analysis. Nucleic Acids Res. 19:1349

EMBL-EBI Array express; https://www.ebi.ac.uk/arrayexpress/

Ensembl Plants; http://plants.ensembl.org/index.html

Fan, L.M., Zhang, W., Chen, J.G., Taylor, J.P., Jones, A.M. and Assmann, S.M. (2008). Abscisic acid regulation of guard-cell K+ and anion channels in Gb and RGS-deficient Arabidopsis lines. Proc. Natl Acad. Sci. 105: 8476– 8481.

Fetchko, M., and Stagljar, I. (2004). Application of the split-ubiquitin membrane yeast two-hybrid system to investigate membrane protein interactions. Methods. 32: 349-362.

Feng, D.R., Liu, B., Li, W.Y., He, Y.M., Qi, K.B., Wang, H.B., and Wang, J.F. (2009). Over-expression of cold-induced plasma membrane protein gene (MpRCI) from plantain enhances low temperature-resistance in transgenic tobacco. Environ Exp Bot. 65:395–402. https://doi.org/10.1016/j.envexpbot.2008.12.009.

Folta, K.M., and Kaufman, L.S. (1999). Regions of the pea Lhcb1*4 promoter necessary for blue-light regulation in transgenic Arabidopsis. Plant Physiol. 120: 747–755

Foo, S.Y. and Nolan, G.P. (1999). NF-κB to the rescue: RELs, apoptosis and cellular transformation. Trends Genet. 15: 229–235.

Frandsen, G.I., Muller-Uri, F., Nielsen, M., Mundy, J., and Skriver, K. (1996). Novel plant Ca2+-binding protein expressed in response to abscisic acid and osmotic stress. J Biol Chem. 271: 343–348

Frandsen, G. I., Mundy, J., and Tzen, J.T.C. (2001). Oil bodies and their associated proteins, oleosins and caleosins. Physiol Plant. 112: 301-307.

Fu, L., Niu, B., Zhu, Z., Wu, S., and Li, W. (2012). CD-HIT: accelerated for clustering the next- generation sequencing data. Bioinformatics. 28:3150–2. https://doi.org/ 10.1093/bioinformatics/bts565.

Fu, J., Zhang, D.F., Liu, Y.H., Ying, S., Shi, Y.S., Song, Y.C., Li, Y., and Wang, T.Y. (2012). Isolation and characterization of maize *PMP3* genes involved in salt stress tolerance. PLoS One. 7(2):e31101.

Galvez, A.F., Gulick, P.J., and Dvorak, J. (1993). Characterization of the early stages of genetic salt stress responses in salt-tolerant *Lophopyrum elongatum*, salt-sensitive wheat, and their amphiploid. Plant Physiol.103: 257-265.

Gautam, N., Downes, G.B., Yan, K., and Kisselev, O. (1998). The G-protein βγ complex. Cell. Signal. 10: 447–455.

Gautam, N., Northup, J., Tamir, H., and Simon, M.I. (1990). G protein diversity is increased by associations with a variety of γ-subunits. Proc. Natl. Acad. Sci. 87: 7973–7977.

Gavuzzi, P., Rizza, F., Palumbo, M., Campanile, R.G., Ricciardi, G.L., and Borghi, B. (2007). Evaluation of field and laboratory predictors of drought and heat tolerance in winter cereals. Canadian J Plant Sci. 77:523–31.

Gawande, N. D., Hamiditabar, Z., Brunetti, S. C., and Gulick, P. J. (2022). Characterization of the heterotrimeric G protein gene families in *Triticum aestivum* and related species. 3 Biotech. 12(4): 99.

Gendreau, E., Traas, J., Demos', T., Crandjean, O., Caboche, M., and Hofte, H. (1997) Cellular basis of hypocotyl growth in *Arabidopsis thaliana*. Plant Physiol. 114:295

Goddard, N.J., Dunn, M.A., Zhang, L., White, A.J., Jack, P.L., and Hughes, M.A. (1993) Molecular analysis and spatial expression pattern of a low temperature-specific barley gene, blt101. Plant Mol Biol. 23:871–9.

Gookin, T.E., and Assmann, S.M. (2014). Significant reduction of BiFC non-specific assembly facilitates in planta assessment of heterotrimeric G-protein interactors. Plant J 80:553–567

Gulick, P.J., and Dvorak, J. (1992). Coordinate gene response to salt stress in *Lophopyrum elongatum*. Plant Physiol. 100:1384–8.

Guo, J., and Chen, J. G. (2008). RACK1 genes regulate plant development with unequal genetic redundancy in Arabidopsis. BMC Plant Biol. 8:108.

Guo, J., Wang, J., Xi, L., Huang, W.D., Liang J., and Chen, J.G. (2009) RACK1 is a negative regulator of ABA responses in Arabidopsis. J Exp Bot. 60(13):3819-33. doi: 10.1093/jxb/erp221.

Hanano, A., Alkara, M., Almousally, I., Shaban, M., Rahman, F., Hassan, M., and Murphy, D. J. (2018). The Peroxygenase Activity of the *Aspergillus flavus* Caleosin, AfPXG, Modulates the Biosynthesis of Aflatoxins and Their Trafficking and Extracellular Secretion via Lipid Droplets. Front. Microbiol. 9:158.

Hanano, A., Bessoule, J.J., Heitz, T., and Blée, E. (2015). Involvement of the caleosin/peroxygenase RD20 in the control of cell death during Arabidopsis responses to pathogens. Plant Signal. Behav. 10:3.

Hanano, A., Burcklen, M., Flenet, M., Ivancich, A., Louwagie, M., Garin, J., and Blée, E. (2006). Plant seed peroxygenase is an original heme-oxygenase with an EF-hand calcium binding motif. J Biol Chem. 281: 33140–33151.

Hauser, F., Li, Z., Waadt, R., and Schroeder, J.I. (2017). SnapShot: abscisic acid signaling. Cell. 171(7): 1708–1708.e0.

Huang, C.Y., Chung, C.I., Lin, Y.C., Hsing, Y.I., and Huang, A.H. (2009). Oil bodies and oleosins in Physcomitrella possess characteristics representative of early trends in evolution. Plant Physiol. 150:1192–1203

Huang, X., and Madan, A. (1999). CAP3: a DNA sequence assembly program. Genome Res. 9: 868–877. doi:10.1101/gr.9.9.868. PMID: 10508846.

Huang, J., Taylor, J.P., Chen, J-G., Uhrig, J.F., Schnell, D.J., Nakagawa, T., Korth, K.L., and Jones, A.M. (2006). The plastid protein THYLAKOID FORMATION1 and the plasma membrane G-protein GPA1 interact in a novel sugar-signaling mechanism in Arabidopsis. Plant Cell. 18: 1226–1238.

Huang, H., Ullah, F., Zhou, D. X., Yi, M., and Zhao, Y. (2019). Mechanisms of ROS Regulation of Plant Development and Stress Responses. Front. Plant. Sci. 10: 800.

Huang, S., Sirikhachornkit, A., Su, X., Faris, J., Gill, B., Haselkorn, R., and Gornicki, P. (2002). Genes encoding plastid acetyl-CoA carboxylase and 3-phosphoglycerate kinase of the Triticum/Aegilops complex and the evolutionary history of polyploid wheat. Proc Natl Acad Sci USA. 99(12):8133–8.

International Wheat Genome Sequencing Consortium. (2018). Science 361. eaar7191 (2018). https://doi.org/10.1126/science.aar7191.

Ito, H., Fukuda, Y., Murata, K., and Kimura, A. (1983). Transformation of intact yeast cells treated with alkali cations. J Bacteriol. 153:163–168

Jefferson, R.A., Kavanagh, T.A., and Bevan, M.W. (1987). GUS fusions: beta-glucoronidase as a sensitive and versatile gene fusion marker in higher plants. EMBO J. 6:3901-3907.

Jiang, P., and Beauchamp, G.K. (2014). Sensing nectar's sweetness. Science. 345: 878. DOI: 10.1126/science.1259175.

Johnston, C.A., Taylor, J.P., Gao, Y., Kimple, A.J., Grigston, J.C., Chen JG., Siderovski, D.P., Jones, A.M., and Willard, F. S. (2007). GTPase acceleration as the rate-limiting step in Arabidopsis G protein-coupled sugar signaling. PNAS. 104:17317-17322.

Jones, A.M. (2002). G-protein-coupled signaling in Arabidopsis. Curr Opin Plant Biol. 5:402–407

Jones, A.M., and Assmann, S.M. (2004). Plants: the latest model system for G-protein research. EMBO Rep. 5: 572-578.

Jones, A.M., Ecker, J.R., and Chen J.G. (2003). A reevaluation of the role of the heterotrimeric G protein in coupling light responses in Arabidopsis. Plant Physiol. 131:1623-1627.

Jones, J.C., Jones, A.M., Temple, B.R., and Dohlman, H.G. (2012). Differences in intradomain and interdomain motion confer distinct activation properties to structurally similar Gα proteins. Proc. Natl. Acad. Sci. 109:7275–7279.

Jukes, T.H., and Cantor, C.R. (1969). Evolution of protein molecules. In Mammalian Protein Metabolism. Edited by H.N. Munro. Academic Press, New York, pp. 21–132.

Kapila, J., De Rycke, R., and Angenon, G. (1997). An Agrobacterium-mediated transient gene expression system for intact leaves. Plant Sci 122:101–108

Karimi, M., Inze, D., and Depicker, A. (2002). GATEWAY™ vectors for Agrobacterium-mediated plant transformation. Trends Plant Sci 7:193–195

Kato, C., Mizutani, T., Tamaki, H., Kumagai, H., Kamiya, T., Hirobe, A., Fujisawa, Y., Yato, H., and Iwasaki, Y. (2004). Characterization of heterotrimeric G protein complexes in rice plasma membrane. Plant J. 38:320–331

Khalil, H.B., Brunetti, S.C., Pham, U.M., Maret, D., Laroche, A., and Gulick, P.J. (2014). Characterization of the caleosin gene family in the Triticeae. BMC Genom. 15: 239.

Khalil, H.B., Wang, Z., Wright, J.A., Ralevski, A., Donayo, A.O., and Gulick, P.J. (2011). Heterotrimeric Gα subunit from wheat (*Triticum aestivum*), GA3, interacts with the calcium-binding protein, Clo3, and the phosphoinositide-specific phospholipase C, PI-PLC1. Plant Mol Biol. 77: 145-158.

Khurana, N., Chauhan, H., and Khurana, P. (2015). Characterization of a chloroplast localized wheat membrane protein (TaRCI) and its role in heat, drought and salinity stress tolerance in *Arabidopsis thaliana*. Plant Gene. 4:45–54.

Kim, Y.Y., Jung, K.W., Yoo, K.S., Jeung, J.U., and Shin, J.S. (2011). A stress-responsive caleosin-like protein, AtCLO4, acts as a negative regulator of ABA responses in Arabidopsis. Plant Cell Physiol. 52:874-884.

Kim, G-T., Tsukaya, H., and Uchimiya, H. (1998). The ROTUNDIFOLIA3gene of *Arabidopsis thaliana* encodes a new member of the cytochrome P-450 family that is required for the regulated polar elongation of leaf cells. Genes Dev. 12:2381–3239

Klopffleisch, K., Phan, N., Augustin, K., Robert, B.S., Booker, K.S., Botella, J.R., Carpita, N.C., Carr, T., Chen, J., Cooke, T.R., Frick-Cheng, A., Fried- man, E.J., Fulk, B., Hahn, M.G., Jiang, K., Jorda, L., Kruppe, L., Liu, C., Lorek, J., McCann, M.C., Molina, A., Moriyama, E.N., Mukhtar, M.S., Mudgil, Y., Pattathil, S., Schwarz, J., Seta, S., Tan, M., Temp, U., Trusov, Y., Urano, D., Welter, B., Yang, J., Panstruga, R., Uhrig, J.F., and Jones, A.M. (2011). Arabidopsis G-protein interactome reveals connections to cell wall carbohydrates and morphogenesis. Mol Syst Biol. 7:532

Koornneef, M., Alonso-Blanco, C., Peeters, A.J. and Soppe, W. (1998a). Genetic control of flowering time in Arabidopsis. Annu. Rev. Plant Physiol. Plant Mol. Biol. 49: 345–370.

Kreps, J.A., Wu, Y., Chang, H-S., Zhu, T., Wang, X., and Harper, J.F. (2002) Transcriptome changes for Arabidopsis in response to salt, osmotic and cold stress. Plant Physiol. 130:2129–2141

Kumar, S., Stecher, G., and Tamura, K. (2007). MEGA7: molecular evolution- ary genetics analysis version 7.0 for bigger datasets. Mol. Biol. Evol. 33: 1870–1874. doi:10.1093/molbev/msw054.

Lachowiec, J., Mason, G. A., Schultz, K., and Queitsch, C. (2018). Redundancy, Feedback, and Robustness in the *Arabidopsis thaliana* BZR/BEH Gene Family. Front. genet. 9: 523. https://doi.org/10.3389/fgene.2018.00523

Lapik, Y.R., and Kaufman, L.S. (2003). The Arabidopsis cupin domain protein AtPirin1 interacts with the G protein a subunit GPA1 and regulates seed germination and early seedling development. Plant Cell. 15:1578-1590.

Lescot, M., Déhais, P., Moreau, Y., De Moor, B., Rouzé, P., and Rombauts, S. (2002). PlantCARE: a database of plant cis-acting regulatory elements and a portal to tools for in silico analysis of promoter sequences. Nucleic Acids Res., Database Issue. 30(1): 325–327. doi:10.1093/nar/30.1. 325.

Leung, J., and Giraudat, J. (1998). Abscisic acid signal transduction. Annu. Rev. Plant Physiol. 49, 199–222 **Levy,**

Y.Y., and Dean, C. (1998) The transition to flowering. Plant Cell. 10: 1973–1989.

Liman, E. R., Zhang, Y. V., and Montell, C. (2014). Peripheral coding of taste. Neuron. 81(5): 984–1000.

Li, Q., Zheng, Q., Shen, W., Cram, D., Fowler, D.B., and Wei, Y. (2015). Understanding the biochemical basis of temperature-induced lipid pathway adjustments in plants. Plant Cell. 27(1): 86–103. doi:10.1105/ tpc.114.134338. PMID: 25564555.

Liu, B., Feng, D., Zhang, B., Mu, P., Zhang, Y., He, Y., Qi, K., Wang, J., and Wang, H. (2012). *Musa paradisica* RCI complements AtRCI and confers Na+ tolerance and K+ sensitivity in Arabidopsis. Plant Sci. 184:102–11.

Liu, Z., Xin, M., Qin, J., Peng, H., Ni, Z., and Yao, Y. (2015). Temporal transcriptome profiling reveals expression partitioning of homeologous genes contributing to heat and drought acclimation in wheat (*Triticum aestivum L.*). BMC Plant Biol. 15: 152. doi:10.1186/ s12870-015-0511-8. PMID: 26092253.

Long, R., Zhang, F., Li, Z., Li, M., Cong, L., Kan,g J., Zhang, T., Zhao, Z., Sun, Y., and Yang, Q. (2015). Isolation and functional characterization of salt-stress induced RCI2-like genes from *Medicago sativa* and *Medicago truncatula*. J Plant Res.128:697–707.

Lu, Q., Tang, X., Tian, G., Wang, F., Liu, K., Nguyen, V., Kohalmi, S.E., Keller, W.A., Tsang, E.W., Harada, J.J., Rothstein, S.J., and Cui, Y. (2010). Arabidopsis homolog of the yeast TREX-2 mRNA export complex: components and anchoring nucleoporin. Plant J. 61(2):259–270

Luo, M.C., Gu, Y.Q., Puiu, D., Wang, H., Twardziok, S.O., Deal, K.R., Huo, N., Zhu, T., Wang, L., Wang, Y., McGuire, P.E., Liu, S., Long, H., Ramasamy, R.K., Rodriguez, J.C., Van, S.L., Yuan, L., Wang, Z., Xia, Z., Xiao, L., Anderson, O.D., Ouyang, S., Liang, Y., Zimin, A.V., Pertea, G., Qi, P., Bennetzen, J.L., Dai, X., Dawson, M.W., Müller, H.G., Kugler, K., Rivarola-Duarte, L., Spannagl, M., Mayer, K.F.X., Lu, F.H., Bevan, M.W., Leroy, P., Li, P., You, F.M., Sun, Q., Liu, Z., Lyons, E., Wicker, T., Salzberg, S.L., Devos, K.M., and Dvořák, J. (2017). Genome sequence of the progenitor of the wheat D genome *Aegilops tauschii*. Nature. 551:492–502.

Malamy, J., and Benfey, P. (1997). Organization and cell differentiation in lateral roots of *Arabidopsis thaliana*. Genes Dev. 124: 33–44.

Marrari, Y., Crouthamel, M., Irannejad, R., and Wedegaertner, P.B. (2007). Assembly and trafficking of heterotrimeric G proteins. Biochemistry. 46:7665–7677.

Maruta, N., Trusov, Y., Chakravorty, D., Urano, D., Assmann, S. M., and Botella, J. R. (2019). Nucleotide

exchange-dependent and nucleotide exchange-independent functions of plant heterotrimeric GTP-binding proteins. Sci. Signal. 12: 606.

Matsuoka, Y. (2011). Evolution of Polyploid Triticum wheats under cultivation: the role of domestication, natural hybridization and allopolyploid speciation in their diversification. Plant Cell Physiol. 52(5): 750– 764. doi:10.1093/pcp/pcr018. PMID: 21317146.

Misra, S., Wu, Y., Venkataraman, G., Sopory, S.K., and Tuteja, N. (2007). Heterotrimeric G-protein complex and G-protein-coupled receptor from a legume (*Pisum sativum*): role in salinity and heat stress and cross-talk with phospholipase C. Plant J 51:656–669

Mitsuya, S., Taniguchi, M., Miyake, H., and Takabe, T. (2005). Disruption of RCI2A leads to over-accumulation of Na+ and increased salt sensitivity in *Arabidopsis thaliana* plants. Planta. 222:1001–9. https://doi.org/10.1007/s00425-005- 0043-9.

Mitsuya, S., Taniguchi, M., Miyake, H., and Takabe, T. (2006). Overexpression of RCI2A decreases Na+ uptake and mitigates salinity-induced damages in *Arabidopsis thaliana* plants. Physiol Plant. 128:95–102.

Medina, J., Ballesteros, M.L., and Salinas, J. (2007). Phylogenetic and functional analysis of Arabidopsis RCI2 genes. J Exp Bot. 58:4333–46.

Medina, J., Catala, R., and Salinas, J. (2001). Developmental and stress regulation of RCI2A and RCI2B, Two Cold-Inducible Genes of Arabidopsis Encoding Highly Conserved Hydrophobic Proteins. Plant Physiol. 125:1655–66.

Mega, R., Abe, F., Kim, J. S., Tsuboi, Y., Tanaka, K., Kobayashi, H., Sakata, Y., Hanada, K., Tsujimoto, H., Kikuchi, J., Cutler, S. R., and Okamoto, M. (2019). Tuning water-use efficiency and drought tolerance in wheat using abscisic acid receptors. Nature plants, 5(2), 153–159.

Meinke, D.W. (2020). Genome-wide identification of EMBRYO -DEFECTIVE (EMB) genes required for growth and development in Arabidopsis. New Phytol. 226: 306-325.

Meng, L-S., Cao, X-Y., Liu, M-Q, and Jiang, J-H. (2017). "The antagonistic or synchronous relationship between ASL/LBD and KNOX homeobox members" Biologia. 72:5.

Moon, J., Suh, S.-S., Lee, H., Choi, K.-R., Hong, C.B., Paek, N.-C., Kim, S.-G. and Lee, I. (2003), The SOC1 MADS-box gene integrates vernalization and gibberellin signals for flowering in Arabidopsis. Plant J. 35: 613-623.

Morsy, M.R., Almutairi, A.M., Gibbons, J., Yun, S.J., and Reyes, B.G. (2005). The OsLti6 genes encoding low-molecular-weight membrane proteins are differentially expressed in rice cultivars with contrasting sensitivity to low temperature. Gene. 344:171–80.

Mouradov, A., Cremer, F. and Coupland, G. (2002) Control of flowering time: interacting pathways as a basis for diversity. Plant Cell. 14: S111–S130.

Naested, H., Frandsen, G.I., Jauh, G.-Y., Hernandez-Pinzon, I., Nielsen, H.B., Murphy, D.J., Rogers, J.C., and Mundy, J. (2000). Caleosins: Ca2+-binding proteins associated with lipid bodies. Plant Mol. Biol. 44: 463–476

Navarre, C., and Goffeau, A. (2000). Membrane hyperpolarization and salt sensitivity induced by deletion of PMP3, a highly conserved small protein of yeast plasma membrane. EMBO J. 19:2515–24.

Nelson, J. C., Sorrells, M. E., Van Deynze, A. E., Lu, Y. H., Atkinson, M., Bernard, M., Leroy, P., Faris, J. D., and Anderson, J. A. (1995). Molecular mapping of wheat: major genes and rearrangements in homoeologous groups 4, 5, and 7. Genetics, 141(2), 721–731. PMID: 8647405

Nilson, S.E., and Assmann, S.M. (2010). The alpha-subunit of the Arabidopsis heterotrimeric G protein, GPA1 is a regulator of transpiration efficiency. Plant Physiol. 152:2067–2077.

Nilsson, O., Lee, I., Blázquez, M.A. and Weigel, D. (1998) Flowering-time genes modulate the response to LEAFY activity. Genetics. 150: 403–410.

Noh, B., Lee, S. H., Kim, H. J., Yi, G., Shin, E. A., Lee, M., Jung, K. J., Doyle, M. R., Amasino, R. M., and Noh, Y. S. (2004). Divergent roles of a pair of homologous jumonji/zinc-finger-class transcription factor proteins in the regulation of Arabidopsis flowering time. The Plant cell. 16(10): 2601–2613.

Okamoto, M., Tanaka, Y., Abrams, S.R., Kamiya, Y., Seki, M., and Nambara, E. (2009). High humidity induces abscisic acid 8'-hydroxylase in stomata and vasculature to regulate local and systemic abscisic acid responses in Arabidopsis. Plant Physiol. 149:825–834.

Orozco-Nunnelly, D.A., Muhammad, D., Mezzich, R., Lee, B-S., Jayathilaka, L., Kaufman, L.S., and Warpeha, K.M. (2014). Pirin1 (PRN1) Is a Multifunctional Protein that Regulates Quercetin, and Impacts Specific Light and UV Responses in the Seed-to-Seedling Transition of *Arabidopsis thaliana*. PLoS One. 9:4.

Oono, Y., Seki, M., Nanjo, T., Narusaka, M., Fujita, M., Satoh, R., Satou, M., Sakurai, T., Ishida, J., Akiyama, K., Lida, K., Maruyama, K., Satoh, S., Yamaguchi-Shinozaki, K., and Shhinozaki, K. (2003). Monitoring expression profiles of Arabidopsis gene expression during rehydration process after dehydration using ca. 7000 full-length cDNA microarray. Plant J. 34:868–887.

Pagnussat, G.C., Yu, H-J., Ngo, Q.A., Rajani, S., Mayalagu, S., Johnson, C.S., Capron, A., Xie, L-F., Ye, D., and Sundaresan, V. (2004) Genetic and molecular identification of genes required for female gametophyte development and function in Arabidopsis. Development. 132: 603-614.

Park, Y.C., Chapagain, S., and Jang, C.S. (2018). A negative regulator in response to salinity in Rice: *Oryza sativa* Salt-, ABA- and drought- induced RING finger protein 1 (OsSADR1). Plant Cell Physiol. 59(3): 575–589. doi:10.1093/pcp/pcy009.

Palanivelu, R., and Preuss, D. (2006). Distinct short-range ovule signals attract or repel *Arabidopsis thaliana* pollen tubes in vitro. BMC plant biol. 6:7. https://doi.org/10.1186/1471-2229:6-7.

Pandey, S. (2019). Heterotrimeric G-protein signaling in plants: con- served and novel mechanisms. Annu Rev Plant Biol 70:213–238. https://doi.org/10.1146/annurev-arplant-050718-100231

Pandey, S., Chen, J.G., Jones, A.M., and Assmann, S.M. (2006). G-protein complex mutants are hypersensitive to abscisic acid regulation of germination and postgermination development. Plant Physiol. 141: 243–256.

Pandey, S., Nelson, D.C., and Assmann, S.M. (2009). Two novel GPCR-type G proteins are abscisic acid receptors in Arabidopsis. Cell. 136:136–148.

Partridge, M., and Murphy, D.J. (2009). Roles of a membrane-bound caleosin and putative peroxygenase in biotic and abiotic stress responses in Arabidopsis. Plant Physiol Bioch. 47:796-806.

Perfus-Barbeoch, L., Jones, A.M., and Assmann, S.M. (2004). Plant heterotrimeric G protein function: insights from Arabidopsis and rice mutants. Curr Op in Plant Biology 7:719–731.

Peng, Y., Chen, L., Li, S., Zhang, Y., Xu, R., Liu, Z., Liu, W., Kong, J., Huang, X., Wang, Y., Cheng, B., Zheng, L., and Li, Y. (2018). BRI1 and BAK1 interact with G proteins and regulate sugar-responsive growth and development in Arabidopsis. Nat Commun. 9:1522.

Peng, J., Richards, D.E., Hartley, N.M., Murphy, G.P., Devos, K.M., Flintham, J.E., Beales, J., Fish, L.J., Worland, A.J., Pelica, F., Sudhakar, D., Christou, P., Snape, J.W., Gale, M.D., and Harberd. N.P. (1999). `Green revolution' genes encode mutant gibberellin response modulators. Nature. 400: 256–261.

Phobius A combined transmembrane topology and signal peptide predictor. Stockholm Bioinformatic Center. http://phobius.sbc.su.se/.

Piazza, M., Taiakina, V., Dieckmann, T., and Guillemette, J.G. (2017). Structural consequences of calmodulin EF hand mutations. Biochemistry 56(7):944–956.

Pingault, L., Choulet, F., Alberti, A., Glover, N., Wincker, P., and Feuillet, C. (2015). Deep transcriptome sequencing provides new insights into the structural and functional organization of the wheat genome. Genome Biol. 16(1): 29.

PLEXdb database; http://www.plexdb.org

Poxleitner, M., Rogers, S. W., Lacey Samuels, A., Browse, J., and Rogers, J. C. (2006). A role for caleosin in degradation of oil-body storage lipid during seed germination. Plant J. 47:6, 917–933.

Purkrtova, Z., Chardot, T., and Froissard, M. (2015). N-terminus of seed caleosins is essential for lipid droplet sorting but not for lipid accumulation. Arch. Biochem. Biophys. 579: 47–54.

Purkrtova, Z., Jolivet, P., Miquel, M., and Chardot, T. (2008). Structure and function of seed lipid-body-associated proteins C. R. Biol. 331(10): 746–754.

Qin, F., Kodaira, K. S., Maruyama, K., Mizoi, J., Tran, L. S., Fujita, Y., Morimoto, K., Shinozaki, K., and Yamaguchi-Shinozaki, K. (2011). SPINDLY, a negative regulator of gibberellic acid signaling, is involved in the plant abiotic stress response. Plant Physiol. 157(4): 1900–1913.

Ramírez-González, R. H., Borrill, P., Lang, D., Harrington, S. A., Brinton, J., Venturini, L., Davey, M., Jacobs, J., Ex F. van., Pasha, A., Khedikar, Y., Robinson, S. J., Cory, A. T., Florio, T., Concia, L., Juery, C., Schoonbeek, H., Steuernagel, B., Xiang, D., Ridout, C. J., Chalhoub, B., Mayer, K. F. X., Benhamed, M., Latrasse, D., Bendahmane, A., International Wheat Genome Sequencing Consortium, Wulff, B. B. H., Appels, R., Tiwari, V., Datla, R., Choulet, F., Pozniak, C. J., Provart, N. J., Sharpe, A. G., Paux, E., Spannag, M., Bräutigam, A., and Uauy, C. (2018). The transcriptional landscape of polyploid wheat. Science. 361:6403. https://doi. org/10.1126/science.aar6089.

Rasband, W.S. (1997–2014). ImageJ, U. S. National Institutes of Health, Bethesda, Maryland, USA, http://imagej.nih.gov/ij/.

Ridha Farajalla, M., and Gulick, P.J. (2007). The alpha-tubulin gene family in wheat (*Triticum aestivum L.*) and differential gene expression during cold acclimation. Genome. 50(5):502–10.

Ritchie, S., and Gilroy, S. (2000). Abscisic acid stimulation of phospholipase D in the barley aleurone is G-protein-mediated and localized to the plasma membrane. Plant Physiol. 124:693–702

Rocha, P.S.C.F. (2015). Plant abiotic stress-related RCI2/PMP3s: multigenes for multiple roles. Planta. 243(1):1–12.

Schmid, M., Davison, T.S., Henz, S.R., Pape, U.J., Demar, M., Vingron, M., Scholkopf, B., Weigel, D., and Lohmann, J.U. (2005). A gene expression map of *Arabidopsis thaliana* development. Nat. Genet. 37:501.

Schreiber, A.W., Sutton, T., Caldo, R.A., Kalashyan, E., Lovell, B., Mayo, G., Muehlbauer, G.J., Druka, A., Waugh, R., Wise, R.P., Langridge, P., and Baumann, U. (2009). Comparative transcriptomics in the Triticeae. BMC Genomics. 10:285. https://doi.org/10.1186/1471-2164-10-285.

Sequencing the *Aegilops tauschii* Genome, pseudomolecules; http://aegilops.wheat.ucdavis.edu/ATGSP/data.php

Shimada, T.L., Shimada, T., and Hara-Nishimura, I. (2010). A rapid and non- destructive screenable marker, FAST, for identifying transformed seeds of *Arabidopsis thaliana*. Plant J. 61:519–528.

Signora L., De Smet I., Foyer C.H., Zhang H. (2001). ABA plays a central role in mediating the regulatory effects of nitrate on root branching in Arabidopsis. Plant J. 28: 655–662

Simpson, G.G., and Dean, C. (2002). Arabidopsis, the Rosetta stone of flowering time? Science. 296: 285–289.

Sprang, S. (2001). GEFs: master regulators of G-protein activation. Trends Biochem. Sci. 26(4): 266–267. https://doi.org/10.1016/s0968-0004(01)01818-7

Sreenivasulu, N., Sopory, S.K., and Kavi Kishor, P.B. (2007). Deciphering the regulatory mechanisms of abiotic stress tolerance in plants by genomic approaches. Gene. 388: 1–13.

Sriram, K., and Insel, P. A. (2018). G Protein-Coupled Receptors as Targets for Approved Drugs: How Many Targets and How Many Drugs? Mol. Pharmacol. 93(4): 251–258.

Steffens, B., and Sauter, S. (2010). G proteins as regulators in ethylene-mediated hypoxia signaling. Plant Signal Behav. 5:375–378.

Steiner, B., Zimmerl, S., Lemmens, M., Adam, G., Till, B., and Schweiger, W. (2017). Functional identification of the wheat gene enhancing mycotoxin detoxification of the major Fusarium resistance QTL Fhb1. Toxins. 9(8): 238. doi:10.3390/toxins9080238.

Studier, F.W. (2005). Protein production by auto-induction in high density shaking cultures. Protein Expr Purif. 41(1):207–234.

Takahashi, S., Katagiri, T., Yamaguchi-Shinozaki, K., and Shinozaki, K. (2000). An Arabidopsis gene encoding a Ca 2+ -binding protein is induced by abscisic acid during dehydration. Plant Cell Physiol. 41:898-903.

Temple, B.R.S., and Jones, A.M. (2007). The plant heterotrimeric G-protein complex. Annu Review Plant Biology. 58:249–266.

The International Wheat Genome Sequencing Consortium (IWGSC). (2014). A chromosome-based draft sequence of the hexaploid bread wheat (*Triticum aestivum*) genome. Science. 345: 1251788. Available from http://www.wheatgenome.org/Tools-and-Resources. 10. 1126/science.1251788. PMID: 25035500.

Thung, L., Chakravorty, D., Trusov, Y., Jones, A. M., and Botella, J. R. (2013). Signaling specificity provided by the *Arabidopsis thaliana* heterotrimeric G-protein γ subunits *AGG1* and *AGG2* is partially but not exclusively provided through transcriptional regulation. PloS One. 8(3): e58503.

Thung, L., Trusov, Y., Chakravorty, D., and Botella, J.R. (2012). Gγ1+Gγ2+Gγ3 = Gβ: The search for heterotrimeric G-protein γ subunits in Arabidopsis is over. J. Plant Physiol. 169: 542–545.

Trusov, Y., Rookes, J.E., Tilbrook, K., Chakravorty, D., Mason, M.G., Anderson, D., Chen, J.G., Jones, A.M. and Botella, J.R. (2007). Heterotrimeric G protein c subunits provide functional selectivity in Gbc dimer signaling in Arabidopsis. Plant Cell. 19: 1235–1250.

Tsuge, T., Tsukaya, H., and Uchimiya, H. (1996). Two independent and polarized processes of cell elongation regulate leaf blade expansion in *Arabidopsis thaliana* (L.) Heynh. Development. 122(5):1589–1600.

Tuteja, N., and Mahajan, S. (2007). Calcium signaling network in plants: an overview. Plant Signal Behav. 2(2):79–85.

Ueguchi-Tanaka, M., Fujisawa, Y., Kobayashi, M., Ashikari, M., Iwasaki, Y., Kitano, H., and Matsuoka, M. (2000). Rice dwarf mutant d1, which is defective in the alpha subunit of the heterotrimeric G protein, affects gibberellin signal transduction. PNAS USA. 97(21): 11638–11643.

Uhrig, J.F., Mutondo, M., Zimmermann, I., Deeks, M.J., Machesky, L.M., Thomas, P., Uhrig, S., Rambke, C., Hussey, P.J., and Hülskamp, M. (2007). The role of Arabidopsis SCAR genes in ARP2-ARP3-dependent cell morphogenesis. Development. 134:967–977.

Ullah, H., Chen, J.G., Temple, B., Boyes, D.C., Alonso, J.M., Davis, KR, Ecker, JR., and Jones A.M. (2003). The β-subunit of the Arabidopsis G protein negatively regulates auxin-induced cell division and affects multiple developmental processes. Plant Cell. 15: 393–40.

Ullah, H., Chen, J.G., Young ,J.C., Im,, K.H., Sussman M.R., and Jones, A.M. (2001). Modulation of cell proliferation by heterotrimeric G protein in Arabidopsis. Science. 292:2066-2069.

Ullah, H., Chen, J.G., Wang, S., and Jones, A.M. (2002). Role of a heterotrimeric G protein in regulation of Arabidopsis seed germination. Plant Physiol. 129:897-907.

Ullah, H., Scappini, E. L., Moon, A. F., Williams, L. V., Armstrong, D. L., and Pedersen, L. C. (2008). Structure of a signal transduction regulator, RACK1, from *Arabidopsis thaliana*. Protein Sci. 17(10): 1771–1780.

Urano, D., Jackson, D., and Jones, AM. (2015). A G protein alpha null mutation confers prolificacy potential in maize. J.Exp.Bot. 66:4511–15.

Urano, D., and Jones, A.M. (2013). "Round Up the Usual Suspects": A Comment on Nonexistent Plant G Protein-Coupled Receptors. Plant Physiol.161:1097-1102.

Urano, D., and Jones, A. M. (2014). Heterotrimeric G protein-coupled signaling in plants. Annu. Rev. Plant Biol. 65: 365–384.

Wang, S., Assmann, S.M., and Fedoroff, N.V. (2008). Characterization of the Arabidopsis heterotrimeric G protein. J Biol Chem. 283:13913–13922

Wang, Y., and Botella, J.R. (2022). Heterotrimeric G Protein Signaling in Abiotic Stress. Plants (Basel). 11(7):876.

Wang, X.Q., Ullah, H., Jones, A.M. and Assmann, S.M. (2001). G protein regulation of ion channels and abscisic acid signaling in Arabidopsis guard cells. Science. 292; 2070–2072.

Warpeha, K.M., Upadhyay, S., Yeh, J., Adamiak, J., Hawkins, S.I., Lapik, Y.R., Anderson, M.B., and Kaufman, L.S. (2007). The GCR1, GPA1, PRN1, NF-Y signal chain mediates both blue light and abscisic acid responses in Arabidopsis. Plant Physiol. 143: 1590–1600.

Weigel, D., and Nilsson, O. (1995). A developmental switch sufficient for flower initiation in diverse plants. Nature. 377, 495–500.

Wendler, W.M., Kremmer, E., Forster, R., and Winnacker, E.L. (1997). Identification of pirin, a novel highly conserved nuclear protein. J. Biol. Chem. 272, 8482–8489.

Wettschureck, N., and Offermanns, S. (2005). Mammalian G proteins and their cell type specific functions. Physiol. Rev. 85(4): 1159–1204.

Whelan, S., and Goldman, N. (2001). A general empirical model of protein evolution derived from multiple protein families using a maximum-likelihood approach. Mol. Biol. Evol. 18: 691–699. doi:10. 1093/oxfordjournals.molbev.a003851. PMID: 11319253.

Wilson, R. N., Heckman, J. W., and Somerville, C. R. (1992). Gibberellin Is Required for Flowering in *Arabidopsis thaliana* under Short Days. Plant Physiol. 100(1), 403–408.

Winter, D., Vinegar, B., Nahal, H., Ammar, R., Wilson, G.V., and Provart, N.J. (2007). An "electronic fluorescent pictograph" browser for exploring and analyzing large-scale biological data sets. PLoS One. 8 (2): e718. doi:10.1371/journal.pone.0000718.

Witherow, S.D., Wang, Q., Konstatin, L., Cabrera, J.L., Chen, J., Willars, G.B., and Slepak, V.Z. (2000). Complexes of the G Protein Subunit Gβ5 with the Regulators of G Protein Signaling RGS7 and RGS9: Characterization in Native Tissues and in Transfected. Cells. J. Biol. Chem. 275: 24872-24880.

Woo, E.J., Dunwell, J.M., Goodenough, P.W., Marvier, A.C., and Pickersgill, R.W. (2000). Germin is a manganese containing homohexamer with oxalate oxidase and superoxide dismutase activities. Nat. Struct. Biol. 7: 1036–1040. PMID: 11062559.

Wulczyn, F.G., Krappmann, D., and Scheidereit, C. (1996). The NFκB/Rel and I κB gene families: mediators of immune response and inflammation. J. Mol. Med. 74: 749–769.

Xiong, L.W., Kleerekoper, Q.K., Wang, X., and Putkey, J.A. (2010) Intra- and interdomain effects due to mutation of calcium-binding sites in calmodulin. J Biol Chem 285(11):8094–8103.

Yan, W., Chen, D., Smaczniak, C., Engelhorn, J., Liu, H., Yang, W., Graf, A., Carles, C. C., Zhou, D. X., and Kaufmann, K. (2018). Dynamic and spatial restriction of Polycomb activity by plant histone demethylases. Nature plants, 4(9), 681–689. https://doi.org/10.1038/s41477-018-0219-5

Ye, Z., Rodriguez, R., Tran, A., Hoang, H., de los Santos D, Brown, S., and Vellanoweth, R. L. (2000). The developmental transition to flowering represses ascorbate peroxidase activity and induces enzymatic lipid peroxidation in leaf tissue in *Arabidopsis thaliana.* Plant Sci.158(1-2), 115–127.

Zhang, C.Q., Nishluchi, S., Liu, S., and Takano, T. (2008). Characterization of two plasma membrane. Protein 3 genes (PutPMP3) from the alkali grass, *Puccinellia tenuiflora* and functional comparison of the rice homologues, OsLti6a/b from rice. BMB Rep. 41:448–54.

Zhang, B., Sztojka, B., Escamez, S., Vanholme, R., Hedenström, M., Wang, Y., Turumtay, H., Gorzsás, A., Boerjan, W., and Tuominen, H. (2019). PIRIN2 suppresses S-type lignin accumulation in a noncell-autonomous manner in Arabidopsis xylem elements. New Phytol. 225(5): 1923–1935.

Zhang, H., Yang, Y., Wang, C., Liu, M., Li, H., Fu, Y., Wang, Y., Nie, Y., Liu, X., and Ji, W. (2014). Large-scale transcriptome comparison reveals distinct gene activations in wheat responding to stripe rust and powdery mildew. BMC genomics, 15(1), 898. PMID: 25318379.

Zhang, H., Zhang, F., Yu, Y., Feng, L., Jia, J., Liu, B., Li, B., Guo, H., and Zhai, J. (2020). A Comprehensive Online Database for Exploring ~20,000 Public Arabidopsis RNA-Seq Libraries. Molecular plant. 13(9): 1231–1233. https://doi.org/10.1016/j.molp.2020.08.001

Zhao, Y., Tong, H., Cai. R., Peng, X., Li, X., Gan, D., and Zhu, S. (2018). Identification and characterization of the RCI2 gene family in maize (*Zea mays*). J Genet. 93:655–66.

Zhao, J., and Wang, X. (2013). Biochemical Analysis of the Interaction Between Phospholipase Dα1 and GTP-Binding Protein α-Subunit from *Arabidopsis thaliana*. Methods Mol Biol. 1043: 21-35. 10.1007/978-1-62703-532-3_3.

Zimmermann, P., Heinlein, C., Orendi, G., and Zentgraf, U. (2006). Senescence-specific regulation of catalases in *Arabidopsis thaliana* (L.) Heynh. Plant Cell Environ. 29: 1049–1060.

Zolla, G., Heimer, Y.M., and Barak, S. (2010). Mild salinity stimulates a stress-induced morphogenic response in *Arabidopsis thaliana* roots. J Exp Bot. 61: 211-24.